

UNIVERSIDADE DE LISBOA
Faculdade de Medicina de Lisboa



**DEVELOPMENT OF AN INNOVATIVE REAL-TIME
ASSAY FOR ANTIMALARIAL SENSITIVITY TESTING**

Maria Sousa Rebelo

Orientador: Prof. Doutor Thomas Hanscheid

Co-orientador: Prof.^a Doutora Maria Manuel Dias Mota

Tese especialmente elaborada para obtenção do grau de Doutor em Ciências Biomédicas
Especialidade Microbiologia e Parasitologia

2017

UNIVERSIDADE DE LISBOA
Faculdade de Medicina de Lisboa



**DEVELOPMENT OF AN INNOVATIVE REAL-TIME ASSAY FOR
ANTIMALARIAL SENSITIVITY TESTING**

Maria Sousa Rebelo

Orientador: Prof. Doutor Thomas Hanscheid

Co-orientador: Prof.^a Doutora Maria Manuel Dias Mota

Tese especialmente elaborada para obtenção do grau de Doutor em Ciências Biomédicas
Especialidade Microbiologia e Parasitologia

Júri

Presidente:

Doutor José Augusto Gamito Melo Cristino, Professor Catedrático e Presidente do Conselho Científico da Faculdade de Medicina da Universidade de Lisboa

Vogais:

- Doutor Martin Peter Grobusch, *Professor (Chair) of Tropical Medicine, Specialist in Internal Medicine, Infectious Diseases, Tropical Medicine of Academic Medical Center, University of Amsterdam, The Netherlands;*
- Doutora Ana Paula Martins dos Reis Arez, Investigadora Auxiliar do Instituto de Higiene e Medicina Tropical da Universidade Nova de Lisboa;
- Doutor Rui Miguel Prudêncio da Cunha Pignatelli, Investigador, *Group Leader* do Instituto de Medicina Molecular, da unidade de investigação associada à Faculdade de Medicina da Universidade de Lisboa;
- Doutora Luísa Miranda Figueiredo, Investigadora, *Group Leader* do Instituto de Medicina Molecular, da unidade de investigação associada à Faculdade de Medicina da Universidade de Lisboa;
- Doutor Mário Nuno Ramos de Almeida Ramirez, Professor Associado com Agregação da Faculdade de Medicina da Universidade de Lisboa;
- Doutor Thomas Hanscheid, Professor Auxiliar com Agregação da Faculdade de Medicina da Universidade de Lisboa; (Orientador).

Bolsa de doutoramento financiada pela Fundação para a Ciência e a Tecnologia
(SFRH/BD/84530/2012)

2017

**As opiniões expressas nesta publicação são da exclusiva
responsabilidade do seu autor.**

**A impressão desta tese foi aprovada pelo Conselho Científico da
Faculdade de Medicina de Lisboa em reunião de 24 de Janeiro de 2017.**

ACKNOWLEDGMENTS

My sincere acknowledgments to my supervisor Prof. Thomas Hanscheid, for teaching me so much, for giving me the opportunity to become a better and more knowledgeable person and for always supporting me whenever I needed. I would also like to thank my co-supervisor Prof. Maria Mota.

I would like to thank Prof. José Melo Cristino, head of the Instituto de Microbiologia, Faculdade de Medicina, Universidade de Lisboa and Prof. Mário Ramirez, group leader of the Molecular Microbiology and Infection Unit.

I would like to acknowledge Prof. Peter Kremsner, the director of the *Centre de Recherches Médicales de Lambaréné* (CERMEL), Dr. Marguerite Loembe the head of the laboraroty at CERMEL and Dr. José Fernandes, physician at Albert Schweitzer Hospital.

I also thank all my colleagues and friends I met in Gabon, who shared with me some of the best moments of my life and who made me thrive in such a challenging environment.

I thank Dr. Howard Shapiro and Prof. David Warhurst for being a constant source of inspiration and for sharing their unlimited knowledge with me.

To Rui Gardner, the ex-head of the flow cytometry facility of *Instituto Gulbenkian de Ciência*.

To previous and current laboratory colleagues, specially to Rosangela Frita, Ana Parreira, Cláudia Sousa, Denise Francisco and Carolina Tempera, who made my life in the laboratory much more pleasant.

Thank you Vanessa Luís, my tutor, for having such a beautiful mind and for sharing all ideas and ideals with me.

To my family, closest friends and, specially, to my better half for unconditional friendship and support. And finally to my four pillars in life: my mother, my father, Antónia e Jota, who will stand by me no matter what.

SUMMARY

Keywords: malaria; antimalarial drug resistance; drug sensitivity testing; hemozoin, flow cytometry.

Antimalarial drug resistance has always been an obstacle in the fight against malaria. Malaria parasites have developed resistance to most available antimalarial drugs and, more recently resistance to artemisinins, the first-line treatment for malaria, is emerging and spreading in Southeast Asia. Artemisinin resistance is characterized by delayed parasite clearance times observed in malaria patients. For now this resistance is considered to be partial by the WHO and artemisinin-combination therapies remain as the mainstay of antimalarial treatment.

In vitro assays are of paramount importance to detect and monitor drug resistance. Several *in vitro* drug assays exist, however their inherent characteristics, such as the use of radioactive or expensive reagents and their long turn-around times limit their application.

The project developed in the context of this thesis aimed to develop a novel drug assay for *Plasmodium* spp. that would overcome some of the limitations of currently available drug assays. The underlying idea was to use hemozoin, a crystal produced by malaria parasites, to measure their own growth or maturation which would allow to detect drug effects.

The hemozoin content increases as parasites mature inside the erythrocytes. Thus, hemozoin constitutes an optimal parasite maturation biomarker. Moreover, it is a birefringent crystal, and as such it is able to depolarize light. The resulting light depolarization can be easily detected by optical methods such as flow cytometry. It was previously shown by our laboratory that in a rodent model of malaria depolarization caused by hemozoin inside infected erythrocytes could be detected using a simple flow cytometric set-up. Moreover, the inhibitory effect of commonly used antimalarial drugs could also be determined after only 6-8 hours of incubation.

The main objectives of the work developed during this thesis was to further develop the flow cytometric detection of hemozoin assay using *P. falciparum in vitro* cultures and to assess its performance *ex vivo*, in the field, using samples from malaria patients.

SUMMARY

A benchtop flow cytometer (Cyflow SL) was modified to allow the detection of light depolarization and it was used for all studies. Other commercially available cytometers (MoFlo, Accuri C6, Attune) were also easily adapted to detect light depolarization, showing that the measurement of this additional parameter can be accomplished in different instruments.

In vitro cultures of *P. falciparum* were established and allowed to further investigate the potential of this novel method. Ring-stage synchronized cultures of *P. falciparum* were incubated with several antimalarial drugs (chloroquine, mefloquine, quinine, artemisinin, artesunate and pyrimethamine). Analysis of depolarizing events, corresponding to parasitized erythrocytes containing hemozoin, allowed the detection of parasite maturation. Furthermore, chloroquine resistance and the inhibitory effect of all antimalarial drugs tested, except for pyrimethamine, could be determined as early as 18 - 24 hours of incubation. The 50% inhibitory concentrations (IC₅₀) obtained at 24 hours of incubation were comparable to previously reported values. However, these values were most of the times higher than the ones obtained with the already validated HRP2 ELISA assay. Indeed, IC₅₀ values may differ considerably between assays. Different assays measure different parameters to assess parasite growth, at different time-points. Moreover, variations in parasite density and hematocrit as well as the stage-dependent action of antimalarial drugs, may influence these values. Altogether, explaining the differences in IC₅₀ values that are commonly observed.

The performance of the hemozoin detection assay in the field was assessed during a 6-month trial performed in Gabon, a malaria endemic country. The trial was conducted in the *Centre de Recherches Médicales de Lambaréné* – Albert Schweitzer Hospital. On site, an existing flow cytometer (Cyflow SL) was modified to detect light depolarization caused by hemozoin. A total of 46 samples from malaria patients were analyzed during this study. Blood samples were incubated with increasing concentrations of chloroquine, artesunate and artemisinin. The percentage of depolarizing cells was used as maturation indicator and measured at 24, 48 and 72 hours of incubation to determine parasite growth and drug effects. Analysis of *ex vivo* cultures of parasites obtained from blood samples of malaria patients showed four different growth profiles. The flow cytometric detection of hemozoin allowed to detect drug effects in 39/46 (85%) of samples. In 25 samples drug effects were

measurable at 24 hours. In the remaining 14 samples parasite maturation was delayed, and thus drug effects were only detected at 48 hours of incubation. Obtained IC₅₀ values showed that chloroquine-resistant parasites were still common and present in Lambaréné, Gabon but they were fully sensitive to artesunate and artemisinin.

Finally, the usefulness of the hemozoin detection assay in the investigation of artemisinin resistance *in vitro* was also assessed. Artemisinin-resistant (MRA-1240) and sensitive (MRA-1239, 3D7) strains were cultured *in vitro*. Parasite maturation was determined based on the flow cytometric detection of hemozoin-containing cells. Two different drug assays were performed: 1) standard drug assay: where ring-stage parasites were continuously incubated with increasing concentrations of dihydroartemisinin (DHA) for 48 hours; and 2) pulse assay: where tightly ring-stage synchronized parasites were incubated with a single high-dose (700 nM) of DHA for 6 hours.

Results showed that at 24 hours of incubation artemisinin-resistant parasites had increased IC₅₀ values, in comparison to the artemisinin-sensitive strains (15 nM and 8 nM, respectively). Moreover, when parasites were exposed to a high-dose of DHA for 6 hours, increased survival rates associated with artemisinin resistance could be detected after only 30 hours of incubation.

Interestingly, it was also observed that artemisinin-resistant parasites do not seem to enter dormancy, as it has been previously suggested by others. Microscopic assessment performed after 72 hours of incubation showed that parasites that survived to a 6-hour exposure to DHA were very close in terms of parasite development to the ones found in the drug free control. Further investigation using more artemisinin-resistant strains is required to determine whether increased IC₅₀ values correlate with the delayed parasite clearance times observed in the patients; and if the underlying mechanisms of artemisinin resistance is or not related to dormancy.

Overall, the work presented in this thesis shows that hemozoin detection by flow cytometry is an alternative, reagent-free and rapid drug assay that overcomes some of the limitations of currently available drug assays for *P. falciparum*. Moreover, it may also be a useful tool in the study of artemisinin resistance both in culture-adapted strains and, possibly in strains obtained directly from patients.

Importantly, this work paves the way for the development and investigation of better

SUMMARY

tools to assess drug effects and monitor drug resistance in *Plasmodium* spp. Several novel hemozoin detection platforms are available or under development and should definitely be further explored for their potential to be used as antimalarial drug assays. Furthermore, combination of hemozoin detection with the measurement of other parameters, such as DNA and RNA content and parasite viability may even provide additional important information to reliably determine the developmental stage and metabolic status of parasites and, consequently, detect drug effects. Hopefully, this would lead to the development of an optimal antimalarial drug assay that could play an important role in the fight against malaria.

RESUMO

Palavras-chave: malária; fármacos anti-maláricos; testes de suscetibilidade a fármacos; hemozoína; citometria de fluxo.

O número de casos e mortes por malária tem vindo a diminuir, de forma considerável, na última década, devido principalmente à disponibilidade de fármacos eficazes no tratamento desta doença e à implementação de medidas de controlo vetorial. No entanto, o parasita da malária desenvolveu resistência à maioria dos fármacos anti-maláricos. Na atualidade, a situação mais alarmante ocorre no Sudeste Asiático e está relacionada com o surgimento de parasitas resistentes à artemisinina, o fármaco base da terapêutica de primeira linha para a malária. A resistência à artemisinina é diferente das resistências observadas anteriormente para outros anti-maláricos e caracteriza-se por um atraso na eliminação do parasita do sangue observado em doentes com malária. Apesar destas observações, é importante referir que esta resistência é considerada pela Organização Mundial de Saúde (OMS) como sendo parcial e as terapêuticas combinadas, baseadas na artemisinina, continuam a ser o pilar do tratamento da malária.

Neste contexto, os testes de suscetibilidade *in vitro* são ferramentas essenciais para detetar e monitorizar o aparecimento de parasitas resistentes. Atualmente, existem vários testes de suscetibilidade *in vitro* para *Plasmodium* spp., o agente etiológico da malária, mas a sua aplicação é limitada por características, como a utilização de reagentes radioativos e dispendiosos, além dos longos tempos de resposta.

O projeto realizado no âmbito desta tese teve como objetivo desenvolver um novo teste de suscetibilidade para *Plasmodium* spp. capaz de ultrapassar algumas das limitações dos testes existentes. A ideia subjacente baseia-se na deteção da hemozoína como método indireto de determinação do efeito de anti-maláricos na maturação do parasita.

A hemozoína é produzida em quantidades crescentes pelos parasitas da malária, durante a sua maturação no interior dos eritrócitos, sendo um cristal birrefringente capaz de despolarizar a luz, constituindo assim um ótimo bio-marcador da maturação do parasita. Por sua vez, a despolarização da luz pode ser detetada por métodos óticos, como a citometria de fluxo. Trabalhos realizados anteriormente no nosso laboratório num modelo animal de malária demonstraram que a despolarização da luz causada pela hemozoína, que se encontra no interior de eritrócitos infectados, pode ser detetada utilizando um protocolo simples baseado em citometria de fluxo. Verificou-se ainda que este método permitiu

RESUMO

detetar a maturação dos parasitas no interior dos eritrócitos, bem como o efeito inibitório dos fármacos anti-maláricos testados, em apenas seis/oito horas de incubação.

O principal objetivo do trabalho realizado, durante este projeto de doutoramento, consistiu em desenvolver este novo teste de suscetibilidade baseado na deteção de hemozoína por citometria de fluxo, utilizando culturas *in vitro* de parasitas de malária que infetam humanos, nomeadamente o *P. falciparum*. Posteriormente, o desempenho deste novo teste foi avaliado *ex vivo*, no campo, utilizando amostras de doentes com malária.

Para isso, um citómetro de fluxo de bancada (Cyflow SL) foi modificado para permitir a deteção da despolarização da luz causada pela hemozoína. Outros citómetros (MoFlo, Accuri C6, Attune), disponíveis no mercado, também foram adaptados, sem dificuldade, para detetar este parâmetro adicional. Não obstante, o Cyflow SL modificado foi o instrumento usado na maioria dos estudos realizados durante este projeto.

Estabeleceram-se culturas *in vitro* de *P. falciparum* que permitiram investigar o potencial da deteção de hemozoína por citometria de fluxo como teste de suscetibilidade aos anti-maláricos. Neste sentido, as culturas de *P. falciparum* foram sincronizadas e os parasitas em forma de anel foram incubados com vários fármacos anti-maláricos (cloroquina, mefloquina, quinino, artemisinina, artesunato e pirimetamina). A análise das células que despolarizam a luz, correspondentes a eritrócitos parasitados que contêm hemozoína, permitiu detetar a maturação do parasita ao longo do tempo, assim como o efeito inibitório de todos os anti-maláricos testados em apenas dezoito/vinte e quatro horas de incubação, à exceção da pirimetamina, cujo efeito foi detetado somente após setenta e duas horas. As concentrações inibitórias de 50% (IC₅₀), calculadas às vinte e quatro horas de incubação, eram comparáveis com os valores previamente reportados usando outros métodos, embora estes valores fossem, na maioria das vezes, superiores aos valores obtidos com o teste de ELISA-HRP2. Sabe-se que os valores de IC₅₀ podem variar de modo considerável entre testes, maioritariamente porque os parâmetros de medição e os tempos de incubação são diferentes consoante o teste usado. Além disso, variações da parasitémia e de hematócrito, bem como a especificidade do fármaco em determinados estádios de desenvolvimento do parasita, também podem influenciar estes valores.

O desempenho do teste de deteção de hemozoína por citometria de fluxo, em amostras de doentes com malária, foi avaliado durante um estudo de seis meses, realizado no Gabão, um país onde a malária é endémica. Neste estudo, o citómetro de fluxo existente no local (Cyflow SL) foi modificado para detetar a despolarização da luz causada pela hemozoína, tendo sido analisado um total de quarenta e seis amostras de doentes com malária. As

amostras de sangue foram incubadas com concentrações crescentes de cloroquina, artesunato e artemisinina e a percentagem de células que despolarizam a luz foi utilizada como indicador de maturação do parasita, tendo sido medida às vinte e quatro, quarenta e oito, e setenta e duas horas de incubação, para determinar o crescimento do parasita e os efeitos dos anti-maláricos testados.

Após a realização de culturas *ex vivo* de parasitas obtidos de amostras de sangue de doentes com malária, observou-se que existiam quatro perfis de crescimento diferentes. Independentemente desta observação, a deteção da hemozoína por citometria de fluxo permitiu determinar o efeito dos fármacos anti-maláricos em trinta e nove das quarenta e seis (85%) amostras. Em vinte e cinco amostras, o efeito dos fármacos foi detetado às vinte e quatro horas. Nas catorze amostras restantes, os parasitas apresentaram um atraso na sua maturação e, por isso, o efeito dos fármacos anti-maláricos foi detetado apenas às quarenta e oito horas de incubação. Os valores de IC₅₀ obtidos revelaram que ainda existem naquela região do Gabão (Lambaréné) parasitas resistentes à cloroquina, mas estes continuam a ser totalmente sensíveis ao artesunato e à artemisinina.

Por último, investigou-se a deteção de hemozoína por citometria de fluxo no estudo da resistência à artemisinina *in vitro*. Para isso, estirpes resistentes (MRA-1240) e sensíveis (MRA-1239, 3D7) à artemisinina foram cultivadas *in vitro*. Uma vez mais, a maturação do parasita foi determinada com base na deteção de eritrócitos com hemozoína por citometria de fluxo. Neste caso, foram realizados dois tipos de ensaios: 1) ensaio de suscetibilidade padrão, no qual os parasitas em forma de anel são incubados com concentrações crescentes de dihidroartemisinina (DHA), durante quarenta e oito horas; 2) ensaio de pulso, em que os parasitas sincronizados em forma de anel são incubados com uma única dose (700 nM) de DHA, durante seis horas.

Os resultados mostraram que, às vinte e quatro horas de incubação, os parasitas resistentes à artemisinina têm valores de IC₅₀ superiores aos observados para as estirpes sensíveis à artemisinina (quinze nM e oito nM, respetivamente). Nos ensaios de pulso, observou-se um aumento na taxa de sobrevivência associado à resistência à artemisinina, após somente trinta horas de incubação. É de salientar que a avaliação microscópica, realizada às setenta e duas horas de incubação, revelou que os parasitas, expostos durante seis horas à DHA, são muito semelhantes, a nível de desenvolvimento, aos parasitas encontrados no controlo sem fármaco. Tal indica que os parasitas resistentes à artemisinina não parecem entrar num estado de dormência, ao contrário do que foi descrito noutros estudos. Será necessária investigação adicional, utilizando mais estirpes resistentes à artemisinina, para determinar:

RESUMO

1) se os valores aumentados de IC50 estão correlacionados com o atraso nos tempos de eliminação do parasita observados nos doentes; 2) se o mecanismo de resistência à artemisinina está ou não relacionado com um processo de dormência.

O trabalho apresentado nesta tese demonstra que a detecção de hemozoína por citometria de fluxo pode ser uma alternativa aos testes de suscetibilidade aos anti-maláricos existentes. Esta abordagem não requer a utilização de reagentes adicionais para a detecção dos parasitas e é um teste relativamente rápido, superando algumas das limitações dos testes de suscetibilidade atualmente disponíveis. Além disso, também pode ser uma ferramenta útil no estudo da resistência à artemisinina, tanto em estirpes adaptadas a crescer *in vitro*, como em estirpes obtidas diretamente de doentes com malária.

Convém referir que atualmente estão disponíveis, ou em desenvolvimento, novas plataformas de detecção de hemozoína que devem ser exploradas relativamente ao seu potencial para utilização como testes de suscetibilidade aos anti-maláricos. Para além disso, a combinação da detecção de hemozoína com a medição de outros parâmetros, como o conteúdo de DNA e RNA e viabilidade do parasita, pode fornecer informações adicionais e relevantes na determinação do efeito inibitório dos fármacos anti-maláricos.

Em conclusão, esperamos que os resultados obtidos durante este projeto possam conduzir ao desenvolvimento do teste de suscetibilidade ideal para *Plasmodium* spp. e que este possa desempenhar um papel importante no combate à malária.

THESIS OUTLINE

The present thesis describes the development and validation of a novel, rapid and reagent-free antimalarial sensitivity assay for *Plasmodium falciparum*.

In **Chapter I**, an overview of the main subjects discussed in this thesis is done to contextualize the theme. The problematic of malaria as a public health disease, the importance of antimalarial drug resistance and the *in vitro* detection of drug resistance is introduced. Furthermore, several aspects about the subject of study (hemozoin) and the technique that was investigated (flow cytometry) are also presented.

In **Chapter II**, the detection of light depolarization caused by hemozoin by flow cytometry is presented and discussed in the context of malaria research. Specific explanations on how to modify different commercially available flow cytometers to detect this additional parameter are given.

Chapter III, describes how the flow cytometric detection of hemozoin can be used to assess drug effects in *P. falciparum* laboratory-adapted strains. Results presented in this chapter show that the inhibitory effect of all antimalarial drugs tested could be detected. Therefore, indicating that the reagent-free and real-time hemozoin detection assay could become a novel assay for the detection of drug effects on *P. falciparum*.

In **Chapter IV**, the performance of the hemozoin detection assay is investigated in the field using samples from malaria patients. Results presented here were obtained from a study conducted in a malaria-endemic country (Gabon) where samples from malaria patients were cultured *ex vivo* with several antimalarial drugs. Drug effects and parasite resistance could be detected in blood samples from malaria patients using the hemozoin detection assay.

In **Chapter V**, the usefulness of the hemozoin assay to detect artemisinin resistance, as characterized by a delay in parasite clearance times in the patients, *in vitro* is investigated. Results are still preliminary but they seem to indicate that increased 50% inhibitory concentrations can be detected in artemisinin-resistant parasites, as well as increased survival rates.

Finally, in **Chapter VI**, an overview, general discussion and conclusions of major findings of the work presented in this thesis is provided. Future perspectives are also discussed.

TABLE OF CONTENTS

ACKNOWLEDGMENTS	i
SUMMARY	iii - vi
RESUMO	vii - x
THESIS OUTLINE.....	xi
TABLE OF CONTENTS.....	xiii - xv
FIGURE AND TABLE INDEX.....	xvii - xx
ABBREVIATIONS.....	xxi -xxii

CHAPTER I – GENERAL INTRODUCTION..... 1 - 62

1. MALARIA.....	1
a. Epidemiology and the disease.....	1
b. Threats to malaria control.....	3
c. Treatment of malaria.....	4
<i>i. Antimalarial drugs – historical overview.....</i>	<i>4</i>
<i>ii. Current guidelines for the treatment of malaria.....</i>	<i>6</i>
<i>iii. New antimalarial drugs.....</i>	<i>8</i>
d. Mechanisms of action of antimalarial drug.....	10
2. ANTIMALARIAL DRUG RESISTANCE.....	12
a. Current status of antimalarial drug resistance.....	13
b. Mechanisms of antimalarial drug resistance.....	16
3. ASSESING ANTIMALARIAL DRUG EFFICACY.....	18
a. Importance of assessing antimalarial drug efficacy.....	18
b. Therapeutic efficacy trials.....	18
c. <i>In vitro</i> assays for antimalarial drug testing.....	20
<i>i. Overview.....</i>	<i>21</i>
<i>ii. Microscopy – the schizont maturation test (WHO microtest).....</i>	<i>21</i>
<i>iii. Radioisotope methods.....</i>	<i>22</i>
<i>iv. Fluorometric assays.....</i>	<i>22</i>
<i>v. Antigen detection by ELISA.....</i>	<i>23</i>
<i>vi. Flow cytometric methods.....</i>	<i>24</i>
d. Interpretation of <i>in vitro</i> results – comparison of different <i>in vitro</i> assays.....	26

TABLE OF CONTENTS

e. Molecular methods.....	29
f. Key practical aspects of antimalarial drug testing.....	29
i. <i>Culturing of P. falciparum</i>	29
ii. <i>Culture-related factors that influence in vitro drug sensitivity</i>	30
iii. <i>Synchronization of parasites</i>	34
4. HEMOZOIN - THE MALARIA PIGMENT.....	34
a. Overview.....	34
b. Formation of hemozoin.....	35
c. Biophysical properties of hemozoin and its use for the study of malaria.....	36
5. FLOW CYTOMETRY.....	37
a. Principles of flow cytometry.....	37
b. Flow cytometry and malaria.....	38
c. Detection of light depolarization by flow cytometry.....	38
6. A NOVEL ANTIMALARIAL DRUG ASSAY FOR <i>PLASMODIUM</i> spp. BASED ON THE FLOW CYTOMETRIC DETECTION OF HEMOZOIN.....	39
7. REFERENCES.....	41
CHAPTER II - FLOW CYTOMETRIC DETECTION OF HEMOZOIN.....	63 - 88
CHAPTER III - DEVELOPMENT OF THE HEMOZOIN DRUG ASSAY USING <i>P. FALCIPARUM</i> LABORATORY-ADAPTED STRAINS.....	89 - 119
CHAPTER IV - VALIDATION OF THE HEMOZOIN DETECTION ASSAY IN THE FIELD USING SAMPLES FROM MALARIA PATIENTS.....	121 - 139
CHAPTER V - USEFULNESS OF THE HEMOZOIN ASSAY TO DETECT ARTEMISININ RESISTANCE.....	141 - 175
1. Introduction.....	141
1.1. Artemisinin-combination therapies.....	141
1.2. Artemisinin-induced dormancy.....	142
1.3. Artemisinin resistance.....	144
1.4. <i>In vitro</i> detection of artemisinin resistance.....	145

1.5. Hemozoin as an alternative assay to detect artemisinin resistance *in vitro*... 146

2. Material and Methods..... 146

3. Results and Discussion..... 151

 3.1. Artemisinin-resistant parasites show increased IC50 values when using the Hz detection assay 151

 3.2. Artemisinin-resistant parasites show increased survival rates in comparison to artemisinins-sensitive strains..... 153

 3.3. Assessment of parasite survival using a simpler protocol for parasite synchronization..... 156

 3.4. Artemisinin-resistant parasites do not seem to enter dormancy..... 158

 3.5. Artemisinin-resistant parasites exhibit altered development patterns..... 166

4. Conclusions..... 168

5. References..... 171

CHAPTER VI – GENERAL CONCLUSION AND FINAL REMARKS..... 177 - 188

PUBLICATIONS..... 189

FIGURE AND TABLE INDEX**Chapter I – General Introduction**

Figure I.1: <i>Plasmodium</i> spp. life cycle.....	2
Figure I.2: Global Portfolio of Antimalarial Medicines (as of 30th June 2016).....	10
Figure I.3: Location of study sites and proportions of patients with artemisinin resistance.....	15
Figure I.4: A representative dose-response curve.....	26
Figure I.5: Hemozoin as a parasite maturation indicator.....	35
Figure I.6: Electron microscopic picture of a <i>P. falciparum</i> infected erythrocyte.....	36
Figure I.7: Granularity/Lobularity plots from the Cell-Dyn 3500.....	39
Figure I.8: Flow cytometric detection of hemozoin and assessment of drug inhibitory effects.....	40

Table I.1: Goals, milestones and targets of the Global technical strategy for Action and Investment to defeat malaria 2016–2030.....	4
Table I.2: Currently used antimalarial drugs.....	7
Table I.3: Current guidelines to treat malaria.....	8
Table I.4: Factors that influence the development of antimalarial drug resistance.....	13
Table I.5: Years of introduction of antimalarial drugs and of their first reports of resistance.....	14
Table I.6: WHO classification of responses to treatment.....	20
Table I.7: Summary of dyes used to study <i>Plasmodium</i> spp. by flow cytometry.	25
Table I.8: Antimalarial activities of several antimalarial drugs determined by different <i>in vitro</i> sensitivity assays against <i>P. falciparum</i> 3D7 strain.....	27
Table I.9: Comparative descriptions of available <i>in vitro</i> sensitivity assays for <i>Plasmodium falciparum</i>	28
Table I.10: Molecular Markers for antimalarial drug resistance.....	29

Chapter II - Flow Cytometric Detection of Hemozoin

Figure II.1: Optical layout of three different bench top flow cytometers modified to detect light depolarization.....	69
Figure II.2: Detection of depolarizing side-scattered light by four different flow cytometers.....	70

FIGURE AND TABLE INDEX

Figure II.3: Detection of intraerythrocytic, intraleukocytic and free hemozoin (Hz).....	70
Figure II.4: Assessing hemozoin depolarization with different wavelengths.....	71
Figure SII.1: Degree of depolarization and developmental stage of <i>P. berghei</i> infected mouse red blood cells.....	78
Figure SII.2: Degree of depolarization and developmental stage of <i>P. falciparum</i> infected red blood cells culture.....	78
Figure SII.3: MoFlo Optical Layout for the 4 different tested wavelengths.....	79
Figure SII.4: Acquisition plots and gating strategy for day 25-03-2014 using Multiline UV.....	80
Figure SII.5: Acquisition plots and gating strategy for day 25-03-2014 using 457 nm.....	80
Figure SII.6: Acquisition plots and gating strategy for day 25-03-2014 using 488 nm.....	81
Figure SII.7: Acquisition plots and gating strategy for day 25-03-2014 using 514 nm.....	81
Table II.1: Samples and protocols used for preparation of samples.....	66
Table SII.1: Separation Index ratios calculated for each wavelength for four different samples.....	82

Chapter III - Development of the Hemozoin Drug Assay using *P. falciparum*

Laboratory-adapted Strains

Figure III.1: Gating for detection of depolarizing parasitized red blood cells in a <i>Plasmodium falciparum</i> culture.....	96
Figure III.2: Growth curves of <i>Plasmodium falciparum</i> (3D7) in culture.....	98
Figure III.3: Effect of chloroquine on the growth curve of <i>P. falciparum</i> sensitive and resistant strains.....	99
Figure III.4: Effect of quinine, mefloquine, artemisinin and a spiroindolone (NITD246) on the growth curve of <i>P. falciparum</i> (3D7).....	100
Figure III.5: Effect of artesunate on the growth curve of <i>P. falciparum</i> (3D7) and the effect of 12 hourly renewing of artesunate during incubation.....	101
Figure III.6: Growth curve of <i>Plasmodium falciparum</i> (3D7) after treatment with pyrimethamine.....	102
Figure SIII.1: Cyflow® flow cytometer and optical bench layout.....	114

Table III.1: Inhibitory concentrations (50%) of several antimalarial drugs against *P. falciparum* 3D7 strain determined by the Hemozoin detection assay at different times of incubation..... 103

Table III.2: Antimalarial activities of several antimalarial drugs determined by the Hemozoin detection assay and the HRP2 assay..... 103

Table SIII.1: Comparative descriptions of available in vitro sensitivity assays for *Plasmodium falciparum*..... 111

Table SIII.2: Antimalarial activities of several antimalarial drugs determined by different in vitro sensitivity assays against *P. falciparum* 3D7 strain..... 112

Chapter IV - Validation of the Hemozoin Detection Assay in the Field using Samples from Malaria Patients

Figure IV.1: Flow cytometry modifications to detect light depolarization..... 124

Figure IV.2: Representative analysis of drug effects assessed after *ex vivo* culture of blood samples from malaria patients..... 129

Figure IV.3: Inhibitory 50% concentrations obtained for artesunate and artemisinin..... 130

Table IV.1: Summarized data of isolates exhibiting different *ex vivo* growth profiles analysed by the hemozoin assay..... 128

Chapter V - Usefulness of the Hemozoin Assay to Detect Artemisinin Resistance

Figure V.1: Artemisinin antimalarial activity in comparison to quinine..... 141

Figure V.2: Current global distribution of artemisinin-based combination therapies as the first-line treatment of uncomplicated falciparum malaria..... 142

Figure V.3: Comparison of dormant and dead parasites after a typical exposure to artemisinin drugs..... 143

Figure V.4: Gating strategy used to detect infected erythrocytes based on depolarization or SYBR green staining..... 147

Figure V.5: Comparison of the two synchronization protocols..... 149

Figure V.6: Inhibitory 50% concentrations of dihydroartemisinin..... 151

Figure V.7: Comparison of artemisinin resistant and sensitive *P. falciparum* strains using different approaches to assess parasite growth and maturation..... 153

Figure V.8: Survival rates of tightly synchronized parasites exposed to a 6-hour pulse of dihydroartemisinin (DHA) 154

FIGURE AND TABLE INDEX

Figure V.9: Survival rates of mildly synchronized parasites exposed to a 6-hour pulse of dihydroartemisinin..... 156

Figure V.10: Representative microscopic pictures of untreated and dihydroartemisinin treated samples at 72 hours of incubation..... 158

Figure V.11: Representative microscopic pictures of untreated and dihydroartemisinin treated samples at 72 hour of incubation..... 158

Figure V.12: Progression of parasitemia in artemisinin-sensitive and artemisinin-resistant parasites after a 6-hour pulse of dihydroartemisinin..... 159

Figure V.13: Representative model of parasite replication after exposure to 6-hour pulse of dihydroartemisinin..... 160

Figure V.14: Parasite development patterns in the absence of drug..... 166

Figure V.15: Parasite development monitored by flow cytometry. The percentage of depolarizing events (hemozoin-containing cells) and SYBR green positive cells (parasitemia) was assessed overtime..... 168

Table V.1: *Kelch 13* gene locus polymorphism associated with delayed parasite clearance..... 155

Table V.2: Summarizing table of mean survival rates for artemisinin-sensitive (3D7 and 1239) and artemisinin-resistant strains (1240)..... 157

Table V.3: Studies that have investigated artemisinin-induced dormancy..... 164

ABBREVIATIONS

ACT – artemisinin-based combination therapy

ART – artemisinin

AS – artesunate

CERMEL – Centre de Recherches Médicales de Lambaréné

CMCM – complete malaria culture medium

CQ – chloroquine

DHA – dihydroartemisinin

DNA – deoxyribonucleic acid

EDTA – ethylenediamine tetraacetic acid

ELISA – Enzyme-Linked Immunosorbent Assay

FACS – Fluorescence-activated cell sorting

FCS – forward scatter

G6PD – Glucose-6-phosphate dehydrogenase

GFP – green fluorescence

HDP – heme detoxification protein

HRP2 – Histidine-rich protein 2

Hz – hemozoin

IC₅₀ – 50% inhibitory concentration

iRBCs – infected red blood cells

IRS – indoor residual spraying

ITNs – insecticide-treated mosquito nets

K13 – kelch 13

LED – light-emitting diode

LLINs – long-lasting insecticidal net

MIC – minimum inhibitory concentration

MMV – Medicines for Malaria Venture

MQ – mefloquine

PABA – para-aminobenzoic acid

PCR – polymerase chain reaction

PfATPase6 – gene encoding *P. falciparum* sarco-endoplasmic reticulum calcium

ATPase 6

Pfcr1 – gene encoding *P. falciparum* chloroquine resistance transporter

ABBREVIATIONS

Pfdhfr – gene encoding *P. falciparum* dihydrofolate reductase

Pfdhps – gene encoding *P. falciparum* dihydropteroate synthase

Pfmdr1 – gene encoding *P. falciparum* multidrug resistance 1 protein

Pfnhe-1 – gene encoding *P. falciparum* Na⁺/H⁺ exchanger

PfPI3K – gene encoding for *P. falciparum* phosphatidylinositol-3-kinase

Pfubp-1 – gene encoding *P. falciparum* deubiquitinating enzyme

PI3P – phosphatidylinositol 3-phosphate

pLDH – parasite lactate dehydrogenase

Pvdhfr – gene encoding *P. vivax* dihydrofolate reductase

Pvdhps – gene encoding *P. vivax* dihydropteroate synthase

Pvmdr1 – gene encoding *P. vivax* multidrug resistance 1 protein

PYR – pyrimethamine

RBCs – red blood cells

RNA – ribonucleic acid

RPMI – Roswell Park Memorial Institute

SSC – side scatter

UV – ultraviolet

WBCs – white blood cells

WHO – World Health Organization

CHAPTER I

GENERAL INTRODUCTION

1. MALARIA

a. Epidemiology and the Disease

Malaria is the most important parasitic disease. In 2015, it was responsible for the death of 438000 people, mainly children under 5 years of age. It is transmitted over 96 countries where 3.2 billion people are at risk [1]. Most cases and deaths occur in Africa, where *P. falciparum* the deadliest of all malaria parasites is dominant. There are five species of the genus *Plasmodium* spp. capable of causing malaria in human beings. Most cases are caused by *P. falciparum* and *P. vivax*, yet *P. malariae*, *P. ovale* and *P. knowlesi* also cause human infections [2].

Malaria is transmitted by *Anopheles* mosquitos. The *Plasmodium* spp. life cycle begins with the inoculation of sporozoites into the skin by infected mosquitos. Through the bloodstream parasites reach the liver, infect hepatocytes and multiply into thousands of parasites, called merozoites. The merozoites will be released into the bloodstream, leading to the blood stage of infection that is characterized by continuous cyclic asexual replication. The liver stage is clinically silent, and symptoms of malaria appear only during the blood stage (Figure I.1).

The symptoms of malaria are nonspecific. They include: headache, fatigue, abdominal discomfort usually followed or accompanied by fever, chills and vomiting. There is no combination of signs and symptoms that distinguish malaria from other causes of fever.

At the early stage of infection, when symptoms start to appear, if prompt effective antimalarial treatment is given full recovery is expected. On the other hand, if treatment is ineffective due to wrong prescription or the use of poor-quality medicines, treatment is delayed, and in the case of *P. falciparum*, progression to severe and potentially lethal malaria can occur. This progression to severe malaria can happen in a matter of hours. Severe malaria manifests with one or more of the following: coma (cerebral malaria), severe anemia, hypoglycemia, metabolic acidosis, acute renal failure or acute pulmonary edema, as reviewed elsewhere [2].

Malaria can also occur during pregnancy and it can have serious consequences both for the unborn child and the mother. Both *P. falciparum* and *P. vivax* can cause placental malaria. Yet, severe cases of *P. vivax* malaria during pregnancy are rare [3]. Placenta malaria can cause low-birth weight (< 2.5 kg), which is associated with increased infant mortality [4]. In high transmission settings mothers may have exacerbated parasitemia but they remain asymptomatic, even though high numbers of infected erythrocytes are accumulated in the placenta. Congenital malaria is rare, but once it happens it clears spontaneously in 62% of

the cases [5]. In regions of unstable malaria transmission, there is increased risk of pregnant women to develop severe *P. falciparum* malaria associated with a mortality rate of roughly 50%. In case of severe disease fetal distress, premature labor and stillbirth can occur. The risk of infant death is high, particularly if maternal malaria occurs during the late pregnancy [6].

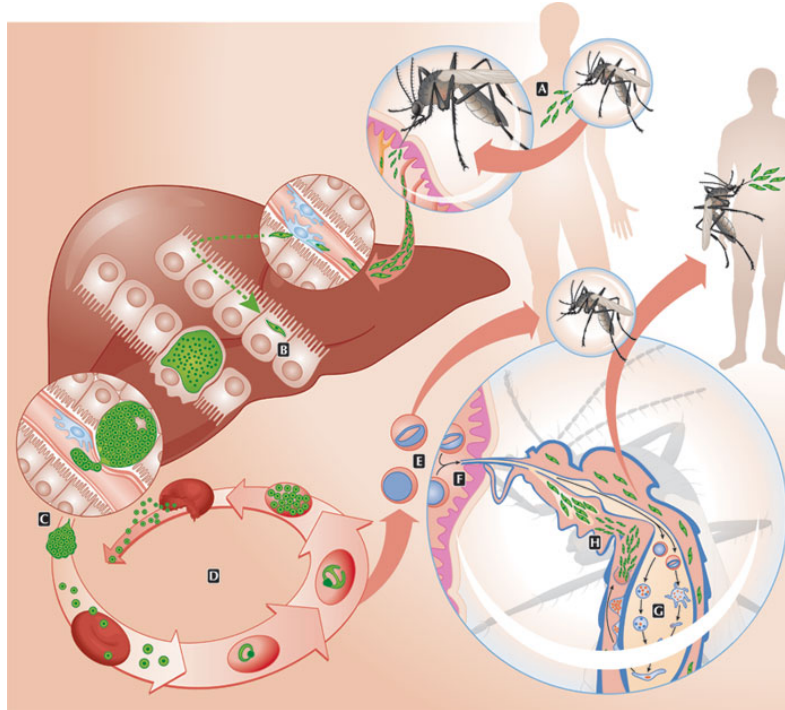


Figure I.1: *Plasmodium* spp. life cycle.

During a blood meal, an anopheline mosquito injects *Plasmodium* spp. sporozoites that will reach the liver through the bloodstream (A). After traversing several hepatocytes—they invade a final one (B). Inside the hepatocyte sporozoites will develop into thousands of merozoites which will be released into the bloodstream (C). Merozoites infect red blood cells and develop from ring-forms to trophozoites and, finally, to schizonts. Schizonts will rupture, releasing merozoites that will re-infect more red blood cells giving rise to a new cycle of asexual replication (D). Occasionally, replication cycles originate female and male gametocytes (E). Through another blood meal, a mosquito ingests gametocytes (F). Fertilization of gametes occurs in the mosquito midgut with the formation of ookinetes and later the oocysts (G). Sporozoites released from the oocyst will migrate to the salivary glands of the mosquito and will be released during the next blood meal. (Adapted from Portugal 2011 - [7])

P. vivax can also lead to severe and sometimes fatal disease. In the last decade, there was an increase in the number of reports describing severe manifestations in *P. vivax* infections. High prevalence of severe anemia associated with *P. vivax* malaria have been described [8–10]. Other severe manifestations including coma, renal failure, hemodynamic shock, severe jaundice, abnormal bleeding and frequent hypoglycemia can occur as well [11–15].

b. Threats to Malaria Control

Even though the number of malaria deaths remain considerably high one must recognize that the scenario of malaria has been worse not too long ago. In 15 years the number of deaths and the incidence of malaria has been reduced by 48% and 18%, respectively [1]. This has mainly been due to cost-effective interventions such as: vector control, chemoprevention and case management.

Vector control strategies reduce the transmission of parasites from humans to mosquitos and then back to humans. This is achieved by the use of insecticide-treated mosquito nets (ITNs) or indoor residual spraying (IRS). Chemoprevention will suppress or treat blood-stage infection in humans and case-management includes prompt diagnosis and treatment. These strategies altogether will greatly contribute for the reduction of transmission and mortality caused by malaria. For instance, a report from a village in Senegal showed that, introduction of effective diagnosis, treatment and vector control (using ITNs) strategies reduced the prevalence of parasites in children from 87% to 0.3% in 12 years [16].

Unfortunately, nature seems to be always a step ahead - some mosquitos have become resistant to some insecticides and malaria parasites have also developed resistance to antimalarial drugs.

P. falciparum resistance to the first-line treatment of malaria, the artemisinins, has now been reported in five countries in the Greater Mekong subregion: Cambodia, Lao People's Democratic Republic, Myanmar, Thailand and Vietnam [17]. This resistance is characterized by a delay on parasite clearance in patients treated with an ACT (artemisinin-combination therapy). Yet patients still respond to treatment, when the partner drug remains effective.

For *P. vivax* malaria, at least one true case of chloroquine resistance has been confirmed in 10 countries: Bolivia, Brazil, Ethiopia, Indonesia, Malaysia, Myanmar, Papua New Guinea, Peru, the Solomon Islands and Thailand [1].

Malaria mosquito vectors are developing resistance to the insecticides used in insecticide-treated mosquito net (ITNs) and indoor residual spraying (IRS), threatening the effectiveness of insecticide-based vector control [1]. Current efforts in global malaria control rely heavily on a single insecticide class: pyrethroids. This is the only class of insecticides used in long-lasting insecticidal net (LLINs) [1, 18]. Pyrethroid resistance was detected in all major malaria vectors [1, 19]. Nevertheless, despite the observed resistance long-lasting insecticidal nets remain effective.

To address remaining threats and emerging challenges, the WHO has developed a *Global technical strategy for malaria 2016–2030*. This strategy sets the very ambitious targets for reductions in malaria cases and deaths and it was developed in close alignment with the *Roll Back Malaria (RBM) Partnership’s Action and Investment to Defeat Malaria 2016–2030 – for a malaria-free world*.

Strong political commitment, robust financing and increased multi-sectorial collaboration are essential if the goals of this agenda are to be met. The previously mentioned threats will have to be continuously addressed and thus, novel tools and optimized approaches are required for the effective and successful accomplishment of malaria elimination by 2030.

Table I.1: Goals, milestones and targets of the Global technical strategy for Action and Investment to defeat malaria 2016–2030 [1].

VISION Goals	A WORLD FREE OF MALARIA		
	Milestones		Targets
	2020	2025	2030
1. Reduce malaria mortality rates globally compared with 2015	At least 40%	At least 75%	At least 90%
2. Reduce malaria case incidence globally compared with 2015	At least 40%	At least 75%	At least 90%
3. Eliminate malaria from countries in which malaria was transmitted in 2015	At least 10 countries	At least 20 countries	At least 35 countries
4. Prevent re-establishment of malaria in all countries that are malaria free	Re-establishment prevented	Re-establishment prevented	Re-establishment prevented

c. TREATMENT OF MALARIA

i. Antimalarial Drugs – Historical Overview

The very first drug used to treat malaria was quinine. Quinine, occurs naturally in the bark of Chinchona trees, that are found in South America. The cinchona bark was introduced into Europe in the 17th century by a Jesuit priest that was returning from a mission in Peru. This miraculous bark relieved feverish symptoms and agues. In fact, this drug has had an extremely important role in colonialism, by reducing the colonial mortality allowing “white men” to establish and survive in the tropics [20]. Because of this quinine was even called as one of the “tools for empire”. Quinine was used for centuries and in fact, it is still an effective drug. However, novel and better drugs have been developed and the use of quinine to cure malaria has decreased.

Synthetic compounds were made available later in the 19th century. By that time the need

for new antimalarial drugs led to the development and search for new effective compounds. Interestingly, methylene blue more commonly known as a dye, was the first synthetic antimalarial. Its antimalarial effect was noticed by Paul Ehrlich, his reasoning was if the dye is able to stain the malaria parasites it may be also toxic to the parasites *in vivo*. In 1891, two patients suffering from malaria were cured using methylene blue – this was the first time that a synthetic drug was ever used in humans [21].

In 1925, plasmoquine was developed by Bayer, this was the first 8-aminoquinoline which proved to be effective in preventing relapses caused by *P. vivax* infections. Later in 1932, mepacrine was developed and showed to be effective against *P. falciparum* malaria. In 1934, H. Andersag, developed a compound known as resochin [22]. This compound seemed promising but it seemed to be too toxic. During the World War II huge efforts were made by American, British and Australian scientists to cooperate in large-scale with the aim of developing new synthetic antimalarial drugs. Around 16000 compounds were synthesized and tested. Interestingly, one of the first compounds to be tested was resochin, which for the second time was considered too toxic. It was only in 1946 that an US clinical trial showed that resochin, now known as chloroquine, had a great activity against malaria parasites. Indeed, chloroquine was then massively used and it was the drug of choice in the WHO Global Eradication Programme of the 1950s and 1960s. Due to its efficacy, affordability and safety chloroquine was considered the best treatment for malaria for many years [23].

During the World War II, several significant scientific advances in the context of antimalarial drugs were made. Soon after the war, primaquine was introduced and proved to be the drug of choice for the prevention of relapses in *P. vivax* malaria, and it still is nowadays [22].

Proguanil was also developed during the war by the British. It actually served as a prototype for the development of pyrimethamine [22].

The antimalarial activity of amodiaquine was discovered in the 1950s. In the mid 1980s, fatal adverse drug reactions were described [24, 25]. However, because of chloroquine resistance amodiaquine was used in Africa and Asia. Currently it is mainly administered in combination with artesunate.

In the 1970's pyrimethamine was introduced in combination with sulfadoxine (Fansidar). This combination is still used today, particularly in intermittent preventative malaria treatment during pregnancy in Africa [26]. The development of mefloquine and atovaquone was also based on prototype compounds that were discovered during the

Vietnam war. Mefloquine was introduced in mid 1970's and was widely used around the world. Resistance to atovaquone can easily emerge and thus, it is used in combination with another drug, namely proguanil (Malarone) [27] .

The current first-line treatment for malaria is based on the artemisinin [26]. Artemisinin is found in a plant called *Artemisia annua* (known as qinghao in China). This plant has been used in traditional Chinese medicine for over 2000 years. It was during the Vietnam War, when a governmental program to screen a library of Chinese plants for their potential antimalarial effect was launched, that the potent antimalarial effect of artemisinin was discovered. Indeed, this research program was initially planned because more militaries were dying of malaria than from fighting the war. In 1972, Tu You You, who has been awarded with a Nobel Prize in 2015, extracted the principal ingredient from the plant and called it qinghaosu (which means essence of qinghao). Artemisinins are the quickest drugs in terms of parasite clearance, affecting up to 10.000-fold reductions in parasite burden every 48 hours [28]. In fact, this feature is of critical benefit in treating severe malaria and reversing its otherwise lethal course [2].

Indeed, it is remarkable that two herbal treatments, cinchona bark and qinghao, were used to treat malaria effectively for hundreds of years before even understanding of the parasite life cycle. Today both quinine (derived from the cinchona bark) and artemisinin (from qinghao) remain of prime importance in the treatment and control of malaria.

ii. Current Guidelines for the Treatment of Malaria

The control of malaria largely depends on drug therapies, and, to a lesser extent, prophylaxis. Table I.2 summarizes the available drugs to treat and/or prevent malaria.

Antimalarial drugs target different stages of the life cycle of malaria parasite and they can be classified as: blood schizonticides (act on the asexual intraerythrocytic stages), tissue schizonticides (kill hepatic schizonts), hypnozoiticides (kill hypnozoites), gametocytocides (destroy intraerythrocytic sexual forms). The majority of the drugs act on the blood (intraerythrocytic) stage.

The choice of the most appropriate treatment is influenced by several factors such as: the causative species, the severity of signs and symptoms, the patients age, immunity status and other risk determining factors (acute or chronic conditions, pregnancy and/or immune impairment). Nevertheless, the primary objective of treating severe malaria is to save life. Other considerations such as minor toxicity or preventing recrudescence are secondary.

Table I.2: Currently used antimalarial drugs (adapted from [29])

Class	Drug	Use	Half-life
4-aminoquinolines	chloroquine	Treatment of non- <i>falciparum</i> malaria	60 days
	amodiaquine	Partner drug for ACT	9–18 days*
	piperaquine	Partner drug for ACT	5 weeks
8-aminoquinolines	primaquine	Radical cure and terminal prophylaxis of <i>P. vivax</i> and <i>P. ovale</i> ; gametocytocidal drug for <i>P. falciparum</i>	5 hours
Arylamino alcohols	quinine	Treatment of <i>P. falciparum</i> and severe malaria	8 – 10 hours
	mefloquine	Prophylaxis or partner drug for ACT	14 – 18 days
	lumefantrine	Partner drug for ACT	3 – 5 days
Sesquiterpene lactone endoperoxides	artemether	ACT: combination with lumefantrine	0.5 – 1.4 hours
	artesunate	Treatment of severe malaria	
	dihydroartemisinin	ACT: combination with piperaquine	
Manich base antifolates	pyronaridine	Combination with artesunate ACT	12 – 14 days
	pyrimethamine-sulfadoxine	Treatment of some chloroquine-resistant parasites or combination with artesunate as ACT	4 – 5 days
Naphtoquinone/antifolate	Atovaquone-proguanil	Combination for prophylaxis and treatment of <i>P. falciparum</i> malaria	2 – 3 days
Antibiotics	doxycycline	Chemoprophylaxis or treatment of <i>P. falciparum</i> malaria	16 – 22 hours
	clindamycin		2 -3 hours

*3 hours (but the antimalarial activity is thought to be exerted by the primary metabolite, monodesethylamodiaquine, which has a half-life of 9–18 days;

The latest guidelines for the treatment of uncomplicated malaria is the use of artemisinin-based combination therapy (ACT). To treat severe malaria the use of several antimalarial drugs, such as artesunate, quinine, artemether, as a single-therapy during 24 hours and, thereafter, complete the treatment with ACTs or with combination therapy of antimalarial drugs with antibiotics (doxycycline, clindamycin) is recommended [26, 30]. More detailed information on treatment regimens is presented in Table I.3.

Table I.3: Current guidelines to treat malaria (adapted from [26])

Treatment of severe malaria
Adults and children with severe malaria (including infants, pregnant women in all trimesters and lactating women) should be treated with intravenous or intramuscular artesunate for at least 24 hours until oral medication can be tolerated. Once the patient has received at least 24 hours of parental therapy and is now able to tolerate oral therapy, treatment should be completed with a 3 day regimen of ACT . If artesunate is not available, artemether in preference to quinine should be used instead.
Treatment of uncomplicated <i>P. falciparum</i> malaria
All children and adults with <i>P. falciparum</i> uncomplicated malaria should be treated with one of the following ACT for 3 days: artemether/lumefantrine, artesunate/amodiaquine, artesunate/mefloquine, dihydroartemisinin/piperaquine or artesunate/sulfadoxine-pyrimethamine. In low-transmission settings, to reduce transmission, a single dose of primaquine with the ACT should be given to patients as well (except pregnant women, infants aged < 6 months and women breastfeeding infants < 6 months). Treatment regimens have to be adjusted in special risk groups, including: first trimester pregnancy, infants with less than 5kg of body weight, patients co-infected with HIV, non-immune travellers and patients with uncomplicated hyperparasitemia.
Treatment of uncomplicated non- <i>P. falciparum</i> malaria
If the malaria species is not known patients should be treated as if they had uncomplicated <i>P. falciparum</i> malaria. In areas where chloroquine is still effective adults and children should be treated with either an ACT or chloroquine . In areas where chloroquine resistance exists, adults and children should be treated with an ACT. Pregnant women in their first trimester who have chloroquine-resistant malaria should be treated with quinine.
Preventing relapse of <i>P. vivax</i> and <i>P. ovale</i> malaria
To prevent relapse either from <i>P. vivax</i> or <i>P. ovale</i> malaria children and adults should be treated with a 14 day course of primaquine , in all transmission settings. The G6PD status of all patients should be used to guide administration. In people with G6PD deficiency, treatment should be done with a higher dose for a shorter period of 8 days. In this case close medical supervision is required. In women who are pregnant or breastfeeding a weekly prophylaxis with chloroquine until delivery or until breastfeeding is completed should be considered.
Chemoprevention for special risk groups
In malaria endemic areas in Africa, intermittent preventive treatment (IPTp) with sulfadoxine-pyrimethamine (SP) should be given to all women in their first or second pregnancy as part of antenatal care. Doses should start in the second trimester and be given at least one month apart, ensuring that at least 3 doses are received. In areas of moderate-to-high malaria transmission in Africa, where SP is still effective, all infants (<12 months of age) should receive SP-IPTi at the time of second and third rounds of vaccination. In areas with highly seasonal malaria transmission in Africa, all children aged <6 years should receive seasonal malaria chemoprevention with a monthly dose of amodiaquine/SP, during each transmission season.

iii. New Antimalarial Drugs

New antimalarial drugs are needed for several reasons. First, available drugs may be limited by drug resistance. It is important to note that even though resistance has been described for most used antimalarial drugs, including artemisinins, the current first line treatment for malaria based on ACTs remains effective. Moreover, effective treatment requires multiple doses. A single-dose effective regimen would offer improved compliance

and allowed to reduce costs. Besides this, most drugs only act on the blood stage and other parasite life-cycle stages such as non-erythrocytic and sexual stages are not affected. More importantly, some drugs have safety limitations. Ideally, antimalarial drugs should be safe in young children and pregnant women. Therefore, investigation and development of novel drugs that may address these issues is crucial to successfully control malaria.

Since the World War II strong efforts were made to discover novel and better antimalarial drugs. However, in the early 1990s many companies have stopped attempting to develop new antimalarial drugs [27]. Between 1975 and 1999 only four of more than a thousand new drugs developed worldwide were antimalarials [31]. In 1999, Medicines for Malaria Venture (MMV) begun and the scenario has changed considerably. This public-private partnership aims to investigate and develop novel, effective drugs against malaria. In fact, MMV has been the main driver of antimalarial drug research and development projects.

The pipeline of drugs targeting malaria include: 1) novel medicines that are based either on already known antimalarial drugs that are now being investigated as potential novel partner drugs for ACTs or new formulations of these compounds for a different route of administration; and 2) completely novel classes of molecules, with potentially different mechanisms of action (Figure I.2).

There are promising new classes of compounds in the pipeline: the KAE069 (cipargamin), KAF156 and ACT-451840.

KAE609 is a spiroindolone antimalarial compound that showed to have a rapid parasite clearance rate in the treatment of *P. falciparum* and *P. vivax* malaria [32]. In fact, it seems to be even more rapid in clearing parasitemia than artemisinins. Moreover, this compound also has gametocytocidal activity detected *in vitro* against *P. falciparum* and thus, may have transmission-blocking properties [33].

The KAF156 represents a new class of antimalarial agents (imidazolopiperazines) [34, 35]. KAF156 has shown potent *in vitro* activity against both asexual and sexual blood stages and against liver stages as well. In a recent clinical study, the rates of parasite clearance after treatment with KAF156 were slightly lower than those associated with artemisinin treatment but still higher than the ones associated with treatment with sulfadoxine–pyrimethamine, atovaquone–proguanil, quinine, or mefloquine [36].

ACT-451840 belongs to a new chemical class of potent antimalarial compounds with a novel mode of action. This novel compound is effective against both *P. falciparum* and *P. vivax* and also against all asexual and sexual stages of *P. falciparum*. It has been shown to have a fast parasite clearance and it has a longer half-life (34 hours) in comparison to

artemisinin (2 hours) [37].

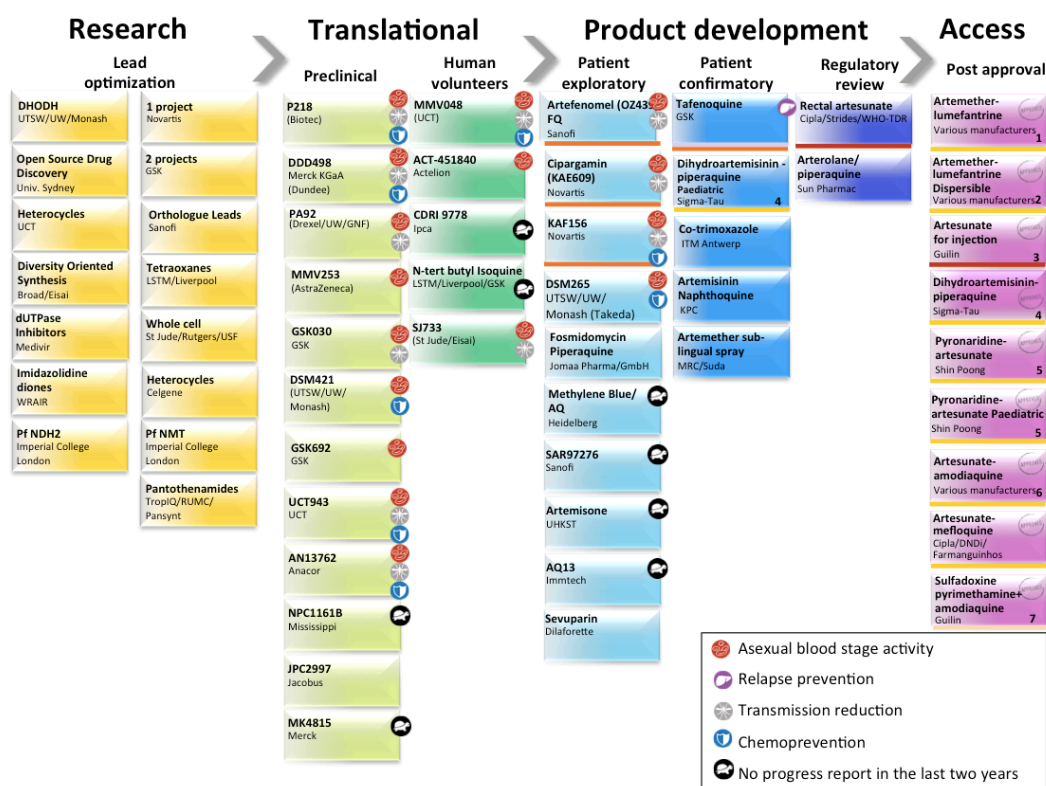


Figure I.2: Global Portfolio of Antimalarial Medicines (as of 30th June 2016).

Several 3-day cure artemisinin based combination therapies are in developments (yellow bars) OZ439/FQ, KAE609, KAF156 and tafenoquine are new compounds to contribute to SERCAP (single-exposure radical cure and prophylaxis) or multiple exposure treatment for multi-drug resistance (orange bars). Tafenoquine has also been shown to be effective against hipnozoites. New treatments for severe malaria under investigation include rectal artesunate and artesunate for injection (Artesun®). A new combination of sulfadoxine-pyrimethamine + amodiaquine (SP+AQ) is being investigated for seasonal malaria chemoprophylaxis. (<http://www.mmv.org/research-development/interactive-rd-portfolio> accessed 28/09/16)

d. Mechanisms of Action of Antimalarial Drugs

The mechanism of action of antimalarial drugs may greatly influence the determination of drug effects in *in vitro* drug assays. Specially, in the context of the work developed in this thesis. As discussed in section 6, the subject of this study is hemozoin, which is the target of action of most antimalarial drugs.

Antimalarial drugs can be grouped, according to its mechanism of action, into compounds that: 1) inhibit the formation of hemozoin 2) inhibit the synthesis of nucleic acid 3) inhibit the mitochondrial respiratory chain and 4) which are not completely understood.

1) Most available antimalarial drugs share the same mechanism of action: inhibition of hemozoin formation. Examples are quinine, chloroquine, amodiaquine, mefloquine,

piperazine and lumefantrine. The exact mechanism of how these drugs inhibit hemozoin formation is far from being resolved, yet it is known that their interaction with heme is essential for the antimalarial activity of these compounds [38, 39]. In this case the death of the parasite results from the accumulation of cytotoxic free heme.

From all the abovementioned drugs the one that has been more extensively investigated is chloroquine, where several mechanisms have been proposed to explain how it interferes with heme detoxification. The first studies suggested that chloroquine causes alkalinization of the food vacuole [40]. Another study challenged this observation and reported that therapeutically achievable levels of chloroquine would induce rather minimal changes in the pH [41] and that such a change could not inhibit hemoglobin degradation [42].

Another explanation was based on the inhibition of peroxidase degradation of heme [43]. It was shown that when heme reacts with H_2O_2 it has catalase and peroxidase activities that contribute to heme degradation [44]. This would be prevented by chloroquine thus, leading to increased levels of H_2O_2 that would cause peroxidative damage to the parasite.

It was also suggested that chloroquine would inhibit heme sequestration by the parasite. Indeed it was shown that quinoline drugs inhibit the formation of both synthetic and native hemozoin [45]. Chloroquine seems to form quinoline-heme complexes that inhibit further extension of hemozoin chains [46]. Thus, it is reasonable to consider that quinolines act by preventing further crystallization of hemozoin, leaving enough free toxic heme to harm the parasite.

2) Folate antagonists, such as sulfadoxine and pyrimethamine, inhibit enzymes of the folate pathway and thus, the synthesis of nucleic acids in the malaria parasite is blocked [39]. Selectivity of action of the malarial enzymes is due to structural and functional differences between them and their human counterparts. The parasite can either synthesize or salvage folate precursors, whereas mammals have no *de novo* synthesis and rely on dietary sources.

3) Atovaquone acts on the mitochondrial electron transfer chain. It was shown to inhibit the respiratory chain of malarial mitochondria at the cytochrome bc₁ complex [47], leading to the collapse of the mitochondrial membrane potential [48].

4) The mechanism of action of some drugs is still not fully understood. In the case of the artemisinins no consensus has been found yet. The most widely accepted view is that artemisinins are pro-drugs which are activated upon cleavage of the endoperoxide ring, after reacting with heme and/or iron(II) oxide [49]. The resulting free radicals are thought to react with susceptible groups within a range of parasite proteins, leading to cellular

damage and killing.

Whether the actual activator of artemisinin is heme or free ferrous iron; or perhaps unstable hemoglobin is still not fully understood [50]. Both iron [51–53] and heme-mediated [54] activation can occur but it seems that the potent activity of artemisinin against trophozoites is likely due to heme-mediated activation. In fact, in the presence of hemoglobinase inhibitors the activity of artemisinins is almost completely abolished [54].

Other modes of action/activation have been proposed. The sarco/endoplasmic reticulum Ca^{2+} ATPase (PfSERCA) was suggested as potential direct target [55, 56]. Yet, its role in artemisinin mechanism of action has been questioned [57, 58].

It was also reported that iron-mediated activation in the mitochondria could lead to inhibition of the electron transport chain and mitochondrial depolarization [59]. Other studies suggested the direct interaction with cofactors involved in maintaining redox homeostasis as an iron-independent pathway of artemisinins activation [60].

More recently, *P. falciparum* phosphatidylinositol-3-kinase (PfPI3K) has been proposed as a direct target of the artemisinins during the ring stage [61]. Nevertheless, other critical targets, including heme, lipids and other proteins, must have a role particularly in other stages of parasite development.

2. ANTIMALARIAL DRUG RESISTANCE

The classical definition of antimalarial drug resistance is “ the ability of a parasite strain to survive and/or multiply despite the administration and absorption of a drug given in doses equal or higher than those usually recommended but within tolerance of the subject”. This definition was modified to specify that the drug in question “must gain access to the parasite or the infected erythrocyte for the duration necessary for its normal action” [62].

Resistance has been documented for most antimalarial drugs and thus, it is, and has always been, a subject of great concern and a major obstacle in the fight against malaria. Drug resistance is complicated with the phenomena of cross-resistance that can occur among drugs that belong to the same chemical family or which have similar modes of action. *P. falciparum* multidrug resistance occurs when the parasite is resistant to more than two antimalarial compounds of different chemical classes and modes of action.

Several factors, summarized in Table I.4, influence the development and spread of drug resistance. One of the most important factors is the inappropriate and widespread use of antimalarial drugs, which will exert a strong selective pressure on malaria parasites.

Table I.4: Factors that influence the development of antimalarial drug resistance (adapted from [63])

1.	The frequency with which the resistance mechanism arises
2.	The fitness cost to the parasite associated with the resistance mechanism
3.	The number of parasites in the human host that are exposed to the drug
4.	The concentrations of drug to which these parasites are exposed (i.e., the doses used and pharmacokinetic properties of the antimalarial drug or drugs)
5.	The pharmacodynamic properties of the antimalarial drug or drugs
6.	The degree of resistance (the shift in the concentration-effect relationship) that results from the genetic changes
7.	The level of host defense (nonspecific and specific immunity)
8.	The simultaneous presence of other antimalarial drugs or substances in the blood that will still kill the parasite if it develops resistance to one drug (i.e., the use of combinations).
9.	Transmission intensity.

Interestingly, antimalarial drug resistance often emerges in the same region, in the Greater Mekong Sub region in Southeast Asia. The reason for this phenomenon is not completely understood but there might be several explanations for this. One of them is the fact that, contrary to Africa, malaria infections are much less common, which allows resistant parasites to survive and reproduce more easily without having much competition from other parasite populations. Another possible explanation is that in Africa most people develop natural immunity to malaria, and in fact only a small number of malaria infected people gets to be treated or exposed to antimalarial drugs. This certainly translates into a much lower drug pressure on the parasite in comparison to Southeast Asia where antimalarial drugs are more widely distributed [64]. In low-transmission settings, as the ones found in Southeast Asia, most infections are symptomatic and thus, more people receive treatment, leading to a greater chance for selection of resistant parasites.

Antimalarial drug resistance greatly affects the global control of malaria in different ways, in terms of: disease burden [8, 65], economic costs [66], distribution of malaria species [67] and access to high-quality treatment [64].

a. Current Status of Antimalarial Drug Resistance

Resistance to antimalarial drugs has been described *P. falciparum*, *P. vivax* and *P. malariae* [64, 68]. While *P. falciparum* has developed resistance to most of antimalarial drugs in current use (Table I.5) [63], *P. vivax* has shown to be resistant to chloroquine [69, 70], primaquine [71] and sulfadoxine-pyrimethamine [72]. Resistance of *P. malariae* to chloroquine was reported in a single study from Indonesia [73].

Table I.5: Years of introduction of antimalarial drugs and of their first reports of resistance (adapted from [74])

Antimalarial drug	Year of introduction	First reported resistance	Location
Quinine	1632	1910	• Thai-Cambodia Border
Chloroquine	1945	1957	• Thai-Cambodia Border • Columbia
Sulfadoxine-pyrimethamine	1967	1967	• Thai-Cambodia Border
Mefloquine	1977	1982	• Thai-Cambodia Border
Artemisinin*	1980s	2008-2009	• Thai-Cambodia Border

* artemisinin resistance as characterized by delayed parasite clearance time.

Resistance of *P. falciparum* to quinine was first described in Brazil [75] and later in Southeast Asia [76]. Yet, resistance to quinine only occurs sporadically in Southeast Asia and Oceania.

Chloroquine-resistant *P. falciparum* malaria has been described in all regions where *P. falciparum* is endemic, except Central America and the Caribbean. However, since its withdrawal there have been signs of decrease of chloroquine resistance in some areas, for instance in Malawi [77, 78], Kenya [79] and Tanzania [80]. While this phenomenon is interesting, caution is still required and widespread reintroduction of chloroquine is not recommended.

Resistance to sulfadoxine-pyrimethamine emerged only 6 months after its introduction and has been reported in Southeast Asia, South America and in Africa. Mefloquine resistance is frequent in Southeast Asia and has also been reported in the Amazon region of South America. Sporadically it occurs in Africa [81].

More recently, resistance to artemisinin, characterized by prolonged parasite clearance times, has been described [82, 83]. Firstly it was reported in Cambodia and Thailand but it has now spread to Myanmar and Vietnam (Figure I.3). The observed delayed parasite clearance phenotype does not translate into increased 50% inhibitory concentrations (IC₅₀) determined by standard *in vitro* assays [83, 84]. In fact, most patients who have delayed parasite clearance following treatment with an ACT still manage to clear their infections. Recently, a molecular marker for artemisinin resistance has been described [85]. Mutations in the kelch13 (K13)-propeller domain are associated with delayed parasite clearance, both *in vitro* and *in vivo*. Even though, further validation is still required, the WHO has updated the definition of artemisinin resistance into: suspected artemisinin resistance, defined as a high prevalence of the delayed parasite clearance phenotype or high prevalence of K13

mutants; and confirmed artemisinin resistance, defined as a combination of both delayed parasite clearance and K13 resistance-validated mutations for the same patient) [86]. Nevertheless, for now artemisinin resistance is officially considered to be partial by the WHO [86].

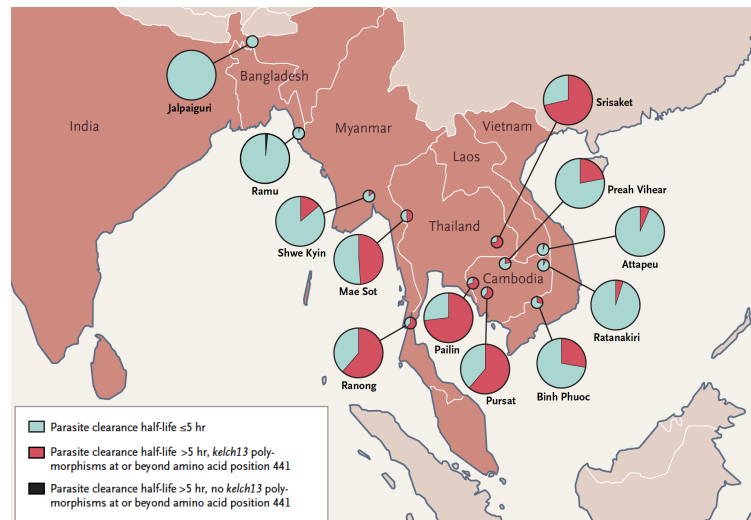


Figure I.3: Location of study sites and proportions of patients with artemisinin resistance. Artemisinin resistance was defined by a parasite clearance half-life longer than 5 hours, with some *Plasmodium falciparum* isolates having *kelch13* polymorphisms (at or beyond amino acid position 441) (adapted from [17]).

P. vivax resistance to chloroquine was first reported in Papua New Guinea and Indonesia but it has also been detected in South America and Asia [87]. Resistance to primaquine has been reported as well, but the data must be interpreted with caution because of many confounding factors, including geographical variations in relapse patterns, unsupervised therapy, parasite tolerance, the risk for reinfection and the difficulty of finding a valid control group [88]. Resistance to sulfadoxine-pyrimethamine in *P. vivax* have also appeared in Asia and the Pacific Islands, where both *P. falciparum* and *P. vivax* coexist [89–91].

In the case of *P. ovale*, *P. malariae* resistance is not well-characterized and it is considered that these parasite remain sensitive to chloroquine. There was only one study in Indonesia that reported resistance of *P. malariae* to chloroquine [73]. Nevertheless, chloroquine is still fully effective against *P. malariae* in Madagascar and against *P. knowlesi* in Malaysia [92, 93].

b. Mechanisms of Antimalarial Drug Resistance

Resistance to antimalarial drugs arises because parasites with genetic changes that confer reduced susceptibility to a specific drug are selected. These genetic changes are either mutations or alterations in the copy number of genes encoding for the parasite target of the drug or for influx/efflux pumps, which influence the concentration of the drugs inside the parasite. In some cases just a single genetic event may be all that is required, in other multiple independent events may be necessary [94].

Chloroquine Resistance

Chloroquine resistance was first noted in the Thai-Cambodian Region in 1957, approximately a decade after its introduction. In Africa, chloroquine resistance was first reported in 1978. By 1989 it had spread throughout the whole African continent. Chloroquine resistance reached the endemic regions in South America in 1980 and in 1989 it was reported in Asia and Oceania. It is now known that the appearance of chloroquine resistance in Africa was not due to a new mutation but instead it was caused by the slow and gradual spread of chloroquine-resistant parasites from Southeast Asia [95].

Resistance to chloroquine is related to an increased capacity of the parasite to expel chloroquine from its digestive vacuole, not allowing the drug to reach the required levels to inhibit the formation of hemozoin [96]. In fact, resistance to chloroquine can be reversed by drugs which interfere with this efflux system [97]. Yet, it remains unclear if parasites resistant to other quinoline drugs have similar mechanisms.

Two genes have been implicated with chloroquine resistance: *pfcr1* (*P. falciparum* chloroquine-resistance transporter) [98] and the *pfmdr1* (*P. falciparum* multi-drug resistant transporter 1) [99]. The *pfcr1* gene is located on chromosome 7 and codes for a vacuolar membrane transporter protein (pfCRT). The *pfcr1* polymorphisms, in particular the K76T mutation has been associated with chloroquine resistance [100] and is a strong marker for predicting it [99, 101]. Cross-resistance of other drugs, such as amodiaquine and quinine, with chloroquine is also influenced by *pfcr1* mutations [99]. The PfCRT K76T polymorphism is thus a validated marker for chloroquine resistance and should also be considered as an indicator for amodiaquine resistance.

The *pfmdr1* gene is localized on chromosome 5 and encodes an ATP-binding cassette (ABC) protein [102]. A point mutation in the *pfmdr1* gene has been linked to chloroquine resistance in some studies [101, 103–105] but not in others [106–108].

Resistance to sulfadoxine-pyrimethamine

Sulfadoxine and pyrimethamine acts synergistically by inhibiting two enzymes that are involved in folate synthesis: dihydropteroate synthetase (DHPS) and dihydrofolatereductase (DHFR), respectively. Mutations in the genes encoding for these enzymes (*pfdhfr* and *pfdhps* genes) are implicated with resistance to sulfadoxine-pyrimethamine [109, 110]. These markers have been useful for tracking sulfadoxine-pyrimethamine resistance across the globe.

Resistance to quinine

Quinine resistance is associated with polymorphisms in several transporters. Polymorphisms in *pfmdr1*, *pfcr1*, and *pfnel1* genes are related to decreased sensitivity to quinine [111].

Resistance to mefloquine

Molecular studies have shown that mefloquine resistance arose in several different places [112]. Resistance to mefloquine is associated with increased copy numbers of the *pfmdr1* gene [113, 114].

Resistance to artemisinin

Resistance to artemisinin differs from what has been observed in resistance against other antimalarial drugs. It is characterized by a delay in parasite clearance time rather than by treatment failure. Furthermore, commonly used *in vitro* assays do not show altered 50% inhibitory concentrations (IC₅₀).

Recently, a potential molecular marker for artemisinin resistance has been described. Genome-wide association studies using field isolates identified regions on chromosome 13 associated with delayed parasite clearance [85, 115]. A mutation in the propeller domain of the *P. falciparum kelch* (K13) gene was associated with delayed parasite clearance after artemisinin therapy in Southeast Asia. Definite evidence that asexual blood-stage parasites harbouring *kelch13* mutations are less susceptible to artemisinin was provided by genome editing study [116]. Non-synonymous polymorphism at the following specific positions: Y493H, R539T, I543T, and C580Y in the kelch repeat region of K13 propeller domain have been associated with artemisinin resistance [85].

Recent studies showed that delayed clearance and K13 mutations are common in parts of Cambodia, Thailand, Myanmar, and Vietnam, but not in other areas of Asia or Africa

[117]. Indeed, in Africa, specific mutations associated with artemisinin resistance were not detected, even though K13 gene polymorphisms and mutations in the propeller domain are also common in African parasites [117]. The molecular function of K13 is still not known. Recently, it was suggested that K13 could be a regulator of polyubiquitination (and thus degradation) of PfPI3K, a recently described potential target of artemisinins [61]. PfPI3K phosphorylates phosphatidylinositol (PI) to produce phosphatidylinositol 3-phosphate (PI3P) in ring-stage parasites. Increased PfPI3K levels were associated with the C580Y mutation in PfKelch13 and were proposed to allow ring-stage parasites survival in the presence of artemisinins [61]. However, this increase is rather modest (2-4 fold) while mutant parasites have shown more than 70-fold resistance to artemisinin [118]. Thus, it is likely that additional factors must be involved in this mechanism of resistance to artemisinin.

3. ASSESING ANTIMALARIAL DRUG EFFICACY

a. Importance of Assessing Antimalarial Drug Efficacy

Resistance to antimalarial drug is of great concern and it hinders the control of malaria. Surveillance is needed in order to facilitate the monitoring and containment of resistant parasites. In fact, monitoring the changing patterns of drug resistant malaria parasites is an essential key component for an efficient control and case management. Recommendations to control the therapeutic efficacy of antimalarial drugs have been made for *P. falciparum*, but also for *P. vivax* [119].

b. Therapeutic Efficacy Trials

In 1965, shortly after chloroquine resistance has emerged the first standardized systems to assess drug responses *in vivo* were developed [120]. These tests were originally developed for chloroquine. In 1996, the WHO developed a new protocol for assessing antimalarial drug efficacy in high transmission areas [121]. Since then, therapeutic efficacy protocols have been updated on a regular basis for high transmission areas and have been validated for low-to-moderate transmission regions as well. The most recent version is from 2009 [122].

In clinical therapeutic efficacy trials a drug is administered to a malaria patient, blood samples are collected at pre-determined times and parasitemia is assessed by microscopic observation of Giemsa-stained blood smear, or less commonly by PCR. Day 0 is traditionally set as the day that the patient is enrolled in the trial and had received the first

dose of medicine. In the case of *P. falciparum* malaria monitoring therapeutic efficacy involves the assessment of clinical and parasitological outcomes for 28 days, in the case of drugs that have an elimination half-life of less than 7 days (chloroquine, amodiaquine, artemisinin derivatives, atovaquone–proguanil, halofantrine, lumefantrine, quinine and sulfadoxine–pyrimethamine), or for 42 days, in the case of drugs with longer half-lives (mefloquine, piperazine) [123]. Standard physical examination will be done on days 0, 1, 2, 3, 7, 14, 21, 28, (35 and 42) [122].

Monitoring of re-appearance of parasites in the blood has to be performed as well. In these cases, PCR genotyping should be used to distinguish recrudescence, associated with treatment failure, from a new infection.

In *P. vivax* malaria assessment of therapeutic responses is more challenging [122]. These parasites produce a dormant liver-stage that causes relapses, which cannot be distinguished from recrudescence or re-infection. In this case, early relapses, which may occur 3 weeks after treatment, or any newly acquired infections should be suppressed by therapeutic doses of antimalarial drugs with longer half-lives, such as chloroquine, mefloquine and piperazine. Thus, reappearance of parasitemia within 28 days of treatment, whether relapse, recrudescence or re-infection, can still be used as a proxy measure of resistance.

The WHO has classified the potential treatment outcomes on the basis of parasitological and clinical assessments performed after a drug had been administered. Accordingly, all patients will be classified as having early treatment failure, late clinical failure, late parasitological failure or an adequate clinical and parasitological response (Table I.6).

The proportion of patients experiencing therapeutic failure during the follow-up period will be used to estimate the efficacy of the drug in question [26]. Once the data has been validated it should be made available to drug policy-makers for action. An antimalarial medicine that is recommended in the national malaria treatment policy should be changed if the total treatment failure rate exceeds 10%. The decline in efficacy can be indeed indicative of drug resistance. Yet, it may also be due to several other reasons thus, complementary studies of pharmacokinetics, *in vitro* drug assays and molecular approaches should be performed to ultimately confirm the existence of drug resistance.

Table I.6: WHO classification of responses to treatment (adapted from [122])

Early treatment failure (ETF)
<ul style="list-style-type: none"> • danger signs or severe malaria on day 1, 2 or 3, in the presence of parasitemia; • parasitemia on day 2 higher than on day 0, irrespective of axillary temperature; • parasitemia on day 3 with axillary temperature ≥ 37.5 °C; • and parasitemia on day 3 $\geq 25\%$ of count on day 0.
Late clinical failure (LCF)
<ul style="list-style-type: none"> • danger signs or severe malaria in the presence of parasitemia on any day between day 4 and day 28 (day 42) in patients who did not previously meet any of the criteria of early treatment failure; • and presence of parasitemia on any day between day 4 and day 28 (day 42) with axillary temperature ≥ 37.5 °C in patients who did not previously meet any of the criteria of early treatment failure.
Late parasitological failure (LPF)
<ul style="list-style-type: none"> • presence of parasitemia on any day between day 7 and day 28 (day 42) with axillary temperature < 37.5 °C in patients who did not previously meet any of the criteria of early treatment failure or late clinical failure
Adequate clinical and parasitological response (ACPR)
<ul style="list-style-type: none"> • absence of parasitemia on day 28 (day 42), irrespective of axillary temperature, in patients who did not previously meet any of the criteria of early treatment failure, late clinical failure or late parasitological failure.

***c. In Vitro* Assays for Antimalarial Drug Testing**

Undoubtedly, *in vivo* tests are essential to provide relevant data to clinicians and health authorities. However, tests of therapeutic efficacy not only require a challenging long follow-up of patients, for at least 28 days, but its outcome might be confounded by the immunity of the patient, pharmacokinetics differences and even possible re-infections. Moreover, ethical considerations preclude the evaluation of new drugs until initial phases of clinical trials are complete and the drug has been approved for clinical use. *In vitro* assays avoid many of these confounding factors and can be used for different purposes, such as:

- for drug development: screening of new compounds, *in vitro* interaction of drug combinations, cross-resistance studies, phenotypic comparisons of pre-treatment and post-treatment isolates, baseline sensitivity to new drugs;
- as a complementary test to determine if drug resistance is the probable cause of therapeutic failure;
- to validate candidate molecular markers of drug resistance;
- to monitor drug resistance: emergence of drug resistance, changing trends of drug sensitivity or resistance over time and space, *in vitro* responses of individual drugs that are currently administered in combination therapies, in particular for drugs that do not have yet a validated molecular marker.

i. Overview

All current antimalarial drug assays are based on *in vitro* culturing of malaria parasites. This technique of culturing *P. falciparum* parasites *in vitro* was only developed in 1976, by Trager and Jensen. Yet, the very first assay to determine antimalarial drug effects *in vitro* was performed in 1922. An isolated *P. falciparum* sample from a patient was incubated *in vitro* and exposed to a single concentration of quinine for 29 hours to demonstrate its schizonticidal effect [124]. In the late 1960s, when the problem of drug resistant malaria emerged, Rieckmann developed the “macrotest” to detect and follow the evolution of chloroquine-resistant *P. falciparum* [125, 126]. The principle of this test was based on sub-optimal short-term cultured method that has been described in 1912, where the crucial point was the maturation from rings to schizonts, without necessarily attaining the ring stage of the second intraerythrocytic cycle [127].

In 1976, *in vitro* culture method for *P. falciparum* underwent a major change and this technical improvement led to an improved version of the “macrotest”, called the microtest. Since then, several novel *in vitro* assays were developed and most of them are still being used nowadays.

ii. Microscopy – The Schizont Maturation Test (WHO microtest)

Microscopy is indeed the technique that has been available for longer and the first *in vitro* drug sensitivity test for *P. falciparum* was based on microscopy, it was known as the microtest [128]. This test was developed by Rieckmann in 1978, shortly after *in vitro* culturing methods for *P. falciparum* had been described. Finger prick capillary blood was collected and incubated with different concentrations of drugs. The amount of young parasite forms that matured into schizonts is assessed after 30-48 hours by microscopy.

A field-applicable standard kit based on Rieckmann’s microtechnique was developed by Wernsdorfer, under WHO sponsorship [129]. Thereafter this assay was known as the WHO microtest. Nowadays, the WHO kit is no longer being produced, yet microscopic assessment of schizont maturation is still used. Nevertheless, microscopic methods are likely to be tedious, time-consuming and more importantly subjective because the decision of whether a parasite is viable or not tends to differ between different examiners. Because of these limitations, several other approaches that rely on specific indicators of parasite growth have been investigated.

iii. Radioisotope Methods

The use of radiolabeled DNA precursors to assess parasite maturation was the first alternative to be investigated. In cultures containing malaria parasites, uninfected erythrocytes and platelets do not synthesize DNA, RNA, proteins or membranes and human leukocytes do not multiply and tend to disintegrate over a few days. Thus, the only actively dividing cells are the parasites themselves. Of the several DNA precursors investigated [³H]Adenosine, [³H]Xanthine and [³H]Hypoxanthine were shown to be incorporated into the nucleic acids of *Plasmodium* spp. parasites. However, [³H]Hypoxanthine is the main purine base used by *P. falciparum* and is the radioisotope used for *in vitro* drug sensitivity assays [130].

The incorporation of [³H]Hypoxanthine is directly proportional to the number of *P. falciparum* infected erythrocytes, when the initial parasitemia ranges between 0.1 and 1% [131, 132]. If the initial parasitemia is higher than 1% incorporation becomes non-linear and is lower than expected. Moreover, it is stage-dependent and follows DNA replication and nuclear division, meaning that during the ring-stage the incorporations is low and it starts increasing as parasites developed into mature throphozoites reaching a maximum with schizont formation [131, 132].

The first radioisotope and semi-automated assay was developed by Desjardins [133] and it still remains as the reference method for *in vitro* antimalarial drug sensitivity testing. Even though it allows an accurate and sensitive determination of drug effects on parasite growth, its main limitation is the use of a radioactive compound that requires sophisticated infrastructure for handling and disposal. Other assays that may overcome this limitation were further investigated and developed.

iv. Fluorometric Assays

This type of assays is based on the principle of DNA labeling with fluorochromes. Infected erythrocytes are incubated with drugs for 48 hours after which erythrocytes are lysed by addition of distilled water or saponin. After centrifugation, the packed pellets are stained with DNA-binding fluorochromes such as Hoechst 33258, PicoGreen®, SYBR® Green I [134–137]. The fluorescence intensity, which is proportional to the amount of DNA in individual samples, is measured with a minifluorometer, fluorescence spectrophotometer or fluorescence activated microplate reader. This procedure may require an additional step of DNA extraction in chloroform to eliminate hemozoin which can cause

quenching. This protocol must be optimized to ensure complete recovery of the total amount of DNA in each sample. Moreover, contaminating human leukocytes must be removed completely. This assay is accurate, rapid but less sensitive in comparison to other methods and it requires an experienced technician to execute it.

v. Antigen Detection by ELISA

Two enzyme-linked immunosorbent assays (ELISAs) based on two different antigens (HRP2 and pLDH) have been developed to assess drug effects in *P. falciparum*. In fact these antigens have been initially investigated for their potential use in the context of malaria diagnosis.

The histidine-rich protein 2 (HRP2) appears to be produced exclusively by *P. falciparum* in the course of its growth and multiplication. It is most actively secreted into the host erythrocyte and to the extracellular environment (plasma, culture medium) during the late ring and trophozoites stages [138]. The levels of HRP2 are closely related with parasite density and development [139]. However, the HRP2 is a stable antigen that persists in patients up to two weeks after effective treatment, despite parasite and fever clearance. In synchronized laboratory-adapted strains levels of HRP2 remain low during the first 48 hours, reaching high levels only at 60 – 72 hours [140]. Assessment of the HRP2 concentration by the end of the 72 hours of incubation represents the cumulative effect of parasite metabolism and it does not seem to increase in parallel with parasite maturation during the first cycle.

A commercial ELISA kit to measure HRP2 is available, however it is expensive (800 USD/10 microtitre plates). Yet, the cost can be reduced by 80% (i.e. about US\$ 100 for 10 plates) by preparing the antibody coated plates in-house [141].

This assay is easy to perform and neither highly specialized equipment nor personnel are required. Moreover, it has a low limit of detection of 0.05% parasitemia. ELISA-based assays can be tedious and time-consuming to perform because they require numerous washing steps. Another limitation is the rather long turn-around time, since it is mandatory for samples to be incubated for 72 hours before the ELISA can be performed.

Another ELISA assay based on the detection and quantification of parasite lactate dehydrogenase (pLDH) was developed. pLDH is a terminal enzyme in the Embden–Meyerhof pathway (glycolysis) of the malaria parasite. The enzymatic activity of pLDH reflects the general metabolic activity of viable parasites. In 1993, Makler et al. developed an assay where by measuring the enzymatic activity of pLDH it was possible to determine

drug activity [142]. Rather high initial parasite densities of 1-2% are required. Subsequent tests with fresh isolates showed that this assay was not sensitive for field application [143]. These limitations led to the development of a new pLDH-based assay. This new approach measures pLDH levels in a double-site enzyme-linked LDH immunodetection (DELI) assay, which was made possible by the development of monoclonal antibodies. This new format is considerably more sensitive and is also field applicable [144]. Nevertheless, limited supplies of monoclonal antibodies constrained the further validation and application of this assay.

vi. Flow Cytometric Methods

By 1987, it had been shown that flow cytometry of DNA and RNA content of parasitized erythrocytes could differentiate stages and, in some cases, species [145, 146]. Since then flow cytometry has been used to study parasite physiology and also response to antimalarial drugs [147–152]. Most of the described flow cytometry methods for drug testing in malaria use fluorescent DNA and RNA stains to detect the parasites [153, 154]. The principle behind this approach is the contrast between host erythrocytes, which most of them lack DNA/RNA, and the malaria parasites, which have DNA/RNA and are thus, readily stained with fluorescent stains. The fluorescent intensity increases in direct proportion to parasite maturation which allows to different asexual development stages. More recent work has also included the use of maturation/viability markers in the context of drug testing [155, 156].

A range of different fluorochromes have been used, such as: thiazole orange, acridine orange, Hoechst 33258 or 33342, SYBR Green I, among others (Table I.7). The latter has been pointed out as the best choice because, contrary to Hoechst 33258 or 33342, it does not require flow cytometers equipped with an ultraviolet laser, which are expensive. Unlike thiazole and acridine orange that bind both to DNA and RNA, SYBR green I is a specific-double stranded DNA dye, therefore excluding the problem of the RNA present in reticulocytes (immature erythrocytes) [137]. This technique is rapid, accurate, highly sensitive, automated and non-radioactive. On the other hand the flow cytometric analysis requires expensive equipment and specialized technicians for maintenance. Even though, nowadays simpler and more affordable flow cytometers have been developed. Another limitation for the use of such method in resource-limited settings is the fact that most flow cytometric approaches rely on the use of nucleic acid stains which are expensive and certainly not readily available in those settings.

Table I.7: Summary of dyes used to study *Plasmodium* spp. by flow cytometry (adapted from [153])

Stain	Marker of	Excitation maximum	Reference
Acridine orange	RNA/DNA	460 nm (RNA) 500 nm (DNA)	[145]
			[157]
Ethidium bromide	RNA/DNA		[158]
			[159]
Dihydroethidium	DNA Live cells	535 nm (DNA) 610 nm (live)	[160]
Hoechst 33258	double-stranded DNA	345 nm	[146]
			[157]
Hoechst 33342	double-stranded DNA	355 nm	[146]
			[161]
			[157]
Propidium iodide	RNA/DNA	535 nm	[162]
SYTO-9	RNA/DNA	486 nm (RNA) 485 nm (DNA)	[157]
SYTO-16	DNA/RNA	494 nm (RNA) 488 nm (DNA)	[163]
			[164]
SYTO-61	DNA/RNA	628 nm	[165]
SYBR green I	double-stranded DNA	488 nm	[157]
			[161]
			[166]
YOYO-1	nucleic acid (high affinity double-stranded DNA)	491 nm	[163]
			[167]
			[168]
SYTOX green	DNA/RNA (distinguish live from dead cells)	504 nm	[169]
Thiazole orange	RNA	509 nm	[170]
Hydroethidine+ Thiazole orange	DNA RNA	536 nm 509 nm	[171]
Hoechst 33342+ Thiazole orange	DNA RNA	355 nm 509 nm	[148]
Hoechst 33342+ Thiazole orange+ DiIc1-5	DNA RNA Membrane potential	355 nm 509 nm 638 nm	[172]
Dihydroethidium + Hoechst 33342	DNA	488 nm + 305 nm	[173]
Dihydroethidium + SYBR green I	DNA	488 nm	[173]
Dihydroethidium + SYBR green	DNA	488 nm	[152]

d. Interpretation of *In Vitro* Results – Comparison of Different *In Vitro* Assays

In vitro assays can be complex and so does their interpretation. Each test has a different end-point and measures the parasite growth differently using: incorporation of radioactive nucleotides or fluorescent stains and production of parasite-specific enzymes or secretion of soluble antigens.

Results from *in vitro* drug assays can be expressed in different ways. Most of them are expressed in terms of which concentration is required to inhibit a specific percentage of parasite growth. Generally, the 50% inhibitory concentration (IC₅₀) is used, but IC₉₀ or the minimal inhibitory concentration (MIC) (synonymous with IC₁₀₀) can also be used. IC₅₀ values are deduced from a sigmoid dose-response curve where the parasite growth is a function of the drug concentration (Figure I.4).

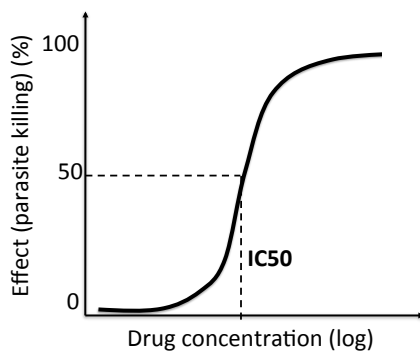


Figure I.4: A representative dose-response curve.

The 50% inhibitory concentration is found on the steepest part of the curve and bisects the distance on the Y-axis between the higher and lower plateaus.

In fact, in malariology the MIC value is a less precise measure than the IC₅₀. This is mainly due to the characteristic growth of malaria parasites and to the inherent limitations of available sensitivity assays. Unlike bacteria, where MIC values are commonly determined, malaria parasites replicate rather slowly in 48 hours cycles. As a consequence, available assays fail to detect small changes in parasites sensitivity to a specific drug. Thus, these small differences in growth inhibition are more reliably detected when determined at the steepest region of the curve, by calculating IC₅₀ values instead of calculating the MIC. Unlike the estimation of IC₅₀ values, the MIC is a fixed cut-off value [130]. Moreover, available assays measure parasite “viability” indirectly and there is no objective measure of growth inhibition like it may happen in bacteriology where the diameter of area cleared of bacterial growth on an agar plate is measured [130].

Even though IC₅₀ values are recommended to assess drug effects it is important to note that results can still differ considerably between different assays or even when using the same assay in different laboratories (Table I.8). The difference between assays is mainly

due to the fact that several different factors, such as hematocrit/erythrocyte volume fraction, initial parasitemia, volume present in the wells will influence parasite growth, both in the presence and absence of drug (Table I.9). Differences observed when using the same assay must be a consequence to inherent differences that exist among different laboratories.

Table I.8: Antimalarial activities of several antimalarial drugs determined by different *in vitro* sensitivity assays against *P. falciparum* 3D7 strain [174]

	Hypoxanthine incorporation	WHO schizont maturation test	SYBR green I plate assay	HRP2 assay
Quinine	47.1 nM [175] 59.9 nM [176] 63 nM [177] 102.3 nM [178]	35 nM [177]	6.9 nM [179]	5.9 nM [179]
Mefloquine	6.1 nM [178] 18.2 nM [175] 34.5 nM [176] 42.6 nM [180]	12.1 nM [181]	9.4 nM [179] 9.5 nM [182] 40.7 nM [183]	8.4 nM [179]
Chloroquine	6 nM [184] 9.6 nM [185] 9.7 nM [178] 11.3 nM [175] 15.7 nM [180] 18.7 nM [176] 29.6 nM [186]	14.79 nM [185]	8.1 nM [179] 11.54 nM [185] 16 nM [187] 22.2 nM [188]	7.5 nM [179] 9.7 nM [185]
Amodiaquine	20.3 nM [189]	7.8 nM [177]		
Artemisinin	10.1 nM [190] 22 nM [180]		9 nM [182]	
Dihydroartemisinin	4.2 nM [186] 5.3 nM [180]		3.78 nM [188] 22.1 nM [183]	2.3 nM [191]
Artesunate	0.4 nM [175] 0.9 nM [176] 1.1 nM [185] 9.4 nM [189]	3.7 nM [185] 5.4 nM [183]	1.9 nM [185] 3.6 nM [188]	1.5 nM (48h) [185] 2.4 nM [191] 2.5 nM (72h) [185]
Atovaquone	0.06 nM [185] 1.1 nM [189] 1.3 nM [180]	0.11 nM [185]	0.06 nM [185]	0.8 nM [185]
Pyrimethamine	5 nM [184] 19.3 nM (48h) [185] 19.4 nM (72h) [185] 78.4 nM [178]	26.3 nM (72h) [185] 32.2 nM (48h) [185]	> 100 nM (48h) [185] 23.9 nM (72h) [185] 7.2 nM [182]	26.6 nM (48 h) [185] 53.9 nM (72h) [185]

Table I.9: Comparative descriptions of available *in vitro* sensitivity assays for *Plasmodium falciparum* [174]

	Schizont maturation test	Hypoxanthine incorporation	Flow cytometric assays	Fluorometric assays	HRP2-ELISA assay
Principle of the assay	Quantification of schizonts	Measurement of parasite DNA			Antigen detection
Time of incubation with the drugs	30h	48h	48h	48 - 96h	72h
Volume of sample to analyze	10 – 50 µL	200 µL	25 - 100 µL	10 – 200 µL	100 µL
Hematocrit	1.5 – 20%	1 – 2.5%	2.5%	1.5 – 2.5%	1.5%
Parasitemia:					
Laboratory strains	1%	0.5%	0.25 – 1%	0.5 - 1%	0.05%
Clinical isolates	0.02%	0.1-0.5%	(n.d.)	0.5 - 1%	0.05%
Required equipment and Infrastructure	Bright field microscope	Scintillation counters and harvesting machine and infrastructure	Flow cytometer	Microplate fluorometer	Microplate spectrophotometer
Advantages	- Requires little equipment.	- Automatic reading of results. - Accurate and sensitive.	- Automatic reading of results. - Accurate and sensitive.	- Simple, does not require specialized personnel. - Accurate.	- Simple, does not require specialized personnel. - Low detection limit (0.05% parasitemias).
Limitations	- Subjective and labor-intensive. - Highly trained personnel.	- Costly equipment. - Handling of radioactive reagents. - Additional incubation with reagents.	- Costly equipment and reagents (e.g.: DNA stains). - Additional incubation with reagents.	- Costly reagents (e.g.: DNA stains). - Additional incubation steps with reagents.	- Costly reagents (e.g.: antibodies). - Additional incubation steps with reagents.

n.d. – not described.

e. Molecular Methods

Molecular assays rely on molecular markers to predict drug resistance. Several molecular markers have been described for some antimalarial drugs including chloroquine, mefloquine, sulfadoxine-pyrimethamine, atovaquone (Table I.10). More recently, a molecular marker for artemisinin resistance, as characterized by delayed parasite clearance, has also been reported but further validation is still required [85]. Similarly to *in vitro* tests, molecular studies are also relevant and useful in monitoring the prevalence of a specific molecular marker in a certain region and thus, monitoring the potential spread of resistant parasites.

Advantages of molecular methods include the need for small volumes of samples, the fact that it does not require *in vitro* incubation of samples with the drugs and it allows the assessment of a large number of samples in a relatively short period of time. More importantly, the transport and storing of samples for molecular analysis can be simply done by using dried blood spots in filter papers. As disadvantages there is the need for sophisticated equipment and training, and most importantly the fact that the number of currently known and validated markers is limited. Nevertheless, molecular methods are valuable surveillance tool for monitoring the occurrence, spread, or intensification of drug resistance.

Table I.10: Molecular Markers for Antimalarial Drug Resistance

	<i>pfcr1</i>	<i>pfmdr1</i>	<i>pfneh1</i>	<i>cyt-b</i>	<i>pfdhfr</i>	<i>pfdhps</i>
Quinine	•	•	•			
Chloroquine	•	•				
Mefloquine		•				
Amodiaquine	•	•				
Lumefantrine		•				
Piperaquine	•					
Atovaquone				•		
Pyrimethamine-sulfadoxine					•	•

pfcr1 (*P. falciparum* chloroquine resistance transporter); *pfmdr1* (*P. falciparum* multidrug resistance transporter 1); *pfneh1* (*P. falciparum* sodium/proton exchanger 1); *cyt-b* (cytochrome b gene); *pfdhfr* (*P. falciparum* dihydrofolate reductase); *pfdhps* (*P. falciparum* dihydropteroate synthetase enzyme)

f. Key Practical Aspects of Antimalarial Drug Testing

i. Culturing of *P. falciparum*

In 1976, Trager and Jansen described a method to reliably culture asexual stages of malaria parasites [192]. Culturing of parasites is an essential step for *in vitro* antimalarial drug

testing because incubation of infected erythrocytes with the drugs is required to assess its inhibitory activity. In fact, vaccine development, investigation of mechanisms of pathogenesis, parasite development and the study of parasite genetics have been greatly impacted by use of *in vitro* cultivation of the malaria parasite.

In vitro cultivation of *P. falciparum* generally requires human erythrocytes, a lipid source and a synthetic medium that provides suitable ionic environment and soluble nutrients. The culture medium for *P. falciparum* consists on RPMI 1640 supplemented with glucose, hypoxanthine, L-glutamine, sodium bicarbonate, HEPES and gentamycin [193].

Detailed information about each culture-related factor that may influence *in vitro* drug testing is presented below.

ii. Culture-related factors that influence in vitro drug sensitivity

No standardize protocol for *in vitro* antimalarial drug testing exists. Different laboratories consider different factors, which can considerably influence the level of drug response (Table I.7 and I.8). Such factors include: modification to the culture medium, the type of serum substitute, the used hematocrit, the initial parasitemias and the incubation conditions.

Culture medium and components

The main *in vitro* assay affected by the culture medium components is the radioisotope assay based on the incorporation of [³H]Hypoxanthine. Unlabeled hypoxanthine is routinely supplemented into to RPMI 1640 medium to optimize the parasite growth in culture. This might influence the maximal incorporation of [³H]Hypoxanthine. At concentrations $\geq 2 \mu\text{mol/l}$ of unlabeled hypoxanthine the incorporation of [³H]Hypoxanthine decreases [130].

The activity of antifolate drugs is also affected by the culture medium. Standard RPMI 1640 contains folic acid (1 mg/l) and PABA (1 mg/l). Both these substrates antagonize the antimalarial activity of antifolate drugs, such as sulfonamides, sulfones, pyrimethamine, trimethoprim and cycloguanil (the biologically active metabolite of proguanil) [130]. Although the “real inhibitory” effect of such drugs may be masked by the presence of folic acid and PABA in the culture medium, IC₅₀ values can still be determined and compared between samples.

Hematocrit: erythrocyte volume fraction

Uninfected erythrocytes are used in *in vitro* drug testing to adjust the initial parasitemia of blood samples. They are essential for the development of the parasite because they obviously provide the location/environment for asexual reproduction but also nutrients for parasite growth [194]. Any blood group can be used since all of them support the growth of erythrocytic stages of malaria [130]. Yet, the use of type O cells may be more adequate because of their compatibility with serum or plasma of all other blood groups. *In vitro* multiplication of *P. falciparum* is higher in freshly collected erythrocytes, independently of the anticoagulant used for its collection [195]. Nevertheless, erythrocytes can be used up to approximately one week after blood collection.

The hematocrit refers to the percentage of volume of red blood cells per total volume of the sample. It is known that increases in the hematocrit, from 1% to 2.5% for example, will lead to an increase in IC₅₀ values as well [196]. Furthermore, when the hematocrit is higher than 2.5% confounding factors can be observed. Because, when using this hematocrit in 96-well plates the parasite growth during 48 hours without medium change is suboptimal due to the depletion of nutrients, poor gas exchange in thick layer of erythrocytes, accumulation of lactic acid or a combination of all these factors [130]. Moreover, some specific assays are directly affected by differences in the hematocrit. For example, incorporation of [³H]Hypoxanthine increases when the hematocrit increases from 1 to 2% but tends to reach a plateau at hematocrits equal or higher than 2.5% [196].

Initial parasitemia

When the parasitemia is higher, using the same hematocrit, the *in vitro* activity of drugs tends to decrease, resulting in higher IC₅₀ values. This is referred as the inoculum effect, which is defined by an increase in the inhibitory drug concentration when greater numbers of parasites are inoculated. It is thought to be the consequence of some drug accumulating inside the parasitized erythrocyte [197] and has been described for most antimalarial drugs like artemisinin, artesunate, chloroquine and mefloquine [198].

Leukocytes

P. falciparum growth is not inhibited by the presence of leukocytes, when this leukocytes were obtained from non-immune healthy donors [199]. Therefore, elimination of leukocytes is unnecessary, and untreated erythrocytes (i.e. with leukocytes) can be used for routine culture.

Even though the presence of leukocytes does not inhibit parasite growth, it can interfere with several *in vitro* drugs assays. Mostly with assays that measure parasite DNA/RNA, such as fluorometry or flow cytometry. Because unlike erythrocytes, leukocytes will have high amounts of DNA/RNA that cannot, or are difficult to, be distinguished from the DNA/RNA of the parasite [153].

In cases the absence of leukocytes is required, blood samples can be treated in order to remove these cells by using CF11 cellulose powder columns, cell affinity chromatography with protein A sepharose or commercial filters [130]. Yet, it should be taken in consideration that leukocyte-free blood prepared by passage over a powdered cellulose column can result in suboptimal parasite growth [199].

Anticoagulants

Several anticoagulants used to collect capillary or venous blood from patients like heparin, acid citrate dextrose and EDTA have been studied. Parasite growth is not affected by any of these anticoagulants if isolates are cultured immediately after blood collection [130]. Yet, others recommend the use of heparin or citrate phosphate dextrose solution (CPD) tubes, claiming that the use of EDTA blood does not support parasite survival [193]. In fact, several reports use EDTA-anticoagulated tubes to collect blood from malaria patients for *ex vivo* drug testing [200–204]. Heparin is also known to reversibly inhibit the invasion of uninfected erythrocytes by merozoites [205], thus as long as the blood is washed before culture it should not affect parasite growth *in vitro*. However, it is known to inhibit the action of taq DNA polymerase [130] and thus, its use should be avoided in molecular studies. Collection tubes containing acid citrate dextrose are designed to be filled completely, and thus the total volume of collected whole blood is altered. No clear consensus seems to exist and different reports mention and use different anticoagulants.

Serum substitutes

Serum factors influence the availability of drug in the blood. Once drugs are administered, the drug is absorbed and enters the bloodstream, some it is bound to blood proteins, in particular albumin, while the rest remains free in circulation. The free part of the drug is the one responsible for drug effects. Each drug will have different proportion of the bound and unbound fractions [130], therefore the type of serum substitute used for *in vitro* culturing of parasites may have a significant impact both on parasite growth but also on drug effect.

Several serum substitutes have been investigated. Fetal calf serum is commercially available and is an affordable alternative to human serum. However, there is wide batch-to-batch variation in its ability to support *P. falciparum* growth *in vitro* [206]. Another alternative is the use of Albumax. This lipid-enriched bovine albumin preparation has been widely tested for culture of malaria parasites and antimalarial drug sensitivity assays. Even though it is the most currently used human serum substitute for *P. falciparum in vitro* cultures, it has also been associated with unpredictable growth of isolates and it may affect the IC₅₀ values obtained for different drugs [196, 206, 207].

Incubation conditions: the period of incubation and the atmosphere

Incubation periods of cultured parasites with the respective drug can differ from 24 to 96 hours, depending on the assay being used and on the drug being tested (Table I.8).

Most assays use as endpoint a period of incubation that precedes the 48 hours. In this case drug effects are determined within the first erythrocytic cycle, this is the case of the schizont maturation test, the hypoxanthine assay and the fluorometric methods. On the other hand, other assays require a prolonged incubation time of 72 hours, such as the ELISA assays, or even 96 hours when drugs have a delayed inhibitory effect on the parasite (e.g. pyrimethamine or antibiotics) [185].

In terms of atmospheres the CO₂ level should be maintained always at 5%, while the O₂ may vary. The currently used culture medium was optimized to have a pH within the physiological range in an atmosphere containing 5% CO₂. Alterations of this concentration will lead to an altered pH, which can influence the IC₅₀ values of pH-dependent drugs like chloroquine. Indeed, studies have shown that an increase in CO₂ concentration will lead to significantly higher IC₅₀ values [208].

On the other hand, O₂ concentrations seem not to affect the IC₅₀ values. Generally, the recommended atmosphere for *P. falciparum* growth *in vitro* include the use of a low O₂ atmosphere, with 5% CO₂ [193]. However, the use of such atmospheres requires gas cylinders and gas-mixing incubators which might not be available in many of the resource-limited settings in malaria endemic countries. The influence of atmospheres on parasite survival after drug treatment has been addressed in a study where an *ex vivo* drug assay was performed using different atmospheres: trigas (5% CO₂, 5% O₂, 90% N₂), 5% CO₂, and candle jar. Results showed no differences in parasite survival using these three atmospheres [84].

iii. Synchronization of parasites

One of the particular features of *P. falciparum* infection in humans is the fact that only young parasite forms (rings) are found in circulation. In *in vitro* cultures of *P. falciparum* all parasite developmental stages (ring-forms, trophozoites and schizonts) are present. Thus, several approaches have been used to synchronize *in vitro* parasite cultures. Generally, they involve combinations of treatments that include: selective killing of mature parasites by sorbitol lysis [209], harvesting of mature stages using a Percoll gradient [210] or using a magnetic column [211, 212].

The use of a 5% sorbitol solution to eliminate mature parasite forms is the most commonly used method [209]. This protocol relies on the lysis of trophozoites and schizonts allowing the continued growth of ring-form parasites.

Percoll density centrifugation can also be used to enrich for mature parasite forms, however separation of late trophozoites, early or late schizonts is not possible [210].

Magnetic cell sorting systems are also used to separate mature forms containing hemozoin. Hemozoin is paramagnetic and thus, when an infected blood sample containing different parasite forms is subjected to a strong magnetic field late-stage parasites containing hemozoin will get retained, while uninfected erythrocytes or young parasites will flow through [211].

Heparin, which reversibly inhibits the invasion of erythrocytes by *P. falciparum* merozoites, has also been used to synchronize cultures [205]. In this case parasites are incubated in the presence of heparin, when almost all of them have progressed to the schizont stage, heparin is removed allowing merozoite invasion to occur. Thus, allowing to obtain parasite cultures with a specific synchronization window. The duration of merozoite invasion can be limited by the addition or removal of heparin [213]. This method is rather recent and it has not been used very often.

4. HEMOZOIN - THE MALARIA PIGMENT

a. Overview

Hemozoin, also known as malaria pigment, is produced by malaria parasites during their growth inside the erythrocytes. During the blood stage the parasites digest up to 80% of hemoglobin present in the erythrocyte [214, 215] in order to gain space to grow [216] and as a source of aminoacids [215]. As a result free toxic heme is produced. In order to detoxify it, the parasite converts it into hemozoin. The content of hemozoin increases as the parasite matures from ring-forms, to trophozoites and, finally to schizonts (Figure I.5).

Similarly to schizonts, gametocytes also have a high content of hemozoin. However, while schizonts have a single granule of hemozoin, in gametocytes the hemozoin is widely distributed.

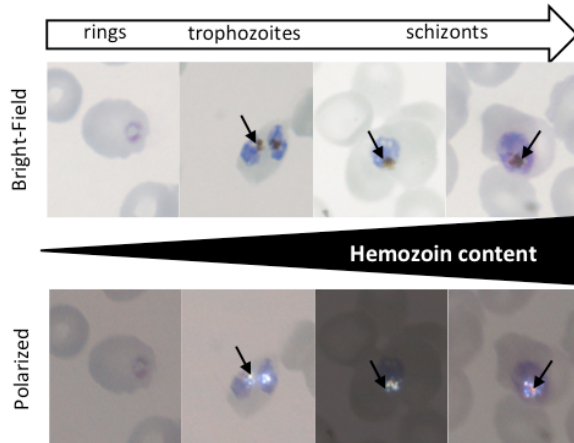


Figure I.5: Hemozoin as a parasite maturation indicator.

The content of hemozoin increases as the parasite matures (arrows). Hemozoin is able to depolarize light, thus using polarized microscopy hemozoin crystals exhibit a shiny appearance.

In fact, hemozoin had a crucial role in the discovery and understanding of malaria, as presented elsewhere [217]. In 1717 Lancini made the first observations of the presence of hemozoin in the spleen and brain in a necropsy of a patient with malaria. In 1847, Meckel made the same observation and assumed that this dark pigment was melanin. Later in 1849, Rudolf Virchow associated this dark pigment with malaria. Yet, it was Laveran who made the ultimate causal relationship between the pigment and the parasite. The pigment was proved to be equivalent to hematin and not melanin in 1911 by Brown.

Hemozoin has also been described in other organisms, such as the blood-sucking insect *Rhodnius prolixus*, in the parasitic worm *Schistosoma mansoni* and in the avian protozoan parasite *Hemoproteus columbae* [218, 219].

Despite the early discovery of hemozoin its mechanism of formation is still not completely understood.

b. Formation of Hemozoin

During the blood stage, the parasite digests hemoglobin and converts the resulting free toxic heme into hemozoin inside its digestive vacuole (Figure I.6). Investigating the process of hemozoin formation inside the parasite is very challenging and thus, most studies have been focused on the structurally and chemically identical β -hematin [220].

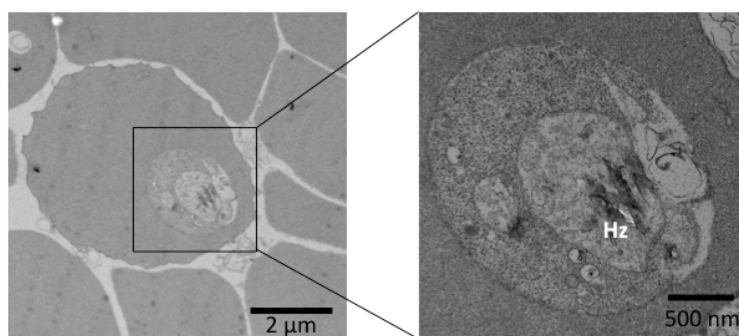


Figure I.6: Electron microscopic picture of a *P. falciparum* infected erythrocyte. Several hemozoin crystals (Hz) can be detected inside the digestive vacuole of the parasite.

Hemozoin is thought to be formed by biomineralization [221, 222]. Biomineralization is the process where deposition of low molecular weight inorganic materials within or outside the cells of living organisms occurs, leading to the formation of inorganic salts. Interestingly, other organisms also use this process as a detoxification mechanism. In the case of hemozoin formation, it has been suggested that the use of the term biocrystallization (instead of biomineralization) is more appropriate [223]. Both enzymes and lipids can be implicated in biomineralization processes. In fact, histidine-rich proteins (HRP) have been suggested to be associated with hemozoin formation [224]. However, parasites that lack these proteins (e.g.: *P. vivax*) can still produce hemozoin [225] and HRPs have been found in small amounts in the parasite food vacuole, where hemozoin is produced [226]. Lipids have also been suggested to be involved in the process of hemozoin formation [227]. Several reports have shown that hemozoin is formed in lipid–aqueous interfaces, providing experimental evidences that support this hypothesis [227–230]. Yet, it was also observed that hemozoin crystals grow on the surface of other hemozoin crystals, suggesting that the process of hemozoin formation could be autocatalytic [218]. More recently, another protein (HDP – heme detoxification protein) that converts heme into hemozoin has been described [231].

In summary, it is still unclear which or if any of these mechanisms is involved in hemozoin crystallization processes *in vivo*. Further studies in this direction are needed to fully elucidate the mechanism of hemozoin production in *Plasmodium* spp.

c. Biophysical Properties of Hemozoin and its Use for the Study of Malaria

Hemozoin crystals are paramagnetic and birefringent. Therefore, they are able to generate small magnetic fields and to change the rotating plane of polarized light, respectively. Due to the fact that Hz is birefringent, it can be detected by optical methods, such as microscopy (Figure I.5) [232, 233] or flow cytometry [174, 234]. Its paramagnetic

property has mainly been used for separating infected erythrocytes from uninfected ones [211, 212]. More recently, systems that exploit both physical properties were developed as alternative malaria diagnosis methods [235–237].

The idea of using hemozoin as a parasite maturation indicator to assess drug effects dates back to 1982. Rieckmann developed a drug assay based on the visual detection of hemozoin, where at the end of 48 hours of incubation the amount of dark-pigmented precipitate (hemozoin) was assessed [238]. However, this assay was not very accurate because of the interference in the final read-out caused by leukocytes agglutination.

The use of hemozoin as a mean to detect the presence of malaria parasites or even its maturation and growth may be a unique opportunity to develop novel and better reagent-free methods for the study of malaria.

5. FLOW CYTOMETRY

a. Principles of Flow Cytometry

Flow cytometry is a powerful technique for the analysis of multiple parameters of individual cells within heterogeneous populations. Measured parameters include the relative size of a particle, granularity or internal complexity and fluorescence. This is accomplished by using an optical-to-electronic system that records how the cell scatters light or emits fluorescence.

As the name indicates, this technique is based on a flow of cells that will pass one at the time through a laser beam. As a cell passes through the laser it will refract or scatter light at all angles. The forward scatter (FCS) refers to the amount of light scattered in the forward direction (less than 10° angles). The magnitude of FCS is proportional to the size of the cell. The side scatter (SSC) refers to the light that is scattered to the side (at a 90° angle). The side-scatter indicates the level of granularity and structural complexity of the cell. The scattered light will reach a detector, which will convert the light intensity into voltages. A combination of filters and beam splitters guide the scattered and fluorescent light to the appropriate detectors.

A flow cytometer is constituted by three main systems: fluidics, optics and electronics. The fluidics system transports particles in a stream allowing them to pass through the laser one at the time. The optics system consists of one or more lasers, which will illuminate the particles passing in the stream, and of optical filters, that will direct the resulting light signals to the respective detectors. Finally, the electronics system will convert the detected light signals into electronic signals that can be processed by the computer (Figure).

Nowadays a wide range of different flow cytometers exist. From expensive and sophisticated instruments to small, simple and affordable versions.

b. Flow Cytometry and Malaria

In 1987 flow cytometry was used for the first time to detect infected erythrocytes (Janse 1987). In this study quantification of DNA and RNA allowed to differentiate parasite species and stages without morphologic information [146]. Due to its speed and to the amount of information it provides, cytometry may become particularly important for the study of malaria parasite growth and invasion since it overcomes some of the limitations of existing methods. Especially, during the last decade flow cytometry has been increasingly used in malaria research with particular focus on the study of parasite physiology and its response to antimalarial drugs [147–149, 152, 239]. Most approaches rely on the use of nucleic acid stains to detect parasite's DNA/RNA (Table I.10). Generally they require either complex multi-parameter analysis or complex protocols of staining to reliably distinguish infected erythrocytes from uninfected [153, 154]. In some they even require the use flow cytometers equipped with UV lasers or with more than one laser – increasing the cost of these methods.

More recently flow cytometric methods based on the detection of hemozoin, produced by malaria parasites, have been described [174, 234, 240, 241]. These methods rely on the fact that hemozoin is able to depolarize light and thus, the resulting light depolarization can be detected by flow cytometry. The detection of hemozoin inside leukocytes have been used for diagnosis and immunological studies [242, 243], while hemozoin inside erythrocytes has mainly been assessed for drug testing purposes [174] and has been the main focus of the work presented in this thesis.

c. Detection of Light Depolarization by Flow Cytometry

In 1987, flow cytometric detection of depolarized light scatter was described for the first time [244]. Initially this was used as a simple and reagent-free mean to distinguish eosinophils from other leukocyte cell population based on the birefringence of the eosinophil granules [244]. This feature was only available on Cell-Dyn automated full-blood-count analysers and other manufacturers of flow cytometers were not allowed to offer this measurement in their instruments because of a patent (US, Patent: 5017497: <http://www.google.com/patents/US5017497> accessed on 02/12/2016).

In 1999, hemozoin-containing monocytes in a blood sample from a malaria patient was detected by a Cell-Dyn hematology analyser [245]. Later other studies reported the detection of hemozoin inside monocytes and neutrophils using the same instruments [234, 240, 242]. In fact the use of hematology analyzers as an alternative tool to diagnose malaria, both in non-endemic and endemic countries, has been investigated and it is extensively reviewed elsewhere [246]. Interestingly, in some of these studies the possibility of detecting hemozoin inside erythrocytes was reported [240, 247] (Figure I.7). This was further investigated and developed in the context of the work presented here in this thesis.

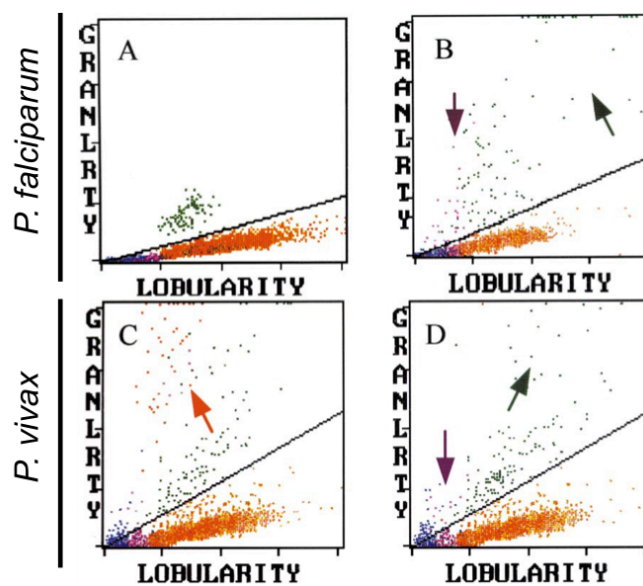


Figure I.7: Granularity/Lobularity plots from the Cell-Dyn 3500.

Granularity is a measure of depolarization (90°-depolarized) and lobularity of 90° light scatter. A normal FBC result is shown with the eosinophil population (green) separated from monocytes (purple), lymphocytes (blue) and neutrophils (orange) (A). A FBC result from a patient with *P. falciparum* malaria (purple dots) shows hemozoin-containing monocytes in the eosinophil area (purple arrow) and an eosinophil population that is abnormally scattered (green arrow) (B). A *P. vivax* infection in a patient with increased osmotic resistance. In “normal lysis” mode many red dots (resistant erythrocytes) with strongly depolarizing content appear in the plot (red arrow) (C). The same sample, as in C, but re-analysed in the “extended lysis” mode where red dots events have disappeared. Changes similar to B, still suggest pigment containing monocytes and granulocytes [240].

6. A NOVEL ANTIMALARIA DRUG ASSAY FOR *PLASMODIUM* spp. BASED ON THE FLOW CYTOMETRIC DETECTION OF HEMOZOIN

The idea of using hemozoin as a parasite maturation indicator was the basis of sensitivity assay developed in the 80’s [238]. Yet, the visual read-out was not ideal and results were

not reliable. However, reports indicating that hemozoin could be detected inside leukocytes by hematology analysers made us revisit Rieckmann's work. This time the subjective visual read-out would be replaced by flow cytometry instead.

Previously, during my master studies, the use hemozoin as a parasite maturation indicator and, consequently as a mean to detect drug effects was assessed in a malaria rodent model (C57BL/6 mice infected with *Plasmodium berghei*). Results showed that indeed it was possible to distinguish between infected and uninfected blood samples based on the flow cytometric detection of hemozoin. Depolarizing cells, which correspond to infected-erythrocytes containing hemozoin, were present in the infected sample but absent in the uninfected one (Figure I.8A and B). Moreover, different degrees of depolarization corresponding to different stages of maturation were observed (Figure I.8B). Drug effects could be determined by assessing the percentage of events that had a high depolarization signal overtime (Figure I.8C) [243].

These promising results led to the work presented in this thesis, where further investigation, development, and validation of the hemozoin detection assay were performed.

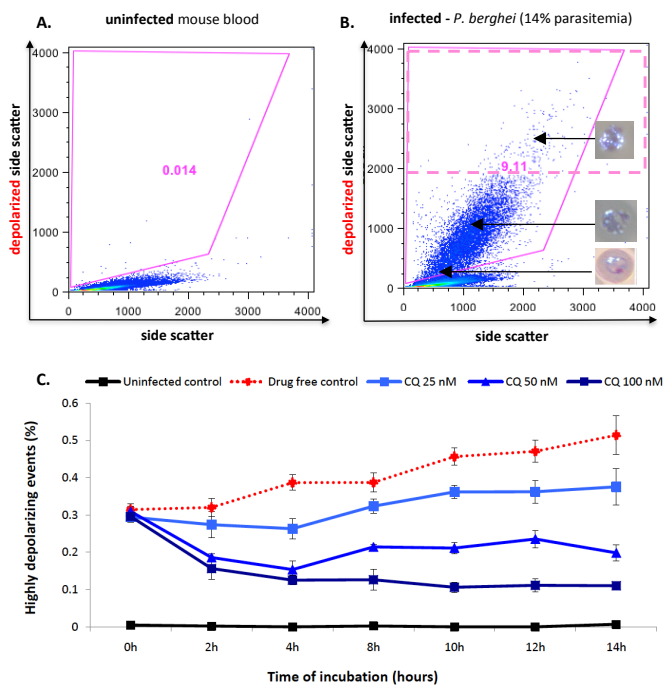


Figure I.8: Flow cytometric detection of hemozoin and assessment of drug inhibitory effects in a malaria rodent model.

Side scatter against depolarized side scatter plots of a blood sample from an uninfected (A) and a *Plasmodium berghei*-infected mouse (B). Solid pink line delineates the depolarizing erythrocyte population and the dashed pink line delineates the population of highly depolarizing events. Increasing concentrations of chloroquine (CQ) were incubated with *P. berghei*-infected erythrocytes. The inhibitory effect of chloroquine can be detected already after 2 hours of incubation. Each point represents the mean of triplicate measurements (\pm one SD) (adapted from [243]).

7. References

1. WHO. (2015) World Malaria Report 2015. World Health Organization, Geneva.
2. White N, Pukrittayakamee S, Hien T, Faiz M, Mokuolu O and Dondorp A. (2014) Malaria. *The Lancet* 22: 723–735.
3. White NJ, Nosten F, Looareesuwan S, Watkins WM, Marsh K, Snow RW, et al. (1999) Averting a malaria disaster. *The Lancet* 353: 1965–1967.
4. Desai M, ter Kuile FO, Nosten F, McGready R, Asamo K, Brabin B, et al. (2007) Epidemiology and burden of malaria in pregnancy. *The Lancet Infectious Diseases* 7: 93–104.
5. Falade C, Mokuolu O, Okafor H, Orogade A, Falade A, Adedoyin O, et al. (2007) Epidemiology of congenital malaria in Nigeria: A multi-centre study. *Tropical Medicine and International Health* 12: 1279–1287.
6. Bardají A, Sigauque B, Sanz S, Maixenchs M, Ordi J, Aponte JJ, et al. (2011) Impact of malaria at the end of pregnancy on infant mortality and morbidity. *Journal of Infectious Diseases* 203: 691–699.
7. Portugal S, Drakesmith H and Mota MM. (2011) Superinfection in malaria: Plasmodium shows its iron will. *EMBO reports* 12: 1233–42.
8. Tjitra E, Anstey NM, Sugiarto P, Warikar N, Kenangalem E, Karyana M, et al. (2008) Multidrug-resistant Plasmodium vivax associated with severe and fatal malaria: A prospective study in Papua, Indonesia. *PLoS Medicine* 5: 0890–0899.
9. Genton B, D’Acromont V, Rare L, Baea K, Reeder JC, Alpers MP, et al. (2008) Plasmodium vivax and mixed infections are associated with severe malaria in children: A prospective cohort study from Papua New Guinea. *PLoS Medicine* 5: 0881–0889.
10. Alexandre MA, Ferreira CO, Siqueira AM, Magalhães BL, Mourão MPG, Lacerda M V., et al. (2010) Severe Plasmodium vivax malaria, Brazilian Amazon. *Emerging Infectious Diseases* 16: 1611–1614.
11. Barcus MJ, Basri H, Picarima H, Manyakori C, Sekartuti, Elyazar I, et al. (2007) Demographic risk factors for severe and fatal vivax and falciparum malaria among hospital admissions in northeastern Indonesian Papua. *The American Journal of Tropical Medicine and Hygiene* 77: 984–991.
12. Lampah DA, Yeo TW, Hardianto SO, Tjitra E, Kenangalem E, Sugiarto P, et al. (2011) Coma associated with microscopy-diagnosed Plasmodium vivax: A prospective study in Papua, Indonesia. *PLoS Neglected Tropical Diseases* 5: 1–7.
13. Manning L, Laman M, Law I, Bona C, Aipit S, Teine D, et al. (2011) Features and

prognosis of severe malaria caused by *Plasmodium falciparum*, *Plasmodium vivax* and mixed plasmodium species in Papua New Guinean children. *PLoS One* 6: e29203.

14. Kochar DK, Das A, Kochar SK, Saxena V, Sirohi P, Garg S, et al. (2009) Severe *Plasmodium vivax* malaria: A report on serial cases from Bikaner in northwestern India. *American Journal of Tropical Medicine and Hygiene* 80: 194–198.

15. Shaikh S, Memon H, Iohano B, Shaikh A, Ahmed I and Baird JK. (2012) Severe disease in children hospitalized with a diagnosis of *Plasmodium vivax* in south-eastern Pakistan. *Malaria journal* 11: 144.

16. Trape J-F, Tall A, Sokhna C, Ly AB, Diagne N, Ndiath O, et al. (2014) The rise and fall of malaria in a West African rural community, Dielmo, Senegal, from 1990 to 2012: a 22 year longitudinal study. *The Lancet Infectious Diseases* 14: 476–88.

17. Ashley E, Dhorda M, Fairhurst RM, Amaratunga C, Lim P, Suon S, et al. (2014) Spread of Artemisinin Resistance in *Plasmodium falciparum* Malaria. *The New England Journal of Medicine* 371: 411–423.

18. WHO. (2015) Conditions for use of long-lasting insecticidal nets treated with a pyrethroid and piperonyl butoxide. World Health Organization, Geneva.

19. Strode C, Donegan S, Garner P, Enayati AA and Hemingway J. (2014) The Impact of Pyrethroid Resistance on the Efficacy of Insecticide-Treated Bed Nets against African Anopheline Mosquitoes: Systematic Review and Meta-Analysis. *PLoS Medicine* 11:.

20. Curtin PD. (1990) The End of the “White Man’s Grave”? Nineteenth-Century Mortality in West Africa. *Journal of Interdisciplinary History* 21: 63–88.

21. Weatherall M. (1991) In Search of a Cure. A History of Pharmaceutical Discovery. *The New England Journal of Medicine* 325:365.

22. Greenwood D. (1995) Conflicts of interest: The genesis of synthetic antimalarial agents in peace and war. *Journal of Antimicrobial Chemotherapy* 36: 857–872.

23. Alkadi HO. (2007) Antimalarial drug toxicity: A review. *Chemotherapy* 53: 385–391.

24. Hatton C, Peto T, Bunch C, Pasvol G, Russell S, Singer C, et al. (1986) Frequency of severe neutropenia associated with amodiaquine prophylaxis against malaria. *The Lancet* 1: 411–414.

25. Neftel KA, Woodtly W, Schmid M, Frick PG and Fehr J. (1986) Amodiaquine induced agranulocytosis and liver damage. *British Medical Journal (Clinical research ed.)* 292: 721–723.

26. WHO. (2015) Guidelines for the treatment of malaria - 3rd edition. World Health Organization, Geneva.

27. Meshnick SR and Dobson MJ. (2001) The History of Antimalarial Drugs. In *Antimalarial Chemotherapy* 15–25.
28. White NJ. (2008) Qinghaosu (artemisinin): the price of success. *Science* 320: 330–4.
29. Cui L, Mharakurwa S, Ndiaye D, Rathod PK and Rosenthal PJ. (2015) Antimalarial Drug Resistance: Literature Review and Activities and Findings of the ICEMR Network. *The American journal of Tropical Medicine and Hygiene* 93: 57–68.
30. Visser BJ, van Vugt M and Grobusch MP. (2014) Malaria: an update on current chemotherapy. *Expert Opinion on Pharmacotherapy* 15: 2219-54.
31. Arrow K, Panosian C and Gelband H. (2004) Saving Lives, Buying Time: Economics of Malaria Drugs in an Age of Resistance.
32. White NJ, Pukrittayakamee S, Phyo AP, Rueangweerayut R, Nosten F, Jittamala P, et al. (2014) Spiroindolone KAE609 for Falciparum and Vivax Malaria. *The New England Journal of Medicine* 371: 403–410.
33. van Pelt-Koops JC, Pett HE, Graumans W, van der Vegte-Bolmer M, van Gemert GJ, Rottmann M, et al. (2012) The spiroindolone drug candidate NITD609 potently inhibits gametocytogenesis and blocks Plasmodium falciparum transmission to anopheles mosquito vector. *Antimicrobial Agents and Chemotherapy* 56: 3544–8.
34. Wu T, Nagle A, Kuhlen K, Gagaring K, Borboa R, Francek C, et al. (2011) Imidazolopiperazines: Hit to lead optimization of new antimalarial agents. *Journal of Medicinal Chemistry* 54: 5116–5130.
35. Leong FJ, Zhao R, Zeng S, Magnusson B, Diagana TT and Pertel P. (2014) A first-in-human randomized, double-blind, placebo-controlled, single- and multiple-ascending oral dose study of novel imidazolopiperazine KAF156 to assess its safety, tolerability, and pharmacokinetics in healthy adult volunteers. *Antimicrobial Agents and Chemotherapy* 58: 6437–6443.
36. White NJ, Duong TT, Uthaisin C, Nosten F, Phyo AP, Hanboonkunupakarn B, et al. (2016) Antimalarial Activity of KAF156 in Falciparum and Vivax Malaria. *New England Journal of Medicine* 375: 1152–1160.
37. Le Bihan A, de Kanter R, Angulo-Barturen I, Binkert C, Boss C, Brun R, et al. (2016) Characterization of Novel Antimalarial Compound ACT-451840: Preclinical Assessment of Activity and Dose–Efficacy Modeling. *PLoS Medicine* 13: e1002138.
38. Mungthin M, Bray PG, Ridley RG and Ward SA. (1998) Central Role of Hemoglobin Degradation in Mechanisms of Action of and Phenanthrene Methanols Central Role of Hemoglobin Degradation in Mechanisms of Action of 4-Aminoquinolines , Quinoline

Methanols, and Phenanthrene Methanols. *Anti-Infective Agents in Medicinal Chemistry* 42: 2973–2977.

39. Olliaro P. (2001) Mode of action and mechanisms of resistance for antimalarial drugs. *Pharmacology & Therapeutics* 89: 207–19.

40. Krogstad DJ, Schlesinger PH and Gluzman IY. (1985) Antimalarials increase vesicle pH in *Plasmodium falciparum*. *The Journal of Cell Biology* 101: 2302–2309.

41. Yayon A, Ioav Cabantchik Z and Ginsburg H. (1985) Susceptibility of human malaria parasites to chloroquine is pH dependent (*Plasmodium falciparum*/food vacuole/lysosomotropic drugs/antimalarials/drug resistance). *Cell Biology* 82: 2784–2788.

42. Jagt DL Vander, Hunsaker LA and Campos NM. (1986) Characterization of a hemoglobin-degrading, low molecular weight protease from *Plasmodium falciparum*. *Molecular and Biochemical Parasitology* 18: 389–400.

43. Loria P, Miller S, Foley M and Tilley L. (1999) Inhibition of the peroxidative degradation of haem as the basis of action of chloroquine and other quinoline antimalarials. *The Biochemical Journal* 339: 363–370.

44. Green D, Xiao L and Lal A. (1996) Formation of hydroxyeicosatetraenoic acids from hemozoin-catalyzed oxidation of arachidonic acid. *Molecular and Biochemical Parasitology* 83: 183–188.

45. O'Neill PM, Bray PG, Hawley SR, Ward SA and Park BK. (1998) 4-Aminoquinolines—past, present, and future: a chemical perspective. *Pharmacology & Therapeutics* 77: 29–58.

46. Sullivan Jr D, Gluzman I, Russell D and Goldberg D. (1996) On the molecular mechanism of chloroquine's antimalarial action. *Proceedings of the National Academy of Sciences* 93: 11865–11870.

47. Vaidya AB, Lashgari MS, Pologé LG and Morrissey J. (1993) Structural features of *Plasmodium* cytochrome b that may underlie susceptibility to 8-aminoquinolines and hydroxynaphthoquinones. *Molecular and Biochemical Parasitology* 58: 33–42.

48. Srivastava IK, Rottenberg H and Vaidya AB. (1997) Atovaquone, a broad spectrum antoparasitic drug, collapses mitochondrial membrane potential in a malarial parasite. *Journal of Biological Chemistry* 272: 3961–3966.

49. O'Neill PM, Barton VE and Ward SA. (2010) The molecular mechanism of action of artemisinin - The debate continues. *Molecules* 15: 1705–1721.

50. Klonis N, Creek DJ and Tilley L. (2013) Iron and heme metabolism in *Plasmodium falciparum* and the mechanism of action of artemisinins. *Current Opinion in Microbiology*

16: 722–727.

51. Meshnick SR, Yang Y, Lima V, Kuypers F, Kamchonwongpaisan S and Yuthavong Y. (1993) Iron-Dependent Free Radical Generation from the Antimalarial Agent Artemisinin (Qinghaosu). *Antimicrobial Agents and Chemotherapy* 37: 1108–1114.
52. Ellis G, Amewu R and Sabbani S. (2008) Two-Step Synthesis of Achiral Dispiro-1, 2, 4, 5-tetraoxanes with Outstanding Antimalarial Activity, Low Toxicity, and High-Stability Profiles. *Journal of Medicinal Chemistry* 51: 2170–2177.
53. Stocks PA, Bray PG, Barton VE, Al-Helal M, Jones M, Araujo NC, et al. (2007) Evidence for a common non-heme chelatable-iron-dependent activation mechanism for semisynthetic and synthetic endoperoxide antimalarial drugs. *Angewandte Chemie - International Edition* 46: 6278–6283.
54. Klonis N, Crespo-Ortiz MP, Bottova I, Abu-Bakar N, Kenny S, Rosenthal PJ, et al. (2011) Artemisinin activity against *Plasmodium falciparum* requires hemoglobin uptake and digestion. *Proceedings of the National Academy of Sciences of the United States of America* 108: 11405–10.
55. Krishna S, Uhlemann A-C and Haynes RK. (2004) Artemisinins: mechanisms of action and potential for resistance. *Drug Resistance Updates* 7: 233–244.
56. Eckstein-Ludwig U, Webb RJ, Van Goethem ID a, East JM, Lee a G, Kimura M, et al. (2003) Artemisinins target the SERCA of *Plasmodium falciparum*. *Nature* 424: 957–961.
57. Cardi D, Pozza A, Arnou B, Marchal E, Clausen JD, Andersen JP, et al. (2010) Purified E255L mutant SERCA1a and purified PfATP6 are sensitive to SERCA-type inhibitors but insensitive to artemisinins. *Journal of Biological Chemistry* 285: 26406–26416.
58. Arnou B, Montigny C, Morth JP, Nissen P, Jaxel C, Møller J V, et al. (2011) The *Plasmodium falciparum* Ca(2+)-ATPase PfATP6: insensitive to artemisinin, but a potential drug target. *Biochemical Society Transactions* 39: 823–831.
59. Wang J, Huang L, Li J, Fan Q, Long Y, Li Y, et al. (2010) Artemisinin directly targets malarial mitochondria through its specific mitochondrial activation. *PLoS One* 5: 1–12.
60. Haynes RK, Cheu KW, Chan HW, Wong HN, Li KY, Tang MMK, et al. (2012) Interactions between Artemisinins and other Antimalarial Drugs in Relation to the Cofactor Model-A Unifying Proposal for Drug Action. *ChemMedChem* 7: 2204–2226.
61. Mbengue A, Bhattacharjee S, Pandharkar T, Liu H, Estiu G, Stahelin R V., et al. (2015) A molecular mechanism of artemisinin resistance in *Plasmodium falciparum* malaria. *Nature* 520: 683–687.

62. Bruce-Peters W, Chwatt L, Black R, Canfield C, Clyde D and Wernsdorfer W. (1986) Chemotherapy of malaria,. World Health Organization.
63. White NJ. (2004) Antimalarial drug resistance. *Journal of Clinical Investigation* 113:1084–1092
64. WHO. (2010) Global Report on Antimalarial Drug Efficacy and Drug Resistance: 2000–2010. World Health Organization, Geneva.
65. Trape JF, Pison G, Preziosi MP, Enel C, Degrees du Lou A, Delaunay V, et al. (1998) Impact of chloroquine resistance on malaria. *Comptes Rendus de l'Académie des Sciences. Série III, Sciences de la Vie* 321: 689–697.
66. Talisuna AO, Bloland P and Alessandro UD. (2004) History , Dynamics , and Public Health Importance of Malaria Parasite Resistance. *Clinical Microbiology Reviews* 17: 235–254.
67. Dash AP, Valecha N, Anvikar AR and Kumar A. (2008) Malaria in India: Challenges and opportunities. *Journal of Biosciences* 33: 583–592.
68. Price RN, Auburn S, Marfurt J and Cheng Q. (2012) Phenotypic and genotypic characterisation of drug-resistant *Plasmodium vivax*. *Trends in parasitology* 28: 522–9.
69. Rieckmann K, Davis D and Hutton D. (1989) *Plasmodium vivax* Resistance to Chloroquine? *The Lancet* 1183–1184.
70. Price RN, von Seidlein L, Valecha N, Nosten F, Baird JK and White NJ. (2014) Global extent of chloroquine-resistant *Plasmodium vivax*: a systematic review and meta-analysis. *The Lancet Infectious Diseases* 14: 982–991.
71. Spudick JM, Garcia LS, Graham DM and Haake DA. (2005) Diagnostic and therapeutic pitfalls associated with primaquine-tolerant *Plasmodium vivax*. *Journal of Clinical Microbiology* 43: 978–981.
72. Marfurt J, de Monbrison F, Brega S, Barbollat L, Müller I, Sie A, et al. (2008) Molecular markers of in vivo *Plasmodium vivax* resistance to amodiaquine plus sulfadoxine-pyrimethamine: mutations in pvdhfr and pvmdr1. *The Journal of Infectious Diseases* 198: 409–417.
73. Maguire JD, Sumawinata IW, Masbar S, Laksana B, Prodjodipuro P, Susanti I, et al. (2002) Chloroquine-resistant *Plasmodium malariae* in south Sumatra, Indonesia. *The Lancet* 360: 58–60.
74. Wongsrichanalai C. (2002) Epidemiology of drug-resistant malaria. *The Lancet Infectious Diseases* 2: 209–218.
75. da Silva AC and Benchimol LJ (2014) Malaria and Quinine Resistance: A Medical and

- Scientific Issue between Brazil and Germany (1907–19). *Medical History* 58: 1–26.
76. Pukrittayakamee S, Supanaranondl W, Looareesuwan S, Vanijanonta S and White NJ. (1994) Quinine in severe falciparum malaria: evidence of declining efficacy in Thailand. *Transactions of the Royal Society of Tropical Medicine and Hygiene* 88: 324–327.
77. Kublin JG, Cortese JF, Njunju M, Mukadam RAG, Wirima JJ, Kazembe PN, et al. (2003) Reemergence of Chloroquine-Sensitive *Plasmodium falciparum* Malaria after Cessation of Chloroquine Use in Malawi. *The Journal of Infectious Diseases* 187: 1870–1875.
78. Laufer MK, Thesing PC, Eddington ND, Masonga R, Dzinjalama FK, Takala SL, et al. (2006) Return of chloroquine antimalarial efficacy in Malawi. *The New England Journal of Medicine* 355: 1959–1966.
- 61 Mwai L, Ochong E, Abdirahman A, Kiara SM, Ward S, Kokwaro G, et al. (2009) Chloroquine resistance before and after its withdrawal in Kenya. *Malaria journal* 8: 106.
79. Alifrangis M, Lusingu JP, Mmbando B, Dalgaard MB, Vestergaard LS, Ishengoma D, et al. (2009) Short report: Five-year surveillance of molecular markers of *Plasmodium falciparum* antimalarial drug resistance in korogwe district, tanzania: Accumulation of the 581G mutation in the *P. falciparum* dihydropteroate synthase gene. *The American Journal of Tropical Medicine and Hygiene* 80: 523–527.
81. Mockenhaupt FP. (1995) Mefloquine resistance in *Plasmodium falciparum*. *Parasitology Today* 11: 248–253.
82. Noedl H, Se Y, Schaecher K, Smith BL, Socheat D and Fukuda MM. (2008) Evidence of artemisinin-resistant malaria in western Cambodia. *The New England Journal of Medicine* 359: 2619–2620.
83. Dondorp A, Nosten F, Yi P, Das D, Phyto A, Tarning J, et al. (2009) Artemisinin Resistance in *Plasmodium falciparum* Malaria. *The New England Journal of Medicine* 361: 455–467.
84. Witkowski B, Amaratunga C, Khim N, Sreng S, Chim P, Kim S, et al. (2013) Novel phenotypic assays for the detection of artemisinin-resistant *Plasmodium falciparum* malaria in Cambodia: in-vitro and ex-vivo drug-response studies. *The Lancet Infectious Diseases* 13: 1043-1049.
85. Ariey F, Witkowski B, Amaratunga C, Beghain J, Langlois A, Khim N, et al. (2014) A molecular marker of artemisinin-resistant *Plasmodium falciparum* malaria. *Nature* 505: 50-55.
86. WHO. (2016) Artemisinin and artemisinin-based combination therapy resistance.

World Health Organization, Geneva.

87. Price RN, Douglas NM and Anstey NM. (2009) New developments in *Plasmodium vivax* malaria: severe disease and the rise of chloroquine resistance. *Current Opinion in Infectious Diseases* 22: 430–435.
88. Baird JK. (2009) Resistance to therapies for infection by *Plasmodium vivax*. *Clinical Microbiology Reviews* 22: 508–534.
89. Miao M, Yang Z, Cui L, Ahlum J, Huang Y and Cui L. (2010) Different allele prevalence in the dihydrofolate reductase and dihydropteroate synthase genes in *Plasmodium vivax* populations from China. *The American Journal of Tropical Medicine and Hygiene* 83: 1206–1211.
90. Auliff A, Wilson DW, Russell B, Qi G, Chen N, Le NA, et al. (2006) Amino acid mutations in *Plasmodium vivax* DHFR and DHPS from several geographical regions and susceptibility to antifolate drugs. *The American Journal of Tropical Medicine and Hygiene* 75: 617–621.
91. Prajapati SK, Joshi H, Dev V and Dua VK. (2011) Molecular epidemiology of *Plasmodium vivax* anti-folate resistance in India. *Malaria Journal* 10: 102.
92. Barnadas C, Ratsimbaoa A, Ranaivosoa H, Ralaizandry D, Raveloariseheno D, Rabekotonorina V, et al. (2007) Short report: Prevalence and chloroquine sensitivity of *Plasmodium malariae* in Madagascar. *The American Journal of Tropical Medicine and Hygiene* 77: 1039–1042.
93. Daneshvar C, Davis TME, Cox-Singh J, Rafa'ee MZ, Zakaria SK, Divis PCS, et al. (2010) Clinical and parasitological response to oral chloroquine and primaquine in uncomplicated human *Plasmodium knowlesi* infections. *Malaria Journal* 9: 238.
94. Valderramos SG, Valderramos JC, Musset L, Purcell LA, Mercereau-Puijalon O, Legrand E, et al. (2010) Identification of a mutant PfCRT-mediated chloroquine tolerance phenotype in *Plasmodium falciparum*. *PLoS Pathogens* 6: 1–14.
95. Sá JM, Twu O, Hayton K, Reyes S, Fay MP, Ringwald P, et al. (2009) Geographic patterns of *Plasmodium falciparum* drug resistance distinguished by differential responses to amodiaquine and chloroquine. *Proceedings of the National Academy of Sciences of the United States of America* 106: 18883–9.
96. Bray, P. G., Howells, R. E., Ritchie, G. Y., Ward SA. (1992) Rapid Chloroquine Efflux Phenotype in Both Chloroquine-Sensitive and Chloroquine- Resistant *Plasmodium falciparum*. *Biochemical Pharmacology* 44: 1317–1324.
97. Martiney JA, Cerami A, Slater AFG and Science WK. (1995) Verapamil Reversal of

Chloroquine Resistance in the Malaria Parasite *Plasmodium falciparum* Is Specific for Resistant Parasites and Independent of the Weak Base Effect. *The Journal of Biological Chemistry* 270: 22393–22398.

98. Wellems TE, Walker-Jonah a and Panton LJ. (1991) Genetic mapping of the chloroquine-resistance locus on *Plasmodium falciparum* chromosome 7. *Proceedings of the National Academy of Sciences of the United States of America* 88: 3382–3386.

99. Menard D, Yapou F, Manirakiza A, Djalle D, Matsika-Claquin MD and Talarmin A. (2006) Polymorphisms in pfcrt, pfmdr1, dhfr genes and in vitro responses to antimalarials in *Plasmodium falciparum* isolates from Bangui, Central African Republic. *The American Journal of Tropical Medicine and Hygiene* 75: 381–387.

100. Fidock DA, Nomura T, Talley AK, Cooper RA, Dzekunov SM, Ferdig MT, et al. (2000) Mutations in the *P. falciparum* digestive vacuole transmembrane protein PfCRT and evidence for their role in chloroquine resistance. *Molecular Cell* 6: 861–871.

101. Djimdé A, Doumbo O, Cortese J, Kayentao K, Doumbo S, Diourté Y, et al. (2001) A molecular marker for chloroquine-resistant falciparum malaria. *The New England Journal of Medicine* 344: 257–263.

102. Duraisingh MT and Cowman AF. (2005) Contribution of the pfmdr1 gene to antimalarial drug-resistance. *Acta Tropica* 94: 181–190.

103. Babiker H, Pringle SJ, Abdel-Muhsin, Mackinnon M, Hunt P and Walliker D. (2001) High-level chloroquine resistance in Sudanese isolates of *Plasmodium falciparum* is associated with mutations in the chloroquine resistance transporter gene pfcrt and the multidrug resistance Gene pfmdr1. *The Journal of Infectious Diseases* 183: 1535–1538.

104. Flüeck TPF, Jelinek T, Kilian AHD, Adagu IS, Kabagambe G, Von Sonnenburg F, et al. (2000) Correlation of in vivo-resistance to chloroquine and allelic polymorphisms in *Plasmodium falciparum* isolates from Uganda. *Tropical Medicine and International Health* 5: 174–178.

105. Price RN, Cassar C, Brockman A, Duraisingh M, Van Vugt M, White NJ, et al. (1999) The pfmdr1 gene is associated with a multidrug-resistant phenotype in *Plasmodium falciparum* from the western border of Thailand. *Antimicrobial Agents and Chemotherapy* 43: 2943–2949.

106. Dorsey G, Kanya MR, Singh a and Rosenthal PJ. (2001) Polymorphisms in the *Plasmodium falciparum* pfcrt and pfmdr-1 genes and clinical response to chloroquine in Kampala, Uganda. *The Journal of Infectious Diseases* 183: 1417–1420.

107. Pillai DR, Labbe AC, Vanisaveth V, Hongvangthong B, Pomphida S, Inkathone S, et

- al. (2001) *Plasmodium falciparum* malaria in Laos: chloroquine treatment outcome and predictive value of molecular markers. *The Journal of Infectious Diseases* 183: 789–795.
108. Chaiyaroj SC, Buranakiti A, Angkasekwinai P, Looareesuwan S and Cowman AF. (1999) Analysis of mefloquine resistance and amplification of pfmdr1 in multidrug-resistant *Plasmodium falciparum* isolates from Thailand. *The American Journal of Tropical Medicine and Hygiene* 61: 780–783.
109. Cowman AF, Morry MJ, Biggs BA, Cross GAM and Foote SJ. (1988) Amino-Acid Changes Linked To Pyrimethamine Resistance in the Dihydrofolate-Reductase Thymidylate Synthase Gene of *Plasmodium falciparum*. *Proceedings of the National Academy of Sciences of the United States of America* 85: 9109–9113.
110. Peterson DS, Walliker D and Wellem TE. (1988) Evidence that a point mutation in dihydrofolate reductase-thymidylate synthase confers resistance to pyrimethamine in falciparum malaria. *Proceedings of the National Academy of Sciences of the United States of America* 85: 9114–9118.
111. Ekland EH and Fidock DA. (2007) Advances in understanding the genetic basis of antimalarial drug resistance. *Current Opinion in Microbiology* 10: 363–370.
112. Vinayak S, Alam M, Sem R, Shah N, Susanti A, Lim P, et al. (2010) Multiple Genetic Backgrounds of the Amplified *Plasmodium falciparum* Multidrug Resistance (pfmdr1) Gene and Selective Sweep of 184F Mutation in Cambodia Sumiti. *The Journal of Infectious Diseases* 201: 1551–1560.
113. Price R, Uhlemann A and Brockman A. (2004) Mefloquine resistance in *Plasmodium falciparum* and increased pfmdr1 gene copy number. *The Lancet* 364.:
114. Price RN, Uhlemann A-C, Van Vugt M, Brockman A, Hutagalung R, Nair S, et al. (2006) Molecular and pharmacological determinants of the therapeutic response to artemether-lumefantrine in multidrug-resistant *Plasmodium falciparum* malaria. *Clinical Infectious Diseases* 42: 1570–1577.
115. Miotto O, Almagro-Garcia J, Manske M, Macinnis B, Campino S, Rockett KA, et al. (2013) Multiple populations of artemisinin-resistant *Plasmodium falciparum* in Cambodia. *Nature Genetics* 45: 648–655.
116. Straimer J, Gnädig NF, Witkowski B, Amaratunga C, Duru V, Ramadani AP, et al. (2014) K13-propeller mutations confer artemisinin resistance in *Plasmodium falciparum* clinical isolates. *Science* 2624: 428–431.
117. Ménard D, Khim N, Beghain J, Adegnika A, Shafiul-Alam M, Amodu O, et al. (2016) A Worldwide Map of *Plasmodium falciparum* K13-Propeller Polymorphisms. *The New*

England Journal of Medicine 374: 2453–64.

118. Dogovski C, Xie SC, Burgio G, Bridgford J, Mok S, McCaw JM, et al. (2015) Targeting the Cell Stress Response of *Plasmodium falciparum* to Overcome Artemisinin Resistance. *PLoS Biology* 13: 1–26.

119. WHO. (2002) Monitoring Antimalarial Drug Resistance. *Report of a WHO consultation*. World Health Organization, Geneva.

WHO. (1965) Resistance of malaria parasites to drugs.

121. WHO. (1996) Assessment of therapeutic efficacy of antimalarial drugs for uncomplicated falciparum malaria in areas with intense transmission. World Health Organization, Geneva.

122. WHO. (2009) Methods for surveillance of antimalarial drug efficacy. World Health Organization, Geneva.

123. Stepniewska K, Taylor WRJ, Mayxay M, Price R, Smithuis F, Guthmann J, et al. (2004) In Vivo Assessment of Drug Efficacy against *Plasmodium falciparum* Malaria: Duration of Follow-Up. *Antimicrobial Agents and Chemotherapy* 48: 4271–4280.

124. Bass C. (1922) Some Observations on the Effect of Quinine upon the Growth of Malaria Plasmodia in Vitro. *The American journal of Tropical Medicine and Hygiene* 2: 289–292.

125. Rieckmann KH. (1971) Determination of the drug sensitivity of *Plasmodium falciparum*. *Journal of the American Medical Association* 217: 573–578.

126. Rieckmann KH and López Antuñaño FJ. (1971) Chloroquine resistance of *Plasmodium falciparum* in Brazil detected by a simple in vitro method. *Bulletin of the World Health Organization* 45: 157–167.

127. Bass C and Johns F. (1912) The cultivation of malarial plasmodia (*Plasmodium vivax* and *Plasmodium falciparum*) in vitro. *The Journal of Experimental Medicine* 16: 567–579.

128. Rieckmann K, Campbell G, Sax L and Mrema J. (1978) Drug sensitivity of *Plasmodium falciparum*. An in-vitro microtechnique. *The Lancet* 1: 22–23.

129. Wernsdorfer WH. (1980) Field evaluation of drug resistance in malaria. In vitro micro-test. *Acta Tropica* 37: 222–227.

130. Basco LK. (2007) Field application of in vitro assays for the sensitivity of human malaria parasites to antimalarial drugs. WHO Press, Geneva, Switzerland.

131. Chulay JD, Haynes JD and Diggs CL. (1983) *Plasmodium falciparum*: assessment of in vitro growth by [3H]hypoxanthine incorporation. *Experimental Parasitology* 55: 138–146.

132. Geary TG, Divo AA and Jensen JB. (1983) An in vitro assay system for the identification of potential antimalarial drugs. *The Journal of Parasitology* 69: 577–83.
133. Desjardins R, Canfield C, Haynes J and Chulay J. (1979) Quantitative Assessment of Antimalarial Activity In Vitro by a Semiautomated Microdilution Technique. *Antimicrobial Agents and Chemotherapy* 16: 710–718.
134. Smeijsters LJ, Zijlstra NM, Franssen FF and Overdulve JP. (1996) Simple, fast, and accurate fluorometric method to determine drug susceptibility of *Plasmodium falciparum* in 24-well suspension cultures. *Antimicrobial agents and chemotherapy* 40: 835–8.
135. Saito-Ito a, Akai Y, He S, Kimura M and Kawabata M. (2001) A rapid, simple and sensitive flow cytometric system for detection of *Plasmodium falciparum*. *Parasitology international* 50: 249–57.
136. Bennett TN, Paguio M, Gligorijevic B, Seudieu C, Kosar AD, Davidson E, et al. (2004) Novel , Rapid , and Inexpensive Cell-Based Quantification of Antimalarial Drug Efficacy. *Society* 48: 1807–1810.
137. Smilkstein M, Sriwilaijaroen N, Kelly JX, Wilairat P and Riscoe M. (2004) Simple and Inexpensive Fluorescence-Based Technique for High-Throughput Antimalarial Drug Screening. *Society* 48: 1803–1806.
138. Noedl H, Wernsdorfer WH, Miller RS and Wongsrichanalai C. (2002) Histidine-Rich Protein II: a Novel Approach to Malaria Drug Sensitivity Testing. *Antimicrobial Agents and Chemotherapy* 46: 1658–1664.
139. Desakorn V, Silamut K, Angus B, Sahassananda D, Chotivanich K, Suntharasamai P, et al. (1997) Semi-quantitative blood and plasma measurement of *Plasmodium falciparum* antigen PfHRP2 in blood and plasma. *Transactions of the Royal Society of Tropical Medicine and Hygiene* 91: 479–483.
140. Noedl H, Wongsrichanalai C, Miller RS, Myint KSA, Looareesuwan S, Sukthana Y, et al. (2002) *Plasmodium falciparum*: Effect of anti-malarial drugs on the production and secretion characteristics of histidine-rich protein II. *Experimental Parasitology* 102: 157–163.
141. Noedl H, Bronnert J, Yingyuen K, Kollaritsch H, Fukuda M and Attlmayr B. (2005) Simple Histidine-Rich Protein 2 Double-Site Sandwich Enzyme-Linked Immunosorbent Assay for Use in Malaria Drug Sensitivity Testing. *Antimicrobial Agents and Chemotherapy* 49: 3575-7.
142. Makler M and Hinrichs D. (1993) Measurement of the lactate dehydrogenase activity of *Plasmodium falciparum* as an assessment of parasitemia. *The American Journal*

of *Tropical Medicine and Hygiene* 48: 205–210.

143. Basco L, Marquet F, Makler M and Le Bras J. (1995) *Plasmodium falciparum* and *Plasmodium vivax*: Lactate dehydrogenase activity and its application for in vitro drug susceptibility assay. *Experimental Parasitology* 80: 260-271.

144. Noedl H. (2003) Malaria drug-sensitivity testing: new assays, new perspectives. *Trends in Parasitology* 19: 175–181.

145. Hare JD. (1986) Two-color flow-cytometric analysis of the growth cycle of *Plasmodium falciparum* in vitro: identification of cell cycle compartments. *Journal of Histochemistry & Cytochemistry* 34: 1651–1658.

146. Janse CJ, van Vianen PH, Tanke HJ, Mons B, Ponnudurai T and Overdulve JP. (1987) *Plasmodium* species: flow cytometry and microfluorometry assessments of DNA content and synthesis. *Experimental Parasitology* 64: 88–94.

147. Jiménez-Díaz MB, Rullas J, Mulet T, Fernández L, Bravo C, Gargallo-Viola D, et al. (2005) Improvement of detection specificity of *Plasmodium*-infected murine erythrocytes by flow cytometry using autofluorescence and YOYO-1. *Cytometry A* 67: 27–36.

148. Grimberg BT, Erickson JJ, Sramkoski RM, Jacobberger JW and Zimmerman P a. (2008) Monitoring *Plasmodium falciparum* growth and development by UV flow cytometry using an optimized Hoechst-thiazole orange staining strategy. *Cytometry A* 73: 546–54.

149. Malleret B, Claser C, Ong ASM, Suwanarusk R, Sriprawat K, Howland SW, et al. (2011) A rapid and robust tri-color flow cytometry assay for monitoring malaria parasite development. *Scientific Reports* 1: 118.

150. Apte SH, Groves PL, Roddick JS, P da Hora V and Doolan DL. (2011) High-throughput multi-parameter flow-cytometric analysis from micro-quantities of *Plasmodium*-infected blood. *International Journal for Parasitology* 41: 1285–1294.

151. Russell B, Malleret B, Suwanarusk R, Anthony C, Kanlaya S, Lau YL, et al. (2013) Field-based flow cytometry for ex vivo characterization of *Plasmodium vivax* and *P. falciparum* antimalarial sensitivity. *Antimicrobial Agents and Chemotherapy* 57: 5170–5174.

152. Wirjanata G, Handayuni I, Prayoga P, Apriyanti D, Chalfein F, Sebayang BF, et al. (2015) Quantification of *Plasmodium* ex vivo drug susceptibility by flow cytometry. *Malaria Journal* 14: 417.

153. Grimberg BT. (2011) Methodology and application of flow cytometry for investigation of human malaria parasites. *Journal of Immunological Methods* 367: 1–16.

154. Shapiro HM, Apte SH, Chojnowski GM, Hänscheid T, Rebelo M and Grimberg BT. (2013) Cytometry in malaria-A practical replacement for microscopy? *Current Protocols in Cytometry* 1–23.
155. Amaratunga C, Neal AT and Fairhurst RM. (2014) Flow cytometry-based analysis of artemisinin-resistant *Plasmodium falciparum* in the ring-stage survival assay. *Antimicrobial Agents and Chemotherapy* 58: 4938–4940.
156. Lelliott PM, Lampkin S, McMorran BJ, Foote SJ and Burgio G. (2014) A flow cytometric assay to quantify invasion of red blood cells by rodent *Plasmodium* parasites in vivo. *Malaria Journal* 13: 100.
157. Izumiyama S, Omura M, Takasaki T, Ohmae H and Asahi H. (2009) *Plasmodium falciparum*: Development and validation of a measure of intraerythrocytic growth using SYBR Green I in a flow cytometer. *Experimental Parasitology* 121: 144–150.
158. Staaloe T, Giha HA, Dodoo D, Theander TG and Hviid L. (1999) Detection of Antibodies to Variant Antigens on. *The Lancet* 336: 329–336.
- 159 Persson KEM, Lee CT, Marsh K and Beeson JG. (2006) Development and Optimization of High-Throughput Methods To Measure *Plasmodium falciparum* -Specific Growth Inhibitory Antibodies *Journal of Clinical Microbiology* 44: 1665–1673.
160. van der Heyde HC, Elloso MM, vande Waa J, Schell K and Weidanz WP. (1995) Use of hydroethidine and flow cytometry to assess the effects of leukocytes on the malarial parasite *Plasmodium falciparum*. *Clinical and Diagnostic Laboratory Immunology* 2: 417–25.
161. Dent AE, Bergmann-Leitner ES, Wilson DW, Tisch DJ, Kimmel R, Vulule J, et al. (2008) Antibody-mediated growth inhibition of *Plasmodium falciparum*: relationship to age and protection from parasitemia in Kenyan children and adults. *PloS One* 3: e3557.
- 162 Pattanapanyasat K, Thaithong S, Kyle DE, Udomsangpetch R, Yongvanitchit K, Hider RC, et al. (1997) Flow cytometric assessment of hydroxypyridinone iron chelators on in vitro growth of drug-resistant malaria. *Cytometry* 27: 84–91.
163. Dahl EL and Rosenthal PJ. (2007) Multiple antibiotics exert delayed effects against the *Plasmodium falciparum* apicoplast. *Antimicrobial Agents and Chemotherapy* 51: 3485–3490.
164. Jiménez-Díaz MB, Mulet T, Gómez V, Viera S, Alvarez A, Garuti H, et al. (2009) Quantitative measurement of *Plasmodium*-infected erythrocytes in murine models of malaria by flow cytometry using bidimensional assessment of SYTO-16 fluorescence. *Cytometry. Part A* :75: 225–35.

165. Fu Y, Tilley L, Kenny S and Klonis N. (2010) Dual labeling with a far red probe permits analysis of growth and oxidative stress in *P. falciparum*-infected erythrocytes. *Cytometry. Part A* 77: 253–263.
166. Karl S, Wong RP, St Pierre TG and Davis TM. (2009) A comparative study of a flow-cytometry-based assessment of in vitro *Plasmodium falciparum* drug sensitivity. *Malaria Journal* 8: 294.
167. Li Q, Gerena L, Xie L, Zhang J, Kyle D and Milhous W. (2007) Development and Validation of Flow Cytometric Measurement for Parasitemia in Cultures of *P. falciparum* Vitrally Stained with YOYO-1. *Cytometry. Part A* 71A: 297–307.
168. Angulo-Barturen I, Jiménez-Díaz MB, Mulet T, Rullas J, Herreros E, Ferrer S, et al. (2008) A murine model of falciparum-malaria by in vivo selection of competent strains in non-myelodepleted mice engrafted with human erythrocytes. *PLoS One* 3: e2252.
169. Chandramohanadas R, Chandramohanadas R, Davis PH, Beiting DP, Harbut MB, Roos DS, et al. (2009) Corrections and Clarifications: Apicomplexan Parasites Co-Opt Host Calpains to Facilitate Their Escape from Infected Cells. *Science* 324: 794–797
170. Makler M, Lee L and Recktenwald D. (1987) Thiazole Orange: A New Dye for Plasmodium Species Analysis. *Cytometry* 8: 568–570.
171. Jouin H, Daher W, Khalife J, Ricard I, Puijalon OM, Capron M, et al. (2004) Double staining of Plasmodium falciparum nucleic acids with hydroethidine and thiazole orange for cell cycle stage analysis by flow cytometry. *Cytometry. Part A* 57: 34–38.
172. Grimberg BT, Jaworska MM, Hough LB, Zimmerman P a and Phillips JG. (2009) Addressing the malaria drug resistance challenge using flow cytometry to discover new antimalarials. *Bioorganic & Medicinal Chemistry Letters* 19: 5452–5457.
173. Malleret B, Claser C, Ong ASM, Suwanarusk R, Sriprawat K, Howland SW, et al. (2011) A rapid and robust tri-color flow cytometry assay for monitoring malaria parasite development. *Scientific Reports* 1: 1–10.
174. Rebelo M, Sousa C, Shapiro HM, Mota MM, Grobusch MP and Hänscheid T. (2013) A Novel Flow Cytometric Hemozoin Detection Assay for Real-Time Sensitivity Testing of *Plasmodium falciparum*. *PLoS One* 8: e61606.
175. Aunpad R, Somsri S, Na-Bangchang K, Udomsangpetch R, Mungthin M, Adisakwattana P, et al. (2009) The effect of mimicking febrile temperature and drug stress on malarial development. *Annals of Clinical Microbiology and Antimicrobials* 8: 19.
176. Lim P, Wongsrichanalai C, Chim P, Khim N, Kim S, Chy S, et al. (2010) Decreased in vitro susceptibility of *Plasmodium falciparum* isolates to artesunate, mefloquine,

chloroquine, and quinine in Cambodia from 2001 to 2007. *Antimicrobial Agents and Chemotherapy* 54: 2135–2142.

177. Chong CR and Sullivan DJ. (2003) Inhibition of heme crystal growth by antimalarials and other compounds: Implications for drug discovery. *Biochemical Pharmacology* 66: 2201–2212.

178. Vivas L, Rattray L, Stewart LB, Robinson BL, Fugmann B, Haynes RK, et al. (2007) Antimalarial efficacy and drug interactions of the novel semi-synthetic endoperoxide artemisone in vitro and in vivo. *Journal of Antimicrobial Chemotherapy* 59: 658–665.

179. Bacon DJ, Latour C, Lucas C, Colina O, Ringwald P and Picot S. (2007) Comparison of a SYBR green I-based assay with a histidine-rich protein II enzyme-linked immunosorbent assay for in vitro antimalarial drug efficacy testing and application to clinical isolates. *Antimicrobial Agents and Chemotherapy* 51: 1172–1178.

180. Duraisingh MT, Roper C, Walliker D and Warhurst DC. (2000) Increased sensitivity to the antimalarials mefloquine and artemisinin is conferred by mutations in the *pfmdr1* gene of *Plasmodium falciparum*. *Molecular Microbiology* 36: 955–961.

181. Wisedpanichkij R, Chaijaroenkul W, Sangsuwan P, Tantisawat J, Boonprasert K and Na-Bangchang K. (2009) In vitro antimalarial interactions between mefloquine and cytochrome P450 inhibitors. *Acta Tropica* 112: 12–15.

182. Plouffe D, Brinker A, McNamara C, Henson K, Kato N, Kuhlen K, et al. (2008) In silico activity profiling reveals the mechanism of action of antimalarials discovered in a high-throughput screen. *Proceedings of the National Academy of Sciences of the United States of America* 105: 9059–9064.

183. Wang Z, Parker D, Meng H, Wu L, Li J, Zhao Z, et al. (2012) In vitro sensitivity of *Plasmodium falciparum* from China-Myanmar border area to major ACT drugs and polymorphisms in potential target genes. *PLoS One* 7: e30927.

184. Reynolds JM, El Bissati K, Brandenburg J, Günzl A and Mamoun C Ben. (2007) Antimalarial activity of the anticancer and proteasome inhibitor bortezomib and its analog ZL3B. *BMC Clinical Pharmacology* 7: 13.

185. Wein S, Maynadier M, Tran Van Ba C, Cerdan R, Peyrottes S, Fraisse L, et al. (2010) Reliability of antimalarial sensitivity tests depends on drug mechanisms of action. *Journal of Clinical Microbiology* 48: 1651–1660.

186. Wong RPM, Karunajeewa H, Mueller I, Siba P, Zimmerman P a and Davis TME. (2011) Molecular Assessment of *Plasmodium falciparum* Resistance to Antimalarial Drugs in Papua New Guinea Using an Extended Ligase Detection Reaction Fluorescent

- Microsphere Assay. *Antimicrobial Agents and Chemotherapy* 55: 798–805.
187. Ramalhete C, Lopes D, Mulhovo S, Molnár J, Rosário VE and Ferreira M-JU. (2010) New antimalarials with a triterpenic scaffold from *Momordica balsamina*. *Bioorganic & Medicinal Chemistry* 18: 5254–5260.
188. He Z, Chen L, You J, Qin L and Chen X. (2010) In vitro interactions between antiretroviral protease inhibitors and artemisinin endoperoxides against *Plasmodium falciparum*. *International Journal of Antimicrobial Agents* 35: 191–193.
189. Johnson JD, Denuff R a, Gerena L, Lopez-Sanchez M, Roncal NE and Waters NC. (2007) Assessment and continued validation of the malaria SYBR green I-based fluorescence assay for use in malaria drug screening. *Antimicrobial Agents and Chemotherapy* 51: 1926–1933.
190. Baniecki ML, Wirth DF and Clardy J. (2007) High-throughput *Plasmodium falciparum* growth assay for malaria drug discovery. *Antimicrobial Agents and Chemotherapy* 51: 716–723.
191. Held J, Soomro S a, Kremsner PG, Jansen FH and Mordmüller B. (2011) In vitro activity of new artemisinin derivatives against *Plasmodium falciparum* clinical isolates from Gabon. *International Journal of Antimicrobial Agents* 37: 485–488.
192. Trager W and Jensen JB. (1976) Human malaria parasites in continuous culture. *Science*.193: 673–5.
193. Moll K, Ljungström I, Perlmann H, Scherf A and Wahlgren M. (2013) *Methods in Malaria Research* 6th edition, Manassas.
194. Schuster FL. (2002) Cultivation of *Plasmodium* spp. *Clinical Microbiology Reviews* 15: 355–364.
195. Kim Y-A, Cha J-E, Ahn S-Y, Ryu S-H, Yeom J-S, Lee H-I, et al. (2007) *Plasmodium falciparum* Cultivation Using the Petri Dish: Revisiting the Effect of the “Age” of Erythrocytes and the Interval of Medium Change. *Journal of Korean Medical Science* 22: 1022.
196. Basco LK. (2004) Molecular epidemiology of malaria in cameroon. XX. Experimental studies on various factors of in vitro drug sensitivity assays using fresh isolates of *Plasmodium falciparum*. *The American Journal of Tropical Medicine and Hygiene* 80: 260-271.
197. Gluzman IY, Schlesinger PH and Krogstad DJ. (1987) Inoculum effect with chloroquine and *Plasmodium falciparum*. *Antimicrobial Agents and Chemotherapy* 31: 32–36.

198. Duraisingh MT, Jones P, Sambou I, von Seidlein L, Pinder M and Warhurst DC. (1999) Inoculum effect leads to overestimation of in vitro resistance for artemisinin derivatives and standard antimalarials: a Gambian field study. *Parasitology* 119: 435–440.
199. Capps T and Jensen J. (1983) Storage Requirements for Erythrocytes Used to Culture *Plasmodium falciparum*. *Journal of Parasitology* 69: 158–162.
200. Lim P, Chim P, Sem R, Nemh S, Poravuth Y, Lim C, et al. (2005) In vitro monitoring of *Plasmodium falciparum* susceptibility to artesunate, mefloquine, quinine and chloroquine in Cambodia: 2001-2002. *Acta Tropica* 93: 31–40.
201. Kaddouri H, Nakache S, Houzé S, Mentré F and Le Bras J. (2006) Assessment of the drug susceptibility of *Plasmodium falciparum* clinical isolates from africa by using a Plasmodium lactate dehydrogenase immunodetection assay and an inhibitory maximum effect model for precise measurement of the 50-percent inhibitory conc. *Antimicrobial Agents and Chemotherapy* 50: 3343–9.
202. Rason MA, Randriantsoa T, Andrianantenaina H, Ratsimbaoa A and Menard D. (2008) Performance and reliability of the SYBR Green I based assay for the routine monitoring of susceptibility of *Plasmodium falciparum* clinical isolates. *Transactions of the Royal Society of Tropical Medicine and Hygiene* 102: 346–51.
203. Legrand E, Volney B, Meynard J-B, Mercereau-Puijalon O and Esterre P. (2008) In vitro monitoring of Plasmodium falciparum drug resistance in French Guiana: a synopsis of continuous assessment from 1994 to 2005. *Antimicrobial Agents and Chemotherapy* 52: 288–298.
204. van Schalkwyk D a, Burrow R, Henriques G, Gadalla NB, Beshir KB, Hasford C, et al. (2013) Culture-adapted Plasmodium falciparum isolates from UK travellers: in vitro drug sensitivity, clonality and drug resistance markers. *Malaria Journal* 12: 320.
205. Boyle M, Wilson D, Richards J, Riglar D, Tetteh K, Conway D, et al. (2010) Isolation of viable Plasmodium falciparum merozoites to define erythrocyte invasion events and advance vaccine and drug development. *Proceedings of the National Academy of Sciences of the United States of America* 107: 14378–14383.
206. Basco LK. (2003) Molecular epidemiology of malaria in Cameroon . XV. Experimental studies on serum substitutes and supplements and alternative culture media for in vitro drug sensitivity assays using fresh isolates of *Plasmodium falciparum*. *The American Journal of Tropical Medicine and Hygiene* 69: 168–173.
207. Ringwald P, Meche FS, Bickii J and Basco LK. (1999) In Vitro Culture and Drug Sensitivity Assay of *Plasmodium falciparum* with Nonserum Substitute and Acute-Phase

- Sera. *Journal of Clinical Microbiology* 37: 700–705.
208. He S, Saito-Ito A, Tanabe K and Matsumura T. (2000) *Plasmodium falciparum*: Effective Use of the CO₂-NaHCO₃ Buffer System for Evaluating Chloroquine Resistance. *Experimental Parasitology* 94: 121–124.
209. Lambros C and Vanderberg JP. (1979) Synchronization of *Plasmodium falciparum* erythrocytic stages in culture. *Journal of Parasitology* 65: 418–420.
210. Rivadeneira EM, Wasserman M and Espinal CT. (1983) Separation and concentration of schizonts of *Plasmodium falciparum* by Percoll gradients. *The Journal of Protozoology* 30: 367–370.
211. Kim CC, Wilson EB and DeRisi JL. (2010) Improved methods for magnetic purification of malaria parasites and haemozoin. *Malaria Journal* 9: 17.
212. Spadafora C, Gerena L and Kopydlowski KM. (2011) Comparison of the in vitro invasive capabilities of *Plasmodium falciparum* schizonts isolated by Percoll gradient or using magnetic based separation. *Malaria Journal* 10: 96.
213. Kobayashi K and Kato K. (2015) A synchronization method using heparin for the in vitro culture of *Plasmodium falciparum*. *Parasitology International* 65: 549–551.
214. Ridley R. (1996) Haemozoin formation in malaria parasites: is there a haem polymerase? *Trends in Microbiology* 4: 253–254.
215. Krugliak M, Zhang J and Ginsburg H. (2002) Intraerythrocytic *Plasmodium falciparum* utilizes only a fraction of the amino acids derived from the digestion of host cell cytosol for the biosynthesis of its proteins. *Molecular and Biochemical Parasitology* 119: 249–256.
216. Francis SE, Sullivan DJJ and Glodberg DE. (1997) Hemoglobin metabolism in the malaria parasite *Plasmodium falciparum*. *Annual Review of Microbiology* 51: 97–123.
217. Hänscheid T, Egan TJ and Grobusch MP. (2007) Haemozoin: from melatonin pigment to drug target, diagnostic tool, and immune modulator. *The Lancet Infectious Diseases* 7: 675–685.
218. Chen MM, Shi L and Sullivan DJ. (2001) Haemoproteus and Schistosoma synthesize heme polymers similar to Plasmodium hemozoin and beta-hematin. *Molecular and Biochemical Parasitology* 113: 1–8.
219. Oliveira MF, Kycia SW, Gomez A, Kosar AJ, Bohle DS, Hempelmann E, et al. (2005) Structural and morphological characterization of hemozoin produced by *Schistosoma mansoni* and *Rhodnius prolixus*. *FEBS Letters* 579: 6010–6016.
220. Egan TJ, Hempelmann E and Mavuso WW. (1999) Characterisation of synthetic β -

haematin and effects of the antimalarial drugs quinidine, halofantrine, desbutylhalofantrine and mefloquine on its formation. *Journal of Inorganic Biochemistry* 73: 101–107.

221. Ziegler J, Linck R and Wright DW. (2001) Heme aggregation inhibitors: Antimalarial drugs targeting an essential biomineralization process. *Studies in Natural Products Chemistry* 25: 327–366.

222. Egan TJ, Mavuso WW and Ncokazi KK. (2001) The mechanism of β -haematin formation in acetate solution. Parallels between hemozoin formation and biomineralization processes. *Biochemistry* 40: 204–213.

223. Hempelmann E and J. Egan T. (2002) Pigment biocrystallization in *Plasmodium falciparum*. *Trends in Parasitology* 18: 11.

224. Sullivan Jr D, Gluzman I and Goldberg D. (1996) Plasmodium Hemozoin Formation Mediated by Histidine-Rich Proteins. *Science* 271: 219–22.

225. Sullivan Jr D. (2002) Theories on malarial pigment formation and quinoline action. *International Journal for Parasitology* 32: 1645–1653.

226. Papalexis V, Siomos M, Campanale N and Guo X. (2001) Histidine-rich protein 2 of the malaria parasite, *Plasmodium falciparum*, is involved in detoxification of the by-products of haemoglobin degradation. *Molecular and Biochemical Parasitology* 115: 77–86.

227. Fitch CD, Cai GZ, Chen YF and Shoemaker JD. (1999) Involvement of lipids in ferriprotoporphyrin IX polymerization in malaria. *Biochimica et Biophysica Acta* 1454: 31–37.

228. Jackson KE, Klonis N, Ferguson DJP, Adisa A, Dogovski C and Tilley L. (2004) Food vacuole-associated lipid bodies and heterogeneous lipid environments in the malaria parasite, *Plasmodium falciparum*. *Molecular Microbiology* 54: 109–122.

229. Egan TJ, Chen JY-J, de Villiers K a, Mabothe TE, Naidoo KJ, Ncokazi KK, et al. (2006) Haemozoin (beta-haematin) biomineralization occurs by self-assembly near the lipid/water interface. *FEBS letters* 580: 5105–5110.

230. Pisciotta JM, Coppens I, Tripathi AK, Scholl PF, Shuman J, Bajad S, et al. (2007) The role of neutral lipid nanospheres in *Plasmodium falciparum* haem crystallization. *The Biochemical Journal* 402: 197–204.

231. Jani D, Nagarkatti R, Beatty W, Angel R, Slebodnick C, Andersen J, et al. (2008) HDP - A novel heme detoxification protein from the malaria parasite. *PLoS Pathogens* 4: e1000053.

232. Jamjoom GA. (1983) Dark-field microscopy for detection of malaria in unstained

- blood films. *Journal of Clinical Microbiology* 17: 717–721.
233. Lawrence C and Olson JA. (1986) Birefringent hemozoin identifies malaria. *American Journal of Clinical Pathology* 86: 360–363.
234. Hänscheid T, Valadas E and Grobusch MP. (2000) Pigment Detection. *Parasitology* 4758: 2000–2002.
235. Newman DM, Heptinstall J, Matelon RJ, Savage L, Wears ML, Beddow J, et al. (2008) A magneto-optic route toward the in vivo diagnosis of malaria: preliminary results and preclinical trial data. *Biophysical Journal* 95: 994–1000.
236. Butykai A, Orbán A, Kocsis V, Szaller D, Bordács S, Tátrai-Szekeres E, et al. (2013) Malaria pigment crystals as magnetic micro-rotors: key for high-sensitivity diagnosis. *Scientific Reports* 3: 1431.
237. Mens PF, Matelon RJ, Nour BYM, Newman DM and Schallig HDFH. (2010) Laboratory evaluation on the sensitivity and specificity of a novel and rapid detection method for malaria diagnosis based on magneto-optical technology (MOT). *Malaria Journal* 9: 207.
238. Rieckmann KH. (1985) Visual in-vitro test for determining the drug sensitivity of *Plasmodium falciparum*. *The Lancet* 1: 1333–1335.
239. Russell B, Malleret B, Suwanarusk R, Anthony C, Kanlaya S, Lau YL, et al. (2013) Field-based flow cytometry for ex vivo characterization of *Plasmodium vivax* and *P. falciparum* antimalarial sensitivity. *Antimicrobial Agents and Chemotherapy* 57: 5170–4.
240. Hänscheid T, Pinto BG, Cristino JM and Grobusch MP. (2000) Malaria diagnosis with the haematology analyser Cell-Dyn 3500: What does the instrument detect? *Clinical and Laboratory Haematology* 22: 259–61.
241. Grobusch MP, Hänscheid T, Krämer B, Neukammer J, May J, Seybold J, et al. (2003) Sensitivity of hemozoin detection by automated flow cytometry in non- and semi-immune malaria patients. *Cytometry B* 55: 46–51.
242. Hänscheid T, Melo-Cristino J and Pinto BG. (2001) Automated detection of malaria pigment in white blood cells for the diagnosis of malaria in Portugal. *The American Journal of Tropical Medicine and Hygiene* 64: 290–292.
243. Frita R, Rebelo M, Pamplona A, Vigarío AM, Mota MM, Grobusch MP, et al. (2011) Simple flow cytometric detection of haemozoin containing leukocytes and erythrocytes for research on diagnosis, immunology and drug sensitivity testing. *Malaria Journal* 10: 74.
244. de Grooth B, Terstappen L, Puppels G and Greve J. (1987) Light-scattering polarization measurements as a new parameter in flow cytometry. *Cytometry* 8: 539–544.

245. Mendelow B V, Lyons C, Nhlangothi P, Tana M, Munster M, Wypkema E, et al. (1999) Automated malaria detection by depolarization of laser light. *British Journal of Haematology* 104: 499–503.
246. Campuzano-Zuluaga G, Hänscheid T and Grobusch MP. (2010) Automated haematology analysis to diagnose malaria. *Malaria Journal* 9: 346.
247. Suh IB, Kim HJ, Kim JY, Lee SW, An SSA, Kim WJ, et al. (2003) Evaluation of the Abbott Cell-Dyn 4000 hematology analyzer for detection and therapeutic monitoring of *Plasmodium vivax* in the Republic of Korea. *Tropical Medicine and International Health* 8: 1074–1081.

CHAPTER II

FLOW CYTOMETRIC DETECTION OF HEMOZOIN

This chapter is published in;

Rebello M, Tempera C, Bispo C, Andrade C, Gardner R, Shapiro HM and Hänscheid T. (2015) Light depolarization measurements in malaria: A new job for an old friend. *Cytometry A* 87:437-45.

Author's contributions:

TH and HMS initiated and ensured follow-up of the project. MR, TH and HMS wrote the manuscript. MR conducted the majority of the experiments. MR and CT performed the measurements with different types of hemozoin, flow cytometric analysis and culture related work. RG, CB and CA performed the sorting experiments, tested the different wavelengths and also revised the manuscript.

1. Abstract

The use of flow cytometry in malaria research has increased over the last decade. Most approaches use nucleic acid stains to detect parasite DNA and RNA and require complex multi-color, multi-parameter analysis to reliably detect infected red blood cells (iRBCs). We recently described a novel and simpler approach to parasite detection based on flow cytometric measurement of scattered light depolarization caused by hemozoin (Hz), a pigment formed by parasite digestion of hemoglobin in iRBCs. Depolarization measurement by flow cytometry was described in 1987; however, patent issues restricted its use to a single manufacturer's hematology analyzers until 2009.

Although we recently demonstrated that depolarization measurement of Hz, easily implemented on a bench top flow cytometer (Cyflow), provided useful information for malaria work, doubts regarding its application and utility remain in both the flow cytometry and malaria communities, at least in part because instrument manufacturers do not offer the option of measuring depolarized scatter. Under such circumstances, providing other researchers with guidance as to how to do this seemed to offer the most expeditious way to resolve the issue.

We accordingly examined how several commercially available flow cytometers (CyFlow SL, MoFLo, Attune and Accuri C6) could be modified to detect depolarization due to the presence of free Hz on solution, or of Hz in leukocytes or erythrocytes Hz from rodent or human blood. All were readily adapted, with substantially equivalent results obtained with lasers emitting over a wide wavelength range. Other instruments now available may also be modifiable for Hz measurement.

Cytometric detection of Hz using depolarization is useful to study different aspects of malaria. Adding additional parameters, such as DNA content and base composition and RNA content, can demonstrably provide improved accuracy and sensitivity of parasite detection and characterization, allowing malaria researchers and eventually clinicians to benefit from cytometric technology.

Keywords: polarization, depolarized side scatter, hemozoin, flow cytometry, malaria, and light depolarization.

2. Introduction

Malaria remains one of the most important parasitic diseases, killing around 700,000 people each year [1]. Reliable detection of parasites and identification of the species are crucial for clinical diagnosis, as well as for many research applications. Both may require differentiation of asexual and sexual forms, determination of different maturation stages, and reliable quantification of parasite density (numbers per unit volume of blood or percentage of infected red blood cells). Antimalarial drug development and assessment of resistance to drugs may additionally require evaluation of parasite metabolic state and viability. Cytometry could potentially provide an alternative to microscopy of Giemsa stained smear [2], the accepted method for diagnosis for over a century.

Malaria parasites growing inside infected erythrocytes (iRBCs) catabolize hemoglobin, producing the strongly absorbing and birefringent pigment hemozoin (Hz). Once the parasite completes its growth cycle in the iRBC, Hz is released and, subsequently ingested by peripheral blood phagocytes [3]. The presence and form of Hz in iRBCs are useful characteristics for distinguishing various species and developmental stages; observation of Hz, known to be associated with malaria, in cells in unstained blood led Alphonse Laveran to the initial discovery of malaria parasites in 1880 [3]. Staining came later.

In addition to strongly absorbing light at wavelengths between 300 and 700 nm, Hz is able to depolarize light and can, as has long been known, be detected by optical methods such as dark-field microscopy [4 – 7] or depolarization microscopy [8, 9]. In the latter, crossed polarizing filters are inserted in the illumination and observation paths of a microscope and bright spots indicate the presence of Hz.

By 1987, it had been shown that flow cytometry of DNA and RNA content of iRBCs could differentiate stages and, in some cases, species [10, 11]. Flow cytometry has since been used to study parasite physiology and response to antimalarial drugs [12 – 17]. This is most often done using fluorescent DNA and RNA stains and complex multi-color, multi-parameter analysis (2, 18); additional maturation/viability markers may also be measured [17, 19].

Also in 1987, it was reported that depolarized light scatter could also be detected by flow cytometry; this was initially recognized as providing a simple, reagent-free means to distinguish eosinophil from neutrophil leukocytes based on the birefringence of eosinophil granules [20]. A patent (US, Patent: 5017497: <http://www.google.com/patents/US5017497> accessed on 01/08/2014) on the procedure was licensed by Abbott Diagnostics (Santa Clara, CA) and used in their Cell-Dyn hematology analyzers; the patent also prevented

manufacturers of research flow cytometers from offering the measurement in their apparatus.

In 1999, it was found that Hz-containing monocytes in the blood of malaria patients could be detected by the Cell-Dyn analyzers [21]. Since then, several other studies have reported the detection of Hz inside monocytes and neutrophils with both those instruments and user-modified research flow cytometers [22 – 25], and the use of hematology analyzers to diagnose malaria in non-endemic and endemic countries has been extensively reviewed elsewhere [26]. Of note, some of these studies reported the possibility of detecting Hz in iRBCs as well [22, 27].

With the patent no longer in force, we recently implemented depolarized scatter measurement on a bench top flow cytometer (Cyflow SL, Partec/Sysmex). This permitted comparing cytometric detection of Hz-containing leukocytes using this cytometer and the Cell-Dyn instrument with microscopy [28, 29]. More importantly, it confirmed that Hz inside iRBCs could be detected, leading to further studies [30 – 31].

Although this work attracted some interest in both the malaria and the flow cytometry communities, questions remained as to whether and how readily depolarized scatter measurements could be easily installed and measured on other common instruments, what kind of Hz can be detected (e.g. free Hz, intraleukocytic Hz, intraerythrocytic Hz from rodent or human parasites), and to what extent aspects of instrument setup, e.g., the laser wavelengths, might interfere with measurements. Addressing these issues, we have now shown that light depolarization caused by Hz from different sources can be easily detected in a variety of flow cytometers. We hope that this will encourage malaria researchers and clinicians to make productive use of the technique.

3. Material and Methods

Samples

Free synthetic Hz, *Plasmodium berghei* (rodent) and *Plasmodium falciparum* (human) infected RBC, as well as Hz containing human peripheral blood mononucleated cells (PBMCs) were analyzed (Table II.1).

P. falciparum infected red blood cells were fixed with 2% paraformaldehyde (PFA) and stained with SYBR green I at 1x (Invitrogen, Carlsbad, USA).

Table II.1: Samples and protocols used for preparation of samples

Samples	Protocol
<i>Plasmodium berghei</i> infected red blood cells [30]	BALB/c mice (Charles River, Spain) were infected with the transgenic <i>P. berghei</i> ANKA (259 cl2) that constitutively expresses GFP during the whole life cycle. Blood samples were collected by cardiac puncture into a heparinized collection tube, as described elsewhere.
<i>Plasmodium falciparum</i> infected red blood cells [32]	<i>P. falciparum</i> 3D7 strain was obtained from MR4 (ATCC, Manassas, VA) and kept in continuous culture according to the recommendations of the Malaria Research and Reference Reagent Resource Center (MR4) and as previously described elsewhere [32]. Cultures were maintained at 5% hematocrit, at 37°C in an atmosphere of 5% CO ₂ .
Intraleukocytic hemozoin [30, 33]	Human peripheral blood mononucleated cells (PBMCs) were incubated with synthetic Hz, as described elsewhere [30]. Briefly, PBMCs were isolated from blood collected from healthy volunteers and placed in a Ficoll gradient (Ficoll-Paque Plus, GE Healthcare, Uppsala, Sweden), where the interface containing the PBMCs was collected after centrifugation. PBMCs were washed, counted and resuspended at a concentration of 5×10^5 PBMC/ml. Synthetic Hz (obtained as explained below) was added at 50 μ M (hme equivalent) and the plate was incubated for 6 hours at 37°C in 5% CO ₂ [33].
Synthetic hemozoin [64, 65]	Synthetic hemozoin was obtained by the method described by Slater et al. (Slater 1991), with some modifications previously reported.

Flow cytometric detection of depolarized side scattered light

Depolarized side scatter detection was implemented using the following flow cytometers (Figures II.1 and II.2):

1) The CyFlow Blue (Sysmex/Partec, Munster, Germany), has a 488 nm excitation laser, and detectors for Forward Scatter (FSC), Side Scatter (SSC), green fluorescence – FL1 (BP 535/35 nm), orange fluorescence – FL2 (BP 590/50 nm) and red fluorescence – FL3 (LP 630 nm). For this study the instrument was modified as described elsewhere [30]. Briefly, two SSC detectors were created, with a 50/50 beam splitter between them. A polarizing filter coupled with a 488 nm filter was placed in front of one of the SSC detectors with the filter's axis of polarization horizontal and therefore orthogonal to the vertical polarization plane of the laser light, allowing the detection of depolarized side scatter.

2) The MoFlo high speed cell sorter (Beckman Coulter, Fort Collins, USA) optical set-up was modified as described in Krämer 2001 and Frita 2011 (23, 30). Briefly, scattered light from a 488 nm laser (200 mW air-cooled Sapphire, Coherent) was split in two using a 95/5 beam splitter to measure normal SSC (5% of the light) and depolarized SSC (95% of the light) by placing a polarization filter with its axis of polarization orthogonally to the

polarization plane of the laser illumination. Both detectors had 488/10 nm bandpass filters; O.D. 1.0 and 2.0 neutral density (ND) filters were, respectively, fitted to the normal and depolarized SSC detectors. SYBR-Green fluorescence, diverted by a 505DCRX dichroic filter ahead of the polarizer, was detected through a 540/30 nm bandpass filter.

3) The Attune Acoustic Focusing Cytometer (Life Technologies, Carlsbad, USA) is equipped with 488 nm and 405 nm lasers with detectors for: FSC, SSC, and six fluorescence regions (BP 530/30, BP 574/26, LP 640, BP 603/48, BP522/31 and BP 450/40). Two SSC detectors were created, with a 50/50 beam splitter between them, and polarizing filters were placed orthogonally to the polarization plane of each laser light, one in front of a detector in the violet laser optical path (VL2) and the other in front of the fluorescence detector of the blue laser path (BL2).

4) The Accuri C6 (BDBiosciences, La Jolla, USA) is equipped with a 488 nm solid state laser and a 640 nm diode laser, detectors for FSC, SSC and four fluorescence detectors with the following optical filters: BP 533/30 (FL1), BP 585/40 (FL2), LP 670 (FL3) and BP 675/25 (FL4). The BP 585/40A fluorescence filter in the FL2 detector was replaced by a 488 nm bandpass filter coupled with a plastic polarizing filter oriented orthogonally to the polarization plane of the laser light, allowing detection of depolarized side scatter.

Measuring depolarized scatter with different wavelengths using a MoFlo

Depolarized side scatter was measured at different wavelengths on a MoFlo using a Coherent Innova I90C Argon laser tuned to multiline UV at 1.10 W, 457 nm at 80 mW, 488 nm at 80 mW, or 514 nm at 80 mW. Each laser line was used separately, but always simultaneously with the main 488 nm Sapphire laser as a control. A mounted Glan-Thompson calcite polarizer with an extinction ratio greater than 100,000:1 (GTH10M, Thorlabs) was placed in front of each secondary laser line. Scattered light from the secondary laser was transmitted through the third instrument pinhole. Normal and depolarized SSC were measured using the corresponding bandpass filters (multiline UV: 350/50 nm; 457 nm: 455/30 nm; 488 nm: 488/10 nm; 514 nm: 510/20 nm; and 640 nm: 630/20 nm) after a 70/30 beam splitter and with an orthogonally positioned polarizer filter in the 70% end of the beam splitter.

The separation Index (SI) $(\text{Median Positive} - \text{Median Negative}) / (2 \times \text{StdDev Negative})$ between the Hz-containing cell population and the uninfected cells was calculated in order to evaluate the capacity of each laser wavelength to resolve these two populations, and compared with the SI measured with the main 488 nm laser. A ratio of 1 indicates there are

no differences in the capacity of the respective wavelength to resolve the Hz-containing cells compared to the main 488 nm laser. One-way ANOVA with $n=4$ for each wavelength was performed to assess whether there were statistical differences between each ratio.

Microscopy

In the *P. berghei* infected sample, sorted cells were centrifuged and transferred to a glass slide, which was then fixed in methanol and Giemsa-stained.

In the case of *P. falciparum*, sorted cells were left to sediment overnight. Supernatant was discarded and a 10 μ l drop of pelleted cells was placed into a glass slide which was immediately covered using a square coverslip. Leica DM5000B (Leica, Solms, Germany) and Leica DM2500 microscopes were used for fluorescence and depolarized microscopy, respectively.

Cell Sorting using the MoFlo

Populations with different levels of depolarization were sorted. The instrument was run at a pressure of 483 kPa (70 psi) with a 70 μ m nozzle and a drop formation frequency of approximately 96 kHz. Sorting rates were typically c.a. 3.5×10^7 cells per hour. Cells were collected into approximately 1 ml of PBS maintained at 4°C.

Flow cytometry data analysis

Flow cytometry results were analyzed using FlowJo software (version 9.0.2, Tree Star Inc., Oregon, USA). Depolarizing events were defined in plots of SSC versus depolarized-SSC as those with a signal above the background observed in the uninfected control.

To assess if the depolarization level would reflect parasite development, parasites tagged with a green fluorescent protein (GFP) in the case of *P. berghei* ANKA or stained with a fluorescent DNA dye (SYBR green I) in the case of *P. falciparum*, were analyzed. To determine SYBR green I or GFP positive cells, green fluorescence (FL1) versus red fluorescence (FL3) plots were used. SYBR green I positive events were established based on a stained uninfected control.

The study involving human samples was approved by the Ethical Committee of the Faculty of Medicine, University of Lisbon. All experiments involving animals were performed in compliance with the relevant laws and institutional guidelines.

4. Results

Detection of light depolarization using different instruments

The Attune, Accuri C6, CyFlow, and MoFlo could all be set up for depolarized side scatter by making a few simple changes to the optics, allowing restoration of the original configuration within a few minutes (Figure II.1). Hz from *P. berghei* iRBC could be successfully detected (Figures II.2, II.3A and SII.1). In fact, a CyFlow instrument located in the rather remote location of Lambaréné, Gabon, was also easily converted and used to investigate indigenous malaria parasites from local patients.

Detection of light depolarization caused by different types of hemozoin

All forms of Hz could be easily detected by measuring depolarized side-scattered light. Intraerythrocytic Hz from both the rodent malaria parasite *P. berghei* and the human malaria parasite *P. falciparum* were detected, although Hz-containing cells of these two species exhibited different levels of depolarized side scatter (Figure II.3B and SII.2). Hz in *P. berghei* iRBC showed higher levels and a wider distribution of depolarization than Hz in *P. falciparum* iRBC. PBMCs containing synthetic Hz also showed a high level of depolarization (Figure II.3C). Free crystals of synthetic Hz could be detected as well and showed a wide range of depolarized side-scatter (Figure II.3D).

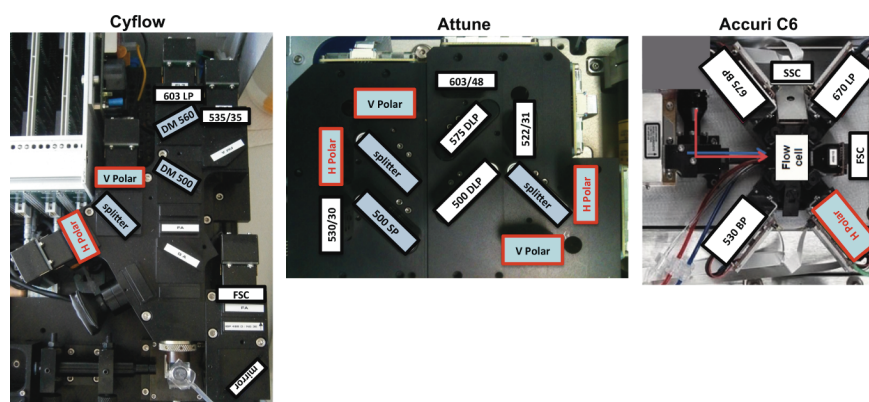


Figure II.1: Optical layout of three different bench top flow cytometers modified to detect light depolarization. Three bench top flow cytometers were adapted to detect light depolarization caused by hemozoin. The Cyflow (Partec) and the Attune (Life Technologies) were modified similarly, briefly: two sides-scatter detectors (SSC) (red boxes) were created by placing a 50/50 beam splitter between them, and a horizontally polarized filter (H polar) was placed in front of one of the SSC detectors. In the Attune this was done twice: for the blue and violet lasers optical paths. The Accuri C6 (BDBiosciences) was easily modified by replacing the emission filter in front of the second detector of fluorescence with a 488 nm filter coupled with a polarizer filter with its axis in the horizontal plane; no further alterations were required. Boxes with the blue background represent the optical components that were modified in comparison to the original set up.

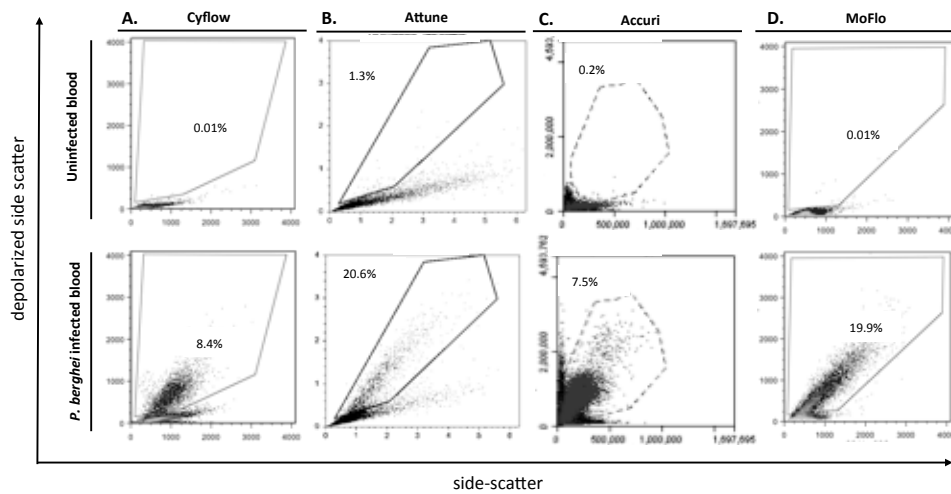


Figure II.2: Detection of depolarizing side-scattered light by four different flow cytometers. Representative plots (side scatter versus depolarized side-scatter) of mouse uninfected red blood cells (RBCs) (top row) and RBCs infected with *Plasmodium berghei* (bottom row). Light depolarization caused by hemozoin was detected in four different cytometers: the Cyflow (A), the Attune (B), the Accuri C6 (C) and the MoFlo (D). Depolarizing cells were selected after establishing a gate using the uninfected controls (top row).

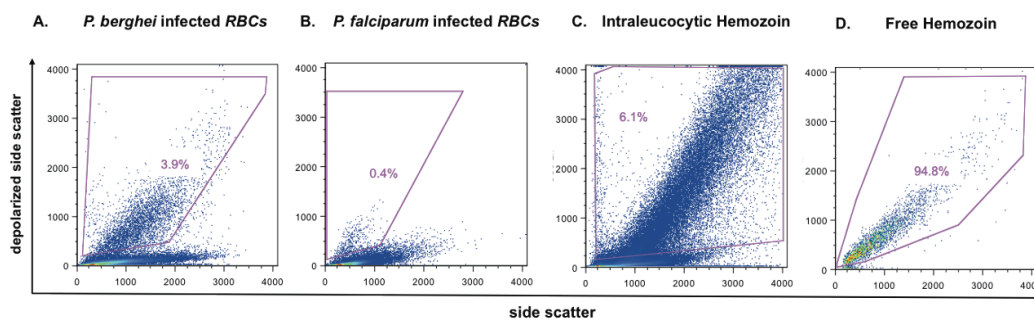


Figure II.3: Detection of intraerythrocytic, intraleukocytic and free hemozoin (Hz). Representative plots (side scatter against depolarized side-scatter) of mouse red blood cells (RBCs) infected with *Plasmodium berghei* (A), human RBCs infected with *Plasmodium falciparum* (B), Hz-containing phagocytes (C) and free synthetic Hz (D), analyzed using a Cyflow. The resulting depolarization of light caused by Hz could be detected in these four different samples, however different degrees of depolarization were observed, possibly indicating a different distribution of Hz crystals within the cells.

Note: Gain values had to be adjusted for the various samples, since they had inherently different characteristics. However, for the depolarized side-scatter parameter the gain values did not differ considerably, ranging from 230 to 280.

Hemozoin induced depolarization at different wavelengths

When depolarized side scatter was measured at several different wavelengths commonly used in flow cytometers, the separation index (SI) ratio obtained with each wavelength in comparison to the SI measured with the main 488 nm was close to one (Figure II.4),

indicating that there appears to be little difference in the detection of depolarizing events, statistically confirmed with one-way ANOVA test (n=4 for each wavelength).

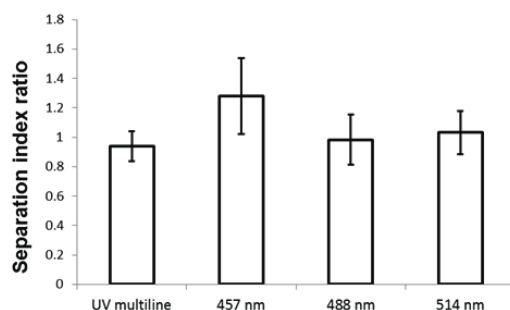


Figure II.4: Assessing hemozoin depolarization with different wavelengths. Bars represent ratios of Separation Index (SI; see Methods) obtained with each wavelength in comparison to the SI measured with the main 488 nm Sapphire laser. A ratio close to one indicates there is no difference, confirmed statistically with one-way ANOVA test (n=4 for each wavelength). Increasing laser power did not improve separation (data not shown).

Identification of *P. berghei* and *P. falciparum* infected RBCs with different degrees of depolarization

In the *P. berghei*-GFP infected RBCs four different populations were selected, designated as non, low, medium and high depolarizing (Figure SII.1). As the depolarization degree increases an increase in the GFP was observed, which indicates that more mature parasites have a higher level of depolarization (Figure SII.1A). Although some overlap in the GFP intensity signal could be observed, there was a clear difference between the highly-depolarizing and non-depolarizing populations, with median values of GFP fluorescence of 1063 and 129, respectively. Microscopic analysis of the sorted populations corroborated this observation, where infected RBCs with immature parasites with no observable Hz were only present in the non-depolarizing population. While, in the high-depolarizing population, only parasites with large amounts of dispersed Hz were present. Interestingly, mature parasites with a single but large clump of Hz could be found in the low and medium-depolarizing populations (Figure SII.1B).

In the case of *P. falciparum* infected RBCs, only two gates were created, designated as SG+/Hz+ (depolarizing) and SG+/Hz- (non-depolarizing) (Figure SII.2). Results showed that the depolarizing population (SG+/Hz+) had a much higher intensity of SYBR green I fluorescence with a median value of 3735 compared to 514 median of the non-depolarizing population (SG+/Hz-), indicating more DNA and thus, reflecting their more advanced stage of development (Figure SII.2A). Bright-field and fluorescence microscopy of SYBR green I showed that mature, multinucleated schizonts were only detected in the depolarizing population, whereas single-nucleated young parasites were only found in the non-depolarizing population (Figure SII.2B).

5. Discussion

Malaria and Flow Cytometry

Cytometry of malaria-infected RBC has been used for (i) monitoring of infected RBC, mainly in mouse models (33 - 38), (ii) characterization of infected RBC (15), (iii) assessment of maturation and/or viability of parasites in infected RBC [10, 13, 14, 16, 17, 39, 40], and (iv) to detect and count *P. falciparum* infected RBC in culture [14, 41 – 43] or from patient blood [44 – 46], with the possibility to distinguish species based on base composition [2, 17].

Reliable discrimination of parasitized RBC from micro-nucleated RBC and/or reticulocytes can, however, be difficult [46]. Usually, this requires elaborate/laborious manipulation steps, such as removal of RNA [12, 33] or the use of a combination of different nucleic acid stains [13, 35], frequently requiring instruments with more than one light source, e.g., UV in the case of the frequently used Hoechst 33342 stain. More complex protocols can be more error-prone.

Hemozoin is a useful and simple parameter to measure

Hz measurement is attractive as an addition and/or an alternative to the range of cytometric measurements now made on malaria parasites. Detection by microscopy using simple polarizing filters [8, 9] or by cytometric depolarized scatter measurement is reagent-free and does not require extensive sample preparation, and thus can easily be done on native samples [31, 32]. Because it is produced throughout schizogony by growing parasites, Hz is an ideal maturation marker [48]. Hz distribution and amount also vary between species and parasite forms. For example, Hz is higher in gametocytes than in most asexual forms of *P. falciparum*, providing aid in identification [6]. Although Hz levels in early *P. falciparum* ring-forms are below the detection thresholds of both dark-field microscopy [49] and flow cytometry [31] when analyzing native samples, it may be detected in bulk in blood after rigorous lysis of the sample [50]. Even though we have shown that free synthetic Hz can be easily detected by flow cytometry (Figure II.3D), we have not investigated detection of free Hz obtained after blood sample lysis. The utility and possible applications of the cytometric Hz detection in phagocytes (Figure II.3C) have been reviewed elsewhere [51].

Detection of light depolarization caused by hemozoin using different flow cytometers

Compact bench top instruments, such as CyFlow SL or the Cube (Partec), the Attune (Life Technologies) or the Accuri C6 (BDBiosciences), which we show are easily modifiable for

Hz (Figures II.1 and II.2), are relatively easy to run in resource-limited environments, making it feasible for cytometric Hz measurement to be more widely used.

The benchtop systems and a MoFlo sorter were all easily modified without any special training and it was easy to return them to their original configurations.

Although patent issues no longer impede modification of flow cytometers for depolarized scatter, a major obstacle has arisen with the common use of fiber optic cables, which do not preserve the polarization of light, in the light collection path(s) for fluorescence and side scatter. It should be noted that, unlike the model we used, the new Attune NxT is equipped with such fiber optics and is therefore not usable to detect depolarized scatter.

The depolarized population detected with the Accuri C6 was not as clearly separated from the non-depolarized population, as was the case with the other instruments (Figure II.2E). The Accuri differs in design from the other systems in several respects; the light that is detected in the depolarized side scatter detector is not at 90° from its original path (Figure II.1), and the detector gains are not easily adjustable by the user. Moreover, the Accuri filters and filter holders are much smaller than those in the Attune, CyFlow, and MoFlo, limiting the choice of optical components initially available to us. We are awaiting arrival of parts for a new filter design that we expect will improve performance.

The use of different beam splitters between the SSC and depolarized SSC seemed to have little, if any influence on the detected population (data not shown). It is noteworthy that placing a 1:100;000 Glan polarizer into the laser illumination path ahead of the cuvette also appeared to have little effect (data not shown). We also found that depolarization was adequately detectable at different wavelengths (Figure II.4), corroborating the report from Krämer *et al* [23] that side scatter light polarization could be detected in a modified MoFlo at wavelengths of 488 nm, 633 nm and 647 nm. They noted that longer wavelengths produced marginally stronger signals. Results obtained from additional excitation wavelengths (UV multiline, 457 nm and 514 nm) did not differ significantly from those obtained using a 488 nm laser (Figure II.4). Indeed, although certain longer wavelengths and perhaps a 95/5 beam splitter or better polarization ratios might be expected to provide better results, the light sources and wavelengths commonly used in flow cytometers, 50/50 beam-splitters, and simple polarizing filters appear sufficient for the measurement of Hz in suspension, inside infected RBCs or inside leukocytes (Figure II.3).

Flow cytometric detection of intraleukocytic and intraerythrocytic hemozoin

At the end of the maturation cycle, schizonts rupture, releasing Hz which is phagocytized by circulating neutrophils and monocytes [52]. After detection of Hz leukocytes using the Cell-Dyn hematology analyzer was reported [21], several studies, reviewed elsewhere (26), addressed the performance and utility of this approach.

Although finding Hz in leukocytes as part of an automated blood count might allow the detection of malaria even in the absence of clinical suspicion, this is still only possible using the Cell-Dyn instruments [53]. These “closed” platforms, which use proprietary reagents, fixed detection and analysis algorithms and provide no ready access to list-mode data are limited in adaptability [23, 26, 29]. However, their detection of intraleukocytic Hz has been correlated with malaria severity [54 – 56], and flow cytometric counts of Hz-containing leukocytes have been shown to be a better marker of disease severity than microscopic counting [28]. Intraleukocytic Hz detection is also potentially applicable to the diagnosis of malaria during pregnancy [9].

Importantly, since Hz has immune modulating effects, as reviewed elsewhere [51], flow cytometric detection/sorting of Hz-containing leukocytes and non-containing leukocytes from the same host might help elucidate further details [30, 51, 57].

Hz detection by microscopy provides the foundation for the slide-based schizont maturation assay, still a mainstay in detecting antimalarial drug resistance in clinical settings. Several flow cytometric procedures analogous to the schizont maturation assay have been described by others [13, 16, 17, 39, 58]; since depolarized scatter measurements were not available on their apparatus, they could not use Hz content as a maturation indicator for stage determination. Instead a combination of DNA and RNA content was employed, providing more precise stage identifications than would be obtained by cytometric detection of DNA content alone but requiring two dyes and two fluorescence measurements.

In a classic schizont maturation assay of *P. falciparum*, initial clinical samples contain little Hz because stages later than early trophozoites are removed from circulation. Parasites in drug-free medium and drug-resistant parasites form Hz as they continue to grow and mature, whereas Hz formation is diminished or absent in parasites cultured in effective concentrations of antimalarial agents. We have shown that schizonts in these contexts are easily distinguished from younger parasites solely based on their level of depolarization (Figure SII.2), measurable without addition of reagents.

We have demonstrated a field-suitable novel flow cytometric assay for antimalarial

susceptibility based on this rationale [30, 32]. This assay has also been shown to detect drug effects on parasite maturation much earlier than any other available technique [32, 59].

Unpublished preliminary experiments with flow cytometers equipped to measure DNA, RNA, and Hz simultaneously in parasitized RBC indicate that although both RNA content and Hz signals increase during maturation, these two parameters are not highly correlated and that measuring both may therefore provide more information about parasite physiology than would measuring only one or the other.

P. berghei- and *P. falciparum*-infected RBC showed different populations with depolarized side scatter signals. It has long been known that the amount, appearance and location of pigment in different species of malaria parasites show wide variations [60]. In *P. berghei* Hz crystals are fine and dispersed granules which only clump together by the end of schizogony (Figure SII.1B, second and third panel from top), while in *P. falciparum* the Hz crystals aggregate as they start to appear (Figure SII.2B, lower panels). Thus, in *P. falciparum* forms with highly dispersed Hz and, consequently, high degree of depolarization are absent. This explanation also fits with the obtained depolarized side scatter signals because side scatter is also a measure of cell granularity [61]. Therefore, it is likely that a parasite containing several small but distributed Hz crystals will have a higher depolarized side scatter signal than a parasite containing a single large clump of Hz.

Microscopy has shown that Hz is also more abundant and dispersed in gametocytes [6] and our analyses of *P. berghei*-infected blood samples showed higher levels of depolarized side scatter in gametocytes (Figure SII.2B). Thus, this approach can eventually be applied to aid in the detection of these sexual forms, which are responsible for transmission. Currently, *in vitro* assays to screen drugs for gametocytes are either based on labor-intensive microscopy or on the analysis of transgenic fluorescent gametocytes by flow cytometry [62 – 64]. Hz detection may be useful to help and develop novel assays for the detection and quantification of gametocytes, with different applications such as, the development and investigation of novel transmission blocking drugs.

Gametocytes differ from sexual forms in that, although their Hz signals are high and may even be higher than those of schizonts, their RNA content is relatively low; our preliminary experiments indicate that cytometry can resolve two gametocyte populations with higher and lower modal RNA content, presumably representing macrogametocytes (female) and microgametocytes (male), the former known to exhibit cytoplasmic basophilia in Giemsa-stained smears, characteristic of RNA staining.

Future Prospects: Malaria Cytometry in Simple Imaging Systems

During the past few years, fluorescence imaging cytometers usable for some multiparameter analyses formerly only possible using flow cytometry, including CD4+ T cell counting in HIV patients and multiplexed bead PCR assays for malaria species identification, have come into use. The DNA and RNA dye measurements typically done in malaria cytometry require less sensitivity, and could be implemented in similar apparatus. A recent report on spectral imaging of malaria-infected cells in a microscope illuminated by multiple LEDs suggests that Hz may be detected efficiently by transmission measurements in the 630-700 nm range [65] without a need to use polarized light; we have also found evidence for this. In addition to its substantially lower cost and complexity, a multiparameter imager for malaria cytometry would offer the considerable advantage of being able to analyze slides. We have just begun work with a prototype of such an instrument.

6. Conclusion

The old parameter of light depolarization measurements has found a new job in malaria. It allows to detect Hz, free in blood or inside iRBCs erythrocytes leukocytes all of which can be used in several applications, such as: (i) detection of Hz-containing leukocytes for diagnostic applications and to unravel malaria-associated immunopathology; (ii) detection of parasitized RBC and determination of species and stages for diagnosis and drug susceptibility determination; and (iii) discrimination of gametocytes and other low-abundance parasite subpopulations. Depolarized light scatter measurements are easily implemented on common benchtop flow cytometers and work across a wide range of illumination wavelengths; equivalent optical measurements for Hz detection can also be made in imaging cytometers. Adding Hz detection to other parameters, such as DNA or RNA content, will provide improved accuracy and sensitivity of parasite detection and allow researchers to expand the use of cytometry in the field of malaria.

7. Acknowledgments

This work was supported by the Luso-American Foundation (FLAD-LACR grant: B-A.V-109-09/07). MR acknowledges FCT for doctoral grant (SFRH/BD/84530/2012).

The authors acknowledge Andrea Tradori from Life Technologies and Daniel Gala from Enzifarma (BD representative in Portugal), who provided us with the measurements on the

Attune and the Accuri C6, respectively, and Grace Chojnowski (Queensland Institute of Medical Research) who gave us additional information regarding the Attune.

8. Supporting Information

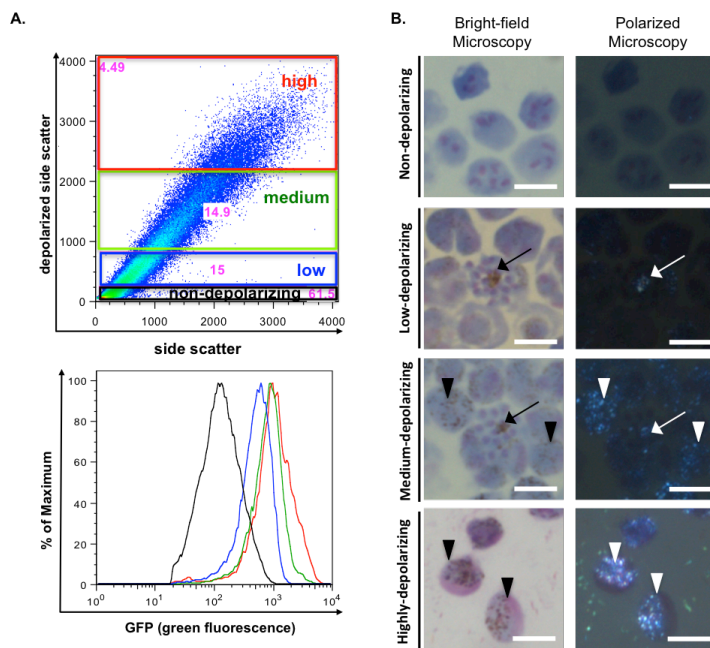


Figure SII.1: Degree of depolarization and developmental stage of *P. berghei* infected mouse red blood cells. Representative flow cytometric plot of side scatter versus depolarized side-scatter (upper plot) and GFP intensity (bottom histogram) of mouse red blood cells (RBCs) infected with *Plasmodium berghei*-GFP (A). Representative pictures of Giemsa-stained smears of FACS sorted cells analyzed by bright field and polarization microscopy are shown in the left and right panel in B, respectively (scale bar = 5 μ m). Populations with increasing levels of depolarization (A, upper plot) show a correspondent increase in

GFP intensity (A, bottom histogram). GFP positive cells were sorted (using a Moflo) based on their degree of depolarization (A). Immature forms were only observed in the non-depolarizing population while mature schizonts with a big clump of hemozoin (Hz) were found both in the low and medium-depolarizing population (arrows) (B). Also in the medium-depolarizing population other parasite forms (gametocytes) with distributed fine granules of Hz were present. However, these forms were more frequent in the high-depolarizing population (arrow heads) (B).

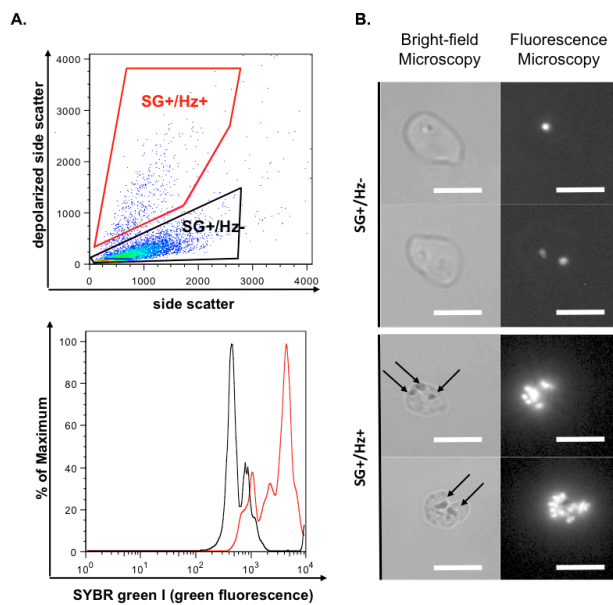


Figure SII.2: Degree of depolarization and developmental stage of *P. falciparum* infected red blood cells culture. Representative plots of side scatter versus depolarized side-scatter (A, upper plot) and SYBR green I intensity (A, bottom histogram) of human red blood cells (RBCs) infected with *Plasmodium falciparum* and stained with SYBR green I (A). Representative pictures of unstained smears of sorted cells analyzed by bright field and fluorescence microscopy (left and right panel in B, respectively) (scale bar = 5 μ m). SYBR green I positive cells were gated and FACS sorted (using a MoFlo) based on their depolarization (hemozoin - Hz): SG+/Hz- (non-depolarizing) and SG+/Hz+

(depolarizing) cells (A). The depolarizing population showed a higher SG intensity than the non-depolarizing. Microscopic observation of the sorted populations showed that single-nucleated immature forms were present only in the non-depolarizing population (B), whereas multi-nucleated schizonts (bright fluorescence spots) with a large clump of Hz (arrows) were exclusively found in the depolarizing population (B).

Hemozoin induced depolarization at different wavelengths

Four different wavelengths were tested (Multiline UV, 457 nm, 488 nm, and 514 nm) using a MoFlo cytometer for the ease of switching optical configurations (see Fig 1). A sample was brought on each different day (total of 4 days) with different parasitemia and Hemozoin (Hz) depolarization was measured for the four tested wavelengths. To address the differences, for each wavelength we measured the sample simultaneously with the main 488 nm laser (Coherent Sapphire 200mW), which is mainly used for all our depolarization measurements.

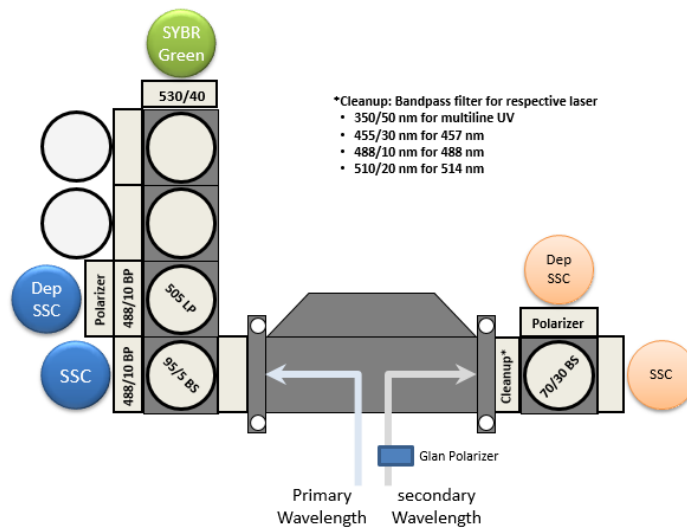


Figure SII.3: MoFlo Optical Layout for the 4 different tested wavelengths. The following figures show the acquisition plots and gate strategy of one representative day to measure the Median channel intensity of the depolarized and non-depolarized populations for the tested and control wavelengths, as well as the standard deviation of the non-depolarized population in the tested and control wavelengths.

CHAPTER II - FLOW CYTOMETRIC DETECTION OF HEMOZOIN

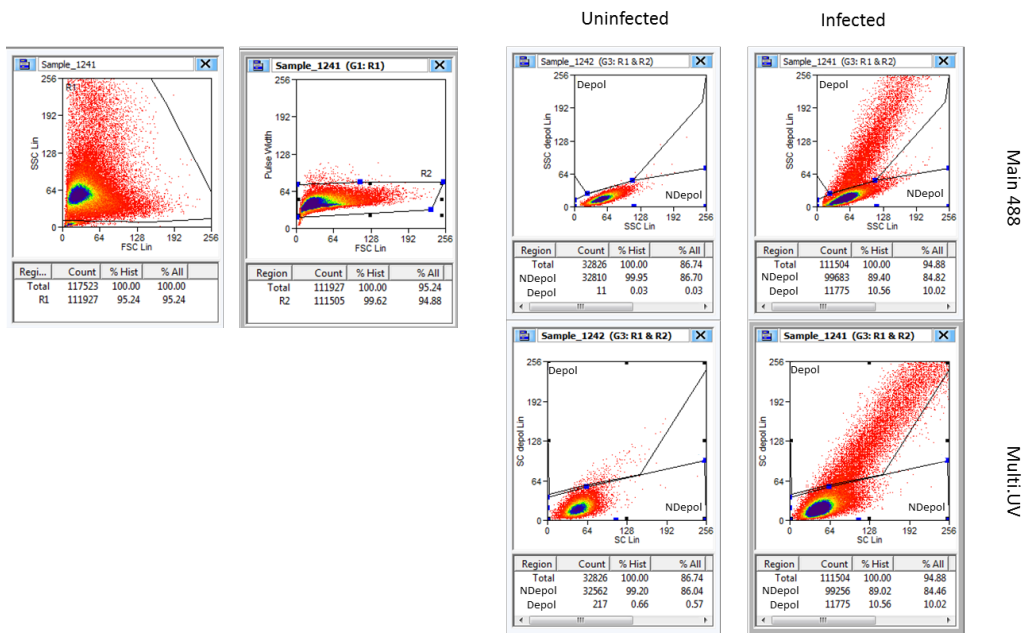


Figure SII.4: Acquisition plots and gating strategy for day 25-03-2014 using Multiline UV.

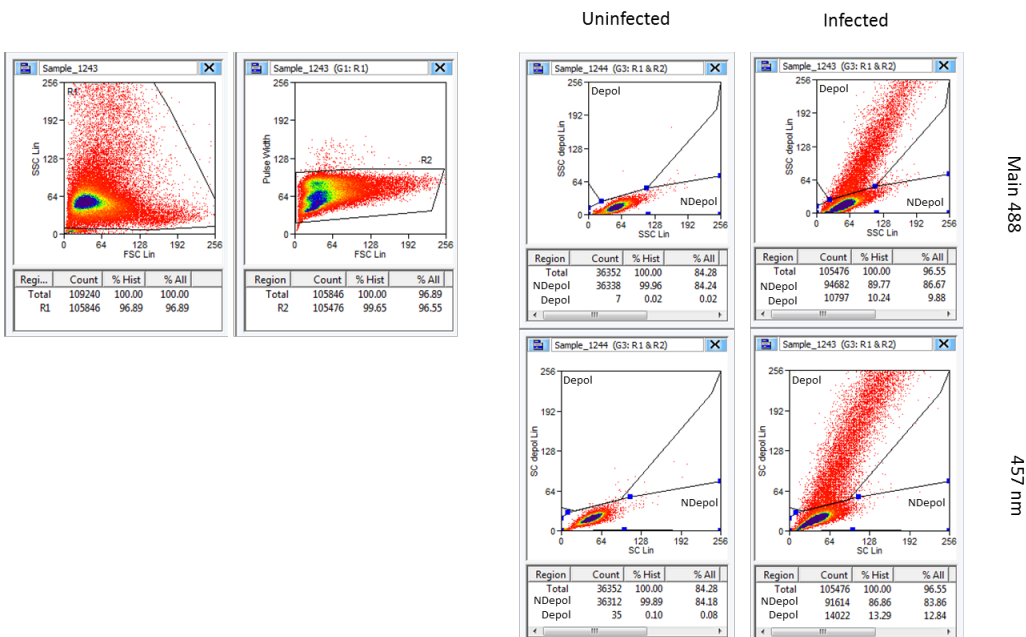


Figure SII.5: Acquisition plots and gating strategy for day 25-03-2014 using 457 nm.

CHAPTER II - FLOW CYTOMETRIC DETECTION OF HEMOZOIN

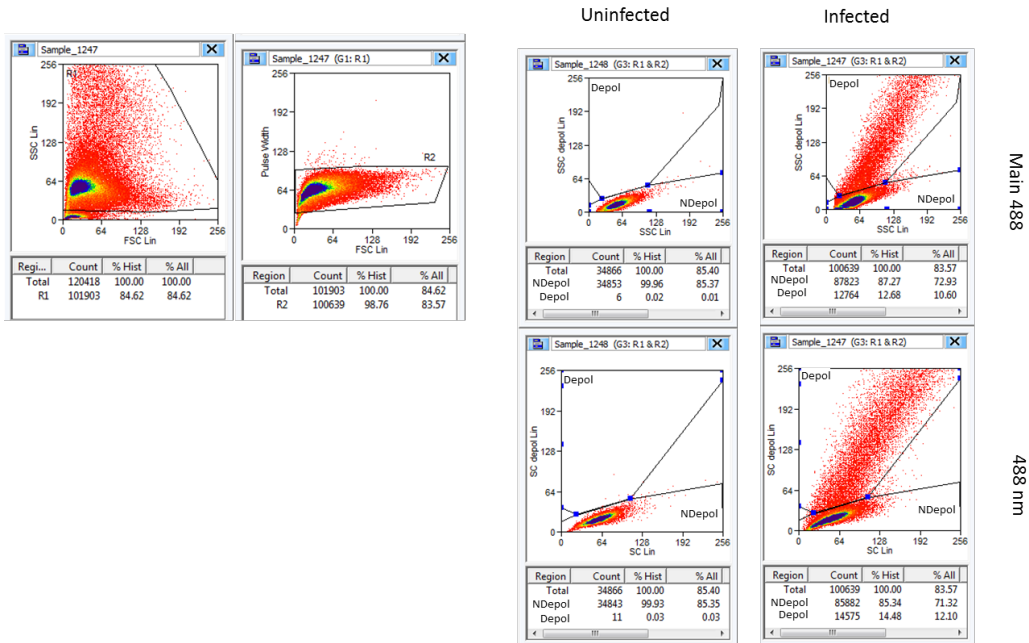


Figure SII.6: Acquisition plots and gating strategy for day 25-03-2014 using 488 nm.

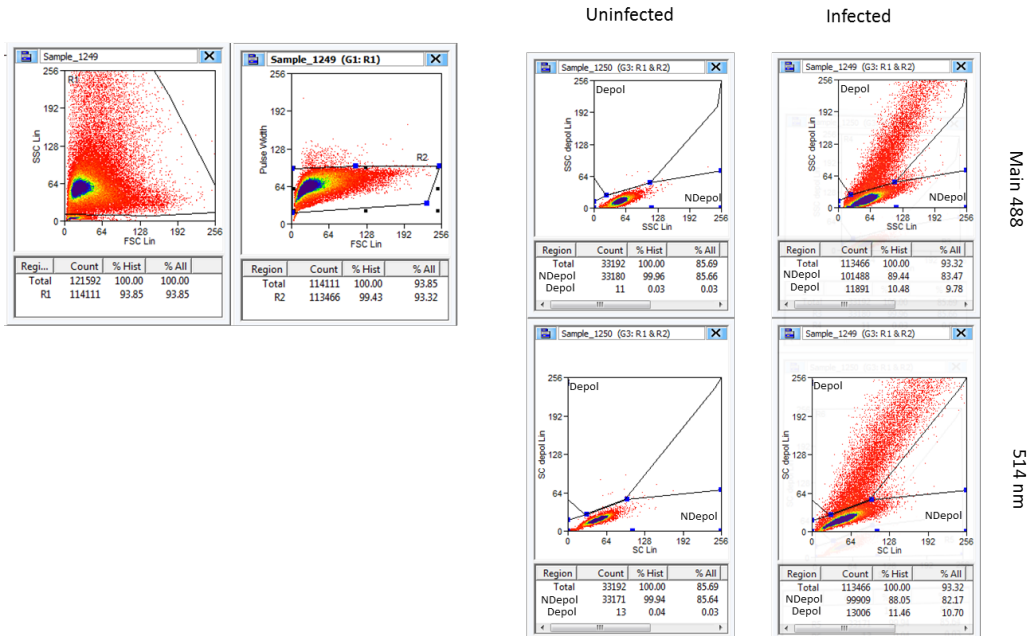


Figure SII.7: Acquisition plots and gating strategy for day 25-03-2014 using 514 nm.

CHAPTER II - FLOW CYTOMETRIC DETECTION OF HEMOZOIN

The values obtained with this strategy are shown in the following table SII for each of the four days, corresponding to four different samples. Separation Index was calculated according to the following equation:

$$\text{Separation Index} = (\text{MFI}_{\text{SC depol Lin [Depol]}} - \text{MFI}_{\text{SC depol Lin [NDepol]}}) / (2 \times \text{SD}_{\text{SC depol Lin [NDepol]}})$$

Table SII: Separation Index ratios calculated for each wavelength for four different samples

Separation Index														
Tested Wav.	Power (W)	Date	sample Parasitemia	Tested Wavelength				Main 488nm (Control)				Tested Wav.	Main 488	Ratio
				Median NDepol	SD NDepol	Median Depol	SD Depol	Median NDepol	SD NDepol	Median Depol	SD Depol			
Multiline UV	1.10	04-02-2014	~ 20%	3	5.18	48	21.89	11	6.65	107	68.96	4.34	7.22	0.60
	1.10	06-02-2014	~ 20%	5	5.11	67	34.83	11	7.04	103	71.05	6.07	6.53	0.93
	1.10	13-02-2014	~ 3%	15	7.79	63	43.58	12	6.48	49	31.47	3.08	2.85	1.08
	1.13	25-03-2014	~ 14%	18	9.76	139	65.23	16	7.00	107	77.35	6.20	6.50	0.95
457nm	0.08	04-02-2014	~ 20%	10	7.03	103	48.53	3	3.41	48	35.45	6.61	6.60	1.00
	0.08	06-02-2014	~ 20%	1	1.75	53	32.18	1	2.25	44	30.48	14.86	9.56	1.55
	0.08	13-02-2014	~ 3%	13	4.36	110	56.00	13	6.67	103	55.35	11.12	6.75	1.65
	0.08	25-03-2014	~ 14%	14	6.70	104	77.19	18	6.01	168	79.94	6.72	12.48	0.54
488nm	0.08	04-02-2014	~ 20%	12	5.31	102	53.63	9	6.55	98	61.45	8.47	6.79	1.25
	0.08	06-02-2014	~ 20%	7	4.01	85	54.84	3	4.00	65	50.38	9.73	7.75	1.25
	0.08	13-02-2014	~ 3%	12	6.23	102	56.29	14	4.58	106	58.43	7.22	10.04	0.72
	0.08	25-03-2014	~ 14%	14	6.64	117	80.65	18	5.66	161	79.81	7.76	12.63	0.61
514nm	0.08	04-02-2014	~ 20%	7	5.23	65	37.52	3	3.21	46	33.02	5.54	6.70	0.83
	0.08	06-02-2014	~ 20%	2	3.25	57	39.32	1	2.02	44	31.95	8.46	10.64	0.79
	0.08	13-02-2014	~ 3%	14	4.70	99	57.39	12	6.22	103	57.21	9.04	7.32	1.24
	0.08	25-03-2014	~ 14%	19	6.10	127	76.77	15	7.25	108	77.37	8.85	6.41	1.38

9. References

1. World Health Organization (2015). World Malaria Report 2013. WHO Press, Geneva.
2. Shapiro HM, Apte SH, Chojnowski GM, Hänscheid T, Rebelo M, Grimberg BT. (2013) Cytometry in malaria – a practical replacement for microscopy? *Current Protocols in Cytometry* Chapter 11: Unit 11.20.
3. Laveran CL. (1880) A newly discovered parasite in the blood of patients suffering from malaria. Parasitic etiology of attacks of malaria In: Kean BH, Mott KE, Russell AJ, eds. Tropical medicine and parasitology. *Classic investigations*, vol 1. Ithaca, NY: Cornell University Press, 1978.
4. Packer H. (1945) The use of darkfield illumination in studies of malaria parasites. *National Malaria Society (U.S.)* 4: 331-340.
5. Jamjoom GA. (1983) Dark-field microscopy for detection of malaria in unstained blood films. *Journal of Clinical Microbiology* 17: 717-721.
6. Jamjoom GA. (1988) Formation and Role of Malaria Pigment. *Reviews of Infectious Diseases* 10: 1029-1034.
7. Wilson BK, Behrend MR, Horning MP, Hegg MC. (2011) Detection of malarial byproduct hemozoin utilizing its unique scattering properties. *Optics Express* 19: 12190-12196.
8. Lawrence C, Olson JA. (1986) Birefringent Hemozoin Identifies Malaria. *American Journal of Clinical Pathology* 86: 360-363.
9. Romagosa C, Menendez C, Ismail MR, Quintó L, Ferrer B, Alonso PL, Ordi J. (2004) Polarisation microscopy increases the sensitivity of hemozoin and *Plasmodium* detection in the histological assessment of placental malaria. *Acta Tropica* 90: 277-284.
10. Hare JD. (1986) Two-Color Flow-cytometric Analysis of the Growth Cycle of *Plasmodium falciparum* in vitro: Identification of Cell Cycle Compartments. *The Journal of Histochemistry and Cytochemistry* 34: 1651-1658.
11. Janse CJ, van Vianen PH, Tanke HJ, Mons B, Ponnudurai T, Overdulve JP. (1987) *Plasmodium* species: flow cytometry and microfluorometry assessments of DNA content and synthesis. *Experimental Parasitology* 64: 88-94.
12. Jiménez-Díaz MB, Rullas J, Mulet T, Fernández L, Bravo C, Gargallo-Viola D, Angulo-Barturen I. (2005) Improvement of detection specificity of Plasmodium-infected murine erythrocytes by flow cytometry using autofluorescence and YOYO-1. *Cytometry A* 67:27-36.

13. Grimberg BT, Erickson JJ, Sramkoski RM, Jacobberger JW, Zimmerman PA. (2008) Monitoring *Plasmodium falciparum* growth and development by UV flow cytometry using an optimized Hoechst-thiazole orange staining strategy. *Cytometry A*. 73: 546-554.
14. Malleret B, Claser C, Ong AS, Suwanarusk R, Sriprawat K, Howland SW, Russell B, Nosten F, Rénia L. (2011) A rapid and robust tri-color flow cytometry assay for monitoring malaria parasite development. *Scientific Reports* 1: 118.
15. Apte SH, Groves PL, Roddick JS, P da Hora V, Doolan DL. (2011) High-throughput multi-parameter flow-cytometric analysis from micro-quantities of plasmodium-infected blood. *International Journal for Parasitology* 41: 1285-1294.
16. Russell B, Malleret B, Suwanarusk R, Anthony C, Kanlaya S, Lau YL, Woodrow CJ, Nosten F, Renia L. (2013) Field-based flow cytometry for ex vivo characterization of *Plasmodium vivax* and *P. falciparum* antimalarial sensitivity. *Antimicrobial Agents and Chemotherapy* 57: 5170-5174.
17. Amaratunga C, Neal AT, Fairhurst RM. (2014) Flow cytometry-based analysis of artemisinin-resistant *Plasmodium falciparum* in the ring-stage survival assay. *Antimicrobial Agents and Chemotherapy* 58: 4938-4940.
18. Grimberg BT. (2011) Methodology and application of flow cytometry for investigation of human malaria parasites. *Journal of Immunological Methods* 367: 1-16.
19. Lelliott PM, Lampkin S, McMorran BJ, Foote SJ, Burgio G. (2014) A flow cytometric assay to quantify invasion of red blood cells by rodent *Plasmodium* parasites in vivo. *Malaria Journal* 13: 100.
20. de Grooth BG, Terstappen LW, Puppels GJ, Greve J. (1987) Light-scattering polarization measurements as a new parameter in flow cytometry. *Cytometry* 8: 539-44.
21. Mendelow BV, Lyons C, Nhlangothi P, Tana M, Munster M, Wypkema E, Liebowitz L, Marshall L, Scott S, Coetzer TL. (1999) Automated malaria detection by depolarization of laser light. *British Journal of Haematology* 104: 499-503.
22. Hänscheid T, Valadas E, Grobusch MP. (2000) Automated malaria diagnosis using pigment detection. *Parasitology Today* 16: 549-51.
23. Krämer B, Grobusch MP, Suttorp N, Neukammer J, Rinneberg H. (2001) Relative frequency of malaria pigment-carrying monocytes of nonimmune and semi-immune patients from flow cytometric depolarized side scatter. *Cytometry* 45: 133-40.
24. Hänscheid T, Melo-Cristino J, Pinto BG. (2001) Automated detection of malaria pigment in white bloodcells for the diagnosis of malaria in Portugal. *The American Journal of Tropical Medicine and Hygiene* 64: 290-92.

25. Scott CS, van Zyl D, Ho E, meyersfeld D, Ruivo L, Mendelow BV and Coetzer TL. (2001) Automated detection of WBC intracellular malaria-associated pigment (Haemozoin) with Abbott Cell-Dyn CD3200 and CD3700 analysers. *Haematology Support and Education* 2: 2-15.
26. Campuzano-Zuluaga G, Hänscheid T, Grobusch MP. (2010) Automated haematology analysis to diagnose malaria. *Malaria Journal* 9: 346.
27. Suh IB, Kim HJ, Kim JY, Lee SW, An SS, Kim WJ, Lim CS. (2003) Evaluation of the Abbott Cell-Dyn 4000 hematology analyzer for detection and therapeutic monitoring of *Plasmodium vivax* in the Republic of Korea. *Tropical Medicine & International Health* 8: 1074-81.
28. Hänscheid T, Frita R, Langin M, Kreamsner PG, Grobusch MP. (2009) Is flow cytometry better in counting malaria pigment-containing leukocytes compared to microscopy? *Malaria Journal* 8: 255.
29. Hänscheid T, Romão R, Grobusch MP, Amaral T, Melo-Cristino J. (2011) Limitation of malaria diagnosis with the Cell-Dyn® analyser: not all haemozoin-containing monocytes are detected or shown. *International Journal of Laboratory Hematology* 33: e14-6.
30. Frita R, Rebelo M, Pamplona A, Vigario AM, Mota MM, Grobusch MP, Hänscheid T. (2011) Simple flow cytometric detection of haemozoin containing leukocytes and erythrocytes for research on diagnosis, immunology and drug sensitivity testing. *Malaria Journal* 10: 74.
31. Rebelo M, Shapiro HM, Amaral T, Melo-Cristino J, Hänscheid T. (2012) Haemozoin detection in infected erythrocytes for *Plasmodium falciparum* malaria diagnosis-prospects and limitations. *Acta Tropica* 123: 58-61.
32. Rebelo M, Sousa C, Shapiro HM, Mota MM, Grobusch MP, Hänscheid T (2013). A novel flow cytometric hemozoin detection assay for real-time sensitivity testing of *Plasmodium falciparum*. *PLoS One* 8: e61606.
33. Barkan D, Ginsburg H, Golenser J. (2000) Optimisation of flow cytometric measurement of parasitaemia in *Plasmodium*-infected mice. *International Journal for Parasitology* 30: 649-653.
34. Jiménez-Díaz MB, Mulet T, Gómez V, Viera S, Alvarez A, Garuti H, Vázquez Y, Fernández A, Ibáñez J, Jiménez M, Gargallo-Viola D, Angulo-Barturen I (2009). Quantitative measurement of Plasmodium-infected erythrocytes in murine models of

malaria by flow cytometry using bidimensional assessment of SYTO-16 fluorescence. *Cytometry A* 75: 225-235.

35. Bhakdi SC, Sratongno P, Chamma P, Rungruang T, Chuncharunee A, Neumann HP, Malasit P, Pattanapanyasat K. (2007) Re-evaluating acridine orange for rapid flow cytometric enumeration of parasitemia in malaria-infected rodents. *Cytometry A* 71: 662-667.

36. Sanchez BA, Mota MM, Sultan AA, Carvalho LH. (2004) Plasmodium berghei parasite transformed with green fluorescent protein for screening blood schizontocidal agents. *International Journal for Parasitology* 34: 485-490.

37. Hein-Kristensen L, Wiese L, Kurtzhals JA, Staalsoe T. (2009) In-depth validation of acridine orange staining for flow cytometric parasite and reticulocyte enumeration in an experimental model using Plasmodium berghei. *Experimental Parasitology* 123: 152-7.

38. Somsak V, Srichairatanakool S, Yuthavong Y, Kamchonwongpaisan S, Uthaipibull C. (2012) Flow cytometric enumeration of Plasmodium berghei-infected red blood cells stained with SYBR Green I. *Acta Tropica* 122: 113-118.

39. Grimberg BT, Jaworska MM, Hough LB, Zimmerman PA, Phillips JG. (2009) Addressing the malaria drug resistance challenge using flow cytometry to discover new antimalarials. *Bioorganic & Medicinal Chemistry Letters* 19: 5452-7.

40. Karl S, Wong RP, St Pierre TG, Davis TM. (2009) A comparative study of a flow-cytometry-based assessment of in vitro Plasmodium falciparum drug sensitivity. *Malaria Journal* 8: 294.

41. Saito-Ito A, Akai Y, He S, Kimura M, Kawabata M. (2001) A rapid, simple and sensitive flow cytometric system for detection of Plasmodium falciparum. *Parasitology International* 50: 249-257.

42. Li Q, Gerena L, Xie L, Zhang J, Kyle D, Milhous W. (2007) Development and validation of flow cytometric measurement for parasitemia in cultures of P. falciparum vitally stained with YOYO-1. *Cytometry A*. 71: 297-307.

43. Bei AK, Brugnara C, Duraisingh MT. (2010) In vitro genetic analysis of an erythrocyte determinant of malaria infection. *The Journal of Infectious Diseases* 202: 1722-1727.

44. van Vianen PH, van Engen A, Thaithong S, van der Keur M, Tanke HJ, van der Kaay HJ, Mons B, Janse CJ. (1993) Flow cytometric screening of blood samples for malaria parasites. *Cytometry* 14: 276-280.

45. Wernli M, Tichelli A, von Planta M, Gratwohl A, Speck B. (1991) Flow cytometric monitoring of parasitaemia during treatment of severe malaria by exchange transfusion. *European Journal of Haematology* 46: 121-123.
46. Campo JJ, Aponte JJ, Nhabomba AJ, Sacarlal J, Angulo-Barturen I, Jiménez-Díaz MB, Alonso PL, Dobaño C. (2011) Feasibility of flow cytometry for measurements of *Plasmodium falciparum* parasite burden in studies in areas of malaria endemicity by use of bidimensional assessment of YOYO-1 and autofluorescence. *Journal of Clinical Microbiology* 49: 968-974.
47. Janse CJ, Van Vianen PH (1994). Flow Cytometry in Malaria Detection. In: *Methods in Cell Biology* 42: 295-318.
48. Rieckmann KH. (1982) Visual in vitro test for determining the drug sensitivity of *Plasmodium falciparum*. *The Lancet* 1: 1333–1335.
49. Delahunst C, Horning MP, Wilson BK, Proctor JL, Hegg MC. (2014) Limitations of haemozoin-based diagnosis of *Plasmodium falciparum* using dark-field microscopy. *Malaria Journal* 13: 147.
50. Orbán A, Butykai Á, Molnár A, Pröhle Z, Fülöp G, Zelles T, Forsyth W, Hill D, Müller I, Schofield L, Rebelo M, Hänscheid T, Karl S, Kézsmárki I. (2014) Evaluation of a novel magneto-optical method for the detection of malaria parasites. *PLoS One* 9: e96981.
51. Boura M, Frita R, Góis A, Carvalho T, Hänscheid T. (2013) The hemozoin conundrum: is malaria pigment immune-activating, inhibiting, or simply a bystander? *Trends in Parasitology* 29: 469-476.
52. Metzger WG, Mordmuller BG, Kremsner PG. (1995) Malaria pigment in leukocytes. *Transactions of the Royal Society of Tropical Medicine and Hygiene* 89: 637–638.
53. Hänscheid T, Pinto BG, Pereira I, Cristino JM, Valadas E. (1999) Avoiding misdiagnosis of malaria: a novel automated method allows specific diagnosis, even in the absence of clinical suspicion. *Emerging Infectious Diseases* 5: 836-838.
54. Phu NH, Day N, Diep PT, Ferguson DJP, White NJ. (1995) Intraleukocytic malaria pigment and clinical severity of malaria in children. *Transactions of the Royal Society of Tropical Medicine and Hygiene* 89: 200-204.
55. Amodu OK, Adeyemo AA, Olumese PE, Gbadegesin RA. (1998) Intraleucocytic malaria pigment and clinical severity of malaria in children. *Transactions of the Royal Society of Tropical Medicine and Hygiene* 92: 54-56.

56. Hänscheid T, Langin M, Lell B, Potschke M, Oyakhirome S, Kremsner PG, Grobusch MP. (2008) Full blood count and haemozoin-containing leukocytes in children with malaria: diagnostic value and association with disease severity. *Malaria Journal* 7: 109.
57. Hänscheid T, Egan TJ, Grobusch MP. (2007) Haemozoin: from melatonin pigment to drug target, diagnostic tool, and immune modulator. *The Lancet Infectious Diseases* 7: 675–685.
58. Suwanarusk R, Russell B, Ong A, Sriprawat K, Chu CS, PyaePhyo A, Malleret B, Nosten F, Renia L. (2015) Methylene blue inhibits the asexual development of vivax malaria parasites from a region of increasing chloroquine resistance. *Journal of Antimicrobial Chemotherapy* 70: 124-129.
59. Noedl H, Wongsrichanalai C, Wernsdorfer WH. (2003) Malaria drug-sensitivity testing: new assays, new perspectives. *Trends in Parasitology* 19: 175–181.
60. Fulton JD, Rimington C. (1953) The Pigment of the Malaria Parasite *Plasmodium berghei*. *Journal of General Microbiology* 8: 157-159.
61. Shapiro HM. (2003) Practical Flow Cytometry – 4th edition. New Jersey. John Wiley & Sons Inc.
62. Dechy-Cabaret O, Benoit-Vical F. (2012) Effects of antimalarial molecules on the gametocyte stage of *Plasmodium falciparum*: the debate. *Journal of Medicinal Chemistry* 55: 10328-10344.
63. Delves MJ, Ramakrishnan C, Blagborough AM, Leroy D, Wells TN, Sinden RE. (2012) A high-throughput assay for the identification of malarial transmission-blocking drugs and vaccines. *International Journal for Parasitology* 42: 999-1006.
64. Peatey CL, Leroy D, Gardiner DL, Trenholme KR. (2012) Anti-malarial drugs: how effective are they against *Plasmodium falciparum* gametocytes? *Malaria Journal* 11: 34.
65. Omucheni DL, Kaduki KA, Bulimo WD, Angeyo HK. (2014) Application of principal component analysis to multispectral-multimodal optical image analysis for malaria diagnostics. *Malaria Journal* 13: 485.

CHAPTER III

DEVELOPMENT OF THE HEMOZOIN DRUG ASSAY USING *P. FALCIPARUM* LABORATORY-ADAPTED STRAINS

This chapter is published in;

Rebelo M, Sousa C, Shapiro HM, Mota MM, Grobusch MP, Hanscheid T. (2013) A novel flow cytometric hemozoin detection assay for real-time sensitivity testing of *Plasmodium falciparum*. *PloS One* 8:e61606.

Author's contributions:

TH conceived the idea, initiated, oversaw and coordinated the completion of the project. MR and CS performed the sensitivity assays of various drugs. MPG, HMS and MMM contributed to the evaluation and provided advice on different aspects of the novel assay and its development, and contributed to writing and revising the final manuscript. MR and TH wrote the manuscript.

1. Abstract

Resistance of *Plasmodium falciparum* to almost all antimalarial drugs, including the first-line treatment with artemisinin, has been described, representing an obvious threat to malaria control. *In vitro* antimalarial sensitivity testing is crucial to detect and monitor drug resistance. Current assays have been successfully used to detect drug effects on parasites. However, they have some limitations, such as the use of radioactive or expensive reagents or long incubation times. Here we describe a novel assay to detect antimalarial drug effects, based on flow cytometric detection of hemozoin (Hz), which is rapid and does not require any additional reagents. Hz is an optimal parasite maturation indicator since its amount increases as the parasite matures. Due to its physical property of birefringence, Hz depolarizes light, hence it can be detected using optical methods such as flow cytometry.

A common flow cytometer was adapted to detect light depolarization caused by Hz. Synchronized *in vitro* cultures of *P. falciparum* were incubated for 48 hours with several antimalarial drugs. Analysis of depolarizing events, corresponding to parasitized red blood cells containing Hz, allowed the detection of parasite maturation. Moreover, chloroquine resistance and the inhibitory effect of all antimalarial drugs tested, except for pyrimethamine, could be determined as early as 18 to 24 hours of incubation. At 24 hours incubation, 50% inhibitory concentrations (IC₅₀) were comparable to previously reported values.

These results indicate that the reagent-free, real-time Hz detection assay could become a novel assay for the detection of drug effects on *Plasmodium falciparum*.

2. Introduction

Resistance of *Plasmodium falciparum* to almost all antimalarial drugs has been observed [1]. In fact, resistance to commonly effective and useful drugs such as chloroquine or sulfadoxine/pyrimethamine has severely compromised their use for malaria control [2]. Alarming, resistance to the currently used first-line treatment compounds, the artemisinins, characterized by a prolonged parasite clearance time [3], has already been reported from South-East-Asia. Consequently, detection and monitoring of drug resistance is of paramount importance.

Traditionally, therapeutic efficacy trials are the gold standard for assessing parasite response to antimalarial drugs. The obvious complexity of these trials led to the development of *in vitro* assays [4]. The major *in vitro* phenotypic assays include the WHO schizont maturation microtest [5], the isotope ($[^3\text{H}]$ -hypoxanthine) incorporation assay [6], the detection of the parasite antigens pLDH [7] or HRP2 [8] by ELISA, and assays using fluorescent DNA dyes, such as SYBR green I [9], YOYO [10], PicoGreen [11] and DAPI [12] with either spectrophotometric or cytometric readout (Table III.S1).

The development of novel antimalarial compounds hinges on assays to determine the inhibitory effects of drugs on the parasite [13]. Although all these assays have been successfully applied to detect drug effects on the parasite, they all have relevant limitations. For example, the WHO microtest is based on the tedious and subjective microscopic observation of parasite maturation [14]. The $[^3\text{H}]$ -hypoxanthine assay requires expensive equipment as well as complex isotope handling precautions and radioactive waste management [6]. All these assays require reagents for parasite detection that are often rather expensive and frequently require a cold chain. Importantly, they also need incubation times of 48 up to 96 hours to reliably detect drug effects [15].

Molecular methods are highly desirable, because they do not depend on viable parasites and have the capacity to provide rapid results. Their major drawback is the limited number of known and validated resistance markers [4]. It is important to note that there is currently no specific *in vitro* test to identify artemisinin resistance, as stated by an expert panel in the WHO Global Plan for Artemisinin Resistance Containment (GPARC) [16].

In this scenario, alternative assays that may overcome the limitations previously mentioned are highly desirable. An assay that would not only allow real-time determination of drug effects during a single parasite cycle but could also detect drug effects in a second or even

third cycle would certainly be a useful tool, permitting the assessment of inhibitory effects of drugs with different times of action.

Malaria pigment, i.e., hemozoin (Hz), is produced in increasing amounts by the parasite during the erythrocytic cycle and, therefore, constitutes an ideal maturation indicator. Hz, the end product of plasmodial hemoglobin metabolism, has been identified as an important modulator of the host's immune response to *Plasmodium* spp., as a marker for disease severity and prognostic factor for disease outcome, and also as an adjuvant diagnostic tool, of particular use regarding the non-immune traveler [17-19]. Hz depolarizes light and can be easily detected thereby without reagents by optical methods including dark-field microscopy [20], polarization microscopy [21] and flow cytometry [22].

In 1999, a study reported that the flow cytometry based full-blood-count analyser, Cell-Dyn® (Abbott, Santa Clara, CA), could detect Hz within leucocytes [23]. More importantly, studies reported that the Cell-Dyn® seemed to detect Hz inside parasitized red blood cells (RBC) [24], [25]. Based on the flow cytometric detection of depolarized side scatter [26], as used in the Cell-Dyn®, we showed that Hz could be detected inside parasitized RBC in *P. berghei* infected rodents [27]. Moreover, *in vitro* parasite maturation, as well as the inhibitory effect of chloroquine and quinine, could be detected after only 6 hours of incubation [27]. Later, we showed that maturation of *P. falciparum* in culture could also be determined [28].

Our present data show how flow cytometric detection of Hz can be used as a novel, reagent-free, real time assay to assess antimalarial drug effects on *P. falciparum*.

3. Material and Methods

All reagents were obtained from Sigma Aldrich (St Louis, Mo, USA), unless stated otherwise.

Flow cytometer modification (depolarized side scatter detection)

The Cyflow® Blue (Partec, Münster, Germany) is a portable (Figure SIII.1), five parameter flow cytometer with blue laser (488 nm) excitation, and detectors for forward scatter (FSC), side scatter (SSC), green fluorescence (FL1), orange fluorescence (FL2) and red fluorescence (FL3). For this study the set-up was modified as described elsewhere [27]. Briefly, two SSC detectors were created, with a 50%/50% beam splitter between them. Then a polarization filter was placed orthogonally (horizontal) to the polarization plane of the laser light (vertical), in front of one of the SSC detectors, allowing the detection of depolarized side scatter (Figure SIII.1). The Cyflow® is equipped with an absolute cell count method (<http://www.partec.com/instrumentation/flow-cytometry.html>, accessed 3/8/2012), which allows determination of the number of particles in 200 μ l of sample. Absolute counts were performed for all experiments to control for possible red blood cell lysis.

Microscopy

Parasitemia, parasite maturation and the synchronicity of parasites in culture were assessed by light microscopic examination of Giemsa-stained blood smears. Air-dried blood smears were fixed in absolute methanol and stained with Giemsa (Merck, Darmstadt, Germany) in a 1:10 dilution in PBS 1x, for 20 minutes.

Plasmodium falciparum continuous cultures

The *Plasmodium falciparum* resistant (Dd2) and susceptible (3D7) strains were grown in recently collected donor erythrocytes in RPMI based complete malaria culture medium (CMCM) according to the recommendations of the Malaria Research and Reference Reagent Resource Center (MR4) [29]. Cultures were maintained at 5% hematocrit, at 37°C in an atmosphere of 5% CO₂. As uninfected controls, erythrocytes from healthy donors were cultured as described above.

Synchronizing *Plasmodium falciparum* continuous cultures

Continuous cultures of *P. falciparum* were cultivated until they reached a parasitemia of >2% with a minimum of 50% rings. They were synchronized by adding 5% sorbitol for 10 minutes-at room temperature as described elsewhere [30]. Briefly, the culture medium was washed away by centrifuging the culture at 1800 rpm, for 5 minutes. Next, 10 mL of 5% sorbitol was added to the pelleted red blood cells and incubated for 10 minutes, at room temperature. Cultures were washed twice in PBS1x by centrifugation at 1800 rpm, for 5 minutes. Finally, CMCM was added to the pelleted cells, and the synchronized culture was incubated for another 48 hours, at 37°C in a 5% CO₂ atmosphere.

Hemozoin detection sensitivity assay

Ring stage synchronized cultures (at least 90% of ring forms) at 2.5% hematocrit and at approximately 1% parasitemia were incubated with antimalarial drugs or with CMCM (used for the drug free and uninfected controls) in 24 or 96 well-plates, for 48 hours, at 37°C in a 5% CO₂ atmosphere.

Quinine, chloroquine, mefloquine, artemisinin, artesunate, and pyrimethamine were purchased from Sigma Aldrich (St Louis, Mo, USA). NITD246 was kindly provided by Dr. Bryan Yeung from the Novartis Institute for Tropical Diseases, Singapore. Stock solutions of chloroquine and quinine were prepared in distilled water, artemisinin and mefloquine in pure methanol (Merck, Darmstadt, Germany), pyrimethamine in absolute ethanol (Merck, Darmstadt, Germany), artesunate in 70% ethanol and NITD246 in pure DMSO.

Doubling concentrations ranging from 6 to 200 nM for chloroquine, 10 to 160 nM for mefloquine, 12 to 200 nM for pyrimethamine and 4 to 64 nM for artesunate and artemisinin were tested. For NITD246 concentrations of 0.1, 0.2, 1 and 2 nM were used, while for quinine concentrations of 3, 12, 50, 200 and 800 nM were tested.

For each flow cytometric measurement approximately 100,000 events were analyzed. A volume of 5 μ L of the blood suspension present in the wells was stained with SYBR green 1x, as described below. To determine the best time point for IC₅₀ calculation, measurements were done at 6-hour intervals over 48 hours for the majority of the drugs tested, except for pyrimethamine which was measured again at 72 hours. All samples were analyzed in triplicate and, for each drug, at least 3 different experiments were performed. In order to investigate possible inoculation effects, artesunate and artemisinin were also investigated at a lower parasitemia of 0.4 and 0.7%, respectively.

To assess if renewing artesunate would influence its effect on parasite growth, cultures were washed and fresh artesunate, at a concentration of 8 nM, was added every 12 hours, during 48 hours of incubation.

To investigate the detection limit of the novel Hz assay, ring-stage synchronized cultures with parasitemias of 0.05%, 0.1%, 0.3%, 0.5%, 0.6% and 1% were incubated for 48 hours. Finally, to assess the performance of the Hz assay with low parasitemias, ring-stage synchronized cultures at 0.3% parasitemia were incubated for 72 hours with increasing concentrations of chloroquine, artesunate and pyrimethamine (as mentioned above). Flow cytometric analysis was performed in 24 hours intervals.

SYBR green I staining

For each measurement 5 μ l of the culture (approximately 800 000 cells) was stained with the DNA-specific dye SYBR green I (Invitrogen, Carlsbad, USA) at 1x. After 20 minutes of incubation, in the dark, the stained sample was immediately analyzed by flow cytometry using a 535/45 nm bandpass filter in front of the detector.

CD235 (glycophorin A) staining

A volume of 10 μ L of a continuous *P. falciparum* culture, at 5% hematocrit, was transferred into a well of a 96 well plate, washed in cold FACS buffer (PBS 1x and 2% bovine albumin serum) and then centrifuged at 1400 rpm, for 3 minutes at 4°C. A volume of 50 μ L of a 1:500 dilution of CD235-Phycoerythrin antibody (eBioscience, San Diego, US) was added to the cells and incubated for 20 minutes on ice in the dark. After a final wash, the cells were re-suspended in PBS 1x and analyzed by flow cytometry using a 610 nm long-pass filter.

Flow cytometric analysis

Flow cytometry results were analyzed using FlowJo software (version 9.0.2, Tree Star Inc., Oregon, USA). The gating scheme used is shown in Figure III.1. The red blood cells in uninfected and infected samples were detected by their characteristic forward (FSC) and side scatter (SSC) properties (Figure III.1A and B).

Staining with the anti-glycophorin A CD235 antibody was used to establish that all events detected represented red blood cells. The antibody was not used for routine analyses.

Depolarizing events were defined in plots of SSC versus depolarized-SSC as those with a signal above the background observed in the uninfected control (Figure III.1C and D).

To determine SYBR green I positive cells, green fluorescence (FL1) versus red fluorescence (FL3) plots were used; these provide better separation between weakly stained and autofluorescent cells than can be obtained from one-dimensional histograms. SYBR green I positive events (Figure III.1F) were established based on a stained uninfected control (Figure III.1E) and had to be adjusted at each time point, always using the uninfected SYBR green stained sample from the corresponding time point.

Histidine-rich protein-2 (HRP2) sensitivity assay

A histidine-rich protein-2 (HRP2) enzyme-linked immunosorbent assay (ELISA) was established and performed according to standard procedures [8], also available on the internet website <http://www.meduniwien.ac.at/user/harald.noedl/malaria/> (accessed 3/8/2012)

Ring-stage synchronized *P. falciparum* cultures, at an initial parasitemia of 0.05% and a 1.5% hematocrit, were incubated with the antimalarial drugs for 72 hours, at 37°C in a 5% CO₂ atmosphere. At the end, samples were frozen at -20°C until the HRP2 ELISA assay was performed.

Briefly, after two freezing and thawing cycles, 100 µL of the lysed sample was transferred to a 96 well-plate pre-coated with MPFM-55A antibody (Immunology Consultants Laboratories, Portland, USA) and incubated for one hour. The cells were washed three times and then incubated for another hour with the secondary antibody, MPFG-55P (Immunology Consultants Laboratories, Portland, USA). Cells were washed again and incubated for 5-10 minutes with the chromogen, TMB One (Biotrend, Köln, Germany). The reaction was stopped by adding sulphuric acid at 1M (Merck, Darmstadt, Germany) and the absorbance was immediately determined using the Infinite M200 plate reader (Tecan, Männedorf, Switzerland), at a wavelength of 450 nm.

To assess a possible inoculum effect of artemisinin, the HRP2 assay was also performed using a parasitemia of 1%.

Data analysis

A nonlinear regression model (sigmoidal dose-response/variable slope) was used to calculate the IC₅₀s, with SigmaPlot - Systat Software (Chicago, IL, USA).

4. Results

Depolarized side scatter detects parasitized red blood cells

Staining with the red blood cell surface marker (CD235) antibody was used to establish that the events detected represented red blood cells. Figure III.1G shows that 99.5% of events detected are red blood cells. Representative dot plots of side scatter versus depolarized side scatter are shown in Figure III.1C and III.1D. At 24 hours of incubation, depolarizing events were very low in the uninfected control (0.027%) (Figure III.1C), but could easily be detected (0.46%) in the infected blood sample (Figure III.1D). The depolarizing events present in the infected sample were also positive for SYBR green I. Analysis of SYBR green I fluorescence intensity showed that the majority of these depolarizing events (79.4%) had high fluorescence (pink line in Figure III.1H) indicating high DNA content and thus, represented parasitized red blood cells with mature parasites. All subsequent results reported in this paper are based on the depolarizing events expressed as a percentage of all events analyzed.

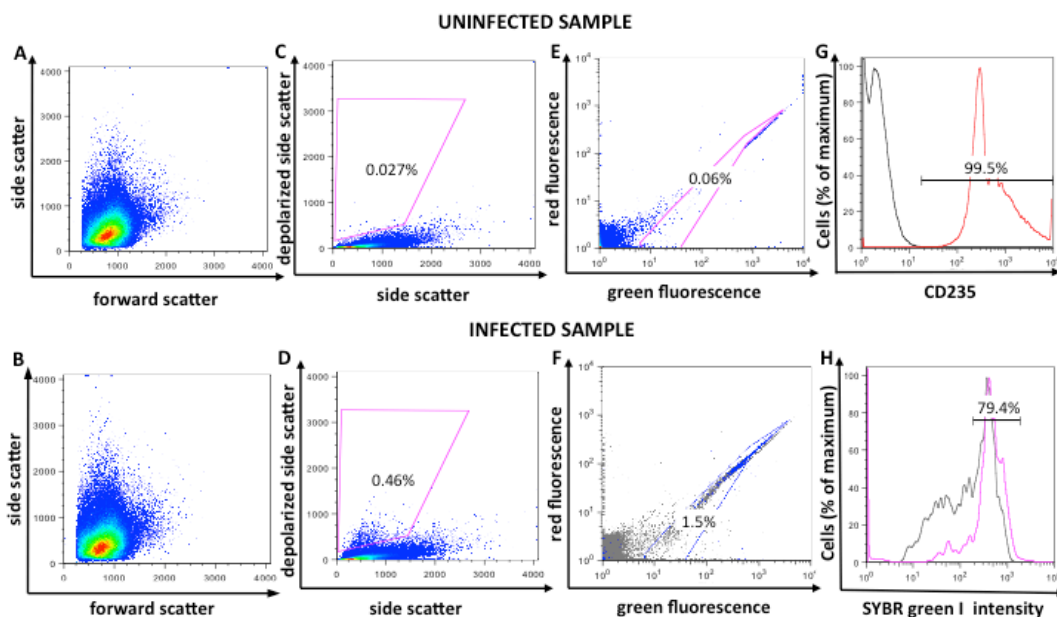


Figure III.1: Gating for detection of depolarizing parasitized red blood cells in a *Plasmodium falciparum* culture.

Flow cytometric analysis of an uninfected and a synchronized *P. falciparum* (3D7) infected culture (1.5% parasitemia) after 24 hours of incubation, stained with SYBR green I. Plots of forward vs. side scatter for the uninfected and infected cultures appear in Figures A and B; corresponding plots of side scatter vs. depolarized side scatter appear in Figures C and D. The gates in Figures C and D identify the depolarizing events.

Figures E and F (see text) illustrate gates defining SYBR green-positive parasitized cells. The blue dots on Figure F represent the depolarizing events.

Staining with the red blood cell surface marker (CD235) shows that 99.5% of events in a stained sample (red line) exhibit fluorescence above the highest level measured in an unstained control

(black line), indicating that the detected events are red blood cells (G).

In the SYBR green I histogram (H) of the infected culture, the overall population (black line) shows a distinct peak with a high fluorescent intensity in the third decade. This peak corresponds mainly to the gated population of depolarizing events (pink line). Because SYBR green I intensity correlates with DNA content and thus with parasite level of maturation, the depolarizing population (pink line) consists mainly (79.4%) of mature parasites. The highly red- and green-fluorescent events visible outside the SYBR green gate just to the right of its apex represent contaminating white blood cells among the donor red cells.

Depolarized Side Scatter detects parasite maturation

We next sought to establish whether this type of analysis would discriminate among different *Plasmodium falciparum* stages. To that end, samples of 100,000 events were analyzed. Determination of the absolute number of cells at each time point showed no evidence for red blood cell lysis. Following the percentage of depolarizing events during 48 hours of incubation, in a ring-stage, synchronized culture (1.4% parasitemia), showed an increase at 18 hours, with a peak at 30 hours and a subsequent decrease (Figure III.2A). The same sample stained with the DNA stain, SYBR green I, showed no change in the percentage of fluorescent events until 30 hours, followed by a steady increase until 48 hours (Figure III.2B). Observation of Giemsa stained blood smears at all time points showed parasite maturation until 30 hours, which coincided with the peak of depolarizing events. Thereafter, from 36 to 48 hours, immature forms were observed, coinciding with a decrease of depolarizing events and an increase of fluorescent events (Figure III.2). These changes reflect parasite growth with the 30 hour peak of depolarization corresponding with the peak of maturation, after which erythrocytes rupture and daughter-merozoites are released along with Hz, explaining the decrease in depolarizing events and the increase in SYBR green I fluorescent events, observed after 30 hours.

The increase in the percentage of depolarizing events over time and the inhibitory effect of chloroquine, artesunate and pyrimethamine could be detected at parasitemias down to 0.3%. At lower parasitemias (0.05 and 0.1%) no clear increase above the background could be detected during the first 48 hours of incubation.

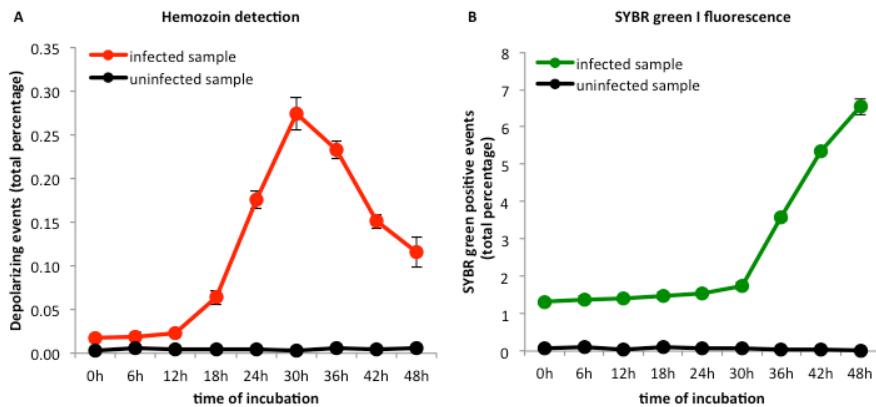


Figure III.2: Growth curves of *Plasmodium falciparum* (3D7) in culture.

Flow cytometric analysis of a synchronized *P. falciparum* (3D7) culture (1.4% parasitemia). The percentages of depolarizing events (A) and SYBR green I positive events (B) were followed for 48 hours in uninfected (black lines in A and B) and infected red blood cells (red line in A and green line in B). Analysis of depolarizing events (Hz-containing parasitized erythrocytes) shows an increase at 18 hours, peaking at 30 hours (A). SYBR green I positive events (parasitized RBC) remain unchanged at 1.4% until 30 hours, after which a steady increase can be noted (B). Hz detection reflects parasite maturation with increasing amounts of Hz until 30 hours, while the parasitemia remains unchanged (SYBR green I positive events). After 30 hours, increasing SYBR green I positive events indicate replication and presence of immature forms, which explains the decrease observed in the depolarizing population. Each time point represents the mean value of triplicate samples \pm one SD. Red blood cell lysis was excluded by absolute cell counts, which remained stable.

Detection of inhibitory effects of chloroquine on sensitive (3D7) and resistant (Dd2) *P. falciparum* strains

Using a chloroquine sensitive strain (3D7), the difference between inhibiting and non-inhibiting concentrations was clearly visible after 18 hours, with the largest difference observed at 30 hours (Figure III.3A). The first sign of drug effect could be consistently detected at 18 hours, where at concentrations of 6 and 12 nM a percentage of 0.1% depolarizing events were observed, while at 25, 50 and 100 nM only 0.004% were detected (Figure III.3A).

In the resistant *P. falciparum* strain (Dd2), chloroquine resistance could clearly be detected at 18 hours after drug exposure, with growth curves of all concentrations following the drug free control (Figure III.3B). At this time point (18 hours), in all drug concentrations around 0.1% depolarizing events were observed, compared to the 0.01% seen at the beginning of the incubation (Figure III.3B).

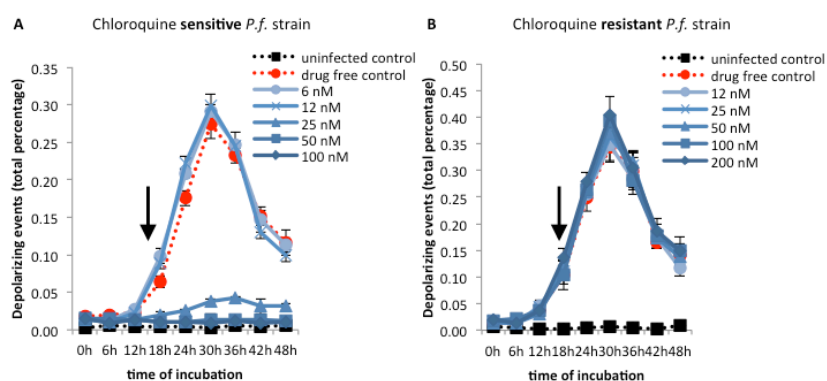


Figure III.3: Effect of chloroquine on the growth curve of *P. falciparum* sensitive and resistant strains.

Synchronous cultures of sensitive (3D7, parasitemia of 1.3%) and resistant (Dd2, parasitemia of 1.4%) *P. falciparum* strains were incubated for 48 hours with doubling concentrations of chloroquine and analyzed at 6 hourly intervals. The inhibitory effect of chloroquine at higher concentrations (>25 nM) is clearly visible (arrow) after 18 hours of incubation (A). The resistant strain can easily be distinguished from the sensitive strain with growth curves of all drug concentrations being identical to the drug free control (B). Each time point represents the mean value of triplicate samples \pm one SD.

Detection of inhibitory effects of other antimalarial drugs

Representative growth curves in the presence of different concentrations of quinine, mefloquine, artemisinin and the spiroindolone NITD246 are shown in Figure III.4. The curves for artesunate are shown in Figure III.5 and those for the slow acting drug, pyrimethamine, are shown in Figure III.6. As was the case with chloroquine, inhibitory concentrations showed a clear effect from 18 hours onwards in three different compound classes: quinolones (quinine and mefloquine), endoperoxides (artemisinin and artesunate) and a spiroindolone (NITD246).

Interestingly, artemisinin showed a delayed growth curve at the 32 nM concentration in comparison to the drug free control (Figure III.4C). The same was observed for artesunate at a lower concentration of 4 nM (Figure III.5A). Of note, the artesunate growth curve at an intermediate concentration of 8 nM showed an initial inhibition with a delayed rise starting after 30 hours and an absence of the typical peak at 24 – 30 hours (Figure III.5A and B). By renewing the artesunate every 12 hours in the culture medium, this delayed rise was lost and the initial inhibition was maintained throughout the 48 hours of incubation (Figure III.5B). In both cases, however, the percentage of SYBR green I positive events remained largely unchanged over the 48 hours of incubation, indicating absence of parasite replication (Figure III.5C). The parasites, previously treated only once with artesunate at 8 nM, were also re-cultured and observed for growth during four days. No growth was

observed during these 4 days, as confirmed by flow cytometry, nor was an increase in either depolarization or SYBR green percentage and intensity observed.

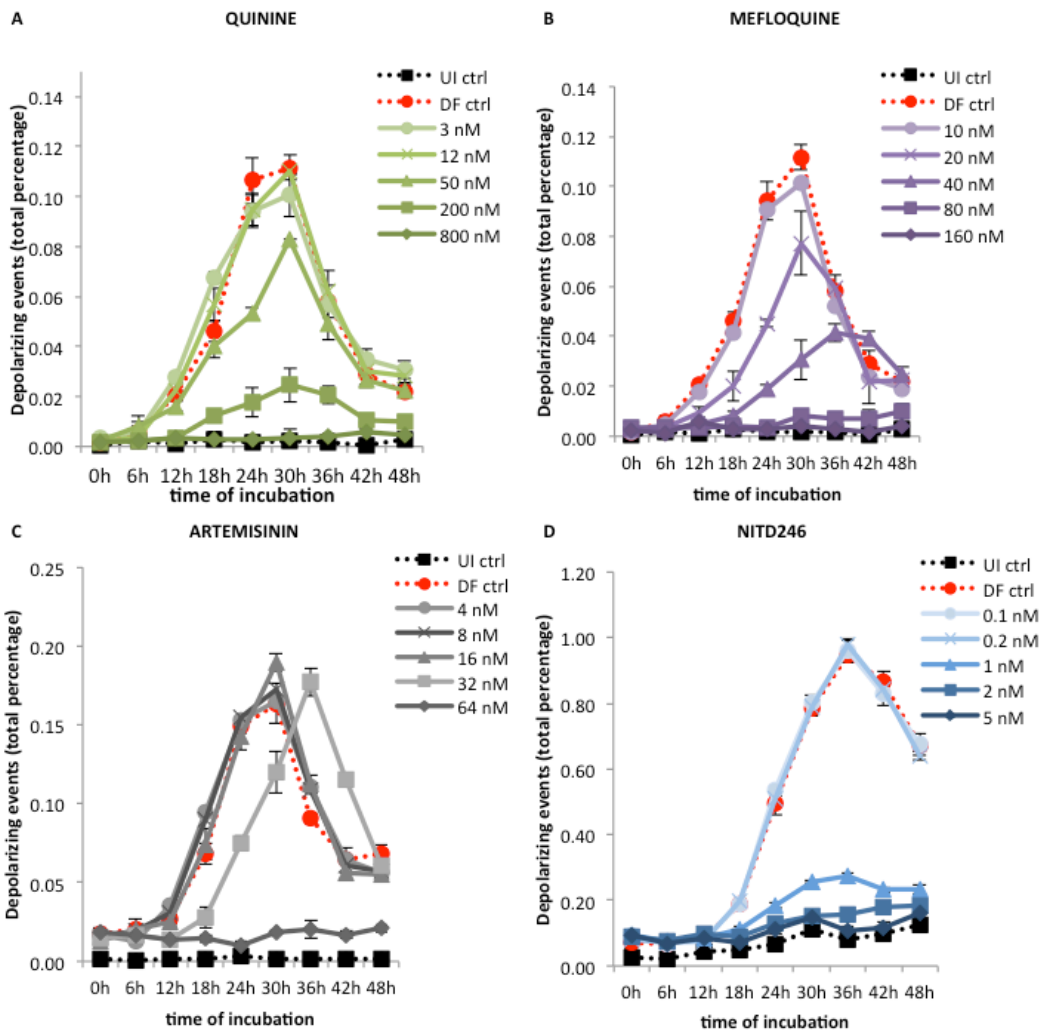


Figure III.4: Effect of quinine, mefloquine, artemisinin and a spiroindolone (NITD246) on the growth curve of *P. falciparum* (3D7).

Synchronous cultures of a *P. falciparum* 3D7 strain were incubated for 48 hours with increasing concentrations of quinine (A), mefloquine (B), artemisinin (C) and NITD246 (D). In all cases the dose-dependent inhibitory effect of the drugs could already be detected at 18 hours by comparing the treated samples (solid lines) with the drug free control (dotted red line). The curves allowed the determination of IC₅₀ values at 24 hours. Of note, artemisinin at 32 nM showed a 6 hour delayed growth curve, from 18 to 42 hours, with the peak of maturation occurring at 36 hours. Each time point represents the mean value of triplicate samples \pm one SD. DF ctrl – drug free control; UI ctrl – uninfected control.

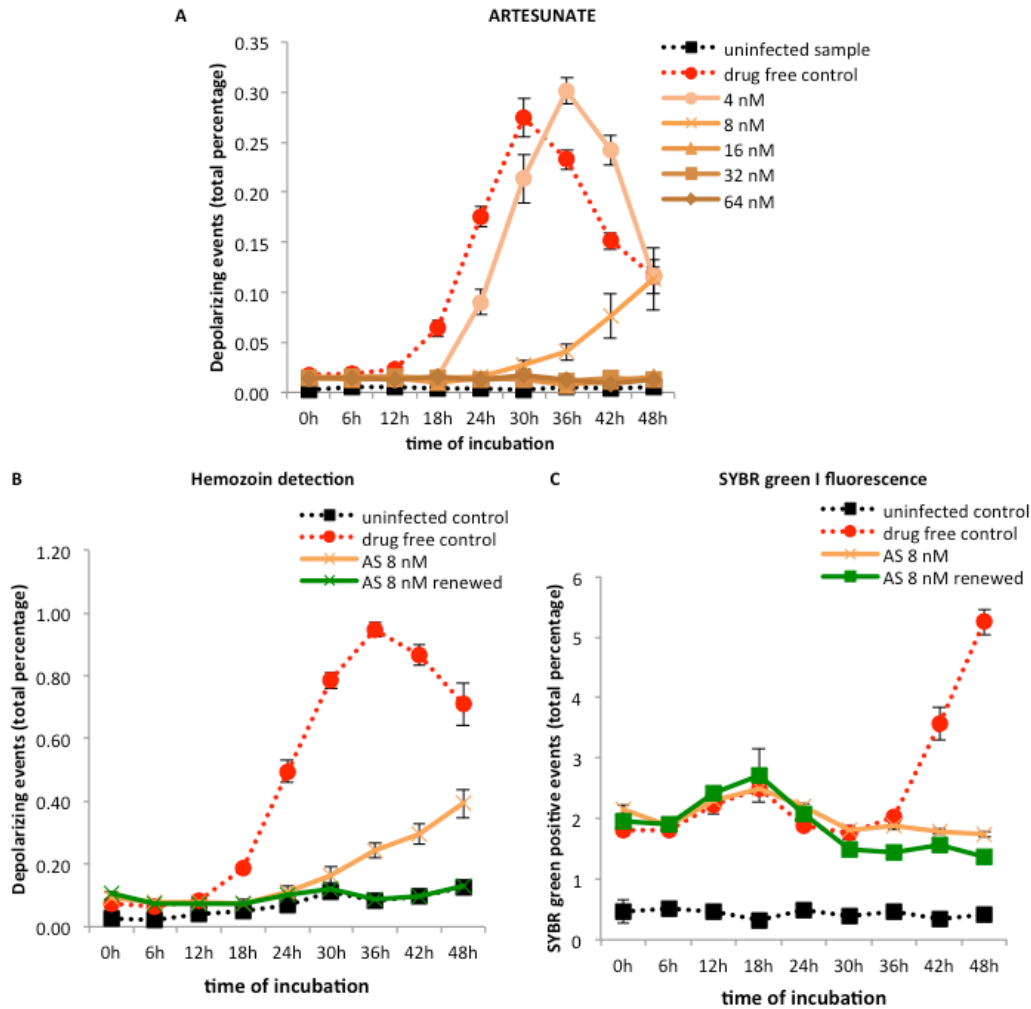


Figure III.5: Effect of artesunate on the growth curve of *P. falciparum* (3D7) and the effect of 12 hourly renewing of artesunate during incubation.

Synchronous cultures of a *P. falciparum* 3D7 strain were incubated for 48 hours with doubling concentrations of artesunate (A) or with a single concentration of 8 nM of artesunate for the whole time or renewed at 12 hour intervals (B and C). Figures A and B show detection of Hz (depolarizing events) while Figure C shows detection of SYBR green I fluorescence (DNA in parasites). The inhibitory effect of artesunate was already detectable after 18 hours of incubation (A). Similar to artemisinin (Figure III.4C), the growth curve of artesunate at 4 nM showed a 6 hourly delayed growth curve from 18 to 42 hours, including a 6 hour delay in the peak, occurring at 36 hours. Interestingly, the growth curve at 8 nM seemed to show inhibition until 30 hours, when a slight increase was observed (A and B). However, renewing artesunate at 12 hourly intervals eliminates this effect (green line in B). The percentage of SYBR green I positive events remained approximately the same during the 48 hours of incubation (C). This indicates that parasites at the non-renewed 8 nM concentration showed some maturation as indicated by Hz detection but were unable to replicate. Each time point represents the mean value of triplicate samples \pm one SD.

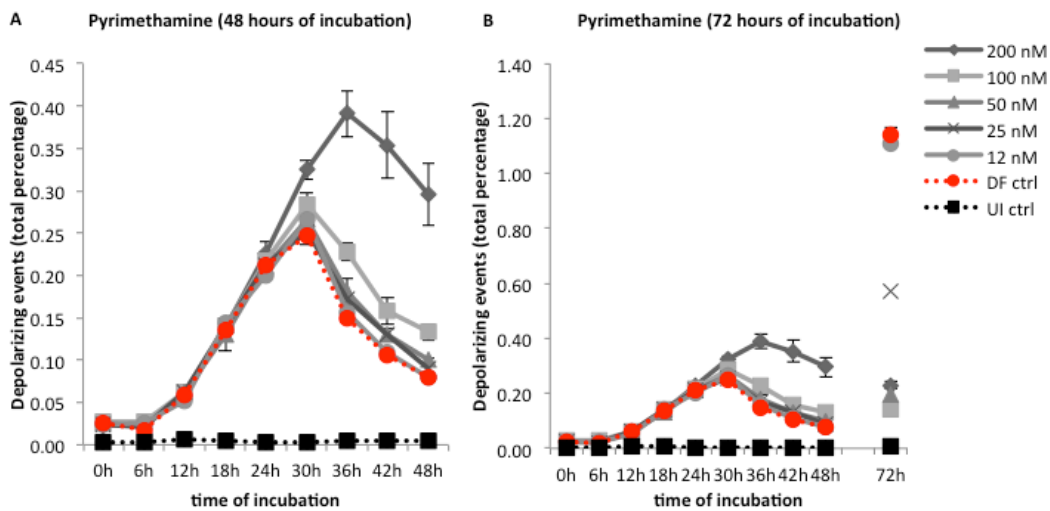


Figure III.6: Growth curve of *Plasmodium falciparum* (3D7) after treatment with pyrimethamine.

Synchronous cultures of a *P. falciparum* 3D7 strain were incubated for 72 hours with doubling concentrations of pyrimethamine. No inhibitory effect could be observed during the first 48 hours at any concentration (A). However, an inhibition was clearly visible at 72 hours (B). This could be explained by the fact that pyrimethamine is a slow acting drug and its effect can only be detected on the second generation, after 48 hours.

Interestingly, the growth curves at all concentrations follow the drug free control after the 30 hour peak, while the curve for 200 nM shows a later peak at 36 hours with a higher number of depolarizing events, compared to the drug free control (A). See discussion for possible explanation. Each time point represents the mean value of triplicate samples \pm one SD. DF ctrl – drug free control; UI ctrl – uninfected control.

IC50 values obtained by the Hemozoin detection assay are comparable with other available assays

To determine the earliest time-point that would allow us to reliably calculate IC50 values, results obtained from the Hz detection assay at different time-points (18, 24, 30 and 36 hours) (Table III.1) were compared with those reported in the literature (Table SIII.2), as well as with results from the already validated HRP2 ELISA assay (Table III.2). This analysis led us to use the 24 hour time point for all subsequent IC50 calculations. The IC50 results for our Hz assay and the HRP2 assay are shown in Table III.2.

Concerning the inoculum effect, no reliable results could be obtained with the HRP2 assay at a parasitemia of 1%, because no differences were observed between the drug treated samples and the drug free control. Using a lower parasitemia in the Hz assay, discrepant results were observed for artemisinin and artesunate: while the IC50 of artesunate remained the same (4 nM) at a parasitemia of 1.3% and 0.4%, the IC50 value for artemisinin decreased from 32 nM at 1.0% parasitemia to 13.2 nM at a parasitemia of 0.7%.

Table III.1: Inhibitory concentrations (50%) of several antimalarial drugs against *P. falciparum* 3D7 strain determined by the Hemozoin detection assay at different times of incubation.

	Time of incubation				
	18h*	24h	30h*	36h*	72h*
Chloroquine	41.9 nM (± 19.3)	34.2 nM (± 8.1)	33.6 nM (± 10.1)	35.9 nM (± 8.9)	29.6 nM (± 7.4)
Quinine	98.5 nM	54.6 nM (± 9)	92.2 nM	142.7 nM	45 nM
Mefloquine	17.2 nM	21.3 nM (± 7)	33.5 nM (± 6.4)	64.9 nM (± 20.2)	19.5 nM
Artemisinin	28.2 nM (± 3.5)	25.6 nM (± 5.9)	34.5 nM (± 5.8)	43.7 nM (± 16)	n.d.
Artesunate	< 4 nM	6.4 nM (± 2.3)	10.8 nM (± 3.6)	12.4 nM (± 6.3)	n.d.
Pyrimethamine	X	X	X	X	25.4 nM (± 10.3)

Mean inhibitory concentration values (50%) ± one standard deviation are presented.

Standard deviation values are not shown for results that were not supported by at least three independent experiments. Time-points identified with (*) were not systematically analyzed, since the 24 hour time-point was used as the preferential time-point to reliably calculate IC50 values (as discussed in the manuscript).

(X) values could not be determined; (n.d.) no data available.

Table III.2: Antimalarial activities of several antimalarial drugs determined by the Hemozoin detection assay and the HRP2 assay.

	Hemozoin detection* 24 hours of incubation	HRP2 72 hours of incubation
Chloroquine	34.2 nM (± 8.1)	22 nM
Quinine	54.6 nM (± 9)	52 nM
Mefloquine	21.3 nM (± 7)	21 nM
Artesunate	6.4 nM (± 2.3)	1.1 nM
Artemisinin	25.6 nM (± 5.9)	11.5 nM
Pyrimethamine	25.4 nM (± 10.3) ¹⁾	30.5 nM
NITD 246	0.8 nM	0.4 nM

The averages of 50 % inhibitory concentration values ± one standard deviation are presented above.

* For the Hemozoin detection assay each drug was tested at least three times (except for the novel compound NITD246).

HRP2 – Histidine-rich protein 2.

1) after 72 hours of incubation

5. Discussion

This study confirms that the optical detection of Hz can be easily achieved by a simple adaptation of a common flow cytometer to allow detection of light depolarization (Figure SIII.1). This study also extends observations [27] that maturation of *P. falciparum* and inhibitory antimalarial drug effects can be assessed by the detection of Hz inside intra-erythrocytic parasites. Although this novel approach is based on previous observations that Hz in parasitized RBC could be detected by flow cytometric methods [24], [27] it should be noted that the idea of using Hz for a sensitivity assay is not new and was described in the 1980s [31]. However, the assay format used a visual readout and appears to have been rather inaccurate because of nonspecific agglutination [32]. Recently, an improvement of this approach has been reported where the Hz produced is measured by a colorimetric method [33]. To do this, the Hz produced by the parasites after 72 hours of incubation is liberated and transformed back into heme before reading the absorbance at 405/750 nm. However, the assay involves multiple manipulation steps, including lysis and several washing steps, which are cumbersome and may introduce variability. In fact, in our hands, the isolation of Hz and quantification of heme requires meticulous attention to accurate pipetting to guarantee reproducible results [34].

Depolarization signal strength and detection limit

The comparison of an uninfected RBC sample with a synchronized *P. falciparum* infected RBC sample at 24 hours of incubation showed a depolarizing population that could be easily identified and gated (Figure III.1C and D). However, the degree of depolarization of the whole population was much lower than previously described for *P. berghei* infected blood samples [27]. A possible explanation for this may be different side scatter signals, which are a measure of cell granularity [35], that could be caused by the different shape and distribution of the Hz crystals within these parasites. A parasite containing several small but distributed Hz crystals will have a higher depolarized side scatter signal than a parasite containing a single big Hz crystal. In fact, during this and previous work, the routine microscopic analysis of Giemsa stained blood smears to control the parasitemia showed that Hz started to appear in small dispersed fine granules in *P. berghei* and only clumped together by the end of schizogony, as previously observed by Warhurst et al. [36], while in *P. falciparum*, Hz crystals aggregate as they start to appear (data not shown). It also appears possible that the depolarization signal can still be improved as a result of

technical modifications to the instrument. The Cyflow® flow cytometer uses a blue laser (488 nm). However, longer wavelengths may increase the depolarization signal as has been described for a red HeNe (633 nm) or Kr⁺ laser (647 nm) [18]. Furthermore, the polarization ratio of most solid-state lasers is usually given as >1:100. If the laser had a higher polarization ratio, as do HeNe and Kr⁺ lasers, positive depolarization signals might be better distinguished from background noise.

To assess parasite maturation and drug effects we chose to use the simple ratio of all identifiable depolarizing events as a percentage of all events analyzed (Figure III.1C and D). Other measurements, like depolarizing intensity, showed no clear advantage (data not shown). A parasitemia of 1% proved to be the optimal parasitemia to detect parasite maturation and growth over 48 hours. Thus, it was used in the Hz detection assay to obtain time-curves when investigating the drug effects in *P. falciparum in vitro* cultures. However, an initial 1% parasitemia is higher than the ones used in other assays, such as the HRP2 or the WHO schizont maturation test, which can use parasitemias as low as 0.02% [8], [37], [38]. However, when investigating the lower detection limit of the Hz assay, parasite maturation and drug effects of chloroquine, artesunate and pyrimethamine could still be clearly detected at parasitemias as low as 0.3%. Nevertheless, this remains higher than the ones used for the HRP2 assay and the WHO schizont maturation test. Still, it is comparable to the parasitemias used in other assays, such as the [3H]-hypoxanthine assay (0.25 – 0.5%) [6] or the SYBR green I assay (0.5 - 1%) [9], [39], [40] (Table SIII.1).

Of note, in all Hz assay experiments, only around 30% of all parasites were typically detected by depolarization measurements (Figure III.1D) as compared to microscopy or SYBR green I fluorescence. The reasons for this are unclear and could be a consequence of the culture not being highly synchronized. At the 30 hour peak of maturation, schizonts as well as some second generation ring forms are present, as confirmed by microscopy; the immature ring forms have insufficient Hz to be reliably detected [28]. Another possible explanation is the already mentioned Hz aggregation that occurs in the mature parasites, which may reduce side scatter intensity.

Certainly, the initial parasitemia of 0.3% required is still a major limitation of this assay if used directly with patient blood samples, some of which may have lower parasitemias [41]. However, further optimization of the assay may lead to an improvement of the detection limit. Nevertheless, future studies conducted in the field will allow us to evaluate the performance of the novel Hz detection assay using *ex vivo* patient samples.

Aspects of parasite maturation

Using a red blood cell surface marker (CD235) (Figure III.1G) and a DNA stain (SYBR green I) we showed that the depolarizing events (Figure III.1F) were indeed infected red blood cells. SYBR green I fluorescent intensity reflects DNA content [42], [43]. Most of the depolarizing events showed high SYBR green I fluorescence (80%), indicating that they were mature parasites (Figure III.1H). Comparing depolarization and fluorescence intensity in a *P. berghei* ANKA infected sample stained with SYBR green I showed, similarly, that the level of depolarization appears to reflect parasite maturation [27].

Usually, the described *P. falciparum* life cycle lasts 42 – 48 hours *in vitro* [44]. Contrary to this, we observed a peak of parasite maturation earlier, at around 30 hours, as reflected by the peak in depolarization (Figure III.2A) followed by a steady increase in SYBR green I positive events indicating replication (Figure III.2B). Corresponding parasite forms were also observed during microscopic observation of Giemsa stained blood smears. This can be explained by the fact that because the assay did not start immediately after re-invasion, the indicated time points correspond to the time post-drug-treatment and not the time post-invasion. Moreover, the fact that cultures were not highly synchronized seem to have contributed to this apparent shorter life cycle. It is known that to obtain highly synchronized cultures, at least one other sorbitol treatment would be needed [45].

After a single synchronization approximately 90% of the parasites are ring forms. However, individual parasites can present differences of several hours in their development. Thus, at the beginning of the experiments, some parasites may have already developed for 12 hours within the ring form population while others are only 6 hours into their development. The microscopic observation of Giemsa stained blood smears at 36 hours gives weight to this reasoning, because both schizonts and second generation ring forms could be observed at this time point.

Drug effects and potential use of the Hz assay

One of the major advantages of the Hz detection assay is the fact that samples can be easily analyzed without further preparation or additional reagents allowing a rapid and easy real-time assessment of parasite maturation and drug effects. For instance other assays, such as the [3H]-hypoxanthine assay, cultures have to be incubated for additional 24 hours with the isotope before measurements are possible [6], [15], [46], [47], [48]. Another advantage is the very early detection of inhibitory drug effects after only 18 hours (Table III.1 and

Figures III.3, III.4 and III.5), in contrast to several other assays, such as the [3H]-hypoxanthine [6], [44] assay, which measures drug effects at 48 hours, and the SYBR green I [15], [40], [49], [50] and the HRP2 [8], [15], [51], [50] assays, which require at least 72 hours.

Although, for example, chloroquine sensitive and resistant strains are easily distinguishable after only 18 hours (Figure III.3) using the Hz assay, the inhibitory effect of the slow acting drug pyrimethamine could only be detected after 72 hours (Figure III.6). This drug has no effect on asexual parasites in the first half of the parasite life cycle (24 hours) [41], [52] and effects can only be detected later in the second parasite generation. For this reason the Hz assay detects slow acting drugs effects, such as pyrimethamine, only after 72 hours of incubation. Interestingly, at concentrations of 200 nM, higher depolarization values were observed after 30 hours (Figure III.6A), which appear to reflect the observed schizont arrest observed by microscopy.

As shown in Table III.1, the Hz detection assay allows determination of a drug's inhibitory concentrations at different time-points during the first and second life cycle, thus extending its potential usefulness.

Artemisinins in the Hz assay

Artemisinin and artesunate growth curves were different from the other tested drugs. At concentrations of 32 nM and 4 nM, respectively, a delayed maturation was observed, starting at 18 hours (Figures III.4C and III.5). However, the SYBR green measurements performed simultaneously indicated that the parasites replicate, reaching approximately the same parasitemia as the drug free control after 48 hours of incubation (data not shown). The reason for this observation remains unclear. Furthermore, samples treated with 8 nM of artesunate showed an initial inhibition with a delayed rise after 30 hours (Figures III.5A and B). SYBR green I measurements, however, did not change over the 48 hour incubation period, indicating that the parasites were somehow able to mature but unable to replicate (Figure III.5C). These parasites, treated a single time with 8 nM of artesunate, were re-cultured in CMCM and no growth could be observed during the following four days. Interestingly, similar behavior has been previously described for artemisinin [53] and was interpreted as a consequence of its rapid degradation [54]. The drug level had to be kept constant by replacing the media with the drug every 24 hours, otherwise the number of viable parasites increased at 96 and 120 hours after drug addition [53]. In fact, renewing the artesunate every 12 hours in the culture medium showed that the inhibition was

maintained throughout the 48 hours of incubation and the delayed rise was lost (Figure III.5B).

Dormancy has been described after treatment with artemisinin, where early stage parasites enter a dormant stage under drug pressure but later regrow [55]. It has been reported that parasites treated with dihydroartemisinin arrested their development shortly after drug exposure, but after 9 days 50% of the parasites managed to resume their growth [58]. Thus, to detect recrudescence of these dormant parasites cultures would have to be monitored for at least 4 life cycles (9 days = 216 hours). Our findings showed a delayed increase during the first life cycle (after 30 hours of incubation), in samples treated with artesunate at 8 nM. Although this might represent the detection dormancy and parasite recrudescence, the data we have obtained so far are not sufficient to confirm or exclude this hypothesis, because these parasites were not monitored for longer than four days. Further investigation is needed to clarify this issue.

Comparison of IC₅₀ values

The IC₅₀ determined by the Hz detection assay were comparable with the ones reported for other, already validated assays (Tables III.1, III.2 and SIII.2). However, slightly higher values were observed for some of the drugs, especially for artesunate, where most publications report values below 2.5 nM [15], [37], [47]. One explanation could be the inoculum effect, i.e., an increase in the inhibitory drug concentration when greater numbers of parasites are inoculated. This is thought to be the consequence of some drug accumulating inside the parasitized RBC [56] and has been described for drugs like artemisinin and artesunate, as well as for chloroquine and mefloquine [57]. In fact, in the Hz assay parasitemias of around 1% were used as compared to other assays, which used parasitemias range from 0.05 to 0.5 % [37], [58]. This might explain the increased IC₅₀ values observed in the Hz detection assay and interestingly, a decrease in the parasitemia from 1.4% to 0.7% led to a decrease in the artemisinin IC₅₀ value from 32 to 13.2 nM. However, no such decrease was observed with artesunate.

It is important to note, that the comparison of IC₅₀ values between assays can be misleading. The IC₅₀ values in the literature vary substantially between assays, even for the same strain. For instances, the standard [3H]-hypoxanthine incorporation assay shows differences of 2 to 23 fold for artesunate (Table SIII.2). Not too surprisingly, one study reported that the reliability of the assays may be influenced by the mechanism of action of

individual drugs [15]. Moreover, variations in parasite density and hematocrit as well as the stage-dependent action of antimalarial drugs, may have a significant impact on the outcome of these sensitivity assays [14], [57].

Assay – prospects, future possibilities

Because the Hz detection assay allows parasite maturation to be monitored in real time, it could possibly be used to investigate drug effects on different parasite developmental stages (stage specificity of drugs). It might also be interesting to assess the performance of the assay with parasite strains that have been reported to show clinical signs of resistance to artemisinins. Since modeling of parasite-clearance curves suggests that artemisinin resistance affects ring-stage parasites more than the more mature parasite stages, thus *in vitro* tests focusing on the inhibition of ring stage parasites could become valuable surveillance tools [58].

The fact that a flow cytometer is required may pose an obstacle to the widespread use of the Hz assay in the field. Furthermore, flow cytometers that use fiber optic cables for light collection, such as the BD LSRFortessa or FACSaria, require relatively elaborate optical modification to detect depolarization. However, detection of depolarization as we have described can be implemented simply on many existing flow cytometers, for example the flow sorter Influx (<http://www.bdbiosciences.com/instruments/influx/features/index.jsp>, accessed 14/08/2012), the Cyflow Cube (Danny Koehler, Partec, Münster, Germany, personal communication), the Life Technologies Attune (Grace Chojnowski, Queensland Institute of Medical Research, Brisbane, Australia, personal communication), and can even be retrofitted to the venerable BD FACSCalibur (Lisa Nichols, Cytex Development, Fremont, CA, USA, personal communication). More importantly, some low-cost flow cytometers for CD4 counts in resource-poor countries could be modified rather easily to detect depolarization, and are already available on site in several African countries (<http://www.partecnorthamerica.com/Press-Release-01Dec2012-b2.html> accessed 22/12/12).

Furthermore, it is now evident [59] that optical measurements of both DNA and Hz can be made in small, robust, simple, widefield multiparameter optical imaging apparatus an order of magnitude less expensive than a typical flow cytometer, using LEDs costing only a few dollars for illumination and employing camera chips only slightly higher in quality than those used in mobile phones as detectors. Signals from all cells in an entire well of an assay microplate can be analyzed in seconds, without the need for precise stage motion or

focus adjustment. Somewhat more elaborate and expensive versions of such devices are already commercially available; minimalist instruments optimized for field use in the resource-poor areas in which malaria is prevalent should arrive within a few years.

In conclusion, the novel Hz detection assay allows parasite maturation to be monitored in real time without the need of further reagents or sample preparation. The assay detects inhibitory drug effects of major antimalarial drug classes after only 18 hours of incubation and permits determination of IC₅₀ values at 24 hours. Future work will have to address the utility of this assay in the field. Issues such as the use of less expensive alternatives to flow cytometry and the application of the assay to such tasks as the determination of stage specific effects of antimalarial drugs will have to be investigated further.

6. Acknowledgements

This work was supported by the Luso-American Foundation (FLAD-LACR grant: B-A.V-109-09/07)

7. Ethical approval

The study was approved by the Ethics Committee of the Medical Faculty of the University of Lisbon.

Erythrocytes were isolated from so-called buffy-coats obtained from the blood bank of the Portuguese Blood Institute (Instituto Português do Sangue – IPS). When producing erythrocyte concentrates for transfusion, the leukocyte-bearing buffy coat fraction, removed by centrifugation, still contains substantial amounts of red blood cells. The buffy coats, which are routinely discarded as they have no further medical use, are in individual packs, devoid of any information regarding the original donor (completely anonymized). We isolated the erythrocytes from these discarded and anonymous buffy coats. The erythrocytes were only used as a culture medium, and therefore no results for any individual donors were obtained, even more so as erythrocytes were often pooled. Thus, given the circumstances, no consent was obtained.

8. Supporting information

Table SIII.1: Comparative descriptions of available *in vitro* sensitivity assays for *Plasmodium falciparum*

	Microtest	Hypoxanthine incorporation	Flow cytometric assays	Fluorometric assays	HRP2 assay
Principle of the assay	Quantification of schizonts	Measurement of parasite DNA			Antigen detection
Time of incubation with the drugs	30h	48h	48h	48 - 96h	72h
Volume of sample to analyze	10 – 50 µL	200 µL	25 - 100 µL	10 – 200 µL	100 µL
Hematocrit	1.5 – 20%	1 – 2.5%	2.5%	1.5 – 2.5%	1.5%
Parasitemias:					
Laboratory strains	1%	0.5%	0.25 – 1%	0.5 -1%	0.05%
Clinical isolates	0.02%	0.1-0.5%	(n.d.)	0.5 - 1%	0.05%
Required equipment and Infrastructure	Bright field microscope	Scintillation counters and harvesting machine and infrastructure	Flow cytometer	Microplate fluorometer	Microplate spectrophotometer
Advantages	- Requires little equipment.	- Automatic reading of results. - Accurate and sensitive.	- Automatic reading of results. - Accurate and sensitive.	- Simple, does not require specialized personnel. - Accurate.	- Simple, does not require specialized personnel. - Low detection limit (0.05% parasitemias).
Limitations	- Subjective and labor-intensive. - Highly trained personnel.	- Costly equipment. - Handling of radioactive reagents. - Additional incubation with reagents.	- Costly equipment and reagents (e.g.: DNA stains). - Additional incubation with reagents.	- Costly reagents (e.g.: DNA stains). - Additional incubation steps with reagents.	- Costly reagents (e.g.: antibodies). - Additional incubation steps with reagents.

(n.d.): no data.

Table SIII.2: Antimalarial activities of several antimalarial drugs determined by different *in vitro* sensitivity assays against *P. falciparum* 3D7 strain

	Hypoxanthine assay	WHO schizont maturation test	SYBR green plate assay	HRP2 assay
Quinine	63 nM [1] 102.3 nM [2] 47.1 nM [3] 59.9 nM [4]	35 nM [1]	6.9 nM [13]	5.9 nM [13]
Mefloquine	42.6 nM [5] 6.1 nM [2] 18.2 nM [3] 34.5 nM [4]	12.1 nM [11]	9.4 nM [13] 9.5 nM [14] 40.7 nM [12]	8.4 nM [13]
Chloroquine	15.7 nM [5] 6 nM [6] 9.7 nM [2] 11.3 nM [3] 18.7 nM [4] 9.6 nM [7] 29.6 nM [8]	14.79 nM [7]	8.1 nM [13] 22.2 nM [15] 16 nM [16] 11.54 nM [7]	7.5 nM [13] 9.7 nM [7]
Amodiaquine	20.3 nM [9]	7.8 nM [1]		
Artemisinin	22 nM [5] 10.1 nM [10]		9 nM [14]	
Dihydroartemisinin	5.3 nM [5] 4.2 nM [8]		3.78 nM [15] 22.1 nM [12]	2.3 nM [17]
Artesunate	1.1 nM [7] 9.4 nM [9] 0.4 nM [3] 0.9 nM [4]	3.7 nM [7] 5.4 nM [12]	1.9 nM [7] 3.6 nM [15]	1.5 nM (48h) [7] 2.5 nM (72h) [7] 2.4 nM [17]
Atovaquone	1.3 nM [5] 1.1 nM [9] 0.06 nM [7]	0.11 nM [7]	0.06 nM [7]	0.8 nM [7]
Pyrimethamine	78.4 nM [2] 5 nM [6] 19.3 nM (48h) [7] 19.4 nM (72h) [7]	32.2 nM (48h) [7] 26.3 nM (72h) [7]	7.2 nM [14] > 100 nM (48h) [7] 23.9 nM (72h) [7]	26.6 nM (48 h) [7] 53.9 nM (72h) [7]

[1] Chong CR, Sullivan DJ Jr. (2003) Inhibition of heme crystal growth by antimalarials and other compounds: implications for drug discovery. *Biochem Pharmacol* 66: 2201-12.

[2] Vivas L, Rattray L, Stewart LB, Robinson BL, Fugmann B, et al. (2007) Antimalarial efficacy and drug interactions of the novel semi-synthetic endoperoxide artemisone *in vitro* and *in vivo*. *J Antimicrob Chemother* 59:658-65.

[3] Aunpad R, Somsri S, Na-Bangchang K, Udomsangpetch R, Mungthin M, et al. (2009) The effect of mimicking febrile temperature and drug stress on malarial development. *Ann Clin Microbiol Antimicrob* 8:19.

[4] Lim P, Wongsrichanalai C, Chim P, Khim N, Kim S, et al. (2010) Decreased *in vitro* susceptibility of *Plasmodium falciparum* isolates to artesunate, mefloquine, chloroquine, and quinine in Cambodia from 2001 to 2007. *Antimicrob Agents Chemother* 54:2135-42.

[5] Duraisingh MT, Roper, C, Walliker D, and Warhurst DC. (2000) Increased sensitivity to the antimalarials mefloquine and artemisinin is conferred by mutations in the *pfmdr1* gene of *Plasmodium falciparum*. *Molecular Microbiology* 36: 955-961.

[6] Reynolds JM, El Bissati K, Brandenburg J, Günzl A, Mamoun CB. (2007) Antimalarial activity of the anticancer and proteasome inhibitor bortezomib and its analog ZL3B. *BMC Clin Pharmacol* 7:13.

[7] Wein S, Maynadier M, Tran Van Ba C, Cerdan R, Peyrottes S, et al. (2010) Reliability of antimalarial sensitivity tests depends on drug mechanisms of action. *J Clin Microbiol* 48: 1651–1660.

- [8] Wong RP, Salman S, Ilett KF, Siba PM, Mueller I, et al. (2011) Desbutyl-lumefantrine is a metabolite of lumefantrine with potent in vitro antimalarial activity that may influence artemether-lumefantrine treatment outcome. *Antimicrob Agents Chemother* 55:1194-8.
- [9] Johnson JD, Denuall RA, Gerena L, Lopez-Sanchez M, Roncal NE, et al. (2007) Assessment and continued validation of the malaria SYBR green I-based fluorescence assay for use in malaria drug screening. *Antimicrob Agents Chemother* 51:1926-33.
- [10] Baniecki ML, Wirth DF, Clardy J (2007). High-throughput *Plasmodium falciparum* growth assay for malaria drug discovery. *Antimicrob Agents Chemother* 51, 716.
- [11] Wisedpanichkij R, Chaijaroenkul W, Sangsuwan P, Tantisawat J, Boonprasert K (2009) In vitro antimalarial interactions between mefloquine and cytochrome P450 inhibitors *Acta Trop* 112:12-5.
- [12] Wang Z, Parker D, Meng H, Wu L, Li J, et al. (2012) In vitro sensitivity of *Plasmodium falciparum* from China-Myanmar border area to major ACT drugs and polymorphisms in potential target genes. *PLoS One* 7:e30927.
- [13] Bacon DJ, Latour C, Lucas C, Colina O, Ringwald P, et al. (2007) Comparison of a SYBR green I-based assay with a histidine-rich protein II enzyme-linked immunosorbent assay for in vitro antimalarial drug efficacy testing and application to clinical isolates. *Antimicrob Agents Chemother* 51:1172-8.
- [14] Plouffe D, Brinker A, McNamara C, Henson K, Kato N. (2008) In silico activity profiling reveals the mechanism of action of antimalarials discovered in a high-throughput screen. *Proc Natl Acad Sci USA* 05:9059-9064.
- [15] He Z, Chen L, You J, Qin L, Chen X. (2010) In vitro interactions between antiretroviral protease inhibitors and artemisinin endoperoxides against *Plasmodium falciparum*. *Int J Antimicrob Agents* 35:191-193.
- [16] Ramalhete C, Lopes D, Mulhovo S, Molnár J, Rosário VE, et al. (2010) New antimalarials with a triterpenic scaffold from *Momordica balsamina*. *Bioorg Med Chem* 18:5254-60.
- [17] Held J, Soomro SA, Kremsner PG, Jansen FH, Mordmüller B (2011) In vitro activity of new artemisinin derivatives against *Plasmodium falciparum* clinical isolates from Gabon. *Int J Antimicrob Agents* 37:485-488.



Figure SIII.1: Cyflow® flow cytometer and optical bench layout

Images in the top row show the components (A) and the optical bench layout (B) of the Cyflow® flow cytometer. The 488 nm laser light is vertically polarized. A horizontally polarized filter is placed in front of a second side scatter detector to allow detection of depolarized light (depol SSC). Images C, D and E show a Cyflow® in the laboratory and being easily packed for transport at the Medical Research Unit of the Albert Schweitzer Hospital in Lambaréné, Gabon. (The subject of the photograph has given written informed consent, as outlined in the PLOS consent form, to publication of the photograph).

9. References

1. Hyde JE. (2007) Drug-resistant malaria - an insight. *The FEBS Journal* 274: 4688-4698.
2. White NJ. (2004) Review series Antimalarial drug resistance. *Trends in Parasitology* 113: 1084-1092.
3. Dondorp A, Nosten F, Yi P, Das D, Phyto A, Tarning J, et al. (2009) Artemisinin Resistance in Plasmodium falciparum Malaria. *New England Journal of Medicine* 361: 455-467.
4. Bloland PB. (2001) Drug resistance in malaria. WHO Press, Geneva, Switzerland.
5. Rieckmann KH, Campbell GH, Sax LJ and Mrema JE. (1978) Drug sensitivity of *Plasmodium falciparum*. An in-vitro microtechnique. *The Lancet* 1: 22-23.
6. Desjardins R, Canfield C, Haynes J and Chulay J. (1979) Quantitative Assessment of Antimalarial Activity In Vitro by a Semiautomated Microdilution Technique. *Antimicrobial Agents and Chemotherapy* 16: 710-718.
7. Makler MT and Hinrichs DJ. (1993) Measurement of the lactate dehydrogenase activity of *Plasmodium falciparum* as an assessment of parasitemia. *The American Journal of Tropical Medicine and Hygiene* 48: 205-210.
8. Noedl H, Wernsdorfer WH, Miller RS and Wongsrichanalai C. (2002) Histidine-Rich Protein II: a Novel Approach to Malaria Drug Sensitivity Testing. *Antimicrobial Agents and Chemotherapy* 46: 1658-1664.
9. Smilkstein M, Sriwilaijaroen N, Kelly JX, Wilairat P and Riscoe M. (2004) Simple and Inexpensive Fluorescence-Based Technique for High-Throughput Antimalarial Drug Screening. *Society* 48: 1803-1806.
10. Li Q, Gerena L, Xie L, Zhang J, Kyle D and Milhous W. (2007) Development and Validation of Flow Cytometric Measurement for Parasitemia in Cultures of *P. falciparum* Vially Stained with YOYO-1. *Cytometry A* 71: 297-307.
11. Corbett Y, Herrera L, Gonzalez J, Cubilla L and Capson TL. (2004) A novel DNA-based microfluorimetric method to evaluate antimalarial drug activity. *The American Journal of Tropical Medicine and Hygiene* 70: 119-24.
12. Baniecki ML, Wirth DF and Clardy J. (2007). High-throughput *Plasmodium falciparum* growth assay for malaria drug discovery. *Antimicrobial Agents and Chemotherapy* 51: 716-723.
13. Wongsrichanalai C. (2002) Epidemiology of drug-resistant malaria. *The Lancet Infectious Diseases* 2: 209-218.

14. Noedl H. (2003) Malaria drug-sensitivity testing: new assays, new perspectives. *Trends in Parasitology* 19: 175–181.
15. Wein S, Maynadier M, Tran Van Ba C, Cerdan R, Peyrottes S, Fraisse L, et al. (2010) Reliability of antimalarial sensitivity tests depends on drug mechanisms of action. *Journal of clinical microbiology* 48: 1651–60.
16. World Health Organization (2011) Global plan for artemisinin resistance containment (GPARC). WHO Press, Geneva.
17. Hänscheid T, Egan TJ and Grobusch MP. (2007) Haemozoin: from melatonin pigment to drug target, diagnostic tool, and immune modulator. *The Lancet Infectious Diseases* 7: 675–85.
18. Krämer B, Grobusch MP, Suttorp N, Neukammer J and Rinneberg H (2001) Relative frequency of malaria pigment-carrying monocytes of nonimmune and semi-immune patients from flow cytometric depolarized side scatter. *Cytometry* 45: 133-40.
19. Grobusch MP, Hänscheid T, Krämer B, Neukammer J, May J, Seybold J, et al. (2003) Sensitivity of hemozoin detection by automated flow cytometry in non- and semi-immune malaria patients. *Cytometry. Part B, Clinical cytometry* 55: 46–51.
20. Jamjoom GA. (1983) Dark-field microscopy for detection of malaria in unstained blood films. *Journal of Clinical Microbiology* 17: 717–721.
21. Lawrence C and Olson JA. (1986) Birefringent hemozoin identifies malaria. *American Journal of Clinical Pathology* 86: 360–363.
22. Hänscheid T, Valadas E and Grobusch MP. (2000) Automated malaria diagnosis using pigment detection. *Parasitology Today* 16:549–551.
23. Mendelow B V, Lyons C, Nhlangothi P, Tana M, Munster M, Wypkema E, et al. (1999) Automated malaria detection by depolarization of laser light. *British journal of haematology* 104: 499–503.
24. Hänscheid T, Pinto BG, Cristino JM and Grobusch MP. (2000) Malaria diagnosis with the haematology analyser Cell-Dyn 3500: What does the instrument detect? *Clinical and laboratory haematology* 22: 259–261.
25. Suh IB, Kim HJ, Kim JY, Lee SW, An SSA, Kim WJ, et al. (2003) Evaluation of the Abbott Cell-Dyn 4000 hematology analyzer for detection and therapeutic monitoring of *Plasmodium vivax* in the Republic of Korea. *Tropical Medicine and International Health* 8: 1074–1081.

26. de Grooth B, Terstappen L, Puppels G and Greve J. (1987) Light-scattering polarization measurements as a new parameter in flow cytometry. *Cytometry* 8: 539–544.
27. Frita R, Rebelo M, Pamplona A, Vigario AM, Mota MM, Grobusch MP, et al. (2011) Simple flow cytometric detection of haemozoin containing leukocytes and erythrocytes for research on diagnosis, immunology and drug sensitivity testing. *Malaria journal* 10: 74.
28. Rebelo M, Shapiro HM, Amaral T, Melo-Cristino and Hanscheid T. (2012) Haemozoin detection in infected erythrocytes for *Plasmodium falciparum* malaria diagnosis—Prospects and limitations. *Acta Tropica* 123: 58– 61.
29. Mphande F, Nilsson Sa and Bolad A. (2008) Culturing of erythrocytic asexual stages of *Plasmodium falciparum* and *P. vivax*. In: Moll K, Ljungström I, Perlmann H, Scherf A, Wahlgren M (Eds.), *Methods in Malaria Research*, fifth ed, pp. 1–3 (Manassas).
30. Lambros C and Vanderberg JP. (1979) Synchronization of *Plasmodium falciparum* erythrocytic stages in culture. *Journal of parasitology* 65: 418–420.
31. Rieckmann KH. (1982) Visual in vitro test for determining the drug sensitivity of *Plasmodium falciparum*. *The Lancet* 1: 1333–1335.
32. Basco LK. (2007) *Field application of in vitro assays for the sensitivity of human malaria parasites to antimalarial drugs*. WHO Press, Geneva, Switzerland.
33. Men TT, Huy NT, Trang DTX, Shuaibu MN, Hirayama K and Kamei K. (2012) A simple inexpensive haemozoin-based colorimetric method to evaluate anti-malarial drug activity. *Malaria Journal* 11: 272.
34. Thomas V, Góis A, Ritts B, Burke P, Hänscheid T and McDonnell G. (2012) A novel way to grow hemozoin-like crystals in vitro and its use to screen for hemozoin inhibiting antimalarial compounds. *PLoS One* 7: e41006.
35. Shapiro HM (2003) *Practical Flow Cytometry – 4th edition*. John Wiley & Sons. New Jersey, USA. Free download available at: <http://www.beckmancoulter.com/wsrportal/wsr/research-and-discovery/products-and-services/flow-cytometry/practical-flow-cytometry/index.htm>
36. Warhurst DC, Homewood CA and Baggaley VC. (1974) The chemotherapy of rodent malaria. XX. Autophagic vacuole formation in *Plasmodium berghei* in vitro. *Annals of Tropical Medicine and Parasitology* 68: 265-281.
37. Held J, Soomro SA, Kremsner PG, Jansen FH and Mordmüller B. (2011) In vitro activity of new artemisinin derivatives against *Plasmodium falciparum* clinical isolates from Gabon. *International Journal of Antimicrobial Agents* 37: 485-488.

38. Ikpa TF, Ajayi JA, Imandeh GN and Usar JI. (2010) Drug resistant *falciparum* malaria in North Central Nigeria. *African Journal of Clinical and Experimental Microbiology* 11: 111-119.
39. Johnson JD, Denuff RA, Gerena L, Lopez-Sanchez M, Roncal NE and Waters NC. (2007) Assessment and continued validation of the malaria SYBR green I-based fluorescence assay for use in malaria drug screening. *Antimicrobial Agents Chemotherapy* 51: 1926-1933.
40. Bacon DJ, Latour C, Lucas C, Colina O, Ringwald P and Picot S. (2007) Comparison of a SYBR green I-based assay with a histidine-rich protein II enzyme-linked immunosorbent assay for in vitro antimalarial drug efficacy testing and application to clinical isolates. *Antimicrobial Agents Chemotherapy* 51: 1172-1178.
41. White NJ. (1997) Assessment of the Pharmacodynamic Properties of Antimalarial Drugs In Vivo. *Antimicrobial Agents Chemotherapy* 41: 1413-1422.
42. Bennett TN, Paguio M, Gligorijevic B and Seudieu C. (2004) Novel, Rapid, and Inexpensive Cell-Based Quantification of Antimalarial Drug Efficacy *Antimicrobial Agents Chemotherapy* 48: 1807-1810.
43. Karl S, Wong RP, St Pierre TG and Davis TM. (2009) A comparative study of a flow-cytometry-based assessment of in vitro *Plasmodium falciparum* drug sensitivity. *Malaria Journal* 8: 294
44. Gritzmacher CA and Reese RT. (1984) Protein and Nucleic Acid Synthesis During Synchronized Growth of *Plasmodium falciparum*. *Journal of Bacteriology* 160: 1165-1167.
45. Schuster FL. (2002) Cultivation of *Plasmodium* spp. *Clinical Microbiology Reviews* 15: 355-364.
46. Lim P, Wongsrichanalai C, Chim P, Khim N, Kim S, Chy S et al. (2010) Decreased in vitro susceptibility of *Plasmodium falciparum* isolates to artesunate, mefloquine, chloroquine, and quinine in Cambodia from 2001 to 2007. *Antimicrobial Agents Chemotherapy* 54: 2135-2142.
47. Aunpad R, Somsri S, Na-Bangchang K, Udomsangpetch R, Mungthin M, Adisakwattana P et al. (2009) The effect of mimicking febrile temperature and drug stress on malarial development. *Annals of Clinical Microbiology and Antimicrobials* 8: 19.
48. Tucker MS, Mutka T, Sparks K, Patel J and Kyle DE. (2012) Phenotypic and genotypic analysis of in vitro-selected artemisinin-resistant progeny of *Plasmodium falciparum*. *Antimicrobial Agents Chemotherapy* 56: 302-314.

49. Vossen MG, Pferschy S, Chiba P and Noedl H. (2010) The SYBR Green I malaria drug sensitivity assay: performance in low parasitemia samples. *American Journal of Tropical Medicine and Hygiene* 82: 398-401.
50. Abiodun OO, Gbotosho GO, Ajaiyeoba EO, Happi CT, Hofer S, Wittlin S et al. (2010) Comparison of SYBR Green I-, PicoGreen-, and [3H]-hypoxanthine-based assays for in vitro antimalarial screening of plants from Nigerian ethnomedicine. *Parasitology Research* 106: 933-939.
51. Wisedpanichkij R, Chaijaroenkul W, Sangsuwan P, Tantisawat J and Boonprasert K. (2009) In vitro antimalarial interactions between mefloquine and cytochrome P450 inhibitors. *Acta Tropica* 112: 12-15.
52. Maerki S, Brun R, Charman SA, Dorn A, Matile H and Wittlin S. (2006) In vitro assessment of the pharmacodynamic properties and the partitioning of OZ277/RBx-11160 in cultures of *Plasmodium falciparum*. *Journal of Antimicrobial Chemotherapy* 58: 52-58.
53. Sanz LM, Crespo B, De-Cózar C, Ding XC, Llergo JL, Burrows JN et al. (2012) *P. falciparum* in vitro killing rates allow to discriminate between different antimalarial mode-of-action. *PLoS One* 7:e30949.
54. Meshnick SR, Taylor TE and Kamchonwongpaisan S. (1996) Artemisinin and the antimalarial endoperoxides: from herbal remedy to targeted chemotherapy. *Microbiological Reviews* 60: 301-315.
55. Teuscher F, Gatton ML, Chen N, Peters J, Kyle DE and Cheng Q. (2010) Artemisinin-induced dormancy in plasmodium falciparum: duration, recovery rates, and implications in treatment failure. *The Journal of Infectious Diseases* 202: 1362-8.
56. Gluzman IY, Schlesinger PH and Krogstad DJ. (1987) Inoculum effect with chloroquine and *Plasmodium falciparum*. *Antimicrobial Agents and Chemotherapy* 31: 32-36.
57. Duraisingh MT, Jones P, Sambou I, von Seidlein L, Pinder M and Warhurst DC. (1999) Inoculum effect leads to overestimation of in vitro resistance for artemisinin derivatives and standard antimalarials: a Gambian field study. *Parasitology* 119: 435-440.
58. Dondorp AM, Fairhurst RM, Slutsker L, Macarthur JR, Breman JG, Guerin PJ et al. (2011) The threat of artemisinin-resistant malaria. *New England Journal of Medicine* 365: 1073-1075.
59. Shapiro HM and Ulrich H. (2010) Overview: Cytometry in malaria: From research tool to practical diagnostic approach? *Cytometry A* 77: 500-501.

CHAPTER IV

VALIDATION OF THE HEMOZOIN DETECTION ASSAY IN THE FIELD USING SAMPLES FROM MALARIA PATIENTS

This chapter is published in;

Rebelo M, Tempera C, Fernandes JF, Grobusch MP and Hänscheid T. (2015) Assessing anti-malarial drug effects ex vivo using the haemozoin detection assay. *Malaria Journal* 14:140.

Author's contributions:

TH, MR and MPG conceived the study. All field experiments were performed by MR. TH and MPG coordinated the project. CT performed the ELISA assays. MPG and JF assisted with obtaining the samples from malaria patients, provided advice on different aspects of the novel assay and its assessment under field conditions. MR and TH wrote the draft manuscript. All authors contributed to the writing, and approved the final manuscript.

1. Abstract

In vitro sensitivity assays are crucial to detect and monitor drug resistance. *Plasmodium falciparum* has developed resistance to almost all anti-malarial drugs. Although different *in vitro* drug assays are available, some of their inherent characteristics limit their application, especially in the field. A recently developed approach based on the flow cytometric detection of hemozoin (Hz) allowed reagent-free monitoring of parasite maturation and detection of drug effects in culture-adapted parasites. In this study, the set-up, performance and usefulness of this novel assay were investigated under field conditions in Gabon.

An existing flow cytometer (Cyflow Blue) was modified on site to detect light depolarization caused by Hz. Blood from malaria patients was incubated for 72 hours with increasing concentrations of chloroquine, artesunate and artemisinin. The percentage of depolarizing red blood cells (RBC) was used as maturation indicator and measured at 24, 48 and 72 hours of incubation to determine parasite growth and drug effects.

The flow cytometer was easily adapted on site to detect light depolarization caused by Hz. Analysis of *ex vivo* cultures of parasites, obtained from blood samples of malaria patients, showed four different growth profiles. In 39/46 samples, 50% inhibitory concentrations (IC₅₀) were successfully determined. IC₅₀ values for chloroquine were higher than 200 nM in 70% of the samples, indicating the presence of chloroquine-resistant parasites. For artesunate and artemisinin, IC₅₀ values ranged from 0.9 to 60 nM and from 2.2 nM to 124 nM, respectively, indicating fully sensitive parasites.

Flow cytometric detection of Hz allowed the detection of drug effects in blood samples from malaria patients, without using additional reagents or complex protocols. Adjustment of the initial parasitaemia was not required, which greatly simplifies the protocol. Although, it may lead to different IC₅₀ values. Further investigation of set-up conditions of the Hz assay, as well as future studies in various settings should be performed to further determine the usefulness of this assay as a tool for rapid resistance testing in malaria-endemic countries.

2. Background

In the last decade the number of malaria deaths has decreased in large part due to the availability of effective treatments, in particular artemisinin combination therapy (ACT) [1]. However, these achievements are in danger and might even be reversed because parasites with prolonged parasite clearance times (PCT), observed in patients treated with ACT, have emerged in Southeast Asia [2, 3]. Indeed, this is considered an early sign of the development of parasite resistance [2, 3] and a major concern in the fight against malaria, as illustrated by the WHO Global Plan for Artemisinin Resistance Containment issued in 2011 [4]. Artemisinin resistance, currently defined as prolonged PCT, has spread across Southeast Asia [5]. Recently, a Vietnamese patient who apparently acquired malaria in Angola failed to respond to intravenous artesunate/clindamycin and an oral ACT after returning to Vietnam [6]. It is not unlikely that it will emerge in sub-Saharan Africa, and drug sensitivities should be monitored pro-actively. In this scenario, *in vitro* sensitivity assays may play a crucial role in future. *In vitro* assays allow reducing host-related factors and thus, provide an objective insight into the intrinsic sensitivity of malaria parasites.

Several phenotypic and genotypic methods have been developed and tried for drug testing in the field [7]. Genetic resistance markers are known for some anti-malarial drugs, but are not yet able to predict sensitivity to all commonly used anti-malarial drugs [8]. Only recently, alterations in the *kelch13* gene were linked to delayed parasite clearance in artemisinin-treated patients [9]. Thus, phenotypic assays continue to be important for detection of resistance and validation of genetic markers. The main phenotypic assays successfully used to detect drug resistance in the field include: (i) the microscopic schizont maturation test [10]; (ii) the incorporation of radioactive hypoxanthine [11]; (iii) ELISA assays for detection of pLDH [12] and HRP2 [13] antigens; and, (iv) fluorescent-based techniques using either fluorometry [14] or flow cytometry [15] to detect parasite DNA/RNA. However, inherent limitations are common, especially during field applications. The supply, handling and disposal of radioactive isotopes are major obstacles. Microscopy is labor-intensive and subjective, although it has a rather quick turn-around time (24-30 hours) when compared to other techniques, especially ELISA-based methods, which can take up to 72 or even 96 hours [16, 17]. Moreover, assays may require the use of, often, expensive antibodies or DNA/RNA stains, highlighting the issues of adequate storage and cold chain as well as limited shelf life.

Regarding flow cytometry, the majority of cytometric methods apply combinations of dyes to reliably detect infected red blood cells (iRBC), which implies a complex multiparameter

analysis [15,18]. Ideally, if parasite maturation was detectable using a direct and simple measurement of a product from the parasite, the need for additional reagents would be avoided.

Hemozoin (Hz) is produced in increasing amounts by the parasite as it matures inside the iRBC, constituting an optimal maturation indicator [10]. Measuring Hz with a simple flow cytometry method allows detection of parasite maturation and drug effects as early as 18 hours after incubation in culture-adapted laboratory strains [19].

The objectives of this study were to evaluate if the Hz detection assay could be easily set up in a remote malaria-endemic area, and to assess whether anti-malarial drug effects could be detected in wild-type strains obtained from malaria patients, using a simple protocol.

3. Material and Methods

The study was carried out at the *Centre de Recherches Médicales de Lambaréné* (CERMEL) in Gabon, a malaria-endemic region in Africa. Ethical approval was obtained from the Institutional Review Board of the Medical Research Unit (CERMEL) of the International Foundation of the Albert Schweitzer Hospital.

Samples

EDTA anti-coagulated blood samples from malaria patients were obtained from the Clinical Analysis Laboratory of the Albert Schweitzer Hospital after the samples had been processed for full blood count (FBC). Malaria diagnosis and parasite loads (number of parasites/ μl of blood) were determined by standard microscopic observation of Giemsa-stained thick blood films. Briefly, parasitemia was quantified by counting the number of parasites per microscopic field from a defined volume of blood (10 μl) spread on a defined area (1.8 cm^2), as described elsewhere [20]. RBCs from these blood samples were washed twice in culture medium before further use.

Flow cytometric detection of depolarized side-scattered light

Flow cytometric analysis was performed using a CyFlow® Blue (Partec, Münster, Germany) available on site. The existing configuration, which was modified on site for this study and is shown in Figure IV.1, consisted of forward scatter (FSC), side scatter (SSC) and three fluorescent detectors (FL1, FL2 and FL3). A set of four optical filters was necessary, as shown in Figure IV.1B: (1) a 500-nm dichroic mirror; (2) a 50:50 beam-

splitter; (3) a 488-nm vertical polarizer; and, (4) a 488-nm horizontal polarizer. Briefly, a 500-nm dichroic mirror (DM) (B1) was placed on the site of the original 540-nm DM and the other original 500-nm DM was replaced by a 50:50 beam-splitter (B2), which allowed the creation of two SSC detectors (Figure IV.1). A 488-nm filter coupled with a polarizer in the same orientation as the incident laser beam (vertical) was placed in front of one of the SSC detectors. Another 488-nm filter coupled with a polarizer perpendicularly orientated in relation to the laser beam (horizontal) was placed in front of the other SSC detector, allowing the detection of light depolarization (Figure IV.1C). The optical components required to modify the optical bench of flow cytometers can be obtained directly from the instruments' manufacturer.

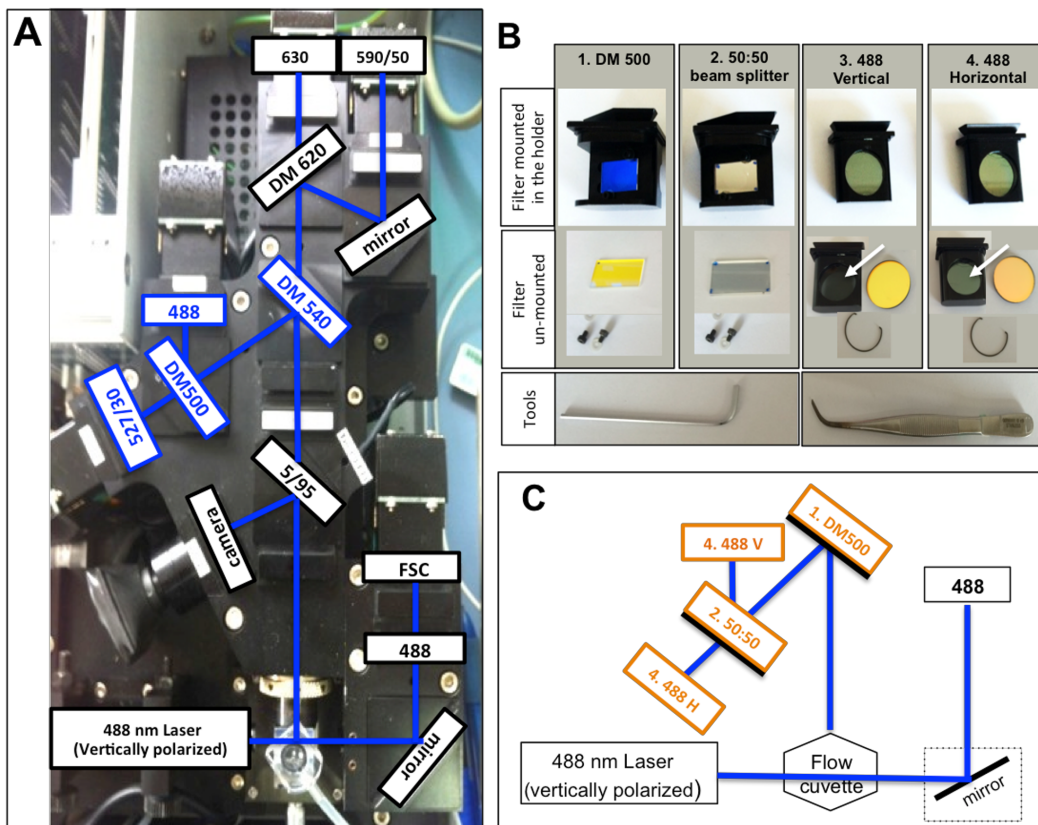


Figure IV.1: Flow cytometry modifications to detect light depolarization.

The optical set-up of the Cyflow (Partec, Münster, Germany) (A) was easily modified to allow the detection of light depolarization. Four optical components from the original set-up (blue boxes in A) had to be replaced by the optical components shown in B, as described in the Methods section. Filters were simply replaced by unscrewing the original ones from the filter holder, or by removing the metallic ring (second row in B). This was accomplished using simple tools (bottom row in B). Note that in this case, polarization filters were glued inside the holder (arrows in B) so that they would not move, since to attain the best depolarization signal polarizers should be perpendicular to each other. The final optical layout to detect light depolarization is presented in C.

Anti-malarial drugs

Samples were tested against different concentrations of chloroquine, artesunate and artemisinin (Sigma Aldrich, St Louis, MO, USA). Stock solutions of chloroquine were prepared in sterile water, and artemisinin and artesunate were prepared in pure methanol. Doubling concentrations, ranging from 25 to 200 nM for chloroquine and from 0.12 to 128 nM for artemisinin and artesunate, were prepared from the stock solutions in complete malaria culture medium (CMCM), which consists of RPMI 1640 supplemented with 25 mM HEPES, 2.4 mM L-glutamine, 50 µg/mL gentamicin, 0.5% w/v Albumax , 11 mM glucose, 1.47 mM hypoxanthine and 37.3 mM NaHCO₃. CMCM. Each drug concentration was tested in triplicate.

Hemozoin detection assay

RBCs obtained from malaria patients were diluted at a hematocrit of 5% in CMCM. To simplify the assay, the parasitaemia was not adjusted so that, eventually, the use of uninfected blood could be avoided. A volume of 100 µL was distributed into the wells of a 96-well plate, previously loaded with 100 µL of anti-malarial drugs at different concentrations, or 100 µL of CMCM for the drug-free controls, respectively. Plates were incubated for 72 hours at 37°C in 5% CO₂ atmosphere. Flow cytometric measurements were performed at 24, 48 and 72 hours of incubation. Parasite maturation from ring-stage to schizonts was assessed based on the increase in the percentage of Hz-containing cells overtime, as described before [19]. To assess parasite replication (re-invasion), the same samples were stained with SYBR green I at 1x (Invitrogen, Carlsbad, CA, USA), as described elsewhere [19].

Histidine-rich protein-2 (HRP2) enzyme-linked immunosorbent assay (ELISA)

For the HRP2-ELISA, RBCs were diluted in CMCM at a hematocrit of 3%. Parasitemia was adjusted to 0.05% using RBCs obtained from healthy volunteer donors. A volume of 100 µL was distributed into the wells of a 96-well plate, previously loaded with 100 µL of anti-malarial drugs at different concentrations or 100 µL of CMCM for the drug-free controls. Plates were incubated for 72 hours at 37°C in 5% CO₂, after which they were frozen at -20°C until the HRP2-ELISA was performed according to standard procedures [21].

Data analysis

Flow cytometry results were analysed using FlowJo software (version 9.0.2, Tree Star Inc., Oregon, USA). Depolarizing events were defined in plots of SSC *versus* depolarized-SSC, as those with a signal above the background observed in the uninfected control (gate in Figure IV.2A and B). To determine SYBR green I-positive cells, green fluorescence (FL1) *versus* red fluorescence (FL3) plots were used. The FL1 detector had a 527/30 band-pass filter and FL2 had a 620-nm long-pass filter. SYBR green I-positive events were established based on a stained uninfected control and had to be adjusted at each time point, always using the uninfected SYBR green I-stained sample from the corresponding time point. A non-linear regression model (sigmoidal dose-response/variable slope) was used to calculate the individual 50% inhibitory concentrations, with SigmaPlot-Systat Software (Chicago, IL, USA). Only those samples with a ≥ 2 ratio of drug-free control to highest drug concentration were included.

4. Results and Discussion

Growth and maturation of wild-type *Plasmodium falciparum* strains

Forty-six samples from malaria patients were analysed during this study. Parasite loads ranged from 50 to 452,000 parasites/ μ L of blood (median of 15,000 parasites/ μ L). *Ex vivo* cultures of infected RBCs showed that parasites had four different growth profiles (Table IV.1): (i) seven samples showed no maturation, as defined by an increase in depolarization; (ii) another eight samples showed maturation at 24 hours and replication at 48 hours; (iii) 17 samples showed maturation at 24 hours but no re-invasion occurred; and, (iv) 14 samples had a delay in parasite growth, with maturation being observed at 48 hours and replication at 72 hours.

One crucial step in the *in vitro* sensitivity assays is the culture of parasites [22]. Maturation of *Plasmodium falciparum* from early rings to late schizonts takes 42-48 hours *in vitro* [23] and consequently, an increase in parasitemia can only be observed every 42-48 hours, after re-invasion of RBCs occurs. Differences in *ex vivo* parasite maturation and replication have already been observed in strains obtained directly from different patients [24,25]. Indeed many factors related to the protocol, the host and the parasite itself might greatly influence the *in vitro* growth of parasites.

Regarding the protocol factors such as the type of anticoagulant used to collect the blood from the patients to the atmosphere where the parasites will be incubated have to be taken into account [7]. During this study EDTA-collected blood was used. Although the use of

EDTA is discouraged by the reference protocol from MR4 [26] it has been shown by different studies that EDTA-collected blood can be successfully used for *ex vivo* drug testing [27-31]. In one of these reports even long-term cultures of parasites present in patients' blood were accomplished [31]. Moreover, the use of specific anticoagulants requires drawing more blood just for the purpose of sensitivity testing. This can be avoided by using EDTA-anticoagulated blood which was obtained as part of the routine FBC analysis, preventing all inherent problems associated with an extra blood drawing.

The incubation atmosphere recommended for *P. falciparum* growth in culture include the use of a low O₂ atmosphere [26]. However, such mixed gas atmospheres may not be available in the resource-limited settings found in malaria endemic countries. Because of this, it has been investigated whether a simple 5% CO₂ atmosphere could be used instead without compromising parasite survival after drug treatment [32]. Results showed no differences in parasite survival using between trigas (5% CO₂, 5% O₂, 90% N₂), candle jar or 5% CO₂ atmospheres [32].

Undoubtedly, host-specific factors, often difficult to control, ranging from the immune response to the presence of pharmacologically active substances might influence the growth of the parasite *in vitro*. Indeed, the fact that some of the patients might already have been treated at the time of blood collection during this study cannot be discarded, possibly explaining some of the differences observed in the parasites' growth profiles. Yet, it is very difficult to control for all these factors and this might not only imply detailed histories, but eventually laboratory test to confirm immune status or presence of drug-metabolites. Perhaps explaining why very few studies on this field are including such detailed information.

Conversely, parasite-related factors may even be more important. The delay between sample collection and processing influences the viability of freshly collected clinical isolates, because it is considerably decreased after a sample has been kept for several hours at room temperature [7]. However, in one study where all 43 samples were cultured within 30 minutes of collection [25], 50% developed into schizonts within 27 hours, while the other half reached schizont stage only between 28 and 63 hours. In this study no correlation between the delay until culture and any of the four parasite growth patterns was observed, supporting the idea that possible host factors may have been more relevant.

Table IV.1: Summarized data of isolates exhibiting different *ex vivo* growth profiles analysed by the hemozoin assay

	Group 1	Group 2	Group 3	Group 4
Growth profile	No maturation	Maturation at 24 hours and replication at 48 hours	Maturation at 24 hours but no replication	Delayed maturation
Number of samples	7	8	17	14
Parasitemia (median; range)	0.01%; 0.001-0.1%	0.3%; 0.2-2.2%	3.5%; 0.2-12%	0.3%; 0.1-1.9%
IC50 Artesunate (mean)	nd	10.5 nM	15.2 nM	5.6 nM
IC50 Artemisinin (mean)	nd	46 nM	47.3 nM	14.4 nM

nd – not determined

IC50 – 50% inhibitory concentration

Note: Results from chloroquine were not presented in this Table because the majority of the samples (32 out of 46) had IC50 values higher than 200 nM. Chloroquine had an inhibitory effect in only four samples from group 3 (IC50 mean = 76.8 nM). In ten samples, chloroquine activity could not be determined.

Detection of anti-malarial drug effects by the hemozoin assay

In *P. falciparum*-infected patients the majority of circulating iRBC are ring forms that contain little or no detectable Hz, as observed in a previous report whereby flow cytometric assessment of Hz these forms could not be detected [33]. This study confirms this observation, as at 0 hours, no difference in depolarizing events was observed between the infected and the uninfected samples (Figure IV.2A and B). Only after incubation the percentage of depolarizing cells increased, indicating higher Hz content and, thus maturation (Figure IV.2B), seen in drug-free controls or drug-resistant parasites. This contrasts with diminished or absent depolarizing events when anti-malarial drugs are effective (Figure IV.2C). Drug inhibitory effects were determined in 39/46 (85%) of samples, in which parasite maturation was observed (groups 2, 3 and 4). In 25 samples (groups 2 and 3), drug effects were measurable at 24 hours, as expected from culture-adapted strains [19]. In the remaining 14 samples (group 4) parasite maturation was delayed; however, it was still possible to detect drug effects at 48 hours of incubation.

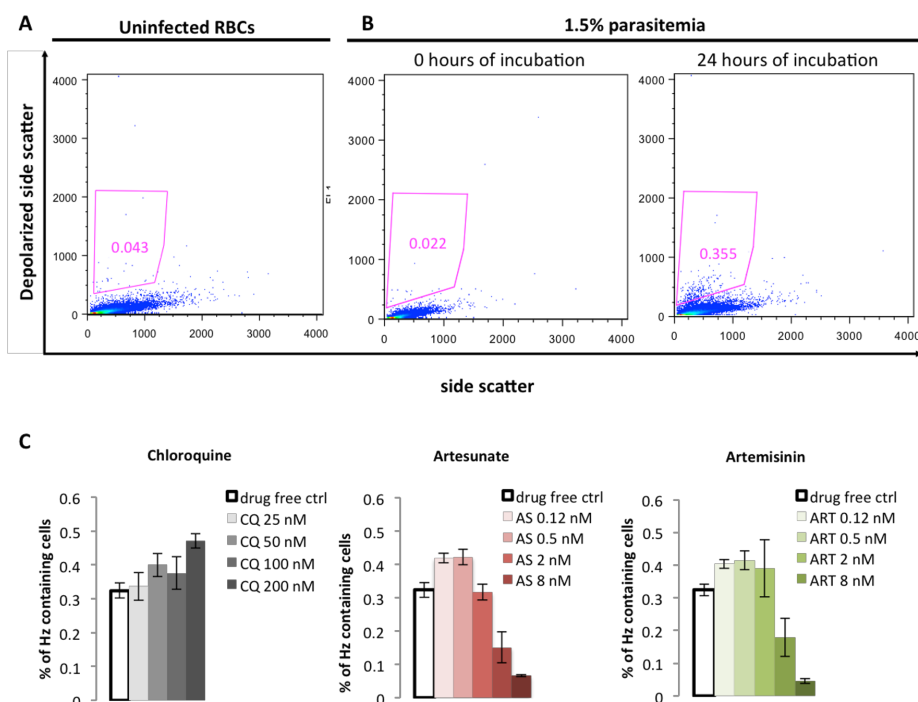


Figure IV.2: Representative analysis of drug effects assessed after *ex vivo* culture of blood samples from malaria patients.

Representative plots of flow cytometric analysis of an uninfected blood sample (A) and a sample from a malaria patient with 1.5% parasitemia (B). At time point 0 of incubation, no difference in depolarizing events is observed between the infected samples and the uninfected control (A and B). However, Hz is produced as the parasite matures, and after 24 hours of incubation an increase in the percentage of depolarizing cells is detected (B) from 0.02 to 0.36. In this example, drug effects could be determined after only 24 hours of incubation (C). Contrary to chloroquine, where resistance was observed, artesunate and artemisinin are still effective drugs (C).

IC50 values of chloroquine and artemisinins

The IC50 values are shown in the Table IV.1. There was a poor correlation between the IC50 values of individual samples and the different assays. In fact, this is commonly observed even when using the same laboratory-adapted strain [19]. Indeed, several factors, such as the initial parasitemia, the hematocrit and the end point for measuring parasite growth can influence IC50 values [7,34]. Samples with higher initial parasitemia (group 3), showed increased IC50 values for artesunate and artemisinin (Table IV.1). Apparently, a higher initial parasitemia may be associated with an increase in inhibitory drug concentration of artemisinin, artesunate, chloroquine, and mefloquine [11], which could explain some of the increase observed in the IC50 values. Interestingly, mean IC50 values for artesunate and artemisinin in isolates that had a delayed growth (group 4) were somewhat lower than in groups 2 and 3, where maturation was detected at 24 hours. This could be due to the different growth profile of drug exposed and non-exposed parasites in group 4. Overall, IC50 values ranged from 0.9 to 60 nM and from 2.2 nM to 124 nM for

artesunate and artemisinin, respectively (Figure IV.3). These values are higher than previously described in the same region, using the HRP-2 assay [35]. Because several assay-related factors can influence IC₅₀ values they may not be directly comparable between different assays [7,34]. In the previous study, the final hematocrit was 1.5% [35], while in the Hz detection assay it was 2.5%. It has been observed that higher hematocrits may cause an increase in IC₅₀ values [34]. Preliminary data using the same culture-adapted strain showed that the IC₅₀ value for dihydroartemisinin increases from 1.7 nM to 7.5 nM when the hematocrit of the sample is raised from 1 to 2.5% (unpublished data).

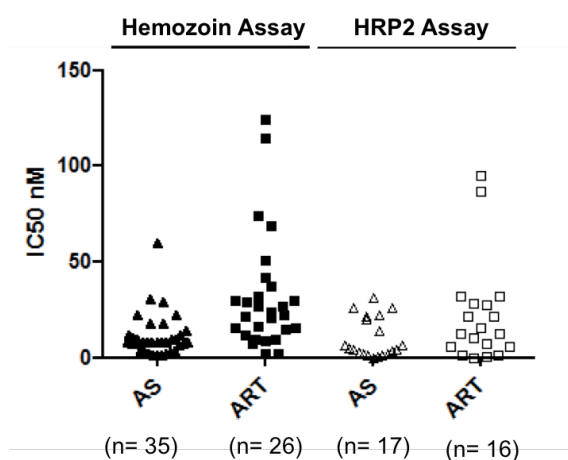


Figure IV.3: Inhibitory 50% concentrations obtained for artesunate and artemisinin.

Using the Hz detection assay, IC₅₀ values for artesunate and artemisinin differed between samples ranging from 0.9 to 60 nM and from 2.2 nM to 124 nM, respectively. IC₅₀ values obtained by the HRP-2 ELISA ranged from 0.6 to 31 nM for artesunate and from 0.6 to 94.8 nM for artemisinin.

For chloroquine, 70% of the samples had IC₅₀ values higher than 200 nM, indicating resistance, which is in line with an earlier reports and which is explained through the high usage of amodiaquine, many years after the use of chloroquine had been curbed and finally abandoned [36,37]. In Malawi [38, 39], Kenya [40] and Tanzania [41], chloroquine resistance decreased after its withdrawal, contrary to the study site, even though chloroquine treatment was discontinued 11 years ago, as observed by others [37,42]. One explanation brought forward is the use of artesunate/amodiaquine, because amodiaquine appears to select mutant *pfcrt* allele, which is responsible for chloroquine resistance [43]. Interestingly, the Hz-detection assay showed in some of the chloroquine-resistant strains that the percentage of Hz-containing cells increased as chloroquine concentration increased as well (Figure IV.2C). It is known that several drugs, especially quinoline-type drugs, directly interact with Hz, as discussed elsewhere [44]. This interaction may lead to alterations in the crystals distribution within the parasite that may affect the depolarized light signal. Recently it has been shown that parasites containing several small but distributed Hz crystals can have a higher depolarized signal than a parasite containing a

single large clump of Hz [45]. In this context it is not unlikely that at higher concentrations of chloroquine some of the drug may interact with Hz avoiding its coalescence. Thus, explaining why at higher concentrations of this drug the signal seems to be increased. Certainly, the mechanism of this observation is not known, and further investigation is required to understand the exact cause of this phenomenon.

During this study the HRP2-ELISA was performed alongside. However, drug effects could only be detected in 17 samples (37%), with IC₅₀ values ranging from 0.6 to 31 nM for artesunate and 0.6 to 94.8 nM for artemisinin (Figure IV.3). This success rate appears to be at the lower end of reported studies with 45% [14], while others had success rates of 75% [46] and 87% [13]. Of note, these samples were collected on purpose to be used exclusively in the scope of these studies. Contrary to this, here, samples were collected for other purposes, which might have contributed to a lower success rate. Furthermore, samples were preselected based on their parasitemias of 0.01% or higher [13], while in this study all samples were included. Apparently, re-invasion of uninfected RBCs (replication) is considered the main criterion for the success of the HRP2 assay [21]. However, even when no schizont maturation is observed after 24 hours of incubation, samples can still be successfully tested by the HRP2 assay [21]. During this study, most results (14 out of 17) were obtained in samples that exhibited delayed-growing parasites (group 4), whereas drug effects were only detected in two samples from groups 1 and 2, and in five samples from group 3.

Indeed, the low detection limit is a major advantage of the HRP2 assay. For instance, the Hz assay failed to determine drug effects in samples from group 1, possibly due to the low parasitaemias present in this group, which were below the previously reported 0.3% detection limit of the Hz assay [19]. On the other hand, when parasitemias are higher than 0.1% [21], samples have to be diluted with uninfected RBCs from healthy donors, which can be a limiting step. Results from group 3, where the parasitemia ranged from 0.2 to 12%, indicate that the Hz detection assay does not seem to require adjustment of the parasitemia to allow the detection of drug effects.

Field applications of flow cytometry

The optical bench of the CyFlow® flow cytometer available on site had a typical configuration common in most small instruments, consisting of one blue-laser (488 nm) and detectors for FSC, SSC and three fluorescences FL1 (green), FL2 (orange) and FL3 (red) (Figure IV.1A). For the detection of light depolarization the original set-up was easily

modified by simply changing the respective filters and mirrors, even taking advantage of the existing filter holders (Figure IV.1B). The optical bench layout required for the detection of light depolarization is simple (Figure IV.1C) and therefore, other instruments should also be easily modifiable, unless they use fiber-optic cables for light collection.

Few studies describe the use of flow cytometry for drug testing in the field [15,47], possibly because of the perceived expense and complexity in setting up and running such instruments. Nowadays the number of simple, robust and portable flow cytometers has increased, including instruments such as the Attune® (Life Technologies, Carlsbad, USA), the Accuri™ C6 (BD Biosciences, La Jolla, USA), the Cyflow Cube 6 (Partec, Münster, Germany), among others. It has been shown that these instruments can be easily modified to detect Hz-caused light depolarization [45] and most of them can be used with an autosampler for higher throughput [48]. Moreover, the initial purchase costs of these instruments have dropped substantially from those practiced before for larger instruments, allowing them to be used and available in the field. Indeed, recent field studies take advantage of this, by using for example the Accuri C6 [15,47]. Even smaller and simpler instruments used for CD4+ T cell counting in HIV-infected patients exist, such as the CyFlow®miniPOC from Partec, which are used in low-resource settings [49]. Although the way was often difficult, cytometry is no longer the very expensive, high-end technology based on bulky instruments. In the future, simple image cytometers might replace flow cytometers, as they seem to perform a broad range of measurements, and eventually parameters such as light depolarization could be detected as well [50,51].

Opening new avenues for anti-malarial drug testing in the field

This study showed that drug effects of clinically relevant anti-malarial drugs as well as resistance to chloroquine could be assessed by simply detecting Hz. This method measures parasite maturation and does not require re-invasion to occur; consequently, results can be obtained earlier than with other currently available methods, except for microscopy. However, microscopy relies on trained observers' ability to detect morphological changes of iRBC [52], which sometimes can be rare. Flow cytometric measurements can provide more objective, reliable and effective results than microscopy, as it has been previously observed in a different context [53]. Moreover, it allows the assessment of additional parameters, such as DNA and RNA content, which can improve parasite detection [51]. Finally, drug effects could be detected without having to decrease the sample's parasitemia. This may greatly simplify the protocol as it avoids the need to obtain blood

from healthy donors. Yet, this seems to lead to increased IC₅₀ values. Thus, whether parasitemia ought to be adjusted or not should be further investigated.

These findings open new avenues for other Hz-detection methods. Interestingly, several Hz detection methods exist [54-58] and they could possibly be used to detect drug effects as early, or even earlier, than the flow cytometric Hz detection.

5. Conclusion

This study conducted in the field showed flow cytometry could be easily implemented and performed in field conditions. Flow cytometric detection of Hz could be used as an alternative tool to assess drug effects on parasites obtained directly from patients' blood samples, without the need for additional reagents or complex protocols. However, further optimization of the Hz assay regarding its set-up conditions, for example, changing the hematocrit, may contribute to obtain IC₅₀ values more comparable to the ones that have been previously reported [13, 59].

Future studies should be performed in various settings, to further investigate the Hz assay and its usefulness as a tool for rapid resistance testing in malaria-endemic countries.

6. Acknowledgements

This work was supported by the Luso-American Foundation (FLAD-LACR grant: B-A.V-109-09/07). MR acknowledges *Fundação para a Ciência e a Tecnologia* for doctoral grant (SFRH/BD/84530/2012) and *Fundação Calouste Gulbenkian* for the Award CAML/Gulbenkian for Travel ACGT fellowship. The authors acknowledge the Albert Schweitzer Hospital's central clinic laboratory staff who provided the samples from malaria patients, the co-directors of CERMEL: Dr Akim Adegniko, Dr Bertrand Lell and Dr Maxime Selidji Agnandji and, finally, Dr Marguerite Massinga Loembe, Head of the CERMEL Research Laboratory.

7. References

1. Kweka EJ, Mazigo HD, Munga S, Magesa SM, Mboera LEG. (2013) Challenges to malaria control and success stories in Africa. *Global Health Perspectives* 1:71-80.
2. Noedl H, Se Y, Schaecher K, Smith BL, Socheat D and Fukuda MM. (2008) Evidence of artemisinin-resistant malaria in western Cambodia. *The New England Journal of Medicine* 359: 2619–2620.
3. Dondorp A, Nosten F, Yi P, Das D, Phyo A, Tarning J, et al. (2009) Artemisinin Resistance in *Plasmodium falciparum* Malaria. *The New England Journal of Medicine* 361: 455–467.
4. WHO. (2011) Global Plan for Artemisinin Resistance containment (GPARC). World Health Organization, Geneva, 2011.
5. Ashley E, Dhorda M, Fairhurst RM, Amaratunga C, Lim P, Suon S, et al. (2014) Spread of Artemisinin Resistance in *Plasmodium falciparum* Malaria. *The New England Journal of Medicine* 371: 411–423.
6. Van Hong N, Amambua-Ngwa A, Tuan NQ, Cuong do D, Giang NT, Van Dung N, et al. (2014) Severe malaria not responsive to artemisinin derivatives in man returning from Angola to Vietnam. *Emerging Infectious Diseases* 20:1199–202.
7. Basco LK. (2007) Field application of in vitro assays for the sensitivity of human malaria parasites to antimalarial drugs. WHO Press, Geneva, Switzerland.
8. Woodrow CJ and Krishna S. (2006) Antimalarial drugs: recent advances in molecular determinants of resistance and their clinical significance. *Cellular and Molecular Life Sciences* 63:1586–1596.
9. Ariey F, Witkowski B, Amaratunga C, Beghain J, Langlois A, Khim N, et al. (2014) A molecular marker of artemisinin-resistant *Plasmodium falciparum* malaria. *Nature* 505: 50-55.
10. Rieckmann K, Campbell G, Sax L and Mrema J. (1978) Drug sensitivity of *Plasmodium falciparum*. An in-vitro microtechnique. *The Lancet* 1: 22–23.
11. Duraisingh MT, Jones P, Sambou I, von Seidlein L, Pinder M and Warhurst DC. (1999) Inoculum effect leads to overestimation of in vitro resistance for artemisinin derivatives and standard antimalarials: a Gambian field study. *Parasitology* 119: 435–440.
12. Basco L, Marquet F, Makler M and Le Bras J. (1995) *Plasmodium falciparum* and *Plasmodium vivax*: Lactate dehydrogenase activity and its application for in vitro drug susceptibility assay. *Experimental Parasitology* 80: 260-271.

13. Noedl H, Attlmayr B, Wernsdorfer WH, Kollaritsch H and Miller RS. (2004) A histidine-rich protein 2-based malaria drug sensitivity assay for field use. *The American Journal of Tropical Medicine and Hygiene* 71:711-714.
14. Bacon DJ, Latour C, Lucas C, Colina O, Ringwald P and Picot S. (2007) Comparison of a SYBR green I-based assay with a histidine-rich protein II enzyme-linked immunosorbent assay for in vitro antimalarial drug efficacy testing and application to clinical isolates. *Antimicrobial Agents and Chemotherapy* 51:1172-1178.
15. Russell B, Malleret B, Suwanarusk R, Anthony C, Kanlaya S, Lau YL, et al. (2013) Field-based flow cytometry for ex vivo characterization of *Plasmodium vivax* and *P. falciparum* antimalarial sensitivity. *Antimicrobial Agents and Chemotherapy* 57: 5170–5174.
16. Noedl H. (2003) Malaria drug-sensitivity testing: new assays, new perspectives. *Trends in Parasitology* 19: 175–181.
17. Wein S, Maynadier M, Tran Van Ba C, Cerdan R, Peyrottes S, Fraisse L, et al. (2010) Reliability of antimalarial sensitivity tests depends on drug mechanisms of action. *Journal of Clinical Microbiology* 48:1651–1660.
18. Grimberg BT, Erickson JJ, Sramkoski RM, Jacobberger JW and Zimmerman PA (2008) Monitoring *Plasmodium falciparum* growth and development by UV flow cytometry using an optimized Hoechst-thiazole orange staining strategy. *Cytometry A* 73:546–554.
19. Rebelo M, Sousa C, Shapiro HM, Mota MM, Grobusch MP, Hänscheid T (2013) A novel flow cytometric hemozoin detection assay for real-time sensitivity testing of *Plasmodium falciparum*. *PLoS One* 8:e61606.
20. Planche T, Krishna S, Kombila M, Engel K, Faucher JF, Ngou-Milama E, et al. (2001) Comparison of methods for the rapid laboratory assessment of children with malaria. *The American Journal of Tropical Medicine and Hygiene* 65:599-602.
21. Noedl H, Bronnert J, Yingyuen K, Kollaritsch H, Fukuda M and Attlmayr B. (2005) Simple Histidine-Rich Protein 2 Double-Site Sandwich Enzyme-Linked Immunosorbent Assay for Use in Malaria Drug Sensitivity Testing. *Antimicrobial Agents and Chemotherapy* 49: 3575-7.
22. Basco LK and Ringwald P (2003) In vitro activities of piperazine and other 4-aminoquinolines against clinical isolates of *Plasmodium falciparum* in Cameroon. *Antimicrobial Agents and Chemotherapy* 47:1391-1394.

23. Gritzmacher CA and Reese RT (1984) Protein and Nucleic Acid Synthesis During Synchronized Growth of *Plasmodium falciparum*. *Journal of Bacteriology* 160:1165–1167.
24. Lopez Antunano FJ and Wernsdorfer WH (1979). In vitro response of chloroquine resistant *Plasmodium falciparum* to mefloquine. *Bulletin of the World Health Organization* 57:663–665.
25. Inaba H, Ohmae H, Kano S, Faarado L, Boaz L, Leafasia J et al (2001) Variation of incubation time in an in vitro drug susceptibility test of *Plasmodium falciparum* isolates studied in the Solomon Islands. *Parasitology International* 50:9–13.
26. Nielsen MA and Staalsoe T (2008) Establishment of long-term in vitro cultures of *Plasmodium falciparum* from patient blood. In: Moll K, Ljungstrom I, Perlmann H, Scherf A, Wahlgren M (Eds.), *Methods in Malaria Research*, 5th edition, Manassas.
27. Lim P, Chim P, Sem R, Nemh S, Poravuth Y, Lim C, et al. (2005) In vitro monitoring of *Plasmodium falciparum* susceptibility to artesunate, mefloquine, quinine and chloroquine in Cambodia: 2001-2002. *Acta Tropica* 93:31–40.
28. Kaddouri H, Nakache S, Houzé S, Mentré F and Le Bras J (2006). Assessment of the drug susceptibility of *Plasmodium falciparum* clinical isolates from Africa by using a *Plasmodium* lactate dehydrogenase immunodetection assay and an inhibitory maximum effect model for precise measurement of the 50% inhibitory concentration. *Antimicrobial Agents and Chemotherapy* 50: 3343–9.
29. Rason MA, Randriantsoa T, Andrianantenaina H, Ratsimbaoa A, Menard D (2008) Performance and reliability of the SYBR Green I based assay for the routine monitoring of susceptibility of *Plasmodium falciparum* clinical isolates. *Transactions of the Royal Society of Tropical Medicine and Hygiene* 102:346–51.
30. Legrand E, Volney B, Meynard JB, Mercereau-Puijalon O, Esterre P (2008) In vitro monitoring of *Plasmodium falciparum* drug resistance in French Guiana: a synopsis of continuous assessment from 1994 to 2005. *Antimicrobial Agents and Chemotherapy* 52: 288–98.
31. van Schalkwyk DA, Burrow R, Henriques G, Gadalla NB, Beshir KB, Hasford C, et al. (2013) Culture-adapted *Plasmodium falciparum* isolates from UK travellers: in vitro drug sensitivity, clonality and drug resistance markers. *Malaria Journal* 12:320.
32. Witkowski B, Amaratunga C, Khim N, Sreng S, Chim P, Kim S, et al. (2013) Novel phenotypic assays for the detection of artemisinin-resistant *Plasmodium falciparum*

malaria in Cambodia: in-vitro and ex-vivo drug-response studies. *The Lancet Infectious Diseases* 13: 1043–1049.

33. Rebelo M, Shapiro HM, Amaral T, Melo-Cristino J, Hanscheid T (2012) Haemozoin detection in infected erythrocytes for *Plasmodium falciparum* malaria diagnosis—Prospects and limitations. *Acta Tropica* 123: 58–61.

34. Basco LK. (2004) Molecular epidemiology of malaria in cameroon. XX. Experimental studies on various factors of in vitro drug sensitivity assays using fresh isolates of *Plasmodium falciparum*. *The American Journal of Tropical Medicine and Hygiene* 80: 260-271.

35. Held J, Soomro SA, Kremsner PG, Jansen FH, Mordmuller B (2011) In vitro activity of new artemisinin derivatives against *Plasmodium falciparum* clinical isolates from Gabon. *International Journal of Antimicrobial Agents* 37: 485–488.

36. Grobusch MP, Adagu IS, Kremsner PG, Warhurst DC (1998) *Plasmodium falciparum*: in vitro chloroquine susceptibility and allele-specific PCR detection of Pfm_{dr}1Asn86Tyr polymorphism in Lambarene, Gabon. *Parasitology* 116: 211–217.

37. Borrmann S, Binder RK, Adegnika AA, Missinou MA, Issifou S, Ramharter M, et al. (2002) Reassessment of the resistance of *Plasmodium falciparum* to chloroquine in Gabon: implications for the validity of tests in vitro vs. in vivo. *Transactions of the Royal Society of Tropical Medicine and Hygiene* 96: 660–663.

38. Kublin JG, Cortese JF, Njunju EM, Mukadam RA, Wirima JJ, Kazembe PN, et al. (2003) Reemergence of chloroquine sensitive *Plasmodium falciparum* malaria after cessation of chloroquine use in Malawi. *The Journal of Infectious Diseases* 187:1870–1875.

39. Laufer MK, Thesing PC, Eddington ND, Masonga R, Dzinjalama FK, Takala SL, et al. (2006) Return of chloroquine antimalarial efficacy in Malawi. *The New England Journal of Medicine* 355:1959–1966.

40. Mwai L, Ochong E, Abdirahman A, Kiara SM, Ward S, Kokwaro G, et al. (2009) Chloroquine resistance before and after its withdrawal in Kenya. *Malaria Journal* 8: 106.

41. Alifrangis M, Lusingu JP, Mmbando B, Dalgaard MB, Vestergaard LS, Ishengoma D, et al. (2009) Five-year surveillance of molecular markers of *Plasmodium falciparum* antimalarial drug resistance in Korogwe District, Tanzania: accumulation of the 581G mutation in the *P. falciparum* dihydropteroate synthase gene. *The American Journal of Tropical Medicine and Hygiene* 80: 523–527.

42. Frank M, Lehnert N, Mayengue PI, Gabor J, Dal-Bianco M, Kombila DU, et al. (2011)

A thirteen-year analysis of *Plasmodium falciparum* populations reveals high conservation of the mutant pfcrt haplotype despite the withdrawal of chloroquine from national treatment guidelines in Gabon. *Malaria Journal* 10: 304.

43. Djimdé AA, Fofana B, Sagara I, Sidibe B, Toure S, Dembele D, et al. (2008) Efficacy, safety, and selection of molecular markers of drug resistance by two ACTs in Mali. *The American Journal of Tropical Medicine and Hygiene* 78: 455–461.

44. Gorka AP, de Dios A and Roepe PD. (2013) Quinoline drug-heme interactions and implications for antimalarial cytostatic versus cytocidal activities. *Journal of Medicinal Chemistry* 56: 5231–5246.

45. Rebelo M, Tempera C, Bispo C, Andrade C, Gardner R, Shapiro M, et al. (2015) Light Depolarization Measurements in Malaria: A New Job for an Old Friend. *Cytometry A* 87: 437–445.

46. Noedl H, Krudsood S, Leowattana W, Tangpukdee N, Thanachartwet W, Looareesuwan S, et al. (2007) In vitro antimalarial activity of azithromycin, artesunate, and quinine in combination and correlation with clinical outcome *Antimicrobial Agents and Chemotherapy* 51: 651–656.

47. Amaratunga C, Neal AT and Fairhurst RM. (2014) Flow cytometry-based analysis of artemisinin-resistant *Plasmodium falciparum* in the ring-stage survival assay. *Antimicrobial Agents and Chemotherapy* 58: 4938–4940.

48. Partec – Cyflow Cube 6. <http://www.sysmex-partec.com/fileadmin/media/pdf/CyFlow-Cube6.pdf>. Accessed: 17 December 2014.

49. Boyle DS, Hawkins KR, Steele MS, Singhal M and Cheng X. (2012) Emerging technologies for point-of-care CD4 T-lymphocyte counting. *Trends in Biotechnology* 30: 45–54.

50. Shapiro HM and Mandy F. (2007) Cytometry in malaria: moving beyond Giemsa. *Cytometry A* 71: 643–645.

51. Shapiro HM, Apte SH, Chojnowski GM, Hänscheid T, Rebelo M and Grimberg BT. (2013) Cytometry in malaria-a practical replacement for microscopy? *Current Protocols in Cytometry* Chapter 11:Unit 11.20.

52. Maguire JD, Lederman ER, Barcus MJ, O'Meara WA, Jordon RG, Duong S, et al. (2006) Production and validation of durable, high quality standardized malaria microscopy slides for teaching, testing and quality assurance during an era of declining diagnostic proficiency. *Malaria Journal* 5: 92.

53. Hänscheid T, Frita R, Längin M, Kremsner PG and Grobusch MP. (2009) Is flow

cytometry better in counting malaria pigment-containing leukocytes compared to microscopy? *Malaria Journal* 8: 255.

54. Mens PF, Matelon RJ, Nour BY, Newman DM and Schallig HD. (2011): Laboratory evaluation on the sensitivity and specificity of a novel and rapid detection method for malaria diagnosis based on magneto-optical technology (MOT). *Malaria Journal* 9: 207.

55. Wilson BK, Behrend MR, Horning MP and Hegg MC. (2011) Detection of malarial byproduct hemozoin utilizing its unique scattering properties. *Opt Express* 2011;19:12190–12196.

56. Lukianova-Hleb EY, Campbell KM, Constantinou PE, Braam J, Olson JS, Ware RE, et al. (2014) Hemozoin-generated vapor nanobubbles for transdermal reagent- and needle-free detection of malaria. *Proceedings of the National Academy of Sciences of the United States of America* 111: 900-5.

57. Orbán A, Butykai A, Molnár A, Pröhle Z, Fülöp G, Zelles T, et al. (2014) Evaluation of a novel magneto-optical method for the detection of malaria parasites. *PLoS One* 9: e96981.

58. Peng WK, Kong TF, Ng CS, Chen L, Huang Y, Bhagat AA, et al. (2014) Micromagnetic resonance relaxometry for rapid label-free malaria diagnosis. *Nature Medicine* 20: 1069-1073.

59. Kreidenweiss A, Kremsner PG and Mordmüller B. (2008) Comprehensive study of proteasome inhibitors against *Plasmodium falciparum* laboratory strains and field isolates from Gabon. *Malaria Journal* 7:187.

CHAPTER V

USEFULNESS OF THE HEMOZOIN ASSAY TO DETECT ARTEMISININ RESISTANCE

1. Introduction

1.1. Artemisinin-combination therapies

The current first-line treatment for malaria is based on artemisinin-combination therapies (ACTs) [1]. Since the introduction of ACTs the burden of malaria has significantly decreased. In fact, in the last 15 years, the number of deaths and the incidence of malaria have been reduced by 48% and 18%, respectively [2].

Artemisinin drugs kill all asexual stages of parasite development in the blood and it is able to reduce the parasite load by up to 10.000-fold per cycle [3]. Moreover, it also affects gametocytes, the forms that are responsible for transmission [4]. Importantly, in addition to its benefits in the treatment of uncomplicated malaria, artesunate is also more effective than quinine in reducing the deaths associated with severe *P. falciparum* malaria (Figure V.1) [5, 6].

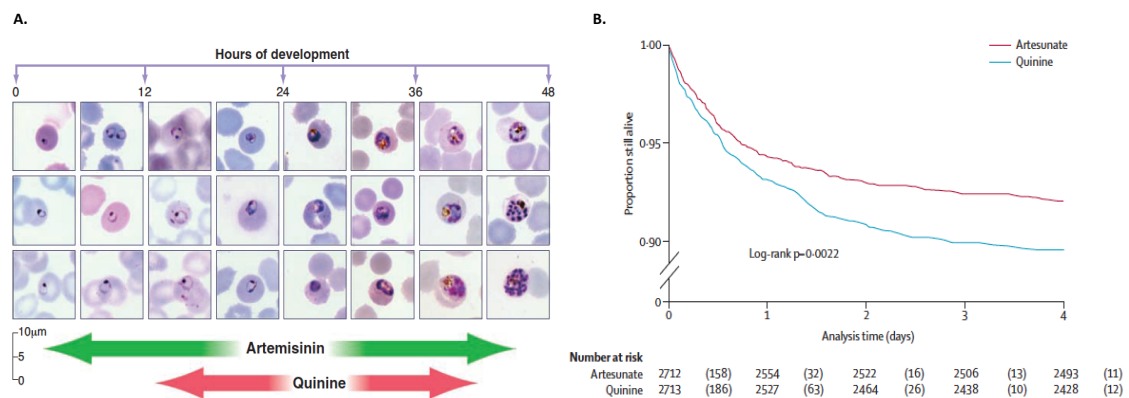


Figure V.1: Antimalarial activity of artemisinin in comparison to quinine.

Representative pictures of blood-stage *P. falciparum* parasites in Giemsa-stained blood smears (A). Parasitized erythrocytes circulate for the first third of the 48-hour cycle and then sequester in capillaries. Artemisinins inhibit development of a broader age range of the parasites than do quinine and other antimalarial drugs. The effect on the young rings prevents their development to the more pathological mature parasites that sequester (A) [4]. Kaplan-Meier curves comparing survival in African children with severe *P. falciparum* malaria treated with either parenteral artesunate or quinine. The numbers in parentheses are the deaths during the indicated time (B) [6].

Despite their potency, if artemisinins are given alone as monotherapy for 3 days, recrudescence rates are high [3, 7, 8]. Extending the treatment for 7 days reduces the recrudescence events but does not eliminate them completely. This is thought to be a consequence of their inherently short *in vivo* half-life (approximately 1 hour) [4]. Combination of artemisinins with a longer-acting partner drug that has a different mode of action (such as lumefantrine, amodiaquine, piperaquine, mefloquine, sulfadoxine–pyrimethamine, and pyronaridine) prevents recrudescence and may also delay the

emergence of drug resistant parasites. The rationale for ACTs is that the highly potent artemisinins will have a rapid onset of action, however they have a very short half-life. Thus, combination with a longer-acting, but less potent, partner drug will allow to kill any remaining parasites over the following 1–2 weeks.

In 2001, the WHO recommended treating uncomplicated malaria with combinations of two unrelated drugs in the form of ACTs. By 2009, 77 of 81 *P. falciparum* malaria-endemic countries had implemented the use of ACTs in their national drug policy program [9].

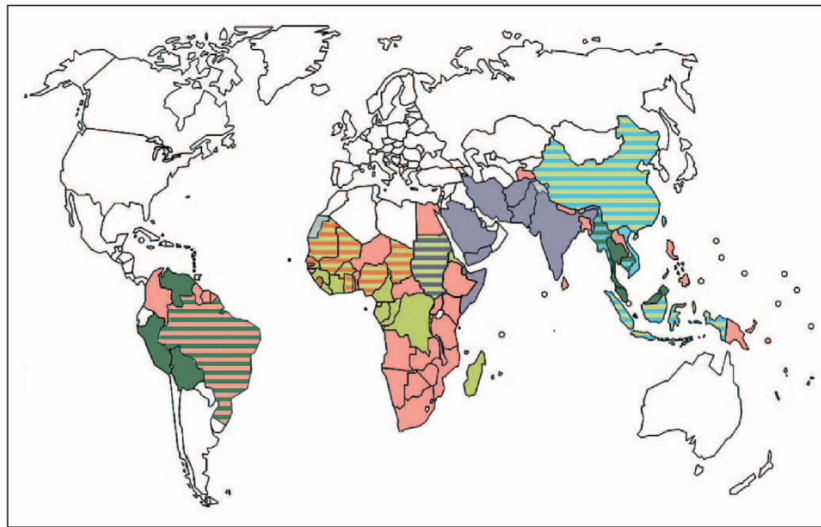


Figure V.2: Current global distribution of artemisinin-based combination therapies as the first-line treatment of uncomplicated falciparum malaria.

This distribution was collated from maps of country-wide artemisinin-based combination therapy use, as published in [1]. ●, artemether–lumefantrine; ●, dihydroartemisinin–piperaquine; ●, artesunate–amodiaquine; ●, artesunate–mefloquine; ●, artesunate–sulphadoxine/pyrimethamine [10].

1.2. Artemisinin-induced dormancy

Artemisinin-induced dormancy has been suggested as the main cause of recrudescence observed in patients treated with artemisinin monotherapies [11].

Artemisinin induced dormancy was reported for the first time in 1996, where dihydroartemisinin (DHA) treated parasites arrested their development at early ring-stage and survived in a dormant form from 3 to 8 weeks, after which they resumed their growth [12]. This led to the hypothesis that artemisinin treated parasites enter a state of dormancy where they are protected from the drug effect and at a later stage, when the drug is no longer present, they recover and resume their growth. More recently, five *P. falciparum* strains with different genetic backgrounds were tested and all became dormant following exposure with high-dose of DHA [13]. However, the recovery rates varied from 0.04% to

1.3% between strains [13]. It was reported that the great majority of dormant parasites die in this state but some recover and become growing parasites with a normal morphology between 3 and 20 days post-treatment [11, 13]. Dormant parasites have been described to exhibit distinct morphological features: “the vacuole is not present, the cytoplasm is condensed and tightened towards the nucleus and the nucleus is condensed” [14]. Nevertheless, microscopic assessment of whether a parasite is dead or dormant can be difficult, as depicted in Figure V.3.

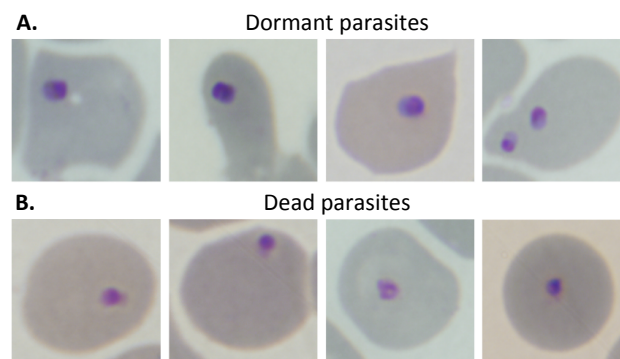


Figure V.3: Comparison of dormant and dead parasites after a typical exposure to artemisinin drugs.

After ring-stage parasites were treated with artemisinin drugs, they became dormant, developed a rounded morphology, and retained blue cytoplasm and red chromatin on a Giemsa smear (A). Dead parasites lacked distinct chromatin and cytoplasm, appearing globular, and they appeared red/purple on a Giemsa smear (B) [14].

Later, dormancy has also been associated with artemisinin resistance [14–16]. Laboratory selected resistant parasites [15] were investigated and it was observed that when dormancy is induced resistant parasites recover faster, leading to an earlier recrudescence [15]. However, artemisinin-induced dormancy occurs in both sensitive and resistant parasites *in vitro* [14, 17] and thus, this phenomenon appear to be independent of drug resistance. Moreover, there have been no reports to date that dormant parasites exist in human infections [11]. Yet, this might be due to the fact that these “abnormal” parasites may be difficult to be distinguished in blood smears from patients. Or it may be that these forms are removed from circulation and the number of dormant parasites found in the blood is too low to be detected [11].

1.3. Artemisinin resistance

The first reports of artemisinin resistance came from two separate efficacy trials conducted in Cambodia, where patients treated with ACTs showed a delay in parasite clearance times [18, 19]. In the first trial, two out of 60 patients had prolonged parasite-clearance times after monotherapy with artesunate. *Ex vivo* IC₅₀ values of these two patients were four-times higher than the ones present in cured patients [18]. The second trial was conducted in Cambodia and Thailand, where both treatment regimens of artesunate monotherapy or artesunate in combination with mefloquine were used. Results showed delayed parasite clearance times in Cambodian patients, suggesting *P. falciparum* parasites isolated from these patients had reduced susceptibility to artesunate. Unlike the first trial, the isolates collected in this trial showed no significant differences in their *in vitro* susceptibility (IC₅₀ values) to DHA or artesunate, when measured using conventional *in vitro* drug assays. Moreover, no correlation between the delayed parasite clearance and putative molecular markers were found [19].

The phenotypic profile of artemisinin resistant parasites differ from what has been observed for other antimalarial drugs, where an increase in IC₅₀ values is usually observed in resistant parasites [20]. Indeed, no correlation between what is observed in the patients can be made with results obtained by the commonly used *in vitro* tests [19]. Moreover, the majority of patients who have delayed parasite clearance following treatment with an ACT still manage to clear their infections [19]. Therefore, artemisinin resistance has been exclusively defined as delayed parasite clearance (e.g. parasite clearance half-life \geq 5 hours) following treatment with an artesunate monotherapy or with an ACT [20, 21]. This is officially named by the WHO as partial resistance [22]. More recently, a molecular marker associated with artemisinin resistance has been described [23]. Mutations in the kelch 13-propeller domain were associated with delayed parasite clearance [24–26]. Even though further validation is still required, this led the WHO to update and divide the definition of artemisinin resistance into: “*suspected artemisinin resistance (defined as a high prevalence of the delayed parasite clearance phenotype or high prevalence of K13 mutants) and confirmed artemisinin resistance (defined as a combination of both delayed parasite clearance and K13 resistance-validated mutations for the same patient)*” [22].

Recent reports indicate that artemisinin resistance has now spread across Southeast Asia [24], but it did not reach the African continent yet [24, 27].

Even though ACTs still cure malaria patients, provided that the partner drug is effective, one must recognize the threat that artemisinin resistance possess in the fight against malaria. It was predicted that artemisinin resistance would cause an excess of 116.000 deaths annually, with medical costs and productivity losses evaluated as 146 million USD and 385 million USD per year, respectively [28]. Moreover, artemisinin resistance may lead to the development of resistance to the partner drugs by allowing higher numbers of parasites to be exposed to the partner drug alone. Consequently, this larger parasite biomass is more likely to develop resistance to the partner drug [20], as it is currently being witnessed in Cambodia for DHA-piperaquine [29–31].

1.4. *In vitro* detection of artemisinin resistance

Standard *in vitro* drug assays fail to detect artemisinin resistance [19]. This may be explained by the fact that only young ring-form parasites exhibit reduced susceptibility to artemisinins [17, 32]. Currently used *in vitro* assays determine drug effects over 48 hours of incubation, reflecting the activity of the drug on all stages of parasite development from rings to mature schizonts. Therefore, results would be relatively unaffected if only a short part of the cycle was affected by the underlying mechanism of resistance. For this reason several modified protocols of currently available drug assays were investigated for their potential to detect artemisinin resistance *in vitro* [33–35].

The first one to be reported was the Ring-Stage-Assay (RSA). This assay format mimics what occurs in treated patients, where parasites are exposed to high concentrations of drug for short periods of 1-2 hours. Thus, in this assay early ring-stage parasites (0-3h of development) are incubated with a 6-hour pulse of DHA at 700 nM [33]. Survival rates of parasites exposed and non-exposed to treatment are calculated based on microscopy. Inherently, this assay is extremely time-consuming, labor-intensive and it requires more than one trained microscopist for the read-out of results.

Another approach based on the RSA was developed. In this case, a DNA and a viability stains were used in combination to detect viable parasites by flow cytometry [34]. The use of such combination allowed to differentiate the population of infected cells into cells containing viable parasites or cells containing non-viable parasites. It was shown that this method performs as well as microscopy and can be used more easily to standardize the collection of RSA data between research groups [34].

A modified 24-hour trophozoite maturation test was developed and compared to the traditional 48-hour schizont maturation test (WHO microtest) [35]. This adaptation was

based on the fact that only ring-forms are less susceptible to artemisinin and thus, it is more likely to be able to detect drug effects at an earlier time-point during parasite development. Indeed, this modified assay showed that IC₅₀ values obtained for the resistant strains were higher than the ones obtained with the standard 48h-schizont maturation test, and that they correlated with parasite clearance half-life, whereas the standard 48-hour test values did not [35]. Even though this adapted version could be used to detect artemisinin resistance, it is also based on microscopic read-out which makes it laborious, slow and requires experienced personnel.

In summary, different approaches have been successful in detecting artemisinin resistance *in vitro*, however the fact that they require either expensive stains or are laborious and time-consuming limits their application.

1.5. Hemozoin as an alternative assay to detect artemisinin resistance *in vitro*

The hemozoin detection assay relies on the detection of hemozoin by flow cytometry to monitor real-time parasite maturation. Therefore, no additional reagents are needed [36]. It has been shown that this method allows to detect drug effects *in vitro* earlier than other available drug assays [36]. It was further validated *ex vivo* in the field using samples from malaria patients [37]. Thus, the hemozoin detection assay may be an alternative assay for artemisinin testing *in vitro* or *ex vivo*.

The main objective of the work presented in this chapter was to investigate the potential and the usefulness of the hemozoin assay in the detection and study of artemisinin resistance *in vitro*.

2. Material and Methods

All reagents were obtained from Sigma Aldrich (St Louis, Mo, USA), unless stated otherwise.

Flow cytometer modification (depolarized side scatter detection)

The Cyflow® Blue (Partec, Münster, Germany) was modified as described elsewhere [38]. Briefly, two side-scatter (SSC) detectors were created, with a 50%/50% beam splitter between them. A polarizer was placed orthogonally (horizontal) to the polarization plane of the laser light (vertical), in front of one of the SSC detectors, allowing the detection of depolarized side scatter.

Microscopy

Parasitemia, parasite maturation and the synchronicity of parasites in culture were assessed by light microscopic examination of Giemsa-stained blood smears. Air-dried blood smears were fixed in absolute methanol and stained with Giemsa (Merck, Darmstadt, Germany) in a 1:10 dilution in 0.4% PBS, for 20 minutes.

Flow cytometric analysis

Parasite maturation was assessed by analyzing the percentage of hemozoin-containing cells (depolarizing events), or by the intensity of SYBR green positive events at different time-points. The parasitemia was determined by assessing by the percentage of SYBR green positive cells.

Flow cytometry results were analyzed using FlowJo software (version 9.0.2, Tree Star Inc., Oregon, USA). Hemozoin-containing cells (depolarizing events) were defined in plots of side scatter (SSC) versus depolarized-SSC as those with a signal above the background observed in the uninfected control (Figure V.4A). To determine SYBR green I positive cells, green fluorescence (FL1) versus red fluorescence (FL3) plots were used (Figure V.4B). SYBR green I positive events were established based on a stained uninfected control and had to be adjusted at each time point, always using the uninfected SYBR green stained sample from the corresponding time point.

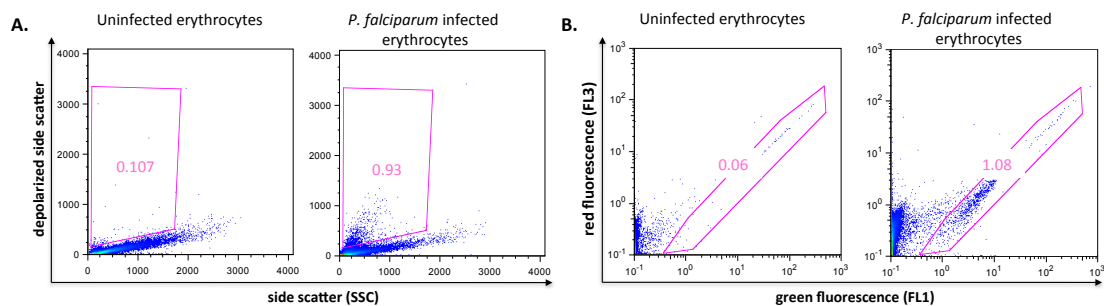


Figure V.4: Gating strategy used to detect infected erythrocytes based on depolarization or SYBR green staining.

Depolarizing events were gated in plots of side scatter versus depolarized-side scatter (A). SYBR green positive cells were gated in plots of green fluorescence (FL1) versus red fluorescence (FL3) (B). In both cases positive events were gated based on the uninfected samples.

Plasmodium falciparum strains

All *Plasmodium falciparum* strains were provided by the Malaria Research and Reference Reagent Resource Center (MR4) for distribution by BEI Resources NIAID, NIH. The

MRA-1239/IPC5188 (artemisinin-sensitive strain) and MRA-1240/IPC5202 (artemisinin-resistant strain) were contributed by Didier Ménard, while the 3D7 (laboratory-adapted strain sensitive to artemisinin) was contributed by Daniel J. Carucci.

Plasmodium falciparum continuous cultures

All *Plasmodium falciparum* strains were grown in recently collected donor erythrocytes in RPMI based complete malaria culture medium (CMCM) according to the recommendations of the Malaria Research and Reference Reagent Resource Center (MR4) [39]. Cultures were maintained at 5% hematocrit, at 37°C in an atmosphere of 5% O₂ and 5% CO₂. As uninfected controls, erythrocytes from healthy donors were cultured as described above.

Tight Synchronization

Culture-adapted parasites were synchronized two to three times with 5% sorbitol at approximately 40-hours intervals, as described elsewhere [40]. Then, synchronous segmenting schizonts were incubated for 15 minutes at 37°C in RPMI-1640 supplemented with 15 U/mL of sodium heparin (Roche, Basel, Switzerland) and then purified on a 35%/75% Percoll gradient, washed in RPMI-1640, and cultured for 3 hours with uninfected erythrocytes. Cultures were treated with 5% sorbitol to eliminate remaining schizonts, adjusted to 2% hematocrit and approximately 1% parasitemia by adding uninfected erythrocytes, and dispensed into 96 well plates. The Ring-Stage-Assay was performed immediately (Figure V.5A).

Mild sorbitol synchronization

When continuous cultures of *P. falciparum* reached a parasitemia of > 2%, with a minimum of 50% rings, the first sorbitol treatment was performed, as described elsewhere [40]. Briefly, the culture medium was discarded after centrifugation of the culture, at 1800 rpm, for 5 minutes. Then, a volume of sorbitol at 5% (corresponding to 10x the volume of the pellet) was added to the pellet and incubated for 10 minutes, at 37°C. Cultures were washed once in RPMI-1640 by centrifugation at 1800 rpm, for 5 minutes. Finally, CMCM was added to the pelleted cells, and the synchronized culture was incubated at 37°C in an atmosphere of 5% O₂ and 5% CO₂.

In this mild synchronization protocol, culture-adapted parasites were synchronized four

times with 5% sorbitol. In the first three times, synchronization was done in approximately 50 hours intervals (to select for younger ring-forms, assuming that the parasite life cycle would be of approximately 48 hours). The last sorbitol was performed after approximately 38h (Figure V.5B).

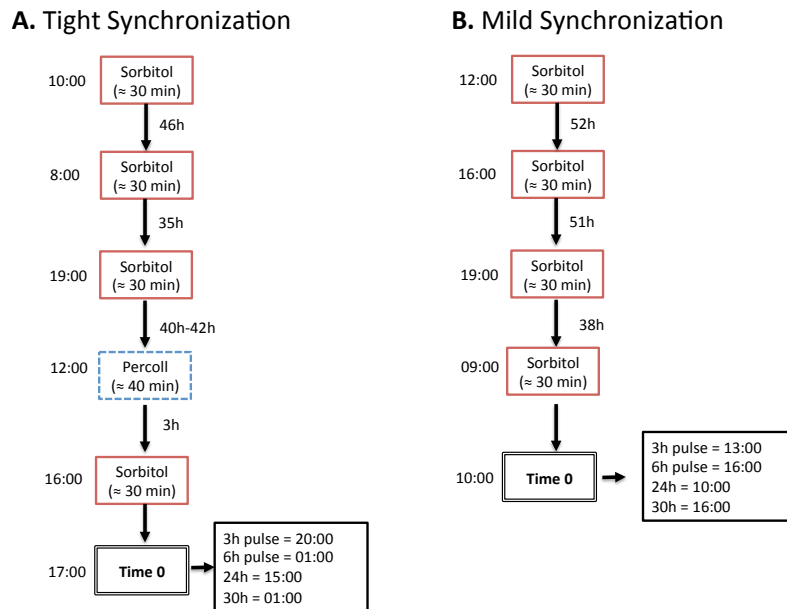


Figure V.5: Comparison of the two synchronization protocols.

Ring-stage assay require the use of tightly synchronized cultures (A). A simple, less laborious synchronization protocol was further investigated (B).

Pulse Assay – based on the Ring-Stage-Assay

Dihydroartemisinin (DHA) in powder was dissolved in DMSO, stored up to 6 months in individual aliquots, at -20°C. In the day of the experiments working solutions of DHA were prepared by diluting the stock solution in CMCM.

Tightly and mildly synchronized ring-form parasites were incubated with 700 nM of DHA. After 6 hours the drug was washed away and infected RBCs were put back in culture with CMCM, as described elsewhere [33]. Parasite maturation and growth was assessed by flow cytometry at 30, 48 and 72 hours. Microscopy determination of parasitemia was performed after 72 hours of incubation. Parasite survival was determined by counting the proportion of viable parasites (in approximately 2000 erythrocytes) that developed into parasites with normal morphology at 72 hours after drug removal. The survival rate was expressed by the ratio of viable parasites in DHA treated samples in comparison to the parasites viable in the drug free control.

Standard Drug Assay

Mildly synchronized ring-form parasites at 2.5% hematocrit and at approximately 1% parasitemia were incubated with increasing concentrations of DHA (0.12, 0.5, 2, 8 and 32 nM), in 96 well-plates, for 72 hours, at 37°C, in a 5% CO₂ and 5% O₂ atmosphere.

For each flow cytometric measurement approximately 100.000 events were analyzed. A volume of 5 µL of the blood suspension present in the wells was stained with SYBR green 1x, as described below. All samples were analyzed in triplicate.

A nonlinear regression model (sigmoidal dose-response/variable slope) was used to calculate the 50% inhibitory concentrations (IC₅₀), with SigmaPlot - Systat Software (Chicago, IL, USA) at specific time-points.

SYBR green I staining

For each measurement 5 µl of the culture (approximately 800.000 cells) was stained with the DNA-specific dye SYBR green I (Invitrogen, Carlsbad, USA) at 1x. After 20 minutes of incubation, in the dark, the stained sample was immediately analyzed by flow cytometry using a 535/45 nm bandpass filter in front of the detector.

3. Results and Discussion

3.1. Artemisinin Resistant parasites show increased IC₅₀ values when using the Hz detection assay

The 50% inhibitory concentrations (IC₅₀) for DHA were calculated for the artemisinin-resistant (1240) and sensitive (1239, 3D7) strains. Two different approaches were used to measure parasite maturation and growth: 1) the percentage of hemozoin-containing cells that depolarize light was assessed after 24 hours of incubation and 2) the percentage of SYBR green positive cells, which reflects the parasitemia, was determined after 48 hours of incubation. Hemozoin depolarizes light and thus can be detected by flow cytometry. As the content of hemozoin increases as parasites mature, assessment of the percentage of depolarizing cells overtime allows to monitor parasite maturation in real-time [36].

Quantification of depolarizing events at 24 hours allowed the detection of increased IC₅₀ values for the ART-resistant strain (average 15 nM) in comparison to the ART-sensitive strains (average 8 nM) (Figure V.6). However, when IC₅₀ values were calculated based on the percentage of SYBR green positive cells (parasitemia) at 48 hours of incubation no difference was observed between strains (Figure V.6).

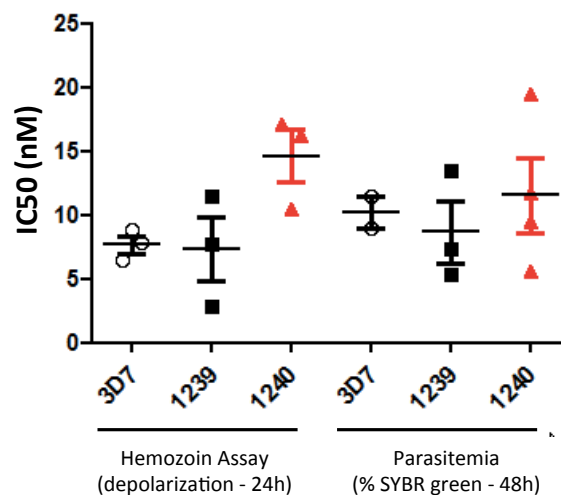


Figure V.6: Inhibitory 50% concentrations of dihydroartemisinin.

Using the hemozoin detection assay (A), IC₅₀ values for the artemisinin-resistant strain (red dots) were higher than the ones obtained for the artemisinin-sensitive strains (3D7 – white dots; 1239 – black dots) at 24 hours of incubation. When parasitemia (% SYBR green positive cells) is assessed after 48 hours incubation, no difference in the IC₅₀s was observed between the different strains.

In fact, one of the hallmarks of artemisinin resistance is precisely the fact that the delayed parasite clearance observed in the patients is not detected by commonly used *in vitro*

assays, including the reference method based on the incorporation of [³H]Hypoxanthine [19, 33]. This can be explained by the fact that only the young ring-forms show reduced susceptibility to DHA [17]. Thus, as currently used *in vitro* assays determine drug effects after 48 hours of incubation, they reflect the activity of the drug on all stages of parasite development. Based on this idea a modified 24-hour trophozoite maturation test was developed and compared to the traditional 48h-schizont maturation test (WHO microtest) [35]. As the name indicates in this assay drug effects were measured earlier at 24 hours of incubation, instead of the conventional 48 hours. IC₅₀ values obtained by the 24-hours trophozoite maturation assay for the resistant strains correlated with parasite clearance half-life, whereas the standard 48-h test values did not [35].

A modified version of the [³H]Hypoxanthine radioactive assay was also developed [14]. In this case, if [³H]Hypoxanthine is added at the same time as the drug, instead of the common addition at 24 or 48 hours after incubation with the drug, any differences in growth of resistant rings would be observed. Results using an *in vitro* derived ART-resistant line of *P. falciparum* showed that these parasite lines had increased IC₅₀ values in comparison to sensitive parasites [14].

3.2. Artemisinin-resistant parasites show increased survival rates in comparison to artemisinins-sensitive strains

Due to the inability of standard *in vitro* drug assays to detect artemisinin resistance, a modified protocol based on a high-dose pulse of DHA for 6 hours, named as the ring-stage assay (RSA) was developed [33]. Here, IC₅₀ values are not calculated (a single drug concentration is tested) and survival rates are determined instead. Results showed that survival rates were associated with parasite clearance times. Fast-clearing (sensitive) parasites had a median 0.23% survival in comparison to 11% in slow-clearing (resistant) parasites [33].

Survival rates were assessed using the previously described RSA protocol [33] and the final read-out was made using four different approaches: 1) the recommended microscopy assessment of parasitemia; 2) the quantification of depolarizing events (Figure V.7A); 3) the determination of SYBR green positive cells (Figure V.7B); and 4) the assessment of SYBR green intensity (Figure V.7C).

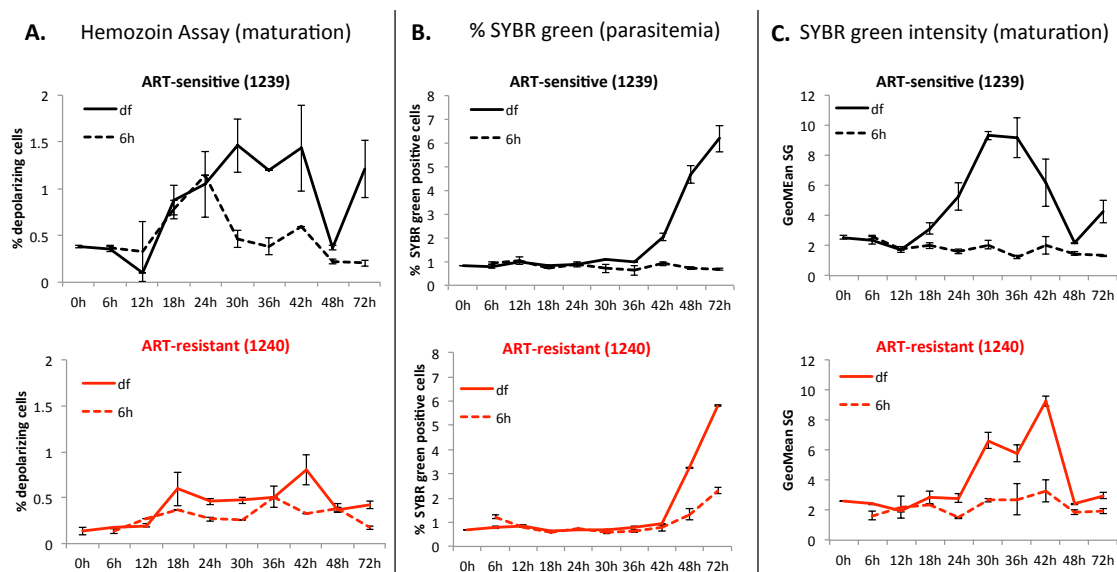


Figure V.7: Comparison of artemisinin resistant and sensitive *P. falciparum* strains using different approaches to assess parasite growth and maturation.

Solid lines represent the drug-free control (df) and dashed lines represent the samples exposed to a 6-hour pulse of dihydroartemisinin at 700nM (6h). Artemisinin (ART)-sensitive samples are presented in black and the ART-resistant strain is represented in red. Parasite maturation assessed by the percentage of depolarizing cells showed a decrease in depolarization after 24h in the ART-sensitive strains (black), while in the ART-resistant parasites (red) the percentage of depolarizing cells is similar to the drug-free control overtime (A). ART-resistant parasites showed an increase in parasitemia after 48h of incubation, whilst the parasitemia of sensitive parasites remains the same overtime (B). No difference between ART-sensitive and ART-resistant strains was detected when parasite maturation was assessed by the intensity of SYBR green positive cells (C).

All tested approaches, with the exception of the determination of SYBR green intensity, allowed to distinguish between ART-resistant and ART-sensitive strains (Figure V.7 and V.8). No further investigation was done based on the SYBR green intensity because it was observed that this approach does not seem to allow to distinguish artemisinin-resistant from sensitive strains.

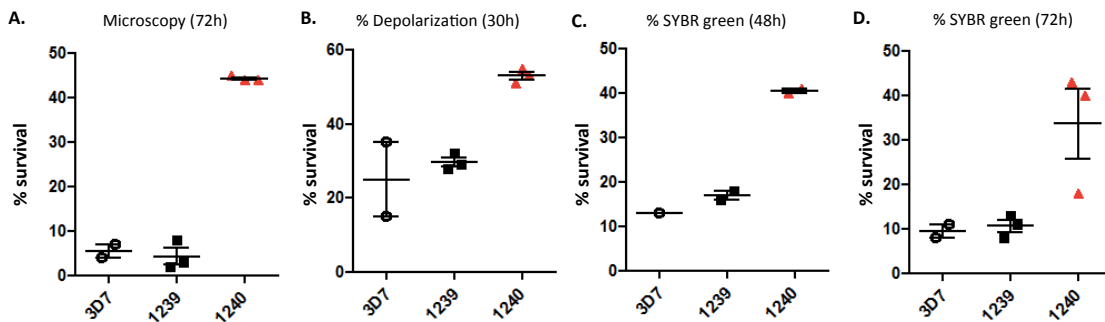


Figure V.8: Survival rates of tightly synchronized parasites exposed to a 6-hour pulse of dihydroartemisinin (DHA).

Survival rates were expressed as ratios of viable parasitemias in DHA-exposed and drug-free samples. Different approaches were used to assess the survival rates of artemisinin-resistant (red) and artemisinin-sensitive (black) strains. In all of them artemisinin-resistant parasites had higher survival rates in comparison to artemisinin-sensitive strains.

Survival rates obtained by the recommended microscopic read-out were of approximately 4% and 44% for the ART-sensitive and ART-resistant strain, respectively (Figure V.8A). These values differed from the ones that were previously described for these same strains (0.1% and 80%). Because artemisinin resistance phenotype appears unstable [35], it was thought that the phenotype could have been partially lost during *in vitro* cultivation. Therefore, two samples with different times in culture (3 and 8 months) were analysed using molecular methods. Results showed that the recently described K13 polymorphism R539T, which is associated with artemisinin resistance [23], was present in both samples, indicating that the tested strain should be resistant to artemisinin (Table V.1). The reason for the observed difference in survival rates is indeed intriguing. However, it should be noted that in several studies survival rates for ART-resistant parasites ranged between 4% - 30%, whereas for ART-sensitive strains values varied from 0.14% - 3% [17, 33, 41].

Table V.1: *Kelch 13* gene locus polymorphism associated with delayed parasite clearance

		M475I (G>A/T/C)	Y493H (T>C)	R539T (G>C)	I543T (T>C)	C580Y (G>A)
Artemisinin-sensitive	3D7	G	T	G	T	G
	1239	G	T	G	T	G
Artemisinin-resistant	1240A (cultured for 3 months)	G	T	C	T	G
	1240B (cultured for 8 months)	G	T	C	T	G

Assessment of depolarizing events at 30 hours showed increased survival rates for both ART-resistant (53%) and ART-sensitive (30%) strains, in comparison to microscopy (Table V.2). The same was observed in the ART-sensitive strains when parasitemia was determined by assessing the percentage of SYBR green positive cells at 48 and 72 hours (17% and 12% respectively). The culture-adapted 3D7 strain (ART-sensitive) was also tested alongside and survival rates were comparable to the ones obtained for the ART-sensitive 1239 strain (Figure V.8 and Table V.2).

The increased survival rates observed in the ART-sensitive strains determined by assessment of the percentage of SYBR green positive cells may be simply explained by the fact that dead parasites may still be accountable in such a measurement, whereas in microscopy they are not. Microscopy assessment accounts only for parasites with a normal morphology. SYBR green is a DNA stain that binds to DNA independently of whether the DNA belongs to viable or a dead parasite. Precisely because of this, another flow cytometric approach was investigated recently, where a viability stain (Mitotracker) was used in combination with SYBR green to allow the quantification of only viable parasites [34]. In this study, results obtained with the flow cytometric read-out were comparable to the ones obtained by microscopy.

Regarding the increased survival rates obtained when assessing the percentage of depolarizing cells no clear explanation has been found yet. However, what certainly may contribute for this is the fact that the detection of depolarizing cells only allows the quantification of parasites that contain a considerably high amount of hemozoin, therefore parasite that are also mature but contain less hemozoin might not be included in this analysis. Moreover, it was observed that at 30 hours of incubation, as an example, only around 30% of the cells that are SYBR green positive do depolarize. This may explain the increased values of survival rates in both sensitive and resistant strains, since the real increase in drug free control samples may be masked by the inability of this method to detect the whole population of infected erythrocytes.

3.3. Assessment of parasite survival using a simpler protocol for parasite synchronization

The synchronization protocol described for the RSA is time-consuming and laborious. It requires complex steps of synchronization, including several sorbitol treatments and one percoll-enrichment to obtain 0-3 hour ring-form parasites (Figure V.5). It has been reported that when older parasites are used instead (9-12 hours or 18-21 hours) the difference in survival rates between resistant and sensitive strains is lost. During this study a simpler synchronization protocol using only the sorbitol synchronization was investigated. In this case, parasites should have around 12 – 20 hours of development. In general, the difference in survival rates between ART-resistant and ART-sensitive strains was more discrete than what was observed when using tightly synchronized cultures. Moreover, in the case of microscopy and flow cytometric assessment of depolarization, results varied considerably between experiments (Figure V.9 and Table V.2). Thus, it seems that discrimination between strains is better when younger and tighter synchronized parasites are used.

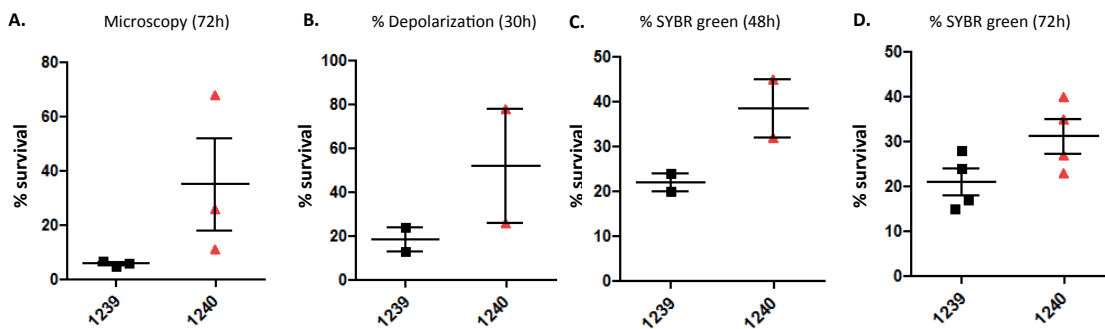


Figure V.9: Survival rates of mildly synchronized parasites exposed to a 6-hour pulse of dihydroartemisinin.

Survival rates were expressed as ratios of viable parasitemias in dihydroartemisinin-exposed and drug-free samples. Different approaches were used to assess the survival rates of artemisinin-resistant (red) and artemisinin-sensitive (black) strains. Artemisinin-resistant parasites had higher survival rates in comparison to artemisinin-sensitive strains in all approaches, yet results differed considerably between experiments.

Interestingly, two other different synchronization protocols have been recently described for the RSA [41]. One is based on the use of three 5% sorbitol treatments, the first two are performed at exactly 46-hour intervals to tighten synchronicity and the last one is done when parasites are between very late schizonts and very early rings to remove the remaining mature forms. The other approach consists on the combination of two sorbitol

treatments followed by a filtration step, where mature schizonts will burst mechanically and free merozoites are obtained and put in culture for 2 hours before drug is added, thus parasites with two hours of development are obtained. In both protocols results were comparable to the RSA standard synchronization protocol [41]. However, the synchronization by filtration leads to low parasitemias of 0.07% and thus, assessment of parasitemia even after 72 hours may be difficult [41]. Nevertheless, the synchronization using only sorbitol treatments seems promising and would certainly be less laborious than the current RSA synchronization protocol.

Table V.2: Summarizing table of mean survival rates for artemisinin-sensitive (3D7 and 1239) and artemisinin-resistant strains (1240).

		3D7	1239	1240	Fold-difference (1240/1239)
Tight Synchronization	microscopy (72h)	5.5 (± 2.1)	4 (± 3.2)	44 (± 0.6)	11
	depolarization (30h)	25 (± 14)	30 (± 2)	53 (± 2)	1.8
	%SYBR green (48h)	13	17 (± 1.4)	40.5 (± 0.7)	2.4
	%SYBR green (72h)	11	12 (± 1.4)	42 (± 2.1)	3.5
Mild Synchronization	microscopy (72h)	nd	6 (± 0.9)	35.1 (± 29.4)	5.9
	depolarization (30h)	nd	19 (± 8)	52 (± 37)	2.7
	%SYBR green (48h)	nd	22 (± 2.8)	38.5 (± 9.2)	1.8
	%SYBR green (72h)	nd	21 (± 6)	31.3 (± 7.7)	1.5

nd: not determined; average values from two or more experiments ± one standard deviation

3.4. Artemisinin-resistant parasites do not seem to enter dormancy

The growth of parasites exposed to a 6-hour pulse of DHA at 700 nM was monitored and compared to drug-free control samples after 72 hours of incubation (Figure V.10 and V.11). Microscopic observation of blood smears showed that indeed the majority of parasites in the ART-sensitive sample arrest their development after drug treatment (Figure V.10 – left panel). In the ART-resistant strain some parasites were also found to be dead/dormant but others managed to survive to drug treatment (Figure V.10 – right panel and V.11B).

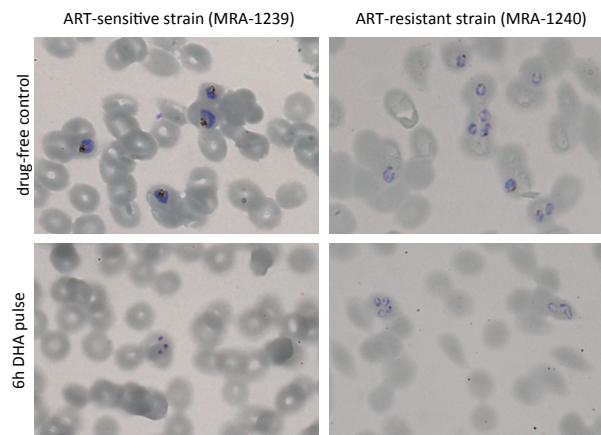


Figure V.10: Representative microscopic pictures of untreated and dihydroartemisinin treated samples at 72 hours of incubation.

Artemisinin (ART)-resistant and ART-sensitive parasites developed as expected in the drug-free control samples (top panels). When treated with 6-hour pulse of dihydroartemisinin (DHA) at 700 nM, most parasites in the ART-sensitive strain were dead/dormant (left – bottom panel). Viable parasites could be detected in the ART-resistant strain (right bottom panel).

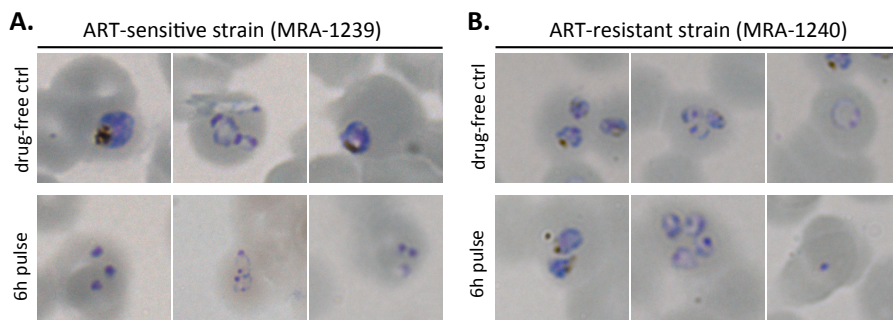


Figure V.11: Representative microscopic pictures of untreated and dihydroartemisinin treated samples at 72 hour of incubation.

Three representative pictures of Giemsa stained blood smears from drug-free control samples and samples exposed for 6-hour to dihydroartemisinin (DHA) at 700 nM. In the artemisinin-sensitive strain most parasites were found dead or dormant at 72 hours of incubation in the treated sample (A). Some parasites managed to survive in the artemisinin-resistant culture that was exposed to DHA (B) and some dead or dormant parasites were also found. The development of parasites that survived treatment was comparable to the one observed in the untreated sample (B).

Interestingly, in the ART-resistant strain not only some parasites were able to survive treatment but they also managed to replicate overtime, leading to an increase of parasitemia (Figure V.12). This was corroborated by the fact that parasites at approximately the same stage of development of the ones present in the drug-free control were found in drug treated samples (Figure V.11B). The number of parasites that survived drug treatment was considerably higher in the ART-resistant strain (44%), in comparison to the ART-sensitive strain (3%) (Figure V.12B).

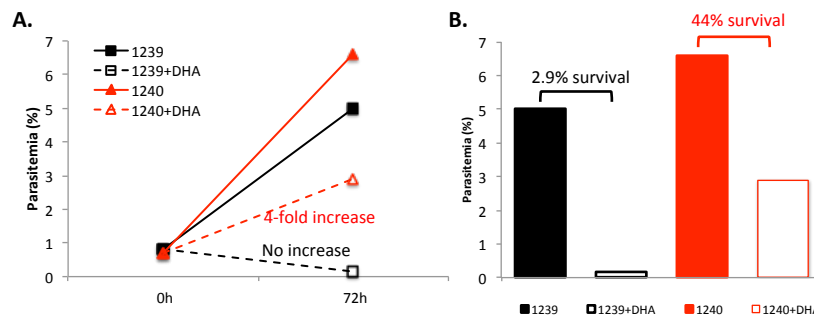


Figure V.12: Progression of parasitemia in artemisinin-sensitive and artemisinin-resistant parasites after a 6-hour pulse of dihydroartemisinin.

The parasitemia of artemisinin-sensitive (1239 - black) and artemisinin-resistant (1240 - red) parasites was monitored after 72 hours of incubation in drug-free samples (solid lines) and in samples treated with 6-hour pulse of dihydroartemisinin (DHA) at 700 nM (dashed line). Artemisinin-resistant parasites showed a 4-fold increase in parasitemia, whereas no increase was detected in artemisinin-sensitive parasites (A). The survival rate was determined by dividing the parasitemia of the drug-free control by the parasitemia of drug exposed samples measured at 72 hours of incubation (B). Artemisinin-resistant parasites had a higher survival rate (44%) than the artemisinin-sensitive strain (2.9%) (B).

These results seem to indicate that upon an effective concentration of DHA most parasites are killed, but not all. This small percentage of parasites that survive treatment will develop and replicate at approximately the same rate as non-treated parasites. However, the percentage of survivor parasites is likely to be below the detection limit of most assays. Thus, depending of depending on the number of parasites that survived treatment, it may take longer for these parasites to grow above the detection limit of the assays. It was observed that the number of viable parasites in the ART-resistant strain is higher than in the ART-sensitive strain. Consequently, ART-resistant parasites show increased levels of parasitemia earlier than the ART-sensitive parasites (Figure V.13), as it was observed in other studies [15, 42]. Based on this, it was hypothesized that ART-resistant parasites manage to survive a 6-hour exposure to a high-dose of DHA by a mechanism that is not associated with dormancy.

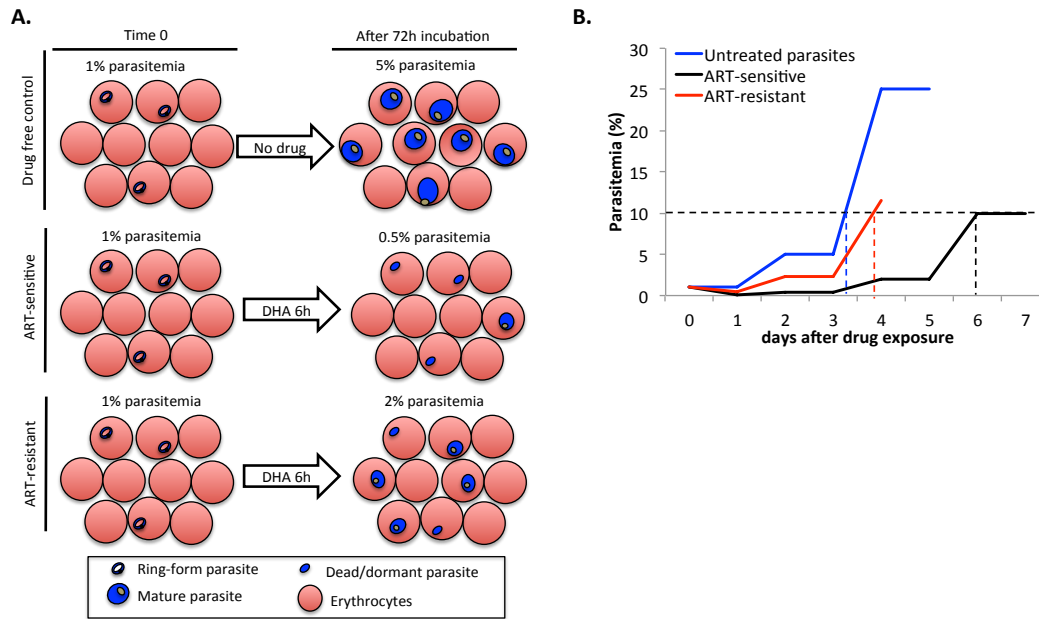


Figure V.13: Representative model of parasite replication after exposure to 6-hour pulse of dihydroartemisinin.

The parasitemia of untreated ring-stage synchronized parasites increase approximately 5-fold after 48 hours of incubation. After a 6-hour pulse with dihydroartemisinin (DHA) at 700 nM most parasites are killed but some manage to survive. The number of parasites that survives drug treatment in the artemisinin-resistance sample is higher than the ones in the artemisinin-sensitive sample (A). Survivor parasites will developed approximately at the same rate as untreated parasites, however due to the reduced numbers of parasites parasitemia will greatly differ between the sensitive and resistant strains (B). For example, resistant parasites manage to reach a 10% parasitemia at day 4 (red line), whereas sensitive parasites will only reach such parasitemia later around day 6 (black line).

Dormancy has been suggested as the underlying mechanism of artemisinin resistance, where ART-resistant parasites manage to survive to DHA exposure by entering state of dormancy or quiescence during which parasites are protected from the drug [11, 16].

The classical definition of quiescence is “a reversible absence of proliferation”, i.e., a non-dividing cell which eventually restarts its cell cycle when conditions become appropriate [43]. In fact, the ability of microorganisms to persist in metabolically inactive states enables survival in unfavorable conditions and it has been described for several human pathogens [44]. For example *Mycobacterium tuberculosis* can enter a dormant state during which they are resistant to drug effects and sometimes to the host immune defenses [45]. In the case of *Plasmodium* spp., parasites arrest their development at the sporozoite stage in the mosquito salivary glands and at the gametocyte stage in the blood. In the case of *P. vivax* and *P. ovale* sporozoites are able to stop their cell cycle in the liver, originating dormant forms known as hypnozoites, which cause relapses weeks to months after the initial infection [46].

Initially, artemisinin-induced dormancy was proposed as the main cause for the high recrudescence rates observed after artemisinin monotherapy [3, 8, 12]. It is widely known that, because of their short half-life, when artemisinins are used alone they fail to eliminate all parasites and recrudescence occurs [3, 7, 8]. Thus, it was hypothesized that artemisinin-treated parasites enter a state of dormancy where they are protected from the drug. After drug effect is no longer present, parasites recover and resume normal growth, causing recrudescence [13]. *In vitro* studies showed that when parasites are exposed to a high-dose of artemisinin (200 ng/mL) the ring-forms arrest their development and enter a dormant state that can last up to 20 days [13]. A computer simulation model that incorporates the ring-stage dormancy, recovery rates, and dose dependency of ART-induced dormancy predicts clinical and parasitological failures at rates comparable to those reported in the field with ART monotherapy [47]. Moreover, dormant parasites morphologically similar to those observed *in vitro* [14] were found *in vivo* in a rodent malaria model following ART treatment [48]. These parasites were shown to be viable because then managed to cause infection after they were transferred into new hosts [48]. All the results presented in these studies suggest that dormancy may be the cause of the high recrudescence associated with artemisinin monotherapy. However, whether dormancy is directly induced by artemisinins is still unclear. Interestingly, dormancy has also been associated with exposure to other drugs such as mefloquine, pyrimethamine and atovaquone [49–51]. This could indicate that dormancy may be an inherent phenomenon that occurs within a parasite population, where “naturally” some parasites will have the ability to persist in the presence of the drug and resume their growth later, instead of being induced by a specific drug. Indeed, this concept is not new and it has been described for bacteria. Bacterial cells escape the effects of antibiotics without undergoing genetic change, these cells are known as persisters [44, 52]. They represent a small fraction of the bacterial population and, unlike resistant cells, these cells do not grow in the presence of antibiotics. Persister cells arise due to a state of dormancy, defined as a state in which cells are metabolically inactive [52]. Exit from this state seems to be unaffected by any external stimuli [44]. However, the mechanism of persister cell formation is not well understood and the metabolic state of these cells is still debated.

The association between dormancy and artemisinin resistance was made for the first time by Witkowski et al [16]. In this study, ART-tolerant strains obtained after *in vitro* drug pressure were exposed to high-doses (9 – 70 μ M) of artemisinin for 48 or 96 hours. Even

though, the majority of parasites died after drug treatment, the ART-resistant strains recovered faster (8 days) than the ART-sensitive strains (16 days). Observations made at 48 hours of incubation indicated that in the ART-resistant parasite culture only rare ring-forms (0.1%) were detected and no mature forms were observed. Later, after 24 and 30 hours of drug removal mature forms are detected, indicating that parasites managed to replicate after drug exposure. These observations led the authors to state that: “drug tolerance is mediated by cell cycle arrest at the ring stage, as they were the only viable forms observed during the 48 hours ART pressure period.” Here, it is assumed that the ring-form parasites observed at 48 hours are parasites that persisted since the beginning of the experiment rather than second-generation ring-forms. To confirm this scheduled sorbitol treatments, that selectively kill all late-parasite stages except ring-forms, were performed five times during the 48 hours of drug exposure and it was observed that parasite survival was not affected by these sorbitol treatments. Yet, it should be noted that parasites used in these experiments were not tightly synchronized. Moreover, sorbitol synchronization selects for parasites with 0-20 hours of development [53]. Thus, even though sorbitol treatments were made five different times during the 48 hours period it may be that some parasites were indeed not affected because they are not in the 0-20 hours developmental period, where the sorbitol is effective, rather than being dormant or arrested. In fact, at this time-point (48 hours of incubation) it would be expected that the majority of parasites would be ring-form parasites. This could be easily concluded by the observation of parasite forms present in the drug-free control sample. Unfortunately, data regarding the drug-free control was not presented nor discussed. Thus, besides considering that parasites arrested their development and were dormant, the hypothesis that some parasites managed to survive to drug exposure and replicated as well as parasites that were not in the presence of the drug should not be discarded.

Later, two other studies reported the same association between artemisinin resistance and dormancy [14, 15]. ART-resistant parasite lines created *in vitro* were used and it was observed that ART-resistant parasites recovered from dormancy faster than ART-sensitive ones [14, 15]. Interestingly, it was found that sensitive parasites enter dormancy as well [14]. Nevertheless, it may be hypothesized that drug-induced dormancy confers a survival advantage which will ultimately select for artemisinin-resistant parasites. Yet, it should be noted that the ART-resistant laboratory parasite lines used in these studies differ from the ART-resistant parasites isolated from patients that have prolonged clearance times. For

example, these strains exhibit increased IC₅₀ values [14, 15], whereas the ones isolated from the patients do not [19].

The correlation of these different findings with the reduced susceptibility of field isolates observed in Cambodia was investigated [54]. Parasites obtained from patients in Pailin (a province of Cambodia where artemisinin resistance has been reported) had higher survival rates in comparison to isolates from Ratanakiri after exposure to 700 nM of DHA [54]. Interestingly, intact arrested ring-form parasites, referred as quiescent parasites, were observed after the ART-resistant strain was exposed with 700 nM DHA for 24 hours. The morphology of these dormant/quiescent parasites differs from what has been previously described, where dormant parasites have been reported to have a smaller cytoplasm and more-condensed chromatin that indeed resemble pyknotic forms rather than ring-forms (Figure V.3) [14, 15].

Moreover, initial *in vitro* studies of dormancy and recovery rates reported that the dormancy observed in parasites after exposure to DHA seems to be rather short (less than 3 days) and that parasites are active enough to be inhibited by a second drug treatment [13]. In this study, synchronous ring-stage parasites were exposed to a 6-hour pulse of DHA at 700 nM, after which a passage through a magnetic column for three consecutive days was performed to eliminate mature forms. It was observed that samples that were exposed to DHA and passed through the magnetic column took longer to recover than the ones that were only exposed to DHA. This delay in recovery indicates that either a small number of parasites are unaffected by the drug or that dormant parasites recover during the first three days and are removed by the magnetic columns. Furthermore, when a combination treatment with artemisinin and mefloquine was investigated, it was observed that the proportion of parasites recovering from treatment with both drugs was decreased by 10-fold as compared to the single treatment with artemisinin, implying that dormant parasites still maintain a basic metabolism since they are still affected by mefloquine.

Table V.3: Studies that have investigated artemisinin-induced dormancy.

Study	Strains	Drug treatment	Findings
Witkwocki <i>et al</i> 2010 [16]	ART-tolerant strains obtained after <i>in vitro</i> drug pressure.	High-dose (9 – 70 μ M) of artemisinin for 48h to 96h.	<ul style="list-style-type: none"> • No differences in IC50 values were observed between the ART-sensitive and ART-resistant strains. • ART-resistant strains recovered faster than ART sensitive when exposed for 48h with the drug, taking 8 and 16 days to reach a parasitemia of 5%, respectively. • The majority of parasites died after drug treatment. <p><u>ART-resistant strain:</u></p> <ul style="list-style-type: none"> • At 48h of incubation with the drug only rare ring-forms (0.1%) were observed in the ART-strain. • 24h and 30h after drug removal mature forms were observed. <p><u>ART-sensitive strain:</u></p> <ul style="list-style-type: none"> • no mature forms could be observed at 24h and 30h after ART removal.
Teuscher <i>et al</i> 2010 [13]	<i>P. falciparum</i> culture-adapted strains W2, D6 and HB3.	6h DHA (700 nM) pulse and passage through a magnetic column for 3 consecutive days to eliminate mature forms.	<ul style="list-style-type: none"> • Higher DHA doses yielded a lower recovery rate. <p><u>Drug exposure but no passage through magnetic column:</u></p> <ul style="list-style-type: none"> • only morphologically abnormal rings and no mature parasite forms were observed in culture for 3 days. • Parasitemia >10% was reached at day 11. <p><u>Drug exposure and passage through magnetic column:</u></p> <ul style="list-style-type: none"> • Parasitemia >10% was reached between day 14 – 19.
Codd <i>et al</i> 2011 [47]	Computer simulation model to assess different regimens of artemisinins in single-dose, 3-day and 7-days treatments.		<ul style="list-style-type: none"> • Dormancy could explain the recrudescence observed after monotherapy with artemisinin. • Repeated treatment reduced dormancy recovery rate and the rate of recrudescence, but a small proportion of treatment failures are still predicted
Teuscher <i>et al</i> 2012 [15]	AL-resistant <i>P. falciparum</i> laboratory strains	6h high-dose AL pulse	<ul style="list-style-type: none"> • AL-resistant parasite strains showed increased IC50 values. • AL-resistant strains recover faster (4 days) than AL-sensitive strains (8 days). • Dormancy occurs in resistant parasites but higher concentrations of drug are needed to induce it.
Tucker <i>et al</i> 2012 [14]	ART-resistant <i>P. falciparum</i> laboratory strains	6h DHA (700 nM) pulse	<ul style="list-style-type: none"> • ART-resistant strains recover faster (3 days) than ART-sensitive strains (4 days). • ART-resistant parasite strains showed increased IC50 values.
Witkwocki <i>et al</i> 2013 [54]	Isolates from Cambodia (ART-resistant and ART-sensitive)	DHA (700 nM) pulses of 6h and 24h.	<ul style="list-style-type: none"> • ART-resistant strains recover faster (3 days) than ART-sensitive strains (more than 6 days). • Quiescent parasites exhibit a different morphology (intact ring-form) than the dormant parasites described by others [14]

ART – artemisinins; AL – Artemisinin; DHA - Dihydroartemisinin

Contrary to what has been described for other microorganisms, such as *Mycobacterium tuberculosis*, it seems that dormancy observed in parasites exposed to artemisinins is rather short and does not cause a full arrest of parasite metabolic activity [13]. Recently it was reported that most metabolic pathways are down regulated in DHA-induced dormant parasites [55]. However, continued transcription of genes encoding apicoplast and mitochondrial proteins was detected, indicating that these dormant parasites are not metabolically quiescent but, even though their growth and replication is arrested [55]. Others have also observed that parasites do not enter dormancy once they are exposed to artemisinins. Indeed, what was shown is that both ART-resistant and ART-sensitive parasites seem to have a dose-dependent growth retardation after being exposed to artemisinin in comparison to the drug-free controls [56, 57].

It is evident that ART-resistant parasites manage to survive to a greater extent to DHA exposure than ART-sensitive parasites. However, it is still unknown why only some of these parasites survive and not all. Dormancy has been widely mentioned as the mechanism behind artemisinin resistance, yet discrepancies between studies and the findings described above seem to indicate that the mechanism associated with artemisinin resistance might not be related to dormancy, at least as it is defined for other organisms. Dormancy implies that organisms are metabolically inactive for long periods of time. This seems not to be the case in the dormancy phenotype observed in *P. falciparum*. Therefore, along with further investigation an update of this definition or the use of a different nomenclature should be considered in the future.

3.5. Artemisinin resistant parasites exhibit altered developmental patterns

It has been described that in the absence of the drug, ART-resistant parasites exhibit an inherent delayed growth *in vitro* in comparison to ART-sensitive parasites [58]. The parasite developmental patterns of the three different strains used in this study were investigated in 6-hour intervals during the whole 48-hour life cycle, in the absence of drug treatment. It was observed that ART-resistant parasites had a delay in parasite development of approximately 6 hours (Figure V.14). This delay was detected both when using tightly (0-3 hours of development) (Figure V.14A) or mildly synchronized (Figure V.14B) (12-20 hours of development) parasites.

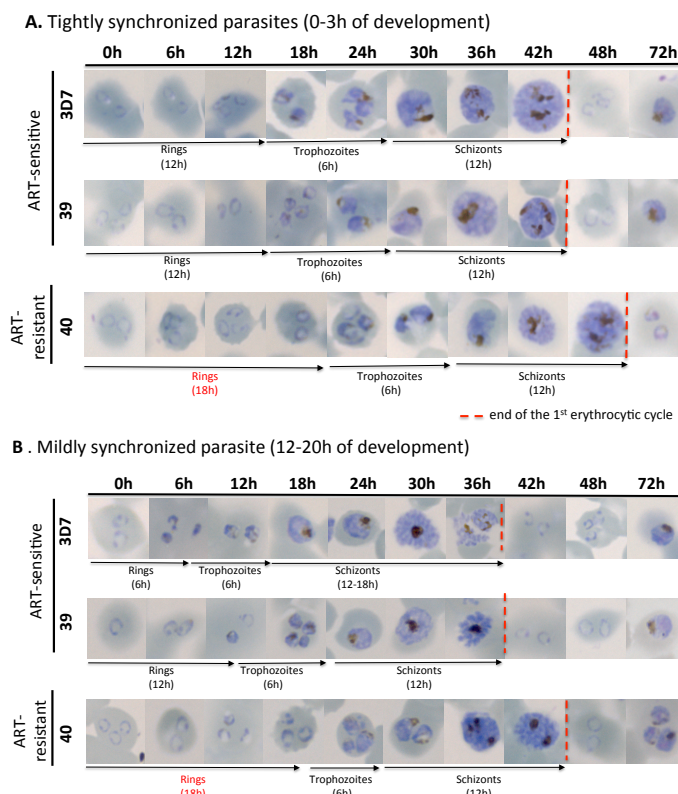


Figure V.14: Parasite developmental patterns in the absence of drug.

The development of parasite in culture was monitored in tightly (A) and mildly synchronized (B) parasites. In both cases, artemisinin-resistant parasites (40) showed a longer cycle of development in comparison to artemisinin-sensitive strains. It seems that this prolonged cycle is associated with a prolonged ring-stage development of 18 hours, instead of the 12 hours observed for the sensitive strains. The duration of the trophozoite stage and the schizont stage seems to be the same between parasite strains.

In fact, it has been described that ART-resistant parasites exhibit a prolonged ring-stage of development and a shorten trophozoite stage, but that the overall duration of the parasite developmental cycle is the same parasites [58]. Contrary to this, obtained results showed

that ART-resistant parasites seem to have a prolonged life cycle of 48 hours in comparison to the 42-hour life cycle observed in ART-sensitive strains (Figure V.14A). The delay in parasite development occurs during the ring stage of development, where ART-resistant parasites have a ring phase of approximately 18 hours, instead of the 12-hour ring-stage duration observed for the ART-sensitive strains. However, no reduction in the duration of the trophozoite stage was observed between strains (Figure V.14).

The potential of the flow cytometric detection of hemozoin to detect delayed parasite growth was investigated. Alongside quantification of parasitemia by flow cytometry was performed as well. The hemozoin detection allowed to distinguish between ART-resistant parasites and ART-sensitive strains only at 72 hours of incubation, when an increase in the percentage of hemozoin-containing cells was observed in the sensitive parasites but not in the resistant ones (Figure V.15A). This reflects what is observed by microscopy, where at 72 hours sensitive parasites are late trophozoites/young schizonts whilst resistant ones are younger ring-forms (Figure V.15A). Assessment of parasitemia by flow cytometry, using SYBR green stained samples, allowed to detect delayed growth at 42 hours of incubation in tightly synchronized parasites, or at 36 hours in mildly synchronized ones (Figure V.15B). In this case, second generation ring-forms are already present at 42 hours in the ART-sensitive strain, whereas in the ART-resistant strain parasites from the second generation only appear later at 48 hours. This explains why the increase in parasitemia (percentage of SYBR green positive cells) is detected at the abovementioned time-points.

The prolonged ring-stage has been suggested as defense mechanism that the parasite develops to cope better once it is in the presence of artemisinin parasites [58]. It is known that young ring-form parasites are the forms that have reduced sensitivity to artemisinins [54] and that these drugs have a short half-life of (~1 hour) [4]. Thus, if parasites could extend this stage until the activity of the drug is lost, it would allow them to resume their growth later. However, not all ART-resistant clones have a prolonged ring phase of development. In fact, it was reported that one resistant clone had an accelerated 36-hour life cycle instead parasites [58]. Thus, further research is needed to elucidate the role of altered parasite growth patterns in the context of artemisinin resistance.

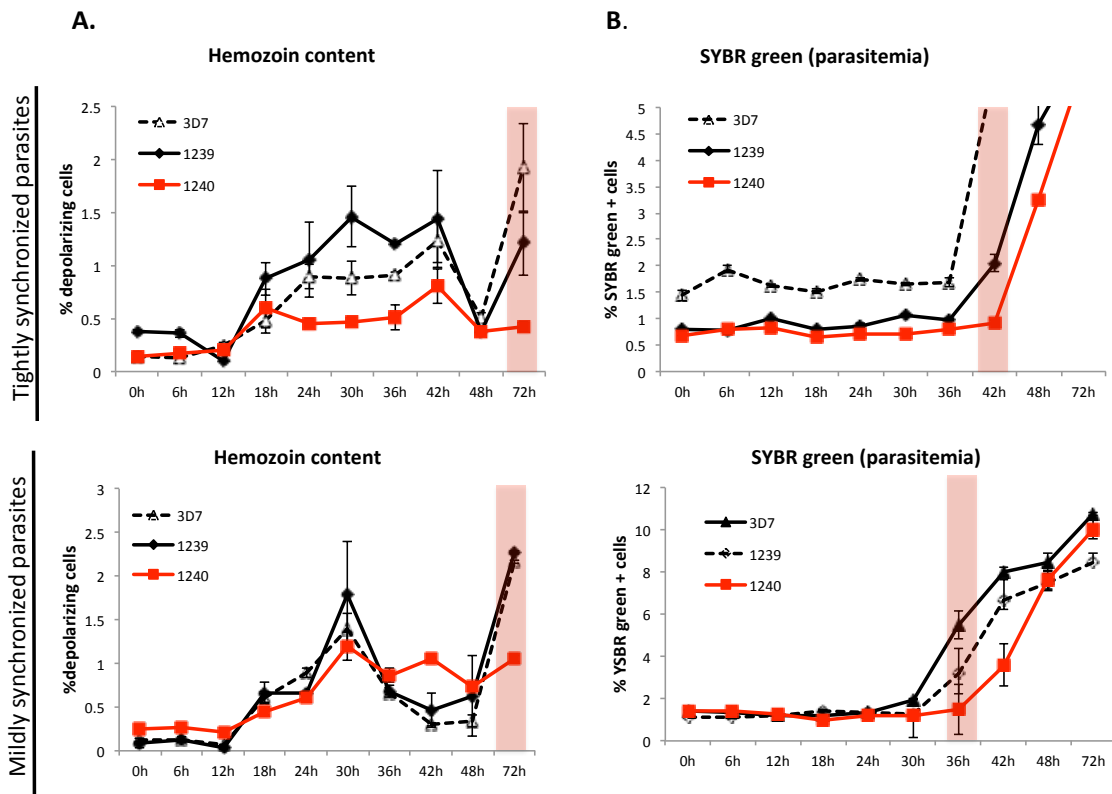


Figure V.15: Parasite development monitored by flow cytometry. The percentage of depolarizing events (hemozoin-containing cells) and SYBR green positive cells (parasitemia) was assessed overtime.

Detection of depolarizing events allowed to distinguish between the slow-growing resistant strain (red line) and the sensitive strain (black line) at 72 hours of incubation (A). At this time sensitive parasites start to mature and produce hemozoin, whilst the resistant parasites did not matured as much. An increase in parasitemia on the sensitive strains but not on the resistant one was detected at 42 and 36 hours in tightly and mildly synchronized parasites, respectively (B).

4. Conclusions

Novel and more practical *in vitro* assays are needed to further investigate artemisinin resistance. Flow cytometry detection of hemozoin may be a useful tool for the *in vitro* investigation of artemisinin resistance. Unlike other available drug assays for *P. falciparum*, the hemozoin assay allows real-time monitoring of parasite maturation and, consequently, drug effects can be detected earlier (at 24 hours of incubation) than most assays. This feature is especially relevant in the case of artemisinin resistance because only the young ring forms seem to be resistant to artemisinin. Therefore, the earlier the assay is able to detect drug effects the better.

Results showed that the hemozoin detection assay allowed to detect increased IC₅₀ values already at 24 hours of incubation. This can possibly allow to distinguish between ART-resistant and ART-sensitive strains based on their respective IC₅₀ values. Moreover, when pulse assays (based on the previously described Ring-Stage-Assay) were performed the flow cytometric readout of parasite maturation (detection of depolarization caused by hemozoin) and parasitemia (percentage of SYBR green positive cells) allowed to detect increased survival rates associated with artemisinin resistance after 30 and 48 hours of incubation, respectively. Yet, obtained survival rates, especially in the ART-sensitive strains, were higher than the ones observed by microscopy at 72 hours. This may be an inherent limitation of the flow cytometric approaches. While microscopy only assesses parasites with a normal morphology and thus, likely to be viable, the quantification of SYBR green positive cells by flow cytometry will also include dead parasites which did not degenerate yet and are still stained by SYBR green. On the other hand, flow cytometric detection of hemozoin only allows the quantification of parasites that have a hemozoin content above a certain threshold and therefore, it is unlikely that all parasites would be detected at a specific time-point. In fact, it was observed that the peak of schizogony (which corresponds to the peak of depolarization) in untreated samples occurred at around 42 hours of incubation. Future experiments should include measurements of parasite maturation at 42 hours of incubation, rather than the 30 hours previously used. This may lead to decreased survival rates, which would be closer to the ones obtained by microscopy at 72 hours.

A simpler synchronization protocol for the pulse assay was also investigated. Although, it was still possible to distinguish between ART-resistant and ART-sensitive parasites, results differed considerably between experiments. Moreover, discrimination between

ART-resistant and ART-sensitive strains was better when younger and tighter synchronized parasites are used.

Interestingly and contrary to some reports, artemisinin resistance does not seem to be related with dormancy. In fact, parasites that survived to drug treatment developed and replicated at approximately the same rate as parasites that were not treated. Yet, these results are preliminary and further demonstration of this observation is required. Future experiments should include the monitoring of parasite maturation in tighter intervals of time (for example 2 to 4 hour intervals). Comparison of parasite development in drug free control samples and in samples exposed for 6-hours to DHA would be more precise and would allow to determine if treated parasites arrest their growth and, if so, when it occurs and for how long.

An additional aspect is that ART-resistant parasites used in this study showed a delayed development in the absence of drug pressure, as it has been previously described. This delay was determined by flow cytometric detection of hemozoin at 72 hours of incubation. Whether this altered growth pattern could allow to distinguish ART-resistant strains from ART-sensitive ones remains unclear and further validation is required. Importantly, previous results from the field-study conducted in Gabon showed that parasites that have similar susceptibility/resistant profiles to the same drug may exhibit differences in *ex vivo* growth. This seems to indicate that the altered parasite growth observed in ART-resistant strains *in vitro* may not be enough to reliably distinguish between ART-sensitive and ART-resistant strains *ex vivo*. Perhaps, one could speculate that the delayed parasite growth is associated to drug resistance in a more general way.

Flow cytometry could be a useful tool to study artemisinin resistance *in vitro*. However, the data set presented here is limited and all observations were made using a single ART-resistant strain (MRA-1240). Indeed, results should be further confirmed using other culture-adapted ART-resistant strains available on the Malaria Research and Reference Reagent Resource Center (MR4). Then, after establishing an optimal *in vitro* protocol the hemozoin detection assay should be tested on site, obviously somewhere in Southeast Asia where artemisinin resistance has been reported. Both ART-sensitive and ART-resistant strains obtained directly from patients with fast and slow-clearing infections should be included. This field-study may allow to clarify some of the remaining doubts and, ultimately, would determine the usefulness of the hemozoin detection assay for the study and detection of artemisinin resistance.

5. References

1. WHO. (2015) Guidelines for the treatment of malaria - 3rd edition.
2. WHO. (2015) World Malaria Report 2015.
3. White NJ. (1997) Assessment of the Pharmacodynamic Properties of Antimalarial Drugs In Vivo. *Antimicrobial Agents and Chemotherapy* 41: 1413–1422.
4. White NJ. (2008) Qinghaosu (artemisinin): the price of success. *Science* 320: 330–4.
5. Dondorp A, Fanello C, Hendriksen I, Gomes E, Seni A, Chhaganlal K, et al. (2005) Artesunate versus quinine for treatment of severe falciparum malaria: a randomised trial. *The Lancet* 366: 1–9.
6. Dondorp AM, Fanello CI, Hendriksen IC, Gomes E, Seni A, Chhaganlal KD, et al. (2010) Artesunate versus quinine in the treatment of severe falciparum malaria in African children (AQUAMAT): An open-label, randomised trial. *The Lancet* 376: 1647–1657.
7. Meshnick SR, Taylor TE and Kamchonwongpaisan S. (1996) Artemisinin and the antimalarial endoperoxides: from herbal remedy to targeted chemotherapy. *Microbiological Reviews* 60: 301–315.
8. Giao PT, Binh TQ, Kager PA, Long HP, Van Thang N, Van Nam N, et al. (2001) Artemisinin for treatment of uncomplicated falciparum malaria: Is there a place for monotherapy? *The American Journal of Tropical Medicine and Hygiene* 65: 690–695.
9. WHO. (2009) World Malaria Report 2009.
10. O'Brien C, Henricha PP, Passia N and Fidock DA. (2012) Recent clinical and molecular insights into emerging artemisinin resistance in *Plasmodium falciparum*. *Current Opinion in Infectious Diseases* 24: 570–577.
11. Cheng Q, Kyle DE and Gatton ML. (2012) Artemisinin resistance in *Plasmodium falciparum*: A process linked to dormancy? *International Journal for Parasitology: Drugs and Drug Resistance* 2: 249–255.
12. Kyle DE and Webster HK. (1996) Postantibiotic effect of quinine and dihydroartemisinin derivatives on *Plasmodium falciparum* in vitro: implications for a mechanism of recrudescence [abstract]. XIVth International Congress for Tropical Medicine and Malaria; 17–22 November 1996; Nagasaki, Japan.
13. Teuscher F, Gatton ML, Chen N, Peters J, Kyle DE and Cheng Q. (2010) Artemisinin-induced dormancy in *Plasmodium falciparum*: duration, recovery rates, and implications in treatment failure. *The Journal of Infectious Diseases* 202: 1362–1368
14. Tucker MS, Mutka T, Sparks K, Patel J and Kyle DE. (2012) Phenotypic and

genotypic analysis of in vitro-selected artemisinin-resistant progeny of *Plasmodium falciparum*. *Antimicrobial Agents and Chemotherapy* 56: 302–314.

15. Teuscher F, Chen N, Kyle DE, Gatton ML and Cheng Q. (2012) Phenotypic changes in artemisinin-resistant *Plasmodium falciparum* lines in vitro: Evidence for decreased sensitivity to dormancy and growth inhibition. *Antimicrobial Agents and Chemotherapy* 56: 428–431.

16. Witkowski B, Lelièvre J, Barragán MJL, Laurent V, Su X, Berry A, et al. (2010) Increased tolerance to artemisinin in *Plasmodium falciparum* is mediated by a quiescence mechanism. *Antimicrobial Agents and Chemotherapy* 54: 1872–1877.

17. Witkowski B, Khim N, Chim P, Kim S, Ke S, Kloeung N, et al. (2013) Reduced artemisinin susceptibility of *Plasmodium falciparum* ring stages in western Cambodia. *Antimicrobial Agents and Chemotherapy* 57: 914–923.

18. Noedl H, Se Y, Schaefer K, Smith BL, Socheat D and Fukuda MM. (2008) Evidence of artemisinin-resistant malaria in western Cambodia. *The New England Journal of Medicine* 359: 2619–2620.

19. Dondorp A, Nosten F, Yi P, Das D, Phyo A, Tarning J, et al. (2009) Artemisinin Resistance in *Plasmodium falciparum* Malaria. *The New England Journal of Medicine* 361: 455–467.

20. Fairhurst RM. (2015) Understanding artemisinin-resistant malaria: what a difference a year makes. *Current Opinion in Infectious Diseases* 28: 417–425.

21. WHO. (2011) Global Plan For Artemisinin Resistance Containment.

22. WHO. (2016) Artemisinin and artemisinin-based combination therapy resistance.

23. Ariey F, Witkowski B, Amaratunga C, Beghain J, Langlois A, Khim N, et al. (2014) A molecular marker of artemisinin-resistant *Plasmodium falciparum* malaria. *Nature* 505: 50–55.

24. Ashley E, Dhorda M, Fairhurst RM, Amaratunga C, Lim P, Suon S, et al. (2014) Spread of Artemisinin Resistance in *Plasmodium falciparum* Malaria. *The New England Journal of Medicine* 371: 411–423.

25. Nyunt MH, Hlaing T, Oo HW, Tin-Oo LLK, Phway HP, Wang B, et al. (2015) Molecular assessment of artemisinin resistance markers, polymorphisms in the K13 propeller, and a multidrug-resistance gene in the Eastern and Western Border Areas of Myanmar. *Clinical Infectious Diseases* 60: 1208–1215.

26. Takala-Harrison S, Clark TG, Jacob CG, Cummings MP, Miotto O, Dondorp AM, et

- al. (2012) Genetic loci associated with delayed clearance of *Plasmodium falciparum* following artemisinin treatment in Southeast Asia. *Proceedings of the National Academy of Sciences of the United States of America* 110: 240–245.
27. Ménard D, Khim N, Beghain J, Adegnika A, Shafiul-Alam M, Amodu O, et al. (2016) A Worldwide Map of *Plasmodium falciparum* K13-Propeller Polymorphisms. *The New England Journal of Medicine* 374: 2453–2464.
28. Lubell Y, Dondorp A, Guérin PJ, Drake T, Meek S, Ashley E, et al. (2014) Artemisinin resistance-modelling the potential human and economic costs. *Malaria Journal* 13: 452.
29. Saunders DL, Vanachayangkul P and Lon C. (2014) Dihydroartemisinin-Piperaquine Failure in Cambodia. *The New England Journal of Medicine* 371: 484–485.
30. Spring MD, Lin JT, Manning JE, Vanachayangkul P, Somethy S, Bun R, et al. (2015) Dihydroartemisinin-piperaquine failure associated with a triple mutant including kelch13 C580Y in Cambodia: An observational cohort study. *The Lancet Infectious Diseases* 15: 683–691.
31. Chaorattanakawee S, Lon C, Jongsakul K, Gawee J, Sok S, Sundrakes S, et al. (2016) Ex vivo piperaquine resistance developed rapidly in *Plasmodium falciparum* isolates in northern Cambodia compared to Thailand. *Malaria Journal* 15: 519.
32. Saralamba S, Pan-Ngum W, Maude RJ, Lee SJ, Tarning J, Lindegardh N, et al. (2011) Intrahost modeling of artemisinin resistance in *Plasmodium falciparum*. *Proceedings of the National Academy of Sciences of the United States of America* 108: 397–402.
33. Witkowski B, Amaratunga C, Khim N, Sreng S, Chim P, Kim S, et al. (2013) Novel phenotypic assays for the detection of artemisinin-resistant *Plasmodium falciparum* malaria in Cambodia: in-vitro and ex-vivo drug-response studies. *The Lancet Infectious Diseases* 13: 1043-1049.
34. Amaratunga C, Neal AT and Fairhurst RM. (2014) Flow cytometry-based analysis of artemisinin-resistant *Plasmodium falciparum* in the ring-stage survival assay. *Antimicrobial Agents and Chemotherapy* 58: 4938–4940.
35. Chotivanich K, Tripura R, Das D, Yi P, Day NPJ, Pukrittayakamee S, et al. (2014) Laboratory detection of artemisinin-resistant *Plasmodium falciparum*. *Antimicrobial Agents and Chemotherapy* 58: 3157–3161.
36. Rebelo M, Sousa C, Shapiro HM, Mota MM, Grobusch MP and Hänscheid T. (2013) A Novel Flow Cytometric Hemozoin Detection Assay for Real-Time Sensitivity Testing of *Plasmodium falciparum*. *PLoS One* 8: e61606.

37. Rebelo M, Tempera C, Fernandes JF, Grobusch MP and Hänscheid T. (2015) Assessing anti-malarial drug effects ex vivo using the haemozoin detection assay. *Malaria Journal* 14:140.
38. Frita R, Rebelo M, Pamplona A, Vigario AM, Mota MM, Grobusch MP, et al. (2011) Simple flow cytometric detection of haemozoin containing leukocytes and erythrocytes for research on diagnosis, immunology and drug sensitivity testing. *Malaria Journal* 10: 74.
39. Mphande F, Nilsson S and Bolad A. (2013) Culturing of erythrocytic asexual stages of *Plasmodium falciparum* and *P. vivax*. In: Moll K, Ljungstrom I, Perlmann H, Scherf A, Wahlgren M (Eds.), *Methods in Malaria Research*, 6th edition, Manassas.
40. Lambros C and Vanderberg JP. (1979) Synchronization of *Plasmodium falciparum* erythrocytic stages in culture. *Journal of Parasitology* 65: 418–420.
41. Kite WA, Melendez-Muniz VA, Moraes Barros RR, Wellems TE and Sa JM. (2016) Alternative methods for the *Plasmodium falciparum* artemisinin ring-stage survival assay with increased simplicity and parasite stage-specificity. *Malaria Journal* 15: 94.
42. Tucker MS, Mutka T, Sparks K, Patel J and Kyle DE. (2012) Phenotypic and Genotypic Analysis of In Vitro-Selected Artemisinin-Resistant Progeny of *Plasmodium falciparum*. *Antimicrobial Agents and Chemotherapy* 56: 302–314.
43. Paloque L, Ramadani AP, Mercereau-Puijalon O, Augereau J and Benoit-Vical F. (2016) *Plasmodium falciparum*: multifaceted resistance to artemisinins. *Malaria Journal* 15: 1–12.
44. Dworkin J and Shah IM. (2010) Exit from dormancy in microbial organisms. *Nature Reviews Microbiology* 8: 890–896.
45. Gengenbacher M and Kaufmann SHE. (2012) *Mycobacterium tuberculosis*: Success through dormancy. *FEMS Microbiology Reviews* 36: 514–532.
46. Price RN, von Seidlein L, Valecha N, Nosten F, Baird JK and White NJ. (2014) Global extent of chloroquine-resistant *Plasmodium vivax*: a systematic review and meta-analysis. *The Lancet Infectious Diseases* 14: 982–991.
47. Codd A, Teuscher F, Kyle DE, Cheng Q and Gatton ML. (2011) Artemisinin-induced parasite dormancy: a plausible mechanism for treatment failure. *Malaria Journal* 10: 56.
48. Lacrue AN, Scheel M, Kennedy K, Kumar N and Kyle DE. (2011) Effects of Artesunate on Parasite Recrudescence and Dormancy in the Rodent Malaria Model *Plasmodium vinckei*. *PloS One* 6: e26689.
49. Nakazawa S, Kanbara H and Aikawa M. (1995) *Plasmodium falciparum*:

Recrudescence of Parasites in Culture. *Experimental Parasitology* 81: 556–563.

50. Nakazawa S, Maoka T, Uemura H, Ito Y and Kanbara H. (2002) Malaria Parasites Giving Rise to Recrudescence In Vitro. *Antimicrobial Agents and Chemotherapy* 46: 958–965.

51. Thapar MM, Gil JP and Björkman A. (2005) In vitro recrudescence of *Plasmodium falciparum* parasites suppressed to dormant state by atovaquone alone and in combination with proguanil. *Transactions of the Royal Society of Tropical Medicine and Hygiene* 99: 62–70.

52. Wood TK, Knabel SJ and Kwan BW. (2013) Bacterial persister cell formation and dormancy. *Applied and Environmental Microbiology* 79: 7116–7121.

53. Xie SC, Dogovski C, Kenny S, Tilley L and Klonis N. (2014) Optimal assay design for determining the in vitro sensitivity of ring stage *Plasmodium falciparum* to artemisinins. *International Journal for Parasitology* 44: 893–899.

54. Witkowski B, Khim N, Chim P, Kim S, Ke S, Kloeung N, et al. (2013) Reduced Artemisinin Susceptibility of *Plasmodium falciparum* Ring Stages in Western Cambodia. *Antimicrobial Agents and Chemotherapy* 57: 914–23.

55. Chen N, LaCrue AN, Teuscher F, Waters NC, Gatton ML, Kyle DE, et al. (2014) Fatty acid synthesis and pyruvate metabolism pathways remain active in dihydroartemisinin-induced dormant ring stages of *Plasmodium falciparum*. *Antimicrobial Agents and Chemotherapy* 58: 4773–4781.

56. Klonis N, Crespo-Ortiz MP, Bottova I, Abu-Bakar N, Kenny S, Rosenthal PJ, et al. (2011) Artemisinin activity against *Plasmodium falciparum* requires hemoglobin uptake and digestion. *Proceedings of the National Academy of Sciences of the United States of America* 108: 11405–11410.

57. Dogovski C, Xie SC, Burgio G, Bridgford J, Mok S, McCaw JM, et al. (2015) Targeting the Cell Stress Response of *Plasmodium falciparum* to Overcome Artemisinin Resistance. *PLoS Biology* 13: 1–26.

58. Hott A, Casandra D, Sparks KN, Morton LC, Castanares GG, Rutter A, et al. (2015) Artemisinin-resistant *Plasmodium falciparum* parasites exhibit altered patterns of development in infected erythrocytes. *Antimicrobial Agents and Chemotherapy* 59: 3156–3167.

CHAPTER VI

CONCLUSION AND FINAL REMARKS

1. Background

Antimalarial drug resistance is a major obstacle in the fight against malaria. In the past the development of resistance to chloroquine led to an increase in the number of cases and deaths from malaria [1, 2]. Substantial gains in malaria control were lost and the reemergence of the disease in many countries occurred due to antimalarial drug resistance [3]. Recently resistance to artemisinin, the basis of the current first-line treatment of malaria, seems to be emerging and is spreading in Southeast Asia [4–6]. However, artemisinin resistance is considered by the WHO as partial resistance and artemisinin-combination therapies (ACTs) are still the mainstay for malaria treatment [7].

In vitro tools to monitor the emergence and spread of resistant malaria parasites are of utmost importance for malaria control. Several different antimalarial drug assays are currently available [8, 9]. However, an optimal approach has not been developed yet. Microscopic assessment of parasite maturation was the first method that allowed the assessment of drug effects on parasites [10]. Even though it is an affordable method and simple to perform, it is subjective and requires experienced personal or special training. Currently, the reference method for antimalarial drug testing is based on the incorporation of radioactive [³H]-hypoxanthine [11]. The use of a radioactive reagent to assess parasite growth is the main limitation of this assay, especially in malaria-endemic countries. Another limitation is the relatively high parasite densities of approximately 0.5% required for this assay [8]. More recently, an ELISA method based on the detection of an antigen from the malaria parasite (the HRP2 antigen) developed in 2002 has been successfully used to assess drug effects [12]. It overcomes some of the limitations of previously mentioned assays as it is easy to perform, it allows the analysis of a large number of samples and it has a low detection limit of 0.05% parasitemia. Yet, it requires the use of expensive reagents (e.g. antibodies), the availability of a cold chain to store samples and/or reagents and it has a long-turn-around time of at least 72 hours. More importantly, lately concerns regarding the fact that some parasites lack the HRP2 gene have emerged and this would certainly limit the application of this assay [13].

In this scenario, it would be ideal if a parasite product could be used to readily assess parasite growth or maturation, avoiding the main limitations of current assays. Hemozoin, a crystal produced by the parasite during its maturation inside the erythrocyte seems to be an optimal candidate. The content of hemozoin increases as parasite matures from ring-forms to trophozoites and, finally, to schizonts. Moreover, hemozoin is a birefringent crystal, and thus it is able to depolarize light. The resulting light depolarization can be

detected by optical methods such as microscopy [14] or flow cytometry [15]. Interestingly, detection of light depolarization by flow cytometry is not new and was developed back in 1986 [15]. However, Abbott Diagnostics patented this feature, and thus it was only available in Abbot's Cell Dyn hematology analyzers. Other manufacturers were not allowed to implement this feature in their machines. In 1999, it was reported for the first time that leukocytes that contain hemozoin could be detected by the Cell-Dyn 3500 hematology analyser [16]. Since then other reports have shown the same [17–20] and the use of hematology analyzers to diagnose malaria has been further investigated, as it is extensively reviewed elsewhere [21]. Importantly, some of these studies reported the possibility of detecting infected erythrocytes that contain hemozoin [20, 22]. This observation led to the hypothesis that if infected erythrocytes that contain hemozoin could be detected, maybe the quantification of these cells overtime would allow to detect parasite maturation and, consequently, drug effects could be determined as well.

Indeed, this idea was already investigated in the past and it was the basis of a drug assay developed by Rieckmann in 1982 [23]. However, the visual read-out of hemozoin formation performed at the time was not accurate enough due to the leukocyte interference.

2. Detection of intra-erythrocytic hemozoin as an alternative drug assay for *Plasmodium* spp.

2.1. Detection of light depolarization by flow cytometry

Hematology analyzers are far from being ideal and practical instruments to be used to further investigate the potential of the flow cytometric detection of hemozoin for antimalarial drug testing. Besides being expensive and bulky, these instruments are closed systems where no modifications can be done. Ideally an affordable, accessible and easy to transport instrument would be a better option. The Cyflow SL (Partec) is a portable benchtop flow cytometer with an accessible optical bench. Modifications of the optical layout can be done easily and it is always possible to switch back to the original optical set-up. This instrument was easily modified to allow the detection of light depolarization caused by hemozoin [24, 25]. In fact, the modification of the optical bench to allow the detection of this additional parameter of light depolarization was also accomplished in other flow cytometers, such as the: MoFlo (Beckman Coulter), Accuri C6 (BD Biosciences) and the Attune (Life Technologies) [25].

2.2. Preliminary proof-of-principle using a rodent malaria model

Rodent malaria parasites, that have high amounts of scattered hemozoin and that were readily available at the institute, were used to determine if the resulting light depolarization caused by hemozoin could be detected by flow cytometry. The main goal was to assess if flow cytometric detection of hemozoin allows to detect drug effects using a rodent malaria model. Indeed, light depolarization caused by hemozoin was detected and it allowed to easily distinguish between infected and uninfected samples. Moreover, measurements of depolarizing events overtime allowed to detect parasite maturation and drug effects [26]. This work was not part of this PhD project but it paved the way for the work that was later developed in the context of this thesis.

2.3. Further development of the flow cytometric detection of hemozoin using the human parasite *P. falciparum*

The aim of this PhD project was to further investigate the flow cytometric detection of hemozoin as a novel antimalarial drug assay. For that *in vitro* cultures of *P. falciparum* were established for the first time at the institute. Investigation of the newly developed drug assay based on the flow cytometric detection of hemozoin using *in vitro* cultures of *P. falciparum* showed that drug effects and drug resistance could be detected earlier than any other available assay, already at 18 hours of incubation [24]. However, limitations of *in vitro* studies using culture-adapted strains included: 1) the fact that hemozoin released during schizont rupture accumulates in the culture and can not be eliminated; and 2) that these parasites have adapted to successfully grow in culture, contrary to parasites that are isolated directly from malaria patients.

Ex vivo culturing of parasites obtained from malaria patients would overcome these limitations and would allow to further elucidate the usefulness of this method as a drug sensitivity assay for *P. falciparum*. Preliminary experiments were done using blood samples from malaria patients returning from endemic countries that were admitted at the *Hospital Santa Maria* [27]. Yet, the number of samples was limited. Moreover, most samples were collected and stored for several days before they were finally analysed by flow cytometry. Thus, they were not in the best conditions to allow further parasite growth *in vitro*.

To overcome this a preliminary field trial in Gabon, a malaria endemic country, was planned. The 6-month field study was conducted at the *Centre de Recherches Médicales de Lambaréné* (CERMEL) which is linked to the Abert Schweitzer Hospital. The Cyflow SL

available on site was successfully modified to detect light depolarization caused by hemozoin. A total of forty-six samples from malaria patients admitted at the Albert Schweitzer Hospital were analysed. Drug inhibitory effects and drug resistance could be detected by the flow cytometric detection of hemozoin, as it was previously observed using *in vitro* cultures of *P. falciparum*. However, IC₅₀ values were higher than the ones obtained when samples were tested using the HRP2-ELISA [25]. Indeed, the same was also detected when culture-adapted strains were tested *in vitro* [24]. Surely the fact that these assays measure parasite growth at different times (24 hours *versus* 72 hours) and using different growth indicators (hemozoin *versus* HRP2-antigen) may explain these differences. Nevertheless, it should be noted that the hemozoin detection assay inherently tends to lead to increased IC₅₀ values. Indeed, comparison of IC₅₀ between different drug assays is difficult since these values can vary considerably between assays [9, 24]. Yet, this becomes less relevant when comparisons are done between results obtained by the same drug assay. Furthermore, not all parasites obtained from malaria patients successfully grew/replicated *ex vivo*. In fact, different growth profiles were observed. It is important to note that tested samples were not specifically collected for the purpose of this study. Thus, information regarding the patients was scarce and might explain some of the differences observed in parasite growth *ex vivo*.

Results obtained during this study served as proof-of-principle of the original idea of using hemozoin detection as a mean to determine drug effects on *P. falciparum*. However, ultimate clinical validation would only be possible by conducting a controlled clinical trial, where a higher number of samples would be tested and detailed information of the patients would be made available.

3. Limitations of flow cytometric detection of hemozoin for antimalarial drug testing

Studies performed in the context of this PhD project showed that the hemozoin detection by flow cytometry allows to monitor parasite maturation and to detect drug effects and drug resistance more rapidly (24 hours) than other available drug assays (48 – 96 hours). Moreover, because it is based on the detection of a parasite product it does not require the use of additional reagents. However, some limitations exist, mainly associated with: 1) a high detection limit of 0.3% parasitemia and 2) the fact that it does not allow the analysis of a high number of samples per day.

Improved detection limits can be obtained by further optimizing the protocol of sample preparation. Preliminary results, which were not presented in this thesis, seem to suggest

that by lysing the erythrocytes, a higher volume of blood sample can be analysed by flow cytometry, and thus depolarizing signals above the background can be detected in samples with parasitemias as low as 0.05% (the same detection limit of the HRP2-ELISA assay).

Flow cytometry is inherently a single-channel instrument, meaning that only a single sample can be analyzed at a time. This implies that a limited and rather reduced number of samples can be analysed in a specific period of time. This is certainly a limitation, specially in validation, epidemiological or drug screening studies where a high number of samples is ought to be tested. Ideally, processing of several samples at the same time would be the best option. High-throughput systems have been developed for flow cytometry [28] and the use of such a system would make the hemozoin assay much more time-efficient. However, these additional systems are expensive and may often require maintenance.

These limitations should be considered and addressed in the future to establish the hemozoin detection assay as a tool for rapid antimalarial resistance testing. In this context and with the aim of investigating better cytometric tools for malaria investigation in resource-limited settings a working group led by Dr. Howard Shapiro was formed at CYTO 2012 Meeting of the International Society for the Advancement of Cytometry (ISAC), held in Leipzig, Germany. Since then, several workshops on Malaria and Cytometry have been held at different meetings to document the current state of malaria cytometry and its applications so further development could be efficiently achieved in the future.

4. Further implementation of hemozoin detection in different contexts

4.1. Image cytometry

Image cytometry may be an alternative to flow cytometric methods. The main difference between these two methods is that one requires a fluidic system (flow cytometry) and the other does not (image cytometry) [29]. Indeed, wide-field image cytometry is now capable of measuring the same parameters that would be measured by flow cytometry, such as DNA, RNA and possibly hemozoin [29]. Wide-field imaging cytometry requires small volumes of blood, short exposure times (no longer than a few seconds) and analysis of data from thousands of cells in one field can be done in few minutes [30]. Overall, an image cytometer is more robust and portable and less complex and costly than a flow cytometer. Furthermore, affordable image cytometers can now be built using cheap materials such as: LED light sources (< 10-100 USD), CMOS or CCD camera chips (~ 25 USD), and

microprocessors similar to those used in smartphones (~ 25 USD) [30]. This would allow to keep the production costs of such devices at low cost, making them affordable for resource-limited settings found in most malaria endemic countries.

Image cytometry could be an alternative method to detect hemozoin and thus, allow to determine drug effects and drug resistance. Currently, a prototype of such an instrument exists; however it has not yet been tested for its potential to detect hemozoin.

4.2. Other novel hemozoin detection technologies

It is important to note that in recent years hemozoin has played a central role in the development of alternative and novel methods to diagnose malaria [31–36]. Indeed, in the 2016's *Malaria Diagnostics Technology and Market Landscape* report it is mentioned that six independent groups have been developing hemozoin-detecting technologies [37]. Even though these methods differ in their technological approach they are based on two unique physical properties of hemozoin: 1) its optical properties - hemozoin crystals scatter and depolarize light in a unique way; and 2) its magnetic properties. Importantly, most of the hemozoin-based technologies are designed to be hand-held devices that use finger-prick collected blood samples [37]. Moreover, no reagents are needed and results are rapidly available (in less than five minutes).

It is known that hemozoin is only detectable in more mature parasite forms and in most *P. falciparum* infections these parasite forms are not found in circulation. We have previously observed that flow cytometric detection of hemozoin does not allow to reliably detect young immature parasite forms found in blood samples from malaria patients [27]. Therefore, hemozoin may not be the ideal marker for diagnosis of *P. falciparum* malaria. Yet, results presented in the context of this thesis show that it may be a useful marker of parasite maturation and, consequently, may allow the detection of drug effects. Definitely novel devices that are able to detect hemozoin should be further explored and investigated for their potential and usefulness as alternative antimalarial drug assays.

A preliminary study using one such device, the Magneto-optical method (MOT) developed by University of Budapest [32, 33], was performed at our laboratory. It was shown that the MOT was able to monitor infection in a rodent model of malaria [34], thus indicating that it might allow the detection of parasite maturation and drug effects as well. Indeed, unpublished data showed that the antimalarial activity of several antimalarial drugs could be detected in *in vitro* cultures of *P. falciparum* after 20 hours of incubation, approximately at the same time as drug effects are detected by flow cytometric detection of

hemozoin. The great advantage of this method in comparison to flow cytometry is its low detection limit of 0.0008% parasitemia [33]. Like in flow cytometry, the MOT device is a single-channel instrument and only a single sample can be measured at a time. However, while by flow cytometry sample acquisition is done in less than a minute, in the MOT method at least five minutes are required. Further optimization of the device should be performed to allow a more rapid sample analysis.

Nevertheless, results obtained with the MOT method reinforces the idea that hemozoin detection, independently of the method or technology used to detect it, is a relevant biomarker for the detection of antimalarial drug effects.

5. Hemozoin detection and artemisinin resistance

The usefulness of the flow cytometric detection of hemozoin was further investigated in the context of artemisinin resistance. One of the hallmarks of artemisinin resistance is that the delayed parasite clearance times observed in patients does not correlate with IC₅₀ values obtained *in vitro*, when conventional drug assays are used [5, 38]. This is thought to be consequence of the fact that artemisinin resistance seems to exist only in young ring-form parasites [39, 40]. All other parasites forms seem to remain susceptible to the drug. Thus, as most *in vitro* drug assays determine drug effects after a whole 48-hour parasite life cycle, results would be relatively unaffected if only a short part of the cycle was affected by the underlying mechanism of resistance [41].

As the flow cytometric detection of hemozoin allows to detect drug effects earlier than any other drug assays, it might be particularly useful for the *in vitro* detection of artemisinin resistance. It was shown that, contrary to other assays, when parasite maturation was assessed by the hemozoin detection assay at 24 hours of incubation, artemisinin-resistant parasites had increased IC₅₀ values in comparison to the ones obtained for the artemisinin-sensitive strains. Moreover, increased survival rates associated with artemisinin resistance were observed after only 30 hours of incubation, instead of the 72 hours described for the previously validated ring-stage assay [38].

Since it was first reported artemisinin resistance has been considered “as a clear and present danger” [42]. For now observed resistance of *Plasmodium falciparum* is considered to be partial by the WHO and artemisinin-combination therapies are still the mainstay of antimalarial treatment [43]. However if the current phenotype spreads to areas with high malaria endemicity, such as the ones found in Sub-Saharan Africa, ACTs may also start failing there. Development of full resistance to the artemisinins may lead to

increased numbers of deaths and morbidity associated with malaria and will certainly jeopardize all efforts and progress made in the last decades in the context of malaria control. As it has been witnessed with the spread of chloroquine resistance in Africa [2], emergence of full resistance to artemisinin would put the life of millions of people at risk again. Better and effective tools to detect artemisinin resistance *in vitro* are needed. Detection of hemozoin may offer a great opportunity to investigate artemisinin resistance. Preliminary results are promising but further optimization using more artemisinin-resistance strains is required. Moreover, validation studies including field trials in Southeast Asia need to be performed to determine the actual usefulness of the flow cytometric detection of hemozoin in the study and detection of artemisinin resistance.

6. Final remarks

Hemozoin has played an important role in the study of malaria since the very beginning. In fact, malaria was discovered by associating the observation of hemozoin in the organs of sick patients and the parasite that caused the disease. For centuries it was thought that hemozoin was a waste product of the parasite, however its importance have increased in the last decades. It is now acknowledged that hemozoin plays an important as an antimalarial drug target [44–46] and as an immune system modulator [47–50]. The work presented in this thesis further shows that hemozoin can also be used for antimalarial drug testing [24–26]. Indeed, detection of hemozoin may offer a great opportunity to further investigate and unravel antimalarial drug resistance.

Flow cytometry is one of the possible approaches to be used in the future. Indeed, simple and affordable instruments are now available and flow cytometric measurements of other parameters, such as DNA content and base composition and RNA content, in addition to hemozoin may provide improved accuracy and sensitivity of parasite detection and characterization [29]. However, an inherent limitation of flow cytometric methods is the fact that only a single sample can be analyzed at a time. This may be overcome by novel technologies or methods that are also able to detect hemozoin [31–36]. In fact, some of such methods are currently available and should definitely be further explored for their potential to detect antimalarial drug effects. Ideally, joint efforts should be made by combining technical knowledge with biological and clinical expertise to allow the efficient development of better *in vitro* tools for antimalarial drug testing that will, ultimately, play a central role in the successful fight against malaria.

7. References

1. Trape JF, Pison G, Preziosi MP, Enel C, Degrees du Lou A, Delaunay V, et al. (1998) Impact of chloroquine resistance on malaria. *Comptes Rendus de l'Académie des Sciences. Série III, Sciences de la Vie* 321: 689–697.
2. Trape JF. (2001) The Public Health Impact of Chloroquine Resistance in Africa. *The American Journal of Tropical Medicine and Hygiene* 64: 12–17.
3. WHO. (2016) Eliminating Malaria. World Health Organization, Geneva.
4. Noedl H, Se Y, Schaecher K, Smith BL, Socheat D and Fukuda MM. (2008) Evidence of artemisinin-resistant malaria in western Cambodia. *The New England journal of medicine* 359: 2619–2620.
5. Dondorp A, Nosten F, Yi P, Das D, Phyto A, Tarning J, et al. (2009) Artemisinin Resistance in *Plasmodium falciparum* Malaria. *The New England Journal of Medicine* 361: 455–467.
6. Ashley E a., Dhorda M, Fairhurst RM, Amaratunga C, Lim P, Suon S, et al. (2014) Spread of Artemisinin Resistance in *Plasmodium falciparum* Malaria. *The New England Journal of Medicine* 371: 411–423.
7. WHO. (2015) Guidelines for the treatment of malaria - 3rd edition. World Health Organization, Geneva.
8. Noedl H. (2003) Malaria drug-sensitivity testing: new assays, new perspectives. *Trends in Parasitology* 19: 175–181.
9. Basco LK. (2007) Field application of in vitro assays for the sensitivity of human malaria parasites to antimalarial drugs. WHO Press, Geneva, Switzerland.
10. Rieckmann K, Campbell G, Sax L and Mrema J. (1978) Drug sensitivity of *Plasmodium falciparum*. An in-vitro microtechnique. *The Lancet* 1: 22–23.
11. Desjardins R, Canfield C, Haynes J and Chulay J. (1979) Quantitative Assessment of Antimalarial Activity In Vitro by a Semiautomated Microdilution Technique. *Antimicrobial Agents and Chemotherapy* 16: 710–718.
12. Noedl H, Wernsdorfer WH, Miller RS and Wongsrichanalai C. (2002) Histidine-Rich Protein II: a Novel Approach to Malaria Drug Sensitivity Testing. *Antimicrobial Agents and Chemotherapy* 46: 1658–1664.
13. WHO. (2016) False-negative RDT results and implications of new reports of *P . falciparum* histidine-rich protein 2 / 3 gene deletions. *Global Malaria Programme - Information Note*. World Health Organization, Geneva.

14. Jamjoom GA. (1983) Dark-field microscopy for detection of malaria in unstained blood films. *Journal of Clinical Microbiology* 17: 717–721.
15. de Grooth B, Terstappen L, Puppels G and Greve J. (1987) Light-scattering polarization measurements as a new parameter in flow cytometry. *Cytometry* 8: 539–544.
16. Mendelow B V, Lyons C, Nhlangothi P, Tana M, Munster M, Wypkema E, et al. (1999) Automated malaria detection by depolarization of laser light. *British Journal of Haematology* 104: 499–503.
17. Hänscheid T, Pinto BG, Cristino JM and Grobusch MP. (2000) Malaria diagnosis with the haematology analyser Cell-Dyn 3500: What does the instrument detect? *Clinical and Laboratory Haematology* 22: 259–261.
- 18 Hänscheid T, Melo-Cristino J and Pinto BG. (2001) Automated detection of malaria pigment in white blood cells for the diagnosis of malaria in Portugal. *The American Journal of Tropical Medicine and Hygiene* 64: 290–292.
19. Grobusch MP, Hänscheid T, Krämer B, Neukammer J, May J, Seybold J, et al. (2003) Sensitivity of hemozoin detection by automated flow cytometry in non- and semi-immune malaria patients. *Cytometry. Part B (Clinical cytometry)* 55: 46–51.
20. Suh IB, Kim HJ, Kim JY, Lee SW, An SSA, Kim WJ, et al. (2003) Evaluation of the Abbott Cell-Dyn 4000 hematology analyzer for detection and therapeutic monitoring of *Plasmodium vivax* in the Republic of Korea. *Tropical Medicine and International Health* 8: 1074–1081.
21. Campuzano-Zuluaga G, Hänscheid T and Grobusch MP. (2010) Automated haematology analysis to diagnose malaria. *Malaria Journal* 9: 346.
22. Hänscheid T, Valadas E and Grobusch MP. (2000) Pigment Detection. *Parasitology* 4758: 2000–2002.
23. Rieckmann KH. (1982) Visual in-vitro test for determining the drug sensitivity of *Plasmodium falciparum*. *The Lancet* 1: 1333–1335.
24. Rebelo M, Sousa C, Shapiro HM, Mota MM, Grobusch MP, Hänscheid T (2013) A novel flow cytometric hemozoin detection assay for real-time sensitivity testing of *Plasmodium falciparum*. *PLoS One* 8:e61606.
25. Rebelo M, Tempera C, Fernandes JF, Grobusch MP and Hänscheid T. (2015) Assessing anti-malarial drug effects ex vivo using the haemozoin detection assay. *Malaria Journal* 14: 140.
26. Frita R, Rebelo M, Pamplona A, Vigario AM, Mota MM, Grobusch MP, et al. (2011) Simple flow cytometric detection of haemozoin containing leukocytes and erythrocytes for

- research on diagnosis, immunology and drug sensitivity testing. *Malaria Journal* 10: 74.
27. Rebelo M, Shapiro HM, Amaral T, Melo-Cristino J and Hänscheid T. (2012) Haemozoin detection in infected erythrocytes for *Plasmodium falciparum* malaria diagnosis-Prospects and limitations. *Acta Tropica* 123: 58–61.
28. Edwards BS, Young SM, Saunders MJ, Bologna C, Oprea TI, Ye RD, et al. (2007) High-throughput flow cytometry for drug discovery. *Expert Opinion on Drug Discovery* 2: 685–696.
29. Shapiro HM, Apte SH, Chojnowski GM, Hänscheid T, Rebelo M and Grimberg BT. (2013) Cytometry in malaria-A practical replacement for microscopy? *Current Protocols in Cytometry* 1–23.
30. Shapiro H. (2011) The Cytometric Future: It Ain't Necessarily Flow! *Methods in Molecular Biology* 699: 471–82.
31. Mens PF, Matelon RJ, Nour BYM, Newman DM and Schallig HDFH. (2010) Laboratory evaluation on the sensitivity and specificity of a novel and rapid detection method for malaria diagnosis based on magneto-optical technology (MOT). *Malaria Journal* 9: 207.
32. Butykai A, Orbán A, Kocsis V, Szaller D, Bordács S, Tátrai-Szekeres E, et al. (2013) Malaria pigment crystals as magnetic micro-rotors: key for high-sensitivity diagnosis. *Scientific Reports* 3: 1431.
33. Orbán Á, Butykai Á, Molnár A, Pröhle Z, Fülöp G, Zelles T, et al. (2014) Evaluation of a novel magneto-optical method for the detection of malaria parasites. *PLoS One* 9: 1–8.
34. Orbán Á, Rebelo M, Molnár P, Albuquerque IS, Butykai A and Kézsmárki I. (2016) Efficient monitoring of the blood-stage infection in a malaria rodent model by the rotating-crystal magneto-optical method. *Scientific Reports* 6: 23218.
35. Peng WK, Kong TF, Ng CS, Chen L, Huang Y, Bhagat AAS, et al. (2014) Micromagnetic resonance relaxometry for rapid label-free malaria diagnosis. *Nature Medicine* 20: 1069–1073.
36. Lukianova-Hleb EY, Campbell KM, Constantinou PE, Braam J, Olson JS, Ware RE, et al. (2014) Hemozoin-generated vapor nanobubbles for transdermal reagent- and needle-free detection of malaria. *Proceedings of the National Academy of Sciences of the United States of America* 111: 900–905.
37. UNITAID - WHO. (2016) Malaria Diagnostics Technology and Market Landscape.
38. Witkowski B, Amaratunga C, Khim N, Sreng S, Chim P, Kim S, et al. (2013) Novel phenotypic assays for the detection of artemisinin-resistant *Plasmodium falciparum*

malaria in Cambodia: In-vitro and ex-vivo drug-response studies. *The Lancet Infectious Diseases* 13: 1043–1049.

39. Saralamba S, Pan-Ngum W, Maude RJ, Lee SJ, Tarning J, Lindegardh N, et al. (2011) Intrahost modeling of artemisinin resistance in *Plasmodium falciparum*. *Proceedings of the National Academy of Sciences of the United States of America* 108: 397–402.

40. Witkowski B, Khim N, Chim P, Kim S, Ke S, Kloeung N, et al. (2013) Reduced Artemisinin Susceptibility of *Plasmodium falciparum* Ring Stages in Western Cambodia. *Antimicrobial Agents and Chemotherapy* 57: 914–23.

41. Dondorp AM, Fairhurst RM, Slutsker L, Macarthur JR, M D JGB, Guerin PJ, et al. (2011) The threat of artemisinin-resistant malaria. *The New England Journal of Medicine* 365: 1073–5.

42. Dondorp AM and Ringwald P. (2013) Artemisinin resistance is a clear and present danger. *Trends in Parasitology* 29: 359–360.

43. WHO. (2016) Artemisinin and artemisinin-based combination therapy resistance.

44. Weissbuch I and Leiserowitz L. (2008) Interplay between malaria, crystalline hemozoin formation, and antimalarial drug action and design. *Chemical Reviews* 108: 4899–914.

45. Chong CR and Sullivan DJ. (2003) Inhibition of heme crystal growth by antimalarials and other compounds: Implications for drug discovery. *Biochemical Pharmacology* 66: 2201–2212.

46. Hempelmann E. (2007) Hemozoin biocrystallization in *Plasmodium falciparum* and the antimalarial activity of crystallization inhibitors. *Parasitology Research* 100: 671–676.

47. Lyke KE, Diallo DA, Dicko A, Kone A, Coulibaly D, Guindo A, et al. (2003) Association of intraleukocytic *Plasmodium falciparum* malaria pigment with disease severity, clinical manifestations, and prognosis in severe malaria. *The American Journal of Tropical Medicine and Hygiene* 69: 253–259.

48. Shio MT, Kassa FA, Bellemare MJ and Olivier M. (2010) Innate inflammatory response to the malarial pigment hemozoin. *Microbes and Infection* 12: 889–899.

49. Hänscheid T, Längin M, Lell B, Pötschke M, Oyakhirome S, Kremsner PG, et al. (2008) Full blood count and haemozoin-containing leukocytes in children with malaria: diagnostic value and association with disease severity. *Malaria Journal* 7: 109.

50. Boura M, Frita R, Góis A, Carvalho T and Hänscheid T. (2013) The hemozoin conundrum: is malaria pigment immune-activating, inhibiting, or simply a bystander? *Trends in parasitology* 29: 469–476.

PUBLICATIONS

As first-author

1. Frita R, **Rebelo M**, Pamplona A, Vigario AM, Mota MM, Grobusch MP, Hänscheid T. Simple flow cytometric detection of haemozoin containing leukocytes and erythrocytes for research on diagnosis, immunology and drug sensitivity testing. *Malar J*. 2011 Mar 31;10:74.
2. **Rebelo M**, Shapiro HM, Amaral T, Melo-Cristino J, Hänscheid T. Haemozoin detection in infected erythrocytes for *P. falciparum* malaria diagnosis – prospects and limitations. *Acta Trop*. 2012;123(1):58-61.
3. **Rebelo M**, Sousa C, Shapiro HM, Mota MM, Grobusch MP, Hänscheid T. A novel flow cytometric hemozoin detection assay for real-time sensitivity testing of *Plasmodium falciparum*. *PlosOne* 2013; 8(4):e61606.
4. **Rebelo M**, Tempera C, Fernandes JF, Grobusch MP, Hänscheid T. Assessing anti-malarial drug effects ex vivo using the haemozoin detection assay. *Malar J*. 2015 Apr 1;14:140.
5. **Rebelo M**, Tempera C, Bispo C, Andrade C, Gardner R, Shapiro HM, Hänscheid T. Light depolarization measurements in malaria: A new job for an old friend. *Cytometry A*. 2015;87(5):437-45.
6. **Rebelo M**, Grenho R, Orban A, Hänscheid T. Hemozoin-based non-invasive diagnosis of malaria: already there? *Emerg Infect Dis*. 2016 Feb;22(2):343-4.
7. **Rebelo M**, Hänscheid T. Flow cytometry for antimalarial drug testing – more than meets the eye. *J Clin Microbiol*. 2016 Mar;54(3):817.
8. Orbán A*, **Rebelo M***, Molnár P, I S Albuquerque, Butykai A, Kézsmárki I. Efficient monitoring of the blood-stage infection in a malaria rodent model by the rotating-crystal magneto-optical method. *Sci Rep*. 2016 Mar 17;6:23218.

As co-author:

9. Hanson KK, Ressurreição AS, Buchholz K, Prudêncio M, Herman J, **Rebelo M**, Beatty WL, Wirth D, Hänscheid T, Moreira R, Marti M, and Mota MM. Torins are potent antimalarials that block replenishment of *Plasmodium* liver stage parasitophorous vacuole membrane proteins. *PNAS* 2013 Jul 23;110(30):E2838-47.
10. Shapiro HM, Apte SH, Chojnowski GM, Hänscheid T, **Rebelo M**, Grimberg BT. Cytometry in malaria – a practical replacement for microscopy? *Curr Protoc Cytom* 2013 Jul;Chapter 11:Unit 11.20.
11. Orbán A, Butykai A, Molnár A, Pröhle Z, Fülöp G, Zelles T, Forsyth W, Hill D, Müller I, Schofield L, **Rebelo M**, Hänscheid T, Karl S, Kézsmárki I. Evaluation of a novel magneto-optical method for the detection of malaria parasites. *PLoS One*. 2014 May 13;9(5):e96981.
12. Hänscheid T, **Rebelo M**, Grobusch MP. Point-of-care tests: where is the point? *Lancet Infect Dis*. 2014 Oct;14(10):922.

METHODOLOGY

Open Access

Simple flow cytometric detection of haemozoin containing leukocytes and erythrocytes for research on diagnosis, immunology and drug sensitivity testing

Rosangela Frita¹, Maria Rebelo¹, Ana Pamplona¹, Ana M Vigario^{1,2}, Maria M Mota¹, Martin P Grobusch^{3,4,5} and Thomas Häscheid^{1,5*}

Abstract

Background: Malaria pigment (haemozoin, Hz) has been the focus of diverse research efforts. However, identification of Hz-containing leukocytes or parasitized erythrocytes is usually based on microscopy, with inherent limitations. Flow cytometric detection of depolarized Side-Scatter is more accurate and its adaptation to common bench top flow cytometers might allow several applications. These can range from the *ex-vivo* and *in-vitro* detection and functional analysis of Hz-containing leukocytes to the detection of parasitized Red-Blood-Cells (pRBCs) to assess antimalarial activity.

Methods: A standard benchtop flow cytometer was adapted to detect depolarized Side-Scatter. Synthetic and *Plasmodium falciparum* Hz were incubated with whole blood and PBMCs to detect Hz-containing leukocytes and CD16 expression on monocytes. C5BL/6 mice were infected with *Plasmodium berghei* ANKA or *P. berghei* NK65 and Hz-containing leukocytes were analysed using CD11b and Gr1 expression. Parasitized RBC from infected mice were identified using anti-Ter119 and SYBR green I and were analysed for depolarized Side Scatter. A highly depolarizing RBC population was monitored in an *in-vitro* culture incubated with chloroquine or quinine.

Results: A flow cytometer can be easily adapted to detect depolarized Side-Scatter and thus, intracellular Hz. The detection and counting of Hz containing leukocytes in fresh human or mouse blood, as well as in leukocytes from *in-vitro* experiments was rapid and easy. Analysis of CD14/CD16 and CD11b/Gr1 monocyte expression in human or mouse blood, in a mixed populations of Hz-containing and non-containing monocytes, appears to show distinct patterns in both types of cells. Hz-containing pRBC and different maturation stages could be detected in blood from infected mice. The analysis of a highly depolarizing population that contained mature pRBC allowed to assess the effect of chloroquine and quinine after only 2 and 4 hours, respectively.

Conclusions: A simple modification of a flow cytometer allows for rapid and reliable detection and quantification of Hz-containing leukocytes and the analysis of differential surface marker expression in the same sample of Hz-containing *versus* non-Hz-containing leukocytes. Importantly, it distinguishes different maturation stages of parasitized RBC and may be the basis of a rapid no-added-reagent drug sensitivity assay.

* Correspondence: thanscheid@fm.ul.pt

¹Instituto de Medicina Molecular, Faculdade de Medicina de Lisboa, Lisbon, Hospital Universitário de Santa Maria, Av. Prof. Egas Moniz, P-1649-028 Lisboa, Portugal

Full list of author information is available at the end of the article

Background

The malaria pigment, or haemozoin (Hz), is gaining increasing attention, as has been reviewed recently [1,2]: (i) Hz production is an important drug target, (ii) Hz appears to have immunomodulatory properties, (iii) detection of Hz-containing leukocytes allows diagnosis of malaria, and (iv) Hz-containing leukocytes appear to be associated with disease severity. However, one important drawback in this area of research is the fact that counting of Hz-containing leukocytes or the detection of Hz-containing parasitized red-blood cells (pRBCs) is based on microscopy [3,4]. This is not only cumbersome, but introduces a significant statistical error if the number of Hz-containing leukocytes is low [5]. An alternative to this is based on the detection of depolarized Side-Scatter by flow cytometry [6]. Hz is birefringent and as a consequence rotates the plane of polarized light, a process called depolarization. LASER light, commonly used in flow cytometers, produces polarized light. Thus, by placing a polarization filter orthogonally (90° rotated) to the plane of the LASER light in front of a second SSC detector allows to detect depolarized light and consequently Hz.

Depolarized SSC detection is incorporated into the Cell-Dyn[®] haematology analysers (Abbott, Santa Clara, CA, USA) to differentiate eosinophils from granulocytes. As a result of this, these instruments detect Hz-containing leukocytes as well as Hz in parasitized red blood cells (pRBC) without need for modifications, [7,8]. Unfortunately, the software analysis and analysis algorithms of the analysers cannot be accessed without the intervention of the manufacturer and thus, studies depended on counting the events (cells) on the instrument's screen or the printout, with consequent data loss and no option for further analysis of the raw data [9]. However, if a simple modification of common flow cytometers created a reliable method for detection and analysis of Hz in leukocytes or pRBC it might open novel approaches for diagnostic applications and research.

For example, flow cytometric counting of Hz-containing leukocytes may be a better marker for disease severity than microscopy based counts [5,10]. Detection and functional analysis of Hz-containing leukocytes may also help to elucidate further aspects on the immunomodulatory properties of Hz. In fact, most *in-vitro* studies use concentrations of Hz that maximize uptake by the majority of monocytes in a given cell population and compare them with a control population that was not exposed to Hz [11]. However, the situation may be different *in vivo*, where both populations coexist. For example, a recent large study, based on microscopy, reported that the median percentage of circulating Hz-containing monocytes was only 2-5% [3].

Interestingly, monocytes are a heterogeneous cell population, even in peripheral blood [12,13], mainly based on the CD14 and CD16 expression: classical "inflammatory" monocytes (CD14⁺/CD16⁻), "intermediate" monocytes (CD14⁺/CD16⁺) and "resident, pro-inflammatory" monocytes (CD14^{dim}/CD16⁺). They also seem to differ functionally [14]. Recent research showed differences in the ratio of these populations in malarious children with different types of malaria [15], as well as differences in surface marker expression and parasite inhibitory action in acute uncomplicated malaria [16]. However, little is known whether Hz phagocytosis contributes to these findings *in vivo*. In fact, the interplay of Hz-containing and non-Hz-containing subpopulations might produce different biological results *in vivo*, when compared to those *in vitro* models, where nearly all monocytes contain Hz.

Another important area for flow cytometric detection of Hz could be the reliable detection of pRBC harbouring different Hz content. This may be useful for sensitivity testing and drug development, because the Hz-content increases proportional to the maturation of the parasite [17].

This paper describes a simple way to modify a standard bench-top flow cytometer to allow depolarized Side-Scatter measurements. The method was then tested for its usefulness to detect Hz-containing leukocytes and erythrocytes and examples for potential applications are presented.

Methods

Flow cytometer modification (depolarized Side Scatter detection)

The CyFlow[®] Blue (Partec, Münster, Germany) is a small, five parameter flow cytometer (Figure 1a) with blue laser (488 nm) excitation, and detectors for Forward Scatter (FSC), Side Scatter (SSC), green fluorescence (FL1), orange fluorescence (FL2) and red fluorescence (FL3) (Figure 1b). For this study the set-up was changed, mainly by creating two SSC detectors, using a 50%/50% beam splitter. Then a polarization filter was placed orthogonally to the polarization plane of the laser light, in front of one of these SSC detectors which allowed the detection of depolarized Side-Scatter. This and other necessary changes are indicated in Figure 1c.

Reagents

All reagents were obtained from Sigma Aldrich (St Louis, Mo, USA), unless stated otherwise. Fluorescein isothiocyanate (FITC) or phycoerythrin (PE) labelled antibodies against surface antigens as well as isotype antibodies (CD14-FITC, CD16-PE, CD11b-FITC, Gr1-PE, TER119-PE, Fc-block) were purchased from

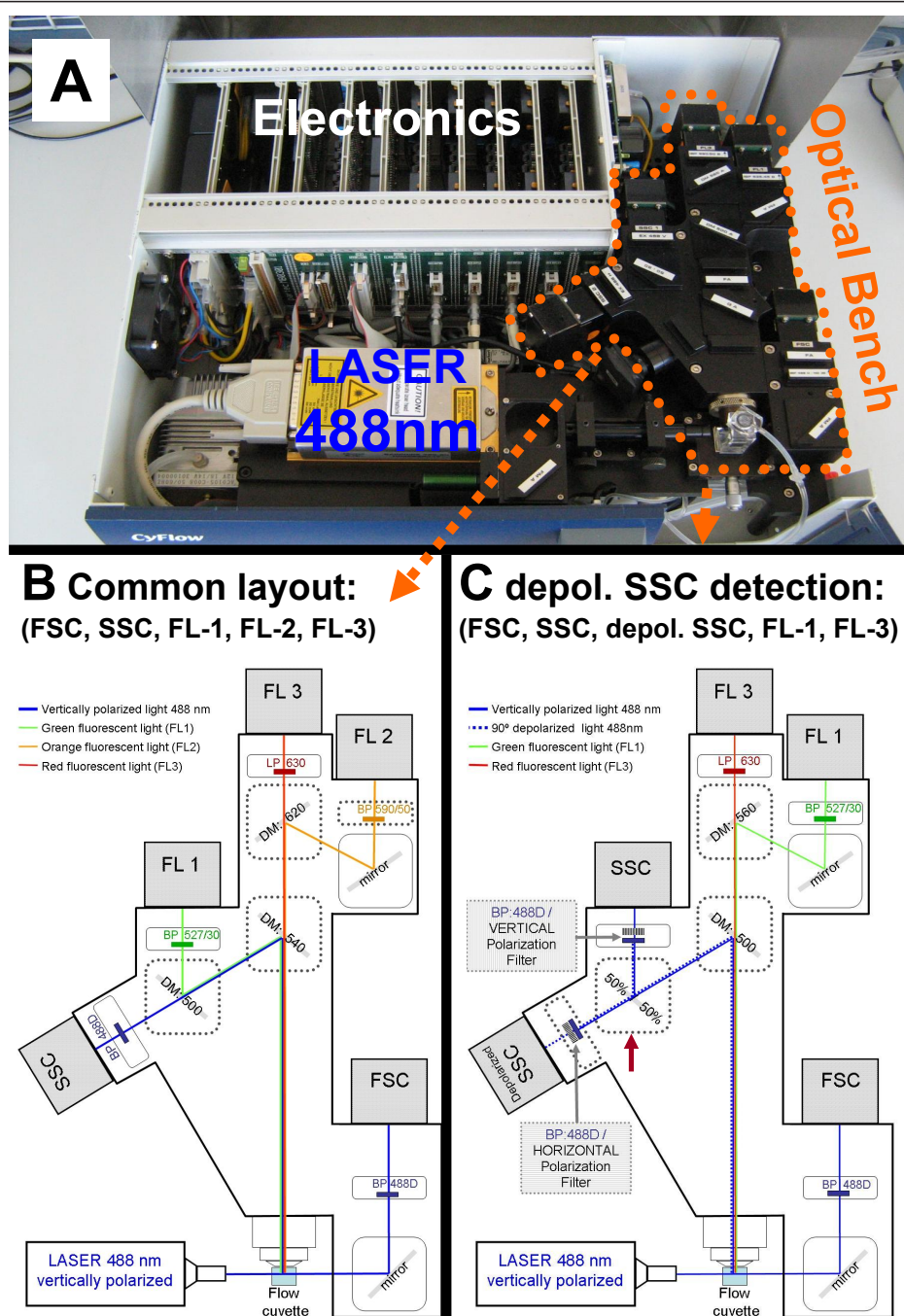


Figure 1 Alterations to the optical bench of a common bench-top flow cytometer which allows detection of depolarized side-scatter. a) The lid of the CyFlow[®] Blue flow cytometer can be easily removed and filters can be swapped by the operator. b) Light path in conventional filter set-up for detection of Forward Scatter (FSC), Side-Scatter (SSC), green (FL-1), orange (FL-2) and red (FL-3) fluorescence. c) Filter set-up that allows detection of depolarized Side-Scatter instead of FL-2 detection. Squares with broken line indicate dichroic mirrors that need to be changed. Red error shows 50%/50% beam splitter. Other beam splitters which divert more light to the depolarized SSC are possible, such as 90%/10% or even 95%/5%. DM = Dichroic Mirror; BP = Bandpass filter, LP = Longpass filter, numbers indicate wavelength in nm.

eBioscience (San Diego, USA). DNase/RNase free ultrapure water, Phosphate buffer saline (PBS), Fetal Bovine Serum (FBS), HEPES and RPMI 1640 were purchased from Gibco (Grand Island, NY). Ultrapure water was obtained with a Milli-Q purification system (Millipore, Madrid, Spain).

Haemozoin preparation and quantification

Synthetic haemozoin (sHz) was prepared by dissolving 1.1 gr of hemin chloride in 70 ml of 0.4 M NaOH and 62 ml of ultrapure water. The heme was then precipitated by the addition of 68 ml of glacial acetic acid. The mixture was heated at 37°C over night to promote the formation of β -haematin. The following day, the formed crystalline synthetic haemozoin (sHz) was washed 5 times in 5% pyridine (in 0.02 M HEPES at pH 7.5) and five times in ultrapure water. Finally, sHz was resuspended in PBS, quantified and stored at 4°C.

Plasmodium falciparum (strain 3D7) haemozoin (Pf-Hz) was purified from a synchronized culture at a parasitaemia of around 3-5%. Infected erythrocytes were spun at 2000 rpm for 10 min and resuspended for 10 min in a mixture of 40 ml ultrapure water with 2 ml of a 1% saponin in water. Cell lysates were then centrifuged at 13,200 rpm for 15 min. The Hz pellets were washed 4x with PBS, resuspended in 1 ml PBS, quantified and stored at 4°C. Both types of Hz showed no DNA contamination and were negative for *Mycoplasma*.

The concentration of Hz was determined as haem content (haem-equivalent) after solubilization in 20 mM NaOH for 1 hour at room temperature. The haem concentration was then determined by luminescence at 400 nm using the QuantiChrom Heme Assay Kit from BioAssay Systems (Hayward CA, USA).

In vitro incubation of human whole blood with synthetic haemozoin

Heparin-anticoagulated blood from healthy human donors was diluted 1:1 in RPMI 1640; and distributed into a 24 well plate. Then sHz was added at 0.01; 0.06 and 0.12 μ mol haem-equivalent/ml. The plate was incubated for 7 hours at 37°C in 5% CO₂. Leucocytes were analysed in triplicates at time 0, 4 and 7 hours.

In vitro incubation of human PBMCs with synthetic and *P. falciparum* haemozoin

Human PBMC were isolated from 40 ml heparin-anticoagulated blood collected from healthy volunteers and after dilution 1:1 in RPMI 1640 and placed in a Ficoll gradient (Ficoll-Paque Plus, GE Healthcare, Uppsala, Sweden). Cells were centrifuged at 700 g for 20 min and the interface containing the PBMCs was collected. The PBMCs were washed, counted and resuspended at a concentration of 1×10^6 PBMC/ml in RPMI 1640

supplemented with 2 mM L-glutamine, 0.05 mg/ml gentamicin and 10% foetal calf serum and distributed into a 24 well plate. Then sHz was added at 0.004 and 0.007 μ moles heme-equivalent/ml and P.f.-Hz was added at 0.002 and 0.004 μ mol haem-equivalent/ml in triplicates. Polystyrene latex beads (0,1 μ m) were diluted from the stock at 10% (vol/vol) to a final concentration of 0.001% and used as control. The plate was incubated for 6 hours at 37°C in 5% CO₂.

Flow cytometric analysis of human leukocytes

EDTA anticoagulated blood was obtained from volunteers and patients for immediate analysis. One hundred μ l of EDTA-anticoagulated blood was incubated for 20 minutes with anti-CD14 and anti-CD16. RBC were then lysed prior to analysis with Whole Blood Lysis Reagent (Partec, Münster, Germany) without further washing.

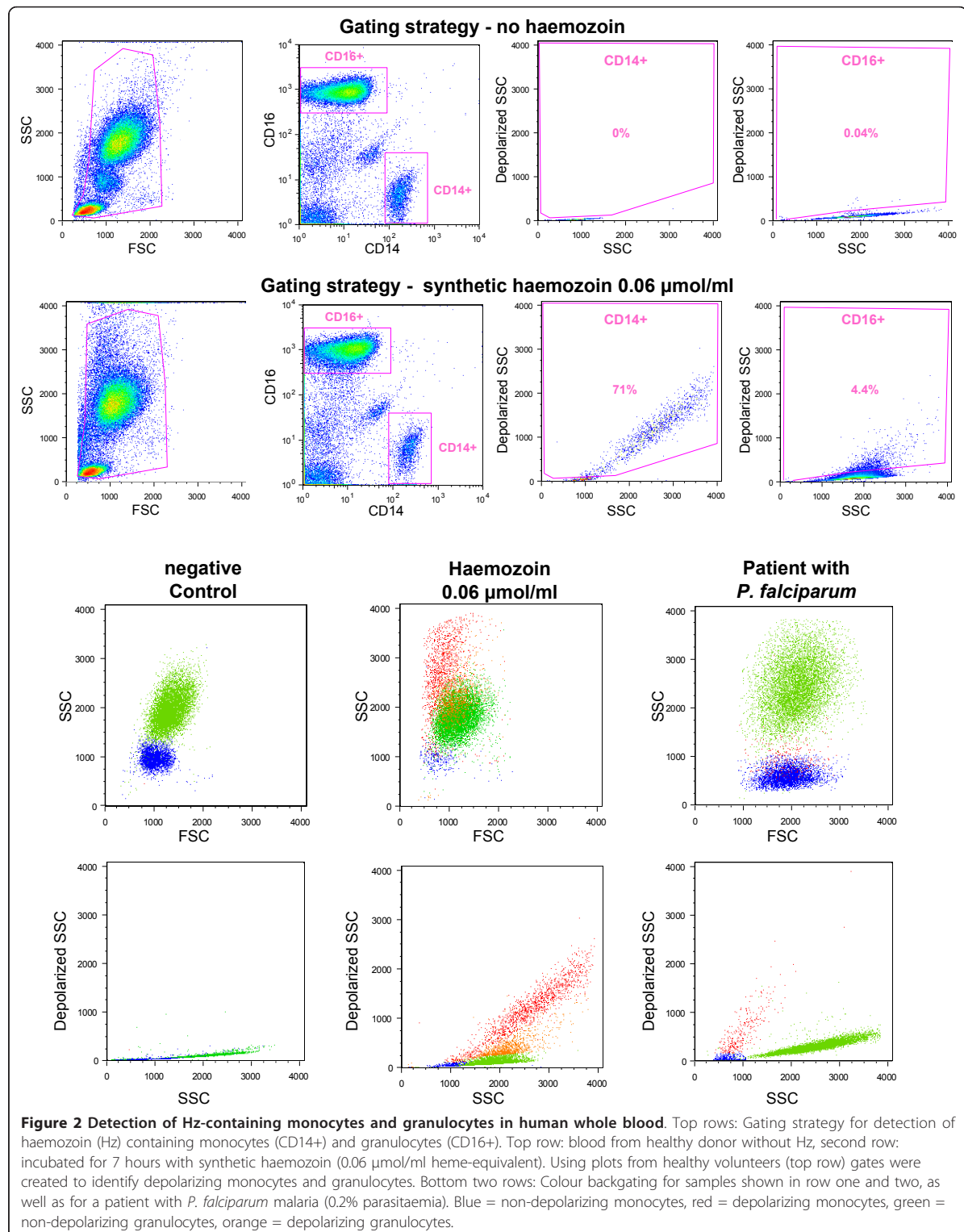
For the *in vitro* whole blood assay 50 μ l were incubated with anti-CD14 and anti-CD16 antibodies. RBC were lysed with BD FACS lysing solution (BD Biosciences, San Jose) for 5 minutes and washed before analysis. PBMCs were labelled as described for the whole blood assay, without erythrocyte lysis. All *in-vitro* samples were performed in triplicate. The gating strategy for monocytes and granulocytes and identification of Hz-containing leukocytes is shown in Figure 2.

Flow cytometric analysis of murine leukocytes

Groups of five C57BL/6 mice (Charles River, Spain) were infected intraperitoneally with *Plasmodium berghei* ANKA (PbA) as model for experimental cerebral malaria or *P. berghei* NK65 (PbNK) as model for hyperparasitaemia. Uninfected and *P. berghei* NK65 infected mice were followed for 18 days. PbA-infected mice were sacrificed on day 5 when showing obvious signs of morbidity. Parasitaemia and flow cytometric analysis of blood was performed on days 3, 5, 12 and 18 post infection. At each time point approximately 25 μ l of blood was collected from a tail vein, incubated with Fc-block and then labelled with anti-CD11b and anti-Gr1. After washing the cells, RBC were lysed with 125 μ l of BD FACS lysing solution (BD Biosciences, San Jose) for 5 min. The cells were washed again, resuspended in FACS buffer and analysed by flow cytometry. Granulocytes and monocytes were analysed as described previously [18], in particular following a protocol that uses Side Scatter, CD11b and Gr1 expression [19] (see: additional file 1 - mouse blood gating strategy.pdf).

Analysis of murine Hz-containing RBC

Mice (C57BL/6) (Charles River, Spain) were infected with *P. berghei* ANKA. Blood samples were collected when mice had a parasitaemia of approximately 5%. RBC were incubated with Fc-block and then labelled



with anti-TER119. After washing the cells, SYBR green I (Invitrogen, Carlsbad, USA) was used to stain the DNA of intraerythrocytic parasites. Briefly, 2.5 μ l of the SYBR Green I solution at 10x was added to a blood suspension of approximately 400,000 cells/mL and incubated for 20 minutes, in the dark.

Anti-malarial drug effect on *P. berghei* infected RBC in-vitro

Blood from infected mice was diluted 1:50 in RPMI medium supplemented with 10% foetal calf serum, 1% non essential amino acids, 1% penicillin/streptomycin, 1% glutamine and 10 mM HEPES, pH 7. The blood suspension was diluted 1:1 in complete RPMI medium and incubated with either chloroquine or quinine for 12 hours in a 24 well plate at 37°C in a 5% CO₂ atmosphere. Chloroquine diphosphate salt or quinine hydrochloride were dissolved in ultrapure water to prepare the stock solution. Final concentrations of 25 nM, 50 nM and 100 nM of chloroquine or 400 nM and 800 nM of quinine were used. Flow cytometric measurements were done during every two hours by diluting 5 μ l of the suspension present in the wells in 1 mL of FACS buffer. The effect of the anti-malarial drugs on the parasites was assessed by quantifying the percentage of highly depolarizing events (hdRBC).

All flow cytometry results were analysed using FlowJo software (version 9.0.2, Tree Star Inc., Oregon, USA).

The study was approved by the Ethical Committee of the Faculty of Medicine, University of Lisbon. All experiments involving animals were performed in compliance with the relevant laws and institutional guidelines.

Results

The Cyflow[®] instrument can be easily adapted to detect depolarized Side-Scatter (depol-SSC) by the operator, without any sophisticated tools or special knowledge. It is only necessary to open the instrument's cover, after releasing four screws, and change the respective filters and dichroic mirrors (Figure 1). This is a very simple procedure that lasts approximately 5 minutes. No special software is necessary and the same set-up (linear) as used for conventional SSC detection is sufficient, although the gain (voltage) of the detectors had to be adjusted.

Detection of Hz-containing leukocytes in human blood

Using anti-CD14 and anti-CD16 it was possible to identify Hz-containing monocytes and granulocytes in whole blood from healthy human volunteers incubated with Hz (Figure 2 and 3) as well as in a sample from a patient with malaria (Figure 2). Importantly, Hz-containing monocytes show much higher Side-Scatter than

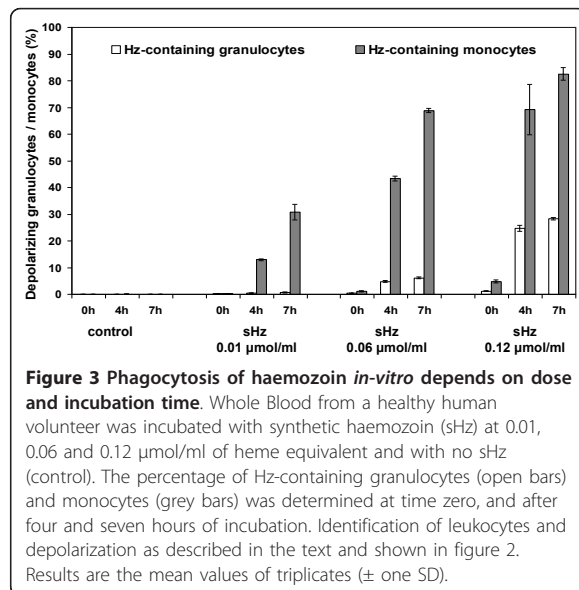


Figure 3 Phagocytosis of haemozoin in-vitro depends on dose and incubation time. Whole Blood from a healthy human volunteer was incubated with synthetic haemozoin (sHz) at 0.01, 0.06 and 0.12 μ mol/ml of heme equivalent and with no sHz (control). The percentage of Hz-containing granulocytes (open bars) and monocytes (grey bars) was determined at time zero, and after four and seven hours of incubation. Identification of leukocytes and depolarization as described in the text and shown in figure 2. Results are the mean values of triplicates (\pm one SD).

normal monocytes, which overlap with the granulocyte population (Figure 2, bottom rows).

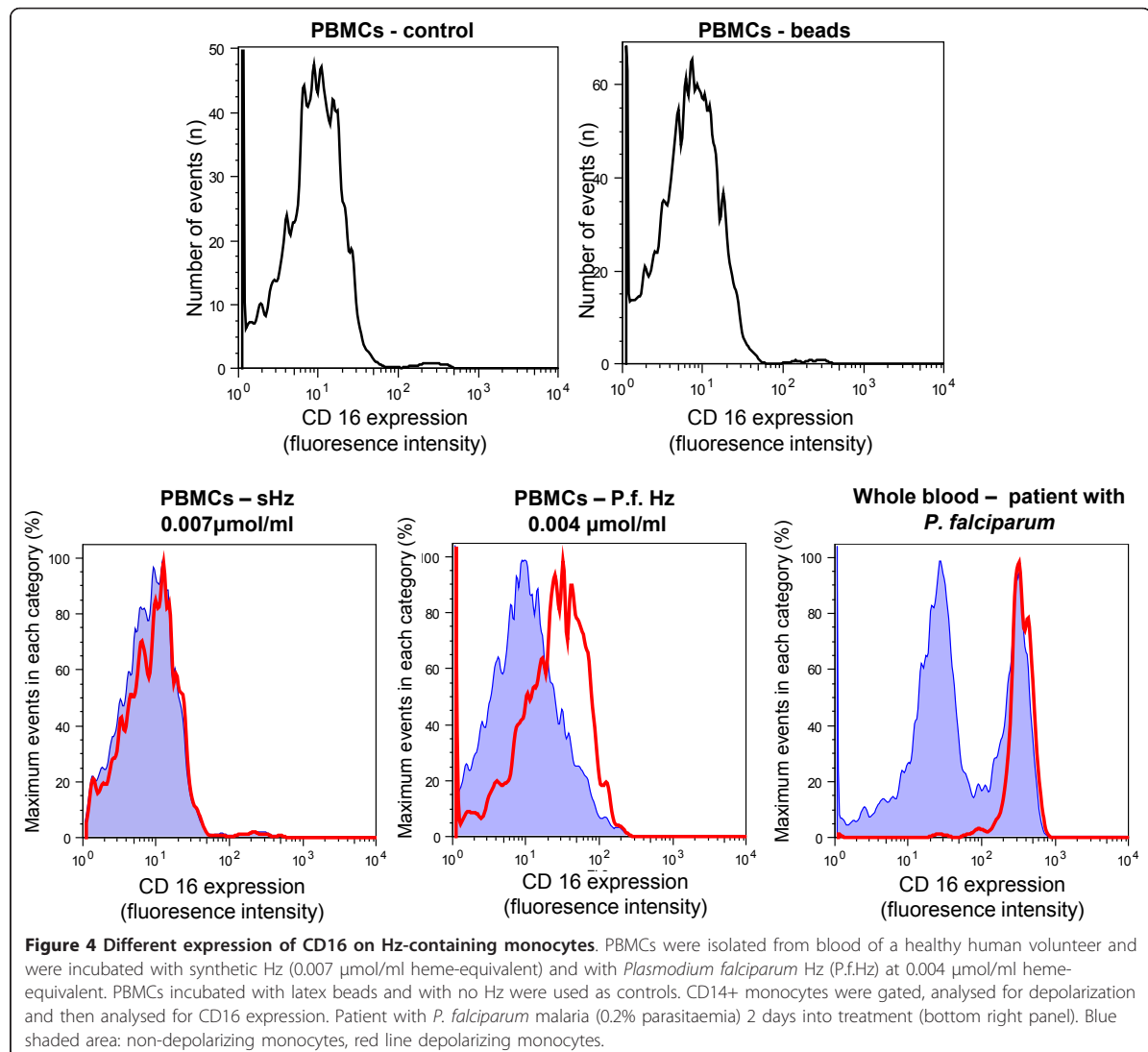
Incubation of whole blood from healthy volunteers with sHz shows that the percentage of Hz-containing monocytes and granulocytes depends on the initial Hz-dose and time of incubation (Figure 3).

In addition, different types of Hz cause distinct expression of CD16 on Hz-containing monocytes, as compared with non-haemozoin containing monocytes in mixed populations (Figure 4, 5). Contrary to the synthetic Hz used in this study, *P. falciparum* derived Hz increases significantly CD16 expression on Hz-containing monocytes from healthy volunteers ($P < 0.01$); Figure 4 and 5). Interestingly, in a single case of *P. falciparum* malaria with 5.4% Hz-containing monocytes, a substantial increase of CD16 expression was noticed and the majority of HZ-containing monocytes were clustered in the CD14+/CD16+ subpopulation (Figure 4, bottom row, right).

Altogether, the data clearly show that a simple alteration in a bench-top flow cytometer for detection of depolarized side-scatter allows quantification of Hz-containing monocytes, which could be easily detected in a case of *P. falciparum* malaria.

Hz-containing murine leukocytes

Using anti-CD11b and anti-Gr1 it was possible to identify Hz-containing monocytes and granulocytes in mouse blood (Figure 6). Mice with PbA infection were sacrificed on day 5 because they developed symptoms compatible with experimental cerebral malaria. Overall, the results show that the percentage of Hz-containing



leukocytes increased when parasitaemia was higher (Figure 6). However, when mice infected with the two different parasite strains were compared when they had a similar parasitaemia, i.e. day 5 for PbA ($5.7 \pm 3.1\%$) and day 12 for PbNK ($7.7 \pm 1.3\%$), PbA infected mice had higher percentages of Hz-containing monocytes than PbNK infected mice (Figure 6, top graph). Also, while the levels of parasitaemia of PbNK at day 18 of infection were significantly higher than the levels of parasitaemia of PbA at day 5 of infection ($28.5 \pm 12\%$ and $5.7 \pm 3.1\%$, respectively, $P < 0.001$) the percentages of Hz-containing monocytes were almost the same (13.3% and 13.0%, respectively). Furthermore, a comparison of the degree of Gr1 expression (low, medium, high) on the Hz-containing monocytes, appeared to

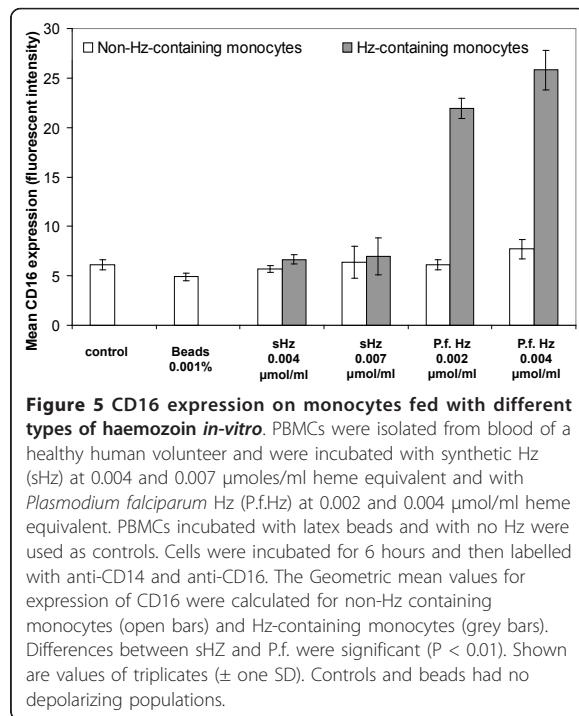
show differences in these two groups of mice at similar parasitaemia (Figure 6, bottom graph).

Interestingly, using CD11b and F4/80 showed that it appears possible to identify Hz-containing tissue macrophages as shown in additional file 2 (Additional file 2 - mouse spleen macrophages.pdf).

Altogether, using two distinct rodent models of infection, Hz-containing monocytes and granulocytes can also be detected in this flow cytometer. Most importantly, the data suggest that the percentage and type of Hz-containing monocytes may also be associated with disease severity.

Detection of Hz in murine pRBCs

Plasmodium accumulates Hz throughout its development stage inside RBCs. The detection of depolarization



was evaluated to determine whether this measurement could be used to detect pRBCs and most importantly to distinguish different pRBC stages. In whole blood from mice infected with *P. berghei* a population of depolarizing events is observed (Figure 7). More than 97% of these events were positive for the RBC marker TER119 (red population, Figure 7E). SYBR green I staining was positive in this population, indicating that the depolarizing erythrocytes contained DNA, and thus were parasitized RBC (pRBC) (Figure 8). Further analysis revealed that events with a higher degree of depolarization also showed a higher degree of SYBR green fluorescence (Figure 8), with several distinct peaks, likely representing different maturation stages of the parasite (ring-forms, early and late trophozoites and schizonts).

Detection of Hz in parasitized murine RBC to assess drug effects

Based on the above findings (Figure 8, gate A), which contained the pRBC with the highest degree of depolarization (hdRBC) and as such contains the most mature parasites, the flow cytometric method was investigated to see if it could be used to rapidly assess drug effects. Thus, the percentage of this hdRBC population was determined over a 12-hour period in an *in-vitro* culture of *P. berghei* pRBC. The results clearly show that the inhibitory effect of chloroquine and quinine is detected in a dose dependent manner throughout time (Figure 9).

Importantly, inhibitory effects were discernable after only two hours for chloroquine and four hours for quinine.

Discussion

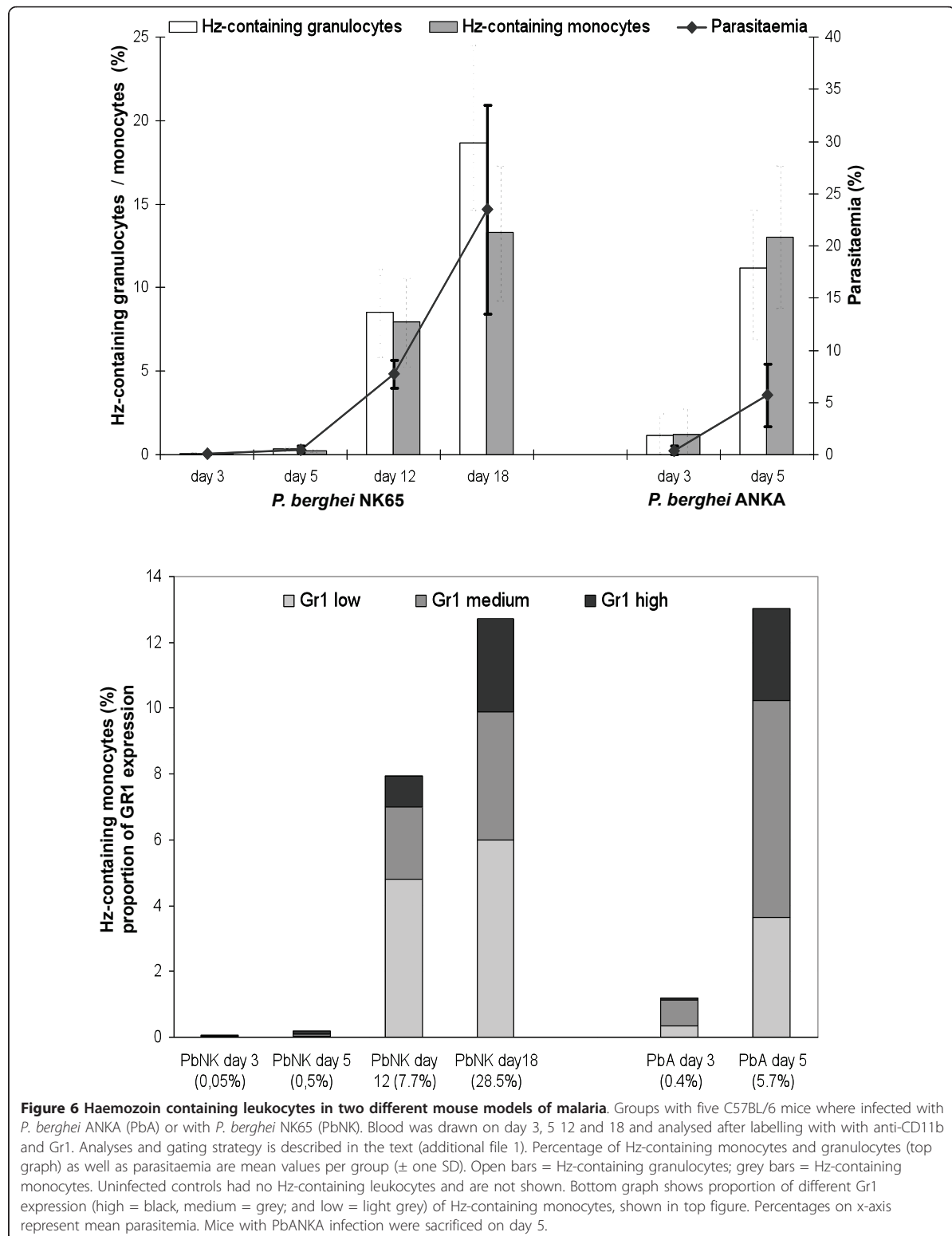
Modification of flow cytometers

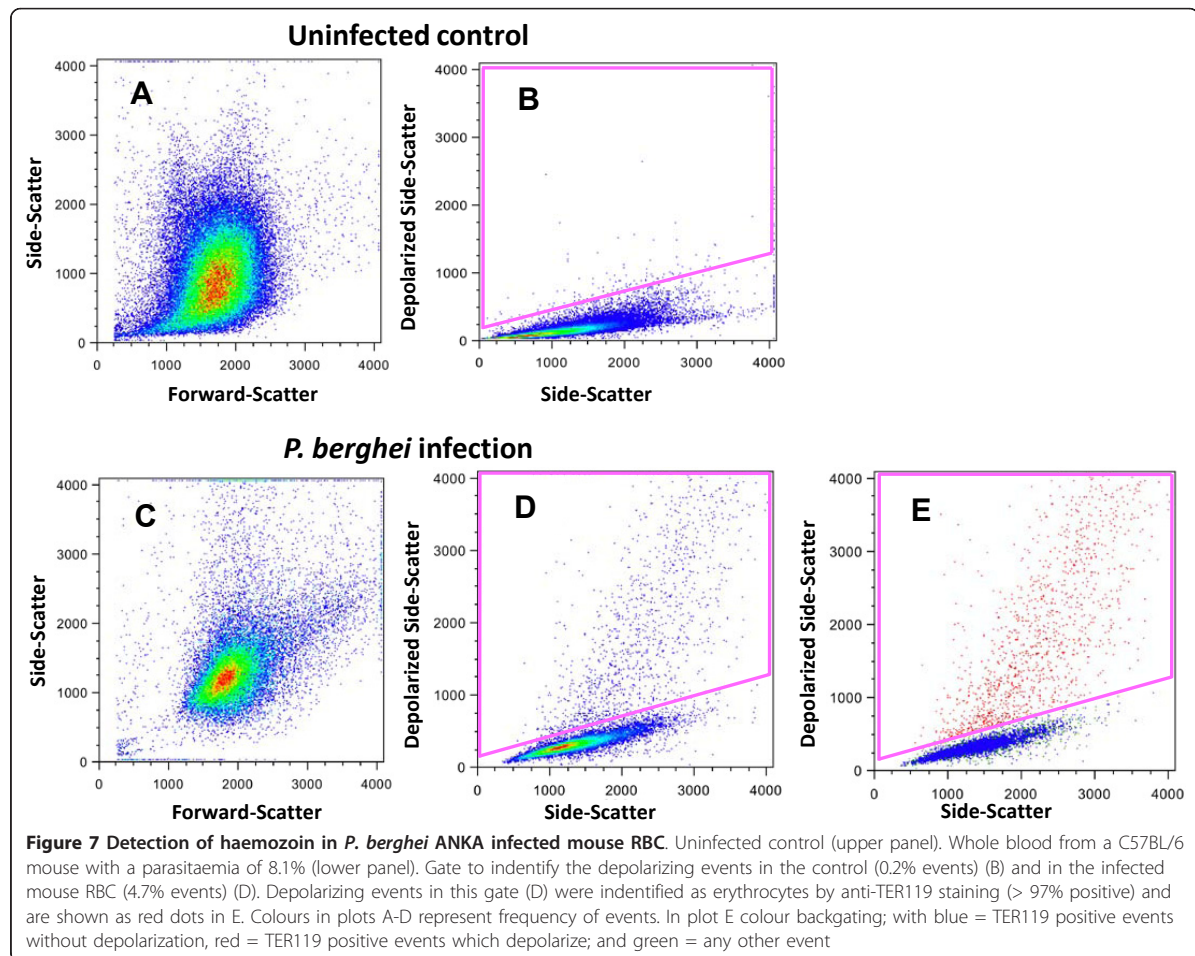
This study shows that a simple modification of a common flow cytometer for the detection of depolarized Side-Scatter, allows the detection of Hz-containing leukocytes and erythrocytes. In fact, a study using a MoFlo[®] high speed cell sorter (Beckman Coulter, Inc, Fullerton, CA), showed that depolarizing leukocytes did contain Hz [20]. However, MoFlo[®] sorters are expensive and sophisticated instruments, and by far not as commonly available as flow cytometers, which are even standard equipment in most research centres in malaria endemic regions nowadays. Nonetheless, the widespread incorporation of this method in common flow cytometers of major manufacturers has somehow been hampered by the fact that the company of the Cell-Dyn[®] instruments held the patent of this method (US patent 5017497) [21]. However, this patent was filed in 1989 and published in 1991, and as such, according to US legislation [22], it expired in March 2009. The necessary filters and dichroic mirrors (Figure 1c) used to change the CyFlow[®] cytometer were obtained for less than €2.000. No special software is necessary and the settings resemble those of the conventional SSC detection, albeit with an increased gain (voltage) of the detector. For the set-up in this study a 50%/50% beam splitter used to divert the respective light to the depolarized SSC and SSC detector (Figure 1, red error). Using a 90%/10% or even 95%/5% beam splitter may increase the signal of the depolarized SCC, without decreasing the quality of the SSC signal.

Any flow cytometer can be modified as described here. However, it should be noted that to modify some flow cytometers, which use fibre optic cables for light collection, for example, the newer Becton Dickinson instruments (Franklin Lakes, NJ, USA), it is necessary to confirm that these cables maintain polarization of the light.

Detection and counting of Hz-containing leukocytes

Hz-containing monocytes and granulocytes could be rapidly determined in fresh human or mouse blood as well as in *in-vitro* phagocytosis experiments involving whole blood or PBMCs. As has been pointed out before, previous studies on the immunological effects of Hz *in-vitro* used diverse quantities of Hz, different incubation times, as well as different types of phagocytic cells [1,2]. Few studies quantified the uptake of Hz by monocytes, although some used a luminescence assay after lysing the monocytes and reported Hz uptake as Hz-





equivalents found in around 8-10 trophozoites per monocyte [23]. However, even less studies mention the percentage of Hz-containing monocytes. In one of these studies confocal microscopy was used and showed that 75% (\pm 31%) of human PBMCs contained Hz after only 180 min, albeit only based on counting a total of \geq 400 cells [11]. Contrary to this, the presented method allows the analysis of ten-thousands of cells to determine rapidly adequate doses of Hz and required incubation times to get the desired percentage of Hz containing leukocytes (Figure 3).

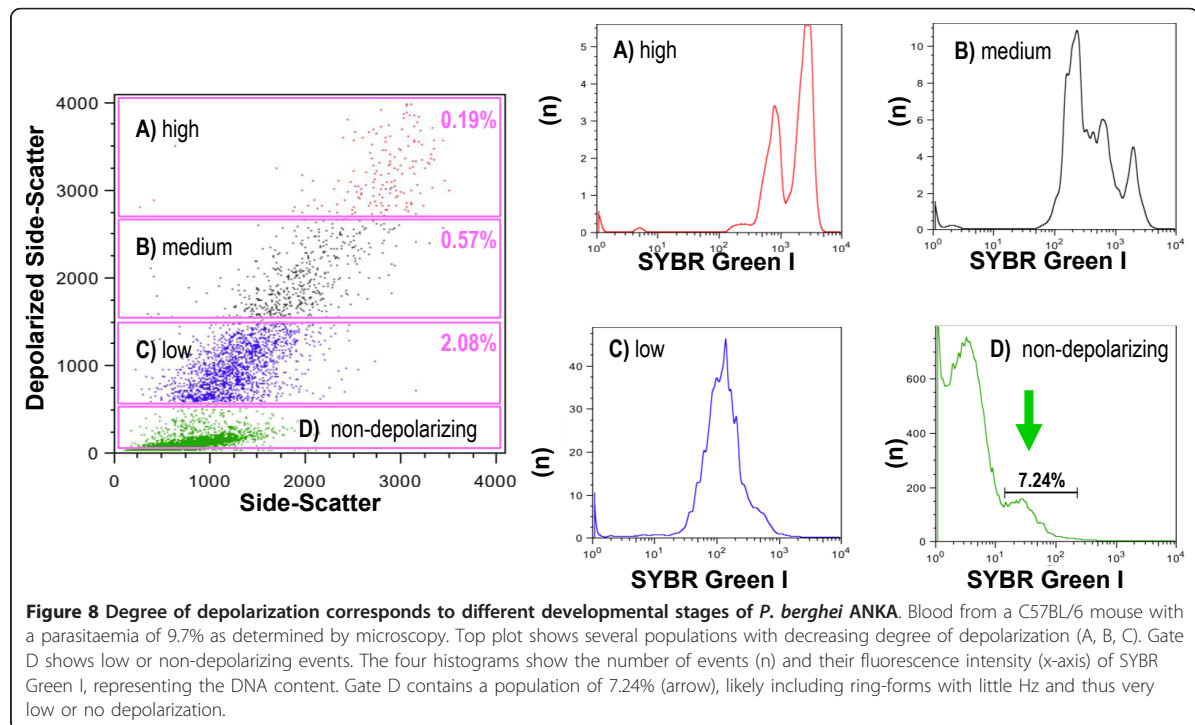
Furthermore, it allows to investigate Hz-containing monocytes from malarious patients who usually have only a few percent of these cells in circulation [3]. For example, considering that in common protocols for the analysis of whole blood, 100 μ l are labelled, and further assuming 1,000 monocytes/ μ l with only 5% of these containing Hz, a total of 5000 Hz-containing cells could be easily analysed using the flow cytometric method proposed here. As previously reported [5,10], this

method also allows to re-address the question if the number of Hz-containing leukocytes is associated with disease severity or certain types of malaria.

In some studies, however, the identification of monocytes was based on the typical monocyte gate in the Forward Scatter (FSC)/SideScatter (SSC) plot [16,20]. One problem with this is that monocytes containing several or larger Hz crystals might thus be excluded from analysis as they have higher SSC and appear superimposed on the granulocyte population (Figure 2), with a possible impact on final results.

Single cell analysis for studies of Hz-containing leukocytes

This may open the possibility to investigate functional differences of Hz-containing and non-containing leukocytes, especially in monocyte subsets found in fresh human blood from malarious patients or in mouse models of malaria. For example, recent papers reported differences in surface markers on CD14/CD16 monocyte



subsets in malarious patients [15,16], or in peripheral blood dendritic cells in children [24]. Measurement of depolarized Side-Scatter and, thus, identification of Hz-containing cells might allow to establish if these cells may have an imported role in the reported results. It would also allow the possibility to study functionally leukocytes on single cell level *in-vitro*, including surface expression or intracellular cytokines, comparing Hz with non-Hz containing leukocytes in the same cell population. In fact, differences in CD16 expression in a mixed population of Hz-containing and non-containing cells were observed (Figures 4 and 5), a finding that differs from a previous report that found no difference in CD16 expression in an *in-vitro* model [25]. Despite recent reports of differences between human and mouse monocytes [26], the current method may also allow to investigate the effects of Hz on phagocytic cells in fresh blood using different mouse models (Figure 6).

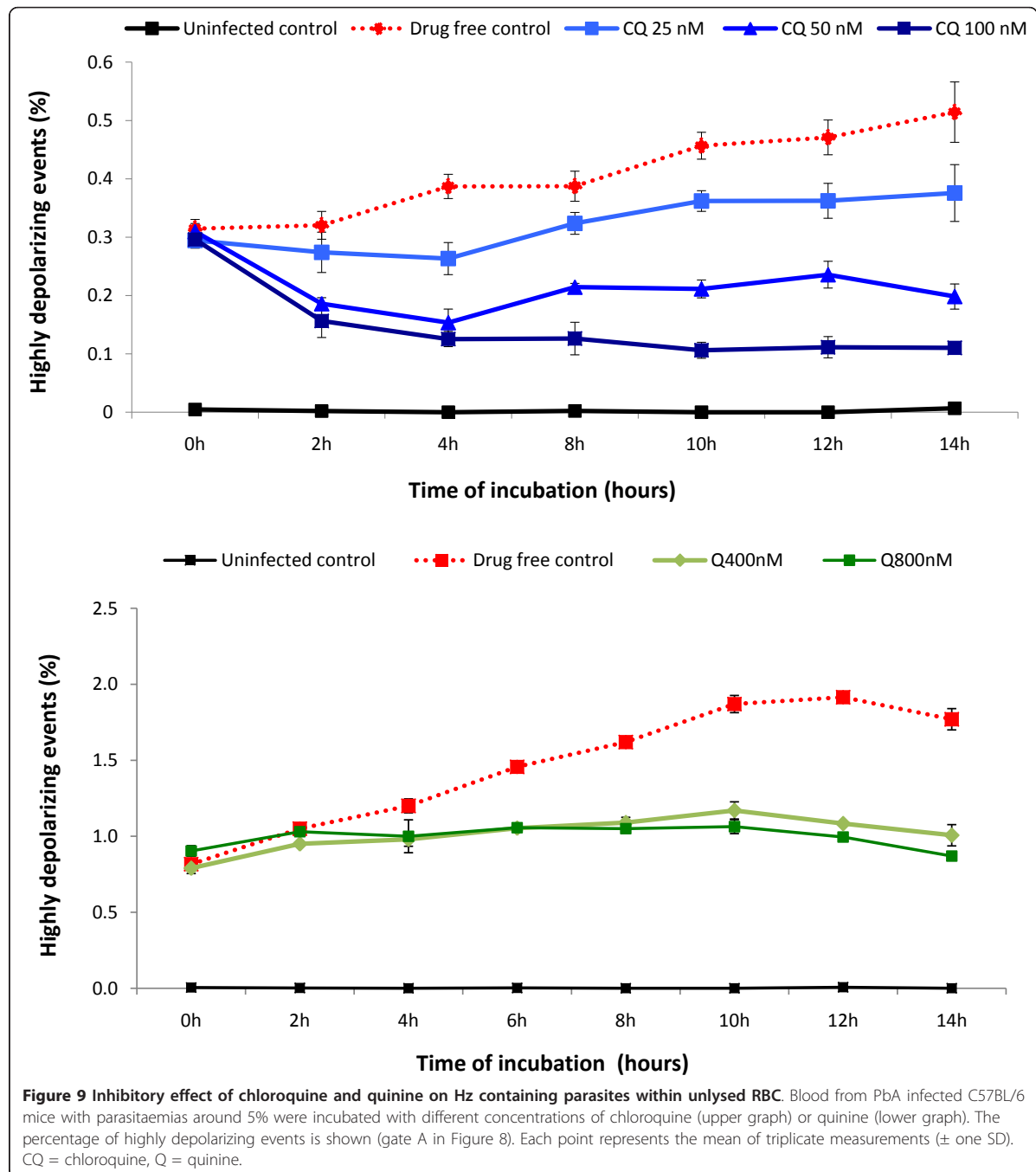
First results (additional file 2) indicate that it appears possible to detect tissue macrophages. This may allow to compare Hz-containing and non-Hz-containing cells from tissues such as spleen, liver or bone marrow which may help to elucidate recent findings, for example, the association of Hz with severe anaemia [27,28]. However, the reliable identification of tissue macrophages may require more than the two antibodies used in this study. In this case, instruments that have several light sources are necessary.

Detection of pRBC and sensitivity testing of antimalarial drugs

Flow cytometric analysis of depolarized Side-Scatter allows to easily detect pRBCs (Figure 7) and distinguish different maturation stages of the parasite (Figure 8). Both findings might serve as the basis for a novel drug sensitivity assay. In fact, the idea to use Hz as a maturation indicator is not new and was tried in a simple visual agglutination test in the 1980s [17]. Apparently, this method did not produce very reliable results, mainly due to leukocyte interference [29]. However, these limitations could be overcome by single-cell flow cytometric analysis.

Currently several drug sensitivity assays for *P. falciparum* exist and have been reviewed elsewhere [29,30]. Nonetheless, all of these assays have some disadvantages, including long turn-around times or the need for additional and often expensive reagents. Interestingly, a recent report concluded that the reliability of some of these assays may depend on the mode of action of the tested drugs [31]. Flow cytometry appears to be a reliable technique to assess parasite maturation and sensitivity to antimalarial drugs. However, protocols reported so far require additional reagents, usually to stain DNA and/or RNA and may even require flow cytometers with more than one light source [32,33].

The presented method is based on the detection of Hz, without the need of any further reagents. Determining the percentage of highly depolarizing RBC (hdRBC)



present in blood samples from infected mice, it was possible to detect the inhibitory effect of chloroquine (CQ) and quinine (Q) after only a few hours of *in-vitro* culture (Figure 9). In this study an experimental model using C57BL/6 mice infected with *P. berghei* was chosen to assure that only maturation of parasites was

measured, because *P. berghei* does not replicate in *in-vitro* cultures [34]. However, although the preliminary results seem promising, further work with different drugs and, most importantly, *P. falciparum* cultures are necessary to evaluate the usefulness of this method as a novel sensitivity assay.

Conclusions

A simple modification of a flow cytometer allows the reliable detection of Hz containing leukocytes and pRBCs. This method facilitates the rapid and reliable detection and counting of Hz-containing leukocytes in human or animal blood. It also allows single cell analysis of Hz-containing *versus* non-Hz-containing leukocytes in the same sample, including functional analysis, both *in-vitro* experiments or using fresh blood. Finally, it detects different maturation stages of parasitized RBC and may be the basis of a rapid no-added-reagent drug sensitivity assay.

Additional material

Additional file 1: Description of flow cytometric gating strategy to identify Hz-containing mouse granulocytes and monocytes.

Additional file 2: Detection of Hz-containing mouse spleen macrophages.

Acknowledgements and Funding

This work was funded by the Fundação para a Ciência e Tecnologia (PIC/IC/83214/2007) and the Fundação Luso Americana (FLAD-LACR grant: B-A-V-109-09/07). Rosângela Frita was supported by the Fundação Glaxo Smith Kline Research with a grant for a doctorate in Infectious Pathology.

Author details

¹Instituto de Medicina Molecular, Faculdade de Medicina de Lisboa, Lisbon, Hospital Universitário de Santa Maria, Av. Prof. Egas Moniz, P-1649-028 Lisboa, Portugal. ²University of Madeira, Funchal, Portugal. ³Infectious Diseases, Tropical Medicine and AIDS, Division of Internal Medicine, Academic Medical Centre, University of Amsterdam, The Netherlands. ⁴Institute of Tropical Medicine, University of Tübingen, Germany. ⁵Medical Research Unit, Hôpital Albert Schweitzer, Lambaréné, Gabon.

Authors' contributions

RF and MR contributed equally to this paper. RF carried out the human and mouse leukocyte studies. MR realized the studies on parasitized RBC and anti-malarious drug effects. AP, AMV and MMM participated in setting up the mouse models and analysing the results. MMM and TH conceived the study, participated in its design and coordination. MPG contributed to the design of the study and the draft of the manuscript. All authors have read the manuscript and approved it.

Competing interests

The authors declare that they have no competing interests.

Received: 1 February 2011 Accepted: 31 March 2011

Published: 31 March 2011

References

- Hänscheid T, Egan TJ, Grobusch MP: Hemozoin: from melatonin pigment to drug target, diagnostic tool, and immune modulator. *Lancet Infect Dis* 2007, **7**:675-685.
- Shio MT, Kassa FA, Bellemare MJ, Olivier M: Innate inflammatory response to the malarial pigment hemozoin. *Microbes Infect* 2010, **12**:889-899.
- Kremsner PG, Valim C, Missinou MA, Olola C, Krishna S, Issifou S, Kombila M, Bwanaisa L, Mithwani S, Newton CR, Agbenyega T, Pinder M, Bojang K, Wypij D, Taylor T: Prognostic value of circulating pigmented cells in african children with malaria. *J Infect Dis* 2009, **199**:142-150.
- Lawrence C, Olson JA: Birefringent hemozoin identifies malaria. *Am J Clin Pathol* 1986, **86**:360-363.
- Hänscheid T, Frita R, Langin M, Kremsner P, Grobusch M: Is flow cytometry better in counting malaria pigment-containing leukocytes compared to microscopy? *Malar J* 2009, **8**:255.
- de Grooth BG, Terstappen LW, Puppels GJ, Greve J: Light-scattering polarization measurements as a new parameter in flow cytometry. *Cytometry* 1987, **8**:539-544.
- Mendelow BV, Lyons C, Nhlangothi P, Tana M, Munster M, Wypkema E, Liebowitz L, Marshall L, Scott S, Coetzer TL: Automated malaria detection by depolarization of laser light. *Br J Haematol* 1999, **104**:499-503.
- Suh I, Kim H, Kim J, Lee S, An S, Kim W, Lim C: Evaluation of the Abbott Cell-Dyn 4000 hematology analyzer for detection and therapeutic monitoring of *Plasmodium vivax* in the Republic of Korea. *Trop Med Int Health* 2003, **8**:1074-1081.
- Hänscheid T, Langin M, Lell B, Potschke M, Oyakhrome S, Kremsner P, Grobusch M: Full blood count and haemozoin-containing leukocytes in children with malaria: diagnostic value and association with disease severity. *Malar J* 2008, **7**:109.
- Shankar AH, Fawzi WW: Moving toward hematological predictors of disease severity in malaria: going with the flow. *Am J Hematol* 2010, **85**:225-226.
- Schwarzer E, Bellomo G, Giribaldi G, Ulliers D, Arese P: Phagocytosis of malarial pigment hemozoin by human monocytes: a confocal microscopy study. *Parasitology* 2001, **123**:125-131.
- Strauss-Ayali D, Conrad SM, Mosser DM: Monocyte subpopulations and their differentiation patterns during infection. *J Leukoc Biol* 2007, **82**:244-252.
- Tacke F, Randolph GJ: Migratory fate and differentiation of blood monocyte subsets. *Immunobiology* 2006, **211**:609-618.
- Skrzeczyńska-Moncznik J, Bzowska M, Loseke S, Grage-Griebenow E, Zembala M, Pryjma J: Peripheral blood CD14high CD16+ monocytes are main producers of IL-10. *Scand J Immunol* 2008, **67**:152-159.
- Ogonda LA, Orago ASS, Otieno MF, Adhiambo C, Otieno W, Stoute JA: The levels of CD16/Fc[gamma] receptor IIIa on CD14+ CD16+ monocytes are higher in children with severe *Plasmodium falciparum* anemia than in children with cerebral or uncomplicated Malaria. *Infect Immun* 2010, **78**:2173-2181.
- Chimma P, Roussillon C, Sratongno P, Ruangveerayuth R, Pattanapanyasat K, Pérignon JL, Roberts DJ, Druihe P: A distinct peripheral blood monocyte phenotype is associated with parasite inhibitory activity in acute uncomplicated *Plasmodium falciparum* malaria. *PLoS Pathog* 2009, **5**:e1000631.
- Rieckmann KH: Visual in-vitro test for determining the drug sensitivity of *Plasmodium falciparum*. *Lancet* 1982, **1**:1333-1335.
- Sunderkötter C, Nikolic T, Dillon MJ, van Rooijen N, Stehling M, Drevets DA, Leenen PJM: Subpopulations of mouse blood monocytes differ in maturation stage and inflammatory response. *J Immunol* 2004, **172**:4410-4417.
- Aging study: Peripheral blood leukocytes (PBL profiles) in 32 inbred strains of mice. [http://phenome.jax.org/db/q?rt=projects/docstatic&doc=Petkova1/Petkova1_Protocol].
- Kramer B, Grobusch M, Suttorp N, Neukammer J, Rinneberg H: Relative frequency of malaria pigment-carrying monocytes of nonimmune and semi-immune patients from flow cytometric depolarized side scatter. *Cytometry* 2001, **45**:133-140.
- Particle discriminator and method, United States Patent 5017497. [<http://www.freepatentsonline.com/5017497.html>].
- How to Calculate Standard Patent Expiry Dates and Data Exclusivity in Key Territories. [http://www.genericsweb.com/How_to_Calculate_Standard_Patent_Expiry_Dates_and_Data_Exclusivity.pdf].
- Giribaldi G, Prato M, Ulliers D, Gallo V, Schwarzer E, Akide-Ndungu OB, Valente E, Saviozzi S, Calogero RA, Arese P: Involvement of inflammatory chemokines in survival of human monocytes fed with malarial pigment. *Infect Immun* 2010, **78**:4912-4921.
- Urban BC, Mwangi T, Ross A, Kinyanjui S, Mosobo M, Kai O, Lowe B, Marsh K, Roberts DJ: Peripheral blood dendritic cells in children with acute *Plasmodium falciparum* malaria. *Blood* 2001, **98**:2859-2861.

25. Schwarzer E, Alessio M, Ulliers D, Arese P: **Phagocytosis of the malarial pigment, hemozoin, impairs expression of major histocompatibility complex class II antigen, CD54, and CD11c in human monocytes.** *Infect Immun* 1998, **66**:1601-1606.
26. Ingersoll MA, Spanbroek R, Lottaz C, Gautier EL, Frankenberger M, Hoffmann R, Lang R, Haniffa M, Collin M, Tacke F, Habenicht AJ, Ziegler-Heitbrock L, Randolph GJ: **Comparison of gene expression profiles between human and mouse monocyte subsets.** *Blood* 2010, **115**:e10-19.
27. Davenport GC, Ouma C, Hittner JB, Were T, Ouma Y, Ong'echa JM, Perkins DJ: **Hematological predictors of increased severe anemia in Kenyan children coinfectd with *Plasmodium falciparum* and HIV-1.** *Am J Hematol* 2010, **85**:227-233.
28. Lamikanra AA, Theron M, Kooij TWA, Roberts DJ: **Hemozoin (malarial pigment) directly promotes apoptosis of erythroid precursors.** *PLoS ONE* 2009, **4**:e8446.
29. Basco L: *Field application of in vitro assays for the sensitivity of human malaria parasites to antimalarial drugs* Geneva: World Health Organization; 2007.
30. Noedl H, Wongsrichanalai C, Wernsdorfer WH: **Malaria drug-sensitivity testing: new assays, new perspectives.** *Trends Parasitol* 2003, **19**:175-181.
31. Wein S, Maynadier M, Tran Van Ba C, Cerdan R, Peyrottes S, Fraisse L, Vial H: **Reliability of antimalarial sensitivity tests depends on drug mechanisms of action.** *J Clin Microbiol* 2010, **48**:1651-1660.
32. Grimberg BT, Jaworska MM, Hough LB, Zimmerman PA, Phillips JG: **Addressing the malaria drug resistance challenge using flow cytometry to discover new antimalarials.** *Bioorg Med Chem Lett* 2009, **19**:5452-5457.
33. Izumiyama S, Omura M, Takasaki T, Ohmae H, Asahi H: ***Plasmodium falciparum*: Development and validation of a measure of intraerythrocytic growth using SYBR Green I in a flow cytometer.** *Exp Parasitol* 2009, **121**:144-150.
34. Janse CJ, Waters AP: ***Plasmodium berghei*: The application of cultivation and purification techniques to molecular studies of malaria parasites.** *Parasitol Today* 1995, **11**:138-143.

doi:10.1186/1475-2875-10-74

Cite this article as: Frita et al.: Simple flow cytometric detection of haemozoin containing leukocytes and erythrocytes for research on diagnosis, immunology and drug sensitivity testing. *Malaria Journal* 2011 10:74.

Submit your next manuscript to BioMed Central and take full advantage of:

- Convenient online submission
- Thorough peer review
- No space constraints or color figure charges
- Immediate publication on acceptance
- Inclusion in PubMed, CAS, Scopus and Google Scholar
- Research which is freely available for redistribution

Submit your manuscript at
www.biomedcentral.com/submit





Haemozoin detection in infected erythrocytes for *Plasmodium falciparum* malaria diagnosis—Prospects and limitations

Maria Rebelo^a, Howard M. Shapiro^b, Teresa Amaral^c, José Melo-Cristino^{a,c}, Thomas Hänscheid^{a,*}

^a Instituto de Medicina Molecular, Faculdade de Medicina, Lisbon, Portugal

^b The Center for Microbial Cytometry, 283 Highland Avenue, West Newton, MA, USA

^c Serviço de Patologia Clínica, Centro Hospitalar Lisboa Norte, Lisbon, Portugal

ARTICLE INFO

Article history:

Received 21 December 2011

Received in revised form 24 February 2012

Accepted 7 March 2012

Available online 22 March 2012

Keywords:

Haemozoin

Erythrocyte

Malaria

Diagnosis

ABSTRACT

Several methods based on the detection of the parasite-specific pigment haemozoin (Hz) in blood are currently being investigated as alternative diagnostic methods for malaria. Although this approach may appear attractive, the fact that in *Plasmodium falciparum* (*P. f.*) malaria, the severity of which should give it the highest diagnostic priority, the fact that most circulating intra-erythrocytic *P. f.* parasites contain little or no Hz raises some concern. We used flow cytometry to investigate the possibilities and limitations of the detection of intra-erythrocytic Hz in malaria infected patient blood samples and in vitro cultures. However, reliable detection of ring-forms or young trophozoites of *P. f.* parasites could not be achieved, although one-quarter of mature parasites could be detected after 24–48 h in culture. Our results strongly suggest that, although it may be useful for monitoring maturation, detection of intra-erythrocytic Hz by flow cytometry will not provide an optimal method for diagnosis of *P. falciparum* malaria.

© 2012 Elsevier B.V. All rights reserved.

1. Introduction

Haemozoin (Hz), an optically birefringent, paramagnetic pigment (Hänscheid et al., 2007), is produced from haem by intra-erythrocytic malaria parasites and is detectable at developmental stages beyond the ring form. It can be visualized more easily using polarization and/or darkfield microscopy, in some instances using either minimally and inexpensively modified standard microscopes or other inexpensive optics (Jamjoom, 1983, 1988; Maude et al., 2009; Wilson et al., 2011). In recent years, automation of this technology, sometimes combined with exploitation of the magnetic properties of Hz (Mens et al., 2010), has been advocated and supported as an approach to rapid and affordable malaria diagnosis, with the potential advantage of providing reagent-free detection of a parasite-specific material.

Flow-cytometry of depolarized side scatter, employed in some automated full-blood-count analysers (Cell-Dyn series; Abbott Diagnostics, Santa Clara, CA) to count eosinophils, which have birefringent granules, also detects Hz in monocytes and neutrophils that have phagocytosed parasitized erythrocytes or Hz. Although the presence of such cells could diagnose malaria with reported sensitivities from 49% to 100% in 13 reviewed studies

(Campuzano-Zuluaga et al., 2010), it is known that Hz-containing phagocytes may be found in blood for days after an acute infection is cured.

The sensitivity of Hz detection for malaria diagnosis, especially in infected erythrocytes, depends on two main factors: (i) the total parasitemia and (ii) the amount of Hz present inside the individual parasites. The latter is strongly dependent on the distribution of developmental stages; immature forms, i.e., rings and young trophozoites, contain little if any detectable Hz. That this could be a limitation for Hz microscopy was noted by Jamjoom (1988); it is of particular concern with respect to *Plasmodium falciparum* (*P. f.*) malaria, in which trophozoites and schizonts are removed from blood by binding to endothelial cells.

Since *P. f.* causes the vast majority of malaria deaths, its rapid diagnosis is critical, and it would be desirable to establish how well a method based on Hz-detection might work in typical clinical samples, which contain few if any mature parasites. For this, a flow cytometry Hz detection method was used (Frita et al., 2011).

2. Material and methods

Reagents were obtained from Sigma–Aldrich (St. Louis, MO, USA), unless stated otherwise.

The *P. falciparum* 3D7 strain was used. Although, this strain has a slow growing nature no difference in haemozoin morphology is observed between different *P. falciparum* clones (Noland et al., 2003). Briefly, the *P. f.* 3D7 strain was grown in recently collected

* Corresponding author at: Instituto de Medicina Molecular, Faculdade de Medicina de Lisboa, Av. Prof. Egas Moniz, P-1649-028 Lisboa, Portugal. Tel.: +351 217999458; fax: +351 217999459.

E-mail address: t.hanscheid@fm.ul.pt (T. Hänscheid).

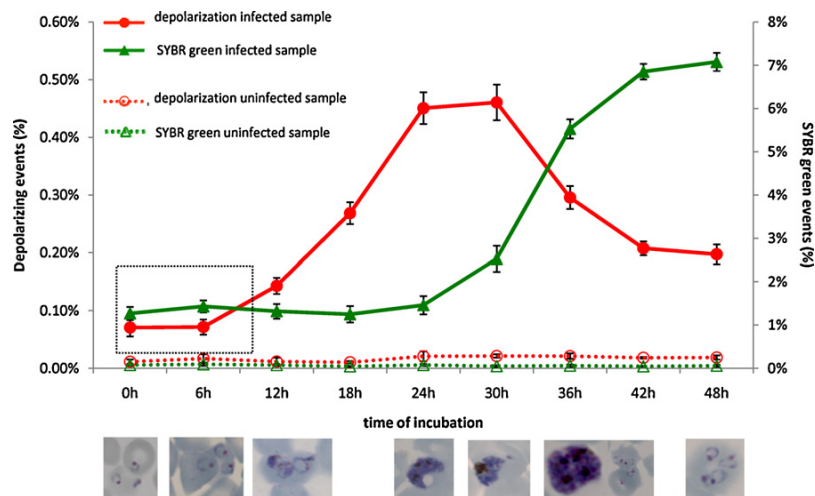


Fig. 1. Growth curve of *P. falciparum* (3D7) in culture. The primary Y-axis (left-hand) corresponds to the percentage of depolarizing events and the secondary Y-axis (right-hand) corresponds to the percentage of SYBR green positive cells. The percentage of depolarizing (red lines) and SYBR green positive events (green lines) were followed for 48 h in non-infected (dotted lines) and *Plasmodium falciparum* infected RBC cultures (solid lines). The initial parasitemia was 1.3% (secondary Y-axis), while the corresponding depolarizing events were only 0.07% (primary Y-axis), at 0 h of incubation. Each time point represents the mean value of triplicate samples \pm one SD. Red blood cell lysis was excluded by total cell counts. The pictures are representative of the parasite stages found at each time point. Within the first 6 h the amount of haemozoin inside intra-erythrocytic parasites, which are the ring forms predominant in the peripheral circulation of patients, is very low (dotted rectangle). (For interpretation of the references to color in this figure legend, the reader is referred to the web version of the article.)

donor erythrocytes in RPMI based complete malaria culture medium (CMCM) according to the recommendations of Malaria Research and Reference Reagent Resource Center (MR4) (Mphande et al., 2008).

As uninfected controls, erythrocytes from healthy donors were cultured as described above. Cultures were maintained at 5% hematocrit at 37°C in an atmosphere of 5% CO₂. The culture was synchronized to ring stages by incubating the red blood cell culture with 5% sorbitol for 10 min, at room temperature (Lambros and Vanderberg, 1979).

After one further life cycle (48 h) parasitemia and hematocrit were adjusted to approximately 1% and 2.5%, respectively and the culture incubated as described above. Measurements were done at 6-h intervals during 48 h. For each measurement 5 μ l of the culture was stained with the highly DNA-specific dye SYBR green I (Invitrogen, Carlsbad, USA) at 1 \times . After 20 min of incubation, the stained sample was immediately analysed using a CyFlow flow cytometer with 488 nm excitation and detectors for Forward Scatter, Side-Scatter (SSC), depolarized SSC and green fluorescence (FL1), as described elsewhere (Frita et al., 2011). Parasitemia was also assessed by microscopic observation of Giemsa-stained thin blood smears.

EDTA anticoagulated blood was obtained from patients with microscopy confirmed *P. f.* malaria from the adjacent hospital, stained with SYBR green I at 1 \times and analysed. The study was approved by the local Ethics Committee.

3. Results

Growth curves for SYBR green I and Hz detection are shown in Fig. 1, representative of six separate experiments performed in triplicate. The percentage of parasites, as determined with SYBR green, remained stable during the first 30 h and increased only after RBC invasion by the second generation of parasites. Contrary to this, the percentage of parasites as determined by Hz-detection remained very low, at around 0.07% during the first 6 h of incubation. The maxima of Hz-containing parasites were detected at 24 h and 30 h, although they only represented 20% and 9% of all parasites, respectively, as determined by SYBR-green.

Fig. 2 shows samples from a healthy donor, a *P. f.* malaria-infected patient, and a ring form-synchronized *P. f.* culture. It is noteworthy that only 2.2% of SYBR green positive events in the culture showed depolarization indicating the presence of Hz. In ten blood samples from patients with *P. f.* malaria only immature forms were found as confirmed by microscopic observation of Giemsa-stained blood smears. In all the cases with young trophozoites being the most mature forms seen. Parasitemias in these samples ranged from 0.5% to 7.0% and no depolarizing events which were also SYBR green positive could be detected above the background (Fig. 2). However, incubating three patient samples for 48 h allowed the detection of a maximum of 2.72% depolarizing events, representing 38% of the SYBR green positive population.

4. Discussion

Although depolarized SSC may be able to detect around one-quarter of mature *P. f.* parasites in culture after 24–48 h of incubation, using the 3D7 laboratory strain or patient blood, it appears difficult if not impossible to reliably detect young immature *P. f.* either in culture or in patient blood using flow cytometric detection of Hz alone on a single cell level (Fig. 2). Thus, optical methods such as the investigated flow cytometric one or those based on Hz microscopy will almost certainly suffer from low sensitivity in the detection of *P. falciparum* malaria, unless additional characteristics of parasites (e.g., DNA content, as in our study) as well as Hz are examined.

The relatively complex magneto-optical (MOT) method (Mens et al., 2010) is said to be capable of detecting haemozoin levels corresponding to 50–100 parasites/ μ L. When applied to 86 known *P. f.* - positive patient samples with parasitemias ranging from 600 to 85,000/ μ L, found 65 (77.4%) as positive, but failed to detect Hz in the remaining 19, with parasitemias between 5680 and 78,000/ μ L. These levels are at least ten times higher than the lowest parasitemias (200–500/ μ L) reported detectable by thin film Giemsa (Ohrt et al., 2008) and fluorescence microscopy (Lenz et al., 2011).

It is not clear that more complex and expensive Hz detection methodology (Scholl et al., 2004; Nyunt et al., 2005; Bélisle

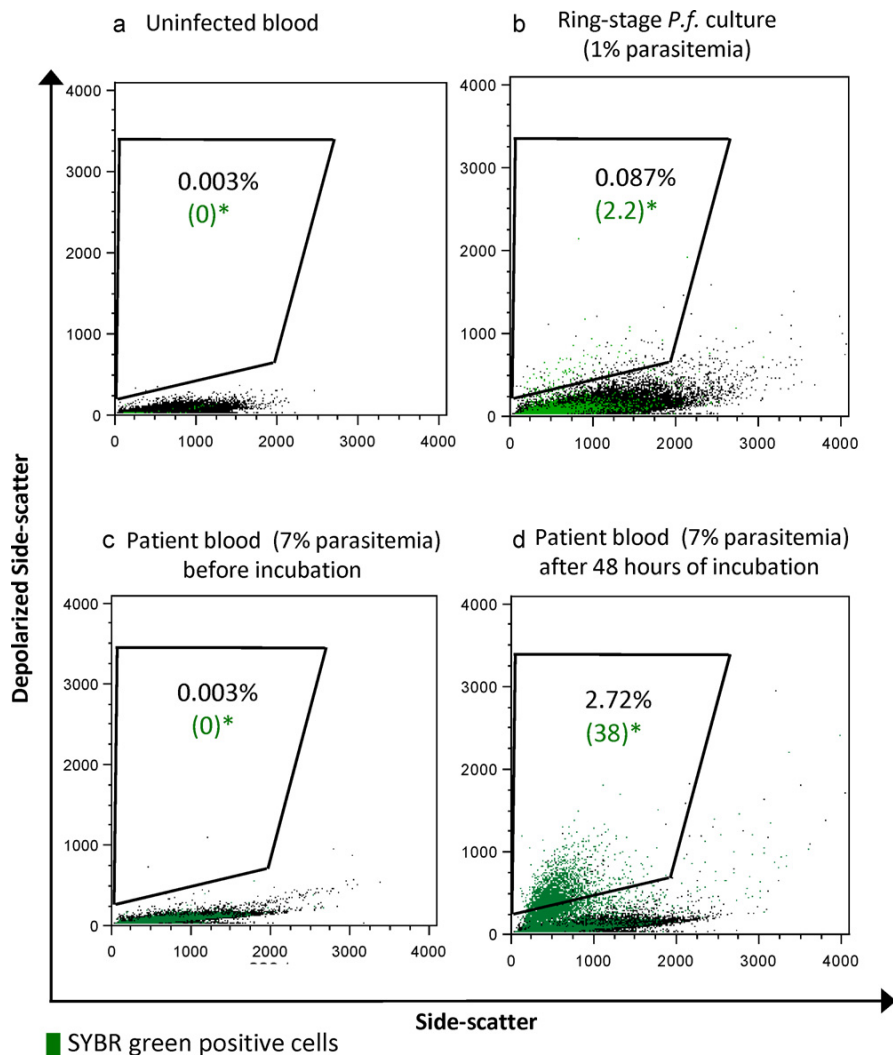


Fig. 2. Detection of immature *P. falciparum* forms. Flow cytometric analysis of uninfected RBC from healthy donor (a), ring-stage synchronized *Plasmodium falciparum* (*P. f.*) culture (b), and a patient blood sample with 7% *P. f.* parasitemia before (c) and after 48 h of incubation (d). The parasite developmental stages present in the patient blood sample were confirmed by microscopy as being ring-form parasites (c). The gate was optimized to select for depolarizing cells above background. SYBR green was used to stain parasites (green dots), which are absent in the uninfected sample and could only be found below the gate in the patient blood sample. In the ring-stage synchronized *P. f.* culture only a small percentage (2.2%) of SYBR green positive cells showed depolarized SSC. In the patient blood sample this percentage was the same as the uninfected control. Only after 48 h of incubation this percentage increased to 38%. *Percentage in brackets represents SYBR green positive events (parasites) which depolarize. (For interpretation of the references to color in this figure legend, the reader is referred to the web version of the article.)

et al., 2008; Karl et al., 2011), more difficult to adapt to field conditions, could improve sensitivity. Of course, all the Hz-based methods may work for the detection of non-*falciparum* strains, where mature forms with abundant Hz are present in circulation, as do flow cytometry based haematology analysers (Campuzano-Zuluaga et al., 2010).

An ideal novel method ought to detect all clinically relevant malaria cases and thus, likely detect parasitemias below the thick blood film. Furthermore it should be rapid, robust and easy, allow parasite quantification and, ideally, speciation. The cost ought to be in the range or below low-cost Rapid-Diagnostic-Tests.

With respect to *P. falciparum* malaria, Hz-detection methods, used alone or combined with other cytometric parameters, may provide a sensitive means of monitoring the maturation of these parasites (and those) of other species, which may be useful in non-diagnostic applications such as monitoring of antimalarial drug effects, as we recently reported (Frita et al., 2011).

In conclusion, Hz detection methods may not be the ideal approach for a novel test to diagnose *P. falciparum* malaria due to the low content of Hz in circulating immature forms. Nevertheless, the multiparameter cytometric methodology used to date with flow cytometers is also now readily transferable to simpler, less expensive widefield imaging cytometers (Shapiro and Perlmutter, 2006; Shapiro and Ulrich, 2010). Thus, we suggest that further investigation along these lines is at least as likely to yield useful and affordable diagnostics, especially for *P. f.*, as is continued work focused solely on Hz detection, particularly in parasitized erythrocytes.

Acknowledgement

This work was supported by the Fundação Luso Americana (FLAD-LACR grant: B-A.V-109-09/07).

References

- Bélisle, J.M., Costantino, S., Leimanis, M.L., Bellemare, M.J., Bohle, D.S., Georges, E., Wiseman, P.W., 2008. Sensitive detection of malaria infection by third harmonic generation imaging. *Biophys. J.* 94, L26–L28.
- Campuzano-Zuluaga, G., Hänscheid, T., Grobusch, M.P., 2010. Automated haematology analysis to diagnose malaria. *Malar. J.* 9, 346.
- Frita, R., Rebelo, M., Pamplona, A., Vigario, A.M., Mota, M.M., Grobusch, M.P., Hänscheid, T., 2011. Simple flow cytometric detection of haemozoin containing leukocytes and erythrocytes for research on diagnosis, immunology and drug sensitivity testing. *Malar. J.* 10, 74.
- Hänscheid, T., Egan, T.J., Grobusch, M.P., 2007. Haemozoin: from melatonin pigment to drug target, diagnostic tool, and immune modulator. *Lancet Infect. Dis.* 7, 675–685.
- Jamjoom, G.A., 1983. Dark-field microscopy for detection of malaria in unstained blood films. *J. Clin. Microbiol.* 17, 717–721.
- Jamjoom, G.A., 1988. Patterns of pigment accumulation in *Plasmodium falciparum* trophozoites in peripheral blood samples. *Am. J. Trop. Med. Hyg.* 39, 21–25.
- Karl, S., Gutiérrez, L., House, M.J., Davis, T.M., St Pierre, T.G., 2011. Nuclear magnetic resonance: a tool for malaria diagnosis? *Am. J. Trop. Med. Hyg.* 85, 815–817.
- Lambros, C., Vanderberg, J.P., 1979. Synchronization of *Plasmodium falciparum* erythrocytic stages in culture. *J. Parasitol.* 65, 418–420.
- Lenz, D., Kremsner, P.G., Lell, B., Biallas, B., Boettcher, M., Mordmüller, B., Adegnika, A.A., 2011. Assessment of LED fluorescence microscopy for the diagnosis of *Plasmodium falciparum* infections in Gabon. *Malar. J.* 10, 194.
- Maude, R.J., Buapetch, W., Silamut, K., 2009. A simplified, low-cost method for polarized light microscopy. *Am. J. Trop. Med. Hyg.* 8, 782–783.
- Mens, P.F., Matelon, R.J., Nour, B.Y., Newman, D.M., Schallig, H.D., 2010. Laboratory evaluation on the sensitivity and specificity of a novel and rapid detection method for malaria diagnosis based on magneto-optical technology (MOT). *Malar. J.* 9, 207.
- Mphande, F., Nilsson, S., Bolad, A., 2008. Culturing of erythrocytic asexual stages of *Plasmodium falciparum* and *P. vivax*. In: Moll, K., Ljungström, I., Perlmann, H., Scherf, A., Wahlgren, M. (Eds.), *Methods in Malaria Research*, fifth ed, pp. 1–3 (Manassas).
- Noland, G.S., Briones, N., Sullivan Jr., D.J., 2003. The shape and size of hemozoin crystals distinguishes diverse *Plasmodium* species. *Mol. Biochem. Parasitol.* 130, 91–99.
- Nyunt, M., Pisciotto, J., Feldman, A.B., Thuma, P., Scholl, P.F., Demirev, P.A., Lin, S.L., Shi, L., Kumar, N., Sullivan Jr., D.J., 2005. Detection of *Plasmodium falciparum* in pregnancy by laser desorption mass spectrometry. *Am. J. Trop. Med. Hyg.* 73, 485–490.
- Ohr, C., O'Meara, W.P., Remich, S., McEvoy, P., Ogutu, B., Mtalib, R., Odera, J.S., 2008. Pilot assessment of the sensitivity of the malaria thin film. *Malar. J.* 7, 22.
- Scholl, P.F., Kongkasuriyachai, D., Demirev, P.A., Feldman, A.B., Lis, S.L., Sullivan Jr., D.J., Kumar, N., 2004. Rapid detection of malaria infection in vivo by laser desorption mass spectrometry. *Am. J. Trop. Med. Hyg.* 71, 546–551.
- Shapiro, H.M., Perlmutter, N.G., 2006. Personal cytometers: slow flow or no flow? *Cytometry A* 69, 620–630.
- Shapiro, H.M., Ulrich, H., 2010. Cytometry in malaria: from research tool to practical diagnostic approach? *Cytometry A* 77, 500–501.
- Wilson, B.K., Behrend, M.R., Horning, M.P., Hegg, M.C., 2011. Detection of malarial byproduct hemozoin utilizing its unique scattering properties. *Opt. Express* 19, 12190–12196.

A Novel Flow Cytometric Hemozoin Detection Assay for Real-Time Sensitivity Testing of *Plasmodium falciparum*

Maria Rebelo^{1,2}, Claudia Sousa¹, Howard M. Shapiro³, Maria M. Mota¹, Martin P. Grobusch^{2,4,5}, Thomas Hänscheid^{1,2*}

1 Instituto de Medicina Molecular, Faculdade de Medicina de Lisboa, Lisbon, Portugal, **2** Centre de Recherches Médicales de Lambaréné - CERMEL, Albert Schweitzer Hospital, Lambaréné, Gabon, **3** The Center for Microbial Cytometry, West Newton, Massachusetts, United States of America, **4** Department of Infectious Diseases, Centre for Tropical and Travel Medicine, Amsterdam Medical Centre, Amsterdam, The Netherlands, **5** Institute of Tropical Medicine, University of Tübingen, Tübingen, Germany

Abstract

Resistance of *Plasmodium falciparum* to almost all antimalarial drugs, including the first-line treatment with artemisinins, has been described, representing an obvious threat to malaria control. *In vitro* antimalarial sensitivity testing is crucial to detect and monitor drug resistance. Current assays have been successfully used to detect drug effects on parasites. However, they have some limitations, such as the use of radioactive or expensive reagents or long incubation times. Here we describe a novel assay to detect antimalarial drug effects, based on flow cytometric detection of hemozoin (Hz), which is rapid and does not require any additional reagents. Hz is an optimal parasite maturation indicator since its amount increases as the parasite matures. Due to its physical property of birefringence, Hz depolarizes light, hence it can be detected using optical methods such as flow cytometry. A common flow cytometer was adapted to detect light depolarization caused by Hz. Synchronized *in vitro* cultures of *P. falciparum* were incubated for 48 hours with several antimalarial drugs. Analysis of depolarizing events, corresponding to parasitized red blood cells containing Hz, allowed the detection of parasite maturation. Moreover, chloroquine resistance and the inhibitory effect of all antimalarial drugs tested, except for pyrimethamine, could be determined as early as 18 to 24 hours of incubation. At 24 hours incubation, 50% inhibitory concentrations (IC50) were comparable to previously reported values. These results indicate that the reagent-free, real-time Hz detection assay could become a novel assay for the detection of drug effects on *Plasmodium falciparum*.

Citation: Rebelo M, Sousa C, Shapiro HM, Mota MM, Grobusch MP, et al. (2013) A Novel Flow Cytometric Hemozoin Detection Assay for Real-Time Sensitivity Testing of *Plasmodium falciparum*. PLOS ONE 8(4): e61606. doi:10.1371/journal.pone.0061606

Editor: Steffen Borrmann, Kenya Medical Research Institute - Wellcome Trust Research Programme, Kenya

Received: October 8, 2012; **Accepted:** March 11, 2013; **Published:** April 24, 2013

Copyright: © 2013 Rebelo et al. This is an open-access article distributed under the terms of the Creative Commons Attribution License, which permits unrestricted use, distribution, and reproduction in any medium, provided the original author and source are credited.

Funding: This work was supported by the Luso-American Foundation (FLAD-LACR grant: B-A.V-109-09/07). The funders had no role in study design, data collection and analysis, decision to publish, or preparation of the manuscript.

Competing Interests: The authors would like to declare that the author HMS is an employee of The Center for Microbial Cytometry. There are no patents, products in development or marketed products to declare. This does not alter the authors' adherence to all the PLOS ONE policies on sharing data and materials.

* E-mail: t.hanscheid@fm.ul.pt

Introduction

Resistance of *Plasmodium falciparum* to almost all antimalarial drugs has been observed [1]. In fact, resistance to commonly effective and useful drugs such as chloroquine or sulfadoxine/pyrimethamine has severely compromised their use for malaria control [2]. Alarmingly, resistance to the currently used first-line treatment compounds, the artemisinins, characterized by a prolonged parasite clearance time [3], has already been reported from South-East-Asia. Consequently, detection and monitoring of drug resistance is of paramount importance.

Traditionally, therapeutic efficacy trials are the gold standard for assessing parasite response to antimalarial drugs. The obvious complexity of these trials led to the development of *in vitro* assays [4]. The major *in vitro* phenotypic assays include the WHO schizont maturation microtest [5], the isotope (³H]-hypoxanthine) incorporation assay [6], the detection of the parasite antigens pLDH [7] or HRP2 [8] by ELISA, and assays using fluorescent DNA dyes, such as SYBR green I [9], YOYO [10], PicoGreen [11] and DAPI [12] with either spectrophotometric or cytometric readout (Table S1).

The development of novel antimalarial compounds hinges on assays to determine the inhibitory effects of drugs on the parasite

[13]. Although all these assays have been successfully applied to detect drug effects on the parasite, they all have relevant limitations. For example, the WHO microtest is based on the tedious and subjective microscopic observation of parasite maturation [14]. The [³H]-hypoxanthine assay requires expensive equipment as well as complex isotope handling precautions and radioactive waste management [6]. All these assays require reagents for parasite detection that are often rather expensive and frequently require a cold chain. Importantly, they also need incubation times of 48 up to 96 hours to reliably detect drug effects [15].

Molecular methods are highly desirable, because they do not depend on viable parasites and have the capacity to provide rapid results. Their major drawback is the limited number of known and validated resistance markers [4]. It is important to note that there is currently no specific *in vitro* test to identify artemisinin resistance, as stated by an expert panel in the WHO Global Plan for Artemisinin Resistance Containment (GPARC) [16].

In this scenario, alternative assays that may overcome the limitations previously mentioned are highly desirable. An assay that would not only allow real-time determination of drug effects during a single parasite cycle but could also detect drug effects in a

second or even third cycle would certainly be a useful tool, permitting the assessment of inhibitory effects of drugs with different times of action.

Malaria pigment, i.e., hemozoin (Hz), is produced in increasing amounts by the parasite during the erythrocytic cycle and, therefore, constitutes an ideal maturation indicator. Hz, the end product of plasmodial hemoglobin metabolism, has been identified as an important modulator of the host's immune response to *Plasmodium* spp., as a marker for disease severity and prognostic factor for disease outcome, and also as an adjuvant diagnostic tool, of particular use regarding the non-immune traveler [17–19]. Hz depolarizes light and can be easily detected thereby without reagents by optical methods including dark-field microscopy [20], polarization microscopy [21] and flow cytometry [22].

In 1999, a study reported that the flow cytometry based full-blood-count analyser, Cell-Dyn[®] (Abbott, Santa Clara, CA), could detect Hz within leucocytes [23]. More importantly, studies reported that the Cell-Dyn[®] seemed to detect Hz inside parasitized red blood cells (RBC) [24], [25]. Based on the flow cytometric detection of depolarized side scatter [26], as used in the Cell-Dyn[®], we showed that Hz could be detected inside parasitized RBC in *P. berghei* infected rodents [27]. Moreover, *in vitro* parasite maturation, as well as the inhibitory effect of chloroquine and quinine, could be detected after only 6 hours of incubation [27]. Later, we showed that maturation of *P. falciparum* in culture could also be determined [28].

Our present data show how flow cytometric detection of Hz can be used as a novel, reagent-free, real time assay to assess antimalarial drug effects on *P. falciparum*.

Methods

All reagents were obtained from Sigma Aldrich (St Louis, Mo, USA), unless stated otherwise.

Flow cytometer modification (depolarized side scatter detection)

The Cyflow[®] Blue (Partec, Münster, Germany) is a portable (Figure S1), five parameter flow cytometer with blue laser (488 nm) excitation, and detectors for forward scatter (FSC), side scatter (SSC), green fluorescence (FL1), orange fluorescence (FL2) and red fluorescence (FL3). For this study the set-up was modified as described elsewhere [27]. Briefly, two SSC detectors were created, with a 50%/50% beam splitter between them. Then a polarization filter was placed orthogonally (horizontal) to the polarization plane of the laser light (vertical), in front of one of the SSC detectors, allowing the detection of depolarized side scatter (Figure S1). The Cyflow[®] is equipped with an absolute cell count method (<http://www.partec.com/instrumentation/flow-cytometry.html>, accessed 3/8/2012), which allows determination of the number of particles in 200 μ l of sample. Absolute counts were performed for all experiments to control for possible red blood cell lysis.

Microscopy

Parasitemia, parasite maturation and the synchronicity of parasites in culture were assessed by light microscopic examination of Giemsa-stained blood smears. Air-dried blood smears were fixed in absolute methanol and stained with Giemsa (Merck, Darmstadt, Germany) in a 1:10 dilution in PBS 1 \times , for 20 minutes.

Plasmodium falciparum continuous cultures

The *Plasmodium falciparum* resistant (Dd2) and susceptible (3D7) strains were grown in recently collected donor erythrocytes in

RPMI based complete malaria culture medium (CMCM) according to the recommendations of the Malaria Research and Reference Reagent Resource Center (MR4) [29]. Cultures were maintained at 5% hematocrit, at 37°C in an atmosphere of 5% CO₂. As uninfected controls, erythrocytes from healthy donors were cultured as described above.

Synchronizing *Plasmodium falciparum* continuous cultures

Continuous cultures of *P. falciparum* were cultivated until they reached a parasitemia of >2% with a minimum of 50% rings. They were synchronized by adding 5% sorbitol for 10 minutes at room temperature as described elsewhere [30]. Briefly, the culture medium was washed away by centrifuging the culture at 1800 rpm, for 5 minutes. Next, 10 mL of 5% sorbitol was added to the pelleted red blood cells and incubated for 10 minutes, at room temperature. Cultures were washed twice in PBS 1 \times by centrifugation at 1800 rpm, for 5 minutes. Finally, CMCM was added to the pelleted cells, and the synchronized culture was incubated for another 48 hours, at 37°C in a 5% CO₂ atmosphere.

Hemozoin detection sensitivity assay

Ring-stage synchronized cultures (at least 90% of ring forms) at 2.5% hematocrit and at approximately 1% parasitemia were incubated with antimalarial drugs or with CMCM (used for the drug free and uninfected controls) in 24 or 96 well-plates, for 48 hours, at 37°C in a 5% CO₂ atmosphere.

Quinine, chloroquine, mefloquine, artemisinin, artesunate, and pyrimethamine were purchased from Sigma Aldrich (St Louis, Mo, USA). NITD246 was kindly provided by Dr. Bryan Yeung from the Novartis Institute for Tropical Diseases, Singapore. Stock solutions of chloroquine and quinine were prepared in distilled water, artemisinin and mefloquine in pure methanol (Merck, Darmstadt, Germany), pyrimethamine in absolute ethanol (Merck, Darmstadt, Germany), artesunate in 70% ethanol and NITD246 in pure DMSO.

Doubling concentrations ranging from 6 to 200 nM for chloroquine, 10 to 160 nM for mefloquine, 12 to 200 nM for pyrimethamine and 4 to 64 nM for artesunate and artemisinin were tested. For NITD246 concentrations of 0.1, 0.2, 1 and 2 nM were used, while for quinine concentrations of 3, 12, 50, 200 and 800 nM were tested.

For each flow cytometric measurement approximately 100,000 events were analyzed. A volume of 5 μ L of the blood suspension present in the wells was stained with SYBR green 1 \times , as described below. To determine the best time point for IC₅₀ calculation, measurements were done at 6 hour intervals over 48 hours for the majority of the drugs tested, except for pyrimethamine which was measured again at 72 hours. All samples were analyzed in triplicate and, for each drug, at least three different experiments were performed. In order to investigate possible inoculation effects, artesunate and artemisinin were also investigated at a lower parasitemia of 0.4 and 0.7%, respectively.

To assess if renewing artesunate would influence its effect on parasite growth, cultures were washed and fresh artesunate, at a concentration of 8 nM, was added every 12 hours, during 48 hours of incubation.

To investigate the detection limit of the novel Hz assay, ring-stage synchronized cultures with parasitemias of 0.05%, 0.1%, 0.3%, 0.5%, 0.6% and 1% were incubated for 48 hours.

Finally, to assess the performance of the Hz assay with low parasitemias, ring-stage synchronized cultures at 0.3% parasitemia were incubated for 72 hours with increasing concentrations of

chloroquine, artesunate and pyrimethamine (as mentioned above). Flow cytometric analysis was performed in 24 hours intervals.

SYBR green I staining

For each measurement 5 μ L of the culture (approximately 800 000 cells) was stained with the DNA-specific dye SYBR green I (Invitrogen, Carlsbad, USA) at 1 \times . After 20 minutes of incubation, in the dark, the stained sample was immediately analyzed by flow cytometry using a 535/45 nm bandpass filter in front of the detector.

CD235 (glycophorin A) staining

A volume of 10 μ L of a continuous *P. falciparum* culture, at 5% hematocrit, was transferred into a well of a 96 well plate, washed in cold FACS buffer (PBS 1 \times and 2% bovine albumin serum) and then centrifuged at 1400 rpm, for 3 minutes at 4°C. A volume of 50 μ L of a 1:500 dilution of CD235-Phycoerythrin antibody (eBioscience, San Diego, US) was added to the cells and incubated for 20 minutes on ice in the dark. After a final wash, the cells were re-suspended in PBS 1 \times and analyzed by flow cytometry using a 610 nm long-pass filter.

Flow cytometric analysis

Flow cytometry results were analyzed using FlowJo software (version 9.0.2, Tree Star Inc., Oregon, USA). The gating scheme used is shown in Figure 1. The red blood cells in uninfected and infected samples were detected by their characteristic forward (FSC) and side scatter (SSC) properties (Figure 1A and 1B).

Staining with the anti-glycophorin A CD235 antibody was used to establish that all events detected represented red blood cells. The antibody was not used for routine analyses.

Depolarizing events were defined in plots of SSC versus depolarized-SSC as those with a signal above the background observed in the uninfected control (Figure 1C and 1D).

To determine SYBR green I positive cells, green fluorescence (FL1) versus red fluorescence (FL3) plots were used; these provide better separation between weakly stained and autofluorescent cells than can be obtained from one-dimensional histograms. SYBR green I positive events (Figure 1F) were established based on a stained uninfected control (Figure 1E) and had to be adjusted at each time point, always using the uninfected SYBR green stained sample from the corresponding time point.

Histidine-rich protein-2 (HRP2) sensitivity assay

A histidine-rich protein-2 (HRP2) enzyme-linked immunosorbent assay (ELISA) was established and performed according to standard procedures [8], also available on the internet website: malaria.farch.net. (<http://www.meduniwien.ac.at/user/harald.noedl/malaria/> assessed 3/8/2012)

Ring-stage synchronized *P. falciparum* cultures, at an initial parasitemia of 0.05% and at 1.5% hematocrit, were incubated with the antimalarial drugs for 72 hours, at 37°C in a 5% CO₂ atmosphere. At the end, samples were frozen at -20°C until the HRP2 ELISA assay was performed.

Briefly, after two freezing and thawing cycles, 100 μ L of the lysed sample was transferred to a 96 well-plate pre-coated with MPFM-55A antibody (Immunology Consultants Laboratories, Portland, USA) and incubated for one hour. The cells were washed three times and then incubated for another hour with the secondary antibody, MPFG-55P (Immunology Consultants Laboratories, Portland, USA). Cells were washed again and incubated for 5–10 minutes with the chromogen, TMB One (Biotrend, Köln, Germany). The reaction was stopped by adding sulphuric acid at

1 M (Merck, Darmstadt, Germany) and the absorbance was immediately determined using the Infinite M200 plate reader (Tecan, Männedorf, Switzerland), at a wavelength of 450 nm.

To assess a possible inoculum effect of artemisinin, the HRP2 assay was also performed using a parasitemia of 1%.

Data analysis

A nonlinear regression model (sigmoidal dose-response/variable slope) was used to calculate the IC₅₀s, with SigmaPlot - Systat Software (Chicago, IL, USA).

Results

Depolarized side scatter detects parasitized red blood cells

Staining with the red blood cell surface marker (CD235) antibody was used to establish that the events detected represented red blood cells. Figure 1G shows that 99.5% of events detected are red blood cells. Representative dot plots of side scatter versus depolarized side scatter are shown in Figure 1C and 1D. At 24 hours of incubation, depolarizing events were very low in the uninfected control (0.027%) (Figure 1C), but could easily be detected (0.46%) in the infected blood sample (Figure 1D). The depolarizing events present in the infected sample were also positive for SYBR green I. Analysis of SYBR green I fluorescence intensity showed that the majority of these depolarizing events (79.4%) had high fluorescence (pink line in Figure 1H) indicating high DNA content and thus, represented parasitized red blood cells with mature parasites.

All subsequent results reported in this paper are based on the depolarizing events expressed as a percentage of all events analyzed.

Depolarized side scatter detects parasite maturation

We next sought to establish whether this type of analysis would discriminate among different *Plasmodium falciparum* stages. To that end, samples of 100,000 events were analyzed. Determination of the absolute number of cells at each time point showed no evidence for red blood cell lysis. Following the percentage of depolarizing events during 48 hours of incubation, in a ring-stage synchronized culture (1.4% parasitemia), showed an increase at 18 hours, with a peak at 30 hours and a subsequent decrease (Figure 2A). The same sample stained with the DNA stain, SYBR green I, showed no change in the percentage of fluorescent events until 30 hours, followed by a steady increase until 48 hours (Figure 2B). Observation of Giemsa stained blood smears at all time points showed parasite maturation until 30 hours, which coincided with the peak of depolarizing events. Thereafter, from 36 to 48 hours, immature forms were observed, coinciding with a decrease of depolarizing events and an increase of fluorescent events (Figure 2). These changes reflect parasite growth with the 30 hour peak of depolarization corresponding with the peak of maturation, after which erythrocytes rupture and daughter-merozoites are released along with Hz, explaining the decrease in depolarizing events and the increase in SYBR green I fluorescent events, observed after 30 hours.

The increase in the percentage of depolarizing events over time and the inhibitory effect of chloroquine, artesunate and pyrimethamine could be detected at parasitemias down to 0.3%. At lower parasitemias (0.05 and 0.1%) no clear increase above the background could be detected during the first 48 hours of incubation.

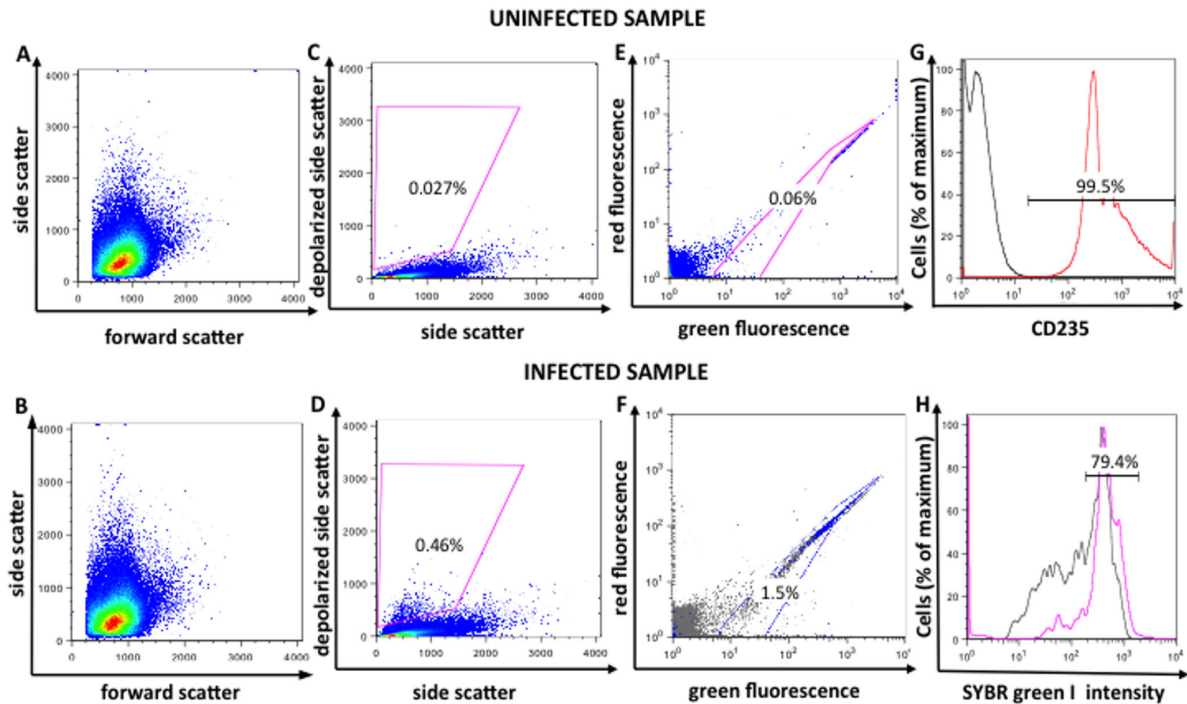


Figure 1. Gating for detection of depolarizing parasitized red blood cells in a *Plasmodium falciparum* culture. Flow cytometric analysis of an uninfected and a synchronized *P. falciparum* (3D7) infected culture (1.5% parasitemia) after 24 hours of incubation, stained with SYBR green I. Plots of forward vs. side scatter for the uninfected and infected cultures appear in Figures A and B; corresponding plots of side scatter vs. depolarized side scatter appear in Figures C and D. The gates in Figures C and D identify the depolarizing events. Figures E and F (see text) illustrate gates defining SYBR green-positive parasitized cells. The blue dots on Figure F represent the depolarizing events. Staining with the red blood cell surface marker (CD235) shows that 99.5% of events in a stained sample (red line) exhibit fluorescence above the highest level measured in an unstained control (black line), indicating that the detected events are red blood cells (G). In the SYBR green I histogram (H) of the infected culture, the overall population (black line) shows a distinct peak with a high fluorescence intensity in the third decade. This peak corresponds mainly to the gated population of depolarizing events (pink line). Because SYBR green I intensity correlates with DNA content and thus with parasite level of maturation, the depolarizing population (pink line) consists mainly (79.4%) of mature parasites. The highly red- and green-fluorescent events visible outside the SYBR green gate just to the right of its apex represent contaminating white blood cells among the donor red cells.
doi:10.1371/journal.pone.0061606.g001

Detection of inhibitory effects of chloroquine on sensitive (3D7) and resistant (Dd2) *P. falciparum* strains

Using a chloroquine sensitive strain (3D7), the difference between inhibiting and non-inhibiting concentrations was clearly visible after 18 hours, with the largest difference observed at 30 hours (Figure 3A). The first sign of drug effect could be consistently detected at 18 hours, where at concentrations of 6 and 12 nM a percentage of 0.1% depolarizing events were observed, while at 25, 50 and 100 nM only 0.004% were detected (Figure 3A).

In the resistant *P. falciparum* strain (Dd2), chloroquine resistance could clearly be detected at 18 hours after drug exposure, with growth curves of all concentrations following the drug free control (Figure 3B). At this time point (18 hours), in all drug concentrations around 0.1% depolarizing events were observed, compared to the 0.01% seen at the beginning of the incubation (Figure 3B).

Detection of inhibitory effects of other antimalarial drugs

Representative growth curves in the presence of different concentrations of quinine, mefloquine, artemisinin and the spiroindolone NITD246 are shown in Figure 4. The curves for artesunate are shown in Figure 5 and those for the slow acting drug, pyrimethamine, are shown in Figure 6. As was the case with

chloroquine, inhibitory concentrations showed a clear effect from 18 hours onwards in three different compound classes: quinolones (quinine and mefloquine), endoperoxides (artemisinin and artesunate) and a spiroindolone (NITD246).

Interestingly, artemisinin showed a delayed growth curve at the 32 nM concentration in comparison to the drug free control (Figure 4C). The same was observed for artesunate at a lower concentration of 4 nM (Figure 5A). Of note, the artesunate growth curve at an intermediate concentration of 8 nM showed an initial inhibition with a delayed rise starting after 30 hours and an absence of the typical peak at 24–30 hours (Figure 5A and B). By renewing the artesunate every 12 hours in the culture medium, this delayed rise was lost and the initial inhibition was maintained throughout the 48 hours of incubation (Figure 5B). In both cases, however, the percentage of SYBR green I positive events remained largely unchanged over the 48 hours of incubation, indicating absence of parasite replication (Figure 5C). The parasites, previously treated only once with artesunate at 8 nM, were also re-cultured and observed for growth during four days. No growth was detected during these four days, as confirmed by flow cytometry, nor was an increase in either depolarization or SYBR green percentage and intensity observed.

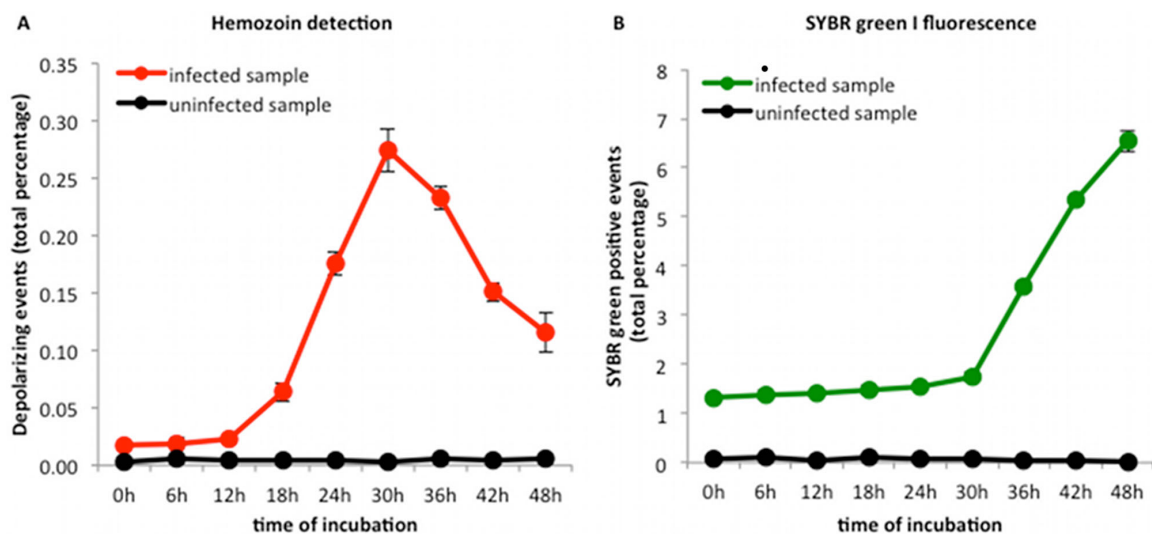


Figure 2. Growth curves of *Plasmodium falciparum* (3D7) in culture. Flow cytometric analysis of a synchronized *P. falciparum* (3D7) culture (1.4% parasitemia). The percentages of depolarizing events (A) and SYBR green I positive events (B) were followed for 48 hours in uninfected (black lines in A and B) and infected red blood cells (red line in A and green line in B). Analysis of depolarizing events (Hz-containing parasitized erythrocytes) shows an increase at 18 hours, peaking at 30 hours (A). SYBR green I positive events (parasitized RBC) remain unchanged at 1.4% until 30 hours, after which a steady increase can be noted (B). Hz detection reflects parasite maturation with increasing amounts of Hz until 30 hours, while the parasitemia remains unchanged (SYBR green I positive events). After 30 hours, increasing SYBR green I positive events indicate replication and presence of immature forms, which explains the decrease observed in the depolarizing population. Each time point represents the mean value of triplicate samples \pm one SD. Red blood cell lysis was excluded by absolute cell counts, which remained stable. doi:10.1371/journal.pone.0061606.g002

Inhibitory effect of slow-acting drugs (pyrimethamine)

Pyrimethamine (Figure 6A and B) required an incubation time of 72 hours to reliably detect drug effects (Figure 6B). Interestingly, while concentrations of 12 to 50 nM followed the drug free

control, the curve of 100 nM showed slightly higher values from 30–48 hours, while the highest concentration of 200 nM showed a marked increase of depolarizing events and a delayed peak at 36 hours, with twice as many events (Figure 6A).

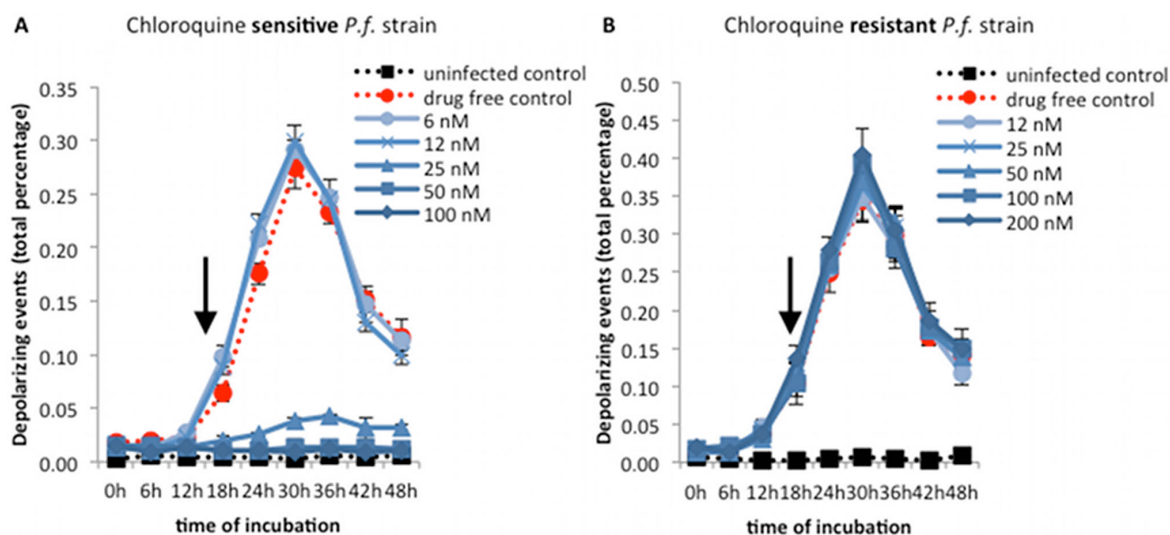


Figure 3. Effect of chloroquine on the growth curve of *P. falciparum* sensitive and resistant strains. Synchronous cultures of sensitive (3D7, parasitemia of 1.3%) and resistant (Dd2, parasitemia of 1.4%) *P. falciparum* strains were incubated for 48 hours with doubling concentrations of chloroquine and analyzed at 6 hourly intervals. The inhibitory effect of chloroquine at higher concentrations (>25 nM) is clearly visible (arrow) after 18 hours of incubation (A). The resistant strain can easily be distinguished from the sensitive strain with growth curves of all drug concentrations being identical to the drug free control (B). Each time point represents the mean value of triplicate samples \pm one SD. doi:10.1371/journal.pone.0061606.g003

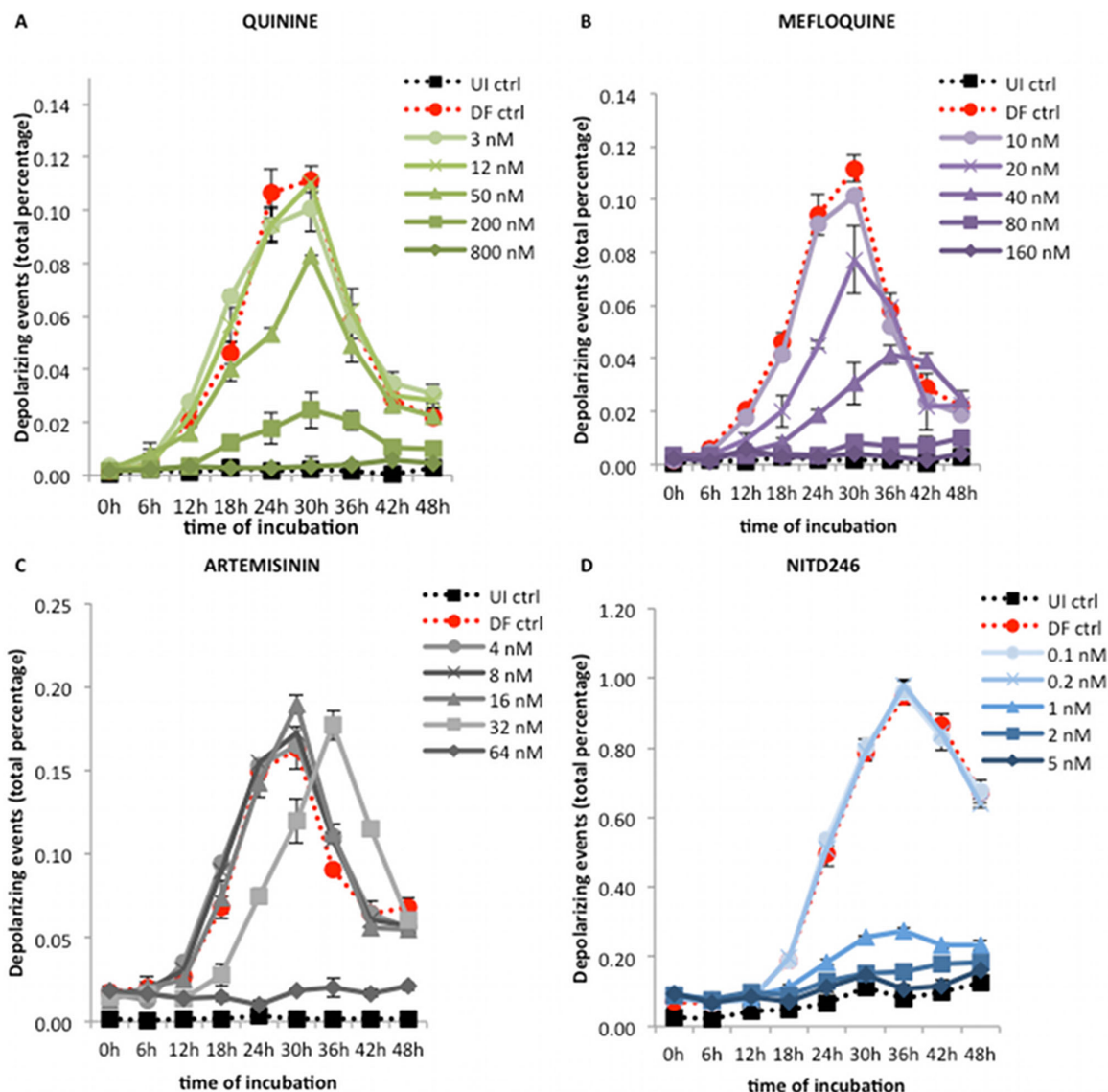


Figure 4. Effect of quinine, mefloquine, artemisinin and a spiroindolone (NITD246) on the growth curve of *P. falciparum* (3D7). Synchronous cultures of a *P. falciparum* 3D7 strain were incubated for 48 hours with increasing concentrations of quinine (A), mefloquine (B), artemisinin (C) and NITD246 (D). In all cases the dose-dependent inhibitory effect of the drugs could already be detected at 18 hours by comparing the treated samples (solid lines) with the drug free control (dotted red line). The curves allowed the determination of IC₅₀ values at 24 hours. Of note, artemisinin at 32 nM showed a 6 hour delayed growth curve, from 18 to 42 hours, with the peak of maturation occurring at 36 hours. Each time point represents the mean value of triplicate samples \pm one SD. DF ctrl – drug free control; UI ctrl – uninfected control. doi:10.1371/journal.pone.0061606.g004

IC₅₀ values obtained by the Hemozoin detection assay are comparable with other available assays

To determine the earliest time-point that would allow us to reliably calculate IC₅₀ values, results obtained from the Hz detection assay at different time-points (18, 24, 30 and 36 hours) (Table 1) were compared with those reported in the literature (Table S2), as well as with results from the already validated HRP2 ELISA assay (Table 2). This analysis led us to use the 24 hour time

point for all subsequent IC₅₀ calculations. The IC₅₀ results for our Hz assay and the HRP2 assay are shown in Table 2.

Concerning the inoculum effect, no reliable results could be obtained with the HRP2 assay at a parasitemia of 1%, because no differences were observed between the drug treated samples and the drug free control. Using a lower parasitemia in the Hz assay, discrepant results were observed for artemisinin and artesunate: while the IC₅₀ of artesunate remained the same (4 nM) at a

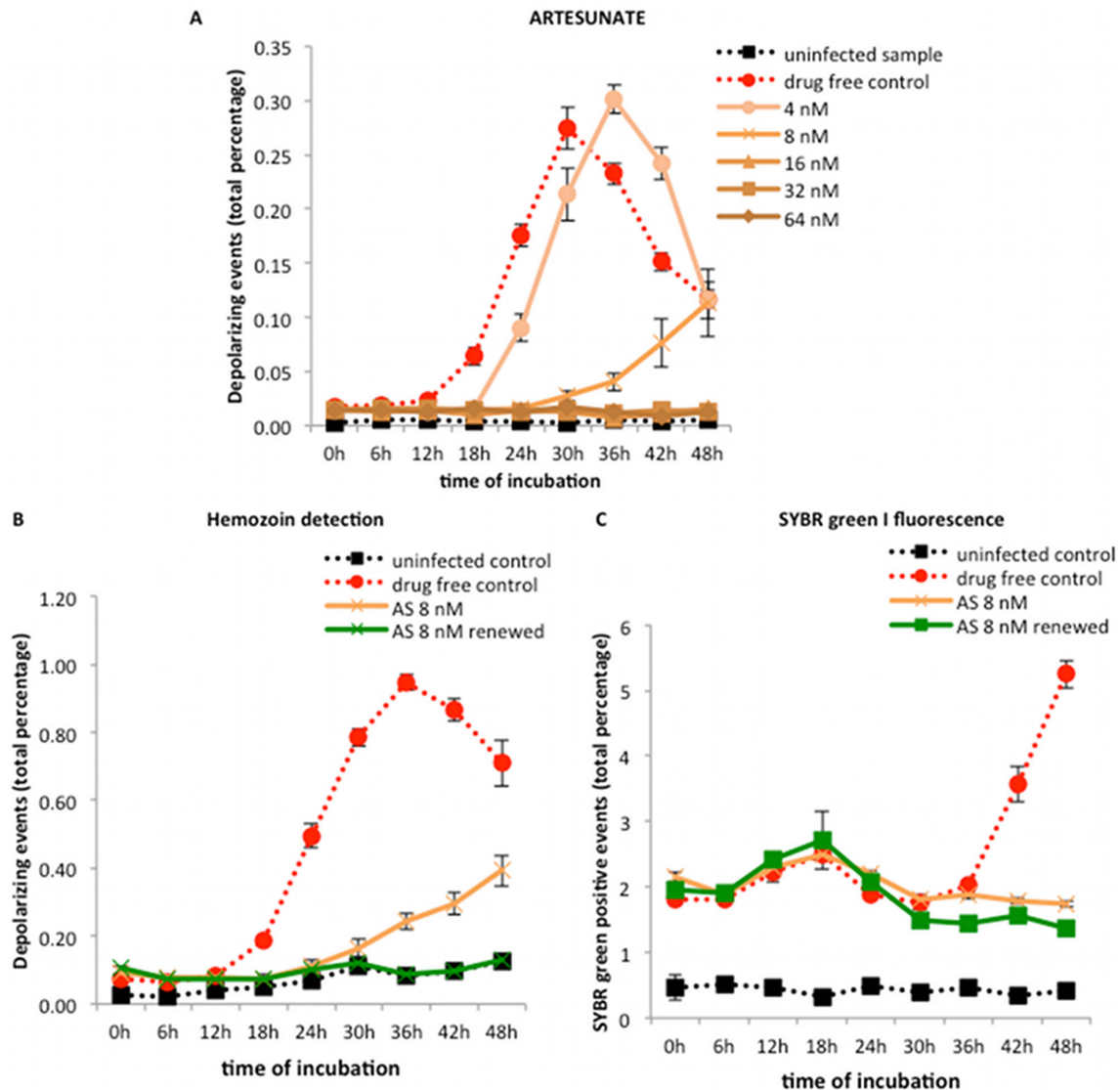


Figure 5. Effect of artesunate on the growth curve of *P. falciparum* (3D7) and the effect of 12 hourly renewing of artesunate during incubation. Synchronous cultures of a *P. falciparum* 3D7 strain were incubated for 48 hours with doubling concentrations of artesunate (A) or with a single concentration of 8 nM of artesunate for the whole time or renewed at 12 hour intervals (B and C). Figures A and B show detection of Hz (depolarizing events) while Figure C shows detection of SYBR green I fluorescence (DNA in parasites). The inhibitory effect of artesunate was already detectable after 18 hours of incubation (A). Similar to artemisinin (Figure 4C), the growth curve of artesunate at 4 nM showed a 6 hourly delayed growth curve from 18 to 42 hours, including a 6 hour delay in the peak, occurring at 36 hours. Interestingly, the growth curve at 8 nM seemed to show inhibition until 30 hours, when a slight increase was observed (A and B). However, renewing artesunate at 12 hourly intervals eliminates this effect (green line in B). The percentage of SYBR green I positive events remained approximately the same during the 48 hours of incubation (C). This indicates that parasites at the non-renewed 8 nM concentration showed some maturation as indicated by Hz detection but were unable to replicate. Each time point represents the mean value of triplicate samples \pm one SD. doi:10.1371/journal.pone.0061606.g005

parasitemia of 1.3% and 0.4%, the IC₅₀ value for artemisinin decreased from 32 nM at 1.0% parasitemia to 13.2 nM at a parasitemia of 0.7%.

Discussion

This study confirms that the optical detection of Hz can be easily achieved by a simple adaptation of a common flow

cytometer to allow detection of light depolarization (Figure S1). This study also extends observations [27] that maturation of *P. falciparum* and inhibitory antimalarial drug effects can be assessed by the detection of Hz inside intra-erythrocytic parasites. Although this novel approach is based on previous observations that Hz in parasitized RBC could be detected by flow cytometric methods [24], [27] it should be noted that the idea of using Hz for a sensitivity assay is not new and was described in the 1980s [31].

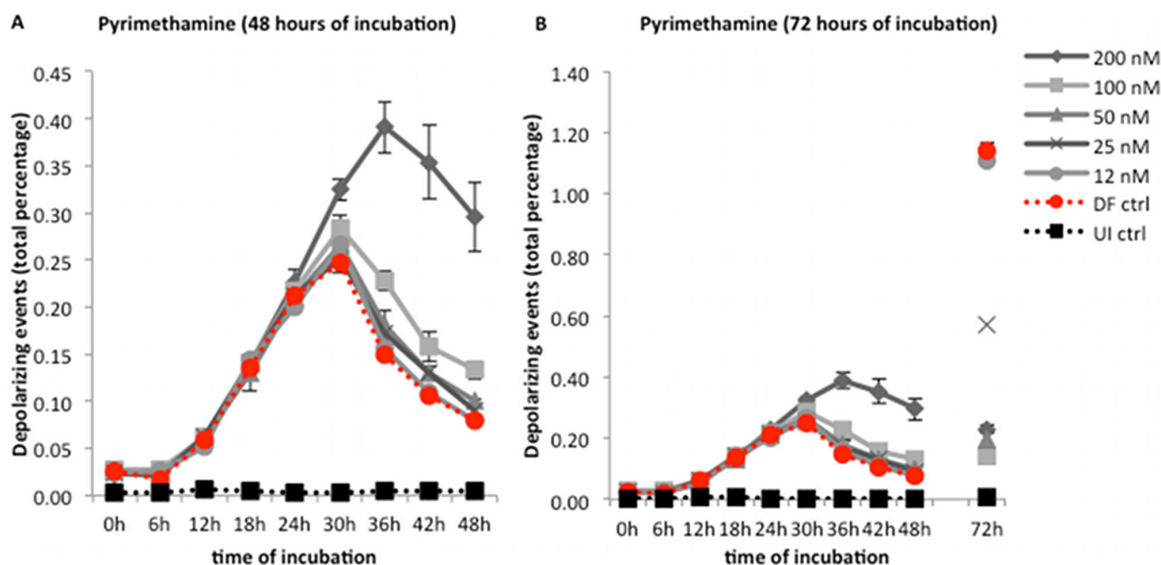


Figure 6. Growth curve of *Plasmodium falciparum* (3D7) after treatment with pyrimethamine. Synchronous cultures of a *P. falciparum* 3D7 strain were incubated for 72 hours with doubling concentrations of pyrimethamine. No inhibitory effect could be observed during the first 48 hours at any concentration (A). However, an inhibition was clearly visible at 72 hours (B). This could be explained by the fact that pyrimethamine is a slow acting drug and its effect can only be detected on the second generation, after 48 hours. Interestingly, the growth curves at all concentrations follow the drug free control after the 30 hour peak, while the curve for 200 nM shows a later peak at 36 hours with a higher number of depolarizing events, compared to the drug free control (A). See discussion for possible explanation. Each time point represents the mean value of triplicate samples \pm one SD. DF ctrl – drug free control; UI ctrl – uninfected control. doi:10.1371/journal.pone.0061606.g006

However, the assay format used a visual readout and appears to

Table 1. Inhibitory concentrations (50%) of several antimalarial drugs against *P. falciparum* 3D7 strain determined by the Hemozoin detection assay at different times of incubation.

	Time of incubation				
	18 h*	24 h	30 h*	36 h*	72 h*
Chloroquine	41.9 nM (\pm 19.3)	34.2 nM (\pm 8.1)	33.6 nM (\pm 10.1)	35.9 nM (\pm 10.1)	29.6 nM (\pm 7.4)
Quinine	98.5 nM	54.6 nM (\pm 9)	92.2 nM	142.7 nM	45 nM
Mefloquine	17.2 nM	21.3 nM (\pm 7)	33.5 nM (\pm 6.4)	64.9 nM (\pm 20.2)	19.5 nM
Artemisinin	28.2 nM (\pm 3.5)	25.6 nM (\pm 5.9)	34.5 nM (\pm 5.8)	43.7 nM (\pm 16)	n.d.
Artesunate	< 4 nM	6.4 nM (\pm 2.3)	10.8 nM (\pm 3.6)	12.4 nM (\pm 6.3)	n.d.

PyrimethamineXXXX25.4 nM(\pm 10.3)

Mean inhibitory concentration values (50%) \pm one standard deviation are presented.

Standard deviation values are not shown for results that were not supported by at least three independent experiments. Time-points identified with (*) were not systematically analyzed, since the 24 hour time-point was used as the preferential time-point to reliably calculate IC50 values (as discussed in the manuscript).

(X) values could not be determined; (n.d.) no data available.

doi:10.1371/journal.pone.0061606.t001

have been rather inaccurate because of nonspecific agglutination [32]. Recently, an improvement of this approach has been reported where the Hz produced is measured by a colorimetric method [33]. To do this, the Hz produced by the parasites after 72 hours of incubation is liberated and transformed back into heme before reading the absorbance at 405/750 nm. However, the assay involves multiple manipulation steps, including lysis and several washing steps, which are cumbersome and may introduce variability. In fact, in our hands, the isolation of Hz and quantification of heme requires meticulous attention to accurate pipetting to guarantee reproducible results [34].

Depolarization signal strength and detection limit

The comparison of an uninfected RBC sample with a synchronized *P. falciparum* infected RBC sample at 24 hours of incubation showed a depolarizing population that could be easily identified and gated (Figure 1D). However, the degree of depolarization of the whole population was much lower than previously described for *P. berghei* infected blood samples [27]. A possible explanation for this may be different side scatter signals, which are a measure of cell granularity [35], that could be caused by the different shape and distribution of the Hz crystals within these parasites. A parasite containing several small but distributed Hz crystals will have a higher depolarized side scatter signal than a parasite containing a single big Hz crystal. In fact, during this and previous work, the routine microscopic analysis of Giemsa stained blood smears to control the parasitemia showed that Hz started to appear in small dispersed fine granules in *P. berghei* and only clumped together by the end of schizogony, as previously observed by Warhurst et al. [36], while in *P. falciparum*, Hz crystals aggregate as they start to appear (data not shown). It also appears possible that the depolarization signal can still be improved as a result of

Table 2. Antimalarial activities of several antimalarial drugs determined by the Hemozoin detection assay and the HRP2 assay.

	Hemozoin detection* 24 hours of incubation	HRP2 72 hours of incubation
Chloroquine	34.2 nM (± 8.1)	22 nM
Quinine	54.6 nM (± 9)	52 nM
Mefloquine	21.3 nM (± 7)	21 nM
Artesunate	6.4 nM (± 2.3)	1.1 nM
Artemisinin	25.6 nM (± 5.9)	11.5 nM
Pyrimethamine	25.4 nM (± 10.3) ¹⁾	30.5 nM
NITD 246	0.8 nM	0.4 nM

The averages of 50% inhibitory concentration values \pm one standard deviation are presented above.

*For the Hemozoin detection assay each drug was tested at least three times (except for the novel compound NITD246).

HRP2 – Histidine-rich protein 2;

¹⁾after 72 hours of incubation.

doi:10.1371/journal.pone.0061606.t002

technical modifications to the instrument. The Cyflow[®] flow cytometer uses a blue laser (488 nm). However, longer wavelengths may increase the depolarization signal as has been described for a red HeNe (633 nm) or Kr⁺ laser (647 nm) [18]. Furthermore, the polarization ratio of most solid-state lasers is usually given as $>1:100$. If the laser had a higher polarization ratio, as do HeNe and Kr⁺ lasers, positive depolarization signals might be better distinguished from background noise.

To assess parasite maturation and drug effects we chose to use the simple ratio of all identifiable depolarizing events as a percentage of all events analyzed (Figure 1C and D). Other measurements, like depolarizing intensity, showed no clear advantage (data not shown). A parasitemia of 1% proved to be the optimal parasitemia to detect parasite maturation and growth over 48 hours. Thus, it was used in the Hz detection assay to obtain time-curves when investigating the drug effects in *P. falciparum* *in vitro* cultures. Still, an initial 1% parasitemia is higher than the ones used in other assays, such as the HRP2 or the WHO schizont maturation test, which can use parasitemias as low as 0.02% [8], [37], [38]. However, when investigating the lower detection limit of the Hz assay, parasite maturation and drug effects of chloroquine, artesunate and pyrimethamine could still be clearly detected at parasitemias as low as 0.3%. Nevertheless, this remains higher than the ones used for the HRP2 assay and the WHO schizont maturation test. Yet, it is comparable to the parasitemias used in other assays, such as the [3H]-hypoxanthine assay (0.25–0.5%) [6] or the SYBR green I assay (0.5–1%) [9], [39], [40] (Table S1).

Of note, in all Hz assay experiments, only around 30% of all parasites were typically detected by depolarization measurements (Figure 1D) as compared to microscopy or SYBR green I fluorescence. The reasons for this are unclear and could be a consequence of the culture not being highly synchronized. At the 30 hour peak of maturation, schizonts as well as some second generation ring forms are present, as confirmed by microscopy; the immature ring forms have insufficient Hz to be reliably detected [28]. Another possible explanation is the already mentioned Hz aggregation that occurs in the mature parasites, which may reduce side scatter intensity.

Certainly, the initial parasitemia of 0.3% required is still a major limitation of this assay if used directly with patient blood samples, some of which may have lower parasitemias [41]. However, further optimization of the assay may lead to an improvement of the detection limit. Nevertheless, future studies conducted in the

field will allow us to evaluate the performance of the novel Hz detection assay using *ex vivo* patient samples.

Aspects of parasite maturation

Using a red blood cell surface marker (CD235) (Figure 1G) and a DNA stain (SYBR green I) we showed that the depolarizing events were indeed infected red blood cells (Figure 1F). SYBR green I fluorescent intensity reflects DNA content [42], [43]. Most of the depolarizing events showed high SYBR green I fluorescence (80%), indicating that they were mature parasites (Figure 1H). Comparing depolarization and fluorescence intensity in a *P. berghei* ANKA infected sample stained with SYBR green I showed, similarly, that the level of depolarization appears to reflect parasite maturation [27].

Usually, the described *P. falciparum* life cycle lasts 42–48 hours *in vitro* [44]. Contrary to this, we observed a peak of parasite maturation earlier, at around 30 hours, as reflected by the peak in depolarization (Figure 2A) followed by a steady increase in SYBR green I positive events indicating replication (Figure 2B). Corresponding parasite forms were also observed during microscopic observation of Giemsa stained blood smears. This can be explained by the fact that because the assay did not start immediately after re-invasion thus, the indicated time points correspond to the time post-drug-treatment and not the time post-invasion. Moreover, the fact that cultures were not highly synchronized seem to have contributed to this apparent shorter life cycle. It is known that to obtain highly synchronized cultures, at least one other sorbitol treatment would be needed [45].

After a single synchronization approximately 90% of the parasites are ring forms. However, individual parasites can present differences of several hours in their development. Thus, at the beginning of the experiments, some parasites may have already developed for 12 hours within the ring form population while others are only 6 hours into their development. The microscopic observation of Giemsa stained blood smears at 36 hours gives weight to this reasoning, because both schizonts and second generation ring forms could be observed at this time point.

Drug effects and potential use of the Hz assay

One of the major advantages of the Hz detection assay is the fact that samples can be easily analyzed without further preparation or additional reagents allowing a rapid and easy real-time assessment of parasite maturation and drug effects. For instance other assays, such as the [3H]-hypoxanthine assay, cultures have to be incubated for additional 24 hours with the

isotope before measurements are possible [6], [15], [46–48]. Another advantage is the early detection of inhibitory drug effects after only 18 hours (Table 1 and Figures 3, 4 and 5), in contrast to several other assays, such as the [3H]-hypoxanthine assay [6], [48], which measures drug effects at 48 hours, the SYBR green I [15], [40], [49], [50] and the HRP2 [8], [15], [37] assays, which require at least 72 hours.

Although, for example, in the Hz assay chloroquine sensitive and resistant strains are easily distinguishable after only 18 hours (Figure 3), the inhibitory effect of the slow acting drug pyrimethamine could only be detected after 72 hours (Figure 6). This drug has no effect on asexual parasites in the first half of the parasite life cycle (24 hours) [41], [51] and effects can only be detected later in the second parasite generation. For this reason the Hz assay detects slow acting drugs effects, such as pyrimethamine, only after 72 hours of incubation. Interestingly, at concentrations of 200 nM, higher depolarization values were observed after 30 hours (Figure 6A), which appear to reflect schizont arrest, which was observed by microscopy.

As shown in Table 1, the Hz detection assay allows determination of a drug's inhibitory concentrations at different time-points during the first and second life cycle, thus extending its potential usefulness.

Artemisinins in the Hz assay

Artemisinin and artesunate growth curves were different from the other tested drugs. At concentrations of 32 nM and 4 nM, respectively, a delayed maturation was observed, starting at 18 hours (Figures 4C and 5A). However, the SYBR green I measurements performed simultaneously indicated that the parasites replicate, reaching approximately the same parasitemia as the drug free control after 48 hours of incubation (data not shown). The reason for this observation remains unclear. Furthermore, samples treated with 8 nM of artesunate showed an initial inhibition with a delayed rise after 30 hours (Figures 5A and 5B). SYBR green I measurements, however, did not change over the 48 hour incubation period, indicating that the parasites were somehow able to mature but unable to replicate (Figure 5C). These parasites, treated a single time with 8 nM of artesunate, were re-cultured in CMC and no growth could be observed during the following four days. Interestingly, similar behavior has been previously described for artemisinin [52] and was interpreted as a consequence of its rapid degradation [53]. The drug level had to be kept constant by replacing the media with the drug every 24 hours, otherwise the number of viable parasites increased at 96 and 120 hours after drug addition [52]. In fact, renewing the artesunate every 12 hours in the culture medium showed that the inhibition was maintained throughout the 48 hours of incubation and the delayed rise was lost (Figure 5B).

Dormancy has been described after treatment with artemisinins, where early stage parasites enter a dormant stage under drug pressure but later regrow [54]. It has been reported that parasites treated with dihydroartemisinin arrested their development shortly after drug exposure, but after 9 days 50% of the parasites managed to resume their growth [54]. Thus, to detect recrudescence of these dormant parasites cultures would have to be monitored for at least four life cycles (9 days = 216 hours). Our findings showed a delayed increase during the first life cycle (after 30 hours of incubation), in samples treated with artesunate at 8 nM. Although this might represent the detection of dormancy and parasite recrudescence, the data we have obtained so far are not sufficient to confirm or exclude this hypothesis, because these parasites were not monitored for longer than four days. Further investigation is needed to clarify this issue.

Comparison of IC50 values

The IC50 determined by the Hz detection assay were comparable with the ones reported for other, already validated assays (Tables 1, 2 and S2). However, slightly higher values were observed for some of the drugs, especially for artesunate, where most publications report values below 2.5 nM [15], [37], [47]. One explanation could be the inoculum effect, i.e., an increase in the inhibitory drug concentration when greater numbers of parasites are inoculated. This is thought to be the consequence of some drug accumulating inside the parasitized RBC [55] and has been described for drugs like artemisinin and artesunate, as well as for chloroquine and mefloquine [56]. In fact, in the Hz assay parasitemias of around 1% were used as compared to other assays, which used parasitemias ranging from 0.05 to 0.5% [6–9], [37–40]. This might explain the increased IC50 values observed in the Hz detection assay and interestingly, a decrease in the parasitemia from 1.4% to 0.7% led to a decrease in the artemisinin IC50 value from 32 to 13.2 nM. However, no such decrease was observed with artesunate.

It is important to note, that the comparison of IC50 values between assays can be misleading. The IC50 values in the literature vary substantially between assays, even for the same strain. For instances, the standard [3H]-hypoxanthine incorporation assay shows differences of 2 to 23 fold for artesunate (Table S2). Not too surprisingly, one study reported that the reliability of the assays may be influenced by the mechanism of action of individual drugs [15]. Moreover, variations in parasite density and hematocrit as well as the stage-dependent action of antimalarial drugs, may have a significant impact on the outcome of these sensitivity assays [14], [56].

Assay – prospects, future possibilities

Because the Hz detection assay allows parasite maturation to be monitored in real time, it could possibly be used to investigate drug effects on different parasite developmental stages (stage specificity of drugs). It might also be interesting to assess the performance of the assay with parasite strains that have been reported to show clinical signs of resistance to artemisinins. Since modeling of parasite-clearance curves suggests that artemisinin resistance affects ring-stage parasites more than the more mature parasite stages, thus *in vitro* tests focusing on the inhibition of ring-stage parasites could become valuable surveillance tools [57].

The fact that a flow cytometer is required may pose an obstacle to the widespread use of the Hz assay in the field. Furthermore, flow cytometers that use fiber optic cables for light collection, such as the BD LSRFortessa or FACSAria, require relatively elaborate optical modification to detect depolarization. However, detection of depolarization as we have described can be implemented simply on many existing flow cytometers, for example the flow sorter Influx (<http://www.bdbiosciences.com/instruments/influx/features/index.jsp>, accessed 14/08/2012), the Cyflow Cube (Danny Koehler, Partec, Münster, Germany, personal communication), the Life Technologies Attune (Grace Chojnowski, Queensland Institute of Medical Research, Brisbane, Australia, personal communication), and can even be retrofitted to the venerable BD FACSCalibur (Lisa Nichols, Cytex Development, Fremont, CA, USA, personal communication). More importantly, some low-cost flow cytometers for CD4 counts in resource-poor countries could be modified rather easily to detect depolarization, and are already available on site in several African countries (http://www.partecnorthamerica.com/Press-Release-01Dec2012-_b_2.html assessed 22/12/12).

Furthermore, it is now evident [58] that optical measurements of both DNA and Hz can be made in small, robust, simple, widefield multiparameter optical imaging apparatus an order of

magnitude less expensive than a typical flow cytometer, using LEDs costing only a few dollars for illumination and employing camera chips only slightly higher in quality than those used in mobile phones as detectors. Signals from all cells in an entire well of an assay microplate can be analyzed in seconds, without the need for precise stage motion or focus adjustment. Somewhat more elaborate and expensive versions of such devices are already commercially available; minimalist instruments optimized for field use in the resource-poor areas in which malaria is prevalent should arrive within a few years.

In conclusion, the novel Hz detection assay allows parasite maturation to be monitored in real time without the need of further reagents or sample preparation. The assay detects inhibitory drug effects of major antimalarial drug classes after only 18 hours of incubation and permits determination of IC50 values at 24 hours. Future work will have to address the utility of this assay in the field. Issues such as the use of less expensive alternatives to flow cytometry and the application of the assay to such tasks as the determination of stage specific effects of antimalarial drugs will have to be investigated further.

Supporting Information

Table S1 Comparative descriptions of available *in vitro* sensitivity assays for *Plasmodium falciparum*.
(DOCX)

References

- Hyde JE (2007) Drug-resistant malaria - an insight. *FEBS J*. 27:4688–4698.
- White NJ (2004) Antimalarial drug resistance. *J Clin Invest* 113:1084–1092.
- Dondorp AM, Nosten F, Yi P, Das D, Phyo AP, et al. (2009) Artemisinin resistance in *Plasmodium falciparum* malaria. *N Engl J Med* 361: 455–467.
- Bloland PB (2001) Drug resistance in malaria. WHO Press, Geneva, Switzerland.
- Rieckmann KH, Campbell GH, Sax LJ, Mrema JE (1978) Drug sensitivity of *Plasmodium falciparum*. An in-vitro microtechnique. *Lancet* 1:22–23.
- Desjardins RE, Canfield CJ, Haynes JD, Chulay JD (1979) Quantitative assessment of antimalarial activity in vitro by a semiautomated microdilution technique. *Antimicrobial Agents and Chemotherapy* 16: 710–718.
- Makler MT, Hinrichs DJ (1993) Measurement of the lactate dehydrogenase activity of *Plasmodium falciparum* as an assessment of parasitemia. *Am J Trop Med Hyg* 48: 205–210.
- Noedl H, Wernsdorfer WH, Miller RS, Wongsrichanalai C (2002) Histidine-rich protein II: a novel approach to malaria drug sensitivity testing. *Antimicrobial Agents and Chemotherapy* 46: 1658–1664.
- Smilkstein M, Sriwilajjaroen N, Kelly JX, Wilairat P, Riscoe M (2004). Simple and inexpensive fluorescence-based technique for high-throughput antimalarial drug screening. *Antimicrobial Agents and Chemotherapy* 48: 1803–1806.
- Li Q, Gerena L, Xie L, Zhang J, Kyle D, et al. (2007) Development and validation of flow cytometric measurement for parasitemia in cultures of *P. falciparum* vitally stained with YOYO-1. *Cytom A* 71: 297.
- Corbett Y, Herrera L, Gonzalez J, Cubilla L, Capson TL (2004) A novel DNA-based microfluorimetric method to evaluate antimalarial drug activity. *Am J Trop Med Hyg* 70:119–24.
- Baniecki ML, Wirth DF, Clardy J (2007). High-throughput *Plasmodium falciparum* growth assay for malaria drug discovery. *Antimicrob Agents Chemother* 51: 716.
- Wongsrichanalai C, Pickard AL, Wernsdorfer WH, Meshnick SR (2002) Epidemiology of drug resistant malaria. *Lancet Infect Dis* 2:209–218.
- Noedl H, Wongsrichanalai C, Wernsdorfer WH (2003) Malaria drug-sensitivity testing: new assays, new perspectives. *Trends in Parasitology* 19: 175–181.
- Wein S, Maynadier M, Tran Van Ba C, Cerdan R, Peyrottes S, et al. (2010) Reliability of antimalarial sensitivity tests depends on drug mechanisms of action. *J Clin Microbiol* 48: 1651–1660.
- World Health Organization (2011) Global path for artemisinin resistance containment (GPARC). WHO Press, Geneva.
- Hanscheid T, Egan TJ, Grobusch MP (2007) Haemozoin: From melatonin pigment to drug target, diagnostic tool and immune-modulator. *The Lancet Infectious Diseases* 7: 675–685.
- Krämer B, Grobusch MP, Suttorp N, Neukammer J, Rinneberg H (2001) Relative frequency of malaria pigment-carrying monocytes of nonimmune and semi-immune patients from flow cytometric depolarized side scatter. *Cytometry* 45:133–40.
- Grobusch MP, Hanscheid T, Kraemer B, Neukammer J, May J, et al. (2003) Diagnosis of malaria by automated detection of malaria pigment in travelers returning to Berlin, Germany. *Clinical Cytometry* 55B: 46–51.

Table S2 Antimalarial activities of several antimalarial drugs determined by different *in vitro* sensitivity assays against *P. falciparum* 3D7 strain.
(DOCX)

Figure S1 Cyflow® flow cytometer and optical bench layout. Images in the top row show the components (A) and the optical bench layout (B) of the Cyflow® flow cytometer. The 488 nm laser light is vertically polarized. A horizontally polarized filter is placed in front of a second side scatter detector to allow detection of depolarized light (depol SSC). Images C, D and E show a Cyflow® in the laboratory and being easily packed for transport at the Centre de Recherches Médicales de Lambaréné – CERME, Lambaréné, Gabon. (The subject of the photograph has given written informed consent, as outlined in the PLOS consent form, to publication of the photograph).
(DOCX)

Author Contributions

Evaluated and provided advice on different aspects of the novel assay and its development, and contributed to writing and revising the final manuscript: MPG HMS MMM. Conceived and designed the experiments: MR HMS MMM MPG TH. Performed the experiments: MR CS. Analyzed the data: MR CS HMS TH. Contributed reagents/materials/analysis tools: MMM TH. Wrote the paper: MR MPG HMS TH.

- Jamjoom GA (1983) Dark-Field Microscopy for Detection of Malaria in Unstained Blood Films. *J Clin Microbiol* 17:717–721.
- Lawrence C, Olson JA (1996) Birefringent Hemozoin Identifies Malaria. *American Journal of Clinical Pathology* 96: 360–363.
- Hanscheid T, Valadas E, Grobusch MP (2000a). Automated malaria diagnosis using pigment detection. *Parasitol Today* 16: 549.
- Mendelow BV, Lyons C, Nhangothi P, Tana M, Munster M, et al. (1999) Automated malaria detection by depolarization of laser light. *Brit J Haematol* 104: 499–503.
- Hanscheid T, Pinto BG, Cristino JM, Grobusch MP (2000b) Malaria diagnosis with the haematology analyser Cell-Dyn 3500: What does the instrument detect? *Clin Lab Haematol* 22:259–261.
- Suh IB, Kim HJ, Kim JY, Lee SW, An SS, et al. (2003) Evaluation of the Abbott Cell-Dyn 4000 hematology analyzer for detection and therapeutic monitoring of *Plasmodium vivax* in the Republic of Korea. *Trop Med Int Health* 8:1074–1081.
- Grooth BG, Terstappen LWMM, Pupples GJ, Greve J (1987) Light-Scattering Polarization Measurements as New Parameter in Flow Cytometry. *Cytometry* 8: 539–544.
- Frita R, Rebelo M, Pamplona A, Vigario AM, Mota MM, et al. (2011) Simple flow cytometric detection of haemozoin containing leukocytes and erythrocytes for research on diagnosis, immunology and drug sensitivity testing. *Malar J* 10:74.
- Rebelo M, Shapiro HM, Amaral T, Melo-Cristino J, Hanscheid T (2012) Haemozoin detection in infected erythrocytes for *Plasmodium falciparum* malaria diagnosis—Prospects and limitations. *Acta Tropica* 123:58–61.
- Mphande F, Nilsson S, Bolad A (2008) Culturing of erythrocytic asexual stages of *Plasmodium falciparum* and *P. vivax*. In: Moll K, Ljungström I, Perlmann H, Scherf A, Wahlgren M (Eds.), *Methods in Malaria Research*, fifth ed, pp. 1–3 (Manassas).
- Lambros C, Vanderberg JP (1979) Synchronization of *Plasmodium falciparum* erythrocytic stages in culture. *J Parasitol* 65:418–420.
- Rieckmann KH (1982) Visual in vitro test for determining the drug sensitivity of *Plasmodium falciparum*. *Lancet* 1:1333–1335.
- Basco LK (2007) Field application of in vitro assays for the sensitivity of human malaria parasites to antimalarial drugs. WHO Press, Geneva, Switzerland.
- Men TT, Huy NT, Trang DTX, Shuaibu MN, Hirayama K, et al. (2012) A simple inexpensive haemozoin-based colorimetric method to evaluate antimalarial drug activity. *Malar J* 11:272.
- Thomas V, Góis A, Ritts B, Burke P, Hanscheid T, et al. (2012) A novel way to grow hemozoin-like crystals in vitro and its use to screen for hemozoin inhibiting antimalarial compounds. *PLoS ONE* 7(7): e41006.
- Shapiro HM (2003) *Practical Flow Cytometry – 4th edition*: John Wiley & Sons. New Jersey, USA.
- Warhurst DC, Homewood CA, Baggaley VC (1974) The chemotherapy of rodent malaria. XX. Autophagic vacuole formation in *Plasmodium berghei* in vitro. *Ann Trop Med Parasitol* 68:265–81.

37. Held J, Soomro SA, Kremsner PG, Jansen FH, Mordmüller B (2011) In vitro activity of new artemisinin derivatives against *Plasmodium falciparum* clinical isolates from Gabon. *Int J Antimicrob Agents* 37:485–488.
38. Ikpa TF, Ajayi JA, Imandeh GN, Usar JI (2010) Drug resistant *falciparum* malaria in North Central Nigeria. *Afr J Clin Exper Microbiol* 11: 111–119.
39. Johnson JD, Denuff RA, Gerena L, Lopez-Sanchez M, Roncal NE, et al. (2007) Assessment and continued validation of the malaria SYBR green I-based fluorescence assay for use in malaria drug screening. *Antimicrob Agents Chemother* 51:1926–33.
40. Bacon DJ, Latour C, Lucas C, Colina O, Ringwald P, et al. (2007) Comparison of a SYBR green I-based assay with a histidine-rich protein II enzyme-linked immunosorbent assay for in vitro antimalarial drug efficacy testing and application to clinical isolates. *Antimicrob Agents Chemother* 51:1172–8.
41. White NJ (1997) Assessment of the Pharmacodynamic Properties of Antimalarial Drugs In Vivo. *Antimicrob Agents Chemother* 41:1413–22.
42. Bennett TN, Paguio M, Gligorijevic B, Seudieu C (2004) Novel, Rapid, and Inexpensive Cell-Based Quantification of Antimalarial Drug Efficacy. *Antimicrob Agents Chemother* 48:1807–10.
43. Karl S, Wong R, Pierre TG, Davis T (2009) A comparative study of a flow-cytometer-based assessment of in vitro *Plasmodium falciparum* drug sensitivity. *Malar J* 8:294.
44. Grizmacher CA, Reese RT (1984) Protein and Nucleic Acid Synthesis During Synchronized Growth of *Plasmodium falciparum*. *J Bacteriol* 160:1165–1167.
45. Schuster FL (2002) Cultivation of *Plasmodium* spp. *Clin Microbiol Rev* 15:355–364.
46. Lim P, Wongsrichanalai C, Chim P, Khim N, Kim S, et al. (2010) Decreased in vitro susceptibility of *Plasmodium falciparum* isolates to artesunate, mefloquine, chloroquine, and quinine in Cambodia from 2001 to 2007. *Antimicrob Agents Chemother* 54:2135–42.
47. Aunpad R, Somsri S, Na-Bangchang K, Udamsangpetch R, Mungthin M, et al. (2009) The effect of mimicking febrile temperature and drug stress on malarial development. *Ann Clin Microbiol Antimicrob* 8:19.
48. Tucker MS, Mutka T, Sparks K, Patel J, Kyle DE (2012) Phenotypic and genotypic analysis of in vitro-selected artemisinin-resistant progeny of *Plasmodium falciparum*. *Antimicrob Agents Chemother* 56:302–14.
49. Vossen MG, Pferschy S, Chiba P, Noedl H (2010) The SYBR Green I malaria drug sensitivity assay: performance in low parasitemia samples. *Am J Trop Med Hyg* 82:398–401.
50. Abiodun OO, Gbotosho GO, Ajaiyeoba EO, Happi CT, Hofer S, et al. (2010) Comparison of SYBR Green I-, PicoGreen-, and [3H]-hypoxanthine-based assays for in vitro antimalarial screening of plants from Nigerian ethnomedicine. *Parasitol Res* 106:933–939.
51. Maerki S, Brun R, Charman SA, Dorn A, Matile H, et al. (2006) In vitro assessment of the pharmacodynamic properties and the partitioning of OZ277/RBx-11160 in cultures of *Plasmodium falciparum*. *J Antimicrob Chemother* 58:52–58.
52. Sanz LM, Crespo B, De-Cózar C, Ding XC, Llergo JL, et al. (2012) *P. falciparum* in vitro killing rates allow to discriminate between different antimalarial mode-of-action. *PLoS One* 7:e30949.
53. Meshnick SR, Taylor TE, Kamchonwongpaisan S (1996) Artemisinin and the antimalarial endoperoxides: from herbal remedy to targeted chemotherapy. *Microbiol Rev* 60: 301–315.
54. Teuscher F, Gatton ML, Chen N, Peters J, Kyle DE, et al. (2010) Artemisinin-induced dormancy in *Plasmodium falciparum*: duration, recovery rates, and implications in treatment failure. *J Infect Dis* 202:1362–8.
55. Gluzman IY, Schlesinger PH, Krogstad DJ (1987) Inoculum effect with chloroquine and *Plasmodium falciparum*. *Antimicrob Agents Chemother* 31:32–6.
56. Duraisingh MT, Jones P, Sambou I, Von Seidlein L, Pinder M, et al. (1999) Inoculum effect leads to overestimation of in vitro resistance for artemisinin derivatives and standard antimalarials: a Gambian field study. *Parasitology* 119: 435–440.
57. Dondorp AM, Fairhurst RM, Slutsker L, Macarthur JR, Breman JG, et al. (2011) The threat of artemisinin-resistant malaria. *N Engl J Med* 365:1073–1075.
58. Shapiro HM, Ulrich H (2010) Overview: Cytometry in malaria: From research tool to practical diagnostic approach? *Cytometry Part A* 77: 500–501.

METHODOLOGY

Open Access

Assessing anti-malarial drug effects *ex vivo* using the haemozoin detection assay

Maria Rebello^{1,2*}, Carolina Tempera¹, José F Fernandes^{2,3,4}, Martin P Grobusch^{2,3,4} and Thomas Häscheid^{1,2,5}

Abstract

Background: *In vitro* sensitivity assays are crucial to detect and monitor drug resistance. *Plasmodium falciparum* has developed resistance to almost all anti-malarial drugs. Although different *in vitro* drug assays are available, some of their inherent characteristics limit their application, especially in the field. A recently developed approach based on the flow cytometric detection of haemozoin (Hz) allowed reagent-free monitoring of parasite maturation and detection of drug effects in culture-adapted parasites. In this study, the set-up, performance and usefulness of this novel assay were investigated under field conditions in Gabon.

Methods: An existing flow cytometer (Cyflow Blue) was modified on site to detect light depolarization caused by Hz. Blood from malaria patients was incubated for 72 hrs with increasing concentrations of chloroquine, artesunate and artemisinin. The percentage of depolarizing red blood cells (RBC) was used as maturation indicator and measured at 24, 48 and 72 hrs of incubation to determine parasite growth and drug effects.

Results: The flow cytometer was easily adapted on site to detect light depolarization caused by Hz. Analysis of *ex vivo* cultures of parasites, obtained from blood samples of malaria patients, showed four different growth profiles. In 39/46 samples, 50% inhibitory concentrations (IC50) were successfully determined. IC50 values for chloroquine were higher than 200 nM in 70% of the samples, indicating the presence of chloroquine-resistant parasites. For artesunate and artemisinin, IC50 values ranged from 0.9 to 60 nM and from 2.2 nM to 124 nM, respectively, indicating fully sensitive parasites.

Conclusion: Flow cytometric detection of Hz allowed the detection of drug effects in blood samples from malaria patients, without using additional reagents or complex protocols. Adjustment of the initial parasitaemia was not required, which greatly simplifies the protocol, although it may lead to different IC50 values. Further investigation of set-up conditions of the Hz assay, as well as future studies in various settings should be performed to further determine the usefulness of this assay as a tool for rapid resistance testing in malaria-endemic countries.

Keywords: Malaria, field trial, Anti-malarial sensitivity testing, Resistance, Flow cytometry, Haemozoin

Background

In the last decade, the number of malaria deaths has decreased in large part due to the availability of effective treatments, in particular artemisinin combination therapy (ACT) [1]. However, these achievements are in danger and might even be reversed because parasites with prolonged parasite clearance times (PCT), observed in patients treated with ACT, have emerged in Southeast

Asia [2,3]. Indeed, this is considered an early sign of the development of parasite resistance [2,3] and a major concern in the fight against malaria, as illustrated by the WHO Global Plan for Artemisinin Resistance Containment issued in 2011 [4]. Artemisinin resistance, currently defined as prolonged PCT, has spread across Southeast Asia [5]. Recently, a Vietnamese patient who apparently acquired malaria in Angola failed to respond to intravenous artesunate/clindamycin and an oral ACT after returning to Vietnam [6]. It is not unlikely that it will emerge in sub-Saharan Africa, and drug sensitivities should be monitored pro-actively. In this scenario, *in vitro* sensitivity assays may play a crucial role in the

* Correspondence: mariarebello@fm.ul.pt

¹Instituto de Medicina Molecular, Faculdade de Medicina de Lisboa, Av Prof Egas Moniz, Lisbon P-1649-028, Portugal

²Centre de Recherches Médicales de Lambaréné - CERMEL, Albert Schweitzer Hospital, Lambaréné, Gabon

Full list of author information is available at the end of the article



future. *In vitro* assays allow reducing host-related factors and thus, provide an objective insight into the intrinsic sensitivity of malaria parasites.

Several phenotypic and genotypic methods have been developed and tried for drug testing in the field [7]. Genetic resistance markers are known for some anti-malarial drugs, but are not yet able to predict sensitivity to all commonly used anti-malarial drugs [8]. Only recently, alterations in the *kelch13* gene were linked to delayed parasite clearance in artemisinin-treated patients [9]. Thus, phenotypic assays continue to be important for detection of resistance and validation of genetic markers. The main phenotypic assays successfully used to detect drug resistance in the field include: (i) the microscopic schizont maturation test [10]; (ii) the incorporation of radioactive hypoxanthine [11]; (iii) ELISA assays for detection of pLDH [12] and HRP2 [13] antigens; and, (iv) fluorescent-based techniques using either fluorometry [14] or flow cytometry [15] to detect parasite DNA/RNA. However, inherent limitations are common, especially during field applications. The supply, handling and disposal of radioactive isotopes are major obstacles. Microscopy is labour-intensive and subjective, although it has a rather quick turn-around time (24–30 hrs) when compared to other techniques, especially ELISA-based methods, which can take up to 72 or even 96 hrs [16,17]. Moreover, assays may require the use of, often, expensive antibodies or DNA/RNA stains, highlighting the issues of adequate storage and cold chain as well as limited shelf life.

Regarding flow cytometry, the majority of cytometric methods apply combinations of dyes to reliably detect infected red blood cells (iRBC), which implies a complex multiparameter analysis [15,18]. Ideally, if parasite maturation was detectable using a direct and simple measurement of a product from the parasite, the need for additional reagents would be avoided.

Haemozoin (Hz) is produced in increasing amounts by the parasite as it matures inside the iRBC, constituting an optimal maturation indicator [10]. Measuring Hz with a simple flow cytometry method allows detection of parasite maturation and drug effects as early as 18 hrs after incubation in culture-adapted laboratory strains [19].

The objectives of this study were to evaluate if the Hz detection assay could be easily set up in a remote malaria-endemic area, and to assess whether anti-malarial drug effects could be detected in wild-type strains obtained from malaria patients, using a simple protocol.

Methods

The study was carried out at the Centre de Recherches Médicales de Lambaréné (CERMEL) in Gabon, a malaria-endemic region in Africa. Ethical approval was obtained from the Institutional Review Board of the

Medical Research Unit (CERMEL) of the International Foundation of the Albert Schweitzer Hospital.

Samples

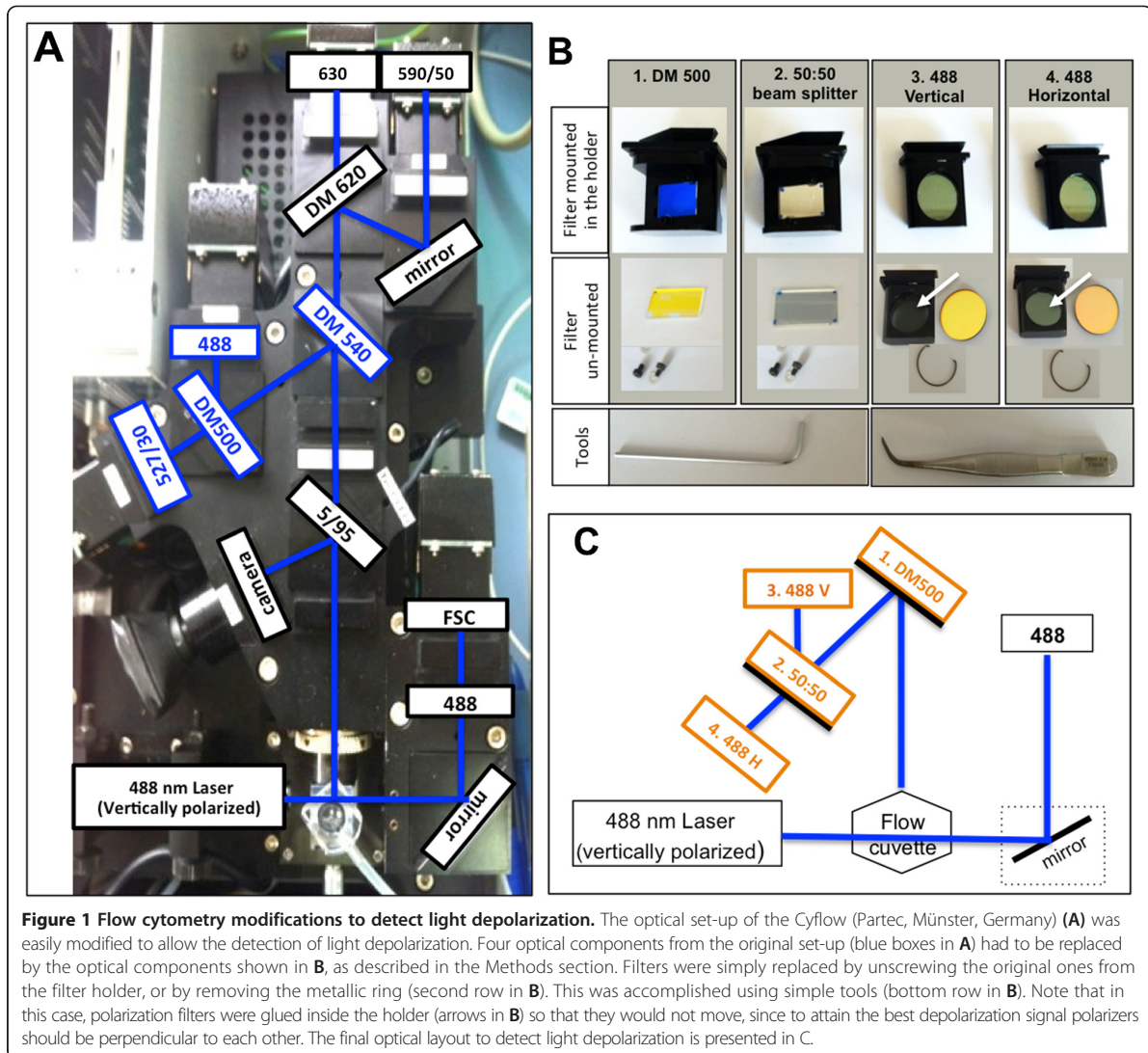
EDTA anti-coagulated blood samples from malaria patients were obtained from the Clinical Analysis Laboratory of the Albert Schweitzer Hospital after the samples had been processed for full blood count (FBC). Malaria diagnosis and parasite loads (number of parasites/ μ l of blood) were determined by standard microscopic observation of Giemsa-stained thick blood films. Briefly, parasitaemia was quantified by counting the number of parasites per microscopic field from a defined volume of blood (10 μ l) spread on a defined area (1.8 cm²), as described elsewhere [20]. RBCs from these blood samples were washed twice in culture medium before further use.

Flow cytometric detection of depolarized side-scattered light

Flow cytometric analysis was performed using a CyFlow[®] Blue (Partec, Münster, Germany) available on site. The existing configuration, which was modified on site for this study and is shown in Figure 1, consisted of forward scatter (FSC), side scatter (SSC) and three fluorescent detectors (FL1, FL2 and FL3). A set of four optical filters was necessary, as shown in Figure 1B: (1) a 500-nm dichroic mirror; (2) a 50:50 beam-splitter; (3) a 488-nm vertical polarizer; and, (4) a 488-nm horizontal polarizer. Briefly, a 500-nm dichroic mirror (DM) (B1) was placed on the site of the original 540-nm DM and the other original 500-nm DM was replaced by a 50:50 beam-splitter (B2), which allowed the creation of two SSC detectors (Figure 1). A 488-nm filter coupled with a polarizer in the same orientation as the incident laser beam (vertical) was placed in front of one of the SSC detectors. Another 488-nm filter coupled with a polarizer perpendicularly orientated in relation to the laser beam (horizontal) was placed in front of the other SSC detector, allowing the detection of light depolarization (Figure 1C). The optical components required to modify the optical bench of flow cytometers can be obtained directly from the instruments' manufacturer.

Anti-malarial drugs

Samples were tested against different concentrations of chloroquine, artesunate and artemisinin (Sigma Aldrich, St Louis, MO, USA). Stock solutions of chloroquine were prepared in sterile water, and artemisinin and artesunate were prepared in pure methanol. Doubling concentrations, ranging from 25 to 200 nM for chloroquine and from 0.12 to 128 nM for artemisinin and artesunate, were prepared from the stock solutions in complete malaria culture medium (CMCM), which consists of RPMI 1640 supplemented with 25 mM HEPES,



2.4 mM L-glutamine, 50 µg/mL gentamicin, 0.5% w/v Albumax, 11 mM glucose, 1.47 mM hypoxanthine and 37.3 mM NaHCO₃.

Each drug concentration was tested in triplicate.

Haemozoin detection assay

RBCs obtained from malaria patients were diluted at a haematocrit of 5% in CMCM. To simplify the assay, the parasitaemia was not adjusted so that, eventually, the use of uninfected blood could be avoided. A volume of 100 µL was distributed into the wells of a 96-well plate, previously loaded with 100 µL of anti-malarial drugs at different concentrations, or 100 µL of CMCM for the drug-free controls, respectively. Plates were incubated for 72 hrs at 37°C in 5% CO₂ atmosphere. Flow cytometric measurements were performed at 24, 48 and 72 hrs of incubation.

Parasite maturation from ring-stage to schizonts was assessed based on the increase in the percentage of Hz-containing cells overtime, as described before [19]. To assess parasite replication (re-invasion), the same samples were stained with SYBR green I at 1x (Invitrogen, Carlsbad, CA, USA), as described elsewhere [19].

Histidine-rich protein-2 (HRP2) enzyme-linked immunosorbent assay (ELISA)

For the HRP2-ELISA, RBCs were diluted in CMCM at a haematocrit of 3%. Parasitaemia was adjusted to 0.05% using RBCs obtained from healthy volunteer donors. A volume of 100 µL was distributed into the wells of a 96-well plate, previously loaded with 100 µL of anti-malarial drugs at different concentrations or 100 µL of CMCM for the drug-free controls. Plates were incubated for

72 hrs at 37°C in 5% CO₂, after which they were frozen at -20°C until the HRP2-ELISA was performed according to standard procedures [21].

Data analysis

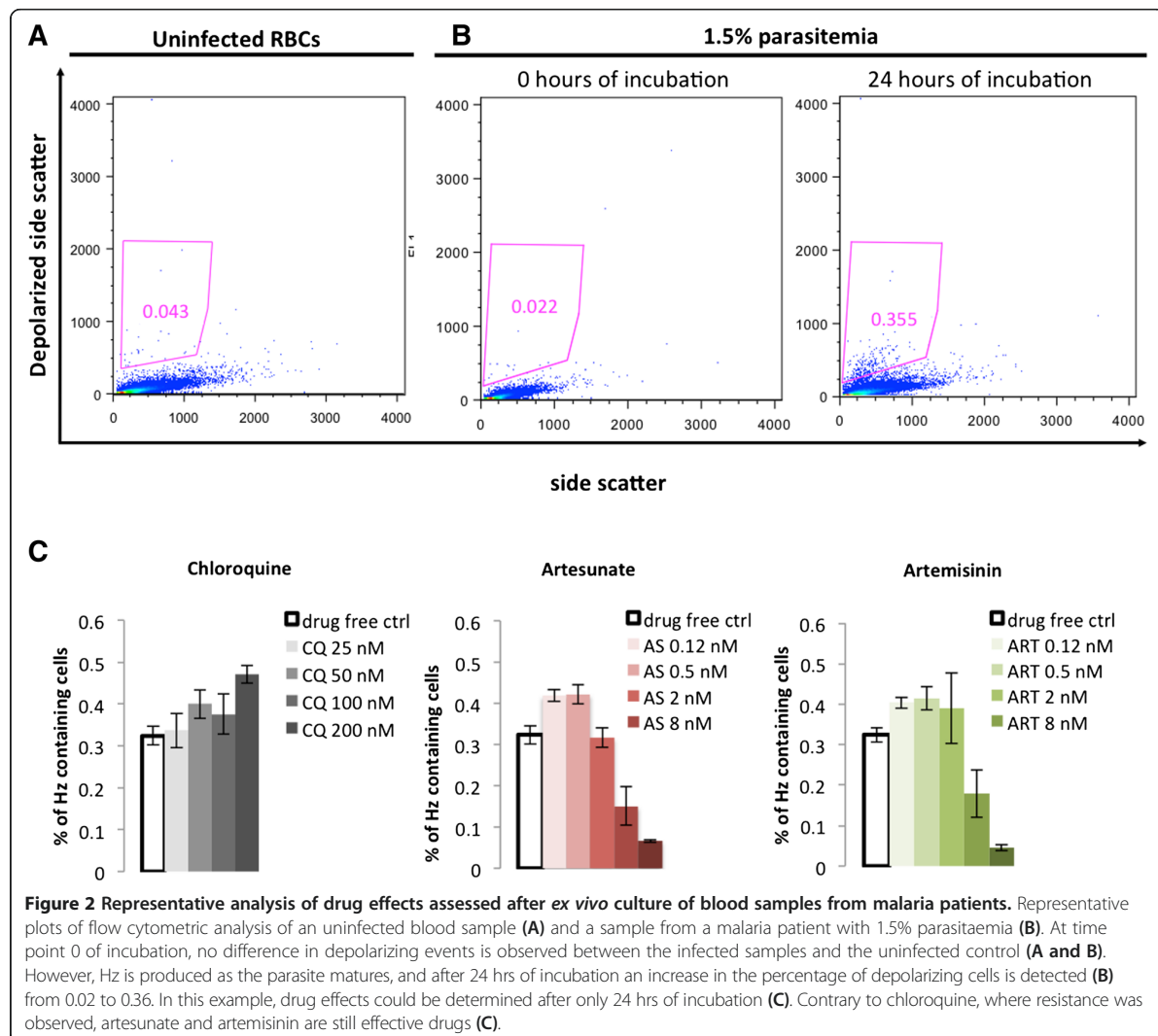
Flow cytometry results were analysed using FlowJo software (version 9.0.2, Tree Star Inc., Oregon, USA). Depolarizing events were defined in plots of SSC versus depolarized-SSC, as those with a signal above the background observed in the uninfected control (gate in Figure 2A and B). To determine SYBR green I-positive cells, green fluorescence (FL1) versus red fluorescence (FL3) plots were used. The FL1 detector had a 527/30 band-pass filter and FL2 had a 620-nm long-pass filter. SYBR green I-positive events were established based on a stained uninfected control and had to be adjusted at each time point, always using the uninfected SYBR green I-stained sample from the corresponding time

point. A non-linear regression model (sigmoidal dose-response/variable slope) was used to calculate the individual 50% inhibitory concentrations, with SigmaPlot-Systat Software (Chicago, IL, USA). Only those samples with a ≥2 ratio of drug-free control to highest drug concentration were included.

Results and discussion

Growth and maturation of wild-type *Plasmodium falciparum* strains

Forty-six samples from malaria patients were analysed during this study. Parasite loads ranged from 50 to 452,000 parasites/μL of blood (median of 15,000 parasites/μL). *Ex vivo* cultures of infected RBCs showed that parasites had four different growth profiles (Table): (i) seven samples showed no maturation, as defined by an increase in depolarization; (ii) another eight samples



showed maturation at 24 hrs and replication at 48 hrs; (iii) 17 samples showed maturation at 24 hrs but no re-invasion occurred; and, (iv) 14 samples had a delay in parasite growth, with maturation being observed at 48 hrs and replication at 72 hrs.

One crucial step in the *in vitro* sensitivity assays is the culture of parasites [22]. Maturation of *Plasmodium falciparum* from early rings to late schizonts takes 42–48 hrs *in vitro* [23] and consequently, an increase in parasitaemia can only be observed every 42–48 hrs, after re-invasion of RBCs occurs. Differences in *ex vivo* parasite maturation and replication have already been observed in strains obtained directly from different patients [24,25]. Indeed many factors related to the protocol, the host and the parasite itself might greatly influence the *in vitro* growth of parasites.

Regarding the protocol factors, such as the type of anticoagulant used to collect the blood from the patients to the atmosphere where the parasites will be incubated, have to be taken into account [7]. During this study EDTA-collected blood was used. Although the use of EDTA is discouraged by the reference protocol from MR4 [26] it has been shown by different studies that EDTA-collected blood can be successfully used for *ex vivo* drug testing [27–31]. In one of these reports even long-term cultures of parasites present in patients' blood were accomplished [31]. Moreover, the use of specific anticoagulants requires drawing more blood just for the purpose of sensitivity testing. This can be avoided by using EDTA-anticoagulated blood, which was obtained as part of the routine FBC analysis, preventing all inherent problems associated with an extra blood drawing.

The incubation atmosphere recommended for *P. falciparum* growth in culture include the use of a low O₂ atmosphere [26]. However, such mixed gas atmospheres may not be available in the resource-limited settings found in malaria endemic countries. Because of this, it has been investigated whether a simple 5% CO₂ atmosphere could be used instead without compromising parasite survival after drug treatment [32]. Results showed no differences in parasite survival between trigas (5% CO₂, 5% O₂, 90% N₂), candle jar or a 5% CO₂ atmosphere [32].

Undoubtedly, host-specific factors, often difficult to control, ranging from the immune response to the presence of pharmacologically active substances might influence the growth of the parasite *in vitro*. Indeed, the fact that some of the patients might already have been treated at the time of blood collection during this study cannot be discarded, possibly explaining some of the differences observed in the parasites' growth profiles. Yet, it is very difficult to control for all these factors and this might not only imply detailed histories, but eventually laboratory test to confirm immune status or presence of drug-metabolites. Perhaps explaining why very few studies on this filed are including such detailed information.

Conversely, parasite-related factors may even be more important. The delay between sample collection and processing influences the viability of freshly collected clinical isolates, because it is considerably decreased after a sample has been kept for several hours at room temperature [7]. However, in one study where all 43 samples were cultured within 30 minutes of collection [25], 50% developed into schizonts within 27 hrs, while the other half reached schizont stage only between 28 and 63 hrs. In this study no correlation between the delay until culture and any of the four parasite growth patterns was observed, supporting the idea that possible host factors may have been more relevant.

Detection of anti-malarial drug effects by the haemozoin assay

In *P. falciparum*-infected patients the majority of circulating iRBC are ring forms that contain little or no detectable Hz, as observed in a previous report whereby flow cytometric assessment of Hz these forms could not be detected [33]. This study confirms this observation, as at 0 hrs, no difference in depolarizing events was observed between the infected and the uninfected samples (Figure 2A and B). Only after incubation the percentage of depolarizing cells increased, indicating higher Hz content and, thus maturation (Figure 2B), seen in drug-free controls or drug-resistant parasites. This contrasts with diminished or absent depolarizing events when anti-malarial drugs are effective (Figure 2C). Drug inhibitory effects were determined in 39/46 (85%) of samples, in which parasite maturation was observed (groups 2, 3 and 4). In 25 samples (groups 2 and 3), drug effects were measurable at 24 hrs, as expected from culture-adapted strains [19]. In the remaining 14 samples (group 4) parasite maturation was delayed; however, it was still possible to detect drug effects at 48 hrs of incubation.

IC₅₀ values of chloroquine and artemisinins

The IC₅₀ values are shown in the Table 1. There was a poor correlation between the IC₅₀ values of individual samples and the different assays. In fact, this is commonly observed even when using the same laboratory-adapted strain [19]. Indeed, several factors, such as the initial parasitaemia, the haematocrit and the end point for measuring parasite growth can influence IC₅₀ values [7,34]. Samples with higher initial parasitaemia (group 3), showed increased IC₅₀ values for artesunate and artemisinin (Table). Apparently, a higher initial parasitaemia may be associated with an increase in inhibitory drug concentration of artemisinin, artesunate, chloroquine, and mefloquine [11], which could explain some of the increase observed in the IC₅₀ values. Interestingly, mean IC₅₀ values for artesunate and artemisinin in isolates that had a delayed growth (group 4) were somewhat

Table 1 Summarized data of isolates exhibiting different *ex vivo* growth profiles analysed by the haemozoin assay

	Group 1	Group 2	Group 3	Group 4
Growth profile	No maturation	Maturation at 24 hrs and replication at 48 hrs	Maturation at 24 hrs but no replication	Delayed maturation
Number of samples	7	8	17	14
Parasitaemia	0.01%;	0.3%;	3.5%;	0.3%;
(median; range)	0.001-0.1%	0.2-2.2%	0.2-12%	0.1-1.9%
IC50 Artesunate (mean)	nd	10.5 nM	15.2 nM	5.6 nM
IC50 Artemisinin (mean)	nd	46 nM	47.3 nM	14.4 nM

nd – not determined.

IC50 – 50% inhibitory concentration.

Note: Results from chloroquine were not presented in this Table because the majority of the samples (32 out of 46) had IC50 values higher than 200 nM.

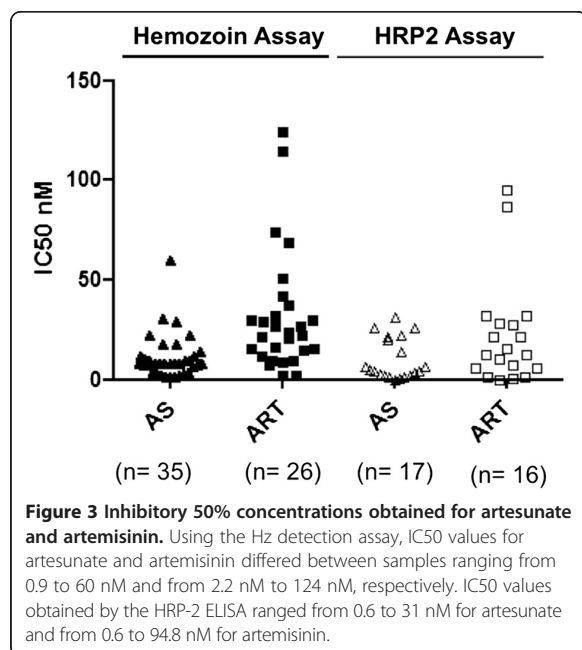
Chloroquine had an inhibitory effect in only four samples from group 3 (IC50 mean = 76.8 nM). In ten samples, chloroquine activity could not be determined.

lower than in groups 2 and 3, where maturation was detected at 24 hrs. This could be due to the different growth profile of drug exposed and non-exposed parasites in group 4. Overall, IC50 values ranged from 0.9 to 60 nM and from 2.2 nM to 124 nM for artesunate and artemisinin, respectively (Figure 3). These values are higher than previously described in the same region, using the HRP-2 assay [35]. Because several assay-related factors can influence IC50 values they may not be directly comparable between different assays [7,34]. In the previous study, the final haematocrit was 1.5% [35], while in the Hz detection assay it was 2.5%. It has been observed that higher haematocrits may cause an increase in IC50 values [34]. Preliminary data using the same culture-adapted strain showed that the IC50 value for dihydroartemisinin increases from 1.7 nM to 7.5 nM when the haematocrit of the sample is raised from 1 to 2.5% (unpublished data).

For chloroquine, 70% of the samples had IC50 values higher than 200 nM, indicating resistance, which is in line with an earlier reports and which is explained through the high usage of amodiaquine, many years after the use of chloroquine had been curbed and finally abandoned [36,37]. In Malawi [38,39], Kenya [40] and Tanzania [41], chloroquine resistance decreased after its withdrawal, contrary to the study site, even though chloroquine treatment was discontinued 11 years ago, as observed by others [37,42]. One explanation brought forward is the use of artesunate/amodiaquine, because amodiaquine appears to select mutant *pfprt* allele, which is responsible for chloroquine resistance [43].

Interestingly, the Hz-detection assay showed in some of the chloroquine-resistant strains that the percentage of Hz-containing cells increased as chloroquine concentration increased as well (Figure 2C). It is known that several drugs, specially quinoline-type drugs, directly interact with Hz, as discussed elsewhere [44]. This interaction may lead to alterations in the crystals distribution within the parasite that may affect the depolarized light signal. Recently it has been shown that parasites containing several small but distributed Hz crystals can have a higher depolarized signal than a parasite containing a single large clump of Hz [45]. In this context it is not unlikely that at higher concentrations of chloroquine some of the drug may interact with Hz avoiding its coalescence. Thus, explaining why at higher concentrations of this drug the signal seems to be increased. Certainly, the mechanism of this observation is not known, and further investigation is required to understand the exact cause of this phenomenon.

During this study the HRP2-ELISA was performed alongside. However, drug effects could only be detected in 17 samples (37%), with IC50 values ranging from 0.6 to 31 nM for artesunate and 0.6 to 94.8 nM for artemisinin (Figure 3). This success rate appears to be at the lower end of reported studies with 45% [14], while others had success rates of 75% [46] and 87% [13]. Of note, these samples were collected on purpose to be used exclusively in the scope of these studies. Contrary



to this, here, samples were collected for other purposes, which might have contributed to a lower success rate. Furthermore, samples were preselected based on their parasitaemias of 0.01% or higher [13], while in this study all samples were included. Apparently, re-invasion of uninfected RBCs (replication) is considered the main criterion for the success of the HRP2 assay [21]. However, even when no schizont maturation is observed after 24 hrs of incubation, samples can still be successfully tested by the HRP2 assay [21]. During this study, most results (14 out of 17) were obtained in samples that exhibited delayed-growing parasites (group 4), whereas drug effects were only detected in two samples from groups 1 and 2, and in five samples from group 3.

Indeed, the low detection limit is a major advantage of the HRP2 assay. For instance, the Hz assay failed to determine drug effects in samples from group 1, possibly due to the low parasitaemias present in this group, which were below the previously reported 0.3% detection limit of the Hz assay [19]. On the other hand, when parasitaemias are higher than 0.1% [21], samples have to be diluted with uninfected RBCs from healthy donors, which can be a limiting step. Results from group 3, where the parasitaemia ranged from 0.2 to 12%, indicate that the Hz detection assay does not seem to require adjustment of the parasitaemia to allow the detection of drug effects.

Field applications of flow cytometry

The optical bench of the CyFlow® flow cytometer available on site had a typical configuration common in most small instruments, consisting of one blue-laser (488 nm) and detectors for FSC, SSC and three fluorescences FL1 (green), FL2 (orange) and FL3 (red) (Figure 1A). For the detection of light depolarization the original set-up was easily modified by simply changing the respective filters and mirrors, even taking advantage of the existing filter holders (Figure 1B). The optical bench layout required for the detection of light depolarization is simple (Figure 1C) and therefore, other instruments should also be easily modifiable, unless they use fiber-optic cables for light collection.

Few studies describe the use of flow cytometry for drug testing in the field [15,47], possibly because of the perceived expense and complexity in setting up and running such instruments. Nowadays the number of simple, robust and portable flow cytometers has increased, including instruments such as the Attune® (Life Technologies, Carlsbad, USA), the Accuri™C6 (BD Biosciences, La Jolla, USA), the Cyflow Cube 6 (Partec, Münster, Germany), among others. It has been shown that these instruments can be easily modified to detect Hz-caused light depolarization [45] and most of them can be used with an autosampler for higher throughput [48]. Moreover, the initial purchase costs of these instruments have dropped substantially from those

practiced before for larger instruments, allowing them to be used and available in the field. Indeed, recent field studies take advantage of this, by using for example the Accuri C6 [15,47]. Even smaller and simpler instruments used for CD4+ T cell counting in HIV-infected patients exist, such as the CyFlow®miniPOC from Partec, which are used in low-resource settings [49]. Although the way was often difficult, cytometry is no longer the very expensive, high-end technology based on bulky instruments. In the future, simple image cytometers might replace flow cytometers, as they seem to perform a broad range of measurements, and eventually parameters such as light depolarization could be detected as well [50,51].

Opening new avenues for anti-malarial drug testing in the field

This study showed that drug effects of clinically relevant anti-malarial drugs as well as resistance to chloroquine could be assessed by simply detecting Hz. This method measures parasite maturation and does not require re-invasion to occur; consequently, results can be obtained earlier than with other currently available methods, except for microscopy. However, microscopy relies on trained observers' ability to detect morphological changes of iRBC [52], which sometimes can be rare. Flow cytometric measurements can provide more objective, reliable and effective results than microscopy, as it has been previously observed in a different context [53]. Moreover, it allows the assessment of additional parameters, such as DNA and RNA content, which can improve parasite detection [51]. Finally, drug effects could be detected without having to decrease the sample's parasitaemia. This may greatly simplify the protocol as it avoids the need to obtain blood from healthy donors. Yet, this seems to lead to increased IC50 values. Thus, whether parasitaemia ought to be adjusted or not should be further investigated.

These findings open new avenues for other Hz-detection methods. Interestingly, several Hz detection methods exist [54-58] and they could possibly be used to detect drug effects as early, or even earlier, than the flow cytometric Hz detection.

Conclusion

This study conducted in the field showed flow cytometry could be easily implemented and performed in field conditions. Flow cytometric detection of Hz could be used as an alternative tool to assess drug effects on parasites obtained directly from patients' blood samples, without the need for additional reagents or complex protocols. However, further optimization of the Hz assay regarding its set-up conditions, for example, changing the haematocrit, may contribute to obtain IC50 values more

comparable to the ones that have been previously reported [13,59].

Future studies should be performed in various settings, to further investigate the Hz assay and its usefulness as a tool for rapid resistance testing in malaria-endemic countries.

Competing interests

The authors have declared that they have no competing interests.

Authors' contributions

TH, MR and MPG conceived the study. All field experiments were performed by MR, TH and MPG coordinated the project. CT performed the ELISA assays. MPG and JF assisted with obtaining the samples from malaria patients, provided advice on different aspects of the novel assay and its assessment under field conditions. MR and TH wrote the draft manuscript. All authors contributed to the writing, and approved the final manuscript.

Acknowledgements

This work was supported by the Luso-American Foundation (FLAD-LACR grant: B-AV-109-09/07). MR acknowledges *Fundação para a Ciência e a Tecnologia* for doctoral grant (SFRH/BD/84530/2012) and *Fundação Calouste Gulbenkian* for the Award CAML/Gulbenkian for Travel ACGT fellowship. The authors acknowledge the Albert Schweitzer Hospital's central clinic laboratory staff who provided the samples from malaria patients, the co-directors of CERME: Dr Akim Adegnika, Dr Bertrand Lell and Dr Maxime Selidji Agnandji and, finally, Dr Marguerite Massinga Loembe, Head of the CERME Research Laboratory.

Author details

¹Instituto de Medicina Molecular, Faculdade de Medicina de Lisboa, Av Prof Egas Moniz, Lisbon P-1649-028, Portugal. ²Centre de Recherches Médicales de Lambaréné - CERME, Albert Schweitzer Hospital, Lambaréné, Gabon. ³Institut für Tropenmedizin, Universität Tübingen, Tübingen, Germany. ⁴Centre of Tropical Medicine and Travel Medicine, Amsterdam Medical Centre, University of Amsterdam, Amsterdam, The Netherlands. ⁵Instituto de Microbiologia, Faculdade de Medicina, Lisbon, Portugal.

Received: 26 December 2014 Accepted: 17 March 2015

Published online: 01 April 2015

References

- Kweka EJ, Mazigo HD, Munga S, Magesa SM, Mboera LEG. Challenges to malaria control and success stories in Africa. *Global Health Perspectives*. 2013;1:71–80.
- Noedl H, Se Y, Schaefer K, Smith BL, Socheat D, Fukuda MM, et al. Evidence of artemisinin-resistant malaria in western Cambodia. *N Engl J Med*. 2008;359:2619–20.
- Dondorp AM, Nosten F, Yi P, Das D, Phyto AP, Tarning J, et al. Artemisinin resistance in *Plasmodium falciparum* malaria. *N Engl J Med*. 2009;361:455–67.
- WHO. Global plan for artemisinin resistance containment (GPARC). Geneva: World Health Organization; 2011.
- Ashley EA, Dhorda M, Fairhurst RM, Amaratunga C, Lim P, Suon S, et al. Spread of artemisinin resistance in *Plasmodium falciparum* malaria. *N Engl J Med*. 2014;371:411–23.
- Van Hong N, Amambua-Ngwa A, Tuan NQ, Cuong Do D, Giang NT, Van Dung N, et al. Severe malaria not responsive to artemisinin derivatives in man returning from Angola to Vietnam. *Emerg Infect Dis*. 2014;20:1199–202.
- Basco LK. Field application of *in vitro* assays for the sensitivity of human malaria parasites to antimalarial drugs. Geneva, Switzerland: WHO Press; 2007.
- Woodrow CJ, Krishna S. Antimalarial drugs: recent advances in molecular determinants of resistance and their clinical significance. *Cell Mol Life Sci*. 2006;63:1586–96.
- Ariey F, Witkowski B, Amaratunga C, Beghain J, Langlois AC, Khim N, et al. A molecular marker of artemisinin-resistant *Plasmodium falciparum* malaria. *Nature*. 2014;505:50–5.
- Rieckmann KH, Campbell GH, Sax LJ, Mrema JE. Drug sensitivity of *Plasmodium falciparum*. An *in-vitro* microtechnique. *Lancet*. 1978;1:22–3.
- Duraisingh MT, Jones P, Sambou I, Von Seidlein L, Pinder M, Warhurst DC. Inoculum effect leads to overestimation of *in vitro* resistance for artemisinin derivatives and standard antimalarials: a Gambian field study. *Parasitology*. 1999;119:435–40.
- Basco LK, Marquet F, Makler MM, Le Bras J. *Plasmodium falciparum* and *Plasmodium vivax*: lactate dehydrogenase activity and its application for *in vitro* drug susceptibility assay. *Exp Parasitol*. 1995;80:260–71.
- Noedl H, Attlmayr B, Wernsdorfer WH, Kollaritsch H, Miller RS. A histidine-rich protein 2-based malaria drug sensitivity assay for field use. *Am J Trop Med Hyg*. 2004;71:711–4.
- Bacon DJ, Latour C, Lucas C, Colina O, Ringwald P, Picot S. Comparison of a SYBR green I-based assay with a histidine-rich protein II enzyme-linked immunosorbent assay for *in vitro* antimalarial drug efficacy testing and application to clinical isolates. *Antimicrob Agents Chemother*. 2007;51:1172–8.
- Russell B, Malleret B, Suwanarusk R, Anthony C, Kanlaya S, Lau YL, et al. Field-based flow cytometry for *ex vivo* characterization of *Plasmodium vivax* and *P. falciparum* antimalarial sensitivity. *Antimicrob Agents Chemother*. 2013;57:5170–4.
- Noedl H, Wongsrichanalai C, Wernsdorfer WH. Malaria drug-sensitivity testing: new assays, new perspectives. *Trends Parasitol*. 2003;19:175–81.
- Wein S, Maynadier M, Tran Van Ba C, Cerdan R, Peyrottes S, Fraisse L, et al. Reliability of antimalarial sensitivity tests depends on drug mechanisms of action. *J Clin Microbiol*. 2010;48:1651–60.
- Grimberg BT, Erickson JJ, Sramkoski RM, Jacobberger JW, Zimmerman PA. Monitoring *Plasmodium falciparum* growth and development by UV flow cytometry using an optimized Hoechst-thiazole orange staining strategy. *Cytometry A*. 2008;73:546–54.
- Rebello M, Sousa C, Shapiro HM, Mota MM, Grobusch MP, Hänscheid T. A novel flow cytometric hemozoin detection assay for real-time sensitivity testing of *Plasmodium falciparum*. *PLoS One*. 2013;8:e61606.
- Planche T, Krishna S, Kombila M, Engel K, Faucher JF, Ngou-Milama E, et al. Comparison of methods for the rapid laboratory assessment of children with malaria. *Am J Trop Med Hyg*. 2001;65:599–602.
- Noedl H, Bronnert J, Yingyuen K, Attlmayr B, Kollaritsch H, Fukuda M. Simple histidine-rich protein 2 double-site sandwich enzyme-linked immunosorbent assay for use in malaria drug sensitivity testing. *Antimicrob Agents Chemother*. 2005;49:3575–7.
- Basco LK, Ringwald P. *In vitro* activities of piperazine and other 4-aminoquinolines against clinical isolates of *Plasmodium falciparum* in Cameroon. *Antimicrob Agents Chemother*. 2003;47:1391–4.
- Gritzmacher CA, Reese RT. Protein and nucleic acid synthesis during synchronized growth of *Plasmodium falciparum*. *J Bacteriol*. 1984;160:1165–7.
- Lopez Antunano FJ, Wernsdorfer WH. *In vitro* response of chloroquine resistant *Plasmodium falciparum* to mefloquine. *Bull World Health Organ*. 1979;57:663–5.
- Inaba H, Ohmae H, Kano S, Faarado L, Boaz L, Leafasia J, et al. Variation of incubation time in an *in vitro* drug susceptibility test of *Plasmodium falciparum* isolates studied in the Solomon Islands. *Parasitol Int*. 2001;50:9–13.
- Nielsen MA, Staalsøe T. *Establishment of long-term in vitro cultures of Plasmodium falciparum from patient blood*. In: Moll K, Ljungstrom I, Perlmann H, Scherf A, Wahlgren M, editors. *Methods in Malaria Research*. 5th ed. Manassas, Virginia: MRA/ATCC; 2008. p. 4–6.
- Lim P, Chim P, Sem R, Nemh S, Poravuth Y, Lim C, et al. *In vitro* monitoring of *Plasmodium falciparum* susceptibility to artesunate, mefloquine, quinine and chloroquine in Cambodia: 2001–2002. *Acta Trop*. 2005;93:31–40.
- Kaddouri H, Nakache S, Houzé S, Mentré F, Le Bras J. Assessment of the drug susceptibility of *Plasmodium falciparum* clinical isolates from Africa by using a *Plasmodium* lactate dehydrogenase immunodetection assay and an inhibitory maximum effect model for precise measurement of the 50-percent inhibitory concentration. *Antimicrob Agents Chemother*. 2006;50:3343–9.
- Rason MA, Randrianntsoa T, Andrianantenaina H, Ratsimbaoa A, Menard D. Performance and reliability of the SYBR Green I based assay for the routine monitoring of susceptibility of *Plasmodium falciparum* clinical isolates. *Trans R Soc Trop Med Hyg*. 2008;102:346–51.
- Legrand E, Volney B, Meynard JB, Mercereau-Pujjalon O, Esterre P. *In vitro* monitoring of *Plasmodium falciparum* drug resistance in French Guiana: a synopsis of continuous assessment from 1994 to 2005. *Antimicrob Agents Chemother*. 2008;52:288–98.
- Van Schalkwyk DA, Burrow R, Henriques G, Gadalla NB, Beshir KB, Hasford C, et al. Culture-adapted *Plasmodium falciparum* isolates from UK travellers: *in vitro* drug sensitivity, clonality and drug resistance markers. *Malar J*. 2013;12:320.

32. Witkowski B, Amaratunga C, Khim N, Sreng S, Chim P, Kim S, et al. Novel phenotypic assays for the detection of artemisinin-resistant *Plasmodium falciparum* malaria in Cambodia: in-vitro and ex-vivo drug-response studies. *Lancet Infect Dis*. 2013;13:1043–9.
33. Rebello M, Shapiro HM, Amaral T, Melo-Cristino J, Hanscheid T. Haemozoin detection in infected erythrocytes for *Plasmodium falciparum* malaria diagnosis—Prospects and limitations. *Acta Trop*. 2012;123:58–61.
34. Basco LK. Molecular epidemiology of malaria in Cameroon. XX. Experimental studies on various factors of *in vitro* drug sensitivity assays using fresh isolates of *Plasmodium falciparum*. *Am J Trop Med Hyg*. 2004;70:474–80.
35. Held J, Soomro SA, Kreamsner PG, Jansen FH, Mordmüller B. *In vitro* activity of new artemisinin derivatives against *Plasmodium falciparum* clinical isolates from Gabon. *Int J Antimicrob Agents*. 2011;37:485–8.
36. Grobusch MP, Adagu IS, Kreamsner PG, Warhurst DC. *Plasmodium falciparum*: *in vitro* chloroquine susceptibility and allele-specific PCR detection of PfmDr1Asn86Tyr polymorphism in Lambarene, Gabon. *Parasitology*. 1998;116:211–7.
37. Borrmann S, Binder RK, Adegnikaa AA, Missinou MA, Issifou S, Ramharter M, et al. Reassessment of the resistance of *Plasmodium falciparum* to chloroquine in Gabon: implications for the validity of tests *in vitro* vs. *in vivo*. *Trans R Soc Trop Med Hyg*. 2002;96:660–3.
38. Kublin JG, Cortese JF, Njunju EM, Mukadam RA, Wirima JJ, Kazembe PN, et al. Reemergence of chloroquine sensitive *Plasmodium falciparum* malaria after cessation of chloroquine use in Malawi. *J Infect Dis*. 2003;187:1870–5.
39. Laufer MK, Thesing PC, Eddington ND, Masonga R, Dzinjalimala FK, Takala SL, et al. Return of chloroquine antimalarial efficacy in Malawi. *N Engl J Med*. 2006;355:1959–66.
40. Mwai L, Ochong E, Abdurahman A, Kiara SM, Ward S, Kokwaro G, et al. Chloroquine resistance before and after its withdrawal in Kenya. *Malar J*. 2009;8:106.
41. Alifrangis M, Lusingu JP, Mmbando B, Dalgaard MB, Vestergaard LS, Ishengoma D, et al. Five-year surveillance of molecular markers of *Plasmodium falciparum* antimalarial drug resistance in Korogwe District, Tanzania: accumulation of the 581G mutation in the *P. falciparum* dihydropteroate synthase gene. *Am J Trop Med Hyg*. 2009;80:523–7.
42. Frank M, Lehnert N, Mayengue PI, Gabor J, Dal-Bianco M, Kombila DU, et al. A thirteen-year analysis of *Plasmodium falciparum* populations reveals high conservation of the mutant pfcr1 haplotype despite the withdrawal of chloroquine from national treatment guidelines in Gabon. *Malar J*. 2011;10:304.
43. Djimdé AA, Fofana B, Sagara I, Sidibe B, Toure S, Dembele D, et al. Efficacy, safety, and selection of molecular markers of drug resistance by two ACTs in Mali. *Am J Trop Med Hyg*. 2008;78:455–61.
44. Gorka AP, De Dios A, Roepe PD. Quinoline drug-heme interactions and implications for antimalarial cytostatic versus cytotoxic activities. *J Med Chem*. 2013;56:5231–46.
45. Rebello M, Tempera C, Bispo C, Andrade C, Gardner R, Shapiro M, et al. Light depolarization measurements in malaria: a new job for an old friend. *Cytometry A* 2015;in press.
46. Noedl H, Krudsood S, Leowattana W, Tangpukdee N, Thanachartwet W, Looareesuwan S, et al. *In vitro* antimalarial activity of azithromycin, artesunate, and quinine in combination and correlation with clinical outcome. *Antimicrob Agents Chemother*. 2007;51:651–6.
47. Amaratunga C, Neal AT, Fairhurst RM. Flow cytometry-based analysis of artemisinin-resistant *Plasmodium falciparum* in the ring-stage survival assay. *Antimicrob Agents Chemother*. 2014;58:4938–40.
48. Partec – Cyflow Cube 6. <http://www.sysmex-partec.com/fileadmin/media/pdf/CyFlow-Cube6.pdf>. Accessed: 17 December 2014.
49. Boyle DS, Hawkins KR, Steele MS, Singhal M, Cheng X. Emerging technologies for point-of-care CD4 T-lymphocyte counting. *Trends Biotechnol*. 2012;30:45–54.
50. Shapiro HM, Mandy F. Cytometry in malaria: moving beyond Giemsa. *Cytometry A*. 2007;71:643–5.
51. Shapiro HM, Apte SH, Chojnowski GM, Hanscheid T, Rebello M, Grimberg BT. Cytometry in malaria—a practical replacement for microscopy? *Curr Protoc Cytom*. 2013;11:11–20.
52. Maguire JD, Lederman ER, Barcus MJ, O'Meara WA, Jordan RG, Duong S, et al. Production and validation of durable, high quality standardized malaria microscopy slides for teaching, testing and quality assurance during an era of declining diagnostic proficiency. *Malar J*. 2006;5:92.
53. Hanscheid T, Frita R, Längin M, Kreamsner PG, Grobusch MP. Is flow cytometry better in counting malaria pigment-containing leukocytes compared to microscopy? *Malar J*. 2009;8:255.
54. Mens PF, Matelon RJ, Nour BY, Newman DM, Schallig HD. Laboratory evaluation on the sensitivity and specificity of a novel and rapid detection method for malaria diagnosis based on magneto-optical technology (MOT). *Malar J*. 2011;9:207.
55. Wilson BK, Behrend MR, Horning MP, Hegg MC. Detection of malarial byproduct hemozoin utilizing its unique scattering properties. *Opt Express*. 2011;19:12190–6.
56. Lukianova-Hleb EY, Campbell KM, Constantinou PE, Braam J, Olson JS, Ware RE, et al. Hemozoin-generated vapor nanobubbles for transdermal reagent- and needle-free detection of malaria. *Proc Natl Acad Sci U S A*. 2014;111:900–5.
57. Orbán A, Butykai A, Molnár A, Pröhle Z, Fülöp G, Zelles T, et al. Evaluation of a novel magneto-optical method for the detection of malaria parasites. *PLoS One*. 2014;9:e96981.
58. Peng WK, Kong TF, Ng CS, Chen L, Huang Y, Bhagat AA, et al. Micromagnetic resonance relaxometry for rapid label-free malaria diagnosis. *Nat Med*. 2014;20:1069–73.
59. Kreidenweiss A, Kreamsner PG, Mordmüller B. Comprehensive study of proteasome inhibitors against *Plasmodium falciparum* laboratory strains and field isolates from Gabon. *Malar J*. 2008;7:187.

Submit your next manuscript to BioMed Central and take full advantage of:

- Convenient online submission
- Thorough peer review
- No space constraints or color figure charges
- Immediate publication on acceptance
- Inclusion in PubMed, CAS, Scopus and Google Scholar
- Research which is freely available for redistribution

Submit your manuscript at
www.biomedcentral.com/submit





Light Depolarization Measurements in Malaria: A New Job for an Old Friend

Maria Rebelo,^{1*} Carolina Tempera,¹ Claudia Bispo,² Claudia Andrade,²
Rui Gardner,² Howard M. Shapiro,³ Thomas Hänscheid¹

¹Molecular Microbiology and Infection Unit, Instituto De Medicina Molecular, Faculdade De Medicina, Lisbon, Portugal

²Cellular Imaging Unit, Instituto Gulbenkian de Ciência, Oeiras, Portugal

³The Center for Microbial Cytometry, 283 Highland Avenue, West Newton, Massachusetts

Received 27 October 2014; Revised 28 January 2015; Accepted 27 February 2015

Grant sponsor: Luso-American Foundation (FLAD-LACR), Grant number: B-A-V-109-09/07

Grant sponsor: FCT, Grant number: SFRH/BD/84530/2012

Additional Supporting Information may be found in the online version of this article.

Correspondence to: Maria Rebelo, Instituto de Medicina Molecular, Faculdade de Medicina de Lisboa, Av. Prof. Egas Moniz, P-1649-028 Lisboa, Portugal
E-mail: mariarebelo@fm.ul.pt

Authors' contributions: Thomas Hänscheid and Howard M Shapiro initiated and ensured follow-up of the project. Maria Rebelo, Thomas Hänscheid and Howard M Shapiro wrote the manuscript. Maria Rebelo and Carolina Tempera performed the measurements with different types of hemozoin, flow cytometric analysis and culture related work. Rui Gardner, Claudia Bispo and Claudia Andrade performed the sorting experiments, tested the different wavelengths and also revised the manuscript.

Published online 00 Month 2015 in Wiley Online Library (wileyonlinelibrary.com)

DOI: 10.1002/cyto.a.22659

• Abstract

The use of flow cytometry in malaria research has increased over the last decade. Most approaches use nucleic acid stains to detect parasite DNA and RNA and require complex multi-color, multi-parameter analysis to reliably detect infected red blood cells (iRBCs). We recently described a novel and simpler approach to parasite detection based on flow cytometric measurement of scattered light depolarization caused by hemozoin (Hz), a pigment formed by parasite digestion of hemoglobin in iRBCs. Depolarization measurement by flow cytometry was described in 1987; however, patent issues restricted its use to a single manufacturer's hematology analyzers until 2009. Although we recently demonstrated that depolarization measurement of Hz, easily implemented on a bench top flow cytometer (Cyflow), provided useful information for malaria work, doubts regarding its application and utility remain in both the flow cytometry and malaria communities, at least in part because instrument manufacturers do not offer the option of measuring depolarized scatter. Under such circumstances, providing other researchers with guidance as to how to do this seemed to offer the most expeditious way to resolve the issue. We accordingly examined how several commercially available flow cytometers (CyFlow SL, MoFLO, Attune and Accuri C6) could be modified to detect depolarization due to the presence of free Hz on solution, or of Hz in leukocytes or erythrocytes from rodent or human blood. All were readily adapted, with substantially equivalent results obtained with lasers emitting over a wide wavelength range. Other instruments now available may also be modifiable for Hz measurement. Cytometric detection of Hz using depolarization is useful to study different aspects of malaria. Adding additional parameters, such as DNA content and base composition and RNA content, can demonstrably provide improved accuracy and sensitivity of parasite detection and characterization, allowing malaria researchers and eventually clinicians to benefit from cytometric technology. © 2015 International Society for Advancement of Cytometry

• Key terms

Key terms: polarization; depolarized side scatter; hemozoin; flow cytometry; malaria; light depolarization

MALARIA remains one of the most important parasitic diseases, killing around 700,000 people each year (1). Reliable detection of parasites and identification of the species are crucial for clinical diagnosis, as well as for many research applications. Both may require differentiation of asexual and sexual forms, determination of different maturation stages, and reliable quantification of parasite density (numbers per unit volume of blood or percentage of infected red blood cells). Antimalarial drug development and assessment of resistance to drugs may additionally require evaluation of parasite metabolic state and viability. Cytometry could potentially provide an alternative to microscopy of Giemsa stained smears (2), the accepted method for diagnosis for over a century.

Malaria parasites growing inside infected erythrocytes (iRBCs) catabolize hemoglobin, producing the strongly absorbing and birefringent pigment hemozoin (Hz).

Table 1. Samples and protocols used for preparation of samples

SAMPLES	PROTOCOL	REFERENCES
<i>Plasmodium berghei</i> infected red blood cells	BALB/c mice (Charles River, Spain) were infected with the transgenic <i>P. berghei</i> ANKA (259 cl2) that constitutively expresses GFP during the whole life cycle. Blood samples were collected by cardiac puncture into a heparinized collection tube, as described elsewhere.	(30)
<i>Plasmodium falciparum</i> infected red blood cells	<i>P. falciparum</i> 3D7 strain was obtained from MR4 (ATCC, Manassas, VA) and kept in continuous culture according to the recommendations of the Malaria Research and Reference Reagent Resource Center (MR4) and as previously described elsewhere (32). Cultures were maintained at 5% hematocrit, at 37 °C in an atmosphere of 5% CO ₂ .	(32)
Intraleukocytic hemozoin	Human peripheral blood mononucleated cells (PBMCs) were incubated with synthetic Hz, as described elsewhere (30). Briefly, PBMCs were isolated from blood collected from healthy volunteers and placed in a Ficoll gradient (Ficoll-Paque Plus, GE Healthcare, Uppsala, Sweden), where the interface containing the PBMCs was collected after centrifugation. PBMCs were washed, counted and resuspended at a concentration of 5 x 10 ⁵ PBMC/ml. Synthetic Hz (obtained as explained below) was added at 50 uM (hme equivalent) and the plate was incubated for 6 h at 37 °C in 5% CO ₂ (33).	(30,33)
Synthetic hemozoin	Synthetic hemozoin was obtained by the method described by Slater et al. (1991), with some modifications previously reported.	(64,65)

Once the parasite completes its growth cycle in the iRBC, Hz is released and, subsequently ingested by peripheral blood phagocytes (3). The presence and form of Hz in iRBCs are useful characteristics for distinguishing various species and developmental stages; observation of Hz, known to be associated with malaria, in cells in unstained blood led Alphonse Laveran to the initial discovery of malaria parasites in 1880 (3). Staining came later.

In addition to strongly absorbing light at wavelengths between 300 and 700 nm, Hz is able to depolarize light and can, as has long been known, be detected by optical methods such as dark-field microscopy (4–7) or depolarization microscopy (8,9). In the latter, crossed polarizing filters are inserted in the illumination and observation paths of a microscope and bright spots indicate the presence of Hz.

By 1987, it had been shown that flow cytometry of DNA and RNA content of iRBCs could differentiate stages and, in some cases, species (10,11). Flow cytometry has since been used to study parasite physiology and response to antimalarial drugs (12–17). This is most often done using fluorescent DNA and RNA stains and complex multi-color, multi-parameter analysis (2,18); additional maturation/viability markers may also be measured (17,19).

Also in 1987, it was reported that depolarized light scatter could also be detected by flow cytometry; this was initially recognized as providing a simple, reagent-free means to distinguish eosinophil from neutrophil leukocytes based on the birefringence of eosinophil granules (20). A patent (US, Patent: 5017497: <http://www.google.com/patents/US5017497> accessed on 01/08/2014) on the procedure was licensed by Abbott Diagnostics (Santa Clara, CA) and used in their Cell-Dyn hematology analyzers; the patent also prevented manu-

facturers of research flow cytometers from offering the measurement in their apparatus.

In 1999, it was found that Hz-containing monocytes in the blood of malaria patients could be detected by the Cell-Dyn analyzers (21). Since then, several other studies have reported the detection of Hz inside monocytes and neutrophils with both those instruments and user-modified research flow cytometers (22–25), and the use of hematology analyzers to diagnose malaria in non-endemic and endemic countries has been extensively reviewed elsewhere (26). Of note, some of these studies reported the possibility of detecting Hz in iRBCs as well (22,27).

With the patent no longer in force, we recently implemented depolarized scatter measurement on a bench top flow cytometer (Cyflow SL, Partec/Sysmex). This permitted comparing cytometric detection of Hz-containing leukocytes using this cytometer and the Cell-Dyn instrument with microscopy (28,29). More importantly, it confirmed that Hz inside iRBCs could be detected, leading to further studies (30,31).

Although this work attracted some interest in both the malaria and the flow cytometry communities, questions remained as to whether and how readily depolarized scatter measurements could be easily installed and measured on other common instruments, what kind of Hz can be detected (e.g., free Hz, intraleukocytic Hz, intraerythrocytic Hz from rodent or human parasites), and to what extent aspects of instrument setup, e.g., the laser wavelengths, might interfere with measurements. Addressing these issues, we have now shown that light depolarization caused by Hz from different sources can be easily detected in a variety of flow cytometers. We hope that this will encourage malaria researchers and clinicians to make productive use of the technique.

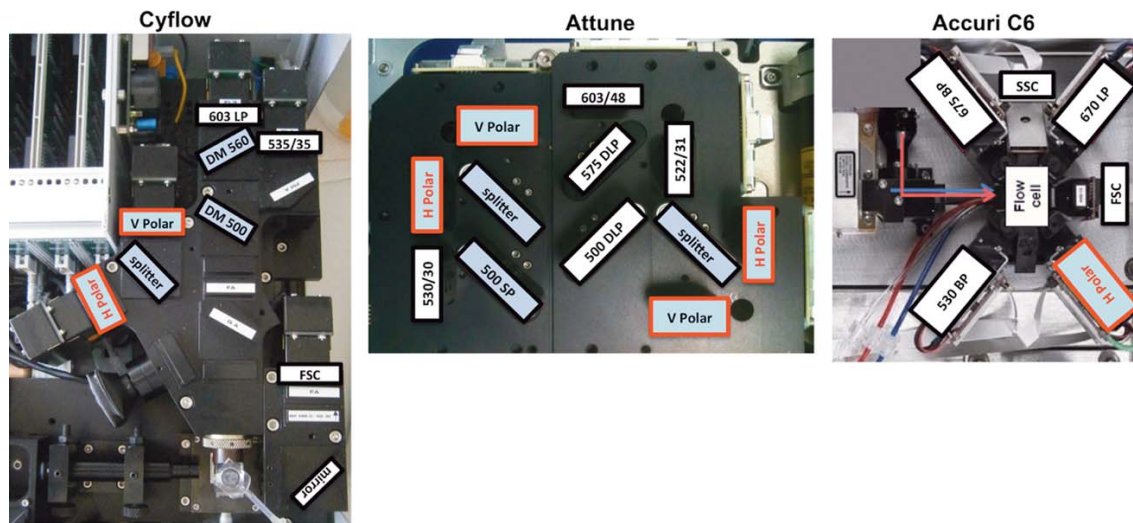


Figure 1. Optical layout of three different bench top flow cytometers modified to detect light depolarization. Three bench top flow cytometers were adapted to detect light depolarization caused by hemozoin. The Cyflow (Partec) and the Attune (Life Technologies) were modified similarly, briefly: two sides-scatter detectors (SSC) (red boxes) were created by placing a 50/50 beam splitter between them, and a horizontally polarized filter (H polar) was placed in front of one of the SSC detectors. In the Attune this was done twice: for the blue and violet lasers optical paths. The Accuri C6 (BD Biosciences) was easily modified by replacing the emission filter in front of the second detector of fluorescence with a 488 nm filter coupled with a polarizer filter with its axis in the horizontal plane; no further alterations were required. Boxes with the blue background represent the optical components that were modified in comparison to the original set up. [Color figure can be viewed in the online issue, which is available at wileyonlinelibrary.com.]

MATERIAL AND METHODS

Samples

Free synthetic Hz, *Plasmodium berghei* (rodent) and *Plasmodium falciparum* (human) infected RBC, as well as Hz containing human peripheral blood mononucleated cells (PBMCs) were analyzed (Table 1).

P. falciparum infected red blood cells were fixed with 2% paraformaldehyde (PFA) and stained with SYBR green I at 1x (Invitrogen, Carlsbad, CA, USA).

Flow Cytometric Detection of Depolarized Side Scattered Light

Depolarized side scatter detection was implemented using the following flow cytometers (Figs. 1 and 2):

The CyFlow Blue (Sysmex/Partec, Munster, Germany), has a 488 nm excitation laser, and detectors for Forward Scatter (FSC), Side Scatter (SSC), green fluorescence—FL1 (BP 535/35 nm), orange fluorescence—FL2 (BP 590/50 nm) and red fluorescence—FL3 (LP 630 nm). For this study the instrument was modified as described elsewhere (30). Briefly, two SSC detectors were created, with a 50/50 beam splitter between them. A polarizing filter coupled with a 488 nm filter was placed in front of one of the SSC detectors with the filter's axis of polarization horizontal and therefore orthogonal to the vertical polarization plane of the laser light, allowing the detection of depolarized side scatter.

The MoFlo high speed cell sorter (Beckman Coulter, Fort Collins, CO, USA) optical set-up was modified as described in Krämer 2001 and Frita 2011 (23,30). Briefly, scattered light

from a 488 nm laser (200 mW air-cooled Sapphire, Coherent) was split in two using a 95/5 beam splitter to measure normal SSC (5% of the light) and depolarized SSC (95% of the light) by placing a polarization filter with its axis of polarization orthogonally to the polarization plane of the laser illumination. Both detectors had 488/10 nm bandpass filters; O.D. 1.0 and 2.0 neutral density (ND) filters were, respectively, fitted to the normal and depolarized SSC detectors. SYBR-Green fluorescence, diverted by a 505DCRX dichroic filter ahead of the polarizer, was detected through a 540/30 nm bandpass filter.

The Attune Acoustic Focusing Cytometer (Life Technologies, Carlsbad, CA, USA) is equipped with 488 nm and 405 nm lasers with detectors for: FSC, SSC, and six fluorescence regions (BP 530/30, BP 574/26, LP 640, BP 603/48, BP522/31 and BP 450/40). Two SSC detectors were created, with a 50/50 beam splitter between them, and polarizing filters were placed orthogonally to the polarization plane of each laser light, one in front of a detector in the violet laser optical path (VL2) and the other in front of the fluorescence detector of the blue laser path (BL2).

The Accuri C6 (BDBiosciences, La Jolla, USA) is equipped with a 488 nm solid state laser and a 640 nm diode laser, detectors for FSC, SSC and four fluorescence detectors with the following optical filters: BP 533/30 (FL1), BP 585/40 (FL2), LP 670 (FL3), and BP 675/25 (FL4). The BP 585/40A fluorescence filter in the FL2 detector was replaced by a 488 nm bandpass filter coupled with a plastic polarizing filter oriented orthogonally to the polarization plane of the laser light, allowing detection of depolarized side scatter.

Measuring Depolarized Scatter with Different Wavelengths Using a MoFlo

Depolarized side scatter was measured at different wavelengths on a MoFlo using a Coherent Innova I90C Argon laser tuned to multiline UV at 1.10 W, 457 nm at 80 mW, 488 nm at 80 mW, or 514 nm at 80 mW. Each laser line was used sepa-

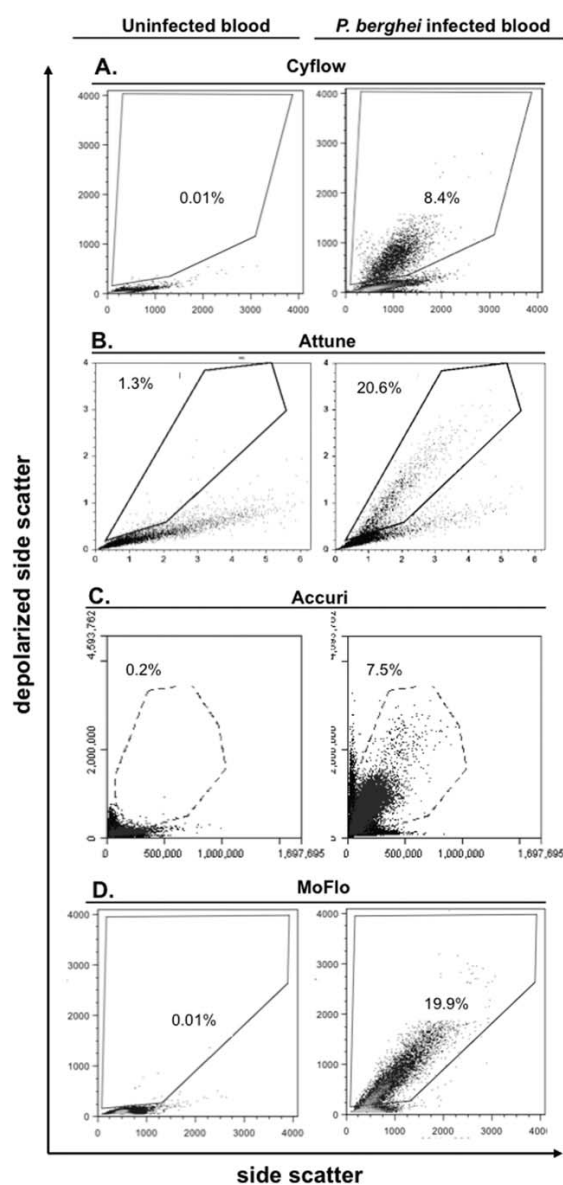


Figure 2. Detection of depolarizing side-scattered light by four different flow cytometers. Representative plots (side scatter versus depolarized side-scatter) of mouse uninfected red blood cells (RBCs) (left row) and RBCs infected with *Plasmodium berghei* (right row). Light depolarization caused by hemozoin was detected in four different cytometers: the Cyflow (A), the Attune (B), the Accuri C6 (C), and the MoFlo (D). Depolarizing cells were selected after establishing a gate using the uninfected controls (left row).

rately, but always simultaneously with the main 488 nm Sapphire laser as a control. A mounted Glan-Thompson calcite polarizer with an extinction ratio >100,000:1 (GTH10M, Thorlabs) was placed in front of each secondary laser line. Scattered light from the secondary laser was transmitted through the third instrument pinhole. Normal and depolarized SSC were measured using the corresponding bandpass filters (multiline UV: 350/50 nm; 457 nm: 455/30 nm; 488 nm: 488/10 nm; 514 nm: 510/20 nm; and 640 nm: 630/20 nm) after a 70/30 beam splitter and with an orthogonally positioned polarizer filter in the 70% end of the beam splitter.

The separation index (SI) (Median Positive – Median Negative)/(2 × StdDev Negative) between the Hz-containing cell population and the uninfected cells was calculated in order to evaluate the capacity of each laser wavelength to resolve these two populations, and compared with the SI measured with the main 488 nm laser. A ratio of 1 indicates there are no differences in the capacity of the respective wavelength to resolve the Hz-containing cells compared to the main 488 nm laser. One-way ANOVA with $n=4$ for each wavelength was performed to assess whether there were statistical differences between each ratio.

Microscopy

In the *P. berghei* infected sample, sorted cells were centrifuged and transferred to a glass slide, which was then fixed in methanol and Giemsa-stained.

In the case of *P. falciparum*, sorted cells were left to sediment overnight. Supernatant was discarded and a 10 μ l drop of pelleted cells was placed into a glass slide which was immediately covered using a square coverslip. Leica DM5000B (Leica, Solms, Germany) and Leica DM2500 microscopes were used for fluorescence and depolarized microscopy, respectively.

Cell Sorting Using the MoFlo

Populations with different levels of depolarization were sorted. The instrument was run at a pressure of 483 kPa (70 psi) with a 70 μ m nozzle and a drop formation frequency of \sim 96 kHz. Sorting rates were typically about 3.5×10^7 cells per hour. Cells were collected into \sim 1 mL of PBS maintained at 4 $^{\circ}$ C.

Flow Cytometry Data Analysis

Flow cytometry results were analyzed using FlowJo software (version 9.0.2, Tree Star, Oregon, USA). Depolarizing events were defined in plots of SSC versus depolarized-SSC as those with a signal above the background observed in the uninfected control.

To assess if the depolarization level would reflect parasite development, parasites tagged with a green fluorescent protein (GFP) in the case of *P. berghei* ANKA or stained with a fluorescent DNA dye (SYBR green I) in the case of *P. falciparum*, were analyzed. To determine SYBR green I or GFP positive cells, green fluorescence (FL1) versus red fluorescence (FL3) plots were used. SYBR green I positive events were established based on a stained uninfected control.

The study involving human samples was approved by the Ethical Committee of the Faculty of Medicine, University of

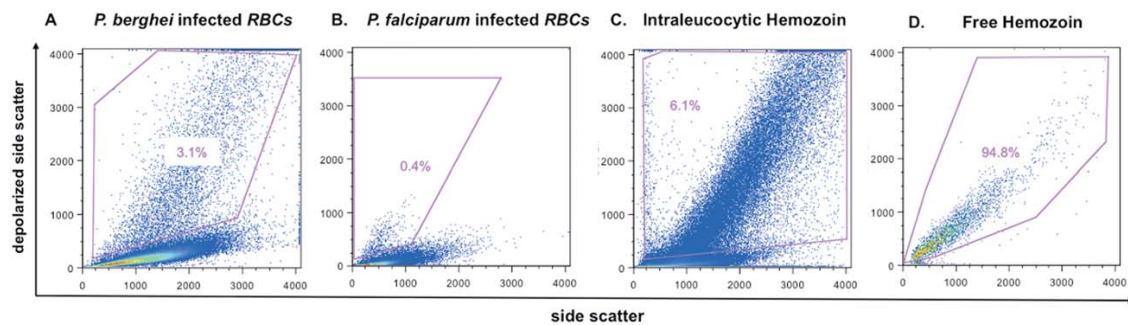


Figure 3. Detection of intraerythrocytic, intraleukocytic and free hemozoin (Hz). Representative plots (side scatter against depolarized side-scatter) of mouse red blood cells (RBCs) infected with *Plasmodium berghei* (A), human RBCs infected with *Plasmodium falciparum* (B), Hz-containing phagocytes (C), and free synthetic Hz (D), analyzed using a Cyflow. The resulting depolarization of light caused by Hz could be detected in these four different samples, however different degrees of depolarization were observed, possibly indicating a different distribution of Hz crystals within the cells. Note: Gain values had to be adjusted for the various samples, since they had inherently different characteristics. However, for the depolarized side-scatter parameter the gain values did not differ considerably, ranging from 230 to 280. [Color figure can be viewed in the online issue, which is available at wileyonlinelibrary.com.]

Lisbon. All experiments involving animals were performed in compliance with the relevant laws and institutional guidelines.

RESULTS

Detection of Light Depolarization Using Different Instruments

The Attune, Accuri C6, CyFlow, and MoFlo could all be set up for depolarized side scatter by making a few simple changes to the optics, allowing restoration of the original configuration within a few minutes (Fig. 1). Hz from *P. berghei* iRBC could be successfully detected (Figs. 2, 3A, and Supporting Information Fig. S1). In fact, a CyFlow instrument located in the rather remote location of Lambaréné, Gabon, was also easily converted and used to investigate indigenous malaria parasites from local patients.

Detection of Light Depolarization Caused by Different Types of Hemozoin

All forms of Hz could be easily detected by measuring depolarized side-scattered light. Intraerythrocytic Hz from both the rodent malaria parasite *P. berghei* and the human malaria parasite *P. falciparum* were detected, although Hz-containing cells of these two species exhibited different levels of depolarized side scatter (Fig. 3B and Supporting Information Fig. S2). Hz in *P. berghei* iRBC showed higher levels and a wider distribution of depolarization than Hz in *P. falciparum* iRBC. PBMCs containing synthetic Hz also showed a high level of depolarization (Fig. 3C). Free crystals of synthetic Hz could be detected as well and showed a wide range of depolarized side-scatter (Fig. 3D).

Hemozoin Induced Depolarization at Different Wavelengths

When depolarized side scatter was measured at several different wavelengths commonly used in flow cytometers, the separation index (SI) ratio obtained with each wavelength in comparison to the SI measured with the main 488 nm was close to one (Fig. 4), indicating that there appears to be little difference in the detection of depolarizing events, statistically

confirmed with one-way ANOVA test ($n=4$ for each wavelength).

Identification of *P. berghei* and *P. falciparum* Infected RBCs with Different Degrees of Depolarization

In the *P. berghei*-GFP infected RBCs four different populations were selected, designated as non, low, medium and high depolarizing (Supporting Information Fig. S1). As the depolarization degree increases an increase in the GFP was observed, which indicates that more mature parasites have a higher level of depolarization (Supporting Information Fig. S1A). Although some overlap in the GFP intensity signal could be observed, there was a clear difference between the highly-depolarizing and non-depolarizing populations, with median values of GFP fluorescence of 1063 and 129, respectively. Microscopic analysis of the sorted populations corroborated this observation, where infected RBCs with immature parasites with no observable Hz were only present in the non-depolarizing population. While, in the high-depolarizing population, only parasites with large amounts of dispersed Hz were present. Interestingly, mature parasites with a single but large clump of Hz could be found in the low and medium-depolarizing populations (Supporting Information Fig. S1B).

In the case of *P. falciparum* infected RBCs, only two gates were created, designated as SG+/Hz+ (depolarizing) and SG+/Hz- (non-depolarizing) (Supporting Information Fig. S2). Results showed that the depolarizing population (SG+/Hz+) had a much higher intensity of SYBR green I fluorescence with a median value of 3735 compared to 514 median of the non-depolarizing population (SG+/Hz-), indicating more DNA and thus, reflecting their more advanced stage of development (Supporting Information Fig. S2A). Bright-field and fluorescence microscopy of SYBR green I showed that mature, multinucleated schizonts were only detected in the depolarizing population, whereas single-nucleated young parasites were only found in the non-depolarizing population (Supporting Information Fig. S2B).

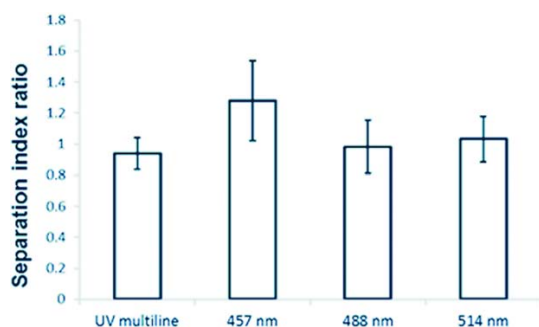


Figure 4. Assessing hemozoin depolarization with different wavelengths. Bars represent ratios of Separation Index (SI; see Methods) obtained with each wavelength in comparison to the SI measured with the main 488 nm Sapphire laser. A ratio close to one indicates there is no difference, confirmed statistically with one-way ANOVA test ($n = 4$ for each wavelength). Increasing laser power did not improve separation (data not shown). Each measurement represents the median value of four samples \pm Standard Error of the Mean. [Color figure can be viewed in the online issue, which is available at wileyonlinelibrary.com.]

DISCUSSION

Malaria and Flow Cytometry

Cytometry of malaria-infected RBC has been used for (i) monitoring of infected RBC, mainly in mouse models (34–39), (ii) characterization of infected RBC (15), (iii) assessment of maturation and/or viability of parasites in infected RBC (10,13,14,16,17,40,41), and (iv) to detect and count *P. falciparum* infected RBC in culture (14,42–44) or from patient blood (45–47), with the possibility to distinguish species based on base composition (2,10,11).

Reliable discrimination of parasitized RBC from micro-nucleated RBC and/or reticulocytes can, however, be difficult (47). Usually, this requires elaborate/laborious manipulation steps, such as removal of RNA (12,34) or the use of a combination of different nucleic acid stains (13,36), frequently requiring instruments with more than one light source, e.g., UV in the case of the frequently used Hoechst 33342 stain. More complex protocols can be more error-prone.

Hemozoin is a Useful and Simple Parameter to Measure

Hz measurement is attractive as an addition and/or an alternative to the range of cytometric measurements now made on malaria parasites. Detection by microscopy using simple polarizing filters (8,9) or by cytometric depolarized scatter measurement is reagent-free and does not require extensive sample preparation, and thus can easily be done on native samples (31,32). Because it is produced throughout schizogony by growing parasites, Hz is an ideal maturation marker (48). Hz distribution and amount also vary between species and parasite forms. For example, Hz is higher in gametocytes than in most asexual forms of *P. falciparum*, providing aid in identification (6). Although Hz levels in early *P. falciparum* ring-forms are below the detection thresholds of both

dark-field microscopy (49) and flow cytometry (31) when analyzing native samples, it may be detected in bulk in blood after rigorous lysis of the sample (50). Even though we have shown that free synthetic Hz can be easily detected by flow cytometry (Fig. 3D), we have not investigated detection of free Hz obtained after blood sample lysis. The utility and possible applications of the cytometric Hz detection in phagocytes (Fig. 3C) have been reviewed elsewhere (33).

Detection of Light Depolarization Caused by Hemozoin Using Different Flow Cytometers

Compact bench top instruments, such as CyFlow SL (Partec), the Attune (Life Technologies) or the Accuri C6 (BD Biosciences), which we show are easily modifiable for Hz (Figs. 1 and 2), are relatively easy to run in resource-limited environments, making it feasible for cytometric Hz measurement to be more widely used.

The benchtop systems and a MoFlo sorter were all easily modified without any special training and it was easy to return them to their original configurations.

Although patent issues no longer impede modification of flow cytometers for depolarized scatter, a major obstacle has arisen with the common use of fiber optic cables, which do not preserve the polarization of light, in the light collection path(s) for fluorescence and side scatter. It should be noted that, unlike the model we used, the new Attune NxT is equipped with such fiber optics and is therefore not usable to detect depolarized scatter.

The depolarized population detected with the Accuri C6 was not as clearly separated from the non-depolarized population, as was the case with the other instruments (Fig. 2E). The Accuri differs in design from the other systems in several respects; the light that is detected in the depolarized side scatter detector is not at 90° from its original path (Fig. 1), and the detector gains are not easily adjustable by the user. Moreover, the Accuri filters and filter holders are much smaller than those in the Attune, CyFlow, and MoFlo, limiting the choice of optical components initially available to us. We are awaiting arrival of parts for a new filter design that we expect will improve performance.

The use of different beam splitters between the SSC and depolarized SSC seemed to have little, if any influence on the detected population (data not shown). It is noteworthy that placing a 1:100;000 Glan polarizer into the laser illumination path ahead of the cuvette also appeared to have little effect (data not shown). We also found that depolarization was adequately detectable at different wavelengths (Fig. 4), corroborating the report from Krämer et al. (23) that side scatter light polarization could be detected in a modified MoFlo at wavelengths of 488, 633, and 647 nm. They noted that longer wavelengths produced marginally stronger signals. Results obtained from additional excitation wavelengths (UV multiline, 457 and 514 nm) did not differ significantly from those obtained using a 488 nm laser (Fig. 4). Indeed, although certain longer wavelengths and perhaps a 95/5 beam splitter or better polarization ratios might be expected to provide better results, the light sources and wavelengths commonly used in

flow cytometers, 50/50 beam-splitters, and simple polarizing filters appear sufficient for the measurement of Hz in suspension, inside infected RBCs or inside leukocytes (Fig. 3).

Flow Cytometric Detection of Intraleukocytic and Intraerythrocytic Hemozoin

At the end of the maturation cycle, schizonts rupture, releasing Hz which is phagocytized by circulating neutrophils and monocytes (51). After detection of Hz leukocytes using the Cell-Dyn hematology analyzer was reported (21), several studies, reviewed elsewhere (26), addressed the performance and utility of this approach.

Although finding Hz in leukocytes as part of an automated blood count might allow the detection of malaria even in the absence of clinical suspicion, this is still only possible using the Cell-Dyn instruments (52). These “closed” platforms, which use proprietary reagents, fixed detection and analysis algorithms and provide no ready access to list-mode data are limited in adaptability (23,26,29). However, their detection of intraleukocytic Hz has been correlated with malaria severity (53–55), and flow cytometric counts of Hz-containing leukocytes have been shown to be a better marker of disease severity than microscopic counting (28). Intraleukocytic Hz detection is also potentially applicable to the diagnosis of malaria during pregnancy (9).

Importantly, since Hz has immune modulating effects, as reviewed elsewhere (33), flow cytometric detection/sorting of Hz-containing leukocytes and non-containing leukocytes from the same host might help elucidate further details (30,33,56).

Hz detection by microscopy provides the foundation for the slide-based schizont maturation assay, still a mainstay in detecting antimalarial drug resistance in clinical settings. Several flow cytometric procedures analogous to the schizont maturation assay have been described by others (13,16,17,40,57); since depolarized scatter measurements were not available on their apparatus, they could not use Hz content as a maturation indicator for stage determination. Instead a combination of DNA and RNA content was employed, providing more precise stage identifications than would be obtained by cytometric detection of DNA content alone but requiring two dyes and two fluorescence measurements.

In a classic schizont maturation assay of *P. falciparum*, initial clinical samples contain little Hz because stages later than early trophozoites are removed from circulation. Parasites in drug-free medium and drug-resistant parasites form Hz as they continue to grow and mature, whereas Hz formation is diminished or absent in parasites cultured in effective concentrations of antimalarial agents. We have shown that schizonts in these contexts are easily distinguished from younger parasites solely based on their level of depolarization (Supporting Information Fig. S2), measurable without addition of reagents.

We have demonstrated a field-suitable novel flow cytometric assay for antimalarial susceptibility based on this rationale (30,32). This assay has also been shown to detect

drug effects on parasite maturation much earlier than any other available technique (32).

Unpublished preliminary experiments with flow cytometers equipped to measure DNA, RNA, and Hz simultaneously in parasitized RBC indicate that although both RNA content and Hz signals increase during maturation, these two parameters are not highly correlated and that measuring both may therefore provide more information about parasite physiology than would measuring only one or the other.

P. berghei- and *P. falciparum*-infected RBC showed different populations with depolarized side scatter signals. It has long been known that the amount, appearance and location of pigment in different species of malaria parasites show wide variations (58). In *P. berghei* Hz crystals are fine and dispersed granules which only clump together by the end of schizogony (Supporting Information Fig. S1B, second and third panel from top), while in *P. falciparum* the Hz crystals aggregate as they start to appear (Supporting Information Fig. S2B, lower panels). Thus, in *P. falciparum* forms with highly dispersed Hz and, consequently, high degree of depolarization are absent. This explanation also fits with the obtained depolarized side scatter signals because side scatter is also a measure of cell granularity (59). Therefore, it is likely that a parasite containing several small but distributed Hz crystals will have a higher depolarized side scatter signal than a parasite containing a single large clump of Hz.

Microscopy has shown that Hz is also more abundant and dispersed in gametocytes (6) and our analyses of *P. berghei*-infected blood samples showed higher levels of depolarized side scatter in gametocytes (Supporting Information Fig. S2B). Thus, this approach can eventually be applied to aid in the detection of these sexual forms, which are responsible for transmission. Currently, *in vitro* assays to screen drugs for gametocytes are either based on labor-intensive microscopy or on the analysis of transgenic fluorescent gametocytes by flow cytometry (60–62). Hz detection may be useful to help and develop novel assays for the detection and quantification of gametocytes, with different applications such as, the development and investigation of novel transmission blocking drugs.

Gametocytes differ from sexual forms in that, although their Hz signals are high and may even be higher than those of schizonts, their RNA content is relatively low; our preliminary experiments indicate that cytometry can resolve two gametocyte populations with higher and lower modal RNA content, presumably representing macrogametocytes (female) and microgametocytes (male), the former known to exhibit cytoplasmic basophilia in Giemsa-stained smears, characteristic of RNA staining.

Future Prospects: Malaria Cytometry in Simple Imaging Systems

During the past few years, fluorescence imaging cytometers usable for some multiparameter analyses formerly only possible using flow cytometry, including CD4+ T cell counting in HIV patients and multiplexed bead PCR assays for malaria species identification, have come into use. The DNA and RNA dye measurements typically done in malaria

cytometry require less sensitivity, and could be implemented in similar apparatus. A recent report on spectral imaging of malaria-infected cells in a microscope illuminated by multiple LEDs suggests that Hz may be detected efficiently by transmission measurements in the 630–700 nm range (63) without a need to use polarized light; we have also found evidence for this. In addition to its substantially lower cost and complexity, a multiparameter imager for malaria cytometry would offer the considerable advantage of being able to analyze slides. We have just begun work with a prototype of such an instrument.

CONCLUSION

The old parameter of light depolarization measurements has found a new job in malaria. It allows to detect Hz, free in blood or inside iRBCs erythrocytes leukocytes all of which can be used in several applications, such as: (i) detection of Hz-containing leukocytes for diagnostic applications and to unravel malaria-associated immunopathology; (ii) detection of parasitized RBC and determination of species and stages for diagnosis and drug susceptibility determination; and (iii) discrimination of gametocytes and other low-abundance parasite subpopulations. Depolarized light scatter measurements are easily implemented on common benchtop flow cytometers and work across a wide range of illumination wavelengths; equivalent optical measurements for Hz detection can also be made in imaging cytometers. Adding Hz detection to other parameters, such as DNA or RNA content, will provide improved accuracy and sensitivity of parasite detection and allow researchers to expand the use of cytometry in the field of malaria.

ACKNOWLEDGMENTS

The authors acknowledge Andrea Tradori from Life Technologies and Daniel Gala from Enzifarma (BD representative in Portugal), who provided with the measurements on the Attune and the Accuri C6, respectively, and Grace Chojnowski (Queensland Institute of Medical Research) who gave the additional information regarding the Attune.

LITERATURE CITED

- World Health Organization. World Malaria Report 2013. Geneva: WHO Press; 2013.
- Shapiro HM, Apte SH, Chojnowski GM, Hänscheid T, Rebelo M, Grimberg BT. Cytometry in malaria—A practical replacement for microscopy? *Curr Protoc Cytom* 2013; Chapter 11:Unit 11.20.
- Laveran CL. A newly discovered parasite in the blood of patients suffering from malaria. Parasitic etiology of attacks of malaria (1880). In: Kean BH, Mott KE, Russell AJ, editors. *Tropical Medicine and Parasitology. Classic Investigations*, vol 1. Ithaca, NY: Cornell University Press; 1978; p 23–26.
- Packer H. The use of darkfield illumination in studies of malaria parasites. *J Natl Malar Soc* 1945;4:331–340.
- Jamjoom GA. Dark-field microscopy for detection of malaria in unstained blood films. *J Clin Microbiol* 1983;17:717–721.
- Jamjoom GA. Formation and role of malaria pigment. *Rev Infect Dis* 1988;10:1029–1034.
- Wilson BK, Behrend MR, Horning MP, Hegg MC. Detection of malarial byproduct hemozoin utilizing its unique scattering properties. *Opt Express* 2011;19:12190–12196.
- Lawrence C, Olson JA. Birefringent hemozoin identifies malaria. *Am J Clin Pathol* 1986;86:360–363.
- Romagosa C, Menendez C, Ismail MR, Quintó L, Ferrer B, Alonso PL, Ordí J. Polarisation microscopy increases the sensitivity of hemozoin and plasmodium detection in the histological assessment of placental malaria. *Acta Trop* 2004;90:277–284.
- Hare JD. Two-color flow-cytometric analysis of the growth cycle of plasmodium falciparum in vitro: Identification of cell cycle compartments. *J Histochem Cytochem* 1986;34:1651–1658.
- Janse CJ, van Vianen PH, Tanke HJ, Mons B, Ponnudurai T, Overdulve JP. Plasmodium species: Flow cytometry and microfluorometry assessments of DNA content and synthesis. *Exp Parasitol* 1987;64:88–94.
- Jiménez-Díaz MB, Rullas J, Mulet T, Fernández L, Bravo C, Gargallo-Viola D, Angulo-Barturen I. Improvement of detection specificity of Plasmodium-infected murine erythrocytes by flow cytometry using autofluorescence and YOYO-1. *Cytometry A* 2005;67A:27–36.
- Grimberg BT, Erickson JJ, Sramkoski RM, Jacobberger JW, Zimmerman PA. Monitoring plasmodium falciparum growth and development by UV flow cytometry using an optimized Hoechst-thiazole orange staining strategy. *Cytometry A* 2008;73A:546–554.
- Malleret B, Claser C, Ong AS, Suwanarusk R, Sriprawat K, Howland SW, Russell B, Nosten F, Rénia L. A rapid and robust tri-color flow cytometry assay for monitoring malaria parasite development. *Sci Rep* 2011;1:118.
- Apte SH, Groves PL, Roddick JS, P da Hora V, Doolan DL. High-throughput multiparameter flow-cytometric analysis from micro-quantities of plasmodium-infected blood. *Int J Parasitol* 2011;41:1285–1294.
- Russell B, Malleret B, Suwanarusk R, Anthony C, Kanlaya S, Lau YL, Woodrow CJ, Nosten F, Renia L. Field-based flow cytometry for ex vivo characterization of *Plasmodium vivax* and *P. falciparum* antimalarial sensitivity. *Antimicrob Agents Chemother* 2013;57:5170–5174.
- Amaratunga C, Neal AT, Fairhurst RM. Flow cytometry-based analysis of artemisinin-resistant *Plasmodium falciparum* in the ring-stage survival assay. *Antimicrob Agents Chemother* 2014;58:4938–4940.
- Grimberg BT. Methodology and application of flow cytometry for investigation of human malaria parasites. *J Immunol Methods* 2011;367:1–16.
- Lelliott PM, Lampkin S, McMorrin BJ, Foote SJ, Burgio G. A flow cytometric assay to quantify invasion of red blood cells by rodent plasmodium parasites in vivo. *Malar J* 2014;13:100.
- de Grooth BG, Terstappen LW, Puppels GJ, Greve J. Light-scattering polarization measurements as a new parameter in flow cytometry. *Cytometry* 1987;8:539–544.
- Mendelow BV, Lyons C, Nhlangothi P, Tana M, Munster M, Wypkema E, Liebowitz L, Marshall L, Scott S, Coetzer TL. Automated malaria detection by depolarization of laser light. *Br J Haematol* 1999;104:499–503.
- Hänscheid T, Valadas E, Grobusch MP. Automated malaria diagnosis using pigment detection. *Parasitol Today* 2000;16:549.
- Krämer B, Grobusch MP, Suttrop N, Neukammer J, Rinneberg H. Relative frequency of malaria pigment-carrying monocytes of nonimmune and semi-immune patients from flow cytometric depolarized side scatter. *Cytometry* 2001;45:133–140.
- Hänscheid T, Melo-Cristino J, Pinto BG. Automated detection of malaria pigment in white bloodcells for the diagnosis of malaria in Portugal. *Am J Trop Med Hyg* 2001;64:290–292.
- Scott CS, van Zyl D, Ho E, Meyersfeld D, Ruivo L, Mendelow BV, Coetzer TL. Automated detection of WBC intracellular malaria-associated pigment (haemozoin) with Abbott Cell-Dyn CD3200 and CD3700 analysers. *Haematol Support Educ* 2001;2:2–15.
- Campuzano-Zuluaga G, Hänscheid T, Grobusch MP. Automated haematology analysis to diagnose malaria. *Malar J* 2010;9:346.
- Suh IB, Kim HJ, Kim JY, Lee SW, An SS, Kim WJ, Lim CS. Evaluation of the Abbott Cell-dyn 4000 hematology analyzer for detection and therapeutic monitoring of *Plasmodium vivax* in the republic of Korea. *Trop Med Int Health* 2003;8:1074–1081.
- Hänscheid T, Frita R, Langin M, Kremsner PG, Grobusch MP. Is flow cytometry better in counting malaria pigment-containing leukocytes compared to microscopy? *Malar J* 2009;8:255.
- Hänscheid T, Romão R, Grobusch MP, Amaral T, Melo-Cristino J. Limitation of malaria diagnosis with the Cell-dyn® analyser: Not all haemozoin-containing monocytes are detected or shown. *Int J Lab Hematol* 2011;33:e14–e16.
- Frita R, Rebelo M, Pamplona A, Vigario AM, Mota MM, Grobusch MP, Hänscheid T. Simple flow cytometric detection of haemozoin containing leukocytes and erythrocytes for research on diagnosis, immunology and drug sensitivity testing. *Malar J* 2011;10:74.
- Rebelo M, Shapiro HM, Amaral T, Melo-Cristino J, Hänscheid T. Haemozoin detection in infected erythrocytes for *Plasmodium falciparum* malaria diagnosis—prospects and limitations. *Acta Trop* 2012;123:58–61.
- Rebelo M, Sousa C, Shapiro HM, Mota MM, Grobusch MP, Hänscheid T. A novel flow cytometric hemozoin detection assay for real-time sensitivity testing of *Plasmodium falciparum*. *PLoS One* 2013;8:e61606.
- Boura M, Frita R, Góis A, Carvalho T, Hänscheid T. The hemozoin conundrum: Is malaria pigment immune-activating, inhibiting, or simply a bystander? *Trends Parasitol* 2013;29:469–476.
- Barkan D, Ginsburg H, Golenser J. Optimisation of flow cytometric measurement of parasitaemia in plasmodium-infected mice. *Int J Parasitol* 2000;30:649–653.
- Jiménez-Díaz MB, Mulet T, Gómez V, Viera S, Alvarez A, Garuti H, Vázquez Y, Fernández A, Ibáñez J, Jiménez M, Gargallo-Viola D, Angulo-Barturen I. Quantitative measurement of Plasmodium-infected erythrocytes in murine models of malaria by flow cytometry using bidimensional assessment of SYTO-16 fluorescence. *Cytometry A* 2009;75A:225–235.
- Bhakti SC, Sratongno P, Chimma P, Rungruang T, Chuncharunee A, Neumann HP, Malasit P, Pattanapanyasat K. Re-evaluating acridine orange for rapid flow cytometric enumeration of parasitemia in malaria-infected rodents. *Cytometry A* 2007;71A:662–667.

37. Sanchez BA, Mota MM, Sultan AA, Carvalho LH. *Plasmodium berghei* parasite transformed with green fluorescent protein for screening blood schizontocidal agents. *Int J Parasitol* 2004;34:485–490.
38. Hein-Kristensen L, Wiese L, Kurtzhals JA, Staalsoe T. In-depth validation of acridine orange staining for flow cytometric parasite and reticulocyte enumeration in an experimental model using *Plasmodium berghei*. *Exp Parasitol* 2009;123:152–157.
39. Somsak V, Srichairatanakool S, Yuthavong Y, Kamchonwongpaisan S, Uthaiyapibull C. Flow cytometric enumeration of *Plasmodium berghei*-infected red blood cells stained with SYBR green I. *Acta Trop* 2012;122:113–118.
40. Grimberg BT, Jaworska MM, Hough LB, Zimmerman PA, Phillips JG. Addressing the malaria drug resistance challenge using flow cytometry to discover new antimalarials. *Bioorg Med Chem Lett* 2009;19:5452–5457.
41. Karl S, Wong RP, St Pierre TG, Davis TM. A comparative study of a flow-cytometry-based assessment of in vitro *Plasmodium falciparum* drug sensitivity. *Malar J* 2009;8:294.
42. Saito-Ito A, Akai Y, He S, Kimura M, Kawabata M. A rapid, simple and sensitive flow cytometric system for detection of *Plasmodium falciparum*. *Parasitol Int* 2001;50:249–257.
43. Li Q, Gerena L, Xie L, Zhang J, Kyle D, Milhous W. Development and validation of flow cytometric measurement for parasitemia in cultures of *P. falciparum* vitally stained with YOYO-1. *Cytometry A* 2007;71A:297–307.
44. Bei AK, Brugnara C, Duraisingh MT. In vitro genetic analysis of an erythrocyte determinant of malaria infection. *J Infect Dis* 2010;202:1722–1727.
45. van Vianen PH, van Engen A, Thaithong S, van der Keur M, Tanke HJ, van der Kaay HJ, Mons B, Janse CJ. Flow cytometric screening of blood samples for malaria parasites. *Cytometry* 1993;14:276–280.
46. Wernli M, Tichelli A, von Planta M, Gratwohl A, Speck B. Flow cytometric monitoring of parasitaemia during treatment of severe malaria by exchange transfusion. *Eur J Haematol* 1991;46:121–123.
47. Campo JJ, Aponte JJ, Nhabomba AJ, Sacarlal J, Angulo-Barturen I, Jiménez-Díaz MB, Alonso PL, Dobaño C. Feasibility of flow cytometry for measurements of *Plasmodium falciparum* parasite burden in studies in areas of malaria endemicity by use of bidimensional assessment of YOYO-1 and autofluorescence. *J Clin Microbiol* 2011;49:968–974.
48. Rieckmann KH. Visual in vitro test for determining the drug sensitivity of *Plasmodium falciparum*. *Lancet* 1982;1:1333–1335.
49. Delahun C, Horning MP1, Wilson BK, Proctor JL, Hegg MC. Limitations of haemozoin-based diagnosis of *Plasmodium falciparum* using dark-field microscopy. *Malar J* 2014;13:147.
50. Orbán A, Butykai Á, Molnár A, Pröhle Z, Fülöp G, Zelles T, Forsyth W, Hill D, Müller I, Schofield L, Rebelo M, Hänscheid T, Karl S, Kézsmárki I. Evaluation of a novel magneto-optical method for the detection of malaria parasites. *PLoS One* 2014;9:e96981.
51. Metzger WG, Mordmuller BG, Kremsner PG. Malaria pigment in leukocytes. *Trans R Soc Trop Med Hyg* 1995;89:637–638.
52. Hänscheid T, Pinto BG, Pereira I, Cristino JM, Valadas E. Avoiding misdiagnosis of malaria: A novel automated method allows specific diagnosis, even in the absence of clinical suspicion. *Emerg Infect Dis* 1999;5:836–838.
53. Phu NH, Day N, Diep PT, Ferguson DJP, White NJ. Intraleukocytic malaria pigment and clinical severity of malaria in children. *Trans R Soc Trop Med Hyg* 1995;89:200–204.
54. Amodu OK, Adeyemo AA, Olumese PE, Gbadegesin RA. Intraleukocytic malaria pigment and clinical severity of malaria in children. *Trans R Soc Trop Med Hyg* 1998;92:54–56.
55. Hänscheid T, Langin M, Lell B, Potschke M, Oyakhrome S, Kremsner PG, Grobusch MP. Full blood count and haemozoin-containing leukocytes in children with malaria: Diagnostic value and association with disease severity. *Malar J* 2008;7:109.
56. Hänscheid T, Egan TJ, Grobusch MP. Haemozoin: From melatonin pigment to drug target, diagnostic tool, and immune modulator. *Lancet Infect Dis* 2007;7:675–685.
57. Suwanarusk R, Russell B, Ong A, Sriprawat K, Chu CS, PyaePhyo A, Malleret B, Nosten F, Renia L. Methylene blue inhibits the asexual development of vivax malaria parasites from a region of increasing chloroquine resistance. *J Antimicrob Chemother* 2015;70:124–129.
58. Fulton JD, Rimington C. The pigment of the malaria parasite plasmodium berghei. *J Gen Microbiol* 1953;8:157–159.
59. Shapiro HM. *Practical Flow Cytometry*, 4th ed. New Jersey: Wiley; 2003.
60. Dechy-Cabaret O, Benoit-Vical F. Effects of antimalarial molecules on the gametocyte stage of *Plasmodium falciparum*: The debate. *J Med Chem* 2012;55:10328–10344.
61. Delves MJ, Ramakrishnan C, Blagborough AM, Leroy D, Wells TN, Sinden RE. A high-throughput assay for the identification of malarial transmission-blocking drugs and vaccines. *Int J Parasitol* 2012;42:999–1006.
62. Peatey CL, Leroy D, Gardiner DL, Trenholme KR. Anti-malarial drugs: How effective are they against *Plasmodium falciparum* gametocytes? *Malar J* 2012;11:34.
63. Omucheni DL, Kaduki KA, Bulimo WD, Angeyo HK. Application of principal component analysis to multispectral-multimodal optical image analysis for malaria diagnostics. *Malar J* 2014;13:485.
64. Slater AF, Swiggard WJ, Orton BR, Flitter WD, Goldberg DE, Cerami A, Henderson GB. An iron-carboxylate bond links the heme units of malaria pigment. *Proc Natl Acad Sci USA* 1991;88:325–329.
65. Thomas V, Gois A, Ritts B, Burke P, Hänscheid T, McDonnell G. A novel way to grow hemozoin-like crystals in vitro and its use to screen for hemozoin inhibiting antimalarial compounds. *PLoS One* 2012;7:e41006.

Transdermal Diagnosis of Malaria Using Vapor Nanobubbles

Maria Rebelo, Rita Grenho, Agnes Orban, Thomas Hänscheid

Author affiliations: Instituto de Medicina Molecular, Lisbon, Portugal (M. Rebelo, R. Grenho, T. Hänscheid); Budapest University of Technology and Economics, Budapest, Hungary (A. Orban); MTA-BME Lendület Magneto-optical Spectroscopy Research Group, Budapest (A. Orban)

DOI: <http://dx.doi.org/10.3201/eid2202.151203>

To the Editor: Establishing reliable noninvasive methods for diagnosis of malaria has been a challenge. Lukianova-Helb et al. should be applauded for developing such a method on the basis of hemozoin (Hz) detection (1). The authors reported a proof of principle and are preparing for “large-scale studies in humans” (2). Such large endeavors should be based on firm evidence, so it is surprising that the results presented were from a single patient, remarkable for the unusual quadruple drug treatment (2). In such a scenario, to compensate for the limited data, the results should be of convincing scientific quality.

However, the case described raises several doubts that could have been addressed, such as the reliability of the diagnosis if only a thin film and a rapid test were used (co-infection excluded) and why parasitemia was not determined at the time of the device test (instead of 4 hours before and 9 hours after). What developmental stages were the

parasites in at the time of the evaluation (for example, already early trophozoites containing Hz or Hz-rich gametocytes)? Why was the patient not re-evaluated to find out if repeated measurements would become appropriately negative (test-of-cure)?

The methods and results used in the study contrast with the extraordinary numbers for the limit of detection (LOD): 0.0001% in human blood and 0.00034% in a rodent model (1,2). However, the LOD is a virtual, inferred parasitemia rate based on the detection of free Hz added to uninfected blood (1). An LOD can be obtained from serially diluted cultures or samples (3). In rodent models, detection of Hz tends to be much easier (4). Moreover, in *Plasmodium falciparum* infections, only immature forms have been observed, with little or no detectable Hz (5).

The prospects of a noninvasive test for malaria are exciting. However, in times of cost restraints, any diagnostic test or intervention should provide sufficiently convincing results before consideration of resource-intensive large-scale trials.

References

1. Lukianova-Hleb EY, Campbell KM, Constantinou PE, Braam J, Olson JS, Ware RE, et al. Hemozoin-generated vapor nanobubbles for transdermal reagent- and needle-free detection of malaria. *Proc Natl Acad Sci U S A*. 2014;111:900–5. <http://dx.doi.org/10.1073/pnas.1316253111>
2. Lukianova-Hleb E, Bezek S, Szigeti R, Khodarev A, Kelley T, Hurrell A, et al. Transdermal diagnosis of malaria using vapor nanobubbles. *Emerg Infect Dis*. 2015;21:1122–7. <http://dx.doi.org/10.3201/eid2107.150089>
3. Orbán Á, Butykai Á, Molnár A, Pröhle Z, Fülöp G, Zelles T, et al. Evaluation of a novel magneto-optical method for the detection of malaria parasites. *PLoS ONE*. 2014;9:e96981. <http://dx.doi.org/10.1371/journal.pone.0096981>

etymologia

Hemozoin [he"mo-zo'in]

From the Greek *haima* (“blood”) + *zoon* (“animal”), hemozoin is a pigment produced by malaria parasites from hemoglobin in the host’s red blood cells. This pigment was first observed by Johann Heinrich Meckel in 1847 in the blood and spleen of a mentally impaired person. In 1849, Rudolf Virchow made the connection to malaria, but it was initially believed that it was produced in the patient’s spleen as a part of the immune response to malaria. In 1880, Charles Louis Alphonse Laveran observed pigmented parasites in the blood of an Algerian soldier and realized that the parasites, not the patient, produce “malaria pigment.” The term “hemozoin” was coined by Louis Westenra Sambon.



Isolated *Plasmodium falciparum* hemozoin, Ernst Hempelmann, via Wikipedia

Sources

1. Janjua RM, Schultka R, Goebbel L, Pait TG, Shields CB. The legacy of Johann Friedrich Meckel the Elder (1724–1774): a 4-generation dynasty of anatomists. *Neurosurgery*. 2010;66:758–71. <http://dx.doi.org/10.1227/01.NEU.0000367997.45720.A6>
2. Sullivan DJ. Theories on malarial pigment formation and quinoline action. *Int J Parasitol*. 2002;32:1645–53. [http://dx.doi.org/10.1016/S0020-7519\(02\)00193-5](http://dx.doi.org/10.1016/S0020-7519(02)00193-5)

Address for correspondence: Ronnie Henry, Centers for Disease Control and Prevention, 1600 Clifton Rd NE, Mailstop E03, Atlanta, GA 30329-4027, USA; email: boq3@cdc.gov

DOI: <http://dx.doi.org/10.3201/eid2202.ET2202>

4. Rebelo M, Tempera C, Bispo C, Andrade C, Gardner R, Shapiro HM, et al. Light depolarization measurements in malaria: A new job for an old friend. *Cytometry A*. 2015;87:437–45. <http://dx.doi.org/10.1002/cyto.a.22659>
5. Rebelo M, Shapiro HM, Amaral T, Melo-Cristino J, Hänscheid T. Haemozoin detection in infected erythrocytes for *Plasmodium falciparum* malaria diagnosis-prospects and limitations. *Acta Trop*. 2012;123:58–61. <http://dx.doi.org/10.1016/j.actatropica.2012.03.005>

Address for correspondence: Thomas Hänscheid, Instituto de Medicina Molecular, Faculdade de Medicina de Lisboa, Av Prof Egas Moniz, P-1649-028 Lisbon, Portugal; email: t.hanscheid@medicina.ulisboa.pt

In Response:

Ekaterina Lukianova-Hleb, Sarah Bezek, Reka Szigeti, Alexander Khodarev, Thomas Kelley, Andrew Hurrell, Michail Berba, Nirbhay Kumar, Umberto D'Alessandro, Dmitri Lapotko

Author affiliations: Rice University, Houston, Texas, USA (E. Lukianova-Hleb, D. Lapotko); Baylor College of Medicine, Houston (S. Bezek, R. Szigeti); Ben Taub General Hospital, Harris Health System, Houston (S. Bezek, R. Szigeti); X Instruments LLC, Fremont, California, USA (A. Khodarev); Precision Acoustics Ltd, Dorset, England, UK (T. Kelley, A. Hurrell); Standa UAB, Vilnius, Lithuania (M. Berba); Tulane University, New Orleans, Louisiana, USA (N. Kumar); Medical Research Council, Banjul, The Gambia (U. D'Alessandro); London School of Hygiene and Tropical Medicine, London, UK (U. D'Alessandro)

DOI: <http://dx.doi.org/10.3201/eid2202.151829>

In Response: The letter by Rebelo et al. (1) that questions our previously described noninvasive malaria diagnostics (2,3) misinterprets both articles. The main objection comes to our alleged call for “large-scale studies in humans”; no such statement appeared in our 2014 article (2), and in the 2015 article (3), we clearly stated that large-scale studies will be considered after the optimization of a new prototype and improving its sensitivity. The authors’ final questioning of our eligibility for resources is a non-scientific opinion.

Concerning the quality of the standard clinical diagnosis, both thin blood film analysis and rapid diagnostic test results were obtained in a certified US clinical laboratory and returned consistent data. The lack of re-evaluation of the patient and the diagnostic timing are indeed limitations but were caused by the clinical restrictions. Our goal in the 2015 article (3) was to demonstrate the first noninvasive diagnosis of malaria in a human, which was achieved. The additional parameters discussed in the letter were not the

subject of this study. Their letter further misinterprets our 2014 study, stating that parasitemia was virtual in that article; in fact, we studied actual infections among mice (2).

The criticism of Rebelo et al. might have been fueled by their own limited detection of hemozoin with flow cytometry and microscopy (4), in which they used parasite cultures and an unspecified number of malaria patients. That the methods they used might not have performed well does not mean that the novel technology we described, based upon a different mechanism, would have the same limitations in detecting hemozoin.

In conclusion, we agree with the need for optimization of the technology and additional testing. We are currently developing and testing our technology in a malaria-endemic country. Nevertheless, the letter by Rebelo et al. does not alter the fact that our novel noninvasive malaria diagnostic technology worked in a human.

References

1. Rebelo M, Grenho R, Orban A, Hänscheid T. Transdermal diagnosis of malaria using vapor nanobubbles [letter]. *Emerg Infect Dis*. 2016; 22:343. <http://dx.doi.org/10.3201/eid2202.151203>
2. Lukianova-Hleb EY, Campbell KM, Constantinou PE, Braam J, Olson JS, Ware RE, et al. Hemozoin-generated vapor nanobubbles for transdermal reagent- and needle-free detection of malaria. *Proc Natl Acad Sci U S A*. 2014;111:900–5. <http://dx.doi.org/10.1073/pnas.1316253111>
3. Lukianova-Hleb E, Bezek S, Szigeti R, Khodarev A, Kelley T, Hurrell A, et al. Transdermal diagnosis of malaria using vapor nanobubbles. *Emerg Infect Dis*. 2015;21:1122–7. <http://dx.doi.org/10.3201/eid2107.150089>
4. Rebelo M, Shapiro HM, Amaral T, Melo-Cristino J, Hänscheid T. Haemozoin detection in infected erythrocytes for *Plasmodium falciparum* malaria diagnosis-prospects and limitations. *Acta Trop*. 2012;123:58–61. <http://dx.doi.org/10.1016/j.actatropica.2012.03.005>

Address for correspondence: Dmitri Lapotko, Rice University, Houston, Texas, USA, 6100 Main St, MS-140, Houston, TX 77005, USA; email: d15@rice.edu

Malaria in French Guiana Linked to Illegal Gold Mining

Vincent Pommier de Santi, Aissata Dia, Antoine Adde, Georges Hyvert, Julien Galant, Michel Mazevet, Christophe Nguyen, Samuel B. Vezenegho, Isabelle Dusfour, Romain Girod, Sébastien Briolant

Author affiliations: Military Center for Epidemiology and Public Health, Marseille, France (V. Pommier de Santi, A. Dia); Direction Interarmées du Service de Santé en Guyane, Cayenne, French

Flow Cytometry for Antimalarial Drug Testing: More than Meets the Eye

Maria Rebelo, Thomas Hänscheid

Instituto de Medicina Molecular, Faculdade de Medicina, Lisbon, Portugal

Resistance to antimalarial drugs has been increasing, with resistance to artemisinins in Southeast Asia being of particular concern. Monitoring resistance requires useful and feasible *in vitro* tests, and Woodrow et al. should be applauded for their report on a two-color flow cytometry assay (1), a right step in the direction of establishing a practical, objective, alternative testing strategy which addresses the shortcomings of other existing assays. Despite the impressive performance of the assay, it should be noted that this assay requires two nucleic acid stains (dihydroethidium and SYBR green), whereas another recent report using this assay format to assess drug sensitivity used only a single stain, which is certainly a desirable improvement (2). Importantly, the authors mention incorrectly that all flow cytometry assays are based on nucleic acid stains (1). A review by Grimberg on this issue already showed that viability stains are a useful alternative (3). Furthermore, our group has shown that the flow cytometric detection of hemozoin (Hz) is a possible reagent-free assay alternative, both *in vitro* for laboratory strains and *ex vivo* in the field (4, 5).

Notably, the use of nucleic acid stains is prone to interference by other cells. The method described requires the removal of white blood cells, since staining DNA/RNA may interfere with measurements. Although this may not require expensive materials, it certainly makes the assay much more complex and labor-intensive.

However, the most relevant question is whether the described flow cytometric assay has the potential to detect artemisinin resistance. In fact, only recently, a very time-consuming and complex assay was described as being able to achieve this, the ring-stage assay (RSA). This method requires a complicated and meticulous synchronization protocol and is based on microscopic readouts (6).

In contrast, flow cytometric detection of Hz allows tracking of parasite maturation in real time and detection of drug effects much earlier than other phenotypic assays. This is very relevant in the case of artemisinin resistance, as the very young parasite forms are responsible for the observed resistance to this drug. Therefore, this approach may be an attractive alternative to consider and investigate in the context of artemisinin resistance testing.

In conclusion, more flow cytometric assays are available than the one described by Woodrow et al. Some need fewer or no detection reagents, such as the Hz assay, which may have the additional advantage of detecting artemisinin resistance. A prudent

approach would be considering all novel approaches, including cytometric detection of Hz, rather than contemplating only flow cytometry solutions with multicolor staining of nucleic acids.

FUNDING INFORMATION

This research received no specific grant from any funding agency in the public, commercial, or not-for-profit sector.

REFERENCES

1. Woodrow CJ, Wangsing C, Sriprawat K, Christensen PR, Nosten F, Rénia L, Russell B, Malleret B. 2015. Comparison between flow cytometry, microscopy, and lactate dehydrogenase-based enzyme-linked immunosorbent assay for *Plasmodium falciparum* drug susceptibility testing under field conditions. *J Clin Microbiol* 53:3296–3303. <http://dx.doi.org/10.1128/JCM.01226-15>.
2. Wirjanata G, Handayani I, Prayoga P, Apriyanti D, Chalfein F, Sebayang B, Kho S, Noviyanti R, Kenangalem E, Campo B, Poespoprodjo J, Price R, Marfurt J. 2015. Quantification of *Plasmodium* ex vivo drug susceptibility by flow cytometry. *Malar J* 14:417. <http://dx.doi.org/10.1186/s12936-015-0940-8>.
3. Grimberg BT. 2011. Methodology and application of flow cytometry for investigation of human malaria parasites. *J Immunol Methods* 367:1–16. <http://dx.doi.org/10.1016/j.jim.2011.01.015>.
4. Rebelo M, Sousa C, Shapiro HM, Mota MM, Grobusch MP, Hänscheid T. 2013. A novel flow cytometric hemozoin detection assay for real-time sensitivity testing of *Plasmodium falciparum*. *PLoS One* 8:e61606. <http://dx.doi.org/10.1371/journal.pone.0061606>.
5. Rebelo M, Tempera C, Fernandes JF, Grobusch MP, Hänscheid T. 2015. Assessing anti-malarial drug effects ex vivo using the haemozoin detection assay. *Malar J* 14:140. <http://dx.doi.org/10.1186/s12936-015-0657-8>.
6. Witkowski B, Amaratunga C, Khim N, Sreng S, Chim P, Kim S, Lim P, Mao S, Sopha C, Sam B, Anderson JM, Duong S, Chuor CM, Taylor WR, Suon S, Mercereau-Puijalon O, Fairhurst RM, Menard D. 2013. Novel phenotypic assays for the detection of artemisinin-resistant *Plasmodium falciparum* malaria in Cambodia: in-vitro and ex-vivo drug-response studies. *Lancet Infect Dis* 13:1043–1049. [http://dx.doi.org/10.1016/S1473-3099\(13\)70252-4](http://dx.doi.org/10.1016/S1473-3099(13)70252-4).

Citation Rebelo M, Hänscheid T. 2016. Flow cytometry for antimalarial drug testing: more than meets the eye. *J Clin Microbiol* 54:817.

[doi:10.1128/JCM.03017-15](http://dx.doi.org/10.1128/JCM.03017-15).

Editor: A. J. McAdam

Address correspondence to Maria Rebelo, maria.rebelo@fm.ul.pt.

For the author reply, see [doi:10.1128/JCM.03158-15](http://dx.doi.org/10.1128/JCM.03158-15).

Copyright © 2016, American Society for Microbiology. All Rights Reserved.

SCIENTIFIC REPORTS

OPEN

Efficient monitoring of the blood-stage infection in a malaria rodent model by the rotating-crystal magneto-optical method

Received: 13 August 2015
Accepted: 26 February 2016
Published: 17 March 2016

Ágnes Orbán^{1,*}, Maria Rebelo^{2,*}, Petra Molnár¹, Inês S. Albuquerque², Adam Butykai¹ & István Kézsmárki¹

Intense research efforts have been focused on the improvement of the efficiency and sensitivity of malaria diagnostics, especially in resource-limited settings for the detection of asymptomatic infections. Our recently developed magneto-optical (MO) method allows the accurate quantification of malaria pigment crystals (hemozoin) in blood by their magnetically induced rotation. First evaluations of the method using β -hematin crystals and *in vitro* *P. falciparum* cultures implied its potential for high-sensitivity malaria diagnosis. To further investigate this potential, here we study the performance of the method in monitoring the *in vivo* onset and progression of the blood-stage infection in a rodent malaria model. Our results show that the MO method can detect the first generation of intraerythrocytic *P. berghei* parasites 66–76 hours after sporozoite injection, demonstrating similar sensitivity to Giemsa-stained light microscopy and exceeding that of flow cytometric techniques. Magneto-optical measurements performed during and after the treatment of *P. berghei* infections revealed that both the follow up under treatment and the detection of later reinfections are feasible with this new technique. The present study demonstrates that the MO method – besides being label and reagent-free, automated and rapid – has a high *in vivo* sensitivity and is ready for in-field evaluation.

The study of human malaria, one of the most widespread infectious diseases of the globe, is an important agenda of today's scientific research. It involves various methods ranging from epidemiological analysis and clinical studies to laboratory model systems such as *in vitro* parasite cultures in human red blood cells (RBCs) and *in vivo* rodent models. Rodent models of malaria have been widely used to study the biology and pathology of malaria (reviewed in ref. 1) as well as for *in vivo* evaluation of novel vaccine and drug candidates^{2,3}. Rodent models were also applied to successfully investigate the host immune response (reviewed in ref. 1) despite their limitations to replicate certain aspects of the human disease^{4,5}.

Under natural conditions the *Plasmodium* life cycle in the mammalian host starts with the inoculation of sporozoites into the skin by parasite-infected mosquitos. After inoculation the parasites rapidly reach the liver where they infect hepatocytes and develop into thousands of exoerythrocytic merozoites. Once released from the hepatocyte, the merozoites infect red blood cells, leading to the blood stage of the infection that is characterized by cyclic asexual replication. The duration of the liver development and the length of the asexual cycle varies between species. In the case of the *P. berghei* rodent parasites investigated here, the asymptomatic liver stage lasts 47–52 hours and the length of one erythrocytic cycle is approx. 24 hours^{6,7}. Experimental challenges can be carried out either via the bites of infected mosquitos, or through the artificial injection of liver-infecting sporozoites or infected erythrocytes. The progression of the blood stage is quantitatively characterized by the percentage of infected RBCs, i.e. the parasitemia.

The reference method of diagnostics, light microscopy of Giemsa-stained thin blood smears, is a labour-intensive procedure relying on the expertise of the investigator. On the other hand, more sensitive molecular methods based on polymerase chain reaction (PCR) are still not used for either the continuous monitoring

¹Department of Physics, Budapest University of Technology and Economics and MTA-BME Lendület Magneto-optical Spectroscopy Research Group, 1111 Budapest, Hungary. ²Instituto de Medicina Molecular, Faculdade de Medicina Universidade de Lisboa, 1649-028 Lisbon, Portugal. *These authors contributed equally to this work. Correspondence and requests for materials should be addressed to Á.O. (email: orban@dept.phy.bme.hu)

of laboratory experiments or for the primary diagnosis of patient samples due to their high running cost^{8,9}. In laboratory studies automated approaches, such as flow cytometry are preferred and extensively used. However, to achieve sufficient sensitivity they often require special dyes combined with complex protocols^{10–12} or transgenic fluorescent protein-expressing parasites^{13–15}. The use of transgenic luciferase expressing parasites has also been shown to accurately evaluate the pre-patent period, i.e. the time between sporozoite inoculation and the appearance of parasites in the peripheral circulation, and the early blood stages in a novel bioluminescent assay¹⁶. However, methods exploiting the chemiluminescent properties, besides being costly, are limited to animal models.

The need for a universally applicable and automated method for diagnostics has motivated extensive research on malaria pigment (hemozoin), a natural biomarker of the infection. In particular, various magnetic and/or optical detection schemes targeting hemozoin have been proposed^{17–21}.

Hemozoin is a micro-crystalline heme compound produced by all *Plasmodium* spp. during the intraerythrocytic stage as they detoxify free heme derived from hemoglobin digestion^{22–24}. The steadily increasing hemozoin content of the parasites acts as an optimal indicator of their maturation during the erythrocytic cycle. Indeed, the hemozoin-based flow cytometric detection of parasite maturation has been utilized in a novel reagent-free drug sensitivity assay as well^{25,26}.

The rotating-crystal magneto-optical (MO) technique determines the concentration of hemozoin crystals via their linear dichroism and magnetic anisotropy²⁷. In our recent study the sensitivity of the method has been evaluated using ring and schizont stages from *P. falciparum* *in vitro* cultures where detection thresholds of 0.0008% and 0.0002% parasitemia have been found, respectively²⁸. These results implied that the MO method is suitable for the high-sensitivity detection of the infection as a laboratory tool or, eventually, as an in-field diagnostic technique.

Here we test the MO method *in vivo* by monitoring the onset of the blood-stage after sporozoite challenge in a malaria mouse model using *P. berghei* parasites. To evaluate the sensitivity of the MO technique light microscopy, PCR and flow cytometry were used as control methods. The clearance of hemozoin during the treatment of *P. berghei* infections was also followed to establish a time-frame after which the MO signal vanishes in successfully treated mice.

Results

Onset of the blood-stage in *P. berghei* infections monitored by the MO method, light microscopy, PCR and flow cytometry.

The onset of the blood-stage following *P. berghei* sporozoite challenges was monitored in three independent experiment series (A, B and C). Mice in series A and B were infected intravenously, while mice in series C were subjected to mosquito bites (for details see Methods). In order to evaluate the sensitivity of the MO method in comparison with standard techniques and to determine the time scale of the first positive detections, blood was drawn from mice starting at the end of the liver stage in approx. 5-hour intervals until the fourth day of blood-stage infection. The blood samples were examined to assess the appearance of the first parasites by thin smear microscopy, flow cytometry and MO measurements i) from 48 h to 132 h post infection (pi) in series A, ii) from 70 h to 132 h pi in series B and iii) from 56 h to 166 h in series C. For the last two methods the detection limit was determined as the average value plus three times the standard deviation of the data measured for the uninfected references (for details see Methods). Additionally, q-PCR measurements were performed in the early time points of the intraerythrocytic parasite development for series A and B.

The Giemsa-stained thin blood films showed the first parasites in the circulation of mice in series A and B between 66–75 h pi with one exception, when parasites were observed only at 85 h pi (Fig. 1a). The first occurrences of positive microscopy results show small variation in these controlled infections and coincide well with the estimated end of the first erythrocytic cycle (approx. 70–75 h). In series C the first parasites were observed in the same time interval (61–71 h pi), however in these cases only single parasites were found in the smears until 76 h pi (Fig. 2a).

Real-time PCR analysis was performed on blood samples drawn from mice in series A between 48–66 h pi and from mice in series B at 70 h pi. Results in Fig. 1c show that the difference in the PCR signal between the infected and non-infected samples becomes significant at 56 h pi, and gradually increases for later samplings. These PCR data are in good agreement with previous findings described by Zuzarte-Luis *et al.*¹⁶ under similar experimental settings and they confirm the onset of the blood stage with the expected high sensitivity.

Flow cytometric analysis was also performed for measurement series A and C (Figs 3 and 4, respectively). In these experiments two different parameters were assessed simultaneously: i) fluorescence of GFP expressing parasites¹³ and ii) depolarized side scattering (DSS) properties of the hemozoin-containing red blood cells^{17,18}. As an inherent advantage of flow cytometry, parasite counts can be determined in both cases directly. However, the number of GFP- and DSS-positive events may quantitatively differ as fluorescence detects all erythrocytic stages¹³, while DSS exposes only that fraction of parasitized RBCs that contain a sufficient amount of hemozoin¹⁷. Accordingly, the GFP positive events are used to assess parasitemia, while the DSS detection, similarly to MO and PCR yields indirect measure of the parasite burden.

The DSS and GFP values for series A, shown in Fig. 3, are scattered below the detection limit until 85–90 h pi, when both signals start to increase monotonically and the onset of the blood stage is confirmed with the first positive parasite counts of 0.04% and 0.12%, respectively. As expected the parasitemia counts determined by fluorescence were higher at any time point than the corresponding DSS values. In summary, both cytometric methods confirmed the onset of the blood-stage in the middle of the second erythrocytic cycle.

The flow cytometric curves of mice in series C show larger individual variation than those in series A (Fig. 4). The GFP and DSS signals exceed the detection limit between 95–120 h pi. In average the first positive GFP and DSS detections can be placed in the beginning and the second half of the 3rd cycle, respectively. The average

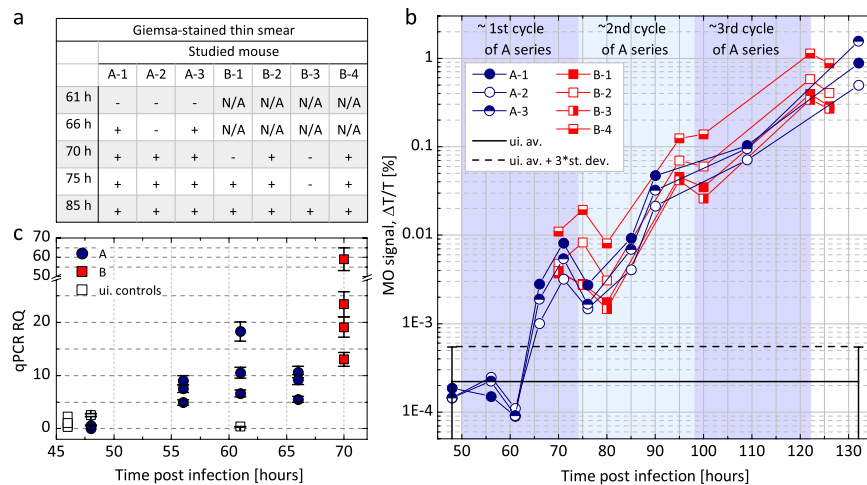


Figure 1. Onset of the blood-stage in series A and B (intravenously infected mice) monitored by light microscopy, the magneto-optical method and q-PCR. (a) Microscopic examination of Giemsa-stained thin blood smears of mice in series A and B. + signals indicate that at least one parasite was found in the whole of the smears (approx. 20–40 fields), – signals mean that no parasites were detected in the smears. (b) The results of the MO measurements. Each circle (square) represents the MO signal of an infected mouse in series A (B) at a given time point after sporozoite injection. The continuous black line represents the average of the MO values of five uninfected control mice measured in all time points. The dashed black line is the detection limit defined as the average plus three times the standard deviation of the uninfected values (for details see Methods section). The MO signals of series A exceed the detection limit at 66 h pi. The MO signals of all mice in series B exceed the detection limit already at the first, 70 h sampling point. The background shading illustrates the estimated layout of the first three erythrocytic cycles of series A. (c) Results of the q-PCR measurements plotted by circles (squares) for series A (B). The error bars represent the standard deviation of technical duplicates. The □ represent measurements on three uninfected controls and the real-time control mouse at 48 h and 61 h.

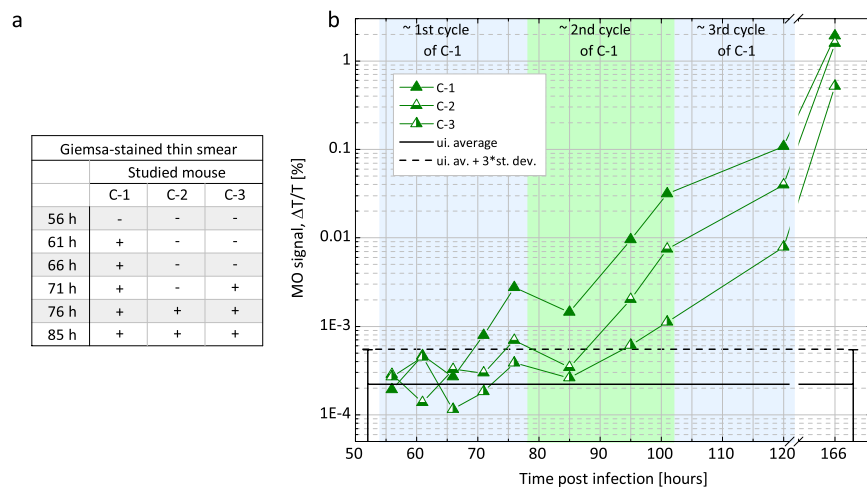


Figure 2. Onset of blood stage infection of series C (mosquito-infected mice) monitored by light microscopy and the magneto-optical method. (a) Microscopic examination of Giemsa-stained thin blood smears of mice in series C. + signals indicate that at least one parasite was found in the whole of the smears (approx. 20–40 fields), while – signals mean that no parasites were detected in the smears. (b) The results of the MO measurements. Each triangle represents the MO signal for a given mouse in series C at a given time point after the mosquito challenge. The continuous black line represents the average of the MO values of five uninfected control mice measured in all time points. The dashed black line is the detection limit defined as the average plus three times the standard deviation of the uninfected values (for details see Methods section). The MO signals of mouse C-1, C-2 and C-3 exceed the detection limit at 71 h, 76 h and 95 h, respectively. The background shading illustrates the estimated layout of the first three erythrocytic cycles.

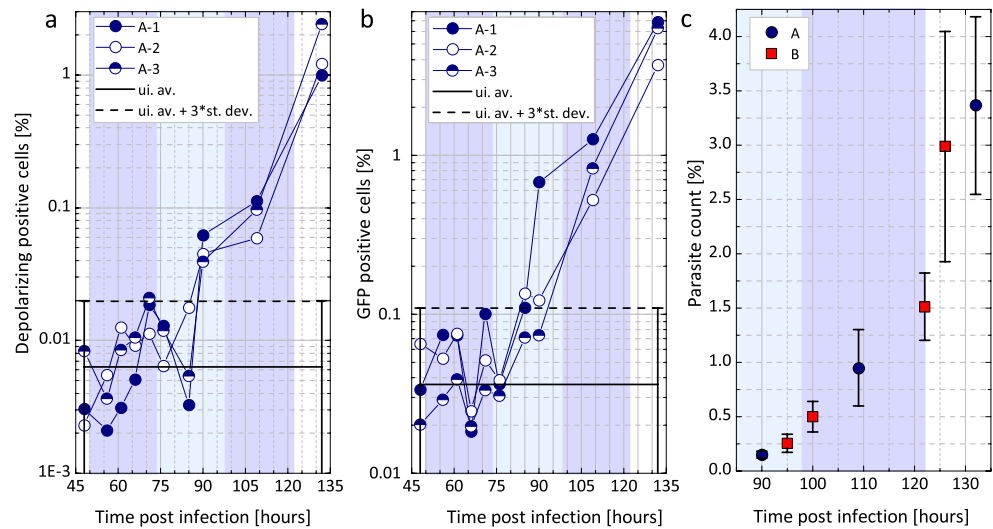


Figure 3. Monitoring parasitemia during the progression of the infection in series A and B via flow cytometry and light microscopy. (a) The results of the DSS measurements. The circles represent the percentages of DSS positive events in the total population of RBC counts for a given mouse in series A. The continuous black line represents the average signal of the uninfected reference, while the dashed black line is the detection limit defined as the average plus three times the standard deviation of the uninfected values (for details see Methods section). The DSS signals of all mice in series A unambiguously exceed the detection limit at 90 h pi. (b) The results of the GFP measurements. The notation of the symbols is the same as in panel (a). The GFP percentages of mouse A-1, A-2 and A-3 exceed the detection limit (dashed line) at 85 h, 85 h and 109 h pi, respectively. The background shading illustrates the estimated layout of the first three erythrocytic cycles. Note the different vertical scales in graphs (a,b). (c) Averaged parasitemia values determined by light microscopy after 90 h pi at the inspected time points of series A (●) and B (■).

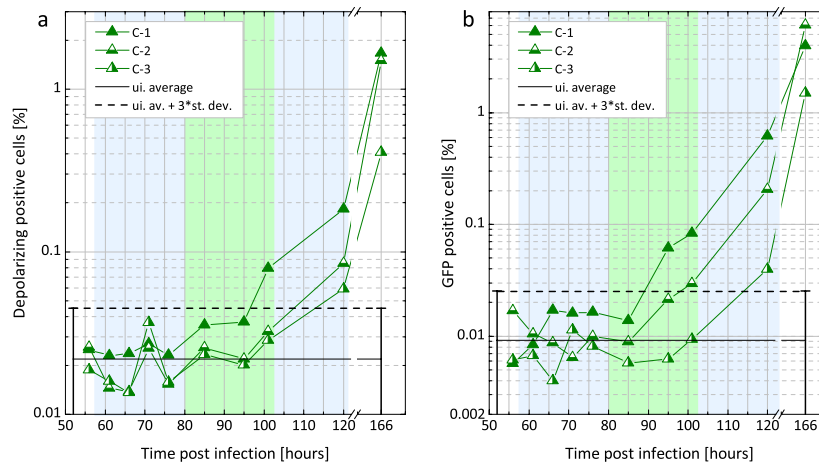


Figure 4. Monitoring parasitemia during the progression of the infection in series C via flow cytometry. (a) The results of the DSS measurements. The triangles represent the percentages of DSS positive events in the total population of RBC counts for a given mouse in series C. The continuous black line represents the average signal of the uninfected references, while the dashed black line is the detection limit defined as the average plus three times the standard deviation of the uninfected values (for details see Methods section). The DSS percentages of mouse C-1, C-2 and C-3 exceed the detection limit at 101 h, 120 h and 120 h pi, respectively. (b) The results of the GFP measurements. The notation of the symbols is the same as in graph (a). The GFP percentages of mouse C-1, C-2 and C-3 exceed the detection limit (dashed line) at 95 h, 100 h and 120 h pi, respectively. The background shading illustrates the estimated layout of the first three erythrocytic cycles. Note the different vertical scales in graphs (a,b).

parasitemia measured by fluorescence at the time points of the first positive detection is approx. 0.04% and the average DSS percentage is 0.07%.

The MO values of the A and B series (Fig. 1b) clearly exceed the detection limit at 66 h pi and 70 h pi, respectively. (Note that no measurements were performed on series B before 70 h pi). The MO measurements of the two series exhibit very similar tendencies and indicate that circulating parasites could be detected by the MO method as early as 66 h pi. The MO signals of the mosquito-infected mice in series C surpass the detection limit in the broad interval of 71–95 h pi. This large variation of the earliest detections is in agreement with the results of microscopy and flow cytometry, and is indeed expected due to the uncontrolled size of the inocula characterizing the natural infections. The delayed detection as compared to the A and B series suggests a lower initial parasite load as seen in the flow cytometric measurements. Nevertheless, the onset of the blood stage still could be detected in the first erythrocytic cycle for two out of three mice.

Monitoring the progression of the blood-stage infection by the MO method. After establishing the first time points of erythrocytic parasite detection by microscopy, PCR, flow cytometry and the MO method, the progression of the infection at later time points was monitored by microscopy, flow cytometry and the MO method until day 6 and 7 pi in series A and C, respectively.

In series A and B the parasitemia values, as measured both by flow cytometry and microscopy, reached the level of 0.1–0.5% on day 4 pi (90–100 h timeframe) similarly to the results of Ploemen *et al.*²⁹, where experiments were performed with similar initial sporozoite loads. In the case of series C this parasitemia range was reached only at the end of the fifth day (120 h) as a result of the considerably lower initial sporozoite load.

In Fig. 1b the MO signals of all three infected mice from series A show the same profile after exceeding the detection limit: the MO signal increases rapidly, interrupted by a distinct drop at 76 h. Following another steadily increasing period a drop of the increase rate can be identified between 90–109 h pi. The same behavior is observed for series B with only slight variations in the positions of the drops, observable at 80 h, 100 h and 125 h. While the drops at the early time points (76 h and 80 h) are clearly visible with a 65% and 75% reduction of the MO signal for series A and B, respectively, at later time points they are less pronounced.

In conclusion, the overall time dependence of the MO signal is very similar in all intravenously initiated infections. These results, supported by similar observations in flow cytometry and microscopy (Fig. 3a–c), suggest that the early blood stages of these controlled infections followed quite similar courses and that this progression could be reliably monitored by the MO measurements.

The MO curves of series C (Fig. 2b) show similar features to that of series A and B, but the signals of the individual animals reveal bigger variation as also found by the reference methods. It can be noted that the MO values of mice C-1 and C-2 exceed the detection limit already in the first erythrocytic cycle as found in series A and B, where mice were infected with considerably higher parasite loads.

The time evolution of the MO signal can be explained by considering that the total hemozoin concentration in the peripheral circulation is measured by this method. This includes crystals present within the parasites, free in circulation and/or inside phagocytic cells at the moment of blood sampling. Consequently, changes in the signal magnitude in the early phases of blood stage development are likely to result from two dynamic processes: i) the continuous production of hemozoin by the circulating parasites increases the MO signal and ii) the clearance of free hemozoin or hemozoin-containing phagocytes decreases the MO signal. If these two processes have comparable rates in a synchronous infection at a given parasite density, the MO signal is expected to pursue the following course: (i) gradual increase from the beginning of the first cycle, (ii) reaching a maximum at the end of the cycle when mature schizonts have maximal hemozoin content, (iii) decrease due to the rupture of iRBCs and the subsequent hemozoin clearance and (iv) turnover and increase due to the hemozoin production of the new generation of parasites.

In *P. berghei* infections the egress of merozoites from hepatocytes is expected around 48–52 h after sporozoite injection^{6,7} and the length of the asexual life cycle is 22–24 h⁷. Accordingly, the first intraerythrocytic cycle is expected to end between 72–76 h pi. This timeframe coincides well with the peak of the MO signal at approx. 72–75 h pi followed by the drop at 76–80 h pi observed both in series A and B. These observations indicate that the first parasites detected by the MO method around 66 h pi were approx. 14–16-hour-old parasites of the first synchronous life cycle. The additional drops observed with approx. 24-hour periodicity indicates that a partial synchronicity is preserved over a couple of cycles. The decreasing magnitude of subsequent drops indicates that synchronicity is eventually lost as known for *P. berghei* infections^{7,30}.

In the first erythrocytic cycle the parasitemia levels were not quantifiable accurately by microscopy or by flow cytometry, but they can be estimated using the parasitemia values measured in the following cycles and the ~10-fold multiplication rate characterizing the first few erythrocytic cycles of the *P. berghei* ANKA parasites^{31,32}. This multiplication rate is also confirmed by the 10-fold increase of the MO values between the ends of consecutive cycles. The average parasitemia for series A and B was in the range of 0.1–0.3% at the end of the second cycle. Accordingly, in these two series the parasitemia level of the first cycle was approx. 0.01–0.03%. For series C, the parasitemia values measured by GFP-detection at the end of the third intraerythrocytic cycle (Fig. 4b) were 0.6%, 0.2% and 0.04% for mouse C-1, C-2 and C-3, respectively. Accordingly, the average parasite loads for the three mice at the time of the first positive MO detection was approx. 0.004%.

Monitoring parasite clearance by the MO method. In this study 5 mice (identified as T-1...5) with severe *P. berghei* infections were treated by the daily administration of chloroquine for seven days. Their MO signal was measured during the treatment and for nine consecutive days in order to study the clearance of the parasites and to determine the time interval after which the MO signal is reduced to the detection level.

The first blood samples were collected from mice T-1, T-3 and T-4 on the first day of treatment (day 0 in Fig. 5). The corresponding parasitemia values, determined by microscopy, were 15%, 20% and 11% and the corresponding

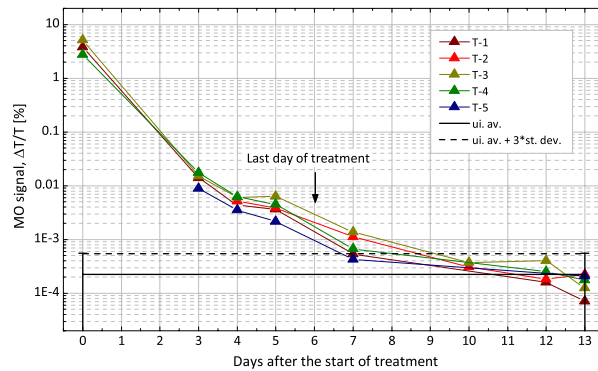


Figure 5. Monitoring parasite clearance during treatment by the MO method. The MO values of five mice were measured during and post treatment (T-series). Each colored triangle represents the MO value of a given mouse on a given day after the start of the treatment. The continuous black line represents the average of the MO values of five uninfected control mice measured in all time points. The dashed black line is the detection limit defined as the average plus three times the standard deviation of the uninfected values (for details see Methods section). The MO values of all treated mice reach the detection limit on day 10 and stay below it for the two consecutive measurements.

MO values were 3.76, 5.20 and 2.78, respectively. Since mice were anemic on the first day of treatment, no further blood collection was performed until the administration of the fourth dose of chloroquine (day 3). Subsequent blood samplings were performed as indicated in Fig. 5.

The MO signals of all the studied mice follow very similar decreasing trends. The substantial decrease in parasitemia ($0.16\% \pm 0.07\%$ and $0.06\% \pm 0.04\%$ on day 3 and 4, respectively) caused by the administration of the first three doses of chloroquine is reflected in the rapid (approximately two orders of magnitude) decrease of the MO signal observed between day 0 and day 3.

On day 5, no viable parasites were observable by light microscopy in any of the mice. Consequently, the MO signal measured between days 5–7 is attributed to hemozoin crystals released from ruptured schizonts remaining in the circulation either freely or inside phagocytes^{33,34}. The clearance rate with an approximate half-life of 24 hours is in agreement with the observations of mid- and long-term hemozoin kinetics reported for *in vivo* *P. berghei* infections³³. By day 10 the MO signals in all treated mice was reduced to the detection limit and remained at this level for the consecutive two days, confirming the absence of the infection and yielding true negative diagnostic results.

Discussion

The rotating-crystal magneto-optical diagnostic method has demonstrated excellent sensitivity to detect low concentrations of synthetic hemozoin crystals²⁷ and low parasite densities of *P. falciparum* *in vitro* cultures²⁸. Besides its *in vitro* sensitivity the method fulfills the most important technical requirements for in-field applicability: the measurement is automated, it is label- and reagent-free, and the device can be designed into a commercially available format^{27,28}. In the present study the *in vivo* efficiency of the method was investigated by comparing its performance to well-known techniques.

In the investigated *P. berghei* infections the first erythrocytic parasites were already detectable at the late ring stage 66 h pi when mice were injected with 50,000 sporozoites. In experiments when mice were subjected to mosquito bites the course of infection showed larger individual variation: in two cases the infection was detected at the end of the first cycle and in one case in the second half of the second cycle. Based on these results we conclude that the performance of the MO method is similar that of light microscopy. This performance is only exceeded by the laboratory-grade q-PCR (with detection as early as 56 h pi). In later time points the quantitative monitoring of the progression of the infection was also feasible with the MO method.

The blood stage of *P. berghei* infections has three important aspects that influence the hemozoin levels observable in the peripheral circulation: (i) the reticulocyte preference; (ii) the asynchronicity of later cycles and (iii) that the late schizonts tend to sequester in organs³⁵. The first two properties are also typical features of the blood stage of *P. vivax* human infections. In this respect the current *P. berghei* experiments can be regarded as a simple model for the MO diagnostics of *P. vivax* infections.

The stage distribution of intraerythrocytic parasites in the case of *P. falciparum* infections, however, is different. In the latter case parasites older than mid-stage trophozoites tend to cytoadhere to the endothelium, thus the young forms present in the circulation contain little or no hemozoin. Clearly, this scenario is different from the *P. berghei* infection model, where only the very late schizonts sequester. However, the present study yielded two results with important implications for the detection of *P. falciparum* infections: (i) the first generation of parasites in the late-ring stage were already detectable and (ii) the MO results obtained during treatment of mice show that there is a substantial amount of hemozoin crystals circulating in the blood stream for a few days after schizont rupture. These observations indicate that the MO method has potential to detect human *P. falciparum* infections as well, either via the lesser amounts of hemozoin present in the blood sample inside the freely circulating late-stage rings or by detecting the hemozoin that is released from the sequestered schizonts after the rupture of

iRBCs. During the treatment of infected mice we found that the period of false positive outcomes after successful treatments is limited to four days implying a similar scenario in the case of human infections.

Though the extrapolation of the results of rodent malaria experiments to human infections is never straightforward, we believe that the present study provides a solid basis for the implementation of in-field tests, which will assess the real performance of the method for the diagnostics of human infections.

Methods

Animals, parasites and treatment. In experiment series A and B, four and three BALB/c mice (Charles River, Spain) were infected, respectively, with the transgenic *P. berghei* ANKA (259cl2) that constitutively expresses GFP during the whole life cycle. Sporozoites were obtained by the disruption of the salivary glands of freshly dissected, infected female *Anopheles stephensi* mosquitoes and collected in DMEM (Dulbecco's Modified Eagle Medium from GIBCO). Mosquitoes were bred at the insect facility of the Instituto de Medicina Molecular. Each mouse was inoculated by the retroorbital injection of 50,000 sporozoites.

Blood was collected from the tail vein according to the following schedule: in series A sampling started at the time point of 48 h pi and it was carried out in 5-hour intervals until 80 h pi; in series B sampling started only at 70 hours pi and two additional samples were taken at 75 h and 80 h pi. After 80 hours blood was collected daily in both series until the 5th day post infection. Blood samples were collected for microscopy, PCR, flow cytometry and the MO method at each time point.

In series C three mice were subjected to five *P. berghei*-infected mosquitos for 20 minutes, individually. The method of blood sampling and its schedule was the same as in series A.

In the treatment measurements (T-series), five mice with severe *P. berghei* ANKA infection were treated by the daily administration of 7 mg/ml of chloroquine for seven days. Mice exhibited anemia on the first days of treatment and thus, no further blood was collected until the administration of the fourth dose of chloroquine (day 3). On this day blood samples from 4 mice were analyzed again by the MO method and by light microscopy. Further blood sampling and analysis was performed on days 4, 5, 7, 10, 12, and 13, as shown in Fig. 5.

Ethics statement. This study was approved by the Ethical Committee of the Faculty of Medicine, University of Lisbon. All experiments involving animals were performed in compliance with the relevant laws and institutional guidelines. Animals were monitored daily and every effort was made to minimize their suffering. Upon completion of the experiments, mice were euthanized by administration of CO₂ followed by cervical dislocation.

Microscopic analysis. Blood parasitemia was monitored by the microscopic analysis of Giemsa-stained thin blood smears at each measured time point. Smears were fixed in absolute methanol and stained with 10% Giemsa-solution prepared in PBS 1X.

The presence of parasites in the early time points, i.e., before 90 h post-infection was determined by light microscopic examination of whole smears (approx. 20–40 fields, i.e. approx. 7,000–14,000 scanned RBCs) with 1000× magnification using a bright-field microscope (Leica, Solms, Germany) performed by two microscopists, independently. At later time points percentages of infected red blood cells and approximate age distribution of the parasites was assessed by light microscopic examination of 5–10 fields (approx. 1800–3600 RBCs).

Magneto-optical measurements. All reagents were purchased from Sigma Aldrich (St Louis, Mo, USA) unless stated otherwise.

For the magneto-optical measurements 30 µl of blood was transferred from each mouse directly into 570 µl of lysis solution (0.066 V/V% Triton X-100 in 3 mM NaOH). The lysed sample was measured after 5 minutes, to enable the hemozoin crystals to be liberated from the RBC's and from the parasites and become homogeneously dispersed in the liquid²⁷. MO measurements were performed using a volume of 450 µl from each lysed sample.

The scheme of the MO setup, as well as the underlying physical principles of the detection method, are described in detail in former studies^{27,28}. Briefly, the lysed sample, filled into a cylindrical sample holder, is inserted into the center of a ring-shaped assembly of permanent magnets, which creates a strong uniform magnetic field ($B = 1\text{ T}$) at the sample position. This magnetic field induces the co-alignment of the hemozoin crystals and when the magnetic ring is rotated, the co-aligned hemozoin crystals follow this rotation. During the measurement polarized light from a laser diode is transmitted through the sample in the direction perpendicular to the plane of the rotating magnetic field. The rotation of the co-aligned dichroic crystals gives rise to a periodic change in the transmitted intensity (ΔT), which – divided by the time-averaged intensity (T) – corresponds to the measured MO signal ($\Delta T/T$ in %). The overall time required for the full MO measurement process is a few minutes.

The level of the detection limit was determined as the mean plus three times the standard deviation of the MO signals measured on the following samples: one control mouse in series A, which was measured at the same time points as the infected ones of the same series; and four controls in series C also measured together with the infected animals of the same series. For clarity we only plot the average of the uninfected values (black line) and the corresponding detection limits (dashed black line) in graphs Figs 1b, 2b and 5. The individual results of the control measurements are plotted in Fig. 3 of the Supplementary information.

DNA extraction and PCR analysis. At the selected time points 5 µl of blood was collected from the tail vein into 200 µl of PBS 1X. DNA extraction was performed using the DNeasy Blood & Tissue Kit (Quiagen, USA), according to the manufacturer's instructions. Real-time PCR analysis was performed in duplicates using 2 µl of DNA and the iTaq Universal SYBR Green Supermix from Bio-Rad according to the manufacturer's instructions. Expression levels of 18 s rRNA were normalized against the housekeeping gene seryl-tRNA synthetase (PbANKA_061540). Gene expression values were calculated based on the $\Delta\Delta C_t$ method. Primer pairs used were: PbA 18S rRNA: 5' GGAGATTGGTTTTGACGTT TATGTG3' and 5'GGAGATTGGTTTTGACGTTTATGTG3'; PBANKA_061540: 5' ATTGCTCAACCTTATCAAACCTG3' and 5'AGCCACATCTGAACAACCG3'.

Flow cytometric measurements. A volume of 5 μ l of blood was collected and diluted in 1 ml of PBS 1X at each time point for each mouse. This blood suspension was analyzed in the CyFlow[®] Blue instrument (Partec, Munster, Germany), which is equipped with a 488 nm excitation laser, and has detectors for forward scatter (FSC), side scatter (SSC), green fluorescence – FL1 (BP 535/35 nm), orange fluorescence – FL2 (BP 590/50 nm) and red fluorescence – FL3 (LP 630 nm). For this study the setup was modified as described previously^{16,17}. Flow cytometry data were analyzed using FlowJo software (version 9.0.2, Tree Star Inc., Oregon, USA). Depolarizing events were defined in plots of side-scatter (SSC) versus depolarized-SSC as those with a signal above the background observed in the uninfected control. GFP positive cells were determined in green fluorescence (FL1) versus red fluorescence (FL3) plots.

In measurement series A one uninfected control was used to define GFP positive cells, which consisted of the ones with green fluorescence levels above the uninfected control. The detection limit of the whole DSS (GFP) measurement series (dashed lines in Fig. 3a,b) was determined as the average plus three times the standard deviation of the DSS (GFP) positive events measured on the uninfected control mouse in all of the investigated time points (not shown in the graphs).

In measurement series C the level of the detection limit (dashed lines in Fig. 4a,b) of the whole DSS (GFP) measurement series was determined as the mean plus three times the standard deviation of the DSS (GFP) positive events measured on the blood samples of four uninfected controls in the same time points as the infected mice (not shown in the graphs).

References

- Zuzarte-Luis, V., Mota, M. M. & Vigário, A. M. Malaria infections: What and how can mice teach us. *J. Immunol. Methods* **410**, 113–122 (2014).
- Mota, M. M., Thathy, V., Nussenzweig, R. S. & Nussenzweig, V. Gene targeting in the rodent malaria parasite *Plasmodium yoelii*. *Mol. Biochem. Parasitol.* **113**, 271–278 (2001).
- Khan, Z. M. & Vanderberg, J. P. Role of host cellular response in differential susceptibility of nonimmunized BALB/c mice to *Plasmodium berghei* and *Plasmodium yoelii* sporozoites. *Infect. Immun.* **59**, 2529–2534 (1991).
- White, N. J., Turner, G. D., Medana, I. M., Dondorp, A. M. & Day, N. P. The murine cerebral malaria phenomenon. *Trends Parasitol.* **26**, 11–15 (2010).
- Craig, A. G. *et al.* The role of animal models for research on severe malaria. *PLoS Pathog.* **8**, e1002401 (2012).
- Landau, I. & Boulard, Y. Life Cycles and Morphology in *Rodent Malaria* (eds Killick-Kendrick, R. & Peters, W.) 53–84 (London: Academic Press, 1978).
- Janse, C. J. & Waters, A. P. *Plasmodium berghei*: The application of cultivation and purification techniques to molecular studies of malaria parasites. *Parasitol. Today* **4**, 138–143 (1995).
- Valkunas, G. *et al.* A comparative analysis of microscopy and PCR-based detection methods for blood parasites. *J. Parasitol.* **94**, 1395–1401 (2008).
- Taylor, S. M. *et al.* High-throughput pooling and real-time PCR-based strategy for malaria detection. *J. Clin. Microbiol.* **48**, 512–519 (2010).
- Lelliott, P. M., Lampkin, S., McMorran, B. J., Foote, S. J. & Burgio, G. A flow cytometric assay to quantify invasion of red blood cells by rodent *Plasmodium* parasites *in vivo*. *Malaria J.* **13**, 100 (2014).
- Jimenez-Diaz, M. B. *et al.* Quantitative measurement of *Plasmodium*-infected erythrocytes in murine models of malaria by flow cytometry using bidimensional assessment of SYTO-16 fluorescence. *Cytometry A* **75**, 225–235 (2009).
- Malleret, B. *et al.* A rapid and robust tri-color flow cytometry assay for monitoring malaria parasite development. *Sci. Rep.* **1**, 118 (2011).
- Franke-Fayard, B. *et al.* A *Plasmodium berghei* reference line that constitutively expresses GFP at a high level throughout the complete life cycle. *Mol. Biochem. Parasitol.* **137**, 23–33 (2004).
- Kenthirapalan, S., Waters, A. P., Matuschewski, K. & Kooij, T. W. Flow cytometry-assisted rapid isolation of recombinant *Plasmodium berghei* parasites exemplified by functional analysis of aquaglyceroporin. *Int. J. Parasitol.* **42**, 1185–1192 (2012).
- Manzoni, G. *et al.* A rapid and robust selection procedure for generating drug-selectable marker-free recombinant malaria parasites. *Sci. Rep.* **4**, 4760 (2014).
- Zuzarte-Luis, V., Sales-Dias, S. & Mota, M. M. Simple, sensitive and quantitative bioluminescence assay for determination of malaria pre-patent period. *Malaria J.* **13**, 15 (2014).
- Rebelo, M., Shapiro, H. M., Amaral, T., Melo-Cristino, J. & Hänscheid, T. Haemozoin detection in infected erythrocytes for *Plasmodium falciparum* malaria diagnosis—Prospects and limitations. *Acta Trop.* **123**, 58–61 (2012).
- Rebelo, M. *et al.* Light depolarization measurements in malaria: A new job for an old friend. *Cytometry A* **87**, 437–445 (2015).
- Karl, S. *et al.* Enhanced detection of gametocytes by magnetic deposition microscopy predicts higher potential for *Plasmodium falciparum* transmission. *Malaria J.* **7**, 66 (2008).
- Mens, P. F., Matelon, R. J., Nour, B. Y. M., Newman, D. M. & Schallig, H. Laboratory evaluation on the sensitivity and specificity of a novel and rapid detection method for malaria diagnosis based on magneto-optical technology (MOT). *Malaria J.* **9**, 207 (2010).
- Lukianova-Hleb, E. Y. Hemozoin-generated vapor nanobubbles for transdermal reagent- and needle-free detection of malaria. *Proc. Nat. Acad. Sci. USA* **111**, 900–905 (2013).
- Fulton, J. D. & Rimington, C. The Pigment of the Malaria Parasite *Plasmodium berghei*. *J. gen. Microbiol.* **8**, 157–159 (1953).
- Francis, S. E., Sullivan, D. J. & Goldberg D. E. Hemoglobin metabolism in the malaria parasite *Plasmodium falciparum*. *Annu. Rev. Microbiol.* **51**, 97–123 (1997).
- Slater, A. F. *et al.* An iron-carboxylate bond links the heme units of malaria pigment. *Proc. Nat. Acad. Sci. USA* **88**, 325–329 (1991).
- Rebelo, M. *et al.* A novel Flow Cytometric hemozoin detection assay for real-time sensitivity testing of *Plasmodium falciparum*. *PLoS ONE* **8**, e61606 (2013).
- Rebelo, M., Tempera, C., Fernandes, J., Grobusch, M. P. & Hänscheid, T. Assessing anti-malarial effects *ex vivo* using the haemozoin detection assay. *Malaria J.* **14**, 140 (2015).
- Butykai, A. *et al.* Malaria pigment crystals as magnetic micro-rotors: key for high-sensitivity diagnosis. *Sci. Rep.* **3**, 1431 (2013).
- Orban A. *et al.* Evaluation of a novel magneto-optical method for the detection of malaria parasites. *PLoS ONE* **9**, e96981 (2014).
- Ploemen, I. H. J. *et al.* Visualisation and quantitative analysis of the rodent malaria liver stage by real time imaging. *PLoS ONE* **4**, 11 (2009).
- Bagnaresi, C. R. *et al.* Unlike the synchronous *Plasmodium falciparum* and *P. chabaudi* infection, the *P. berghei* and *P. yoelii* asynchronous infections are not affected by melatonin. *Int. J. Gen. Med.* **2**, 47–55 (2009).
- Janse, C. J. *et al.* Waters AP: Malaria parasites lacking eef1a have a normal S/M phase yet grow more slowly due to a longer G1 phase. *Mol. Microbiol.* **50**, 1539–51 (2003).

32. Matz, J. M., Matuschewski, K. & Kooij, T. W. A. Two putative protein export regulators promote Plasmodium blood stage development *in vivo*. *Mol. Biochem. Parasitol.* **191**, 44–52 (2013).
33. Frita, R. *et al.* Simple flow cytometric detection of haemozoin containing leukocytes and erythrocytes for research on diagnosis, immunology and drug sensitivity testing. *Malaria J.* **10**, 74 (2011).
34. Boura, M., Frita, R., Góis, A., Carvalho, T. & Hänscheid, T. The hemozoin conundrum: is malaria pigment immune-activating, inhibiting, or simply a bystander? *Trends Parasitol.* **10**, 469–476 (2013).
35. Franke-Fayard, B., Fonager, J., Braks, A., Khan, S. M. & Janse, C. J. Sequestration and tissue accumulation of human malaria parasites: Can we learn anything from rodent models of malaria? *PLoS Pathog* **6**, e1001032 (2010).

Acknowledgements

We thank Thomas Hänscheid for the continuous support of the project and critical reading of the manuscript. We thank Carolina Tempera and Vanessa Zuzarte-Luis for their kind help during the experiments. This work was supported by the Hungarian Research Funds OTKA #K108918.

Author Contributions

A.O., M.R., P.M. and I.S.A. performed the experiments. A.O., M.R., I.S.A. and I.K. analyzed the data. A.O., M.R., A.B. and I.K. wrote the manuscript. A.O. and A.B. developed the magneto-optical setup. M.R., I.K. and A.O. designed the experiments. I.K. supervised the project. All authors read and approved the final form of the manuscript.

Additional Information

Supplementary information accompanies this paper at <http://www.nature.com/srep>

Competing financial interests: The authors declare no competing financial interests.

How to cite this article: Orbán, Á *et al.* Efficient monitoring of the blood-stage infection in a malaria rodent model by the rotating-crystal magneto-optical method. *Sci. Rep.* **6**, 23218; doi: 10.1038/srep23218 (2016).



This work is licensed under a Creative Commons Attribution 4.0 International License. The images or other third party material in this article are included in the article's Creative Commons license, unless indicated otherwise in the credit line; if the material is not included under the Creative Commons license, users will need to obtain permission from the license holder to reproduce the material. To view a copy of this license, visit <http://creativecommons.org/licenses/by/4.0/>

Torins are potent antimalarials that block replenishment of *Plasmodium* liver stage parasitophorous vacuole membrane proteins

Kirsten K. Hanson^{a,1}, Ana S. Ressurreição^b, Kathrin Buchholz^c, Miguel Prudêncio^a, Jonathan D. Herman-Ornelas^c, Maria Rebelo^a, Wandy L. Beatty^d, Dyann F. Wirth^c, Thomas Hänscheid^a, Rui Moreira^b, Matthias Marti^c, and Maria M. Mota^{a,1}

^aInstituto de Medicina Molecular, Faculdade de Medicina, Universidade de Lisboa, 1649-028 Lisboa, Portugal; ^bMed.UL, Faculdade de Farmácia, Universidade de Lisboa, 1649-003 Lisboa, Portugal; ^cDepartment of Immunology and Infectious Diseases, Harvard School of Public Health, Boston, MA 02115; and ^dWashington University School of Medicine, St. Louis, MO 63110

Edited* by Louis H. Miller, National Institutes of Health, Rockville, MD, and approved May 23, 2013 (received for review April 2, 2013)

Residence within a customized vacuole is a highly successful strategy used by diverse intracellular microorganisms. The parasitophorous vacuole membrane (PVM) is the critical interface between *Plasmodium* parasites and their possibly hostile, yet ultimately sustaining, host cell environment. We show that torins, developed as ATP-competitive mammalian target of rapamycin (mTOR) kinase inhibitors, are fast-acting antiplasmodial compounds that unexpectedly target the parasite directly, blocking the dynamic trafficking of the *Plasmodium* proteins exported protein 1 (EXP1) and upregulated in sporozoites 4 (UIS4) to the liver stage PVM and leading to efficient parasite elimination by the hepatocyte. Torin2 has single-digit, or lower, nanomolar potency in both liver and blood stages of infection *in vitro* and is likewise effective against both stages *in vivo*, with a single oral dose sufficient to clear liver stage infection. Parasite elimination and perturbed trafficking of liver stage PVM-resident proteins are both specific aspects of torin-mediated *Plasmodium* liver stage inhibition, indicating that torins have a distinct mode of action compared with currently used antimalarials.

host-parasite interactions | malaria | protein trafficking | *P. falciparum*

The population at risk for developing malaria is vast, comprising some 3.3 billion people particularly in sub-Saharan Africa and Southeast Asia, with mortality estimates ranging from 655,000 to 1,200,000 (1). Widespread resistance has limited the therapeutic utility of most existing antimalarial drugs, and artemisinin, the highly efficacious cornerstone of artemisinin combination therapies, appears to be at risk for the same fate (2). The need for new antimalarial chemotherapeutic strategies is thus acute.

Plasmodium spp., the causative agents of malaria, have a complex life cycle with alternating motile-nonreplicative and sessile-replicative forms in both mammal and mosquito. In the mammalian host, *Plasmodium* invades and replicates inside two very distinct cell types: hepatocytes and red blood cells (RBCs). In mammals, the *Plasmodium* life cycle is initiated by a motile sporozoite that invades a hepatocyte, where it resides for 2–14 d, multiplying into >10,000 merozoites in a single cycle (3). Once released into the bloodstream, each of these motile merozoites will infect an RBC and, within 1–3 d, generate 10–30 new merozoites, which will contribute to the continuous cycle of blood stage infection that causes the symptoms, morbidity, and mortality of malaria.

These two stages of mammalian infection, despite taking place in distinct cell types and having an orders-of-magnitude difference in parasite replication, do share common features. In both, the motile “zoite” invades the host cell through formation of a parasitophorous vacuole (PV). Both stages grow and replicate exclusively within the confines of the PV, and the parasitophorous vacuole membrane (PVM), which is populated with parasite proteins, constitutes the physical host–parasite interface throughout development. Unlike the vacuoles of many intracellular pathogens

including *Leishmania*, *Chlamydia*, *Mycobacteria*, and *Legionella* (4, 5), the *Plasmodium* vacuole, like that of *Toxoplasma gondii*, does not fuse with host lysosomes and is not acidified (6). This is not unsurprising in the context of *Plasmodium* development in an RBC, which lacks endomembrane system trafficking and, indeed, lysosomes. The highly polarized hepatocyte, however, has extensive vesicular transport networks (7) and can target intracellular pathogens residing in a vacuole (8), suggesting that the exoerythrocytic form (EEF) may need to resist host cell attack.

Although the PVM is thought to be critical for *Plasmodium* growth in both the hepatocyte and the RBC contexts, its cellular roles remain elusive. The importance of several *Plasmodium* PVM-resident proteins, however, has been conclusively demonstrated in both blood and liver stages. Attempts to generate exported (*exp*)1 and *Plasmodium* translocon of exported protein (*ptex*)150 knockout parasites in *Plasmodium falciparum* failed (9, 10), revealing that these are both essential proteins for the blood stage, whereas *Plasmodium berghei* and *Plasmodium yoelii* mutants lacking *up-regulated in sporozoites (uis)3* or *uis4* fail to complete liver stage development (11, 12). These PVM-resident proteins, and thus the PVM itself, are performing functions that are crucial for *Plasmodium* growth, but delineating the functions of individual PVM-resident proteins has proven as difficult as identifying the cellular processes mediated by the PVM.

Significance

***Plasmodium* parasites have two distinct intracellular growth stages inside the mammalian host—the first stage, which is clinically silent, in liver hepatocytes, and the second, which causes the symptoms of malaria, in red blood cells. This study reports the discovery of a class of antimalarial compounds called torins, which are extremely potent inhibitors of both intracellular stages of *Plasmodium*. We show that torins block trafficking of liver stage parasite proteins to the physical host–parasite interface, called the parasitophorous vacuole membrane (PVM), and that without continuous trafficking of PVM-resident proteins, the parasite is subject to elimination by its host hepatocyte.**

Author contributions: K.K.H., D.F.W., and M.M.M. designed research; K.K.H., K.B., M.P., J.D.H.-O., M.R., and W.L.B. performed research; A.S.R. and R.M. contributed new reagents/analytic tools; K.K.H., K.B., M.P., J.D.H.-O., M.R., W.L.B., D.F.W., T.H., M.M., and M.M.M. analyzed data; and K.K.H. and M.M.M. wrote the paper.

The authors declare no conflict of interest.

*This Direct Submission article had a prearranged editor.

Freely available online through the PNAS open access option.

¹To whom correspondence may be addressed. E-mail: khanson@fm.ul.pt or mmota@fm.ul.pt.

This article contains supporting information online at www.pnas.org/lookup/suppl/doi:10.1073/pnas.1306097110/-DCSupplemental.

The one process in which both the centrality of the PVM is known and evidence for the participation of specific PVM proteins exists is the export of parasite proteins to the RBC. A cohort of parasite proteins that are involved in extensive physiological and structural modifications of the infected RBC (iRBC) is exported into the iRBC cytoplasm and beyond (13). Five proteins have been identified as components of PTEX, the proposed export machinery at the iRBC PVM (9). Although liver stage protein export has been shown for the Circumsporozoite (CS) protein (14) and PTEX components are expressed in *P. falciparum* EEFs (15), a role for parasite protein export into the hepatocyte remains speculative; the host hepatocyte may not require the extensive structural remodeling that the iRBC does.

Conversely, however, the hepatocyte, with its extensive vesicular transport network, intuitively constitutes a more hostile host environment than the RBC, and there is evidence that the liver stage PVM may play a crucial role in preventing host cell-mediated parasite killing, as it does in *Toxoplasma gondii* (16). Support for a protective role for the liver stage PVM comes from knockout parasites that fail in the earliest steps of PVM formation and remodeling. Sporozoites lacking the p52/p36 gene pair invade hepatocytes successfully, but fail in PVM formation (17, 18) and are severely reduced in abundance midway through liver stage development. Parasites lacking *slarp/sap* (19, 20), a regulator of early liver stage development, fail to express UIS4 and exported protein 1 (EXP-1), along with other parasite proteins, and are also eliminated at the beginning of infection.

Acquisition of resources from the host-cell environment, an unambiguous requirement for an obligate intracellular parasite like *Plasmodium*, is a function ascribed to the PVM in both mammalian stages. The PVM allows the free passage of molecules (21, 22), presumably through proteinaceous pores, which may contribute to acquisition of host nutrients and disposal of parasite waste products. Members of the early transcribed membrane protein (ETRAMP) family, single-pass transmembrane proteins conserved among *Plasmodium* spp., which are highly expressed and developmentally regulated in both blood and liver stage parasites (23, 24), could be candidates for mediating uptake of host resources. Such a role in lipid uptake has indeed been proposed for the *P. berghei* ETRAMP UIS3 on the basis of its interaction with host-cell L-FABP (liver fatty acid binding protein) (25).

Although *Plasmodium* parasites must use host resources to support their own growth in both mammalian stages, the single cycle replicative output of the liver stage parasite is vastly greater than that of the blood stage, which may reflect a similarly increased need for host resources. In this respect, the hepatocyte constitutes far superior “raw material” compared with the RBC; hepatocytes are not only metabolically active, but also highly versatile cells, which are capable of altering uptake, storage, production, and degradation of a wide array of macromolecules in response to cellular and organismal requirements. The presence of a growing *Plasmodium* parasite is sensed by the host hepatocyte, which responds with activation of cellular stress responses and altered metabolism (26, 27). The mammalian target of rapamycin (mTOR) kinase integrates signals from amino acids, stress, oxygen, energy, and growth factors and responds by altering cellular protein and lipid synthesis, as well as autophagy (28). As such, we sought to determine how inhibition of host mTOR signaling would affect *Plasmodium* liver stage development. Here we show that torins, a single structural class of mTOR inhibitors, are highly potent antiparasitodal compounds targeting both mammalian stages in vitro and in vivo. Independent of host-cell mTOR, torins impair trafficking of *Plasmodium* liver stage PVM-resident proteins, revealing the fast turnover of these proteins at the liver stage PVM, and provoke elimination of liver stage parasites.

Results

Torins Potently Inhibit *Plasmodium* Liver and Blood Stages. We first tested whether *Plasmodium* infection could be modulated by inhibition of host mTOR signaling using two unrelated mTOR inhibitors (see Table S1 for structures, reviewed in ref. 29): rapamycin, a naturally occurring macrolide that is an allosteric mTOR inhibitor, and Torin1, a tricyclic benzonaphthridinone developed through medicinal chemistry efforts as an ATP-competitive inhibitor (30). We plated two human hepatoma cell lines, Huh7 and HepG2, and infected the cells with GFP-expressing *P. berghei* sporozoites. Two hours after infection, by which time sporozoite invasion is completed, cells were switched into medium containing 250 nM of either rapamycin or Torin1. Control cells were treated with DMSO alone (vehicle control). Infection parameters were quantified by flow cytometry 48 h after sporozoite addition. In both cell lines, the effects of the two mTOR inhibitors were strikingly different. Treatment with rapamycin led to a modest increase in the proportion of infected cells (number of GFP+ cells) (Fig. 1A), or parasite development (Fig. 1B), as indicated by the geometric mean of the GFP signal intensity, which correlates with parasite development (31). Treatment with Torin1, however, eliminated the vast majority of parasites in both cell lines (Fig. 1A; HepG2 $P < 0.0001$) and blocked the development of those few that remained (Fig. 1B; HepG2 $P < 0.0001$). These results were confirmed by microscopy, and representative examples of control, rapamycin-treated, and the rare remaining Torin1-treated EEFs are shown in Fig. 1C.

A Torin1 analog with properties more amenable to large-scale synthesis and in vivo use was recently reported (32). We next synthesized and tested this analog, Torin2, for antiparasitodal activity. Dose–response analysis revealed that Torin2 is an ~100-fold more potent an inhibitor of *Plasmodium* liver stage growth than Torin1; the calculated cellular EC₅₀ of Torin1 and Torin2 for parasite development was 106 nM 95% confidence interval (CI) 101–107 nM and 1.1 nM (95% CI 0.95–1.33 nM), respectively (Fig. 1D). Furthermore, a single dose of 10 mg/kg Torin2, administered to mice 2 h after infection with 10,000 sporozoites, led to a highly significant reduction in *Plasmodium* liver load (Fig. 1E, $P < 0.0001$) 40 h postinfection. In a controlled physiological infection model with infection initiated by 500 *P. berghei*-GFP sporozoites, the same 10 mg/kg dose of Torin2 was curative. Control mice became blood stage positive by flow cytometry detection of GFP from day 4 to 6 postinfection, but none of the Torin2-treated animals ever developed blood parasitaemia by day 11 (Fig. 1F). The flow cytometry data were confirmed by microscopic examination of thin blood smears for all of the Torin2-treated animals.

The discrepancy between the extremely potent inhibition of *P. berghei* EEFs by the torins and the slight (and opposing) effects of rapamycin led us to wonder whether the antiparasitodal activity of the torins was really mediated by host mTOR. As a first step in addressing this, we tested if the inhibitory effects of the torins would extend to *P. falciparum* asexual blood stages, as the mature enucleate RBCs in which *P. falciparum* replicates have no catabolic capacity for mTOR to stimulate. Torin1 (200 nM) and Torin2 (10 nM) were added to synchronized *P. falciparum* 3D7 ring stages, and parasite replication and reinvasion were assessed by flow cytometry 48 h later. iRBCs were identified based on SYBR green labeling of *P. falciparum* DNA. Strikingly, both Torin1 and Torin2 blocked parasite development and completely prevented reinvasion, as evidenced by the static parasitemia, compared with the DMSO-treated control (Fig. 2A, $P < 0.0001$ for both Torin1 and Torin2 vs. control). Using a different cytometry-based assay and the P2G12 clone of *P. falciparum* 3D7 (33), we performed dose–response assays and determined the Torin2 EC₅₀ for asexual blood stages to be 1.4 nM (95% CI 1.31–1.59 nM) (Fig. 2B). Torin2 is also highly potent against early gametocytes, with a slightly lower EC₅₀ of 6.62 nM (95% CI 4.59–9.54 nM). (Table S1). We next

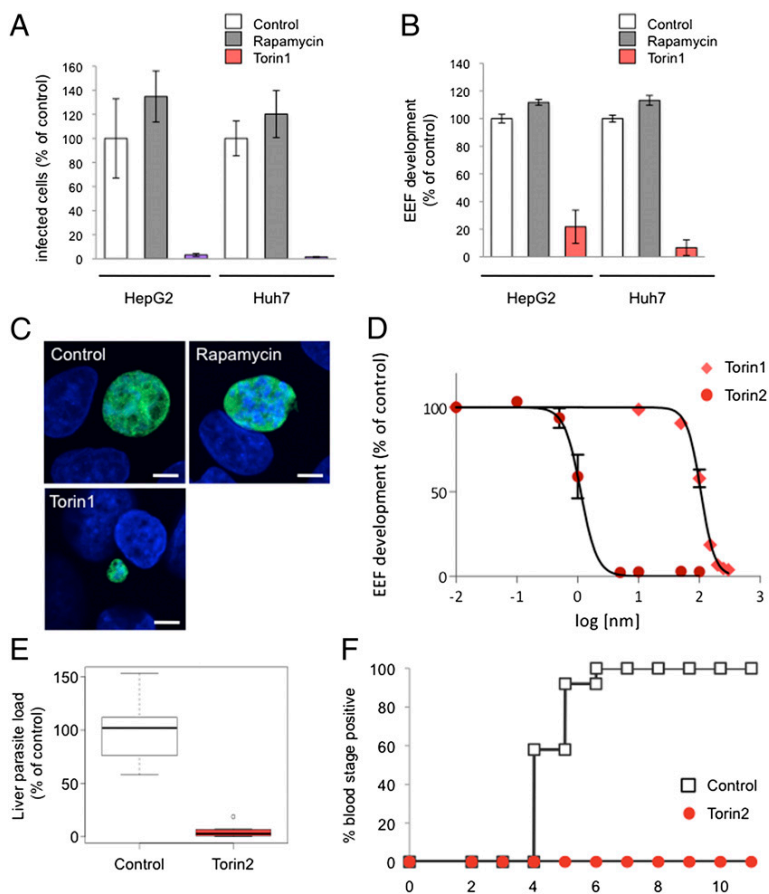


Fig. 1. Torins are antiplasmodial compounds with nanomolar potency against *Plasmodium* liver stages and are capable of curing infection. (A–C) Effect of mTOR inhibitors, rapamycin, and Torin1 on *P. berghei* liver stage infection. HepG2 or Huh7 cells infected with *P. berghei*-GFP sporozoites on the day after seeding. Torin1, rapamycin, or DMSO (vehicle as control) were added 2 h after infection and remained present until 48 h after sporozoite addition, when samples were processed for flow cytometry (A and B) or microscopy (C). Data from technical triplicates of the DMSO control were averaged, and the mean was set to 100%; all samples were then normalized to this value. Mean \pm SD from one representative experiment is shown. (A) The number of GFP+ events detected represents the number of infected cells. (B) The geometric mean of the GFP signal, known to correlate with parasite growth, represents EEF development. (C) Representative confocal images. Huh7 cells were fixed and labeled with anti-PbHSP70 (*P. berghei* heat shock protein 70) (EEF, green) and DAPI (nuclei, blue). (D) Dose-dependent effects of Torin1 and Torin2 on *P. berghei* liver stage infection. HepG2 cell infection analyzed by flow cytometry 48 h later, as in B. Each data point represents $n = 3$ biological triplicates. Four-variable curve fitting was carried out using GraphPad Prism. (E) Effect of a single Torin2 oral dose on parasite liver load. C57BL/6 mice were infected i.v. with 10,000 Pb-GFP sporozoites and given 10 mg/kg Torin2 suspended in sunflower oil or an equivalent dose of sunflower oil alone 2 h after infection. Each point represents a single animal ($n = 3$ independent experiments); mean \pm SD is indicated for each group. (F) Effect of a single Torin2 oral dose on prepatency period. C57BL/6 mice were infected i.v. with 500 Pb-GFP sporozoites and given 10 mg/kg Torin2 suspended in sunflower oil or an equivalent dose of sunflower oil alone 2 h after infection. Animals were monitored daily for appearance of parasitaemia in the blood by flow cytometry. Data are from three independent experiments with a total of 12 animals in each group.

tested whether Torin2 would be capable of antimalarial activity against the blood stage of *P. berghei* in vivo. C57BL/6 mice infected with *P. berghei*-GFP iRBCs were treated with a single oral dose of 10 mg/kg Torin2 on day 4 after infection when the parasitaemia had reached 3%. All control mice succumbed to experimental cerebral malaria by day 7, whereas the majority of the Torin2-treated group did not (Fig. 2C), a highly significant difference in survival ($P < 0.0001$). The single Torin2 dose also led to a highly significant blunting of parasitaemia (Fig. 2D, $P < 0.0001$). Overall, our data demonstrate that torins are similarly effective and potent against both blood and liver stage *Plasmodium* parasites in vitro and in vivo. Thus, the mediator of the antimalarial activity must be present in both of these host–parasite settings.

Inhibition of Host mTOR Signaling by Other Means Does Not Phenocopy the Antiplasmodial Effects of Torins. The ability of torins to potentially target both liver and blood stages of *Plasmodium* infection suggested a direct effect on the parasite and not on host mTOR. We sought to further test this hypothesis using chemical and genetic means to reduce host mTOR activity in hepatoma cells.

First, we evaluated the ability of PP242, another highly specific ATP-competitive mTOR inhibitor that is structurally unrelated to the torins (34), to inhibit *Plasmodium* liver stages. Treatment with 2.5 μ M PP242 [concentration showing complete inhibition of mTORC1 and mTORC2 signaling in cellular assays (34)] did not reduce either infected hepatocyte number or *Plasmodium* liver stage growth (Fig. 3A and B). Likewise, addition of PP242 to *P. falciparum*-synchronized 3D7 ring stages had no impact on blood stage development and reinvasion (Fig. 3C).

We next turned to siRNA knockdown of mTORC1 components in hepatoma cells. siRNA oligonucleotide pools targeting human *mTOR* or *raptor* transcripts were introduced by reverse transfection and the knockdown cells infected with GFP-expressing *P. berghei* sporozoites 48 h later. siRNA-mediated knockdown of neither mTOR nor raptor could phenocopy the dramatic reduction of infected cells or parasite development observed with Torin2 treatment (Fig. 3D and E). EEF morphology 24 h after infection was also comparable across the control, mTOR, and raptor knockdown cells (Fig. 3F). Taken together, our data strongly suggest that the target mediating the antiplasmodial effects of torins is not the host cell mTOR kinase, but rather is parasite-encoded.

Torin2 Is Not Permissive to Generation of Drug-Resistant Parasite Lines in Vitro. To identify the target of Torin2, we attempted to generate drug-resistant mutants in *P. falciparum* blood stage parasites. We first determined that the multidrug-resistant Dd2 strain of *P. falciparum* retained Torin2 sensitivity, with an EC_{50} of 0.7 nM (95% CI 0.48–1.02 nM) in asexual blood stage growth assays (35). We then performed resistance selection with clonal Dd2 ring stage parasites, exposing them to $10\times EC_{50}$ (7 nM) Torin2 for 8 d. When parasites failed to recrudescence 60 d after this treatment, we varied the length of selection to optimize the mutation-selection window. We achieved parasite recrudescence in 4 of 32 independent selection attempts and only with exposure times of 48 h or less (summarized in Table 1). Remarkably, the four selected strains all failed to display any resistance phenotype by SYBR dose–response or decrease in time to recrudescence in subsequent repetitions of the selection protocol (Table 1). We, and others, have used these selection

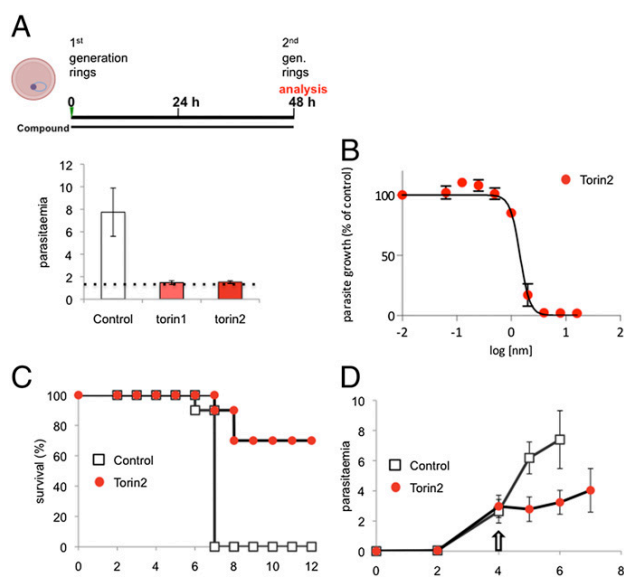


Fig. 2. Torins potently inhibit *Plasmodium* blood stage infection. (A) Effect of Torin1 and Torin2 in *P. falciparum* blood stage in vitro cultures. Synchronized *P. falciparum* 3D7 ring stage parasites were treated with 200 nM Torin1, 10 nM Torin2, or DMSO (vehicle control); reinvasion was analyzed after SybrGreen labeling of parasite DNA 48 h later. Data represent mean \pm SD of three independent experiments. Starting parasitaemia are represented by dotted line. (B) Dose-dependent effect of Torin2 on *P. falciparum* blood growth. Data represent mean \pm SD of three independent experiments. (C and D) Effect of a single 10-mg/kg oral dose of Torin2 administered on day 4 after infection of C57BL/6 mice with 1×10^6 Pb-GFP-parasitized RBC on survival (C) and parasitaemia (D). Animals were monitored daily for malaria-associated pathology (experimental cerebral malaria symptoms), and parasitaemia was analyzed by flow cytometry. (C) Cumulative survival curve for three independent experiments; $n = 10$ mice for control and Torin2-treated groups. (D) Parasitaemia; each point represents the mean \pm SD from three independent experiments.

methodologies to raise resistance to antimalarials that act on a variety of targets within the parasite's cytosol and mitochondria (36, 37). In contrast, Torin2 pressure has thus far failed to induce a stable resistance phenotype after varied, repeated attempts, suggesting that additional unbiased approaches will be necessary to elucidate the drug target(s).

Plasmodium Growth Is Inhibited by Torin2 Throughout Liver Stage Development. With the evidence leaning toward torins acting directly on *Plasmodium* spp., we sought to gain insight into the killing mechanism by asking when the target(s) of Torin2 antiplasmodial activity are present in liver stages. We first varied compound treatment windows to target different stages of parasite invasion and development during liver stage infection. Initially, we checked whether Torin2 treatment of HepG2 cells 2 h before sporozoite addition could impact either sporozoite invasion or EEF development. Torin2 pretreatment did not alter either parasite numbers or development, as assayed 24 h after infection (Fig. S1A). We next tested if Torin2 treatment concomitant with sporozoite addition would affect parasite invasion and again found no effect; comparable amounts of cells were infected (GFP+) after 2 h, demonstrating that sporozoite invasion occurs normally in the presence of Torin2 (Fig. S1B). Next, sporozoites were allowed to complete invasion of HepG2 cells, and then 10 nM Torin2 was added for varying time periods (as schematized in Fig. 4A) corresponding roughly to “early PVM remodeling” (2 h), trophozoite (6 h), and schizont (24 h) stages of intrahepatocyte development. Infection was analyzed 50 h after sporozoite addi-

tion by flow cytometry, and none of the Torin2 treatment periods was found to significantly increase HepG2 cell death (Fig. S1C). As previously shown, continuous incubation of infected cells with 10 nM Torin2 after sporozoite invasion results in near-complete parasite elimination (Fig. 4A). Remarkably, a mere 4-h incubation with 10 nM Torin2 from 2 to 6 h after infection was also capable of eliminating more than 90% of all parasites (Fig. 4A); Torin2 treatment from 6 to 24 h postinfection was similarly effective (Fig. 4A). The very few developing EEFs under the 2- to 6- or 6- to 24-h conditions showed slightly reduced development compared with the control (Fig. 4B). Interestingly, when Torin2 treatment was initiated only after the start of schizogony (24–50 h), fewer parasites were eliminated, with parasite numbers about 60% of the control (Fig. 4B). However, in this treatment group, EEF development showed the strongest inhibition—to 30% of control levels (Fig. 4B); on an individual level, these parasites show aberrant development and fail to form merozoites (Fig. S1D). Our data demonstrate that Torin2 is a potent inhibitor of all phases of *Plasmodium* EEF development through late schizogony. Torin2-treated parasite elimination, however, occurred efficiently only when EEFs were exposed to Torin2 before the onset of schizogony.

Torin2 Treatment Leaves the PVM Structurally Intact, but Lacking PVM-Resident Proteins. A number of gene-knockout parasite lines that successfully invade hepatocytes exist, but fail during PVM establishment or remodeling and are rapidly eliminated (11, 12, 17–20, 38). Given this phenotypic parallel to the effects of Torin treatment, which also does not affect the invasion

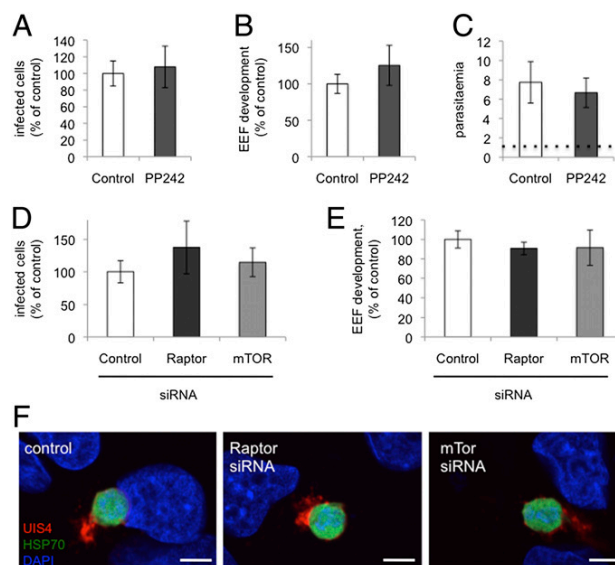


Fig. 3. mTOR inhibition by other means does not phenocopy the antiplasmodial effect of torins. (A and B) Effect of PP242 on inhibition of liver stage infection. Infected HepG2 cells were treated with 2.5 μ M PP242 2 h after sporozoite addition, and the infection was analyzed by flow cytometry 48 h later, as in Fig. 1. Data represent mean \pm SD three independent experiments. (C) Effect of PP242 on blood stage infection. Synchronized *P. falciparum* 3D7 rings were treated with 2.5 μ M PP242 or DMSO (identical control data set as in Fig. 2A), and reinvasion was analyzed after SybrGreen labeling of parasite DNA 48 h later. Data represent mean \pm SD of three independent experiments. (D–F) Effect of siRNA-mediated knockdown of raptor or mTOR on liver stage infection. Validated siRNA pools were reverse-transfected into HepG2 cells, which were infected with sporozoites 2 d later and analyzed by flow cytometry as described above or with immunofluorescence analysis (IFA) 24 h after sporozoite addition. (F) Representative images with PbHSP70 (green), UIS4 (red), and DAPI (blue).

Table 1. Torin2 is refractory to repeated attempts at resistance selection in vitro

Selection strategy	Recrudescence of parasites	Days to recrudescence (first/second/third round)*	Fold EC ₅₀ (nM)**
10x EC ₅₀ , 192 h	0/8	NA	NA
10x EC ₅₀ , 144 h	0/4	NA	NA
20x EC ₅₀ , 48 h	0/4	NA	NA
pulsed three times			
20x EC ₅₀ , 48 h	1/7	26/24/30	1.04
20x EC ₅₀ , 36 h	1/3	26/23/30	0.93
20x EC ₅₀ , 24 h	2/4	22/24/31	1.14
20x EC ₅₀ , 12 h	0/2	NA	NA

Asexual Dd2 parasites were subjected to varied step-wise intermittent selection protocol with 10x EC₅₀ Torin2.

*Number of days for each independent selection to return to 1% parasitemia. The time to recrudescence for subsequent rounds of selection is expressed separately for the first/second/third round of selections and expressed as the average of the number of days when multiple independent selections were performed with identical protocols.

**Parental Dd2 strain EC₅₀ is 0.7 nM (0.48,1.02). Values expressed as fold change over Dd2 EC₅₀.

process itself, but leads to parasite elimination, we wondered if Torin2 treatment might be altering the parasite PVM, or alternatively, if infected cells were selectively rendered nonviable by a brief Torin2 treatment. To this end, we used a live imaging setup to address two questions: (i) Are infected cells viable after Torin2 treatment? and (ii) Is the PVM maintained intact after Torin2 treatment? To that end, we infected HepG2 cells with *P. berghei*-GFP sporozoites and used the vital dye tetramethylrhodamine, ethyl ester (TMRE), which labels mitochondria with an intact membrane potential, to assess host-cell mitochondrial activity and unambiguously identify intracellular EEFs. Additionally, we used the vital DNA dye Hoechst 33258, which freely labels host-cell DNA or free sporozoites, which lack a PVM, but is unable to label the DNA of developing EEFs until maturation-induced PVM changes occur late in liver stage development (39). Torin2 was added 2 h after infection, and the cells were imaged 6 h later, after TMRE and Hoechst 33258 labeling. Based on our earlier data (Fig. 4B), the vast majority of Torin2-treated EEFs are ultimately nonviable after such a treatment. In both control and Torin2-treated cells, the 8-h EEFs developed in host cells with normal nuclear morphology and active mitochondria (Fig. S2A). Importantly, the EEF nuclei are not labeled by Hoechst 33258 in either drug-treated or control

cells (Fig. S2A), although the nuclei of extracellular sporozoites that have failed to invade clearly are an indication that Torin2-treated EEFs reside in an intact PVM. To confirm this interpretation, we used transmission electron microscopy (TEM) to investigate PVM integrity in EEFs that were exposed to Torin2 from 2 to 8 h after infection. As expected, the 8-h control EEFs were uniformly PVM-positive (Fig. 5A). Torin2-treated parasites were also clearly surrounded by a PVM in all cases (Fig. 5A) and tended to have more parasite PM waviness and intracellular complexity (e.g., membranous whorls) than the control parasites observed.

Given that the PVM appeared intact in Torin2-treated infected cells, we next checked whether *Plasmodium* proteins known to localize to the PVM were altered after exposure to Torin2. UIS4, which is already transcribed in mature salivary gland sporozoites (40), is localized to the PVM throughout development inside the hepatocyte (11). Using UIS4-specific antiserum, we confirmed that 2 h after infection UIS4 was already localized to the PVM; the peak UIS4 signal is clearly outside of the parasite soma delineated by *P. berghei* heat shock protein 70 (HSP70) antibody staining (Fig. 5B). Torin2 treatment initiated 2 h after infection is thus acting upon developing parasites already enclosed in UIS4-positive PVMs. Surprisingly, we found that 6 h of Torin2 treatment completely abolished the PVM localization of UIS4. In stark contrast to both the pretreated 2-h parasites and the 8-h control parasites, UIS4 is found exclusively within the parasite soma in Torin2-treated parasites (Fig. 5B).

Torins are potent antiplasmodials throughout liver stage development, so we next investigated whether or not Torin2 treatment could induce mislocalization of PVM-resident proteins in more mature parasites. Infected HepG2 cells were treated with 10 nM Torin2 during a 12-h window starting 16 h after infection, and localization of both UIS4 and EXP1, another known PVM-resident protein [also called Hep17 (41)], was assessed in 28 h EEFs. As expected, UIS4 and EXP1 were localized almost completely outside of the parasite soma in control 28-h EEFs (Fig. 5C). Again, Torin2 treatment led to a dramatic mislocalization of UIS4, with signal largely found in the parasite soma in 28-h EEFs (Fig. 5C), although some residual UIS4 could also be observed in the host-cell cytoplasm. EXP1 localization was also completely perturbed by Torin2 treatment, with a PVM (control) to soma (Torin2-treated) shift paralleling that of UIS4 (Fig. 5C). Additionally, Torin1 treatment also induces mislocalization of UIS4 to the parasite soma (Fig. S2B). These data imply that torins act against *Plasmodium* by altering the localization of PVM-resident proteins.

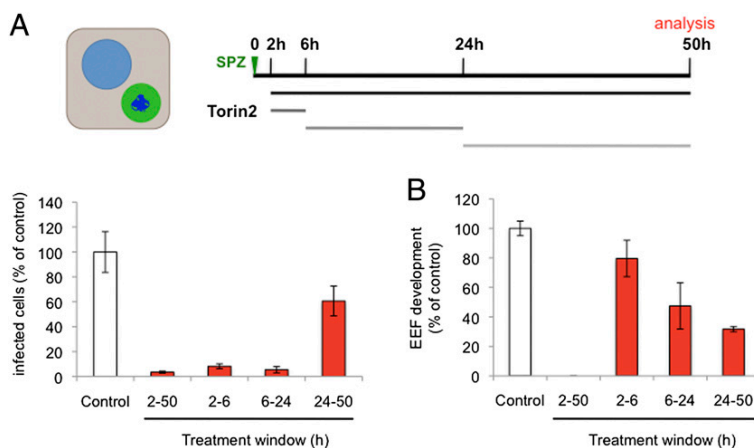


Fig. 4. *Plasmodium* growth is inhibited by Torin2 throughout liver stage development. (A and B) Effects of Torin2 throughout *P. berghei* liver stage development in vitro. Infected HepG2 cells were treated with 10 nM Torin2 or DMSO (vehicle control) as indicated in the schematic illustration, and the infection analyzed by flow cytometry 50 h after sporozoite addition, as in Fig. 1. Data represent mean \pm SD of quadruplicates from one representative experiment with all conditions processed in parallel.

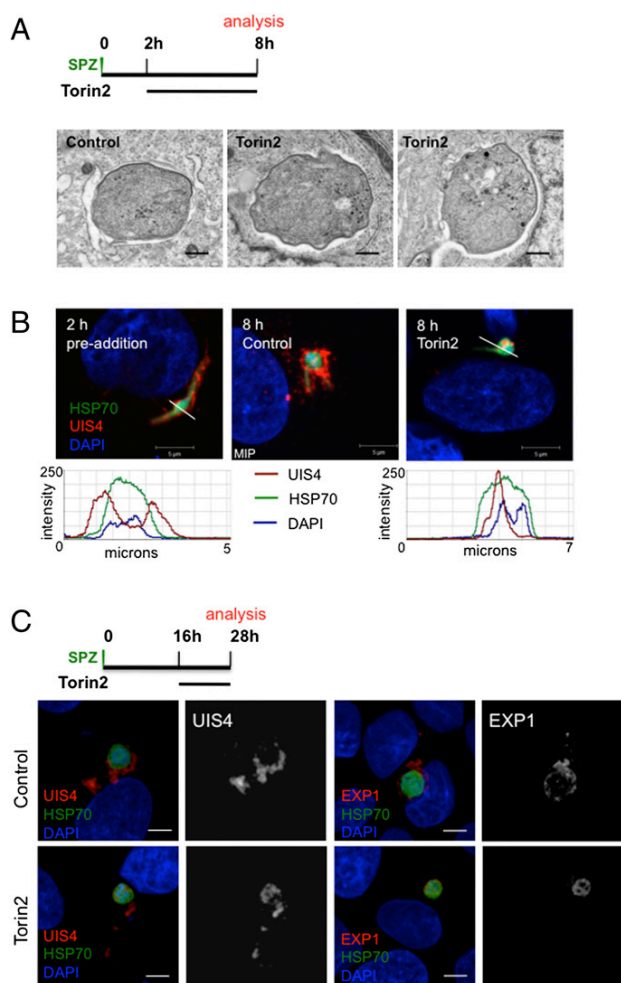


Fig. 5. Torin2 treatment leaves the PVM structurally intact but lacking PVM-resident proteins. (A and B) Effect of Torin2 treatment on the PVM and UIS4 localization in young liver stage trophozoites. Schematic illustrates experimental setup. (A) Representative images of TEM of 8-h EEFs after Torin2 or DMSO (control) treatment. (B) IFA at 2 h (control, single confocal slice) and at 8 h in control [maximum intensity projection (MIP)] and Torin2-treated cells [single confocal slice (HSP70, green; DAPI, blue; UIS4, red)]. Fluorescence intensity graphs of the trajectory indicated by the white lines in the preaddition and Torin2-treated images show the relative spatial intensity peaks of the three fluorophores. (C) Effect of Torin2 treatment on UIS4 and EXP1 during early liver stage schizogony. Schematic illustrates experimental setup. MIPs of the entire EEF are shown for A–C.

EEF Elimination and PVM-Resident Protein Mislocalization Are Not General Aspects of Liver Stage Inhibition by Antimalarials, Indicating a Distinct Mechanism of Action for Torins. Although a comprehensive study of the activity of currently used antimalarials against rodent liver stage parasites has been carried out (42), we lack such information on a phenotypic level, leading us to wonder whether parasite clearance is the inevitable outcome for EEFs that are rendered nonviable during the first hours of intrahepatocyte development. To address this, we first confirmed the elimination of Torin2-treated parasites in HepG2 cells by microscopy; continuous exposure to Torin2 initiated after sporozoite invasion results in a complete absence of developing EEFs 48 h later. We then compared Torin2 side by side with the recently identified antiplasmodial decoquinatate, which has the same mechanism of action (MoA) as atovaquone (43, 44), the most

potent antimalarial in clinical use effective in the liver stage (42). We chose to focus on decoquinatate as its potency is more similar to that of Torin2 than that of atovaquone. Treatment of infected HepG2 cells 2 h after sporozoite invasion with either 10 nM Torin2 or 26 nM decoquinatate ($10\times EC_{50}$) resulted in complete *Plasmodium* inhibition. Torin2 eliminated EEFs, as expected (Fig. 6A, $P < 0.0001$), whereas decoquinatate led to a modest reduction in the number of EEFs present 50 h after infection (Fig. 6A, $P < 0.05$). Furthermore, a 6-h treatment with decoquinatate from 2 to 8 h after infection was phenotypically equivalent to the 2- to 50-h treatment (Fig. S3). Despite the persistence of decoquinatate-treated EEFs, they appear to be arrested very early in development (Fig. 6A, $P < 0.0001$), a phenotype we have confirmed by microscopy in primary mouse hepatocytes (Fig. 6B). EEF elimination is thus not a default outcome of parasite nonviability early in development, but rather reflects a specific aspect of the torin-treated EEF phenotype. This provides an intriguing parallel to the phenotypes described for those mutant parasites that successfully invade hepatocytes, but fail during PVM establishment or remodeling and are rapidly eliminated (17–20).

We next checked if the mislocalization of PVM-resident proteins induced by the torins could be a previously unnoted feature of pharmacological inhibition/killing of *Plasmodium* liver stages, also provoked by known antimalarials active against the liver stages. We tested this hypothesis by evaluating UIS4 and EXP1 localization in infected cells treated with representative members of the classes, in terms of both chemical structure and MoA, of currently known antimalarials (42). Primaquine, pyrimethamine, and decoquinatate were individually added to HepG2 cells 20 h after infection at $10\times EC_{50}$ concentrations. Ten hours later, coverslips were fixed and processed for immunofluorescence. Compared with the control and Torin2 conditions (Fig. 6C), decoquinatate-treated parasites retained robust anti-UIS4 labeling of the PVM but, notably, EXP1 staining was nearly abolished (Fig. 6C), a feature we also noted in mouse primary hepatocytes (Fig. 6B). In the primaquine- and pyrimethamine-treated cells, both PVM-resident proteins were properly localized (Fig. 6C). Additionally, PVM-resident proteins remain properly localized in cells treated with the known liver stage inhibitors genistein (45), lopinavir (46), and cyclosporin A (47), as well as with the PI3K inhibitor LY294002 and rapamycin (Fig. S4). Furthermore, Torin2 treatment from 2 to 4 h postinfection is sufficient to mislocalize UIS4, but is reversible, in terms of both parasite growth and UIS4 localization at 48 h postinfection (Fig. 6D). Additionally, cycloheximide treatment (10 $\mu\text{g}/\text{mL}$), which blocks translation and is a potent antiplasmodial compound (48), during the same 2 h window is uniformly lethal for the developing EEFs, which do not grow after this time period; this lethality is not accompanied by a penetrant defect in UIS4 localization as assayed at either 4 or 50 h after infection (Fig. 6D). Thus, PVM-protein mislocalization is definitively not a consequence of parasite death.

As such, we conclude that both parasite elimination and altered localization of PVM resident proteins are specific phenotypes of torin-mediated *Plasmodium* liver stage inhibition, which strongly indicates that torins have a distinct MoA from currently used antimalarials.

***Plasmodium* Liver Stage Parasites Require Replenishment of PVM-Resident Proteins for Viability.** As the alteration of PVM-resident protein localization was not a general consequence of antimalarial activity against EEFs, we sought to determine the mechanism by which Torin2 provokes the mislocalization of these proteins.

Trafficking of blood stage *P. falciparum* proteins to specific organelles, the vacuolar space, PVM, and beyond into the iRBC itself has been a subject of intense study (49). Brefeldin A (BFA), an inhibitor of eukaryotic ADP-ribosylation factor (ARF) GTPases and the retrograde Golgi-ER trafficking that they mediate in many species, including *Plasmodium* (50), blocks export of knob-

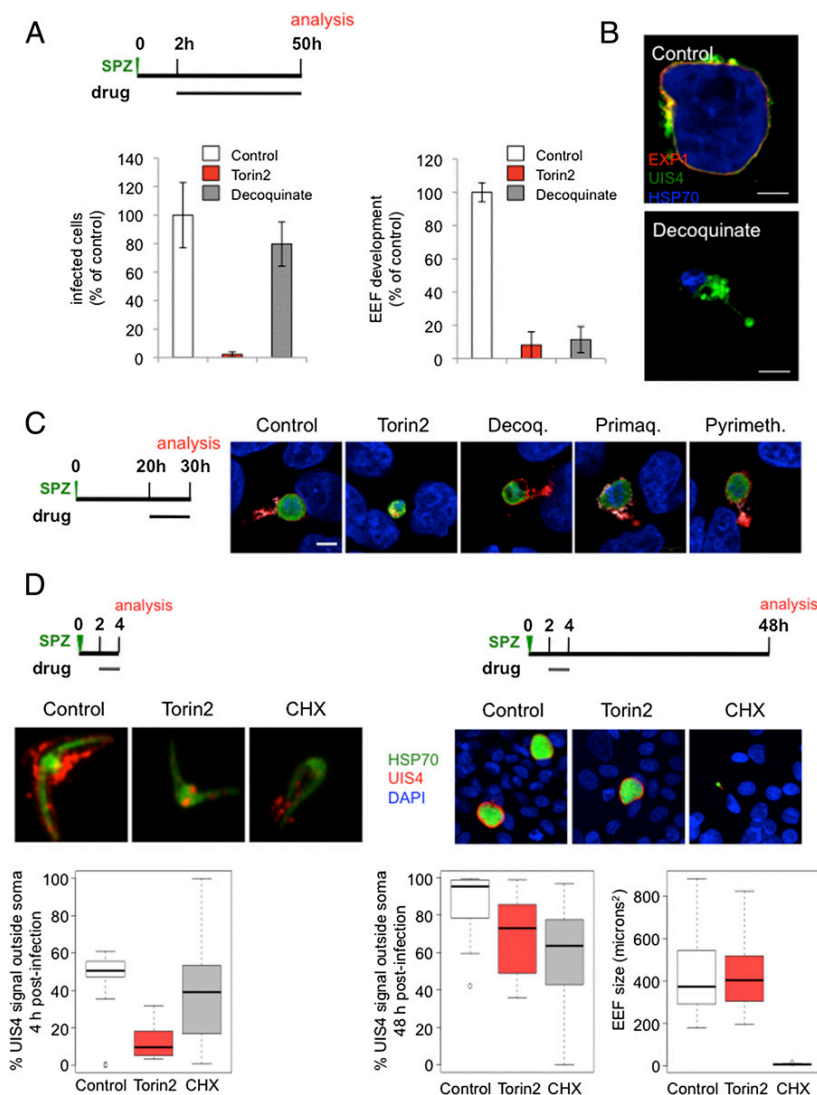


Fig. 6. EEF elimination and PVM-resident protein-trafficking defects are torin-specific phenotypes, not general aspects of liver stage inhibition by antimalarials. (A and B) Effects of decoquinat and Torin2 on EEF numbers and development. (A) Schematic of treatment and analysis. Infected HepG2 cells analyzed by flow cytometry at 50 h after sporozoite addition. Mean of $n = 3$ biological experiments, each condition in triplicate. (B) Mouse primary hepatocytes infected ex vivo with EXP1 (red), UIS4 (green), and HSP70 (blue) labeling. (C) Effect of current antimalarial classes active against the liver stage at the onset of schizogony. Schematic illustrates experimental setup; representative confocal images shown with UIS4 (red), EXP1 (white), PbHSP70 (green), and DAPI (blue) labeling. (D) Effects of 2 h Torin2 or cycloheximide treatment on UIS4 localization and EEF development. Schematic illustrates experimental setup. Representative confocal images of control (DMSO), Torin2-, and cycloheximide-treated EEFs labeled with anti-UIS4 (red), anti-PbHSP70 (green), and DAPI (blue) 4 and 48 h postinfection. Quantification of the proportion of UIS4+ pixels not overlapping PbHSP70 in 20 EEFs from each condition at 4 and 48 h postinfection; quantification of EEF area 48 h postinfection.

associated histidine-rich protein (KAHRP), *P. falciparum* erythrocyte membrane protein 1 (PfEMP1) (51), and EXP1 (52) among other proteins in blood stage parasites. Nothing is known about the trafficking pathways used by the liver stage parasite, so we tested whether UIS4 trafficking to the PVM proceeds through a BFA-sensitive pathway. We added BFA to HepG2 cells 2 h after infection, when UIS4 is already present in the PVM. After BFA (5 μ M) treatment for 6 h postsporozoite invasion, UIS4 is found inside the parasite soma as in Torin2-treated parasites (Fig. 7A). Compared with Torin2 treatment, which causes UIS4 to accumulate in discrete intracellular puncta (Fig. 7A) during the same window, BFA causes UIS4 to accumulate in what appears to be a more continuous distribution within the parasite soma. As UIS4 colocalizes with the microneme marker thrombospondin-related anonymous protein (TRAP) in mature salivary gland sporozoites (40) and as TRAP is maintained in puncta throughout the majority of liver stage development (53), we tested whether UIS4 relocated into TRAP-positive structures upon Torin2 or BFA treatment. The data clearly show that UIS4 and TRAP do not substantially colocalize in control, BFA-, or Torin2-treated cells (Fig. S5A).

Most strikingly, BFA treatment, which blocks only protein secretion, phenocopied the complete loss of PVM-localized UIS4 seen in the Torin2-treated parasites (Fig. 7A). We quantified the distribution of UIS4 and found that, on average, 62% of the UIS4 signal is present outside of the parasite soma in 8-h control EEFs, whereas BFA or Torin2 treatment resulted in >95% overlap of UIS4 and HSP70 in the parasite soma (Fig. 7B). We extended these results to *P. berghei* EEFs developing inside murine primary hepatocytes ex vivo (Fig. S5B); UIS4 and EXP1 trafficking to the PVM is BFA- and Torin2-sensitive in young liver stage schizonts (Fig. S5B), and both PVM-resident proteins are also concomitantly depleted from the PVM.

Taken together, our data support a model (Fig. 7C) in which Torin2 treatment prevents secretion of liver stage PVM-resident proteins, leading to their accumulation inside the EEF soma. This block in secretion causes the PVM to be left devoid of PVM-resident proteins, particularly in trophozoites, which leads to parasite elimination by the host hepatocyte.

Discussion

This study reports that torins, developed as ATP-competitive mammalian mTOR kinase inhibitors, are extremely potent inhib-

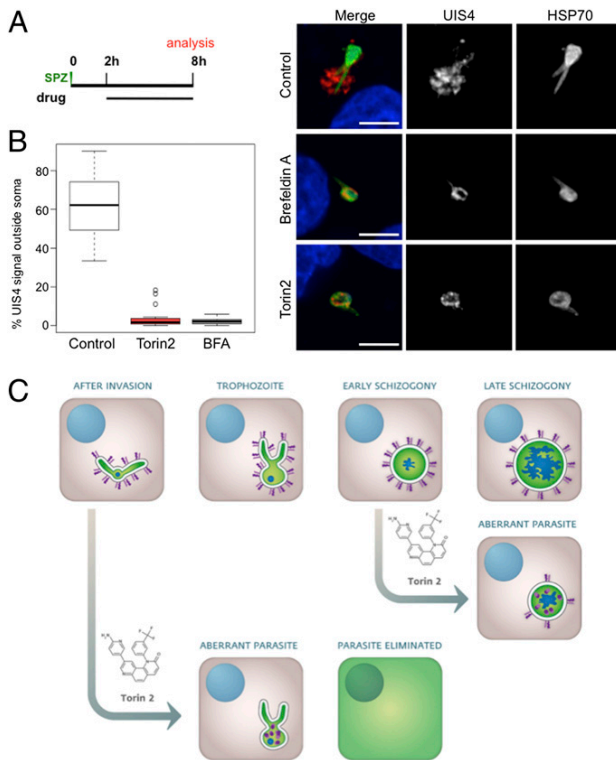


Fig. 7. *Plasmodium* liver stage parasites require replenishment of PVM-resident proteins for viability. (A and B) Comparative effects of Torin2 and BFA on UIS4 trafficking to the PVM in young liver stage trophozoites. Schematic illustrates experimental setup. (A) Representative confocal images of control (methanol, BFA vehicle), Torin2-, and BFA-treated EEFs labeled with anti-UIS4 (red), anti-PbHSP70 (green), and DAPI (blue). (B) Quantification of the proportion of UIS4+ pixels not overlapping PbHSP70 in 20 EEFs from each condition. DMSO and methanol, the vehicle controls for Torin2 and BFA, respectively, are grouped together as control. (C) Model of Torin2 liver stage MoA.

itors of both the liver and blood stages of *Plasmodium* parasites. Although we first tested Torin1 (together with rapamycin) to investigate the role of host hepatocyte mTOR signaling in liver stage *Plasmodium* infection, our data as a whole provide extremely strong support for a parasite-encoded target mediating the antiplasmodial activity of the torins. We present three lines of evidence that suggest that host-cell mTOR is not the mediator of the antiplasmodial activity of the torins. First, unrelated small-molecule mTOR inhibitors (rapamycin and PP242) or siRNA-mediated reduction of mTOR signaling both fail to inhibit *Plasmodium* liver stage infection. Strong evidence that host mTOR is uninvolved comes from the nonequivalence of PP242 and torins. Both cause complete inhibition of mTORC1 and mTORC2 activity (30, 32, 34). The chemical structures of the two compounds are not at all similar although, as we show here, neither are their effects on liver or blood stage *Plasmodium* infection. Second, torins inhibit both liver and blood stage parasites, with Torin2 maintaining a near identical EC_{50} for the two stages and for different *Plasmodium* species. Although it is easy to envisage mechanisms by which reduction of host hepatocyte mTOR signaling could alter liver stage *Plasmodium* development, this is not the case for the iRBC. The mature RBC lacks the capacity for both protein and lipid synthesis, as well as gene expression, and although mTOR has been found in the RBC “hidden proteome,” no evidence of functional protein exists (54). Third, torins are able to alter the localization of *Plasmodium* proteins during liver stage infection, an effect very un-

likely to be mediated by a host protein. As a whole, our data point unequivocally to a *Plasmodium*-encoded molecule or molecules, conserved across the genus and expressed in all mammalian stages, as the target of the antiplasmodial activity of Torin1 and Torin2.

Sequence homology queries of current *Plasmodium* genome assemblies show that no *Plasmodium* orthologs of mTOR exist, and indeed the PI3K-like protein kinase family, of which mTOR is a member, is not found (55, 56). The *P. berghei* proteins showing the highest sequence similarity to human mTOR are the single predicted phosphatidylinositol-3-kinase (PI3K) (PBANKA_111490) and the two predicted phosphatidylinositol-4 kinases (PI4Ks) (PBANKA_110940 and PBANKA_072200), which show conservation primarily in the kinase catalytic domain. Although little is known about the activity of the two predicted *Plasmodium* PI4Ks, PbPI3K is an essential gene (57), and treatment with the known PI3K inhibitors wortmannin and LY294002 reduced PI3P production by PbPI3K in vitro and inhibited blood stage parasite growth (58). LY294002 does not phenocopy Torin2 inhibition of *P. berghei* liver stages, however, and the inhibition of *P. falciparum* replication by wortmannin and LY294002 (58) is much more modest than what we observed with either Torin1 or Torin2.

Our data clearly show that Torin2 is a potent antimalarial with in vivo activity against both liver and blood stages, capable of curing liver stage infection with a single, well-tolerated oral dose. Still, given its demonstrated potent inhibition of human mTOR, we cannot, and do not, see Torin2 itself as a lead compound; further medicinal chemistry elaboration will be necessary to realize a torin analog as a suitable antimalarial lead. Nevertheless, torins represent a new antimalarial chemotype that certainly warrants further medicinal chemistry investigation due to the following highly desirable properties: (i) versatility: Torin2 targets both liver and blood stages, and is active against immature gametocytes; (ii) speed of action: torins render *P. falciparum* parasites nonviable in a single blood stage cycle and short treatment windows are sufficient to kill liver stage parasites; (iii) distinct MoA from currently utilized antimalarials: none of the compounds in current clinical use which are active against *Plasmodium* liver stages provoke PVM trafficking defects; and (iv) Torin2 retains potency against the multidrug resistant Dd2 strain of *P. falciparum*, and is not amenable to in vitro resistance generation, in contrast to most antimalarials in current clinical use and leading candidates (36, 37, 59–63). Additionally, the mediator(s) of the antiplasmodial activity of the torins is clearly druggable in vivo during both mammalian stages.

Although the value of torin analogs for human antimalarial use will rely on future medicinal chemistry elaboration, the utility of torins for probing PVM function and protein-trafficking pathways in the *Plasmodium* EEF is immediate. *Plasmodium* parasites contain many unusual cellular compartments and have evolved strategies to direct proteins not only to these but also to destinations outside of the parasite soma—from the PV to the host-cell membrane itself. The transport pathways that the blood stage parasite uses to direct proteins to these diverse locations has been a subject of intense study; whereas specific trafficking pathways and molecular determinants ultimately mediate protein movement to discrete locations—i.e., the vacuolar space, the Maurer’s clefts in the iRBC cytoplasm, the digestive vacuole, or the PVM—most secreted proteins seem to initially follow a common, canonical BFA-sensitive ER-Golgi route in the blood stage parasites (49). As such, it is perhaps not surprising that UIS4 and EXP1 trafficking to the liver stage PVM requires the canonical BFA-sensitive ER-Golgi transport route, as we have demonstrated. Still, it highlights the fact that the parasite does use this, and undoubtedly other core pathways, throughout all mammalian stages. It remains to be determined whether the EEF uses the same parasite-encoded molecules for acquisition of host hepatocyte resources that the blood stage parasite uses in remod-

elling the “inert” RBC or whether components of the host hepatocyte vesicular trafficking networks are co-opted by the parasite.

Comparing BFA- and Torin2-treated EEFs, we find clear commonalities and subtle differences in phenotype. When either drug is added after sporozoite invasion and initial UIS4-positive PVM establishment, both treatments result in complete loss of UIS4 at the PVM 6 h later, as well as intracellular accumulation of UIS4. BFA blocks ER to Golgi trafficking by inhibiting the *P. falciparum* orthologue of Arf1 (64). BFA-treated blood stage parasites form a hybrid ER- Golgi compartment (65) that accumulates proteins utilizing the canonical secretory pathway. We interpret the similarity of BFA- and Torin2-treated EEF phenotypes as highly suggestive that Torin2, like BFA, causes a failure in anterograde protein trafficking. The compartment in which UIS4 is retained appears qualitatively different, however, with Torin2 treatment leading to the appearance of small puncta of UIS4 and BFA treatment leading to a more continuous distribution of UIS4 inside the parasite soma. Future characterization of the intracellular location in which PVM-resident proteins accumulate after Torin2 treatment may help shed light on which trafficking step is inhibited by Torin2.

Localization of a membrane protein to a specific compartment can be achieved by either its retention at, or continuous transport to, the compartment. Most intriguingly, our data illustrate that UIS4 and EXP1 must be continuously transported to the PVM throughout at least the first 30 h of liver stage development. Several fascinating questions arise from this: Are UIS4 and EXP1 “lost” to the host cell during EEF development? Are UIS4 and EXP1 subject to retrograde trafficking back into the PV or parasite soma? Are these dynamics generalizable to all liver stage PVM-resident proteins, or do they reflect the specific functions of EXP1 and UIS4? Whether or not torin treatment alters protein trafficking in *Plasmodium* asexual and sexual blood stages also remains to be established.

Proteins that are known to populate the nascent PVM of the invading *P. falciparum* merozoite are synthesized during the preceding schizont stage and stored in the apical organelles of the merozoite before release in the invasion process (66). The translocon components HSP101, PTEX150, and EXP2 are examples of this; they are found in the dense granules of merozoites, but will be associated with the PVM throughout the subsequent cycle post-invasion (67). The sporozoite invasion process is assumed to be analogous to that of the merozoite. During the transit of the *Plasmodium* sporozoite from the bite site to the hepatocytes, UIS4 is stored inside the sporozoite where it colocalizes with TRAP (40), apparently in the micronemes, and is discharged only once the sporozoite is in the process of hepatocyte invasion. We clearly demonstrate that the pool of UIS4 that initially populates the young EEF PVM is gone after 6 h of either Torin2 or BFA treatment. As BFA is not thought to affect retrograde trafficking, it is very unlikely that this indicates a block in UIS4 recycling from the parasite soma to the PVM, suggesting that this pool of UIS4 has been degraded either by the host cell or the parasite itself. However, this is not the case with the translocon components in the iRBC, in which the initial pool of proteins released from the dense granules appears to be stably retained at the PVM throughout blood stage development, with further synthesis and trafficking not required (67).

Although it is clear that the blood stage parasite is actively secreting proteins, such as the stage-specific ETRAMPS (24), to

the PVM throughout development, more investigation will be required to determine if some blood PVM proteins show dynamics like those of UIS4, and indeed whether EXP1 itself is similarly dynamically localized to the blood stage PVM. The hypothesis that PVM protein turnover would be related to protein function is attractive, but as the liver stage PVM also must contend with extensive interactions with hepatocyte components (22, 68), it remains possible that the host cell itself dictates the turnover of the liver stage PVM-resident proteins that we have examined.

Regardless of whether host or parasite ultimately drives the turnover of the liver stage PVM-resident proteins that we have studied, their replenishment at the PVM via continued expression and secretion through the early schizont stage, at the least, is crucial for parasite viability. Clearly, the trafficking route to the liver stage PVM and the molecular players that mediate it, as well as the protective role of the PVM, constitute fascinating avenues for future research into *Plasmodium* biology, as well as antimalarial drug development.

Experimental Procedures

See detailed version in *SI Experimental Procedures*.

Plasmodium Liver Stage Assays. GFP-expressing *P. berghei* sporozoites were added to HepG2 or Huh7 cells cultured in 24-well plates. Infected cells were processed and analyzed by flow cytometry as described in ref. 31.

A total of 10,000 *P. berghei*-GFP sporozoites were injected i.v. into C57BL/6 mice; 2 h later, a 10-mg/kg dose of Torin2 was given orally as a sunflower oil slurry. Control animals received an equal dose of oil. Livers were harvested 44 h after infection, mRNA was extracted, and liver parasite load was determined by quantitative RT-PCR of *P. berghei* 18s rRNA.

Plasmodium Blood Stage Assays. *P. falciparum* strains were cultured in vitro, and parasite proliferation was determined by flow cytometry.

To test the antimalarial properties of Torin2 in vivo, 1×10^6 *P. berghei*-GFP iRBCs were injected intraperitoneally into C57BL/6 mice, and parasitaemia was monitored by flow cytometry. Torin2 (10 mM) in DMSO was diluted in PBS, and 10 mg/kg was given orally on day 4 postinfection when parasitaemia was above 3%. Control animals received equal doses of DMSO in PBS.

For resistance selection, $\sim 10^9$ parasites were subject to a stepwise intermittent selection protocol beginning with $10 \times EC_{50}$ for various exposure-time windows. Optimal resistance-selection conditions were obtained that selected against the majority of parasites, but allowed recrudescence of resistant parasites within 60 d. Upon recrudescence, additional selection rounds were conducted to optimally obtain clones uninhibited by Torin2.

Immunofluorescence and Microscopy. Infected cells were fixed in 4% paraformaldehyde (wt/vol) for 10 min at room temperature, permeabilized, blocked in 2% BSA (wt/vol), and incubated with 1° antibodies. After washing, appropriate 2° antibodies were added, and coverslips were mounted in Fluoromount. All images were acquired on Zeiss confocal microscopes.

ACKNOWLEDGMENTS. We thank Ana Parreira for mosquito production and infection; Fernanda Baptista for laboratory support; and Liliana Mancio, Vanessa Luis, and Ghislain Cabal for advice and reagents. Additionally, we are grateful to Volker Heussler, Stefan Kappe, and Miguel Seabra for providing antisera, and to David Sabatini for providing Torin1. This work was supported by Fundação para a Ciência e Tecnologia (FCT, Portugal) Grants PTDC/SAU-GMG/100313/2008 and EXCL/IMI-MIC/0056/2012, and European Research Council funding (to M.M.M.). K.K.H. was supported by funds from the European Community's Seventh Framework Programme (FP7/2007-2013) Marie Curie IntraEuropean Fellowship Grant PIEF-GA-2008-221854 and FCT Grant SFRH/BPD/40989/2007.

- Murray CJL, et al. (2012) Global malaria mortality between 1980 and 2010: A systematic analysis. *Lancet* 379(9814):413–431.
- O'Brien C, Henrich PP, Passi N, Fidock DA (2011) Recent clinical and molecular insights into emerging artemisinin resistance in *Plasmodium falciparum*. *Curr Opin Infect Dis* 24(6):570–577.
- Prudêncio M, Rodriguez A, Mota MM (2006) The silent path to thousands of merozoites: The *Plasmodium* liver stage. *Nat Rev Microbiol* 4(11):849–856.
- Moradin N, Descoteaux A (2012) Leishmania promastigotes: Building a safe niche within macrophages. *Front Cell Infect Microbiol* 2:121.
- Kumar Y, Valdivia RH (2009) Leading a sheltered life: Intracellular pathogens and maintenance of vacuolar compartments. *Cell Host Microbe* 5(6):593–601.
- Lingelbach K, Joiner KA (1998) The parasitophorous vacuole membrane surrounding *Plasmodium* and *Toxoplasma*: An unusual compartment in infected cells. *J Cell Sci* 111 (Pt 11):1467–1475.

7. Wang L, Boyer JL (2004) The maintenance and generation of membrane polarity in hepatocytes. *Hepatology* 39(4):892–899.
8. Bast A, et al. (2011) Defense mechanisms of hepatocytes against *Burkholderia pseudomallei*. *Front Microbiol* 2:277.
9. de Koning-Ward TF, et al. (2009) A newly discovered protein export machine in malaria parasites. *Nature* 459(7249):945–949.
10. Maier AG, et al. (2008) Exported proteins required for virulence and rigidity of *Plasmodium falciparum*-infected human erythrocytes. *Cell* 134(1):48–61.
11. Mueller AK, et al. (2005) *Plasmodium* liver stage developmental arrest by depletion of a protein at the parasite-host interface. *Proc Natl Acad Sci USA* 102(8):3022–3027.
12. Mueller AK, Labaied M, Kappe SH, Matuschewski K (2005) Genetically modified *Plasmodium* parasites as a protective experimental malaria vaccine. *Nature* 433(7022):164–167.
13. Maier AG, Cooke BM, Cowman AF, Tilley L (2009) Malaria parasite proteins that remodel the host erythrocyte. *Nat Rev Microbiol* 7(5):341–354.
14. Singh AP, et al. (2007) *Plasmodium* circumsporozoite protein promotes the development of the liver stages of the parasite. *Cell* 131(3):492–504.
15. Vaughan AM, et al. (2012) Complete *Plasmodium falciparum* liver-stage development in liver-chimeric mice. *J Clin Invest* 122(10):3618–3628.
16. Hunn JP, Feng CG, Sher A, Howard JC (2011) The immunity-related GTPases in mammals: A fast-evolving cell-autonomous resistance system against intracellular pathogens. *Mamm Genome* 22(1–2):43–54.
17. Labaied M, et al. (2007) *Plasmodium yoelii* sporozoites with simultaneous deletion of P52 and P36 are completely attenuated and confer sterile immunity against infection. *Infect Immun* 75(8):3758–3768.
18. van Dijk MR, et al. (2005) Genetically attenuated, P36p-deficient malarial sporozoites induce protective immunity and apoptosis of infected liver cells. *Proc Natl Acad Sci USA* 102(34):12194–12199.
19. Silvie O, Goetz K, Matuschewski K (2008) A sporozoite asparagine-rich protein controls initiation of *Plasmodium* liver stage development. *PLoS Pathog* 4(6):e1000086.
20. Aly AS, et al. (2008) Targeted deletion of SAP1 abolishes the expression of infectivity factors necessary for successful malaria parasite liver infection. *Mol Microbiol* 69(1):152–163.
21. Desai SA, Rosenberg RL (1997) Pore size of the malaria parasite's nutrient channel. *Proc Natl Acad Sci USA* 94(5):2045–2049.
22. Bano N, Romano JD, Jayabalasingham B, Coppens I (2007) Cellular interactions of *Plasmodium* liver stage with its host mammalian cell. *Int J Parasitol* 37(12):1329–1341.
23. MacKellar DC, Vaughan AM, Aly AS, DeLeon S, Kappe SH (2011) A systematic analysis of the early transcribed membrane protein family throughout the life cycle of *Plasmodium yoelii*. *Cell Microbiol* 13(11):1755–1767.
24. Spielmann T, Ferguson DJ, Beck HP (2003) etramps, a new *Plasmodium falciparum* gene family coding for developmentally regulated and highly charged membrane proteins located at the parasite-host cell interface. *Mol Biol Cell* 14(4):1529–1544.
25. Mikolajczak SA, Jacobs-Lorena V, MacKellar DC, Camargo N, Kappe SH (2007) L-FABP is a critical host factor for successful malaria liver stage development. *Int J Parasitol* 37(5):483–489.
26. Albuquerque SS, et al. (2009) Host cell transcriptional profiling during malaria liver stage infection reveals a coordinated and sequential set of biological events. *BMC Genomics* 10:270.
27. Chattopadhyay R, et al. (2011) Early transcriptional responses of HepG2-A16 liver cells to infection by *Plasmodium falciparum* sporozoites. *J Biol Chem* 286(30):26396–26405.
28. Laplante M, Sabatini DM (2012) mTOR signaling in growth control and disease. *Cell* 149(2):274–293.
29. Guertin DA, Sabatini DM (2009) The pharmacology of mTOR inhibition. *Sci Signal* 2(67):pe24.
30. Thoreen CC, et al. (2009) An ATP-competitive mammalian target of rapamycin inhibitor reveals rapamycin-resistant functions of mTORC1. *J Biol Chem* 284(12):8023–8032.
31. Prudêncio M, Rodrigues CD, Ataíde R, Mota MM (2008) Dissecting in vitro host cell infection by *Plasmodium* sporozoites using flow cytometry. *Cell Microbiol* 10(1):218–224.
32. Liu Q, et al. (2011) Discovery of 9-(6-aminopyridin-3-yl)-1-(3-(trifluoromethyl)phenyl)benzo[h][1,6]naphthyridin-2(1H)-one (Torin2) as a potent, selective, and orally available mammalian target of rapamycin (mTOR) inhibitor for treatment of cancer. *J Med Chem* 54(5):1473–1480.
33. Buchholz K, et al. (2011) A high-throughput screen targeting malaria transmission stages opens new avenues for drug development. *J Infect Dis* 203(10):1445–1453.
34. Feldman ME, et al. (2009) Active-site inhibitors of mTOR target rapamycin-resistant outputs of mTORC1 and mTORC2. *PLoS Biol* 7(2):e38.
35. Van Tyne D, et al. (2011) Identification and functional validation of the novel antimalarial resistance locus PF10_0355 in *Plasmodium falciparum*. *PLoS Genet* 7(4):e1001383.
36. Dharía NV, et al. (2009) Use of high-density tiling microarrays to identify mutations globally and elucidate mechanisms of drug resistance in *Plasmodium falciparum*. *Genome Biol* 10(2):R21.
37. Rottmann M, et al. (2010) Spiroindolones, a potent compound class for the treatment of malaria. *Science* 329(5996):1175–1180.
38. Vera IM, Beatty WL, Sinnis P, Kim K (2011) *Plasmodium* protease ROM1 is important for proper formation of the parasitophorous vacuole. *PLoS Pathog* 7(9):e1002197.
39. Sturm A, et al. (2009) Alteration of the parasite plasma membrane and the parasitophorous vacuole membrane during exo-erythrocytic development of malaria parasites. *Protist* 160(1):51–63.
40. Kaiser K, Matuschewski K, Camargo N, Ross J, Kappe SH (2004) Differential transcriptome profiling identifies *Plasmodium* genes encoding pre-erythrocytic stage-specific proteins. *Mol Microbiol* 51(5):1221–1232.
41. Doolan DL, et al. (1996) Identification and characterization of the protective hepatocyte erythrocyte protein 17 kDa gene of *Plasmodium yoelii*, homolog of *Plasmodium falciparum* exported protein 1. *J Biol Chem* 271(30):17861–17868.
42. Delves M, et al. (2012) The activities of current antimalarial drugs on the life cycle stages of *Plasmodium*: A comparative study with human and rodent parasites. *PLoS Med* 9(2):e1001169.
43. Nam TG, et al. (2011) A chemical genomic analysis of decoquinatone, a *Plasmodium falciparum* cytochrome b inhibitor. *ACS Chem Biol* 6(11):1214–1222.
44. da Cruz FP, et al. (2012) Drug screen targeted at *Plasmodium* liver stages identifies a potent multistage antimalarial drug. *J Infect Dis* 205(8):1278–1286.
45. Cunha-Rodrigues M, et al. (2008) Genistein-supplemented diet decreases malaria liver infection in mice and constitutes a potential prophylactic strategy. *PLoS ONE* 3(7):e2732.
46. Hobbs CV, et al. (2009) HIV protease inhibitors inhibit the development of preerythrocytic-stage *Plasmodium* parasites. *J Infect Dis* 199(1):134–141.
47. Meister S, et al. (2011) Imaging of *Plasmodium* liver stages to drive next-generation antimalarial drug discovery. *Science* 334(6061):1372–1377.
48. Gershon PD, Howells RE (1986) Mitochondrial protein synthesis in *Plasmodium falciparum*. *Mol Biochem Parasitol* 18(1):37–43.
49. Deponte M, et al. (2012) Wherever I may roam: Protein and membrane trafficking in *P. falciparum*-infected red blood cells. *Mol Biochem Parasitol* 186(2):95–116.
50. Cray JL, Haldar K (1992) Brefeldin A inhibits protein secretion and parasite maturation in the ring stage of *Plasmodium falciparum*. *Mol Biochem Parasitol* 53(1–2):185–192.
51. Wickham ME, et al. (2001) Trafficking and assembly of the cytoadherence complex in *Plasmodium falciparum*-infected human erythrocytes. *EMBO J* 20(20):5636–5649.
52. Nacer A, Berry L, Slomianny C, Mattei D (2001) *Plasmodium falciparum* signal sequences: Simply sequences or special signals? *Int J Parasitol* 31(12):1371–1379.
53. Jayabalasingham B, Bano N, Coppens I (2010) Metamorphosis of the malaria parasite in the liver is associated with organelle clearance. *Cell Res* 20(9):1043–1059.
54. D'Alessandro A, Righetti PG, Zolla L (2010) The red blood cell proteome and interactome: An update. *J Proteome Res* 9(1):144–163.
55. Brown JR, Auger KR (2011) Phylogenomics of phosphoinositide lipid kinases: Perspectives on the evolution of second messenger signaling and drug discovery. *BMC Evol Biol* 11:4.
56. Ward P, Equinet L, Packer J, Doerig C (2004) Protein kinases of the human malaria parasite *Plasmodium falciparum*: The kinome of a divergent eukaryote. *BMC Genomics* 5:79.
57. Tawk L, et al. (2010) Phosphatidylinositol 3-phosphate, an essential lipid in *Plasmodium*, localizes to the food vacuole membrane and the apicoplast. *Eukaryot Cell* 9(10):1519–1530.
58. Vaid A, Ranjan R, Smythe WA, Hoppe HC, Sharma P (2010) PfPI3K, a phosphatidylinositol-3 kinase from *Plasmodium falciparum*, is exported to the host erythrocyte and is involved in hemoglobin trafficking. *Blood* 115(12):2500–2507.
59. Oduola AM, Milhous WK, Weatherly NF, Bowdre JH, Desjardins RE (1988) *Plasmodium falciparum*: Induction of resistance to mefloquine in cloned strains by continuous drug exposure in vitro. *Exp Parasitol* 67(2):354–360.
60. Ritchie GY, et al. (1996) In vitro selection of halofantrine resistance in *Plasmodium falciparum* is not associated with increased expression of Pgh1. *Mol Biochem Parasitol* 83(1):35–46.
61. Eastman RT, Dharía NV, Winzeler EA, Fidock DA (2011) Piperaquine resistance is associated with a copy number variation on chromosome 5 in drug-pressured *Plasmodium falciparum* parasites. *Antimicrob Agents Chemother* 55(8):3908–3916.
62. Korsinczyk M, et al. (2000) Mutations in *Plasmodium falciparum* cytochrome b that are associated with atovaquone resistance are located at a putative drug-binding site. *Antimicrob Agents Chemother* 44(8):2100–2108.
63. Barnes DA, Foote SJ, Galatis D, Kemp DJ, Cowman AF (1992) Selection for high-level chloroquine resistance results in deamplification of the *pfmdr1* gene and increased sensitivity to mefloquine in *Plasmodium falciparum*. *EMBO J* 11(8):3067–3075.
64. Baumgartner F, Wiek S, Paprotka K, Zauner S, Lingelbach K (2001) A point mutation in an unusual Sec7 domain is linked to brefeldin A resistance in a *Plasmodium falciparum* line generated by drug selection. *Mol Microbiol* 41(5):1151–1158.
65. Elmendorf HG, Haldar K (1993) Identification and localization of ERD2 in the malaria parasite *Plasmodium falciparum*: Separation from sites of sphingomyelin synthesis and implications for organization of the Golgi. *EMBO J* 12(12):4763–4773.
66. Cowman AF, Berry D, Baum J (2012) The cellular and molecular basis for malaria parasite invasion of the human red blood cell. *J Cell Biol* 198(6):961–971.
67. Bullen HE, et al. (2012) Biosynthesis, localization, and macromolecular arrangement of the *Plasmodium falciparum* translocon of exported proteins (PTEx). *J Biol Chem* 287(11):7871–7884.
68. Gomes-Santos CS, et al. (2012) Highly dynamic host actin reorganization around developing *Plasmodium* inside hepatocytes. *PLoS ONE* 7(1):e29408.

Cytometry in Malaria—A Practical Replacement for Microscopy?

UNIT 11.20

Howard M. Shapiro,¹ Simon H. Apte,² Grace M. Chojnowski,² Thomas Hänscheid,³ Maria Rebelo,³ and Brian T. Grimberg⁴

¹The Center for Microbial Cytometry, West Newton, Massachusetts

²Queensland Institute of Medical Research, Brisbane, Queensland, Australia

³Instituto de Medicina Molecular, Faculdade de Medicina da Universidade de Lisboa, Lisbon, Portugal

⁴Center for Global Health and Diseases, Case Western Reserve University School of Medicine, Cleveland, Ohio

ABSTRACT

Malaria, caused by protozoan *Plasmodium* parasites, kills ~800,000 people each year. Exact figures are uncertain because presumptive diagnoses are often made without identifying parasites in patients' blood either by microscopy, using Giemsa's century-old stain, or by simpler tests that are ultimately dependent on microscopy for quality control. Microscopy itself relies on trained observers' ability to detect subtle morphological features of parasitized red blood cells, only a few of which may be present on a slide. Quantitative and objective flow cytometric measurements of cellular constituents such as DNA, RNA, and the malaria pigment hemozoin are now useful in research in malaria biology and pharmacology, and can provide more reliable identification of parasite species and developmental stages and better detection of low-density parasitemia than could microscopy. The same measurements can now be implemented in much smaller, simpler, cheaper imaging cytometers, potentially providing a more accurate and precise diagnostic modality. *Curr. Protoc. Cytom.* 65:11.20.1-11.20.23. © 2013 by John Wiley & Sons, Inc.

Keywords: flow cytometry • fluorescence • hemozoin • image cytometry • malaria • microscopy • polarized light

INTRODUCTION

Malaria has to date had far more influence on cytometry than cytometry has had on malaria. Although cytometry—in the sense of detecting, counting, measuring, and characterizing cells—was initiated by van Leeuwenhoek, Hooke, and other early microscopists in the late 1600s, the cellular culprits involved in malaria and other diseases were not identified for another 200 years. The clinical features of malaria had been described millennia earlier, however. Molecular biology recently confirmed (Hawass et al., 2010) that Tutankhamun harbored the same protozoan malaria parasite, *Plasmodium falciparum*, that has killed large numbers of other young Africans annually since his time. Even today, the precise numbers of malaria infections and deaths worldwide remain uncertain because diagnoses are often made without confirming the presence of parasites in patients' blood (World Health Organization, 2011; Murray et al., 2012).

The current less-than-24-karat “gold standard” method for malaria parasite detection uses high-magnification microscopy to examine blood smears stained with a dye mixture developed by Gustav Giemsa in 1904. Quantification of parasite density, i.e., the number of parasites per unit volume of blood, provides some measure of the severity of malaria infection, and sequential density determinations are recommended to assess treatment progress in severe cases. Density measurements also provide critical objective data to malaria researchers studying the effects of drugs and biologicals on parasite growth and development in cultures and in animals, and to clinicians and epidemiologists analyzing data from trials of vaccines and other preventive and therapeutic interventions.

Quality assurance programs for diagnostic malaria microscopy now aim at a lower limit of detection of 100 to 200 parasites/μl (World Health Organization, 2008, 2010). Although

Current Protocols in Cytometry 11.20.1-11.20.23, July 2013

Published online July 2013 in Wiley Online Library (wileyonlinelibrary.com).

DOI: 10.1002/0471142956.cy1120s65

Copyright © 2013 John Wiley & Sons, Inc.

Microbiological
Applications

11.20.1

Supplement 65

experienced microscopists can detect fewer than 50 parasites/ μl , they typically examine no more than 0.1 μl of blood, making quantification imprecise, even at the higher densities (O'Meara et al., 2006, 2007). For some purposes, e.g., the determination of whether or not malaria has been eliminated from a geographic region or population, investigators would need to examine blood from asymptomatic individuals. They would also need to be able to detect densities no higher than 5 to 10/ μl . The time requirements alone make it impractical to consider microscopy for this application; molecular methods, although effective, have not yet been made robust and affordable enough for routine use in the field.

Until about 1950, cytometry was microscopy and microscopy was cytometry, providing the only means of detecting individual cells—malaria parasites included—in blood or any other material. By 1960, the first simple flow cytometers—electro-optical and electronic instruments capable of counting red blood cells (erythrocytes, RBCs) and white blood cells (leukocytes, WBCs)—had found their way into both clinical and research laboratories in places in which they were affordable and in which trained personnel and the infrastructure needed to keep the apparatus functioning were available. The identification of different types of WBCs and other nucleated cells and of malaria parasites in blood, however, still required microscopy of stained smears, in both rich and poor countries.

Since the 1970s, increasingly sophisticated apparatus and techniques for flow and image cytometry—using reagents far more specific than any available in Giemsa's time—have become well established in other contexts, and have been used for the detection and characterization of many cell types found at low densities in blood and other specimens. Malaria microscopy remains unchanged; even in well-equipped clinical and research laboratories in affluent countries, malaria diagnosis, epidemiology, and the development of new diagnostics, drugs, and vaccines still critically rely on a technique that is essentially neither informed nor transformed by any scientific or technological advances made during the past 108 years—including electric lighting!

Although cytometric apparatus has been commercially available for over 50 years, and more than 140,000 papers involving its use have been published to date, fewer than 300 have described flow or image cytometry of malaria parasites, and only a handful of inves-

tigators and laboratories worldwide combine expertise in both malaria and cytometry. During the past decade, however, modern cytometry has come into increasing use in malaria research for investigations of the physiology of parasites and their responses to antimalarials. It is also now feasible to take relatively compact cytometers into the field for epidemiologic work, e.g., the detection of low-level parasitemia using either cell-based (Campo et al., 2011) or molecular methods, in many places in which malaria causes significant morbidity and mortality.

A great deal is now known about which cytologic characteristics, or parameters, of malaria parasites can be best used to detect them, identify different species and developmental stages, and determine the effects of pharmacologic and immunologic agents on growth and development. Different groups of investigators have developed increasingly sophisticated protocols for multiparameter cytometric analysis of the parasites (Hare, 1986; Hare and Bahler, 1986; Pattanapanyasat et al., 1993; Jouin et al., 1995, 2004; Wongchotigul et al., 2004; Grimberg et al., 2008, 2009; Izumiyama et al., 2009; Karl et al., 2009; Ch'ng et al., 2010; Apte et al., 2011; Campo et al., 2011; Gerena et al., 2011; Malleret et al., 2011; Boissière et al., 2012; Jogdand et al., 2012; Jun et al., 2012; Kaushansky et al., 2012; Philipp et al., 2012; Clark et al., 2013; Sinnis et al., 2013). There have been no systematic multicenter collaborative studies to establish the relative merits of different protocols, however, nor have serious attempts been made to determine which of a variety of various reagents, or probes, and reagent combinations would be optimal for use with a given instrument.

It is important to note that, although conventional cytometric technology has been too costly and complex to be considered as a replacement for malaria microscopy until recently, now some newer field-capable apparatus—primarily imaging instruments using light-emitting diodes (LEDs) for illumination and digital camera chips for detection—can implement the same proven measurements that are being done in flow cytometers. The new systems are sufficiently small, simple, robust, energy efficient, and inexpensive to be feasible for use in routine malaria diagnosis, even in resource-limited settings.

Similar instruments are already in use in such environments for CD4+ T cell counting in HIV-infected patients. The actual

implementation of CD4 counting on a world-wide scale required decades of effort on the part of hundreds of scientists and clinicians in dozens of countries (Mandy et al., 2002). Initially, it was necessary to know what cellular characteristics to measure, what reagents to use, and how to analyze the data. Equally important, it was necessary to implement training and quality assurance programs. The same processes will be required to make malaria cytometry more widely usable and reliable as a research tool and eventually enable it to replace microscopy, yielding substantial improvements in sensitivity, accuracy, and precision of parasite density determination, whether for diagnosis, epidemiology, or research.

As a first step in this direction, we convened a brief Workshop on Malaria Cytometry at the CYTO 2012 Meeting of the International Society for the Advancement of Cytometry (ISAC), held in Leipzig, Germany, in June 2012. At the workshop we agreed to cooperate on further work and to document the current state of malaria cytometry and its prospects for further development and application. The present work, in which we have tried to provide background information comprehensible from the points of view of both malariologists and cytometrists, represents our consensus.

Practical Flow Cytometry (Shapiro, 2003), now available online in free downloadable PDF format, provides details of cytometry hardware, software, and the associated reagent technology. Specific cytometry applications in malaria are the subject of an extensive recent review by Grimberg (Grimberg, 2011). Malaria diagnosis and some relevant biology are discussed at length in Garcia's text (Garcia, 2007).

BEGINNINGS: MIASMA TO GIEMSA

Malaria had a profound influence on the early development of modern medical science. A number of authors have provided enjoyable narratives about this time (de Kruif, 1926; Desowitz, 1991; Garfield, 2001). More scholarly accounts (Clark, 1983; Bosch and Rosich, 2008; Gaynes, 2011) supply additional detail.

Giemsa, Paul Ehrlich, and the others who optimized mixtures of synthetic dyes to improve the visualization of malaria parasites in blood from the 1880s on had the disease to thank for their palette of stains. The Americas, free of malaria until the conquistadores and their African slaves brought parasites there, yielded an often-curative tree bark that made its way across the Atlantic via native healers

and European priests. The "Jesuit powder" and extracts containing its active ingredient, quinine, remained the only effective agents for the treatment and prophylaxis of malaria (or any other serious disease) for centuries thereafter. Quinine, with or without gin added to increase its palatability, sustained the British Empire and others, but producing enough of the drug was not a simple matter of growing money on trees.

By the mid-1850s, William Perkin, a teenaged chemistry student in London, had attempted to synthesize quinine from aniline and had failed. His reaction product was the intensely colored purple dye, mauve. The dye was the first of a long line of commercially successful synthetic textile dyes, and the impetus for an international chemical industry initially driven by the demands of fashion. Within a few decades, some synthetic dyes would be used to stain cells, including those harboring malaria parasites, and, shortly thereafter, to treat malaria and other infectious diseases. Many of the dye-manufacturing companies would become more widely known as producers of drugs, some of which even now double as biological stains.

By the 1850s, improvements in microscopes had facilitated the development and acceptance of the cell theory. In Germany, Rudolf Virchow played a central role in moving the study of disease to the cellular level. Virchow's assistant, Karl Weigert, Ehrlich's older cousin, was among the first to use synthetic dyes to improve the visualization of cells and tissues by microscopy, inspiring his younger relative to explore differential staining of cells and their components by dyes with differing chemical properties and contrasting colors. By 1878, Ehrlich had used combinations of acidic dyes such as eosin and basic dyes such as methylene blue to identify and classify different types of WBCs in peripheral blood.

The identification of disease-specific cellular pathogens also began in the 1870s. Robert Koch led the way, applying dyes to stain bacteria, and taking advantage of what would now be called beta-tester status to obtain sub-stage condensers, oil immersion objectives, and other newly developed products from the Zeiss works before they became commercially available. He also introduced photography to document results more objectively than could be done with drawings. With the help of Ehrlich's methylene blue staining technique, Koch discovered the causes of anthrax and tuberculosis. By 1882, Ehrlich and Koch had developed stains for the "acid-fast"

Mycobacteria, different species of which caused tuberculosis and leprosy. They inspired Christian Gram's subsequent work on bacterial staining.

Stains were not involved in Alphonse Laveran's 1880 discovery of malaria parasites in blood, however. Malaria was itself named for the "bad air" thought by many to be its primary cause; by 1880, several microbiologists claimed to have identified a causative bacterium, but had not made their case. Laveran, a French military doctor working in Algeria, examined fresh unstained blood, attempting to discover the origins of a dark pigment then known for over a century to be present in the tissues and blood of malaria sufferers. His observation of motile, pigment-containing particles substantially larger than bacteria led him to believe that a highly pleomorphic parasite was responsible. Laveran's findings were viewed skeptically for several years, until more widespread use of oil immersion objectives and staining enabled others to confirm the existence of malaria parasites and identify different stages of their development (Laveran, 1907).

It also became possible to detect subtle differences in parasite morphology that correlated with long-known differences in the clinical course of malaria, suggesting that more than one species of parasite might be involved in the human disease. Working with a bird malaria, the British military doctor Ronald Ross elucidated the complex development of the parasite and its transmission through the bites of specific mosquito species. Ross and Laveran received Nobel Prizes in Medicine in 1902 and 1907, respectively. Ross's bitter rival, Giovanni Battista Grassi, who, with others in Italy, established the causative role of *P. falciparum* in the most severe form of the human disease and its transmission by mosquitoes of the genus *Anopheles*, was not similarly rewarded; the feud, over a century old, still provides fuel for disputes among malariologists.

Having found that malaria parasites take up methylene blue, Ehrlich speculated that the dye might exert selective toxicity against them and in 1891 reported antimalarial action in several cases. He had already established close ties to the dye industry in his search for better stains to facilitate diagnosis; his subsequent successful demonstration of what he named chemotherapy motivated companies to modify molecules to treat diseases. The new drug industry provided Ehrlich with over six hundred

compounds to test for activity against syphilis; this first "high-throughput screen" yielded two effective treatments.

Methylene blue itself is still occasionally used as an antimalarial, but does not, either by itself or combined with eosin, produce optimal staining of malaria parasites in blood smears. Between 1891 and 1904, several improvements in staining were made, initially by Malachowski and Romanowsky, and ultimately by Giemsa. All involved the addition of azure dyes—themselves oxidation products of methylene blue—to the eosin-methylene blue mixture. Dye interactions in the azure-augmented stains color parasite cytoplasm an intense blue and nuclei a contrasting red, facilitating identification of the earliest stages of malaria parasites in RBCs. Giemsa's dye combination, still almost universally used for malaria diagnosis by microscopy, is among the easiest to prepare and among the most consistent in its staining properties.

This stain has also remained the standard for morphologic hematology. Over a century later, we might wonder how the malaria tail managed to wag the hematology dog. Many people now have many reasons to look at cells in blood, in both the clinic and the laboratory, and relatively few of us have any occasion to look for or at malaria parasites. That was not the case at the turn of the twentieth century, however. To be sure, the anemias and the leukemias were known by then, as were elevations in the numbers of WBCs associated with infection. In addition, the utility of the first hemacytometers, which counted blood cells in graduated chambers of defined volume, was appreciated. However, although microscopy could provide diagnostic and prognostic information about a range of blood disorders, at that time no treatments were known for most of them. Malaria, considerably more widespread than it is today, could be treated with quinine if diagnosed by microscopy, with subsequent clearance of parasites from the blood confirmed by further microscopy. It thus made sense to optimize staining procedures for blood to facilitate malaria diagnosis.

THE PARASITES: THEN AND NOW

In 1904 the staining patterns observable in blood cells and malaria parasites revealed chemical differences among different cell types and among different intracellular structures, but the biological, chemical, and biochemical details were almost completely unknown. Few suspected that the component

molecules of cells were as large as we now know proteins and nucleic acids to be. In addition, most of their lower-molecular-weight building blocks had not been discovered. The details of cellular and nuclear division had only been worked out in the previous two decades; it was clear that cell nuclei contained an acidic component that would bind basic dyes such as methylene blue and azure B, and that both nucleus and cytoplasm contained varying amounts of proteins, which bound eosin, and acidic materials, which bound the basic dyes. The parasites themselves have changed little since 1904; the acquisition of genes for resistance to antimalarials, perhaps the most significant difference, had no discernible effect on morphology.

By Giemsa's time, it was known that malaria parasites go through only part of their life cycle in the blood. Sporozoites, each containing a single nucleus, are the infective stage resulting from the parasite reproductive cycle in the mosquito vector. Sporozoites are introduced into a human or animal host's blood by a mosquito's bite. The sporozoites invade liver cells, becoming trophozoites, which accumulate cytoplasm, and later schizonts, which undergo multiple rounds of asexual nuclear reproduction (schizogony), and segment into multiple merozoites, each with one nucleus. Rupture of the infected liver cell releases merozoites into the blood, where one or more can infect a RBC.

Within RBCs, merozoites become haploid "ring stage" trophozoites, and then mature into schizonts, all the while feeding on the RBCs' hemoglobin and converting it into hemozoin, the "malaria pigment." Like those in the liver, trophozoites in RBCs initially accumulate cytoplasm. Most develop into schizonts, which segment into uninucleate merozoites, each of which can initiate additional rounds of schizogony in a previously uninfected RBC. A minority of trophozoites develop into male (micro-) and female (macro-) gametocytes, which are ingested by mosquitoes to continue the life cycle, eventually yielding sporozoites.

The overall theme of parasite development described above has recognizable variations; among other things, the timing is different for different species. The development of parasites in both the liver and the blood is synchronized, and the release of parasites and cellular debris produces the characteristic "ague"—a symptom complex including chills, sweating, and fever. Although malaria is frequently diagnosed based solely on the presenting clinical features and their time course, it is rec-

ommended that parasites be demonstrated in blood for definitive diagnosis and that density be monitored by microscopy to establish the efficacy of treatment in severe cases.

Human Malaria Parasite Species: Now at Six

Three distinct clinical pictures of malaria had been known for centuries before the parasite was discovered. By 1904, correlations between these and parasite morphology in patients' blood had allowed investigators to distinguish three species of the genus now called *Plasmodium*.

***P. falciparum* (Pf)**

Most malaria deaths result from the "malignant tertian (i.e., occurring roughly every third day) malaria" caused by Pf, in which symptoms may show 36- to 48-hr periodicity or may occur continuously. The parasite infects RBCs of all ages. Pf also differs from other parasite species in that RBCs infected with trophozoites and later intraerythrocytic stages express surface antigens that bind to endothelium; these infected cells are thereby sequestered, i.e., removed from circulating blood, and may obstruct small blood vessels in various organs, notably the brain and placenta. Cerebral malaria is involved in most deaths caused by Pf.

***Plasmodium vivax* (Pv)**

Pv is responsible for "benign tertian malaria," a relatively mild disease in which symptoms occur at intervals of roughly 48 hr. Pv can produce hypnozoites, a stage that can remain dormant in the liver for long periods of time (months to decades). Pv infects young RBCs (reticulocytes), and was thought to require the presence of the Duffy blood group antigen on the host cell for infection. It is now known, however, that there are Pv strains that can infect Duffy-negative individuals.

***P. malariae* (Pm)**

Pm causes "benign quartan malaria," which is relatively mild but has a cycle of 72 hr, or every fourth day. Pm infects older RBCs.

Since 1904, three other species of *Plasmodium* have been demonstrated to cause malaria in humans.

***P. ovale* (Po)**

Po, identified in the 1920s as the cause of a mild tertian malaria, has recently been demonstrated to comprise two distinct species,

P. ovale curtisi and *P. ovale wallikeri* (Fuehrer et al., 2012). They are not distinguishable by morphology and both resemble Pv. Like Pv, the Po species infect younger RBCs and may produce long-lived hypnozoites.

***P. knowlesi* (Pk)**

Pk (Cox-Singh, 2012) was identified in the 1920s as a cause of malaria in monkeys; occasional human cases have been reported from the 1960s on. In the past decade, substantial numbers of human Pk infections, some severe, have been recognized to occur in Southeast Asia; many were initially misdiagnosed as due to *P. malariae*. The range into which the parasite is likely to expand is limited because it is only transmissible by a small number of geographically restricted mosquito species. Pk has a 24-hr cycle and can infect RBCs of all ages.

Pk and Pf can be maintained in long-term culture in monkey and human RBCs; efforts are now under way to develop long-term culture methods for Pv, which has the broadest geographic distribution and probably infects the largest number of people. The great majority of the 600,000 to 1,000,000 malaria deaths estimated to occur annually however, are due to Pf. Pm and the Po species, which altogether account for no more than 10% of malaria infections, have not been grown in culture.

BIOLOGY, MICROSCOPY, AND CYTOMETRY: PARAMETERS, PROBES, AND PROTOCOLS

A substantial fraction of malaria microscopy and almost all malaria cytometry involve the detection and characterization of small numbers of parasites or parasitized blood cells against a background of much larger numbers of normal blood cells. A necessary first step in developing an appropriate methodology is to identify the physical and chemical characteristics, or parameters, that are most useful in distinguishing parasites and parasitized cells from other constituents of blood and in discriminating among parasite species. In microscopy or cytometry of cultured parasites or blood cells from experimental animals or human subjects, it is generally not necessary to identify the parasite species involved; in diagnosis, this is critical.

None of the dyes used in the Giemsa stain and its relatives is specific for any chemical constituent of a malaria parasite or, indeed, of any other cell type. For that reason, it is necessary in malaria microscopy, as it is in iden-

tifying different types of WBCs in Giemsa-stained smears, to discern the sizes, shapes, colors, and textures of various constituents of cells and to combine that information to identify a parasite or cell. In malaria, information relevant to species identification may come not only from the size, shape, and texture of the nucleus or nuclei and cytoplasm, and the presence or absence of various cytoplasmic structures, but also from the numbers of different developmental stages encountered, the modal number of nuclei per schizont, and the presence or absence and form of the malaria pigment, hemozoin. Discerning the morphologic details of both blood cells and parasites either visually or with interactive or automated image analysis requires that a well-prepared and -stained smear be examined at high magnification (1000 \times) using an oil immersion lens.

Species Identification: Cell-, Sequence-, and Antibody-Based Diagnostic Approaches

The visual identification of parasite species relies on morphologic clues that are generally more subtle than the ones microscopists need to distinguish among developmental stages. There is no guarantee, however, that every example of a given stage of a given parasite species will match those “textbook pictures” of that stage and species that are typically found in instructional materials for microscopists. As a respected text (Garcia, 2007) puts it: “Note: Without the appliqué forms, Schüffner’s dots, multiple rings per cell, and other developing stages, differentiation among the species can be very difficult. It is obvious that the early rings of all four species can mimic one another very easily.” Simultaneous infection with more than one parasite species is not uncommon; such mixed infections are difficult to diagnose with microscopy.

Sequence information collected to date has yielded molecular reagents that are usable for the identification and discrimination of all six known human malaria parasite species. Such reagents are frequently employed in multiplexed bead assays done by flow cytometry and, more recently, by image cytometry. Molecular assays using DNA amplification can detect very low parasite densities and are viewed as more reliable than microscopy for species identification. At present, however, such assays are too complex and costly for routine use.

Specific parasite proteins provide the targets for antibody-based rapid diagnostic tests (RDTs), which were introduced in the 1980s.

The tests detect parasite antigens with “dipsticks” or other simple visual indicators. Although acceptable for the diagnosis and, to some extent, identification of parasite species, RDTs are ineffective at densities below 100 to 200/μl, and do not quantify accurately. They are less effective at detecting Pv than Pf, and unreliable for the detection of Pm and the Po species (Murray et al., 2008; McMorroo et al., 2011). Because they deteriorate when improperly stored, RDTs are reliable only when quality control can be provided by microscopy.

Pf can be identified by RDTs detecting histidine-rich protein 2 (HRP2), which is expressed in and on blood stages. This protein, however, can remain detectable in blood for several weeks after an infection has been adequately treated. It has also been established that some strains of Pf, notably several found in South America, do not express HRP2 at all; this further limits the utility of the protein as a marker.

Nonspecific antibodies to the malaria parasite aldolase have been used in RDTs and combined with HRP2 antibodies in tests that discriminate Pf infections from mixed infections and from infections with other parasite species. There are also RDTs that use monoclonal antibodies against parasite lactate dehydrogenase (pLDH); levels of this protein correlate sufficiently well with the presence and level of viable parasites to be used for antimalarial drug screening and the assessment of antimalarial antibody activity as well as for diagnosis. The range of available anti-pLDH antibodies now includes some that are monospecific and others that are reactive with all or a subset of parasite species.

If one accepts the accuracy of species identification now available using molecular reagents, cumulative anecdotal evidence suggests that even the best and most experienced malaria microscopists fall short of infallibility (Barber et al., 2013). We therefore think it unlikely that computer processing of high-resolution images of Giemsa-stained material, advocated in some quarters, will provide an effective replacement for malaria microscopy. Instead, we favor an approach based on simpler but far more reliable quantification of relevant parameters of parasites and parasitized cells that takes advantage of what has been learned since Giemsa’s time.

The Cellular and Molecular Ecology of Blood

By the mid-1800s investigators understood that counting blood cells could provide clin-

ically useful information. RBCs are the most abundant (~5,000,000/μl whole blood); their very numbers require that a sample be diluted a hundredfold or more. This permits a microscopist to count individual cells in a known volume using a hemacytometer and thereafter calculate the RBC concentration in whole blood from the number counted and the known dilution factor.

Circulating RBCs do not normally contain DNA. Like other blood cells, RBCs are formed in the bone marrow; unlike WBCs, they normally extrude their nuclei before entering circulation. At this point, some of the ribosomes used earlier in RBC development for the synthesis of hemoglobin and other proteins remain in the cytoplasm. Ehrlich himself established that basic dyes would precipitate a stained network, or reticulum, in these young RBCs, giving them the name of reticulocytes. The dye-binding material, which disappears during the cells’ first day or two in circulation, is now known to be ribosomal RNA.

Blood platelets (thrombocytes) are actually cell fragments that break off from large multinucleated megakaryocytes in the bone marrow, and contain neither nuclei nor detectable DNA. They may, however, contain small amounts of ribosomal RNA during their first days in circulation. Platelets, normally present at concentrations of 100,000 to 400,000/μl, are much smaller (volume a few tens of fl) than either RBCs (typical volume ~90 fl) or WBCs (typical volume at least ~200 fl) and are easily distinguishable from RBCs and WBCs by their size.

The typical WBC concentration in normal blood is 5000 to 10,000/μl, meaning that only one or two WBCs accompany each 1000 RBCs. Although their hemoglobin content makes RBCs simple to discriminate from WBCs by microscopy or cytometry, most modern automated cell counters, which simply measure cell size, do not make the distinction and instead include WBCs in RBC counts, with negligible effects on accuracy. WBC counts with either hemacytometers or automated counters are typically done on whole blood diluted ~1:10 with a solution containing chemicals that lyse the RBCs. WBCs contain nuclei, each of which carries two copies of the genome, or approximately 6000 Mbp of DNA in humans.

Since it is not necessary to distinguish subcellular details when using hemacytometers to visually count RBCs and WBCs, total magnifications of 100× or less are typically used. Visual discrimination and counting of

different types of WBCs—the differential leukocyte count or “diff”—requires substantially higher magnification, as noted above.

Giemsa's and the related dye mixtures derived from Ehrlich's work produce characteristic staining patterns in WBCs, defining five major types. The three types, called granulocytes, contain cytoplasmic granules and have lobulated nuclei when mature. The granules of eosinophils stain most intensely with acid dyes, and those of basophils stain most intensely with basic dyes. Those of neutrophils, the most common granulocytes, stain with both acid and basic dyes. Mononuclear cells include lymphocytes, which typically are smaller and rounder than granulocytes and have relatively round nuclei and scanty cytoplasm; and monocytes, which generally are larger than granulocytes, less round, and have larger and less round nuclei.

Although color information allows different types of granulocytes to be identified unequivocally, assessment of the maturity of granulocytes by their degree of nuclear lobularity and discrimination between lymphocytes and monocytes require careful examination of morphologic details. This is typically done at 1000 \times on a slide made by smearing 1 to 2 μ l of blood in a thin film occupying an area of 2 to 4 cm^2 . The quality with which morphology is preserved varies in different areas of a smear; in those areas best suited for cell identification, most WBCs fit within a circle \sim 20 μ m in diameter, and most RBCs fit within a circle $<$ 10 μ m in diameter.

The relatively small size of malaria parasites—particularly ring stages, whose detection is critical in diagnosis—also demands high-magnification microscopy of high-quality smears, which allows an observer to best appreciate the morphologic characteristics necessary to detect parasites and distinguish species. Ring stages, which are actually biconcave discs, are typically about 1/3 the diameter of the RBCs in which they are found. The optical resolution practically attainable with oil immersion lenses is on the order of 0.25 μ m; if this resolution were to be maintained in a digitized image of a ring-form parasite, the image would contain no more than 200 pixels, many of which would represent the clear central space and therefore provide relatively little significant morphologic information. The option of making digital images became available only in the late 1950s; until then, identification of blood cells, parasites, and any other formed elements that might be found in blood required microscopy.

Significant Parameters in Malaria Cytometry

Nucleic Acids: DNA and RNA content

Although the involvement of nuclear replication in the developmental cycle of malaria parasites was recognized by 1904, the quantification of RNA and DNA would have been uninformative at that time; the nature of these macromolecules and their critical roles in cell growth were unsuspected then and indeed not fully appreciated until the 1960s. The staining characteristics that have made it possible for microscopists from Ehrlich on to distinguish RBCs containing malaria parasites from unparasitized RBCs depend on the binding of basic dyes to nucleic acids, but neither methylene blue nor azure B, the basic dyes essential in Giemsa's stain, has particularly specific staining properties. Both of these dyes stain DNA, without a strong preference for A-T or G-C base pairs, and also RNA, making precise quantification of either nucleic acid in Giemsa-stained material impossible.

By 1952, both UV microspectrophotometry and staining with the DNA- and RNA-specific methyl green-pyronin Y dye combination had been used to document increases in both DNA and RNA content during schizogony in RBCs (Lewert, 1952). By 1986, a flow cytometric method for DNA and RNA quantification using acridine orange was used to confirm this, and to demonstrate by cell sorting that all parasite developmental stages in RBCs could be identified based on DNA and RNA content alone, without recourse to any morphologic information (Hare, 1986; Hare and Bahler, 1986). This was again shown in 2008 (Grimberg et al., 2008), using a combination of Hoechst 33342, a compound that stains DNA stoichiometrically in living cells, and thiazole orange, originally developed for flow cytometric reticulocyte counting and established to be RNA-specific in the presence of the Hoechst dye (Jouin et al., 1995, 2004; Grimberg et al., 2008). A schematic of DNA and RNA content levels observed in a culture of *P. falciparum* (Pf) in human RBCs appears in Figure 11.20.1.

Uninfected mature RBCs, as noted above, contain little or no DNA or RNA, and their Hoechst 33342 and thiazole orange fluorescence signals are essentially indistinguishable from those of unstained RBCs. Cells with one or two rings contain little RNA (they are estimated to have only \sim 10,000 ribosomes) and one or two copies of the genome (23.3 or 46.6 Mbp DNA in the case of Pf). Uninfected

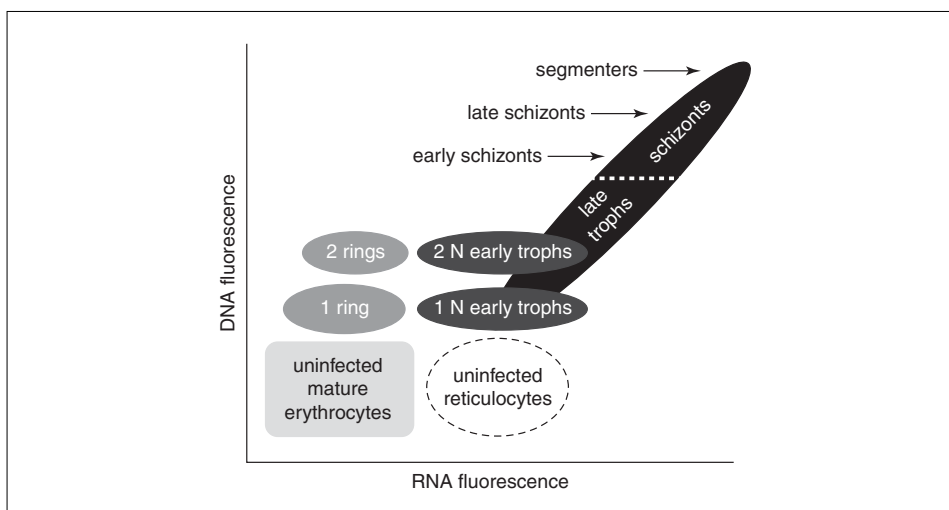


Figure 11.20.1 Typical appearance of a plot of DNA content (UV-excited blue Hoechst 33342 fluorescence) and RNA content (blue-excited green thiazole orange fluorescence) of a population of RBCs infected with Pf. Both DNA and RNA content are displayed on logarithmic scales. Gametocytes are not shown. From Grimberg et al. (2008).

reticulocytes are estimated to contain 50,000 to 100,000 ribosomes, and thus show considerably more thiazole orange fluorescence than is detected in either uninfected mature RBCs or RBCs containing ring forms. RBCs containing early trophozoites contain one or two copies of the genome, and therefore have DNA content equal to those of the RBCs containing corresponding ring stages; their RNA content corresponds to that of uninfected reticulocytes. Both DNA and RNA content increase as parasites pass from the trophozoite to the schizont stage. The overall pattern of increasing DNA and RNA content with parasite development, originally observed by microscopy in Pv decades ago, and shown in Pf above, is also apparent in flow cytometry of cultured Pk. The correlation between morphologic features of these species and those of Pm and the two Po species strongly suggests that the latter three species, which thus far do not appear to have been subjected to multiparameter cytometric analysis, would manifest similar patterns of DNA and RNA content during development.

In various contexts, DNA and RNA content can be used to detect malaria parasites and/or to determine the effects of drugs and immune manipulation on their growth and development. Any of these tasks can be done far more effectively by cytometry than by microscopy, primarily because cytometry is far more accurate and precise for quantification, but also because of the limitations of some of the probes used for detection. DNA could originally be quantified only by Feulgen staining

(which removed the bases and thus lost sequence information) or by its UV absorption near 260 nm (which required treatment of samples with RNase, since RNA absorbs at the same wavelength). Instrumentation was necessary; visual quantification is imprecise and 260 nm is invisible to humans. The methyl green/pyronin dye combination (introduced, ironically enough, by Ehrlich, although its advantages were not appreciated until well after his death) stains DNA green and RNA reddish purple with great specificity, facilitating relative comparisons of DNA content by microscopy, as is done when schizont nuclei are counted.

In current practice, however, quantification of DNA and RNA is most frequently done using fluorescent dyes. Those first demonstrated to be effective were, for the most part, compounds developed early in the 20th century by the dye companies that by then had evolved into drug companies. The Hoechst 33342 dye now widely preferred for DNA staining in unfixed cells, and referred to in Figure 11.20.1, is one such compound. Many newer dyes, however, were designed specifically for analytical purposes, usually by systematic modification of the structures of compounds previously found useful. Thiazole orange, the RNA dye of Figure 11.20.1, coincidentally exemplifies this class of dyes; it was made to allow blood reticulocyte counting to be done on the large base of flow cytometers equipped with 488-nm lasers. Pyronin Y itself can be used as a fluorescent RNA stain when combined with DNA stains

such as Hoechst 33342 (which, incidentally, has DNA-binding properties nearly identical to those of methyl green) (Shapiro, 1981).

A single 23 to 27-Mbp malaria parasite genome can easily bind several million molecules of a DNA dye; larger genomes, such as those in human cells, may bind hundreds of millions. A single ribosome can bind hundreds of molecules of an RNA dye, suggesting that RNA signals from a ring-form-parasitized cell would come from at least one million molecules. Thus, DNA and RNA detection can easily be accomplished by simple fluorescence microscopes and imagers as well as by flow cytometers.

Hemozoin

The association of the “malaria pigment” hemozoin (Hz) with the disease (Hänscheid et al., 2007) antedates the first observation of the parasites by more than a century, and played a direct role in Laveran’s initial discovery. It is now known that Hz formation serves the parasite by detoxifying heme, which is produced as it feeds on the hemoglobin in RBCs. The amount of Hz present in parasitized cells therefore increases as the parasite passes through succeeding developmental stages; little or none is typically detectable in ring forms, while late-stage schizonts and gametocytes contain large quantities.

Hz can be detected and at least partially quantified without the use of reagents. It is paramagnetic, making it possible to use magnets to enrich and separate parasite stages containing the pigment (Karl et al., 2008, 2009; Kim et al., 2010). Hz is also optically birefringent, i.e., capable of changing the plane of polarization of incident light. When observed in unstained or stained blood by transmitted light microscopy using unpolarized light, it appears as brownish-yellow particles. Inserting crossed polarizing filters in the illumination and observation paths of the microscope darkens the field of view except where Hz is present; its birefringence produces bright spots (Lawrence and Olson, 1986). Suitable polarizing filters are widely available and relatively inexpensive; lenses from polarizing sunglasses have been used successfully (Maude et al., 2009). Hz particles also appear as relatively bright spots when observed using dark-field microscopy without polarization. The most pronounced contrast with the background is obtained when polarized light is used for dark-field illumination and samples are observed through a filter with a polarization plane perpendicular to that of the incident light.

This combination is also employed for Hz detection in flow cytometers, in which a side scatter (SSC) signal is measured in a plane of polarization orthogonal to that of the illuminating laser beam (conventional SSC signals are measured in the same plane as the beam). Until recently, the only flow cytometers equipped to do this were Abbott’s (<http://www.abbott.com/>) Cell-Dyn hematology analyzers. The depolarized SSC signal in these analyzers was used to detect eosinophil WBCs, which have birefringent granules, although they do not contain Hz. A now-lapsed patent on depolarized SSC measurement, exclusively licensed to Abbott while in effect, prevented other flow cytometer manufacturers from implementing the feature in their machines.

From the 1990s on, several groups of investigators found that in addition to detecting eosinophils, the Cell-Dyn instruments would register depolarized SSC signals from granulocytic and monocytic WBCs that contained Hz by virtue of having phagocytized parasitized RBCs (Mendelow et al., 1999; Grobusch et al., 2003; Hänscheid et al., 2011). Such cells had previously been visualized on slides; their relative rarity makes it difficult to estimate their abundance precisely enough to clarify their clinical significance. Flow cytometry, in principle, made it possible to quantify Hz-containing WBCs more precisely by analyzing much larger blood samples; however, the hematology analyzers were not readily modifiable to do this. Depolarized SSC measurements can now be implemented in other flow cytometers without legal impediment; many commercially available instruments can be modified to do them (Frita et al., 2011). In some cases, e.g., the Accuri (BD Biosciences) C6 instrument and some from Partec, a user can make the modification in minutes using inexpensive optical components.

The use of Hz detection alone in either blood or tissue for malaria diagnosis, potentially manageable without the use of a reagent, has attracted numerous investigators, and substantial funding has been made available for the approach. Some cautions are in order, however. It is already known that detectable Hz can be found in human WBCs for many weeks after an active malarial infection has resolved, and that the material can persist in animal tissues for months (Frita et al., 2012). Furthermore, Hz may be produced by parasites other than malaria, e.g., schistosomes and some filaria. While they are much less common causes of infection than are malaria parasites, they

occur with significant frequency in many places heavily burdened by malaria.

Lastly, in *P. falciparum* (Pf) infection, RBCs harboring the late trophozoite and schizont stages—which contain most of the Hz—also express surface antigens that adhere to endothelial cells and lead the parasitized cells to be removed from circulation. As a rule, >95% of circulating parasitized RBCs in Pf-infected patients are ring forms containing little or no detectable Hz, although some will be encountered in circulating gametocytes. A flow cytometric study measuring depolarized SSC and DNA in blood from Pf-infected patients found no parasitized RBC with detectable Hz signals (Rebello et al., 2012). Since the use of magnetic fields to concentrate malaria parasites—in or outside RBCs—from blood depends entirely on whether the parasites contain Hz, magnetic separation would be unlikely to increase the sensitivity of a solely Hz-based Pf diagnostic.

Cytometric detection and quantification of Hz can nonetheless be valuable in malaria diagnosis when combined with the measurement of other parameters, notably DNA and RNA content. Moreover, although the literature now contains descriptions of several highly complex and expensive measurement methods, Hz detection using polarized light can, as noted above, be implemented simply and cheaply in either image or flow cytometers. As one might expect, given the established utility of Hz observation in microscopy, cytometric quantification of Hz improves the ability to discriminate among various developmental stages and is likely to aid in distinguishing species. It is already known that a number of antimalarials interfere with Hz production in susceptible parasite strains, and recent evidence suggests that monitoring this by cytometry may produce a relatively simple and effective means of detecting the emergence of drug resistance (Rebello et al., 2013).

Mitochondrial Membrane Potential ($\Delta\Psi_m$) and Other Physiologic Characteristics; Viability

Malaria parasites contain mitochondria; the single mitochondrion that enters an RBC in a merozoite is reproduced during schizogony. Each of the resulting new generation of merozoites is haploid and contains a single mitochondrion. Energized mitochondria in all cell types maintain a difference in electrical potential of ~ 120 mV between their interior and the cytosol, with the interior negative; this mitochondrial membrane poten-

tial ($\Delta\Psi_m$) decreases to zero or near zero in the presence of metabolic inhibitors such as the proton ionophore carbonyl cyanide *m*-chlorophenyl hydrazone (CCCP). The mitochondria in blood stages of plasmodia, like those in trypanosomes and unlike those in almost all animal cells, are not primarily involved in energy metabolism but instead use their membrane potential-derivable energy in biosynthesis, primarily of pyrimidines.

Note that $\Delta\Psi_m$ can be measured cytometrically using fluorescent dyes that carry a single positive charge and are sufficiently lipid-soluble to be able to pass through cytoplasmic and mitochondrial membranes. The less lipophilic representatives of this class of dyes, e.g., tetramethylrhodamine ethyl ester (TMRE), partition across membranes in accordance with the Nernst equation; at 37°C, the ratio of dye concentrations inside and outside the membrane increases by a factor of 10 for every 60 mV of membrane potential. More lipophilic dyes, e.g., rhodamine 123 and cyanines, exhibit higher ratios of interior to exterior concentrations than would be predicted by the Nernst equation.

Mitochondrial de-energization and the accompanying decrease in $\Delta\Psi_m$ occur early in apoptosis in many cell types, and have also been observed in parasites exposed to a number of antimalarial drugs, including chloroquine and atovaquone. Both dihexyloxycarbocyanine (DiOC₆(3)) and hexamethylindodicarbocyanine (DiIC₁(5)) can be used as $\Delta\Psi_m$ indicators (Shapiro et al., 1979; Grimberg et al., 2009; Grimberg, 2011). In cells exposed to concentrations of 1 to 10-nM dye, most fluorescence comes from mitochondria. The dye now in widest use, however, is 5,5',6,6'-tetrachloro-1,1',3,3'-tetraethylbenzimidazolcarbocyanine iodide (JC-1). When applied at micromolar concentrations, this normally green fluorescent dye becomes sufficiently concentrated in energized mitochondria to form red fluorescent aggregates. Measurements of red and green fluorescence and the ratio of both provides a more precise indicator of $\Delta\Psi_m$ than can be obtained by measuring a single emission wavelength. JC-1 has been used to examine $\Delta\Psi_m$ in malaria parasites (Ch'ng et al., 2010).

Most eukaryotic cells have many mitochondria; microscopy or image cytometry would be necessary to detect a condition in which some were energized and some not. The mitochondria in RBCs typically lose function as the cells mature; a parasitized RBC will therefore

typically contain only one energizable mitochondrion for each nucleus, allowing a measurement of DNA content to be used to normalize fluorescence measurements of $\Delta\Psi_m$. The presence of an energized mitochondrion in a parasitized cell provides evidence that the parasite is metabolically viable, but does not speak to its reproductive viability.

Furthermore, the loss of $\Delta\Psi_m$ itself does not establish that an intracellular parasite is apoptotic. The characteristics commonly used in conjunction with $\Delta\Psi_m$ as apoptosis indicators in cultured animal cell lines include membrane phosphatidylserine (PS) exposure, detected with fluorescent annexin V, and permeability to various nucleic acid dyes. The cytoplasmic membranes of parasitized RBCs, although known to contain exposed PS and to therefore bind annexin V, retain sufficient structural integrity to prevent annexin V from reaching the parasite cytoplasmic membrane. Similarly, it is the RBC membrane that determines whether a permeability indicator dye such as propidium iodide can reach the outside of the parasite.

Other parameters measurable by cytometry, e.g., intracellular and intraorganelle pH, content of ions such as Ca^{++} , and levels of redox-related metabolites such as reactive oxygen species (ROS), glutathione, and total $-SH$ groups, are of interest with respect to the physiology of parasites. The multicompartmental nature of parasitized RBCs, composed as they are of RBCs containing membrane-bounded parasites within which there are a variety of membrane-bounded organelles, may make it necessary to use relatively high-resolution imaging apparatus to distinguish signals from molecules of the same indicator in different compartments.

Physiologic parameters such as $\Delta\Psi_m$ are meaningful only in cells that are at least potentially viable. There are some probes that can be applied to cells in that condition that will bind covalently and withstand subsequent fixation, thereby providing at least some indication of the cells' initial physiologic status (Jogdand et al., 2012). This approach would almost certainly be necessary if a parameter such as $\Delta\Psi_m$ were to be considered for diagnostic applications.

Activities of some intracellular enzymes may be detectable however, not only in nonviable cells but also in those that have been permeabilized and/or fixed, using chromogenic or fluorogenic substrates. The fluorogenic substrates most widely used in cytometry are

simple esters of fluorescein and its carboxylated derivatives carboxyfluorescein and calcein; the esters are nonfluorescent and sufficiently lipophilic to diffuse readily through intact cell membranes. Once inside, they are hydrolyzed by nonspecific esterases present in almost all cells, forming fluorescent products containing negatively charged carboxyl groups, which do not readily cross intact membranes. Although esterases in cells with damaged membranes may hydrolyze the esters, the resulting products do not accumulate in sufficient quantity to render these cells fluorescent. Thus, intracellular fluorescence after exposure to fluorescein esters, although often described as an indicator of "viability," actually only establishes the integrity of the cytoplasmic membrane. Other chromogenic and fluorogenic substrates, e.g., tetrazolium dyes, have been used to determine metabolic activity; still others detect the activity of hydrolytic enzymes unique to unique cell types such as monocytes and more general classes such as stem cells.

Protein Structure: Labeled Antibodies and Fluorescent Proteins

By the late 1960s, when analytical flow cytometers and cell sorters were first applied to the problem of differential WBC counting, it was clear that the simple acid-basic dye mixtures in Giemsa's and related stains could not provide the information necessary to distinguish classes of lymphocytes that had been shown to play different roles in the function of the immune system. The fluorescent antibody technique, first developed in the 1940s, provided an obvious means of identifying small numbers of protein molecules in and/or on cells using the high-powered lasers that had recently become available. From the late 1970s on, initial successes in this area led to the exploitation of monoclonal antibodies as specific reagents. When these were used in the early 1980s to define the cellular basis of HIV infection and AIDS and provide a reliable indicator of disease progression, flow cytometry became an essential clinical method, at least for those who could afford and maintain the apparatus.

Today's most complex flow cytometers can simultaneously detect a few thousand molecules of each of ten or more well-defined antigens on single cells. Their simpler predecessors facilitated the discovery of effective antiviral therapies for HIV. From 2000 on, the global effort to extend treatment to HIV

patients in resource-poor countries has motivated the development of a range of progressively simpler apparatus for counting CD4+ T lymphocytes. As noted above, such apparatus for these regions now includes small field-portable fluorescence imaging cytometers that are orders of magnitude smaller, simpler, and cheaper than the far more elaborate flow systems that are now used in malaria research. The imaging instruments can detect signals from fewer than 5,000 fluorescently labeled antibody molecules above background; newer antibody labels should provide even higher sensitivity.

Monoclonal antibodies that detect species-specific parasite protein epitopes are now used in RDTs. Although levels of proteins such as aldolase, HRP2, and pLDH may vary considerably from case to case, antibodies to the latter have been detected by fluorescence microscopy, and biochemical analysis suggests that at least a few tens of thousands of molecules are expressed even in ring-form-parasitized cells. They should therefore be detectable by simple imaging systems as well as by flow cytometers, potentially making it possible for thousands of instruments now in place in the field to be adapted for parasite density determination, diagnostic and otherwise.

The practical development of fluorescent proteins as research tools was, like that of monoclonal antibodies, facilitated by the availability of cytometric apparatus, including high-resolution imaging and confocal microscopes as well as flow cytometers. Although the proteins have proven useful for research applications in malaria (Tilley et al., 2007; Vorobjev et al., 2012), they are substantially less likely than antibodies to be practical for diagnosis.

Nucleic Acid Sequence and Base Composition

Complete genome sequences are now available for three of the six human malaria parasites. The *P. falciparum* genome contains 23.3 Mbp of DNA, with 80.6% in the form of A-T pairs; few other organisms approach this A+T percentage. The *P. vivax* genome contains 26.8 Mbp of DNA, 57.7% in the form of A-T pairs. The *P. knowlesi* genome contains 23.5 Mbp of DNA, 62.5% as A-T pairs. The genomes of *P. malariae* and both *P. ovale* species are estimated to be between 25 and 27 Mbp in size; A+T percentages for these species are not precisely known. Hap-

loid nuclei contain a single copy of the parasite genome.

Although DNA sequence information is widely regarded as capable of providing definitive malaria diagnoses, molecular methods are not yet sufficiently simple and inexpensive enough to replace microscopy. The earliest molecular reagents demonstrated to provide highly sensitive malaria species identification were probes for ribosomal RNA (rRNA) sequences specific to *P. falciparum*. Although autoradiography was initially used for their detection, it is now relatively commonplace to employ fluorescent in situ hybridization (FISH) and flow or image cytometry for the purpose in other contexts. The FISH probes are typically combined with DNA stains, allowing nonspecifically clumped probes to be identified as such by their lack of association with small amounts of DNA comparable in size to the genomes of target organisms. The principal drawback to the use of either FISH probes or fluorescent antibodies lies in the relative lack of abundance of binding sites for them in individual parasites, which typically contain no more than a few tens of thousands of copies of either rRNA sequences or species-specific proteins. Even ring-form parasites can, by contrast, bind millions of molecules of DNA dyes and at least hundreds of thousands of molecules of RNA dyes, providing much stronger fluorescence signals, making detection easier and quantification more precise. Also, nucleic acid dyes are, in general, substantially cheaper and more stable than antibodies and nucleic acid sequence probes, and staining procedures are considerably faster and simpler.

Old and newer cytometric data now suggest that base composition-selective DNA dyes could be used to achieve a genome-based species-specific diagnosis in both flow and image cytometers. Molecular biologists found in the early 1960s that the melting temperature at which double-helical DNA could be broken into single strands depended on the percentages of A-T and G-C pairs, which, respectively, are held together by two and three hydrogen bonds. This allowed the base composition of the DNA of a variety of organisms to be determined relatively simply from melting curves. The nucleic acid binding characteristics of a number of different dyes and drugs could then be determined by analysis of their spectra when associated with different natural and synthetic polynucleotides.

The Hoechst dyes 33258 and 33342 and some related compounds, all originally developed and evaluated as antimalarials, were found to fluoresce strongly only when bound to multiple A-T pairs in DNA. Other drugs such as chromomycin A3 and mithramycin were found to bind with resultant fluorescence only to G-C pairs in DNA. The addition of Hoechst 33258 to mixtures of DNA with substantially different percentages of A-T pairs facilitated ultracentrifugal separation, and was employed in late 1987 to purify *P. falciparum* DNA subsequently used to create sequence-specific probes for the organism (Dame and McCutchan, 1987).

Hoechst 33258 had also been used earlier in 1987 to stain human RBCs infected with *P. falciparum* and *P. vivax* for flow cytometry (Janse et al., 1987), with the former yielding fluorescence signals >21% higher than the latter, precisely as would be predicted from the A-T percentages and genome sizes, neither of which were known at the time. The predicted signal intensities from RBCs infected with *P. knowlesi* would be almost 27% lower than those from Pf-infected RBCs. Although intensity differences of less than 30% are not reliably detectable by eye, much smaller differences are routinely measured cytometrically. Breeders now inseminate cattle using bull sperm sorted into highly enriched X-chromosome-bearing and Y-chromosome-bearing fractions based on a difference of less than 4% in Hoechst dye fluorescence.

Even smaller base composition differences are detectable using combinations of an A-T selective dye with one that has a G-C preference. Two-parameter sorting of human metaphase chromosomes stained with Hoechst 33258 and chromomycin A3 was used to prepare the first chromosome-specific libraries used in the Human Genome Project. This dye combination was also used to identify different bacterial species by base composition and was shown to provide reliable quantification of A+T percentage. Such analyses do not demand use of high-powered, high-priced cell sorters; base composition differences between trypanosomal strains, which would be expected to yield roughly the same fluorescence intensities as would malaria parasites, can be detected on smears using relatively modest fluorescence imaging cytometry apparatus (Mühlpfordt et al., 1985; Mühlpfordt and Berger, 1989, 1990).

The best information now available suggests that base composition measurements

done in such apparatus can reliably discriminate *P. falciparum* from *P. vivax* and *P. knowlesi* and probably distinguish between the latter two species, achieving a specificity equivalent to that obtained with sequence-specific probes but using only relatively inexpensive, simple dyes. The imaging instruments could easily be used to measure the genome sizes and base compositions of the two *P. ovale* species and *P. malariae* by analyzing blood smears from patients with diagnoses confirmed by molecular methods. The utility of DNA base composition measurements for identifying these species could therefore be determined within a few months.

REPLACING MALARIA MICROSCOPY WITH CYTOMETRY: WHAT TO MEASURE AND HOW

Microscopy and Cytometry: Multiparameter Analysis in Stage Identification and Diagnosis

Cell identifications made on the basis of morphologic characteristics visualized by microscopy are of necessity a level removed from those that are made using flow or image cytometry to quantify specific cellular constituents. However, both observers and cytometrists, whether identifying cells by stage and species or determining their functional status, typically consider more than one cellular characteristic. An observer will identify a malaria parasite as a ring stage because of its size and shape, relatively scant cytoplasm, the presence of a single nucleus, and the absence of Hz. Cytometric identification of trophozoites and schizonts can be made by quantification of DNA and RNA content. The former is very highly correlated with the number of nuclei and the latter reflects the amount of cytoplasm present; Hz might or might not be measured, but size and shape information are unnecessary.

The visual identification of gametocytes, particularly the crescent forms that gave the species name to *P. falciparum*, is almost entirely based on morphology, although the presence of Hz also provides a clue. Cytometric quantification of DNA and RNA would reveal a DNA content about twice that of a single genome (Janse et al., 1988), and also would demonstrate the presence of a much larger amount of RNA in female (macro-) than in male (micro-) gametocytes. The difference in RNA content accounts for the more

pronounced blue color of the cytoplasm in Giemsa-stained macrogametocytes. Cytometry would also detect relatively large depolarized SSC signals from gametocytes because of their substantial Hz content; they are the only parasite forms with near-diploid DNA that contain significant amounts of the pigment. Morphologic information would, as in the case of ring forms, be unnecessary for cytometric identification of gametocytes.

All of the parameters mentioned above as relevant to the detection and identification of malaria parasites, i.e., DNA content, base composition, and sequence; and the contents of RNA, hemozoin, and various specific proteins, can be measured accurately and precisely by light transmission, fluorescence, and/or scattering. Whether the measurements are made on liquid samples in a flowing stream or a counting chamber, or on dry samples in smears on slides, the basic analytical problem remains one of detecting and quantifying small amounts of light originating from small regions of space. In 1904, the detection task could only be done by a human observer using a powerful microscope. A century later, although humans remain severely limited in their capacity to quantify light intensity, the more accurate and precise instrumental methods for doing so do not depend on either high magnification or high resolution.

Problems with Microscopy 1: The Sampling Statistics Numbers Game

Even before Giemsa developed what became the definitive stain for blood smears, it had become clear that malaria diagnosis presented problems different from those encountered in blood cell counting, because the levels of parasites present in blood were frequently far lower than was the case for even relatively uncommon types of WBCs and RBCs.

If it is assumed that any malaria parasites seen on a patient's blood smear come from the patient, detection of even a single parasite would indicate the presence of parasitemia. Reliable quantification of parasite density, however, requires counting a number of parasites in a defined volume of blood, and precision depends on the number actually counted. The relevant statistical distribution is Poisson's: the standard deviation (SD) of a count of n objects is $n^{1/2}$ (i.e.),

$$\sqrt{n}$$

even in the absence of any other sources of variability. The percent coefficient of variation (CV), i.e., 100 times the SD divided by the count, defines the best attainable precision of the count. In order to reduce the minimal attainable CV on a density measurement to 10 percent, it is necessary to count 100 parasites; at a density of 100/ μ l, this would require the examination of 1 μ l of blood.

In a modern microscope, the area of a high-power field (HPF) seen with 10 \times eyepieces and a 100 \times oil immersion lens is \sim 0.025 mm²; in older instruments, a single HPF encompassed \sim 0.02 mm². Thus, a 10 \times 20-mm area of a thin smear or film containing 1 μ l of blood would contain 10,000 HPF. At a density of 100/ μ l, the target lower level of detection for microscopy, only 100, or 0.002%, of the \sim 5,000,000 RBCs in 1 μ l of blood contain parasites; it would be necessary to examine 0.01 μ l of blood, or 100 HPF, to encounter a single parasite.

Ronald Ross himself, realizing that the detection of parasites at low densities in thin blood smears would require hours of observation, suggested in 1903 (Ross, 1903) that in addition to the thin smear, a thicker one be made that contained 10 to 20 μ l of blood. He observed that washing an unfixed thick smear with distilled water would remove the hemoglobin from most of the RBCs, enabling parasites to be seen. It remains common practice to prepare both thin and thick smears, examining 200 HPF in both and 500 HPF in the thick smear if no parasites are seen in 200 HPF. By 1910, Ross had refined his methodology (Ross and Thomson, 1910), allowing the actual volume of blood in a thick smear to be estimated relatively precisely by dispensing it from a calibrated capillary tube, typically distributing 1 μ l over a 5 \times 5-mm area, comprising 1250 HPF. Allowing 3 sec/HPF, the entire volume of blood could be searched in an hour, although, as Ross noted, "the identification of the plasmodia [in the thick smear] requires considerable practice."

In recent years, it has been established that the distilled water wash step may remove 60% to 90% of parasites from an unfixed thick smear; gametocytes, typically accounting for only a small percentage of parasites in any case, appear to be lost preferentially in washing. Since even the best thick smears typically do not present parasites in a fashion in which morphological differences between species are as easily distinguished as is possible with thin

smears; however, a good case can be made for the use of fixed thin smears alone (Ohr et al., 2008).

Problems with Microscopy 2: The Resolution Requirement

The relative nonspecificity of the Giemsa stain demands that the human observer process high-magnification, high-resolution images to extract information about the species and stage of any parasites encountered on the slide. We have already noted that equivalent or superior information, independent of morphology, can be obtained using flow cytometers, without the need for high magnification or resolution. Assuming for the moment, however, that computer image analysis of Giemsa-stained slides could be made as accurate as flow cytometry, the collection of data itself would require relatively complex and expensive hardware. It would be necessary for an automated stage to move in increments of no more than a few micrometers in two directions to bring hundreds of high-power fields into the range of the objective lens, and for an automated focusing mechanism to move in submicrometer increments to acquire a properly focused image of each field. A high-power microscope made from a mobile phone, using a spring clip in which to hold a slide and human rather than binary digits for motion control, is unlikely to provide any significant improvement in malaria diagnosis.

Problems with Microscopy 3: Fluorescence Cannot Be Used Optimally

Almost all staining procedures for flow cytometry employ fluorescent dyes and/or labels; it is the quantification of multiple cellular constituents by whole-cell fluorescence measurements in different spectral regions that provides the information needed to identify different cell types and characterize their physiologic states.

The light collection lenses used in flow cytometers are similar in their optical characteristics to the “high dry” and oil immersion lenses used in microscopes. The lens characteristic critical in flow cytometry, however, is numerical aperture, or light-gathering power. Although there are flow cytometers available at premium prices that can provide medium-resolution images of single cells, a more typical instrument collects light equally accurately and precisely from the thin “slice” of a cell on

which it is focused and from the adjacent out-of-focus areas. These instruments do not form an image in which cellular details can be recognized.

Fluorescence measurements of stained cells using either flow cytometers or imaging systems typically yield signals high enough above a background level to make it substantially easier to detect small numbers of dye molecules in or on cells than would be the case with absorption or extinction measurements. Absorption and extinction by particles near or below the optical resolution limit are essentially undetectable; fluorescence and light scattering by particles substantially smaller than the resolution limit, down to the level of individual virions, microvesicles, and even single dye molecules, can be detected in suitably configured apparatus.

Fluorescence microscopes were not available in 1904; until around 1940, they required expensive and relatively power-hungry light sources such as carbon arcs and mercury and xenon arc lamps, and were therefore inaccessible in many places with a high incidence of malaria. From the 1940s on, improvements in incandescent lamp technology made microscopes more affordable and somewhat more energy efficient; since the “Giemsa Centennial” in 2004, high-power LEDs, efficient enough to be run for hours on batteries, have become preferred illumination sources for fluorescence (and other) microscopy as well as for automotive, home, and industrial lighting. Although an LED-illuminated fluorescence microscope must still be run in a dark environment, the addition of a video camera allows a human observer to work in a lighted area.

From the 1920s on, fluorescent dyes were evaluated as stains for blood cells, malaria parasites, and bacteria. Their most notable recent application to public health problems in resource-poor countries has been for the diagnosis of tuberculosis based on the acid-fast nature of the mycobacterial cell wall. It had been known for almost 70 years that using the fluorescent dye auramine O rather than the carbol fuchsin Ziehl-Neelsen absorption method to stain sputum slides typically allowed smaller numbers of organisms to be detected more rapidly using lower (high-dry instead of oil immersion) magnification. A number of manufacturers offer microscope adapters and inexpensive fluorescence microscopes that are equipped with blue LEDs for excitation and yellow filters for observation. This apparatus

is suitable for detecting malaria parasites in acridine orange-stained blood as well as for TB microscopy with auramine O. At least one microscope, the CyScope (Partec), can be equipped with a UV LED for excitation and a blue emission filter, allowing the detection of parasites using the relatively DNA-specific stain DAPI.

Since a human nucleus contains several hundred times as much DNA as a ring-form parasite and almost ten times as much as a schizont with 20 to 30 nuclei, it is not a challenge for a human observer to distinguish parasites from WBC on the basis of the fluorescence intensity of a DNA stain. It would be substantially harder to discriminate between DNAs of different base compositions using a pair of DNA stains. As long as the human observer is involved, it is also necessary to work with a magnified image. Although a single field observed at 40 \times encompasses 6.25 times the area of a 100 \times field, allowing observation time to be shortened by roughly the same factor, the human, even dark-adapted and sitting in a dark room, would be unlikely to be able to detect fluorescence from a stained ring-form parasite when looking at a "life-size" (1 \times magnification) slide.

A further disadvantage of fluorescence microscopy vis-à-vis fluorescence cytometry lies in the tendency of fluorescent dyes to bleach and fade, especially when exposed to the high-intensity excitation used in microscopy and cytometry. Giemsa and other absorption stains leave a much larger amount of dye in stained cells than do typical fluorescence staining procedures; this in itself often makes it difficult to quantify stain intensity by absorption because Beer's law is violated. The large amounts of absorption dyes in cells are, however, easily observable using much less intense illumination than would typically be optimal for fluorescence excitation, so significant fading does not occur even after prolonged illumination. Although there are some chemical treatments that retard the bleaching and fading of fluorescent stains, one typically notices a progressive decrease in the intensity of cells after even a minute or two of scanning a slide. This effectively prevents visual quantification of fluorescence with any precision. In a flow cytometer, the sample flow rate is controlled; cells are not exposed to an illuminating beam until they pass through it for measurement, and all cells spend nearly the same time in the beam, allowing fluorescence intensities from different cells to be compared.

Fluorescence Image Cytometry: Throughput Going Up, Costs Going Down

Quantitative fluorescence microscopy at the whole-cell level can be done by restricting both the illumination and the microscope field of view to an area not too much larger than the area of the cells to be measured, and sequentially positioning individual cells using phase microscopy or an equivalent dye-independent, contrast-enhancing technique and illumination at a wavelength at which the relevant fluorescent dyes do not absorb significantly. Fluorescence measurements can then be made when an excitation source is turned on, or its light is allowed to reach the cell, for only a relatively brief, defined period of time.

This slow process, typically consuming at least several seconds for the measurement of a single cell, was unavoidable when photodiodes or photomultiplier tubes (PMTs) were the only detectors available and extended sources (e.g., arc lamps) were the only available excitation sources. It is possible to speed up the analysis process considerably by examining a larger field of view containing more than one cell, provided cells are well enough separated in space for signals from them to be distinguished. A diode or PMT detector can be used if a laser, focused to a small spot and scanned across the area of the field, is used for illumination; this is analogous to a flow cytometer except that the beam is brought to the cells instead of the cells being brought to the beam. Although such laser-scanning cytometry reduces analysis time to a small fraction of a second per cell, the apparatus incorporates both the costly and complex illumination and light detection components used in a flow cytometer and the precision stage motion and focus control hardware needed in an automated microscope.

If a lamp or LED is used to illuminate a field containing several cells, it becomes more logical to use one or more digital cameras as fluorescence detectors. In this case, it is necessary to use a fluorescence standard such as a dyed slide to measure variations in excitation intensity over the field, providing a normalization factor for raw fluorescence intensity measurements.

This allows reasonably sensitive and precise measurements to be done in standard fluorescence microscopes; it has, moreover, been established that, as is also the case in flow cytometry, the precision of such measurements may be maintained when cells are out of focus.

Using a multimegapixel digital camera chip as a detector overcomes the limitations of the human visual system, demonstrably allowing precise and sensitive quantitative whole-cell measurements of large numbers of cells dispersed on a slide or in a counting chamber to be made at $1\times$ magnification, with all cells in the sample being illuminated simultaneously. Such wide-field imaging cytometry was first demonstrated in the early 1990s when the available digital cameras cost over \$10,000 and the laser and arc lamp sources suitable for excitation were only slightly less expensive, making the apparatus very much simpler than a flow cytometer but not significantly less costly. An equivalent instrument could now be made using LEDs—available at wavelengths ranging from UV to IR and costing only tens of dollars—for illumination and similarly priced camera and microprocessor chips for detection and the very rudimentary image analysis required. Wide-field imaging cytometry requires exposure times no longer than a few seconds; data from thousands of cells in a field can be analyzed in minutes.

Based on the well-established relationships between component costs and finished product costs for similar biomedical apparatus, an image cytometer of the type just described could be sold for no more than a few thousand U.S. dollars. The device could examine $1\ \mu\text{l}$ of blood smeared over a $1\ \text{cm}^2$ area of a slide without requiring either sample movement or focus adjustment, making detection of one or more parasites 95% likely even at a density of $5/\mu\text{l}$. Obviously, the device could be put to use for a wide range of other measurements now made by flow cytometry.

Problems with Flow Cytometry

Reviews of experimental approaches to improving malaria detection, density determination, and diagnosis frequently describe flow cytometry as not only complex and expensive, which it is, but also as imprecise and not particularly sensitive for detecting low parasite densities. We regard the latter characterization as unfair. The small sample of publications dealing with this application, with the earliest dating to the 1970s, have used a wide range of preparative procedures and instruments, with the choice of dyes restricted more often than not by the capabilities of the apparatus available. Much of the earlier work was done using flow cytometers that had only one light source: a 488-nm argon ion laser. The flow cytometers also used nucleic acid dyes that were not par-

ticularly specific for DNA or RNA. This made it difficult to distinguish cells bearing early-stage parasites from reticulocytes. As noted above and illustrated in Figure 11.20.1, the use of DNA- and RNA-specific dyes facilitates this distinction. The addition of measurement parameters, e.g., Hz content, would be expected to increase the specificity and sensitivity of detection, and the small amount of data accumulated by the few laboratories now capable of making such measurements points in this direction. Long ago, flow cytometry was shown to be capable of detecting tumor cells seeded into blood at densities of $1/10,000,000$ WBC (Gross et al., 1995); equivalent performance in malaria would detect 1 parasite/ μl .

Although flow cytometers designed for research and relatively sophisticated clinical immunophenotyping procedures are reasonably well suited to measuring cells from human blood and the immune system, and flow cytometers designed for clinical hematology labs are optimized for the examination of blood cells, no production apparatus of either type comes equipped to measure DNA, RNA, and hemozoin content, let alone DNA base composition and the sequence and content of proteins such as pLDH. Almost all instruments could measure DNA and a specific protein; many could also be adapted to measure RNA and hemozoin. Base composition measurement is problematic because the required base-sensitive DNA dyes require excitation with UV or violet light. Neither wavelength is available on most flow cytometers; adding UV illumination also typically adds at least \$10,000 to the cost of an instrument.

The effect of anemia, particularly iron deficiency anemia, on the course of malaria has been of great interest for some time; a recent paper describes flow cytometric measurement of the labile iron pool in parasitized RBCs (Clark et al., 2013), and it would be of great interest to examine the growth of parasites in RBCs with different hemoglobin contents. However, although one type of existing flow cytometric hematology analyzer (Advia; Siemens Healthcare) can measure hemoglobin, the procedure uses relatively complex optics that cannot readily be added to any existing research flow cytometer, and the hematology analyzers cannot readily be adapted for fluorescence measurements of other relevant parameters such as DNA and RNA. Although an instrument capable of the combined measurements could be built for substantially less than the cost of a

moderately sophisticated commercial research flow cytometer, it has been difficult to convince anybody to pay for it.

At a more mundane level, we note that flow cytometers, even those adapted to use less fluid in their specimen transport mechanisms, consume fairly large volumes of clean, particle-free water or saline, and that access to clean water is limited in many of the malaria-prone areas in which affordable cytometric apparatus for malaria diagnosis and research is most needed. Wide-field image cytometry, which is now capable of measuring the relevant parameters, requires minimal quantities of water and reagents, and the apparatus is less complex and costly, and more robust and portable, than flow cytometry, and is likely to remain so for the foreseeable future.

THE CYTOMETRIC FUTURE IN MALARIA DIAGNOSIS, RESEARCH, AND EPIDEMIOLOGY

At this writing, we are unaware of the existence of any wide-field image cytometers optimized for multiparameter measurements of malaria parasites. We have defined the capabilities of the necessary apparatus during development projects targeting other diagnostic and research applications. Fine-tuning an instrument configuration for malaria work could be accomplished within months, given a supply of unstained patient blood smears containing parasite species identified by nucleic acid sequence and smears from cultured *P. falciparum*, *P. knowlesi*, and—should it become available—*P. vivax*. It would then become possible to put prototypes into the field.

We have been asked about the feasibility of using the installed base of flow cytometers for malaria diagnosis. There are, at present, several thousand such instruments now in use in the field for CD4 counting; most of these relatively simple systems measure fluorescence in two spectral regions and some add a forward or side scatter signal. The fluorescence measurements are sufficiently sensitive to detect a few thousand molecules of each of two antibody labels. Any more complex fluorescence flow cytometer used in either a clinical or research laboratory can almost certainly measure the same two spectral regions with at least equivalent sensitivity.

As noted above, determination of a parasite density of 100/μl with a theoretical minimum percent CV of 10% requires counting at least 100 parasites, which will be distributed among the roughly 5,000,000 RBCs in 1 μl

of whole blood. The simpler flow cytometers, e.g., CD4 counters, may count no more than 5,000 “events” per sec, where an “event” is defined as occurring when a selected “trigger” signal rises above a preset threshold level. In almost all malaria cytometry, the trigger signal is a scatter signal, with the threshold set to include RBCs, but to exclude platelets and smaller particles. Analysis of 5,000,000 RBCs in this case will require 1,000 sec, or 16.7 min. Since the actual flow rate of diluted sample through the cytometer is likely to be no more than 1 μl/sec, the blood sample will have to be diluted 1:1,000 before it is introduced into the cytometer.

The BD Biosciences FACSCount CD4 counter measures only two fluorescence signals. The trigger signal comes from the label on an antibody against the CD3 antigen, the presence of which defines a T cell. The CD4+ T cell count is obtained by counting only those “events,” i.e., T cells, for which there is corresponding signal in the other fluorescence channel, indicating expression of the CD4 antigen. The blood sample is not lysed; however, since the RBCs do not express CD3 antigen, the apparatus is “blind” to them. If the blood sample is diluted 1:10, and the CD4+ T cell count is 1000/μl, it will take only 10 sec to detect 1000 CD4+ T cells, and, even at a count of 50/μl, 100 cells would be counted in 20 sec.

In attempting to detect malaria parasitemia at low levels, it would be advantageous to use a relatively low dilution of blood in order to be able to analyze 1 μl in a minute or two; the trigger signal would have to be chosen to keep the event rate below 5000/sec. The use of a signal from a DNA-specific fluorescent dye would be optimal. RBCs and platelets do not contain DNA; WBCs and nucleated RBCs contain several hundred times as much DNA as do ring-form parasites and almost ten times as much as do the latest-stage schizonts. If blood were diluted 1:10, 0.1 μl of blood would be analyzed each second. With a normal WBC count, no more than 1000 trigger events would come from WBCs, whereas, at a parasite density of 100/μl, only 10 trigger events would be generated by parasitized RBCs. Although small amounts of free DNA are present in blood, their size is typically well under 1 Mbp, so a threshold setting of ~15 Mbp would prevent either free DNA or any bacteria present in blood from generating trigger events because of septicemia or contamination. Nucleated RBCs present at levels of tens of thousands/μl might require that blood be

further diluted; the events they generated, however, would not be confused with any generated by parasitized RBCs. DNA events associated with malaria parasites in the range of 20 Mbp to a few hundred Mbp could also arise if other parasites, e.g., trypanosomes, were present in blood; potential interference would, however, come from micronucleated reticulocytes, which are not normally found in blood.

Micronuclei, also called Howell-Jolly bodies, are chromosomal fragments that remain in RBCs as they enter circulation after incomplete extrusion of the nucleus. Micronucleated reticulocytes typically contain a few times as much DNA as does a single malaria parasite genome; the actual amount is highly variable, however, whereas ring-form-parasitized RBCs contain one, sometimes two, and occasionally three copies of a genome of well-defined size. Many CD4 counters use green (532 or 546-nm) lasers for excitation; these are typically effective at exciting a number of DNA-specific dyes, including DRAQ5 and Vybrant DyeCycle Ruby. Both of these fluoresce at ~670 nm, allowing the shorter fluorescence wavelength (~580 nm) to be used to detect a weaker signal, e.g., one from a fluorescent antibody.

Although the signal from a DNA dye would detect any parasites present in a blood sample, that signal alone would be unlikely to permit reliable discrimination among parasite species; it might also not completely distinguish parasitized RBC from micronucleated reticulocytes. The base composition-specific dyes thus far shown to be usable for discriminating *P. falciparum* DNA from *P. vivax* and *P. knowlesi* DNA require UV or violet excitation—capabilities that are not widely available in simpler flow cytometers. Although one could use sequence-specific rRNA probes for species identification, they are relatively scarce and expensive, and sample preparation would require nucleic acid hybridization. It therefore seems preferable to us to adapt monoclonal antibodies to parasite antigens, which are already well characterized as components of RDTs, for species identification by flow cytometry. Since the diagnosis of *P. falciparum* takes precedence, one might first run a sample stained with DNA dye and antibody to the pLDH of that species, or to HRP2. If specific antigens were not found, one could stain additional aliquots with antibodies to multiple species. If antigen expression is sufficiently uniform, it might also be possible to use different dilutions of panspecific and/or species-

specific antibodies together in a multiplex assay that would allow detection and species identification to be done from a single tube.

The strategy just described could be used with even the simplest flow cytometers for diagnosis, for following parasite clearance on therapy, and for determining low parasite densities for epidemiologic purposes. A simple flow cytometer could also be used with a combination of DNA- and RNA-specific dyes (the yellow fluorescent pyronin Y probably represents a good choice for the latter) to determine resistance to antimalarials by examining the growth of patient-derived parasites in short-term culture. This represents the cytometric analog of the schizont maturation assay (World Health Organization, 2001), which was first developed for *P. falciparum*, but it was also subsequently modified to work with *P. vivax*, eliminating the drawbacks of the associated microscopy.

Of course, more complex flow cytometers can be used for more complex assays, for example, combining DNA, base composition, RNA, hemozoin, and membrane potential measurements. We have already noted that several of these measurements could also be done simultaneously in a much simpler and less expensive wide-field image cytometer, overcoming the economic and infrastructure problems associated with flow cytometry (Basco, 2007), but that no such image cytometers now exist. We should now also point out that we do not know of more than ten flow cytometers worldwide that are presently configured for the full range of measurements. Dozens of these image cytometers could be built for the cost of a single additional high-end flow cytometer.

Economic realities have recently forced substantial reductions in the funds available to deal with all aspects of malaria; we remain optimistic that the right kind of cytometry might actually make it easier for microscopists to work within current fiscal constraints, putting affordable and sustainable technology where the malaria is and empowering those most directly affected by the disease to deal with it more effectively.

ACKNOWLEDGEMENTS

S.H.A. and G.M.C. were supported in part by grants from the National Health and Medical Research Council (Australia) and the Australian Centre for Vaccine Development (ACVD).

B.G. was supported by the NIH (AI079388), the CWRU School of Medicine Vision Fund, and the International Society for Advancement of Cytometry Scholars Program.

T.H. and M.R. were supported in part by the Fundação para a Ciência e a Tecnologia (PIC/IC/291 83214/2007).

H.M.S.'s unsupported malaria work has gotten by with more than a little help from his friends.

We thank Martin Grobusch for his helpful review of an earlier version of this work, Jane Carlton for bringing us up to date on the current status of parasite genome sequencing, and the late Michael Makler for discussions of malaria RDTs and the relevant antibody technology.

LITERATURE CITED

- Apte, S.H., Groves, P.L., Roddick, J.S., P. da Hora, V., and Doolan, D.L. 2011. High-throughput multi-parameter flow-cytometric analysis of micro-quantities of plasmodium-infected blood. *Int. J. Parasitol.* 41:1285-1294.
- Barber, B.E., William, T., Grigg, M.J., Yeo, T.W., and Anstey, N.M. 2013. Limitations of microscopy to differentiate *Plasmodium* species in a region co-endemic for *Plasmodium falciparum*, *Plasmodium vivax* and *Plasmodium knowlesi*. *Malar. J.* 12:8.
- Basco, L.K. 2007. Field Application of In Vitro Assays for the Sensitivity of Human Malaria Parasites to Antimalarial Drugs. World Health Organization, Geneva.
- Boissière, A., Arnathau, C., Duperray, C., Berry, L., Lachaud, L., Renaud, F., Durand, P., and Prugnolle, F. 2012. Isolation of *Plasmodium falciparum* by flow-cytometry: Implications for single-trophozoite genotyping and parasite DNA purification for whole-genome high-throughput sequencing of archival samples. *Malar. J.* 11:163.
- Bosch, F. and Rosich, L. 2008. The contributions of Paul Ehrlich to pharmacology: A tribute on the occasion of the centenary of his Nobel Prize. *Pharmacology* 82:171-179.
- Campo, J.J., Aponte, J.J., Nhabomba, A.J., Sacarlal, J., Angulo-Barturen, I., Jiménez-Díaz, M.B., Alonso, P.L., and Dobaño, C. 2011. Feasibility of flow cytometry for measurements of *Plasmodium falciparum* parasite burden in studies in areas of malaria endemicity by use of bidimensional assessment of YOYO-1 and autofluorescence. *J. Clin. Microbiol.* 49:968-974.
- Ch'ng, J.-H., Kotturi, S.R., Chong, A. G.-L., Lear, M.J., and Tan, K.S.-W. 2010. A programmed cell death pathway in the malaria parasite *Plasmodium falciparum* has general features of mammalian apoptosis but is mediated by clan CA cysteine proteases. *Cell Death Dis.* 1:e26.
- Clark, G., and Kasten, F.H. 1983. History of Staining, 3rd ed. Williams & Wilkins, Baltimore, Maryland.
- Clark, M., Fisher, N.C., Kasthuri, R., and Cerami Hand, C. 2013. Parasite maturation and host serum iron influence the labile iron pool of erythrocyte stage *Plasmodium falciparum*. *Br. J. Haematol.* 161:262-269.
- Cox-Singh, J. 2012. Zoonotic malaria: *Plasmodium knowlesi*, an emerging pathogen. *Curr. Opin. Infect. Dis.* 25:530-536.
- Dame, J.B. and McCutchan, T.F. 1987. *Plasmodium falciparum*: Hoechst dye 33258-CsCl ultracentrifugation for separating parasite and host DNAs. *Exp. Parasitol.* 64:264-266.
- De Kruif, P. 1926. Microbe Hunters (republished 1996). Harcourt, San Diego.
- Desowitz, R.S. 1991. The Malaria Capers: Tales of Parasites and People. Norton, New York.
- Frita, R., Rebelo, M., Pamplona, A., Vigarío, A.M., Mota, M.M., Grobusch, M.P., and Hänscheid, T. 2011. Simple flow cytometric detection of haemozoin containing leukocytes and erythrocytes for research on diagnosis, immunology and drug sensitivity testing. *Malar. J.* 10:74.
- Frita, R., Carapau, D., Mota, M.M., and Hänscheid, T. 2012. In vivo hemozoin kinetics after clearance of *Plasmodium berghei* infection in mice. *Malar. Res. Treat.* 2012:373086.
- Fuehrer, H.-P., Stadler, M.-T., Buczolic, K., Blöeschl, I., and Noedl, H. 2012. Two techniques for simultaneous identification of *Plasmodium ovale curtisi* and *Plasmodium ovale wallikeri* by use of the small-subunit rRNA gene. *J. Clin. Microbiol.* 50:4100-4102.
- Garcia, L.S. 2007. Diagnostic Medical Parasitology, 5th ed. ASM Press, Washington, D.C.
- Garfield, S. 2001. Mauve. Norton, New York.
- Gaynes, R.P. 2011. Germ Theory: Medical Pioneers in Infectious Diseases. ASM Press, Washington, D.C.
- Gerena, Y., Gonzalez-Pons, M., and Serrano, A.E. 2011. Cytofluorometric detection of rodent malaria parasites using red-excited fluorescent dyes. *Cytometry A* 79:965-972.
- Grimberg, B.T. 2011. Methodology and application of flow cytometry for investigation of human malaria parasites. *J. Immunol. Methods* 367:1-16.
- Grimberg, B.T., Erickson, J.J., Sramkoski, R.M., Jacobberger, J.W., and Zimmerman, P.A. 2008. Monitoring *Plasmodium falciparum* growth and development by UV flow cytometry using an optimized Hoechst-thiazole orange staining strategy. *Cytometry A* 73:546-554.
- Grimberg, B.T., Jaworska, M.M., Hough, L.B., Zimmerman, P.A., and Phillips, J.G. 2009. Addressing the malaria drug resistance challenge using flow cytometry to discover new antimalarials. *Bioorg. Med. Chem. Lett.* 19:5452-5457.

- Grobusch, M.P., Hänscheid, T., Krämer, B., Neukammer, J., May, J., Seybold, J., Kun, J.F.J., and Suttorp, N. 2003. Sensitivity of hemozoin detection by automated flow cytometry in non- and semi-immune malaria patients. *Cytometry B* 55:46-51.
- Gross, H.-J., Verwer, B., Houck, D., Hoffman, R.A., and Recktenwald, D. 1995. Model study detecting breast cancer cells in peripheral blood mononuclear cells at frequencies as low as 10^{-7} . *Proc. Natl. Acad. Sci. U.S.A.* 92:537-541.
- Hänscheid, T., Egan, T.J., and Grobusch, M.P. 2007. Haemozoin: From melatonin pigment to drug target, diagnostic tool, and immune modulator. *Lancet Infect. Dis.* 7:675-685.
- Hänscheid, T., Romão, R., Grobusch, M.P., Amaral, T., and Melo-Cristino, J. 2011. Limitation of malaria diagnosis with the Cell-Dyn[®] analyser: Not all haemozoin-containing monocytes are detected or shown. *Int. J. Lab. Hematol.* 33:e14-16.
- Hare, J.D. 1986. Two-color flow-cytometric analysis of the growth cycle of *Plasmodium falciparum* in vitro: Identification of cell cycle compartments. *J. Histochem. Cytochem.* 34:1651-1658.
- Hare, J.D. and Bahler, D.W. 1986. Analysis of *Plasmodium falciparum* growth in culture using acridine orange and flow cytometry. *J. Histochem. Cytochem.* 34:215-220.
- Hawass, Z., Gad, Y.Z., Ismail, S., Khairat, R., Fathalla, D., Hasan, N., Ahmed, A., Elleithy, H., Ball, M., Gaballah, F., Wasef, S., Fateen, M., Amer, H., Gostner, P., Selim, A., Zink, A., and Pusch, C.M. 2010. Ancestry and pathology in King Tutankhamun's family. *JAMA* 303:638-647.
- Izumiyama, S., Omura, M., Takasaki, T., Ohmae, H., and Asahi, H. 2009. *Plasmodium falciparum*: Development and validation of a measure of intraerythrocytic growth using SYBR Green I in a flow cytometer. *Exp. Parasitol.* 121:144-150.
- Janse, C.J., van Vianen, P.H., Tanke, H.J., Mons, B., Ponnudurai, T., and Overdulve, J.P. 1987. *Plasmodium* species: Flow cytometry and microfluorometry assessments of DNA content and synthesis. *Exp. Parasitol.* 64:88-94.
- Janse, C.J., Ponnudurai, T., Lensen, A.H.W., Meuwissen, J.H.E.Th., Ramesar, J., Van der Ploeg, M., and Overdulve, J.P. 1988. DNA synthesis in gametocytes of *Plasmodium falciparum*. *Parasitology* 96:1-7.
- Jogdand, P.S., Singh, S.K., Christiansen, M., Dziegiel, M.H., Singh, S., and Theisen, M. 2012. Flow cytometric readout based on Mitotracker Red CMXRos staining of live asexual blood stage malarial parasites reliably assesses antibody dependent cellular inhibition. *Malar. J.* 11:235.
- Jouin, H., Goguet de la Salmonière, Y.O., Behr, C., Huyin Qan Dat, M., Michel, J.C., Sarthou, J.L., Pereira da Silva, L., and Dubois, P. 1995. Flow cytometry detection of surface antigens on fresh, unfixated red blood cells infected by *Plasmodium falciparum*. *J. Immunol. Methods* 179:1-12.
- Jouin, H., Daher, W., Khalife, J., Ricard, I., Puijalon, O.M., Capron, M., and Dive, D. 2004. Double staining of *Plasmodium falciparum* nucleic acids with hydroethidine and thiazole orange for cell cycle stage analysis by flow cytometry. *Cytometry A* 57:34-38.
- Jun, G., Lee, J.-S., Jung, Y.-J., and Park, J.-W. 2012. Quantitative determination of *Plasmodium parasitemia* by flow cytometry and microscopy. *J. Korean Med. Sci.* 27:1137-1142.
- Karl, S., David, M., Moore, L., Grimberg, B.T., Michon, P., Mueller, I., Zborowski, M., and Zimmerman, P.A. 2008. Enhanced detection of gametocytes by magnetic deposition microscopy predicts higher potential for *Plasmodium falciparum* transmission. *Malar. J.* 7:66.
- Karl, S., Davis, T.M.E., and St-Pierre, T.G. 2009. A comparison of the sensitivities of detection of *Plasmodium falciparum* gametocytes by magnetic fractionation, thick blood film microscopy, and RT-PCR. *Malar. J.* 8:98.
- Kaushansky, A., Rezakhani, N., Mann, H., and Kappe, S.H.I. 2012. Development of a quantitative flow cytometry-based assay to assess infection by *Plasmodium falciparum* sporozoites. *Mol. Biochem. Parasitol.* 183:100-103.
- Kim, C.C., Wilson, E.B., and DeRisi, J.L. 2010. Improved methods for magnetic purification of malaria parasites and haemozoin. *Malar. J.* 9:17.
- Laveran, A. 1907. Protozoa as causes of diseases. Nobel lecture (<http://www.nobelprize.org/>).
- Lawrence, C. and Olson, J.A. 1986. Birefringent hemozoin identifies malaria. *Am. J. Clin. Pathol.* 86:360-363.
- Lewert, R.M. 1952. Nucleic acids in Plasmodia and the phosphorus partition of cells infected with *Plasmodium gallinaceum*. *J. Infect. Dis.* 91:125-144.
- Malleret, B., Claser, C., Ong, A.S.M., Suwanarusk, R., Sriprawat, K., Howland, S.W., Russell, B., Nosten, F., and Rénia, L. 2011. A rapid and robust tri-color flow cytometry assay for monitoring malaria parasite development. *Sci. Rep.* 1:118.
- Mandy, F., Nicholson, J., Autran, B., and Janossy, G. 2002. T-cell subset counting and the fight against AIDS: Reflections over a 20-year struggle. *Cytometry* 50:39-45.
- Maude, R.J., Buapetch, W., and Silamut, K. 2009. A simplified, low-cost method for polarized light microscopy. *Am. J. Trop. Med. Hyg.* 81:782-783.
- McMorrow, M.L., Aidoo, M., and Kachur, S.P. 2011. Malaria rapid diagnostic tests in elimination settings can they find the last parasite? *Clin. Microbiol. Infect.* 17:1624-1631.
- Mendelow, B.V., Lyons, C., Nhlangothi, P., Tana, M., Munster, M., Wypkema, E., Liebowitz, L., Marshall, L., Scott, S., and Coetzee, T.L. 1999. Automated malaria detection by depolarization of laser light. *Br. J. Haematol.* 104:499-503.

- Mühlpfordt, H. and Berger, J. 1989. Characterization and grouping of *Trypanosoma brucei brucei*, *T.b. gambiense* and *T.b. rhodesiense* by quantitative DNA-cytofluorometry and discriminant analysis. *Trop. Med. Parasitol.* 40:1-8.
- Mühlpfordt, H. and Berger, J. 1990. Characterization and grouping of *Trypanosoma cruzi* stocks by DNA base-specific fluorochromes and discriminant analysis. *Parasitol. Res.* 76:319-325.
- Mühlpfordt, H., Berger, J., and Glaser, N. 1985. Cytofluorometry as a method for the differentiation of trypanosomes. *Trop. Med. Parasitol.* 36:135-139.
- Murray, C.J.L., Rosenfeld, L.C., Lim, S.S., Andrews, K.G., Foreman, K.J., Haring, D., Fullman, N., Naghavi, M., Lozano, R., and Lopez, A.D. 2012. Global malaria mortality between 1980 and 2010: A systematic analysis. *Lancet* 379:413-431.
- Murray, C.K., Gasser, R.A. Jr., Magill, A.J., and Miller, R.S. 2008. Update on rapid diagnostic testing for malaria. *Clin. Microbiol. Rev.* 21:97-110.
- O'Meara, W.P., Barcus, M., Wongsrichanalai, C., Muth, S., Maguire, J.D., Jordan, R.G., Prescott, W.R., and McKenzie, F.E. 2006. Reader technique as a source of variability in determining malaria parasite density by microscopy. *Malar. J.* 5:118.
- O'Meara, W.P., Hall, B.F., and McKenzie, F.E. 2007. Malaria vaccine efficacy: The difficulty of detecting and diagnosing malaria. *Malar. J.* 6:36.
- Ohr, C., O'Meara, W.P., Remich, S., McEvoy, P., Ogutu, B., Mtalib, R., and Odera, J.S. 2008. Pilot assessment of the sensitivity of the malaria thin film. *Malar. J.* 7:22.
- Pattanapanyasat, K., Udomsangpet, R., and Webster, H.K. 1993. Two-color flow cytometric analysis of intraerythrocytic malaria parasite DNA and surface membrane-associated antigen in erythrocytes infected with *Plasmodium falciparum*. *Cytometry* 14:449-454.
- Philipp, S., Oberg, H.-H., Janssen, O., Leippe, M., and Gelhaus, C. 2012. Isolation of erythrocytes infected with viable early stages of *Plasmodium falciparum* by flow cytometry. *Cytometry A* 81:1048-1054.
- Rebelo, M., Shapiro, H.M., Amaral, T., Melo-Cristino, J., and Hänscheid, T. 2012. Haemozoin detection in infected erythrocytes for *Plasmodium falciparum* malaria diagnosis—prospects and limitations. *Acta Trop.* 123:58-61.
- Rebelo, M., Sousa, C., Shapiro, H.M., Mota, M.M., Grobusch, M.P., and Hänscheid, T. 2013. A novel flow cytometric hemozoin detection assay for real-time sensitivity testing of *Plasmodium falciparum*. *PLoS One* 8:e61606.
- Ross, R. 1903. An improved method for the microscopical diagnosis of intermittent fever. *Lancet* 161:86.
- Ross, R. and Thomson, D. 1910. Some enumerative studies on malarial fever. *Proc. Royal Soc. London B* 83:159-173.
- Shapiro, H.M. 1981. Flow cytometric estimation of DNA and RNA content in intact cells stained with Hoechst 33342 and pyronin Y. *Cytometry* 2:143-150.
- Shapiro, H.M. 2003. *Practical Flow Cytometry*, 4th ed. Wiley-Liss, Hoboken, N.J.
- Shapiro, H.M., Natale, P.J., and Kametsky, L.A. 1979. Estimation of membrane potentials of individual lymphocytes by flow cytometry. *Proc. Natl. Acad. Sci. U.S.A.* 76:5728-5730.
- Sinnis, P., De La Vega, P., Coppi, A., Krzych, U., and Mota, M.M. 2013. Quantification of sporozoite invasion, migration, and development by microscopy and flow cytometry. *Methods Mol. Biol.* 923:385-400.
- Tilley, L., McFadden, G., Cowman, A., and Klonis, N. 2007. Illuminating *Plasmodium falciparum*-infected red blood cells. *Trends Parasitol.* 23:268-277.
- Vorobjev, I.A., Buchholz, K., Prabhat, P., Ketman, K., Egan, E.S., Marti, M., Duraisingh, M.T., and Barteneva, N.S. 2012. Optimization of flow cytometric detection and cell sorting of transgenic *Plasmodium* parasites using interchangeable optical filters. *Malar. J.* 11:312.
- Wongchotigul, V., Suwanna, N., Krudsood, S., Chindanon, D., Kano, S., Hanaoka, N., Akai, Y., Maekawa, Y., Nakayama, S., Kojima, S., and Looareesuwan, S. 2004. The use of flow cytometry as a diagnostic test for malaria parasites. *Southeast Asian J. Trop. Med. Public Health* 35:552-559.
- World Health Organization. 2001. *In vitro* micro-test (mark III) for the assessment of the response of *Plasmodium falciparum* to chloroquine, mefloquine, quinine, amodiaquine, sulfadoxine/pyrimethamine and artemisinin. World Health Organization, Geneva.
- World Health Organization. 2008. *Malaria Microscopy Quality Assurance Manual*, Version 1. World Health Organization, Geneva.
- World Health Organization. 2010. *Parasitological confirmation of malaria diagnosis: Report of a WHO technical consultation Geneva, 6-8 October 2009*. World Health Organization, Geneva.
- World Health Organization. 2011. *World Malaria Report 2011*. World Health Organization, Geneva.



Evaluation of a Novel Magneto-Optical Method for the Detection of Malaria Parasites

Ágnes Orbán¹, Ádám Butykai¹, András Molnár¹, Zsófia Pröhle¹, Gergő Fülöp¹, Tivadar Zelles², Wasan Forsyth³, Danika Hill^{3,4}, Ivo Müller³, Louis Schofield^{3,5}, Maria Rebelo⁶, Thomas Hänscheid⁶, Stephan Karl³, István Kézsmárki^{1,7*}

1 Department of Physics, Budapest University of Technology and Economics, Budapest, Hungary, **2** Department of Oral Biology, Semmelweis University, Budapest, Hungary, **3** Infection and Immunity Division, Walter and Eliza Hall Institute of Medical Research, Parkville, Victoria, Australia, **4** Department of Medical Biology, University of Melbourne, Parkville, Victoria, Australia, **5** Queensland Tropical Health Alliance Australian Institute of Tropical Health and Medicine James Cook University, Douglas, Queensland, Australia, **6** Instituto de Medicina Molecular, Faculdade de Medicina, Lisbon, Portugal, **7** Condensed Matter Research Group of the Hungarian Academy of Sciences, Budapest, Hungary

Abstract

Improving the efficiency of malaria diagnosis is one of the main goals of current malaria research. We have recently developed a magneto-optical (MO) method which allows high-sensitivity detection of malaria pigment (hemozoin crystals) in blood via the magnetically induced rotational motion of the hemozoin crystals. Here, we evaluate this MO technique for the detection of *Plasmodium falciparum* in infected erythrocytes using in-vitro parasite cultures covering the entire intraerythrocytic life cycle. Our novel method detected parasite densities as low as ~40 parasites per microliter of blood (0.0008% parasitemia) at the ring stage and less than 10 parasites/ μL (0.0002% parasitemia) in the case of the later stages. These limits of detection, corresponding to approximately 20 pg/ μL of hemozoin produced by the parasites, exceed that of rapid diagnostic tests and compete with the threshold achievable by light microscopic observation of blood smears. The MO diagnosis requires no special training of the operator or specific reagents for parasite detection, except for an inexpensive lysis solution to release intracellular hemozoin. The devices can be designed to a portable format for clinical and in-field tests. Besides testing its diagnostic performance, we also applied the MO technique to investigate the change in hemozoin concentration during parasite maturation. Our preliminary data indicate that this method may offer an efficient tool to determine the amount of hemozoin produced by the different parasite stages in synchronized cultures. Hence, it could eventually be used for testing the susceptibility of parasites to antimalarial drugs.

Citation: Orbán Á, Butykai Á, Molnár A, Pröhle Z, Fülöp G, et al. (2014) Evaluation of a Novel Magneto-Optical Method for the Detection of Malaria Parasites. PLoS ONE 9(5): e96981. doi:10.1371/journal.pone.0096981

Editor: Stuart Alexander Ralph, University of Melbourne, Australia

Received: November 16, 2013; **Accepted:** April 15, 2014; **Published:** May 13, 2014

Copyright: © 2014 Orbán et al. This is an open-access article distributed under the terms of the Creative Commons Attribution License, which permits unrestricted use, distribution, and reproduction in any medium, provided the original author and source are credited.

Funding: This work was supported by Hungarian Research Funds OTKA K108918, TAMOP-4.2.1.B-09/1/KMR-2010-0001, by NHMRC grants GNT1021544 and GNT1043345 awarded to Ivo Müller and by NHMRC grants GNT637406 and GNT1058665 awarded to Louis Schofield. Stephan Karl is supported through an NHMRC early career research fellowship (GNT1052760). The funders had no role in study design, data collection and analysis, decision to publish, or preparation of the manuscript.

Competing Interests: Co-author Ivo Müller is a PLOS ONE Editorial Board member. This does not alter the authors' adherence to PLOS ONE Editorial policies and criteria.

* E-mail: kezsmark@dept.phy.bme.hu

Introduction

Although research activities aim at developing novel methods for high-sensitivity diagnosis of malaria, only a few of these approaches are feasible for clinical and in-field diagnosis. The two main diagnostic methods currently in practice are the antigen-based detection of malaria parasites using rapid diagnostic tests (RDT) and the microscopic observation of infected red blood cells in blood smears [1–4]. The detection limits of RDT and light microscopy have been reported to be approximately 100 parasites/ μL and 5–50 parasites/ μL , respectively [1,5–7], corresponding to parasitemia levels of around 0.002% and 0.0001–0.001%. RDT are becoming more affordable, however, they cannot provide a quantitative measure of parasitemia. Presently they do not possess sufficient sensitivity to detect low-level infections which are very common in endemic settings along with the false positive samples due to the presence of parasite protein (HRP2) even after resolving the infection. On the other hand, light

microscopy is time and labor intensive and the detection threshold of 5 parasites/ μL is rather limited to ideal conditions such as good-quality blood films, highly trained microscopists and high-powered microscopes; most of which are rarely present in real life practice. Most routine diagnostic laboratories achieve approximately 50 parasites/ μL and can detect about 50% of malaria cases [6,8,9].

Molecular methods such as polymerase chain reaction (PCR) assays surpass the performance of RTD and light microscopy [10,11]. However, they often require expensive equipment and reagents, highly trained laboratory personnel and are prone to contamination [12]. Although real-time PCR has a detection limit corresponding to a few parasites per μL of blood [13,14], it is not yet a practical method for routine diagnosis under field conditions.

The idea to take advantage of the unique magnetic properties of malaria pigment (hemozoin) and to use it as an alternative target of optical diagnosis has been proposed by several groups [15–19]. Hemozoin is a micro-crystalline heme compound produced by malaria parasites as they detoxify free heme derived from

hemoglobin digestion [20]. Our recent study using synthetic hemozoin crystals suspended in blood demonstrated that the rotating-crystal magneto-optical (MO) diagnostic method can detect hemozoin concentrations down to 15 pg/ μL [15]. Using data describing the rate of hemoglobin digestion by *P. falciparum* available in the literature [21–23], this threshold concentration was estimated to be equivalent to a parasite density of ≤ 30 parasites/ μL in infected blood provided that the entire amount of hemozoin produced by the parasites is released into the lysed cell suspension.

However, the situation in malaria infection and thus the requirements for diagnostic applications are different. One aspect is that in *Plasmodium falciparum* infections only early developmental forms, such as rings and early trophozoites, are usually found in the peripheral circulation, since later developmental stages sequester in the capillaries [24]. Furthermore, the shape and size of hemozoin crystals may be different for synthetic and naturally grown crystals and also depend on the developmental stages of the parasites as well as the parasite species [25–27]. Since the MO method detects only hemozoin crystals released into suspension which can be magnetically rotated, the aggregation of the crystals or their binding to other components of lysed blood could influence the sensitivity of this technique.

In the present study we aimed to address these issues by evaluating the performance of the MO technique using synchronized cultures of *P. falciparum* and to investigate the limit of detection in samples with low levels of parasitemia, which would establish its potential usefulness for field trials. (For a short description of the MO approach see the Materials and Methods section.).

Results and Discussion

Parasite Cultures

We investigated the sensitivity and detection threshold of the rotating-crystal MO method using two cultures (A and B) with different maturity distributions of the parasites. The distributions of the parasites among the different stages – early-ring, late-ring, early-trophozoite, late-trophozoite, early-schizont and late-schizont stages – in the two cultures are displayed in Fig. 1 together with light microscopy images of parasites representative of these stages.

Culture A had a total parasite density of $P \approx 3.1 \times 10^5$ parasites/ μL . Parasite stage distribution corresponded to the beginning of the parasite life cycle following synchronization with mostly ring stages and some early trophozoites. This culture, referred to as the *ring stage culture* in the following, is representative to the distribution of parasite blood stages most often encountered in natural *P. falciparum* infections.

Culture B had a lower total parasite density of $P \approx 2.8 \times 10^4$ parasites/ μL . Parasite stage distribution corresponded to the verge of the first and second parasite life cycles where some of the parasites were still in the schizont form but most of them, following invasion, already turned to early-stage rings of the next generation. Since the main hemozoin content present in this culture was formed during the first life cycle with a dominant contribution from schizont stage parasites [21–23], we will refer to it as the *schizont stage culture*. Schizont stage parasites are not normally found in the peripheral blood during human *P. falciparum* infection due to their sequestration in small capillary blood vessels [24]. However, this stage restriction is not present in other, non-sequestering, species of human malaria parasites such as *P. vivax* [28].

Limit of Detection

The MO signal, the measure of hemozoin content within the lysed cell suspension, is shown in Fig. 2 for dilution series of culture A and culture B. The 20 serial 2-fold dilutions of the two cultures using uninfected erythrocytes allowed for the MO signal to be assessed over 6 orders of magnitude of parasitemia. As a general trend in Fig. 2A, the MO signal varies proportionally to the parasitemia level and the signal for each sample shows a gradual decrease with increasing frequencies of the rotating magnetic field. This frequency dependence is in agreement with previous results obtained for synthetic hemozoin crystals suspended in blood and originates from the viscosity of the lysed cell suspension hindering fast rotations of the crystals [15].

Samples from the dilution series of culture B exhibited higher MO signals as compared to dilutions of culture A with the same level of parasitemia reflecting the increase in intracellular hemozoin content over the course of the parasite life cycle. Although the overall frequency dependence of the MO signal is similar for the two cultures, the more pronounced decrease with increasing frequency found for the dilutions of culture B is likely due to the larger crystal size formed in schizont stage parasites.

In order to determine the limit of detection limit for our method, the MO signal at 20 Hz was plotted versus parasitemia (and parasite density) in Fig. 2B for the dilution series of the ring and schizont stage cultures. For reference, we also measured uninfected blood samples using the same protocol. These showed a residual MO signal of $\Delta T/T \approx 4 \times 10^{-4}$ % in average as indicated in Fig. 2B. This value corresponds to the mean limit of detection of our method. At low levels of parasite density (P), namely for samples with $P \leq 10$ parasites/ μL from the dilution series of the ring stage culture, the signal does not further decrease with decreasing parasitemia but approaches the residual level observed for the uninfected samples. Hence, this residual MO signal is not related to hemozoin. We note that the frequency dependence of the residual MO signal differs from the hemozoin-dependent MO signal dominant at higher concentrations. (See curves corresponding to the ring stage sample with $P = 9.5$ parasites/ μL , the schizont stage sample with $P = 0.5$ parasites/ μL and the uninfected samples in Fig. 2A.).

For highly diluted ring stage samples with $P \leq 10$ parasites/ μL , where the MO signal is independent of the parasite density, we found that the standard deviation of the MO signal from the mean limit of detection (represented by the signal level of uninfected samples) is $\Delta T/T \approx 1.6 \times 10^{-4}$ %. Assuming Gaussian distribution for the residual MO signal values, the 95% confidence level of the mean limit of detection for ring stage samples is $\Delta T/T \approx 7.2 \times 10^{-4}$ % corresponding to a parasite density of ~ 40 parasites/ μL . This is equivalent to a parasitemia level of 0.0008%. The scattering of the data is larger for schizont stage samples. In that case we estimated the 95% confidence level of the mean limit of detection to be $\Delta T/T \approx 2 \times 10^{-3}$ % corresponding to a parasite density of ~ 10 parasites/ μL or a parasitemia of 0.0002%.

The presence of a frequency-dependent residual MO signal indicates that some components of lysed blood can be magnetically oriented and rotated similarly to the hemozoin crystals. We have also studied freshly drawn blood following the same lysis protocol. The residual MO signal observed in that case was considerably lower than found for either the ring or schizont stage samples, which were measured following the freeze-thaw-lysis procedure (see Fig. 2 and also Fig. S1 of the Supporting Information S1). The noise floor of our equipment, shown for pure water in Fig. 2, is nearly frequency independent and about one order of magnitude smaller than the residual signal from fresh blood. This enables

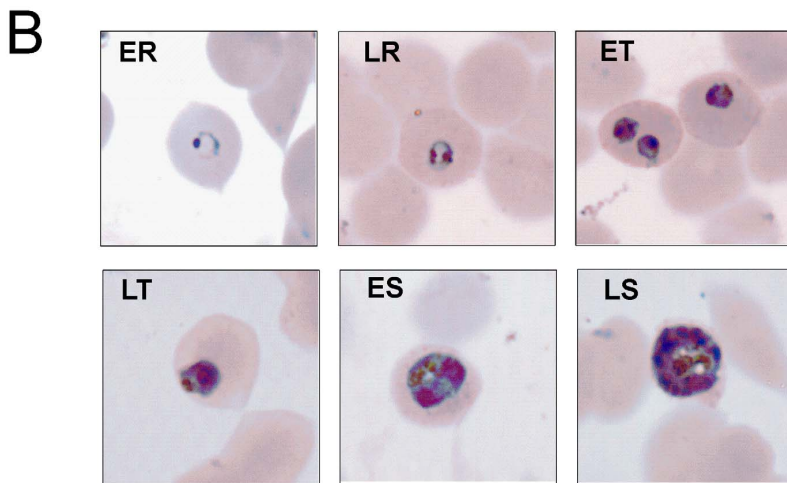
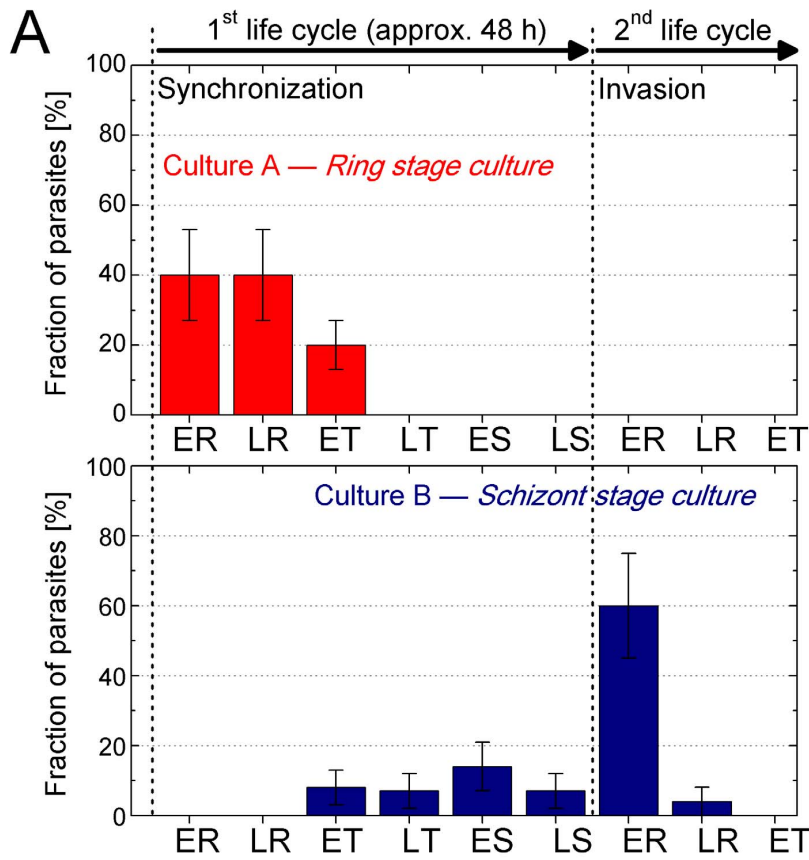


Figure 1. Distribution of parasite life cycle stages in the two *Plasmodium falciparum* cultures used in the present study. Panel A: The *ring stage culture* contained early rings, late rings and some early trophozoites of the first generation after synchronization. The *schizont stage culture* was on the verge of the first and second life cycles where most of the schizont stages have already turned to early ring stages of the second generation following invasion. Therefore, the ring stage culture contained only the hemozoin present in the parasites up to the early trophozoite stage, while the schizont stage culture had the entire hemozoin content formed during one generation of parasites with the largest portion produced by schizonts. Panel B: Light microscopy images of Giemsa stained thin blood films containing infected red blood cells with parasites in different stages of maturity (taken from these two cultures). In both panels the labels ER, LR, ET, LT, ES and LS correspond to early-ring, late-ring, early-trophozoite, late-trophozoite, early-schizont and late-schizont stages, respectively.
doi:10.1371/journal.pone.0096981.g001

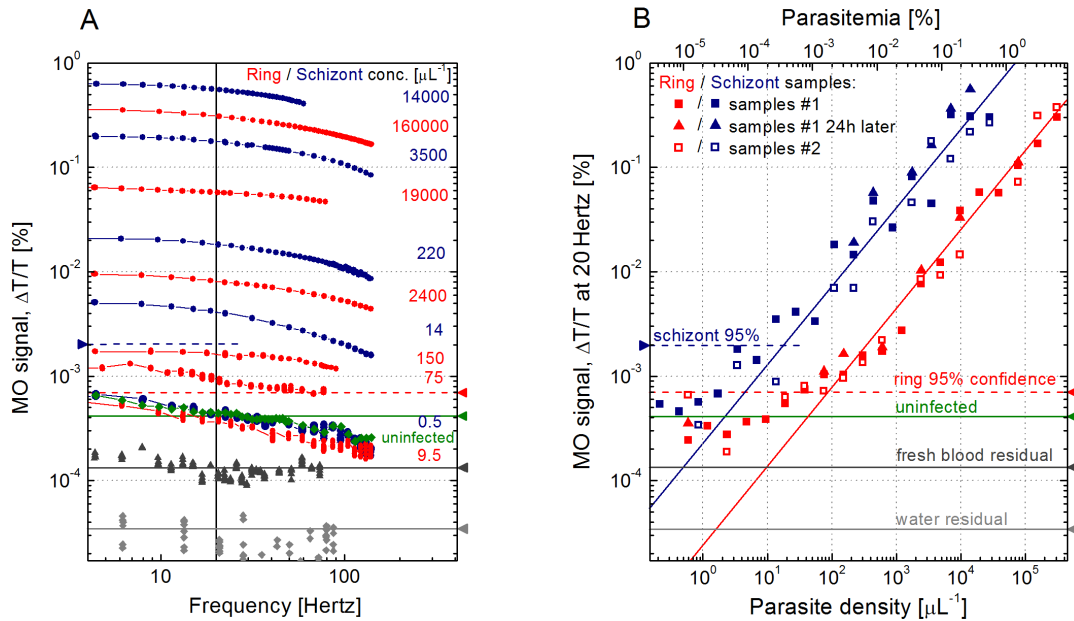


Figure 2. Magneto-optical (MO) detection of parasitemia in synchronized *Plasmodium falciparum* cultures. Panel A: Red and blue curves show the frequency dependent MO signal for samples from the ring and schizont stage cultures, respectively, with various levels of parasite density given in μL^{-1} units on the right of the respective curves. The green curves show the signal from uninfected reference samples. Data plotted with triangles and diamonds are the residual signal from freshly hemolyzed uninfected blood and water, respectively. The frequency scale corresponds to the rotation speed of the magnetic field. Panel B: Red and blue squares in panel B are the MO signal values measured at 20 Hz – indicated by a vertical solid line in panel A – for the dilution series prepared from the original ring and schizont stage cultures, respectively. Solid and open squares correspond to the duplicate samples labeled as samples #1 and samples #2. Triangles indicate the results obtained by re-measuring samples #1 with 24 h delay. The solid lines following the trend of the MO signal at higher parasite densities for ring (red line) and schizont (blue line) samples are guides for the eye. For ring and schizont stage samples with parasite densities lower than 10 parasites/ μL and 1 parasites/ μL , respectively, the MO signal does not further decrease. The green horizontal line shows the residual MO signal of uninfected blood, which is the mean detection limit of our method. The 95% confidence levels of this mean detection limit for the ring and schizont stage samples are indicated by red and blue dashed lines, respectively. Correspondingly, for ring and schizont stage samples with parasite density higher than 40 parasites/ μL and 10 parasites/ μL , respectively, the diagnosis is positive with a confidence of at least 95%. The background signal for freshly hemolyzed uninfected blood and water are also shown by dark and light grey lines. All these horizontal indicators are also shown in panel A for reference. The upper horizontal scale shows the corresponding levels of parasitemia.
doi:10.1371/journal.pone.0096981.g002

further improvement of the detection limit provided that the residual MO signal from blood can be reduced by optimizing blood sample treatment.

Sequential MO measurements performed on the same sample at different time intervals up to one hour gave identical results. In several cases we confirmed the reproducibility of the protocol by repeating the measurement for duplicate samples labeled as samples #1 and samples #2 in Fig. 2B. When samples were re-measured after being stored for 24 hours at 4°C and sonicated for 30 minutes prior to the MO measurements, typically an increase of the MO signal of not more than 10–30% was observed. Additional data about the effect of sonication on the MO signal, given in Fig. S1 of the Supporting Information S1, show that sonication increases the MO signal. We found that the elimination of the entire freeze-thaw-sonication process from the protocol reduces the MO signal by 30–40%. In this case, the lowest level of parasitemia still detectable with a confidence of 95% is approximately 0.0012% for ring stage parasites. Thus, the use of the clearing solution alone appears to be sufficient if fresh blood samples are used. Nevertheless, it seems beneficial to use sonication, where available, especially when screening samples with very low parasitemias.

Hemozoin Concentration of the Cultures

The hemozoin content of the two cultures can be roughly estimated from the parasite density and the stages of parasite development specified in Fig. 1. Ring and early trophozoite stages respectively convert about 3–5% and 15–20% of the total hemoglobin in the infected red blood cells to hemozoin [21,22]. Parasites in the schizont stage convert about 50–70% of hemoglobin to hemozoin [20,29,30]. Using these hemoglobin conversion rates, we calculated the hemozoin concentrations of the undiluted ring and schizont stage cultures and compared them to the amounts estimated based on our MO reference data previously obtained for synthetic hemozoin [15]. These values are listed in Table 1. According to the estimate based on the MO signal, the lowest hemozoin concentration still measurable by our MO setup using the present protocol is ~ 20 pg/ μL , which is close to the threshold reported for artificial crystals [15]. (This concentration refers to the original hemozoin content of blood samples before the 20-fold dilution performed prior to MO measurements.)

The estimate based on the MO signal gives lower values for the hemozoin content of both cultures than the estimate based on the hemoglobin conversion rates quoted above. The comparison between electron microscopy images of natural and synthetic hemozoin crystals, shown in Fig. 3, implies that this difference

Table 1. Using the hemozoin conversion rates reported in the literature for the different parasite stages (rings: 3–5%, trophozoites: 15–20%, and schizonts: 50–70%) [20–22,29,30] and the stage distribution of the parasites (Fig. 1), we estimated the hemozoin content of culture A (ring stage culture) and culture B (schizont stage culture).

	Estimated hemozoin content based on literature	Estimated hemozoin content from MO measurements
Culture A ($P = 3.1 \times 10^5$ parasites/ μL)	17–25 ng/ μL	6 ng/ μL
Culture B ($P = 2.8 \times 10^4$ parasites/ μL)	14–23 ng/ μL hemozoin	9 ng/ μL

The lower and upper values of the hemozoin content correspond to the lower and upper values of the conversion rates quoted above. Note that the cultures have different parasite densities. We also estimated the hemozoin concentration of the two cultures based on MO signal using the conversion factor $c_{\text{H2}} = 1 \text{ ng}/\mu\text{L} \rightarrow \Delta T/T = 1.4\%$ between the hemozoin concentration and the low-frequency ($\sim 1 \text{ Hz}$) MO signal previously determined for artificial hemozoin crystals suspended in blood [15].

doi:10.1371/journal.pone.0096981.t001

arises from the different size of the two types of crystals. The natural crystallites in this study were considerably smaller (with typical lengths of ~ 200 – 500 nm) than the synthetic ones (~ 500 – 900 nm) used in our former work [15]. The weaker frequency dependence of the MO signal observed in the present study indicates that natural crystals are able to follow the rotation of the magnetic field up to higher frequencies than the synthetic ones due to their reduced size. Furthermore, the comparison between the natural crystals within the parasites and those extracted from the cultures confirms no major change either in the size or in the morphology of the crystals due to our lysis-sonication protocol.

We have also studied the change in the hemozoin concentration during the maturation of parasites using additional cultures. Our preliminary results (displayed in Fig. S2–S4 of the Supporting Information S1) show the gradual increase of the hemozoin content during the maturation of the parasites and imply that hemozoin is present in ring stages in agreement with recent works [31–33].

Conclusions

The potential of exploiting hemozoin as a magnetic biomarker for malaria diagnosis has stimulated extended research over the last few decades. Taking advantage of the paramagnetic nature of hemozoin, several approaches have been proposed to improve the sensitivity of existing methods e.g., by magnetic separation of malaria infected erythrocytes from whole blood prior to diagnosis [16,34–36]. More recently, new techniques have emerged, which directly use hemozoin as target material for magnetic diagnosis. These techniques include detection of depolarized side-scatter in flow cytometry [37], electrochemical magneto immunoassays [38], magnetically enriched surface enhanced resonance Raman spectroscopy [39,40], acousto-optic detection [31] and magneto-optical detection using polarized light [17,18,41]. Among them, to the best of our knowledge, our rotating crystal MO diagnostic technique is the first realized in a cost-effective and compact format with excellent sensitivity.

In the present study, the detection limit of our rotating-crystal MO diagnostic technique was found to be ~ 40 parasites/ μL and ~ 10 parasites/ μL for ring and schizont stage parasites, respectively. These limits of detection are below the threshold currently achievable with RDT (>100 parasites/ μL) and are within the same range as the limits of expert microscopy for malaria diagnosis (5 – 50 parasites/ μL) [1]. For the present set of blood samples, which were kept frozen and thawed before the measurement, the performance of the method was limited by a residual MO signal due to some part of the lysed cell suspension. This residual MO signal obscures the genuine MO signal of hemozoin at parasite

densities lower than the limits quoted above. Preliminary results indicate that for measurements on freshly lysed blood samples, which is the condition relevant to instant diagnosis, the detection limit of our rotating crystal MO platform could be further improved.

Limitations of our diagnostic technique include i) the possibility of false positive detections due to the presence of hemozoin in the blood, e.g. contained within white blood cells [42], for extended periods of time after an infection has been cleared and ii) the possibility of false negative results in case an infection only contains very early ring stage parasites with little or no hemozoin. Furthermore, methods targeting only hemozoin as a marker for infection cannot distinguish between different malaria species. However, the specificity of our MO diagnostic scheme, owing to variations in the typical size and morphology of hemozoin crystals produced by different species, needs to be evaluated by a comparative study on various *Plasmodium species*. We emphasize that only studies on field isolates will be able to elucidate the impact of these possible confounding factors and the present study is the basis for such field-based trials.

It is currently believed that without active case detection of asymptomatic malaria infections, malaria eradication will be impossible or very difficult to achieve [6]. However, there are no diagnostic tools for rapidly screening hundreds of people per day, on-site and with high sensitivity [43]. In principle, the rotating-crystal MO diagnostic method has the potential to fulfill these requirements as it is cost-effective, rapid and highly sensitive. However, rigorous field based assessment of the method's performance as well as further method development will have to be conducted in order to judge the value of this method.

Our preliminary results (see the Supporting Information S1) show that the present methodology may provide an efficient in-vitro laboratory tool to test the susceptibility of the parasites to novel or clinically relevant antimalarial drugs by monitoring the effect of drugs on the rate of hemozoin formation [44]. The scope of this technique may also cover the study or diagnosis of other human diseases, such as schistosomiasis, which are also caused by blood-feeding organisms producing hemozoin similarly to malaria parasites [45–48].

Materials and Methods

Parasite Culture

P. falciparum parasites (laboratory adapted strain 3D7) were cultured following the method of Trager and Jensen with modifications [49]. The culture medium was RPMI 1640 with L-glutamine (GIBCO cat # 31800) supplemented with $2 \text{ mg}/\text{mL}$ NaHCO (Merck, cat # 106329), $25 \text{ mg}/\text{L}$ gentamicin (Pfizer, cat

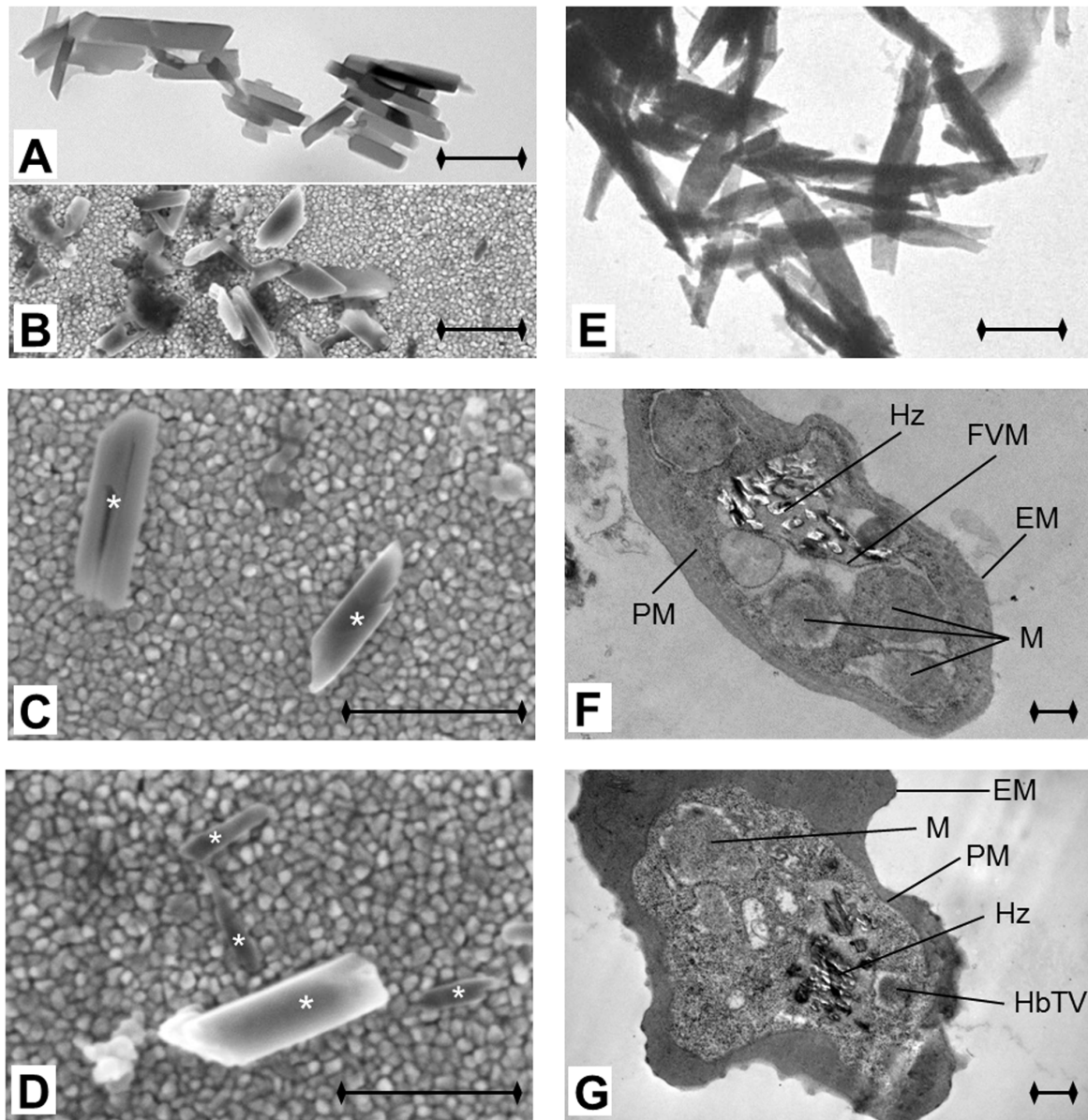


Figure 3. Hemozoin crystals observed by electron microscopy in-situ and after isolation. The transmission electron microscopy (TEM) image in panel A and scanning electron microscopy (SEM) images in panels B, C and D show hemozoin crystals extracted from the samples previously used for the MO measurements. The granular background of the SEM images comes from the gold coating of the glass substrate. Individual crystals in panels C and D are marked with asterisks. The length of the black bar at the bottom right corner of each panel is 500 nm. The typical length of the extracted hemozoin crystals ranges from 200 nm to 500 nm. For comparison, a TEM image of synthetic hemozoin crystals used in our previous MO study [15] is shown in panel E. These synthetic crystals have more elongated shape with a typical length of 500–900 nm. Panels F and G display TEM images of intact infected erythrocytes in the schizont stage. Distinct components of the parasite and the erythrocyte can be observed including the erythrocyte membrane (EM), parasite membrane (PM), food vacuole membrane (FVM), merozoites (M), hemoglobin transport vesicles (HbTV), knobs (K) and hemozoin (Hz).

doi:10.1371/journal.pone.0096981.g003

61022027), 50mg/L hypoxanthine (Calbiochem, cat # 4010), 25 mM HEPES (SAFC, cat # 90909C) and 10% pooled O+ human serum (mixed blood groups, Australian Red Cross Blood Service). Cultures were maintained at 4% hematocrit with changes of culture medium every 48 hours and diluted with uninfected O+

red blood cells when the parasitemia exceeded 5%. Parasites were maintained in an atmosphere of 5% CO₂ and 1% O₂ in N₂. Parasite cultures were kept in stage synchrony by applying the 5% Sorbitol method, first described by Lambros and Vanderberg [50]. Hemozoin liberated from late stage parasites by the synchroniza-

tion process was removed by washing the cells in RPMI medium after the Sorbitol induced cell lysis and before re-establishment of the culture. Cultures A and B were harvested ~0 hour and ~40 hours after synchronization of the culture and prepared for the MO study according to the following protocol.

Parasite stages and densities were determined by counting the number of parasites in the following 6 stages: early ring (ER), late ring (LR), early trophozoites (ET), late trophozoites (LT), early schizonts (ES) and late schizonts (LS). For this determination 5000 red blood cells were counted on Giemsa stained thin blood films. Parasite density values were calculated from the parasitemia values based on the assumption that 1 μL of blood contains 5×10^6 red blood cells at 50% hematocrit [1]. For both cultures, 2-fold dilution series were prepared in duplicate and adjusted to a volume of 200 μL at a hematocrit of 50%, using human erythrocytes (Red Cross blood bank, Royal Melbourne Hospital, VIC, Australia). Blood lysates were prepared from the dilutions by freeze-thawing twice and were stored at -80°C until they were shipped for MO measurement to Hungary. The sample set also contained uninfected reference samples.

Blood Treatment Prior MO Diagnosis

After thawing the lysates they were diluted 20-fold in distilled water, to give a final volume of 4 mL. After adding 100 μL of a red cell lysis buffer (2.5 V/V% Triton X-100 (Sigma-Aldrich, Budapest, Hungary) in 0.1 M NaOH (Sigma-Aldrich, Budapest, Hungary)) the sample was sonicated for 30 minutes to dissociate potential aggregates prior to measurement. MO signals were recorded on 1 mL volumes taken from the samples immediately after sonication. The possible effect of storage was assessed by re-measuring samples after 20 to 120 minutes kept at room temperature and after 24 hours kept at 4°C .

Magneto-optical Measurements

MO measurements were performed blinded. Signals were recorded using 1 mL from each lysed sample. The prototype of the rotating magnet setup as well as the underlying physical principles of the detection method are described in our previous study [15]. In brief, the sample is inserted into an assembly of permanent magnets arranged in a ring. This creates a strong homogenous magnetic field ($B=1\text{ T}$) at the center where the sample is inserted and allows the alignment of the crystals. When the magnetic ring is rotated, the co-aligned hemozoin crystals follow this rotation. Polarized light from a laser diode is transmitted through the sample in the direction perpendicular to the plane of the rotating magnetic field. The rotation of the co-aligned dichroic crystals gives rise to a periodic change in the transmitted intensity (ΔT), which – divided by the time-averaged intensity (T) – corresponds to the MO signal.

In fact, we demonstrated that the MO signal is proportional to the concentration of synthetic hemozoin crystals in the sample [15]. The MO signal was measured with increasing rotational speed values of the magnet, in the range of 1–130 Hertz. Our

previous study showed that a good signal-to-noise ratio is observed in the range of 10–30 Hertz [15], and thus 20 Hertz was chosen to investigate the limit of detection. However, the measurement of the MO signal in the rotation frequency range of 1–130 Hertz was performed for two reasons: i) the frequency-dependence of the signal may provide information about the size distribution of the freely rotating crystals and ii) the frequency-dependence may give additional information at very low hemozoin concentrations and help to differentiate between infected samples and uninfected controls.

Electron Microscopy

For transmission electron microscopy (TEM), parasite samples were fixed in resin blocks and 70–120 nm thin sections were cut using a Leica EM UC6 microtome (Leica Microsystems, North Ryde, NSW, Australia) and brought onto carbon coated copper TEM grids (ProSciTech, Thuringowa, Qld., Australia). The TEM grids were then stained with 5% uranyl acetate for 15 minutes and Reynold's lead citrate solution for 5 minutes. For synthetic hemozoin, the aqueous suspension of crystals was dropped onto formvar membrane (purchased from Sigma-Aldrich) and brought onto carbon coated copper TEM grids. TEM was conducted on a JEOL 2100 TEM (JEOL Inc., Tokyo, Japan).

For scanning electron microscopy (SEM), the samples giving the highest MO signal were used and hemozoin crystals were extracted following the method of Chen and coworkers [45]. The dark brown pellet obtained by this method was re-suspended in 80 μL water. For SEM imaging small droplets of the suspension containing the hemozoin crystals were applied to gold coated glass slides without further purification or treatment. The droplets were dried overnight at room temperature. The SEM images were acquired on a LEO 1540XB electron microscope using the in-lens detector. The accelerating voltage was set to 3 kV and the viewing angle was perpendicular to the gold surface. For details of the method see the Supporting Information S1.

Supporting Information

Supporting Information S1 Supporting information file containing Figs. S1–S4 and supporting text. (PDF)

Acknowledgments

The authors acknowledge assistance with electron microscopy by L. Kyriliak, M. Saunders, J. Shaw and facilities of the Center of Microscopy, Characterization and Analysis at The University of Western Australia.

Author Contributions

Conceived and designed the experiments: IK SK. Performed the experiments: AO AB AM ZP GF TZ WF DH MR SK IK. Analyzed the data: AO AB LS IM TH SK IK. Contributed reagents/materials/analysis tools: WF DH MR. Wrote the paper: IK SK.

References

- Moody A (2002) Rapid diagnostic tests for malaria parasites. *Clinical Microbiology Reviews* 15: 66–78.
- Hanscheld T (1999) Diagnosis of malaria: a review of alternatives to conventional microscopy. *Clinical and Laboratory Haematology* 21: 235–245.
- Payne D (1988) Use and limitations of light-microscopy for diagnosing malaria at the primary health-care level. *Bulletin of the World Health Organization* 66: 621–626.
- Wongsrichanalai C, Barcus MJ, Muth S, Sutamihardja A, Wernsdorfer WH (2007) A review of malaria diagnostic tools: Microscopy and rapid diagnostic test (rdt). *American Journal of Tropical Medicine and Hygiene* 77: 119–127.
- Maltha J, Gillet P, Jacobs J (2013) Malaria rapid diagnostic tests in endemic settings. *Clinical Microbiology and Infection* 19: 399–407.
- Alonso PL, Barnwell JW, Bell D, Hanson K, Mendis K, et al. (2011) A research agenda for malaria eradication: Diagnoses and diagnostics. *Plos Medicine* 8: e1000396.
- O'Meara WP, Remich S, Ogutu B, Lucas M, Mtalib R, et al. (2006) Systematic comparison of two methods to measure parasite density from malaria blood smears. *Parasitology Research* 99: 500–504.
- Okell LC, Ghani AC, Lyons E, Drakeley CJ (2009) Submicroscopic infection in *Plasmodium falciparum*-endemic populations: A systematic review and meta-analysis. *Journal of Infectious Diseases* 200: 1509–1517.

9. Perkins MD, Bell DR (2008) Working without a blindfold: the critical role of diagnostics in malaria control. *Malaria Journal* 7: s5.
10. Coleman RE, Sattabongkot J, Promstaporn S, Maneechai N, Tippayachai B, et al. (2006) Comparison of pcr and microscopy for the detection of asymptomatic malaria in a plasmodium falciparum/vivax endemic area in thailand. *Malaria Journal* 5: 121.
11. Snounou G (1996) Detection and identification of the four malaria parasite species infecting humans by pcr amplification. *Methods in Molecular Biology* 50: 263–291.
12. Tangpukdee N, Duangdee C, Wilairatana P, Krudsood S (2009) Malaria diagnosis: A brief review. *Korean Journal of Parasitology* 47: 93–102.
13. Owusu-Ofori AK, Betson M, Parry CM, Stothard JR, Bates I (2013) Transfusion-transmitted malaria in ghana. *Clinical Infectious Diseases* 56: 1735–1741.
14. Khairnar K, Martin D, Lau R, Ralevski F, Pillai DR (2009) Multiplex real-time quantitative pcr, microscopy and rapid diagnostic immuno-chromatographic tests for the detection of plasmodium spp: performance, limit of detection analysis and quality assurance. *Malaria Journal* 8: 284.
15. Butykai A, Orban A, Kocsis V, Szaller D, Bordacs S, et al. (2013) Malaria pigment crystals as magnetic micro-rotors: key for high-sensitivity diagnosis. *Scientific Reports* 3: 1431.
16. Karl S, David M, Moore L, Grimberg BT, Michon P, et al. (2008) Enhanced detection of gametocytes by magnetic deposition microscopy predicts higher potential for plasmodium falciparum transmission. *Malaria Journal* 7: 66.
17. Mens PF, Matelon RJ, Nour BYM, Newman DM, Schallig H (2010) Laboratory evaluation on the sensitivity and specificity of a novel and rapid detection method for malaria diagnosis based on magneto-optical technology (mot). *Malaria Journal* 9: 207.
18. Newman DM, Heptinstall J, Matelon RJ, Savage L, Wears ML, et al. (2008) A magneto-optic route toward the in vivo diagnosis of malaria: Preliminary results and preclinical trial data. *Biophysical Journal* 95: 994–1000.
19. Zimmerman PA, Thomson JM, Fujioka H, Collins WE, Zborowski M (2006) Diagnosis of malaria by magnetic deposition microscopy. *American Journal of Tropical Medicine and Hygiene* 74: 568–572.
20. Francis SE, Sullivan DJ, Goldberg DE (1997) Hemoglobin metabolism in the malaria parasite plasmodium falciparum. *Annual Review of Microbiology* 51: 97–123.
21. Moore LR, Fujioka H, Williams PS, Chalmers JJ, Grimberg B, et al. (2006) Hemoglobin degradation in malaria-infected erythrocytes determined from live cell magnetophoresis. *Faseb Journal* 20: 747–749.
22. Orjih AU, Fitch CD (1993) Hemozoin production by plasmodium-falciparum - variation with strain and exposure to chloroquine. *Biochimica Et Biophysica Acta* 1157: 270–274.
23. Becker K, Tilley L, Vennerstrom JL, Roberts D, Rogerson S, et al. (2004) Oxidative stress in malaria parasite-infected erythrocytes: host-parasite interactions. *International Journal for Parasitology* 34: 163–189.
24. Cooke BM, Coppel RL (1995) Cytoadhesion and falciparum-malaria - going with the flow. *Parasitology Today* 11: 282–287.
25. Slater AFG, Swiggard WJ, Orton BR, Flitter WD, Goldberg DE, et al. (1991) An iron carboxylate bond links the heme units of malaria pigment. *Proceedings of the National Academy of Sciences of the United States of America* 88: 325–329.
26. Noland GS, Briones N, Sullivan DJ (2003) The shape and size of hemozoin crystals distinguishes diverse plasmodium species. *Molecular and Biochemical Parasitology* 130: 91–99.
27. Jaramillo M, Bellemare MJ, Martel C, Shio MT, Contreras AP, et al. (2009) Synthetic plasmodiumlike hemozoin activates the immune response: A morphology - function study. *Plos One* 4: e6957.
28. Carvalho BO, Lopes SCP, Nogueira PA, Orlandi PP, Bargieri DY, et al. (2010) On the cytoadhesion of plasmodium vivax-infected erythrocytes. *Journal of Infectious Diseases* 202: 638–647.
29. Hackett S, Hamzah J, Davis TME, St Pierre TG (2009) Magnetic susceptibility of iron in malaria-infected red blood cells. *Biochimica Et Biophysica Acta-Molecular Basis of Disease* 1792: 93–99.
30. Weissbuch I, Leiserowitz L (2008) Interplay between malaria, crystalline hemozoin formation, and antimalarial drug action and design. *Chemical Reviews* 108: 4899–4914.
31. Lukianova-Hleb EY, Campbell KM, Constantinou PE, Braam J, Olson JS, et al. (2014) Hemozoin-generated vapor nanobubbles for transdermal reagent- and needle-free detection of malaria. *Proceedings of the National Academy of Sciences of the United States of America* 111: 900–905.
32. Nam J, Huang H, Lim H, Lim C, Shin S (2013) Magnetic separation of malaria-infected red blood cells in various developmental stages. *Analytical Chemistry* 85: 7316–7323.
33. Abu Bakar N, Klonis N, Hanssen N, Chan C, Tilley L (2010) Digestive-vacuole genesis and endocytic processes in the early intraerythrocytic stages of plasmodium falciparum. *Journal of Cell Science* 123: 441–450.
34. Paul F, Roath S, Melville D, Warhurst DC, Osisanya JOS (1981) Separation of malaria-infected erythrocytes from whole-blood - use of a selective high-gradient magnetic separation technique. *Lancet* 2: 70–71.
35. Carter V, Cable HC, Underhill BA, Williams J, Hurd H (2003) Isolation of plasmodium berghei ookinetes in culture using nycodenz density gradient columns and magnetic isolation. *Malaria Journal* 2: 35.
36. Karl S, Davis TME, St Pierre TG (2011) Short report quantification of plasmodium falciparum gametocytes by magnetic fractionation. *American Journal of Tropical Medicine and Hygiene* 84: 158–160.
37. Frita R, Rebelo M, Pamplona A, Vigario AM, Mota MM, et al. (2011) Simple flow cytometric detection of haemozoin containing leukocytes and erythrocytes for research on diagnosis, immunology and drug sensitivity testing. *Malaria Journal* 10: 74.
38. Castilho MD, Laube T, Yamanaka H, Alegret S, Pividori MI (2011) Magneto immunoassays for plasmodium falciparum histidine-rich protein 2 related to malaria based on magnetic nanoparticles. *Analytical Chemistry* 83: 5570–5577.
39. Yuen C, Liu Q (2012) Magnetic field enriched surface enhanced resonance raman spectroscopy for early malaria diagnosis. *Journal of Biomedical Optics* 17: 017005.
40. Hobro AJ, Konishi A, Coban C, Smith NI (2013) Raman spectroscopic analysis of malaria disease progression via blood and plasma samples. *Analyst* 138: 3927–3933.
41. Newman DM, Matelon RJ, Wears ML, Savage LB (2010) The in vivo diagnosis of malaria: Feasibility study into a magneto-optic fingertip probe. *Ieee Journal of Selected Topics in Quantum Electronics* 16: 573–580.
42. Schwarzer E, Bellomo G, Giribaldi G, Ulliers D, Aresè P (2001) Phagocytosis of malarial pigment haemozoin by human monocytes: a confocal microscopy study. *Parasitology* 123: 125–131.
43. Baird JK (2010) Eliminating malaria-all of them. *Lancet* 376: 1883–1885.
44. Rebelo M, Sousa C, Shapiro H, Mota MM, et al. (2013) A novel flow cytometric hemozoin detection assay for real-time sensitivity testing of plasmodium falciparum. *Plos One* 8: e61606.
45. Chen MM, Shi LR, Sullivan DJ (2001) Haemoproteus and schistosoma synthesize heme polymers similar to plasmodium hemozoin and beta-hematin. *Molecular and Biochemical Parasitology* 113: 1–8.
46. Oliveira MF, d'Avila JCP, Tempone AJ, Soares J, Rumjanek FD, et al. (2004) Inhibition of heme aggregation by chloroquine reduces schistosoma mansoni infection. *Journal of Infectious Diseases* 190: 843–852.
47. Oliveira MF, d'Avila JC, Torres CR, Oliveira PL, Tempone AJ, et al. (2000) Haemozoin in schistosoma mansoni. *Molecular and Biochemical Parasitology* 111: 217–221.
48. Karl S, Gutierrez L, Lucyk-Maurer R, Kerr R, Candido RRF, et al. (2013) The iron distribution and magnetic properties of schistosoma eggshells: Implications for improved diagnostics. *Plos Neglected Tropical Diseases* 7: e2219.
49. Trager W, Jensen JB (1976) Human malaria parasites in continuous culture. *Science* 193: 673–675.
50. Lambros C, Vanderberg JP (1979) Synchronization of plasmodium-falciparum erythrocytic stages in culture. *Journal of Parasitology* 65: 418–420.

Point-of-care tests: where is the point?

A recurrent theme in the Review by Paul Drain and colleagues¹ is the dichotomy between point-of-care (POC) tests and their laboratory counterparts, which implies that these tests can be used outside the laboratory. Certainly, rapid diagnostic tests (RDTs) for malaria are an example of a POC test; however, loop-mediated isothermal amplification (LAMP) for malaria has also been touted as a possible POC test.^{2,3} This discrepancy raises an important question: where is the point of care? For example, GeneXpert (Cepheid, CA, USA) MTB/RIF needs basic laboratory infrastructure, shifting the POC from a remote area to a peripheral laboratory.⁴ By contrast, RDTs allow efficient diagnosis of malaria at the POC, even in remote communities, far away from laboratories or hospitals. Despite the analytical advantage of nucleic acid-based tests like LAMP, basic laboratory infrastructure is needed, meaning that it cannot be used at the same proximity to the POC as RDTs can.

Authors of one review define the setting where POC tests can be used, ranging from home to community, health post, peripheral laboratory, and finally hospital.⁴ Malaria tests are deemed POC tests in four of these five categories. Oddly, this approach seems to turn almost any existing malaria diagnostic test into a POC test, and the POC into a so-called area of care, which is somehow contradictory in itself. The effect of this approach is the inflationary use of the term POC test because there is little, if any, difference to a standard laboratory-based test.

Where or what is the POC for malaria patients, and what defines it? At least, tests would need to have some quantifiable degree of suitability for being a POC test? On the Foundation for Innovative New Diagnostics website,⁵ LAMP is categorised as a "district and sub-district level" test, whereas the term POC is mentioned in the context of RDTs.

These questions are not mundane because the term point-of-care could be no longer useful. The term could even be misused in an attempt to capture increasingly competitive research funding or could misinform implementation strategies in times of tight budgets. In conclusion, and notwithstanding the many useful suggestions, criteria, and definitions provided, we believe that the otherwise highly valuable review by Drain and colleagues should have addressed this POC (point of consideration) more elaborately.

We declare no competing interests.

*Thomas Häscheid, Maria Rebelo, Martin P Grobusch
t.häscheid@medicina.ulisboa.pt

Instituto de Microbiologia, Faculdade de Medicina de Lisboa, P-1649-028 Lisbon, Portugal (TH); Instituto de Medicina Molecular, Faculdade de Medicina de Lisboa, Lisbon, Portugal (MR); and Center for Tropical Medicine and Travel Medicine, Department of Infectious Diseases, Division of Internal Medicine, Academic Medical Center, University of Amsterdam, Amsterdam, Netherlands (MPG)

- 1 Drain PK, Noubary F, Freedberg KA, et al. Diagnostic point-of-care tests in resource limited settings. *Lancet Infect Dis* 2014; **14**: 239–49.
- 2 Cordray MS, Richards-Kortum RR. Emerging nucleic acid-based tests for point-of-care detection of malaria. *Am J Trop Med Hyg* 2012; **87**: 223–30.
- 3 Abdul-Ghani R, Al-Mekhlafi AM, Karanis P. Loop-mediated isothermal amplification (LAMP) for malarial parasites of humans: would it come to clinical reality as a point-of-care test? *Acta Trop* 2012; **122**: 233–40.
- 4 Pai NP, Vadnais C, Denking C, Engel N, Pai M. Point-of-care testing for infectious diseases: diversity, complexity, and barriers in low- and middle-income countries. *PLoS Med* 2012; **9**: e1001306.
- 5 Foundation for innovative new diagnostics. About us. <http://www.finddiagnostics.org/about> (accessed Feb 27, 2014).

Paul Drain and colleagues¹ proposed a standard set of criteria to assess the diagnostic accuracy, clinical effect, and costs of point-of-care (POC) tests in low-income countries (LICs). We agree with the authors on the need to improve access to rapid diagnostics in LICs, and we add several factors based on our own research on POC testing for common infections through our work at the

Mercy Hospital Research Laboratory in Bo, Sierra Leone.

First, POC tests are already available in some LICs for many infections not listed in panel 1 of the Review, including hepatitis B virus² and typhoid.³ The cost effectiveness of POC tests improves when test kits for locally common infections can be purchased in bulk, and the positive predictive value associated with high incidence and prevalence could improve assessment of the test's diagnostic accuracy in LIC settings.

Second, we add to the authors' comments on the scarcity of research on real-world use of POC tests by calling for further comparisons of laboratory-based with community-based and home-based tests. The effectiveness of POC tests in all three settings—the clinic, community, and home—needs further testing and validation. Reports of POC test studies need to describe environmental factors, such as temperature and storage conditions, that might affect the test results, and discuss socioeconomic and educational or literacy challenges that could have an effect on test results in all of these venues.

Third, clear eligibility criteria should be included for clinicians, patients, and families who might be considering use of POC tests so that these users will know when use of these tests is appropriate. A high number of valid positive results will improve the perceived value of the tests for future POC use. Additionally, test kits designed for community-based or home-based use should include clear instructions on appropriate treatment for those with both a positive or negative test, who might need to consult with a clinician for additional tests. The goal of testing outside of care centres should be to shorten the time to initiation of appropriate treatment, which might need the results of several different tests, especially if a person with an apparent infection or other illness has a negative result for an infectious disease POC test.